

Title	Palladium and manganese catalysis in C-H activation
Authors	Mackey, Katrina
Publication date	2020-04
Original Citation	Mackey, K. 2020. Palladium and manganese catalysis in C-H activation. PhD Thesis, University College Cork.
Type of publication	Doctoral thesis
Rights	© 2020, Katrina Mackey. - https://creativecommons.org/licenses/by-nc-nd/4.0/
Download date	2023-05-07 18:08:09
Item downloaded from	http://hdl.handle.net/10468/10912



UCC

University College Cork, Ireland
Coláiste na hOllscoile Corcaigh

Palladium and Manganese Catalysis in C-H Activation



University College Cork
Coláiste na hOllscoile Corcaigh

Katrina Mackey, B.Sc.

A thesis presented for the degree of
Doctor of Philosophy
to

National University of Ireland, Cork

School of Chemistry
University College Cork

Supervisor: Dr. Gerard P. McGlacken

Head of School: Dr. Humphrey Moynihan

April 2020

Table of Contents

Chapter 1: Introduction

1.1 Aryl-aryl bond formation	1
1.2 Direct arylation <i>via</i> C-H activation	2
1.2.1 Literature examples of double C-H activation	4
1.3 Mechanisms of direct arylation	7
1.4 Aims and Objectives (Chapter 2)	8
1.5.1 Biological importance of targeted heterocycles	10
1.5.2 Literature examples of palladium catalysed direct arylation of 2-pyrone analogues and 2-coumarin analogues	11
1.6.1 Biological significance of dibenzofurans	14
1.6.2 Previous synthesis of dibenzofurans	15
1.6.3 Literature examples of palladium catalysed intramolecular double C-H activation for the synthesis of dibenzofurans	16
1.7.1 Aims and Objectives (Chapter 3)	19
1.7.2 Literature examples on the direct arylation of <i>ortho</i> -halo diarylethers	20
1.7.3 Nitrogen based ligands in direct arylation reactions	22
1.8 References	24

Chapter 2: Cyclisation of 4-phenoxy-2-coumarins, 2-pyrones and other heterocycles *via* double C-H activation

2.1 Preface	26
2.2 Background	26
2.2.1 Synthesis of 4-phenoxy-2-pyrone substrates	26
2.2.2 Optimisation of double C-H activation reaction conditions	27
2.2.3 Optimisation of reaction conditions performed on diphenylamine and benzophenone	29
2.2.4 Optimisation of reaction conditions performed on 4-phenoxy-2-pyrone	31
2.3.1 Synthesis of substrates (2-pyrones)	33
2.3.2 Demonstration of substrate scope for double C-H activation of 2-pyrones	35
2.3.3 Synthesis of substrates (2-coumarins)	42

2.3.4 Demonstration of substrate scope for double C-H activation of 2-coumarins	44
2.3.5 Structure elucidation of the major and minor <i>meta</i> -fluoro benzofuro- chromenone regioisomers	50
2.4.1 Proposed mechanism for Conditions A	57
2.4.2 Monitoring of double C-H activation by NMR spectroscopy for Conditions B	58
2.5 Three-step synthesis of flemichapparin C	66
2.6 Double C-H activation of 2(1 <i>H</i>)-quinolone analogue	70
2.6.1 Synthesis of starting material	70
2.6.2 Cyclisation of the 4-phenoxy-quinolone substrate	74
2.7.1 Investigation into alternative solvents	75
2.7.2 Investigation into alternative oxidants	76
2.8 Conclusion	78
2.9 Expansion of double C-H activation methodology	78
2.10 Dibenzofurans (Background)	80
2.11 Synthesis of diarylether substrates	80
2.12.1 Demonstration of substrate scope for double C-H activation of mono-substituted diarylethers	85
2.12.2 Demonstration of substrate scope for double C-H activation of di-substituted diarylethers	88
2.12.3 Substrates which proved difficult to cyclise	90
2.13 Investigation of <i>N</i> -linker for double C-H activation	91
2.14 Synthesis of starting materials	91
2.15.1 Double C-H activation of <i>N</i> -methyl diphenylamine substrates	93
2.15.2 Double C-H activation of 3-methoxy diphenylamine	94
2.16 Conclusion	96
2.17 References	98
Chapter 3: Synthesis of dibenzofurans <i>via</i> intramolecular direct arylation of <i>ortho</i>-bromo diarylethers	
3.1 Preface	101
3.2 Background	101
3.3 Ligand identification	103

3.4 Optimisation of reaction conditions	106
3.5 Synthesis of <i>ortho</i> -bromo diarylether starting materials	109
3.5.1 Starting material synthesis <i>via</i> nucleophilic aromatic substitution	109
3.5.2 Starting material synthesis <i>via</i> Chan-Lam-Evans arylation of phenols and phenyl boronic acids	113
3.5.3 Starting material synthesis using iodonium salts	119
3.6.1 Demonstration of substrate scope for direct arylation of <i>ortho</i> -bromo diarylethers	124
3.6.2 Substrates that proved difficult to cyclise	127
3.7.1 Investigation into electron rich substrates	128
3.7.2 Re-optimisation of direct arylation conditions for electron rich substrates	132
3.7.3 Difficulties encountered during the purification of crude material	139
3.8 Additional substrates examined under the reaction conditions	141
3.9 Mechanism for the direct arylation of <i>ortho</i> -bromo diarylethers	142
3.10 Conclusion and future work	146
3.11 References	148
Chapter 4: Introduction	
4.1 Manganese catalysed C-H activation	152
4.2 Aims and Objectives	154
4.3.1 Literature examples of manganese catalysed C-H activation: addition to aldehydes	155
4.3.2 Literature examples of manganese/base system for C-H activation reactions: alkyne coupling partners	155
4.3.3 Manganese catalysed C-H activation: olefin coupling partners	159
4.3.4 Manganese catalysed hydroarylation of aldehydes, ketones and imines	162
4.4 Mechanistic papers on manganese catalysed C-H activation	162
4.5 Literature examples of manganese/acid systems for C-H activation reactions	163
4.6 References	170

Chapter 5: Synthesis of manganese carbonyl phosphine complexes and their application in C-H activation reactions

5.1 Preface	175
5.2 Background	175
5.3.1 Ligand design	175
5.3.2 Choice of ligand for manganese	175
5.3.3 Synthesis of manganese carbonyl phosphine complexes	176
5.3.4 Bonding in metal carbonyl phosphine complexes	179
5.3.5 Spectroscopic and single crystal x-ray results	180
5.4.1 Investigation of manganese carbonyl phosphine complexes in C-H activation reactions	190
5.4.2 Synthesis of <i>N</i> -(2-pyridyl) indole	199
5.4.3 Investigation into alternative coupling partners for manganese catalysis	201
5.5.1 Manganese catalysed hydroarylation of ketones	206
5.5.2 Results and discussion	207
5.5.3 Reaction monitoring	209
5.5.4 Reaction sampling	210
5.5.5 Analysis of the ¹ H NMR spectra of the crude reaction mixtures	210
5.5.6 Catalyst deactivation	214
5.5.7 Reduction of catalyst loading	216
5.5.8 Mechanistic discussion	216
5.5.9 Hydroarylation reaction investigated with ethyl pyruvate	220
5.5.10 Concluding remarks	220
5.6 Additional reactions investigated	222
5.7 Conclusion and future work	223
5.8 References	226
Concluding remarks	230
Chapter 6: Experimental	
6.1 General information	231
6.1.1 Analysis of known and novel compounds	231

6.2 Synthesis of starting materials	233
6.2.1 Preparation of 4-bromo-6-methyl-2 <i>H</i> -pyran-2-one (23)	233
6.2.2 General procedure for preparation of 4-phenoxy-6-methyl-2 <i>H</i> -pyran-2-ones (24, 30-40)	233
6.2.3 Preparation of 4-bromo-2-coumarin (54)	239
6.2.4 General procedure for preparation of 4-phenoxy-2-coumarins (55-68)	239
6.2.5 Synthesis of quinolone starting materials	246
6.2.6 Preparation of 4-bromo-7-methoxy-2-coumarin (88)	248
6.2.7 Preparation of 4-(benzo[<i>d</i>][1,3]dioxol-5-yl)-7-methoxy-2 <i>H</i> -chromen-2-one (89)	249
6.2.8 Preparation of mono-substituted diarylethers (102-113)	250
6.2.9 Procedure for preparation of bis(3-methylphenyl) iodonium triflate (121)	256
6.2.10 Procedure for preparation of di-substituted diarylethers (112-126) <i>via</i> bis(3-methylphenyl) iodonium triflate (121)	257
6.2.11 Procedure for preparation of diphenyliodonium tetrafluoroborate salt (129)	260
6.2.12 Procedure for preparation of 3-phenoxy benzaldehyde (116) <i>via</i> diphenyliodonium tetrafluoroborate salt (129)	261
6.2.13 General procedure for preparation of diphenylamines (144-146)	261
6.2.14 Procedure for preparation of 3-chloro diphenylamine (148)	263
6.2.15 General procedure for preparation of <i>N</i> -methyl diphenylamines (149-151)	264
6.3 Synthesis of starting materials for direct arylation of <i>ortho</i> -bromo diarylethers	266
6.3.1 Procedure for synthesis of 6-substituted-4-phenoxy-quinolone ligands (159-161)	266
6.3.2 Procedure for preparation of 6-methoxy-quinoline <i>N</i> -oxide (162)	268
6.3.3 Procedure for preparation of 1-bromo-2-(4-nitrophenoxy) benzene (163)	268

6.3.4 General procedure for preparation of 1-bromo-2-(4-methylphenoxy) benzene (164) and 1-bromo-2-(4-methylphenoxy) benzene (167)	269
6.3.5 General procedure for preparation of 2-bromo diarylethers <i>via</i> Chan-Lam-Evans coupling	270
6.3.6 General procedure for preparation of diphenyliodonium tetrafluoroborate salts (177-179)	279
6.3.7 General procedure for preparation of 2-bromo diarylethers <i>via</i> diphenyl iodonium tetrafluoroborate salts (177-182)	276
6.3.8 General procedure for preparation of 2-bromo diphenylamine (195)	281
6.3.9 Procedure for synthesis of 4-(2-bromophenoxy) pyridine (197)	281
6.3.10 Procedure for synthesis of 4-(bromophenoxy) pyridine <i>N</i> -oxide (198)	282
6.4 Palladium catalysed intramolecular double C-H activation	283
6.4.1 General procedure for intramolecular double C-H activation of 2-coumarins, 2-pyrones and related heterocycles. Synthesis of compounds 25, 41, 73-85	283
6.4.2 General procedure for intramolecular double C-H activation of diarylethers. Synthesis of compounds 131-137	297
6.5 Palladium catalysed intramolecular direct arylation of <i>ortho</i> -bromo diarylethers	305
6.5.1 General procedure for intramolecular direct arylation of <i>ortho</i> -bromo diarylethers. Synthesis of compounds 16, 199-211, 215	305
6.6 Synthesis of manganese carbonyl phosphine complexes and their application in C-H activation reactions	313
6.6.1 General procedure for preparation of tetracarbonyl manganese phosphine complexes (223-225)	313
6.6.2 General procedure for preparation of tricarbonyl phosphine complexes (226-229)	314
6.6.3 Synthesis of starting materials	317
6.6.4 General procedure for preparation of compounds 263 and 264	318

Declaration

This is to certify that the work I am submitting is my own and has not been submitted for another degree, either at University College Cork or elsewhere. All external references and sources are clearly acknowledged and identified within the contents. I have read and understood the regulations of University College Cork concerning plagiarism.

Katrina Mackey

Katrina Mackey

30/04/20

Date

Acknowledgements

Firstly, I would like to extend my appreciation to my supervisor Dr. Gerard McGlacken for giving me the opportunity to do a PhD in his research group. I am very grateful for all the skills and knowledge that I have gained under your supervision. Thank you for your encouragement, support and enthusiasm over the last number of years. I am also extremely grateful to the SSPC and Science Foundation Ireland for funding this research.

I would like to express my thanks to all of the staff in the School of Chemistry, who provide all of the invaluable services that we rely on to get our work done. Thanks to Dr. Dan McCarthy, Dr. Lorraine Bateman and Dr. Denis Lynch for NMR services, Dr. Florence McCarthy and Mick O'Shea for mass spectrometry, Barry O'Mahony and Noel Browne for microanalysis and Derry Kearney for glass blowing services. Thanks also to the technical staff, Dr. Matthias Jauch, Dr. Trevor Carey, Tina Kent, Denis Duggan, Johnny Ryan and Noel Browne.

To all members of the GMG group, past and present, it has been an honour and privilege to have gained invaluable tools, wisdom and friendship over the last number of years, both inside and outside the lab. To Leti, I am forever grateful to have had the opportunity to work with you, You have taught me so much, from how to master the art of column chromatography, to how to be a thorough and efficient chemist. You are an extremely hard working person and your endless humour and positive attitude always made the lab a better place to work. To Aisling, I don't think I have met a more determined and efficient individual. Thank you for all your support and guidance over the last few years. Rachel, thank you for all your kindness, advice and friendship, particularly over the last three years. Thank you for always listening to me and helping me on my project. I thoroughly enjoyed chatting about food and coffee! Your words of wisdom have helped me in my journey over the last few months. To Rafa, Eoin and Marie-Therese, who were part of the GMG group when I started my PhD, thanks for passing on some of your knowledge and experience. To Davy, thanks for all your help, in particular on the direct arylation project. It was a hard slog!

To Emma and Aobha, I am so glad ye have joined the group. I have really enjoyed the last two years of my PhD. Aobha, thanks for proof reading my thesis. I always enjoyed chatting to you about food and fitness with you. Thanks for all your healthy treats that you baked and shared with everyone. To Emma, thank you for being such a kind and caring person. You are always

thinking of others and willing to help everyone out when needed. Thanks to Peter for all the riveting discussions in the lab. It was great to chat to somebody who has a keen interest in all sports. The discussions about doping were a particular highlight. And to all the researchers on the 4th floor of the Kane and 2nd floor of the Cavanagh, I wish you every success in the future.

To all my teammates on the Cork camogie team, past and present, I would not be the person I am today if it was not for ye. Ye have always taken a keen interest in my PhD research and have been very supportive. Sport has taught me many life lessons. I truly understand how hard work, discipline and persistence are the key to success.

Julia, I am not sure if what I write here will even cover what you have done for me and how you have helped me become the person I am today. You are the greatest friend I could of asked for. Thanks for all your advice and your willingness to listen to anything I have to say. During tough times and good times, I could always turn to you and for that I am truly grateful.

To my sister Pamela, thanks for always being there for me and for being my best friend. You have always pushed me and provided me with extra motivation to be the best person I can be. We have been through many journeys together and there are many more ahead. To my sisters Caroline and Jessica, thanks for all the support throughout my years in UCC. It is very much appreciated. Patrick, I could not have met a kinder and more caring person than you. Thanks for listening to me procrastinating over the last few months! You always see the positives in life and have taught me to appreciate the simpler things in life. I look forward to the many adventures that lay ahead.

To my mum, I am truly grateful for everything you have done for me over the last 28 years of my life. You are strong, caring and independent woman. I am grateful for all your advice and support. You have always taught me to be myself and to have an independent mind. I hope I have made you a proud mother.

For my father, John

Abstract

Direct arylation *via* C-H activation has emerged as a powerful tool for the construction of new aryl-aryl bonds and provides an alternative to classical cross coupling procedures. Double C-H activation in particular, represents a more sustainable approach in terms of waste, cost and atom economy. 2-Pyrone and 2-coumarin analogues represent privileged biological scaffolds and possess broad spectrum biological activity. Importantly, there have been limited reports of catalytic methods involving the C-H activation of 2-pyrones and 2-coumarins. The cyclisation of 2-pyrones and 2-coumarins *via* double C-H activation is described in Chapter 2 of this thesis. The synthesis of a library of 2-pyrone and 2-coumarin substrates was achieved using this methodology. Excellent yields were achieved for the 2-coumarin substrates and some good regioselectivity was obtained for both the 2-pyrone and 2-coumarin analogues. The developed double C-H activation reaction conditions also facilitated a three step synthesis of flemichapparin C. The application of this methodology was then transferred to the synthesis of *meta*-substituted dibenzofurans. A variety of mono- and di-substituted diarylethers were efficiently cyclised in good to excellent yields.

In Chapter 3, the cyclisation of mono-halogenated diarylethers *via* single C-H activation to produce dibenzofurans is discussed. Previous methods for the synthesis of dibenzofurans *via* transition metal-mediated catalysis suffer from a number of drawbacks. Thus, focus was targeted at addressing many of the limitations existing with the current protocols for the intramolecular direct arylation of diarylethers. Substrates with electron withdrawing groups were particularly well tolerated and yields of up to 99% were observed.

The final section of this thesis involved the synthesis and application of a number of carbonyl manganese phosphine complexes. The vast majority of C-H activation protocols involve the use of precious 4d or 5d transition metal catalysts. However, many of these metals are now classed as 'finite raw materials'. Clearly, there is an urgent need to alleviate the worldwide reliance on precious metals, especially palladium. The cost effective and sustainable nature of earth abundant first row transition metals, renders the development of C-H activation protocols using inexpensive 3d metal catalysts a particularly attractive alternative. In recent years, Mn catalysed C-H activation has gained considerable momentum as a more environmentally benign and economically attractive alternative to typically used transition

metal based catalysts. Despite this, most reports on Mn catalysed C-H activation utilise the commercially available $\text{MnBr}(\text{CO})_5$ and $\text{Mn}_2\text{CO}_{10}$ pre-catalysts. The CO ligand cannot be optimised, and this represents the bottle-neck for the expansion of Mn catalysis. In contrast to more commonly studied metals such as Pd, there has yet to be widespread study of the influence of ligands in Mn(I)-catalysis, in many reaction types including C-H bond activation. This represents a significant gap in the State-of-the Art. Thus, the future of Mn catalysed C-H activation requires the development of new tuneable ligands for Mn, analogous to the past developments in Pd catalysis. The work in Chapter 5 involved the synthesis of a range of tetracarbonyl- and tricarbonyl Mn phosphine complexes. The complexes were fully characterised by spectroscopic, single crystal structure X-ray analysis and elemental analysis and applied in a number of C-H activation reactions. Critically, it was demonstrated that these carbonyl Mn phosphine complexes are catalytically competent in a proof-of-principle reaction; the hydroarylation of *N*-(2-pyridyl)indole with ethyl trifluoropyruvate.

Preface

This thesis contains work which has been published after peer review, or which is in the process of publication. A full list of publications arising from this thesis is provided in Appendix I.

Abbreviations and Acronyms

α	alpha
Å	ångström
Ac	acetyl
AcOH	acetic acid
AMLA	ambiphilic metal-ligand assistance
anal.	analysis
approx.	approximately
aq	aqueous
Ar	aryl
β	beta
BF ₃ .OEt ₂	boron trifluoride diethyl etherate
br s	broad singlet
Bu	butyl
<i>ca</i>	circa
°C	Celsius degrees
C	carbon
¹³ C NMR	carbon nuclear magnetic resonance
CDC	cross-dehydrogenative coupling
CMD	concerted metallation-deprotonation
conc.	concentrated
COSY	correlation spectroscopy
Cp	cyclopentadienyl
Cy	cyclohexyl
δ	NMR chemical shift
d	doublet
D	dimensional
DABCO	1,4-diazabicyclo[2.2.2]octane
dba	dibenzylideneacetone
DBU	1,8-diazabicyclo[5.4.0]undec-7-ene
DCE	dichloroethane
DCM	dichloromethane
dd	doublet of doublets
ddd	doublet of doublets of doublets
deg	degree
DEPT	distortionless enhancement by polarisation transfer
DFT	density functional theory
DMA	dimethylacetamide
DMAP	4-dimethylaminopyridine
DMF	dimethylformamide
DMSO	dimethylsulfoxide
dq	doublet of quartets

dt	doublet of triplets
dppp	1,3-bis(diphenylphosphino)propane
<i>e.g.</i>	for example
EDG	electron-donating group
<i>ee</i>	enantiomeric excess
equiv.	equivalent(s)
EAM	earth abundant metals
ESI	electrospray ionisation
Et	ethyl
<i>et al.</i>	and others
etc.	et cetera
EWG	electron withdrawing group
<i>fac</i>	facial
FT-IR	Fourier-transform infrared spectroscopy
FDA	Food and Drug Administration
g	gram(s)
GC	gas chromatography
h	hour(s)
¹ H NMR	proton nuclear magnetic resonance
HetAr	heteroaryl
HOESY	heteronuclear overhauser enhancement spectroscopy
HMBC	heteronuclear multiple-bond correlation spectroscopy
HRMS	high-resolution mass spectrometry
HSQC	heteronuclear single-quantum correlation spectroscopy
Hz	Hertz
HFIP	hexafluoroisopropanol
<i>i</i>	iso
<i>i.e.</i>	that is
I	nuclear spin
IR	infrared
<i>J</i>	coupling constant
KIE	kinetic isotope effect
L	litre
LRMS	low resolution mass spectrometry
m	multiplet
<i>m</i>	meta
<i>mer</i>	meridional
M	metal
	molar
<i>m/z</i>	mass-to-charge ratio
max	maximum
<i>m</i> -CPBA	<i>m</i> -chloroperoxybenzoic acid
Me	methyl
MeCN	acetonitrile

MS	mass spectrometry
mg	milligram
MHz	megahertz
min	minute
mL	millilitre
mmol	millimole
mol	mole
	molecular
mol%	mole percent
m.p.	melting point
MS	mass spectrometry
MW	microwave
ν_{max}	frequency of maximum absorption
Na^tOBu	sodium <i>tert</i> -butoxide
NBS	<i>N</i> -bromosuccinimide
NBO	natural bond orbital
<i>n.d.</i>	not determined
NHC	<i>N</i> -heterocyclic carbene
NIS	<i>N</i> -iodosuccinimide
NMP	<i>N</i> -methyl-2-pyrrolidone
NMR	nuclear magnetic resonance
NOE	nuclear Overhauser effect
NOESY	nuclear Overhauser enhancement spectroscopy
<i>o</i>	ortho
<i>o/n</i>	overnight
π	type of orbital, electron
<i>p</i>	para
^{31}P NMR	phosphorus nuclear magnetic resonance
$\text{PCy}_3\cdot\text{HBF}_4$	tricyclohexyl phosphine tetrafluoroborate
Ph	phenyl
PhD	Doctorate of Philosophy
PIDA	diacetoxy iodobenzene
PIFA	bis-(trifluoroacetoxy) iodobenzene
PivOH	pivalic acid
PivO^-	pivalate
P_2O_5	phosphorus pentoxide
ppm	parts per million
Pr	propyl
PTSA	<i>p</i> -toluenesulfonic acid
$\text{P}^t\text{Bu}_3\cdot\text{HBF}_4$	tri- <i>tert</i> butyl phosphine tetrafluoroborate
q	quartet
RDS	rate-determining step
R.T.	room temperature
σ	type of orbital

s	singlet
S _E Ar	electrophilic aromatic substitution
SPhos	2-dicyclohexylphosphino-2',6'-dimethoxy biphenyl
t	triplet
	time
td	triplet of doublets
<i>tert</i>	tertiary
TBAB	tetrabutylammonium bromide
TBHP	<i>tert</i> -butyl hydroperoxide
TFA	trifluoroacetic acid, trifluoroacetate
TfOH	trifluoromethanesulfonic acid, triflic acid
TLC	thin layer chromatography
TMHD	2,2,6,6-tetramethyl-3,5-heptadione
TOF LC-MS	time-of-flight liquid-chromatography mass spectrometry
Tol	tolyl
TON	turnover number
T	temperature
Ts	tosyl, 4-toluene sulfonyl
UV	ultraviolet
$\bar{\nu}$	wavenumber
wt.	weight
w/v	weight by volume
X	halogen
Zn	zinc

Chapter 1: Introduction

1.1 Aryl-Aryl bond formation

The biaryl motif is a predominant substructure of many pharmaceutically relevant and biologically active compounds (**Figure 1**) such as the anti-inflammatory Felbinac **1**, the anti-hypertensive Losartan **2**, as well as the anti-cancer drug Imatinib **3**. In addition, the motif is an integral part of important agrochemicals such as the anti-fungal agent, Boscalid **4**. As a consequence, the utility of the biaryl motif has driven the discovery of highly efficient aryl-aryl bond forming methodologies.

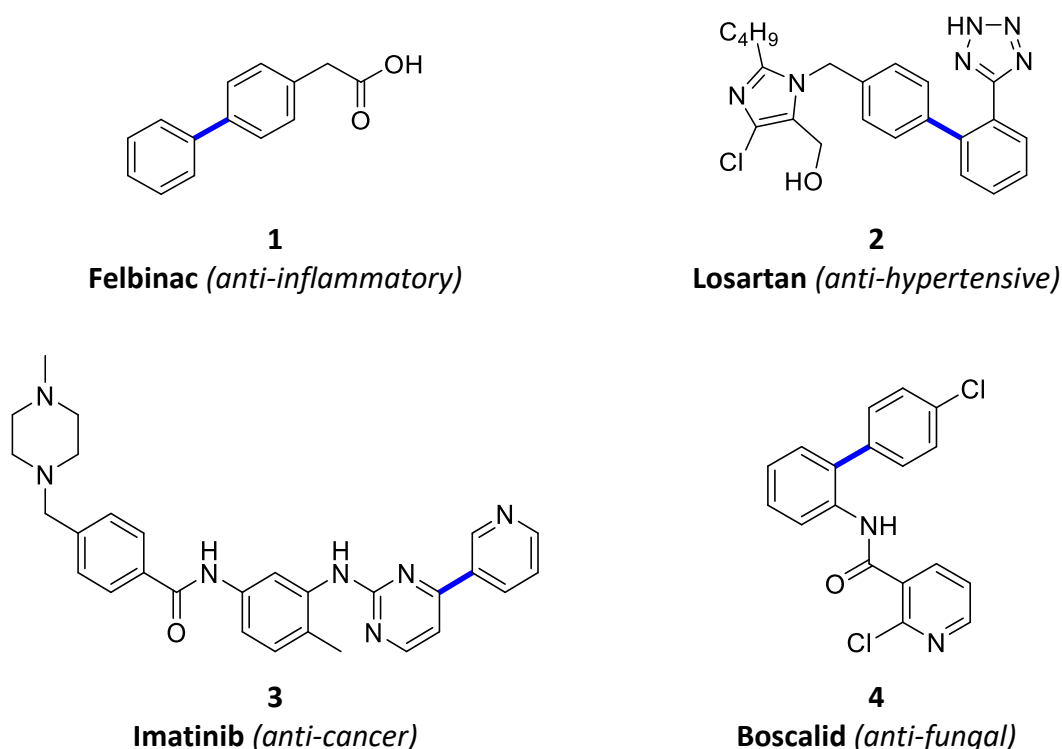


Figure 1. Importance of biaryl structural motif in pharmaceutical products.

Traditionally, the most common and reliable methods to create an aryl-aryl bond require pre-functionalisation of both coupling partners, utilising an aryl halide (or pseudohalide) with an organometallic reagent (e.g. Stille, Negishi, Suzuki-Miyaura reactions) (**Scheme 1 (iii)**).¹⁻⁴ Whilst high yields and selectivities can be obtained *via* these traditional methods, they inherently suffer from a number of drawbacks. Firstly, the preparation of pre-activated substrates often involves several steps which is time consuming and an inefficient process in terms of waste, cost and atom economy. Furthermore, the organometallic and/or organohalide coupling partners required for Suzuki-Miyaura or Stille reactions are not always

readily available. The latter problem is especially prevalent in intramolecular cross-coupling reactions.

As a general guide, there are three main steps in the catalytic cycles of coupling processes which are all mediated by palladium⁰ (Pd^0 , which is ligated: Pd^0L_n) (**Figure 2**). The first step involves **oxidative addition** of the organohalide to Pd^0 to give a Pd^{II} intermediate species. This intermediate can then undergo **transmetallation** with an organometallic reagent to give another Pd^{II} species, with loss of a by-product (salt or other metal halogen species). Finally, **reductive elimination** gives the final aryl-aryl product and allows for regeneration of the Pd^0 species.

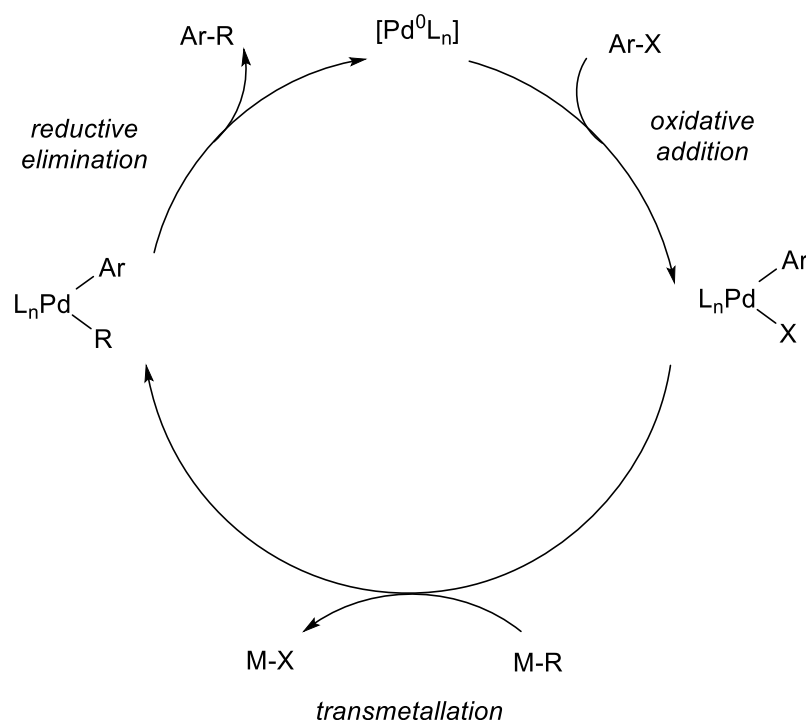


Figure 2. General catalytic cycle for palladium catalysed cross-coupling reactions.

1.2 Direct arylation *via* C-H activation

In recent years, direct arylation *via* C-H activation has proved a valuable alternative to traditional cross-coupling reactions (**Scheme 1**). Direct arylation is a method of biaryl synthesis whereby carbon-carbon bond formation occurs through cleavage of a C-H bond in the presence of a transition metal. The terms C-H activation and C-H functionalisation have been used interchangeably in the literature.⁵ It is noteworthy that the term C-H activation is

used throughout the course of this thesis. Specifically, C-H activation is used to describe reactions between a C-H bond and a transition metal complex to generate discrete 'activated' L_nM-R intermediates that do not involve free radicals, carbocations or carbanions.⁶⁻⁸ The activated L_nM-R intermediate is then functionalised and the catalyst regenerated.

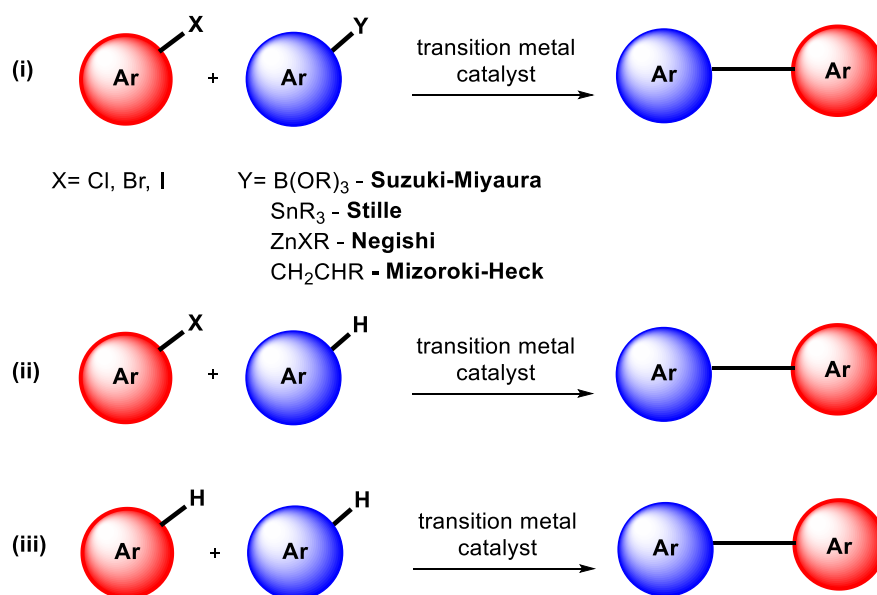
In contrast to traditional cross-coupling procedures, direct arylation protocols avoid the installation of activating groups in one or both of the coupling partners and thereby reduce the associated waste products.⁹⁻¹⁰ As a result, modern methods to synthesise new compounds *via* C-H activation are on the published 'Wanted List' of top pharmaceutical companies.¹¹

The most atom economic approach¹² would involve the coupling of two aryl C-H bonds (**Scheme 1 (iii)**). Ideally, the only by-products here are hydrogen gas or water. However, there are challenges associated with this approach:

(1) Aromatic C-H bonds are thermodynamically stable and chemically inert (for example, the homocoupling of benzene to give biphenyl and dihydrogen is thermodynamically disfavoured by 13.8 kJ mol^{-1}).¹³

(2) Attaining site selective C-H activation in the presence of a number of C-H bonds within a molecule often poses significant regioselectivity and chemoselectivity problems.⁹⁻¹⁰

Alternatively, a chemical compromise is reached whereby one of the coupling partners is pre-activated (single C-H activation) (**Scheme 1 (ii)**).⁵ This is a more widely adopted approach and can be carried out in an intramolecular or intermolecular fashion.^{10, 14} Regioselectivity can be controlled in terms of a directing group strategy and also manipulation of the steric and electronic properties of the system.^{5, 9} A number of examples of this approach will be discussed in this introduction.

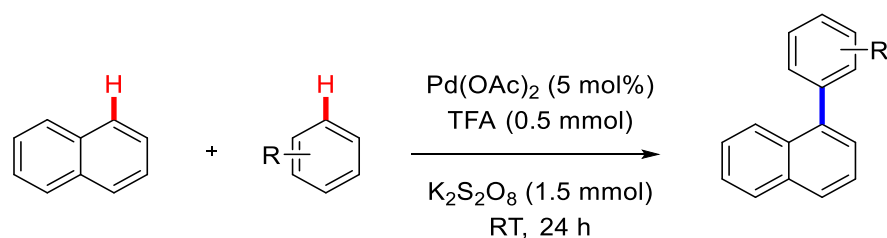


Scheme 1. Methodologies for Ar-Ar bond formation.

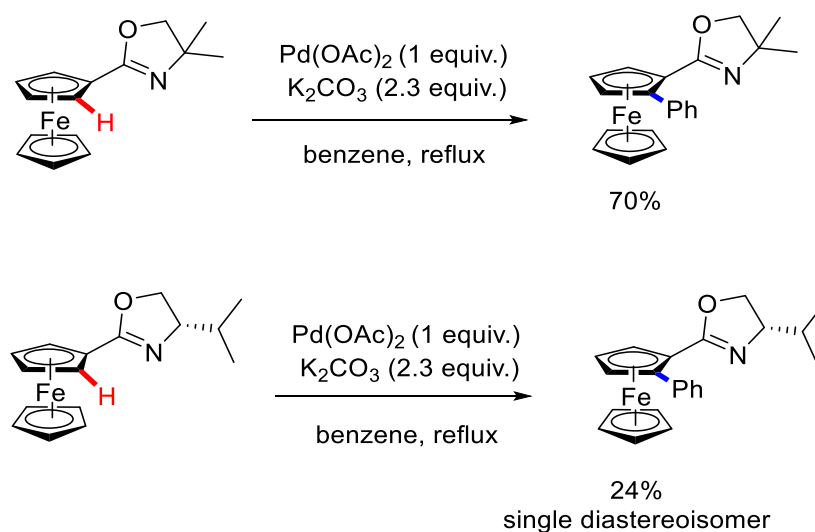
1.2.1 Literature examples of double C-H activation

One of the first reports of biaryl formation *via* a double C-H activation involved the oxidative cross-coupling of simple arenes (**Scheme 2**) published by Lu and co-workers in 2006.¹⁵ Subsequently, You and Xia carried out a direct arylation (*via* a double C-H activation) of simple arenes with ferrocenyl oxazolines in the presence of a stoichiometric amount of Pd(OAc)₂ (**Scheme 2**).¹⁶

(i) Lu, *Organomet. Chem.* 2006, 25, 5973-5975.



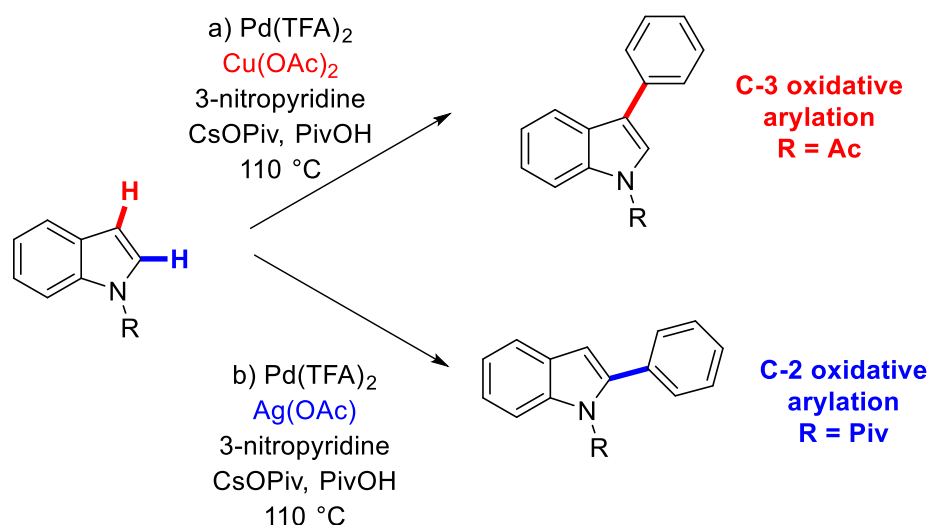
(ii) Xia, *Organomet. Chem.* 2007, 26, 4869-4871.



Scheme 2. Intermolecular direct arylation *via* double C-H activation of simple arenes and ferrocene.

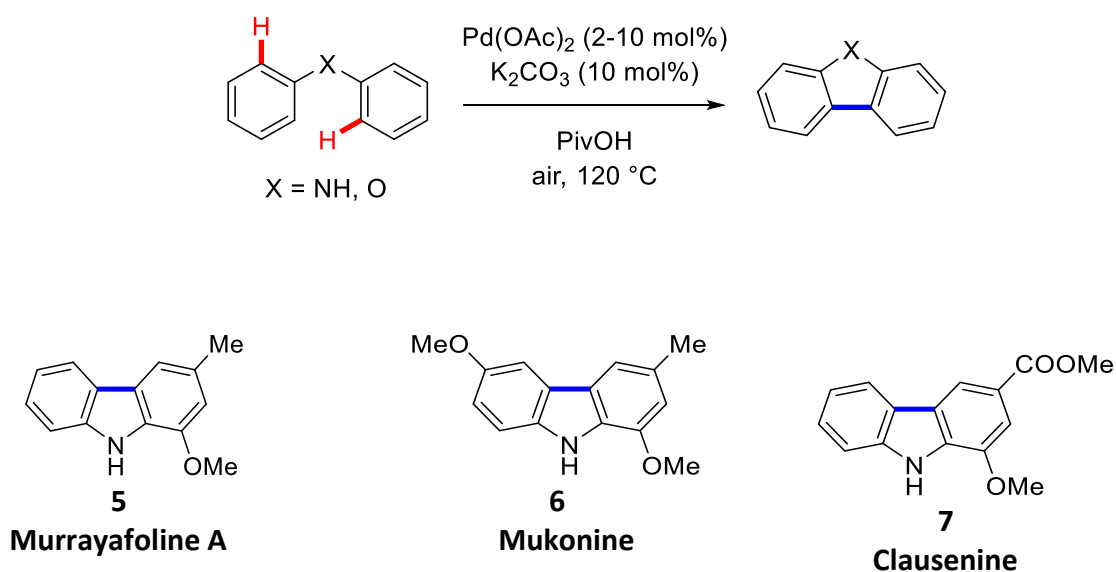
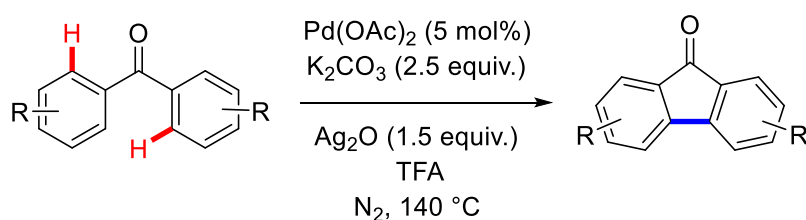
Following on from these seminal reports, in 2007, the Fagnou group achieved a much more practical and selective aryl-H-aryl-H cross-coupling.¹⁷ They applied their methodology to the reaction of unactivated arenes with *N*-alkyl indoles, with yields of up to 84% reported (**Scheme 3**). Fagnou's palladium (Pd) catalysed oxidative cross-coupling allows access to both C-3 and C-2 arylindoles by varying the terminal oxidant, in combination with $\text{Pd}(\text{TFA})_2$ as catalyst and the use of catalytic quantities of 3-nitropyridine and caesium carbonate. The authors also state that changing from *N*-acetyl indole to *N*-pivalyl indole played an important role in the selectivity of the reaction.¹⁷

(i) Fagnou, *J. Am. Chem. Soc.* 2007, 129, 12072-12073.



Scheme 3. Fagnou's direct arylation of *N*-alkyl indoles and unactivated benzenes *via* double C-H activation. Reaction conditions: a) $\text{Pd}(\text{TFA})_2$ (10 mol%), 3-nitropyridine (10 mol%), CsOPiv (40 mol%), $\text{Cu}(\text{OAc})_2$ (3 equiv.), PivOH (6 equiv.). b) $\text{Pd}(\text{TFA})_2$ (10 mol%), 3-nitropyridine (10 mol%), CsOPiv (40 mol%), AgOAc (2.2 equiv.), PivOH (6 equiv.).

In 2008, Fagnou and co-workers reported an intramolecular Pd catalysed oxidative biaryl synthesis under air using pivalic acid as the reaction solvent.¹⁸ This methodology was used in the synthesis of three naturally occurring carbazole products: Murrayafoline A (**5**), Mukonine (**6**) and Clausenine (**7**) (**Scheme 4, (i)**). Following on from this, Shi and co-workers made significant progress towards more sustainable routes to biaryls. In 2012, they reported the first Pd catalysed dual C-H activation of benzophenones to form fluorenone derivatives by oxidative dehydrogenative cyclisation (**Scheme 4, (ii)**).¹⁹ Excellent yields and functional group compatibility were reported.

(i) Fagnou, *J. Org. Chem.* 2008, 73, 5022-5028(ii) Shi, *Org. Lett.*, 2012, 14, 4850-4853**Scheme 4.** Literature examples of direct arylation *via* double C-H activation.**1.3 Mechanisms of direct arylation**

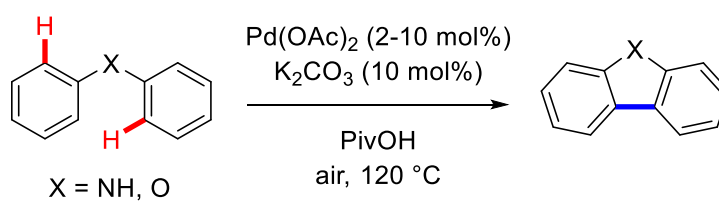
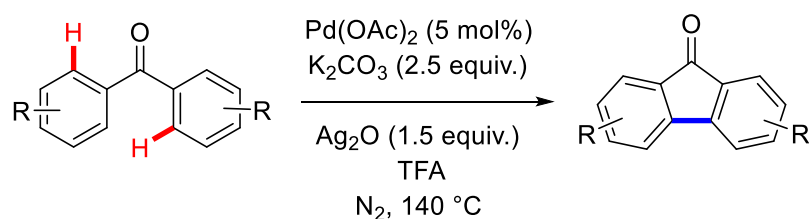
In the context of Pd catalysed direct arylation, several mechanisms have been proposed for the C-H bond cleavage step.^{9, 20-21} These include oxidative C-H insertion observed for late transition metals in low oxidation states, electrophilic aromatic substitution ($S_E\text{Ar}$): selective for electron rich substrates, Heck-type (carbometalation) and Concerted Metallation Deprotonation²² (CMD) or also known as Ambiphilic Metal Ligand Activation²³ (AMLA). CMD type C-H functionalisations show a preference for acidic C-H bonds. However, the intimate reaction mechanism may switch from reaction to reaction as the substrate, solvent, base, ligand and additives are changed.

1.4 Aims and objectives (Chapter 2)

The focus of **Chapter 2** and **Chapter 3** of this thesis is the development of new strategies for the C-H functionalisation of important biological compounds. **Chapter 2** is directed at exploring more environmentally benign C-H functionalisations and application of this methodology on delicate molecular frameworks. A key inspiration for this research was the work previously reported by the groups of Fagnou¹⁸ and Shi¹⁹ (**Figure 3 (i-ii)**). Chapter 3 describes efforts toward the development of ligand accelerated C-H functionalisation of diarylethers as a route to dibenzofurans.

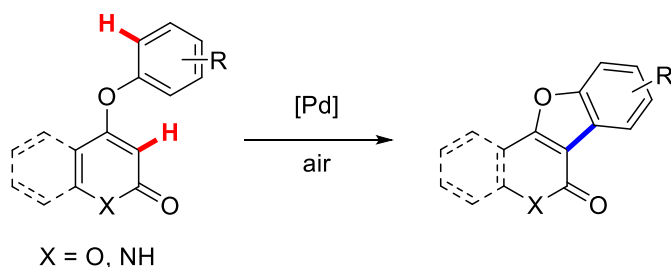
The functionalisation of 2-pyrones and 2-coumarins is highly sought after and has attracted attention due to the interesting biological and pharmacological properties associated with these compounds. Classical cross-coupling reactions such as the Suzuki-Miyaura, Negishi and Stille reactions provide access to such targets. However, despite their importance in various fields there has been very few reports of any catalytic methods involving the C-H functionalisation of 2-pyrones and 2-coumarins. Previously, our lab has reported a palladium catalysed intramolecular **single C-H activation** of 4-phenoxy-2-pyrones and 4-phenoxy-2-coumarins to afford 1*H*-pyrano[4,3-*c*]benzofuran-1-one and 6*H*-benzofuro[3,2-*c*]chromen-6-one products.²⁴⁻²⁷ Although there has been progress in the field of double C-H activation in recent years, it has mainly been achieved on more robust substrates. Thus, there have been limited reports of effective catalytic systems which can perform this type of transformation on more privileged biological scaffolds. Hence, the key goal of **Chapter 2** is the palladium catalysed double C-H activation of 4-phenoxy-2-pyrones and 4-phenoxy-2-coumarins as a novel route to 1*H*-pyrano[4,3-*c*]benzofuran-1-ones and 6*H*-benzofuro[3,2-*c*]chromen-6-ones (**Figure 3 (iii)**). Additionally, this methodology was extended to dibenzofurans which will also be discussed in **Chapter 2 (Figure 3 (iii))**.

Inspiration for this work

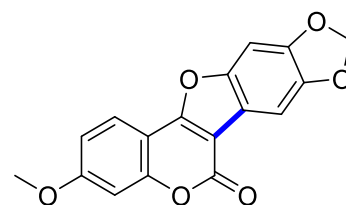
(i) Fagnou, *J. Org. Chem.* 2008, 73, 5022-5028(ii) Shi, *Org. Lett.*, 2012, 14, 4850-4853

(iii) This work

2-pyrones and 2-coumarins



flemichapparin C in three steps



Dibenzofurans

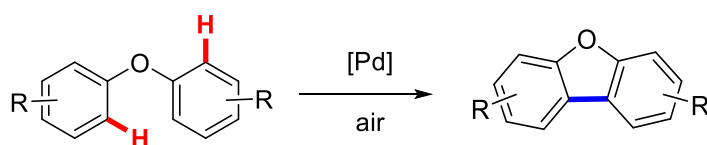


Figure 3. (i-ii) Palladium catalysed intramolecular double C-H activation of robust heterocyclic scaffolds and (iii) privileged biological scaffolds as well as less reactive diarylethers described in **Chapter 2** of this thesis.

1.5.1 Biological importance of targeted heterocycles

2-Pyrone (**8**) is a six membered cyclic unsaturated ester (**Figure 4**). 2-Pyrones have similar chemical and physical properties to both alkene and aromatic compounds. It is a highly abundant moiety in bacteria, plant, insect and animal systems.²⁸ Naturally occurring 2-pyrones include bufadienolides, peripyrone, herbarins, coumarins, etc. Bufadienolides are an important group of steroids containing the 2-pyrone moiety. For example, bufalin (**11**) is a cardio active C-24 steroid that exhibits a variety of biological activities and is of particular importance in regulating cardiovascular function. More recently, bufalin (**11**) is known to induce cell cycle arrest and apoptosis in many cancer cells. For this reason it is now considered a candidate drug for cancer chemotherapy (**Figure 5**).²⁸

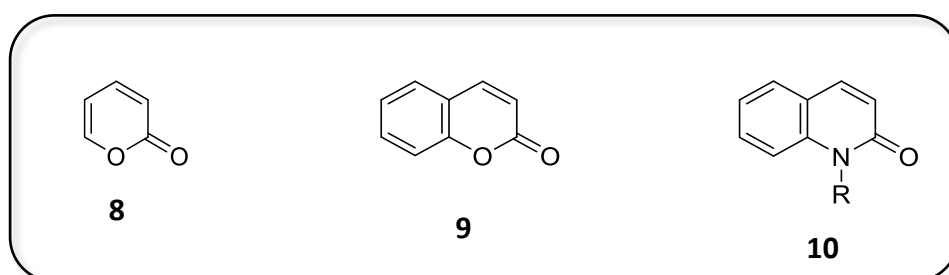


Figure 4. 2-(1H)-pyrone and structurally related heterocycles.

Coumarins (**9**) (sometimes referred to as 2-coumarins, although the '2' is not required) are a class of compounds that are also known as benzopyrones and are structurally related to pyrones (**Figure 4**). Both synthetic and naturally occurring molecules containing the 4-substituted coumarin moiety have exhibited interesting biological and pharmacological properties.²⁸ Of particular interest are 4-aryl coumarins. The synthesis and isolation of 4-aryl coumarins has received much attention for a number of years due to their anti-HIV, anti-malarial and anti-bacterial activity.²⁹ A number of coumarins isolated from the bark of *Ochrocarpos punctatus* have shown to exhibit broad spectrum cytotoxicity against the A2780 human ovarian cancer cell line.³⁰ The blockbuster drug warfarin (**12**) is also a simple 4-hydroxy-2(1H)-coumarin derivative (**Figure 5**).²⁸ The structurally related 2(1H)-quinolone motif (**10**) is considered a privileged biological scaffold (**Figure 4**) and quinolones are among the most important synthetic anti-bacterial drugs.³¹⁻³² For example, Ciprofloxacin (**13**) is a second generation fluoroquinolone antibiotic (**Figure 5**). In addition, quinolones possess a number of other important biological traits.³³

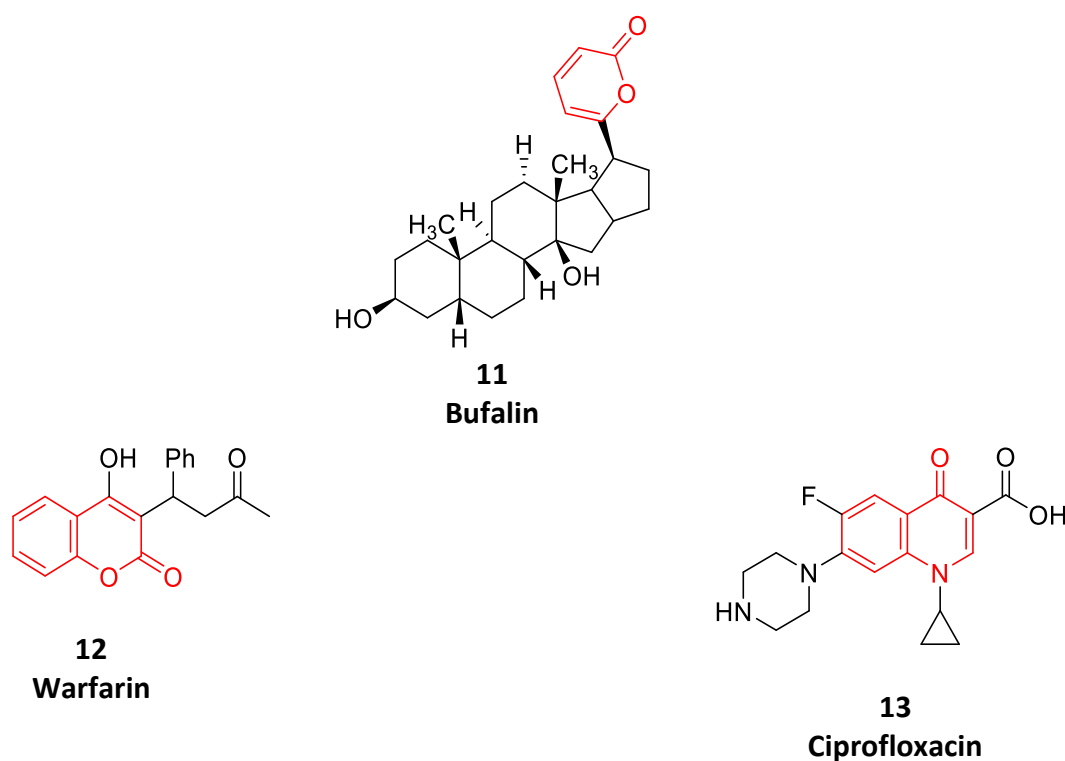


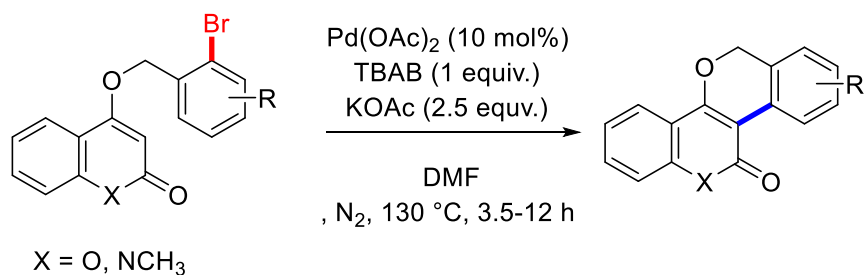
Figure 5. Examples of biologically active compounds containing the 2-pyrone, 2-coumarin and 4-quinolone moiety.

1.5.2 Literature examples of palladium catalysed direct arylation of 2-pyrone analogues and 2-coumarin analogues

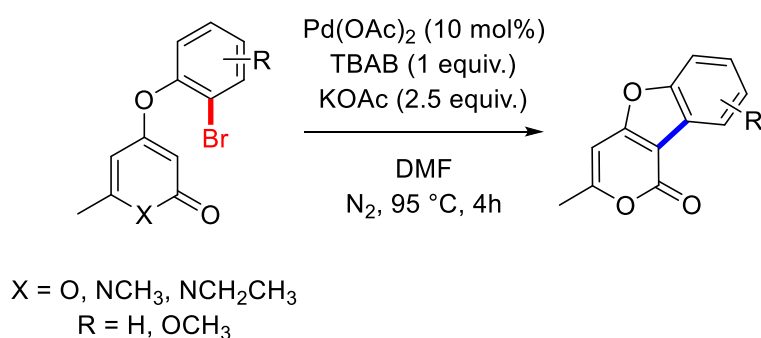
A number of protocols for the C-H activation of 2-pyrone substrates to give five and six membered heterocycles have been developed by Majumdar,³⁴⁻³⁵ Fairlamb³⁶ and McGlacken.^{24-25, 27} Depending on the reaction conditions, these reactions have been proposed to proceed *via* a CMD type mechanism or a Heck-type carbopalladation of the 2-pyrone framework.

In 2007 and 2008, Majumdar and co-workers successfully carried out an intramolecular arylation of 2-pyrone, 2-coumarin, 2-quinolone and 2-pyridone derivatives using a Pd⁰ catalyzed intramolecular Heck-type process (**Scheme 5**).³⁴⁻³⁵ This was an improvement on an existing methodology by the same group utilising tin hydrides *via* a proposed radical mechanism.³⁷

(i) Majumdar, *Synthesis*, 2007, 11, 1707-1711.

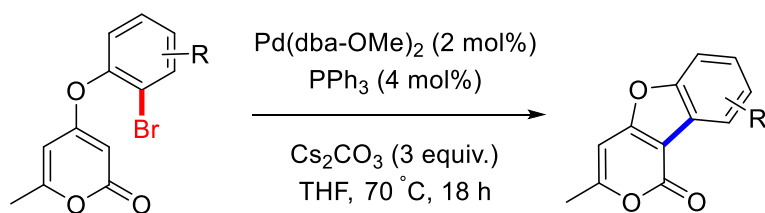


(ii) Majumdar, *Can. J. Chem.* 2008, 86, 325-332.



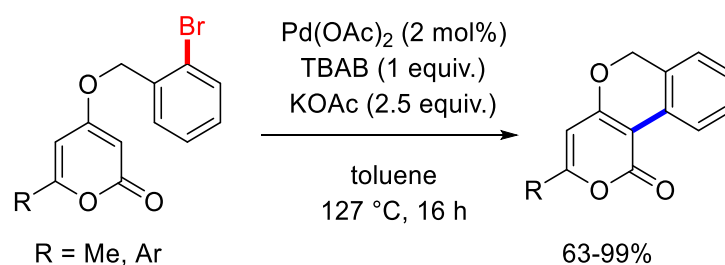
Scheme 5. The intramolecular arylation of 2-pyrone and related heterocycles.

Two years later, Fairlamb reported the catalytic C-H functionalization of 2-pyrones³⁶ with regioselectivity observed for the C-3 position (**Scheme 6**). The authors proposed a Heck-Type mechanism involving carbopalladation of the 2-pyrone framework.



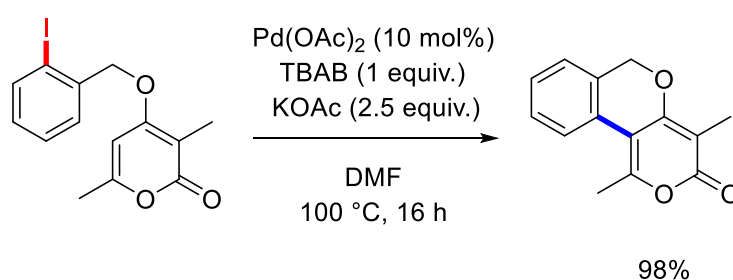
Scheme 6. The C-H functionalization of 2-pyrones.

Fairlamb and McGlacken subsequently reported the intramolecular arylation of 2-pyrones without added phosphine ligands in 2014.²⁴ Excellent yields were obtained under the reaction conditions and the methodology could also be extended to include 2-pyridones, 2-coumarins and quinolones (**Scheme 7**) enabling access to potential biologically active candidates.



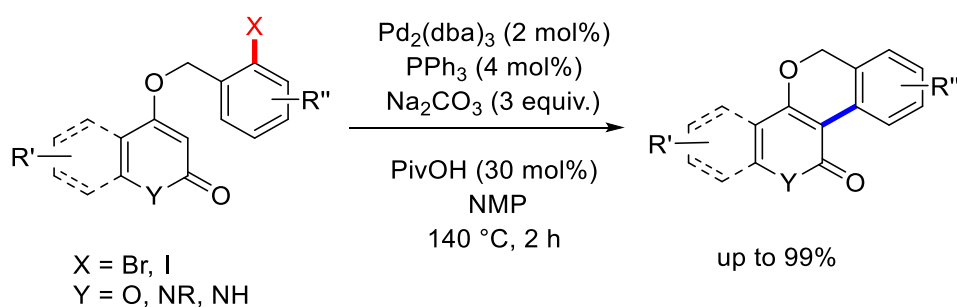
Scheme 7. Intramolecular direct arylation of 2-pyrones at C-3 to give six-membered rings.

The C-5 cyclised product could also be formed if the C-3 position was blocked with a methyl group for example (**Scheme 8**).²⁴



Scheme 8. Intramolecular direct arylation of 2-pyrones at C-5 to give six-membered rings.

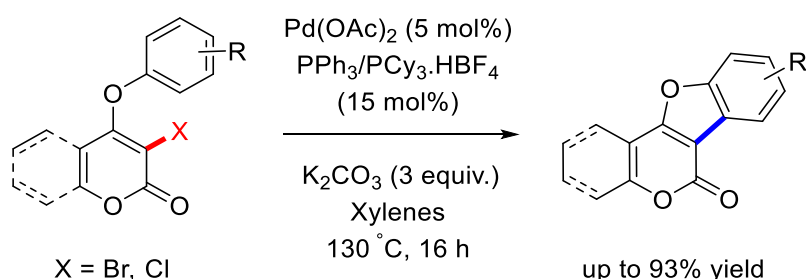
McGlacken and co-workers subsequently developed a complimentary set of conditions for the intramolecular direct arylation of 2-pyrones and other related heterocycles using a Pd^0 source and pivalic acid as a crucial additive (**Scheme 9**). Mechanistic work carried out suggested that the reaction probably proceeds *via* a CMD type pathway.²⁷



Scheme 9. Intramolecular direct arylation of 2-pyrones and related heterocycles to give six-membered rings.

Subsequently, McGlacken and co-workers successfully reported the palladium catalysed intramolecular direct arylation of 3-bromo-2-pyrones and 3-chloro-2-pyrones. A change in phosphine ligand and increased loading of base was required for the 3-chloro substrates to

undergo successful coupling (**Scheme 10**). This methodology was extended to 2-coumarins and applied to the synthesis of the natural product flemichapparin C.^{25, 38}

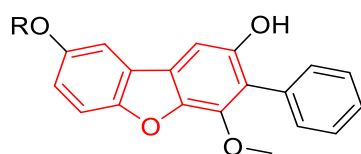


Scheme 10. Intramolecular direct arylation of 3-halo-2-pyrones and 2-coumarins.

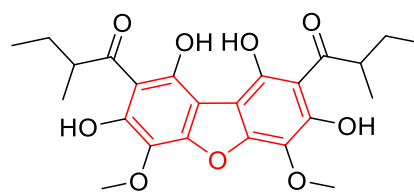
The second aim of **Chapter 2** is focused on applying our double C-H activation protocol to molecular frameworks which are more commonly found in drug molecules and natural products.

1.6.1 Biological significance of dibenzofurans

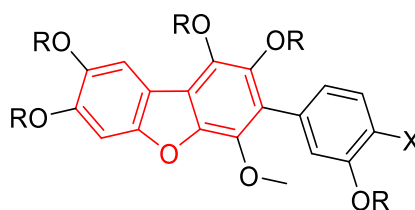
As previously mentioned, the biaryl motif is a predominant structural feature in many natural and synthetic pharmacologically active compounds.³⁹ In particular, dibenzofuran derivatives are an important class of structural motifs and are found in many natural products, bioactive molecules and pharmaceuticals. Significant biological activity has been exhibited by many members of this class of compounds, with a large number of naturally occurring dibenzofurans possessing anti-cancer, anti-inflammatory, anti-bacterial (Rhodomyrtosin (**14**)), anti-malarial and anti-oxidant properties (**Figure 6**).⁴⁰⁻⁴³ As a result, significant efforts have been directed towards their total synthesis. However, the synthesis of dibenzofurans is often limited by tedious steps, a lack of functional group tolerance and substrate availability.⁴⁴



kekokorin D R = H
kekokorin E R = CH₃
(*anti-cancer*)



14
Rhodomyrtosin B
(*anti-bacterial*)



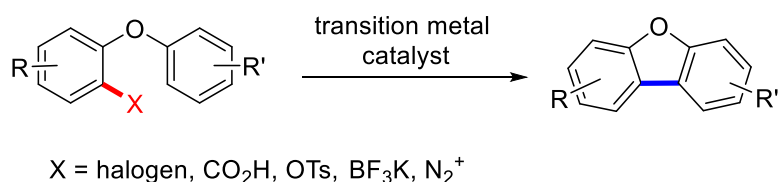
boletopsins
R = H, CH₃, Ac; X = H, OH
(*anti-inflammatory*)

Figure 6. Selected bioactive compounds bearing the dibenzofuran motif.

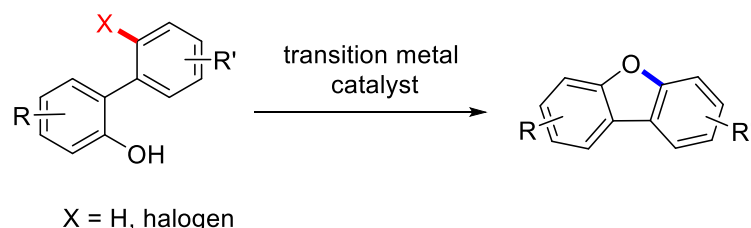
1.6.2 Previous synthesis of dibenzofurans

To date, several approaches have emerged for the synthesis of the dibenzofurans. In general, there are two main protocols as well as a few other miscellaneous methods:⁴⁵ **i)** transition metal catalysed carbon-carbon bond formation *via* cyclisation of 2-substituted phenoxy benzenes^{14, 18, 46-53} and **ii)** Cu or Pd catalysed *O*-arylation of 2-arylphenols (**Scheme 11**).⁴⁴ Nevertheless, these methods suffer from a number of significant drawbacks such as substrate dependence, tedious purification, unsatisfactory regioselectivity, limited substrate scope and harsh reaction conditions.^{44, 49, 51-52}

i) Transition metal catalysed carbon-carbon bond formation



ii) Pd or Cu catalysed O-arylation

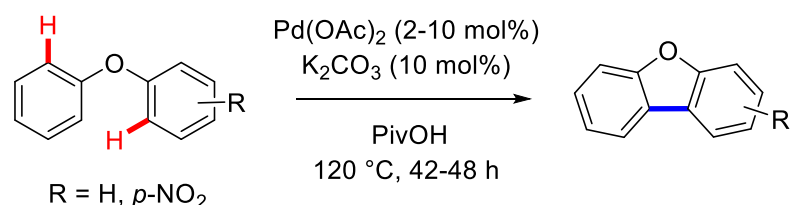
**Scheme 11.** Representative approaches to dibenzofuran synthesis.**1.6.3 Literature examples of palladium catalysed intramolecular double C-H activation for the synthesis of dibenzofurans**

Although a number of reports for the synthesis of dibenzofurans *via* transition metal catalysed carbon-carbon bond formation have emerged in the last number of years, literature examples of dibenzofuran synthesis *via* palladium catalysed double C-H activation of diarylethers are scarce and only scattered examples have been reported (**Scheme 12**). In addition, many of these methods of methods suffer from a number of drawbacks (*vide supra*).⁴⁴⁻⁴⁵

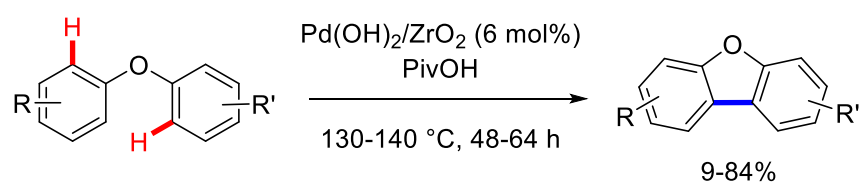
Invaluable advances were made by Fagnou and co-workers in 2008 whereby a new set of reaction conditions for intramolecular palladium catalysed oxidative carbon-carbon bond formation under air were developed.¹⁸ The authors state that the use of pivalic acid as the reaction solvent resulted in greater reproducibility, higher yields and allowed for a broader substrate scope. However, this work was mainly limited to the synthesis of carbazole containing compounds with only two examples of dibenzofurans just reported. Then in 2014, an interesting protocol for the synthesis of carbazoles and dibenzofurans *via* double C-H activation was reported by Ishida and co-workers using a heterogeneous metal oxide-supported palladium hydroxide catalyst (Pd(OH)₂/ZrO₂).⁵⁴ This was found to be an efficient catalyst in terms of catalytic activity and selectivity toward the synthesis of carbazoles and a number of dibenzofurans. Finally, in 2017, Wang and co-workers reported the synthesis of 6*H*-benzo[*c*]chromenes *via* palladium catalysed intramolecular dehydrogenative coupling of

two aryl C-H bonds.⁵⁵ This protocol uses molecular oxygen as the terminal oxidant, HFIP as solvent and was carried out at a relatively low temperature of 55 °C. Again however, the substrate scope was limited and the reaction was extended to the construction of only two dibenzofurans. Encouraged by the success of our optimised double C-H activation protocol on the 2-pyrone and 2-coumarin scaffolds, we envisioned that this same strategy could be applied to the construction of dibenzofuran motifs.

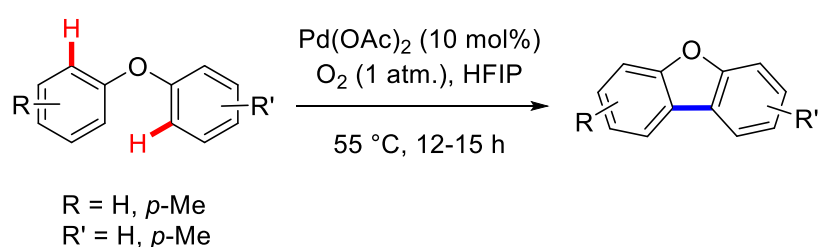
(i) Fagnou, *J. Org. Chem.* 2008, 73, 5022-5028



(ii) Ishida, *Appl. Cat. B. Environ.* 2014, 150, 523-531



(iii) Wang, *Org. Lett.* 2017, 19, 798-801



Scheme 12. Palladium catalysed intramolecular double C-H activation of diarylethers.

In summary, the application of our optimised double C-H activation methodology to a number of 2-pyrone and 2-coumarin substrates will be outlined in **Chapter 2** of this thesis. As previously discussed, there is limited applicability of this methodology on more delicate 2-pyrone and 2-coumarin molecular frameworks. A broad range of functional group compatibility has been observed and the three-step synthesis of the natural product flemichapparin C is also detailed in **Chapter 2**. Our second goal was to apply this double C-H

activation methodology as a new route to dibenzofurans. Particular interest was focused on regioselective aspects of the reaction. The scope and limitations of the reaction will also be discussed.

1.7.1 Aims and objectives (Chapter 3)

The cyclisation of mono-halogenated diarylethers *via* C-H activation is a particularly useful route to form dibenzofurans. Considering the problems associated with traditional and dehydrogenative coupling reactions,^{5, 9, 13} the development of a chemical compromise, which involves the coupling of an aryl-X with an aryl-H, would seem the ideal methodology in many cases. However, many limitations exist with the current protocols, which will be discussed in the following section. Thus, the key goal of **Chapter 3** was focused on addressing the challenges associated with the current methodologies. Particular emphasis was placed on the development of a set of reaction conditions which would drive the reaction to completion and subsequently alleviate purification difficulties.

This work

Dibenzofuran synthesis

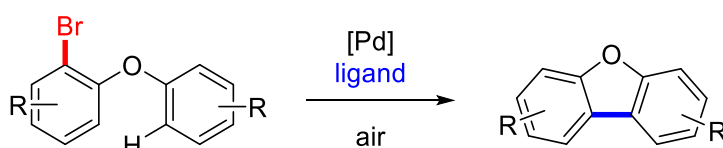
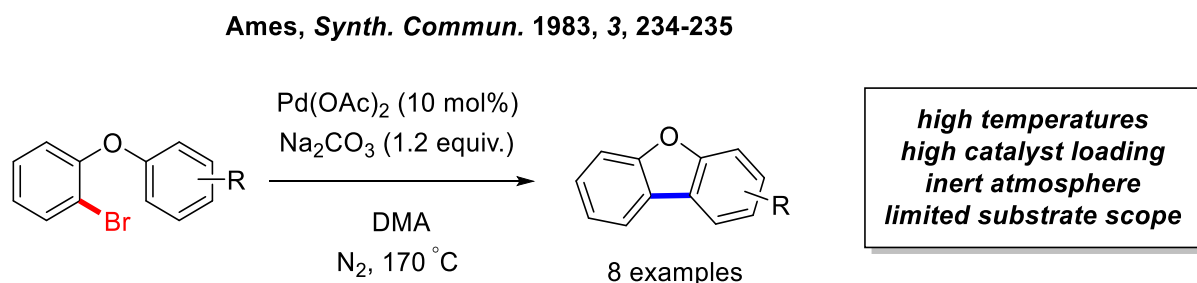


Figure 7. Focus of this research.

1.7.2 Literature examples on the direct arylation of *ortho*-halo diarylethers

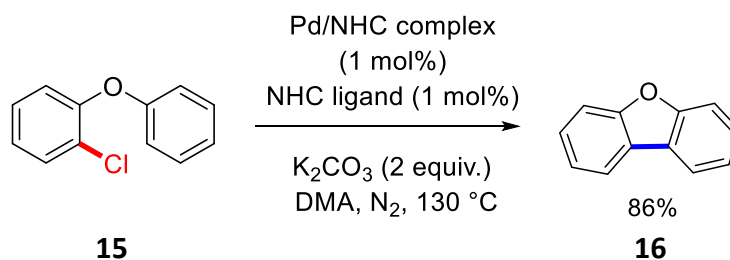
Seminal work carried out by Ames and co-workers in the 1980s led to the development of a convenient method for the cyclisation of substituted 2-bromo diarylethers with no added ligand (**Scheme 13**).⁴⁶



Scheme 13. Intramolecular direct arylation of *ortho*-halo diaryl ethers.

Subsequent work by Fagnou and co-workers utilised an *N*-heterocyclic carbene/Pd catalyst system to promote direct arylation of *ortho*-chloro diarylether (**15**) to produce dibenzofuran (**16**) as well as 6*H*-benzo-[*c*]-chromene systems (**Scheme 14**).⁴⁷

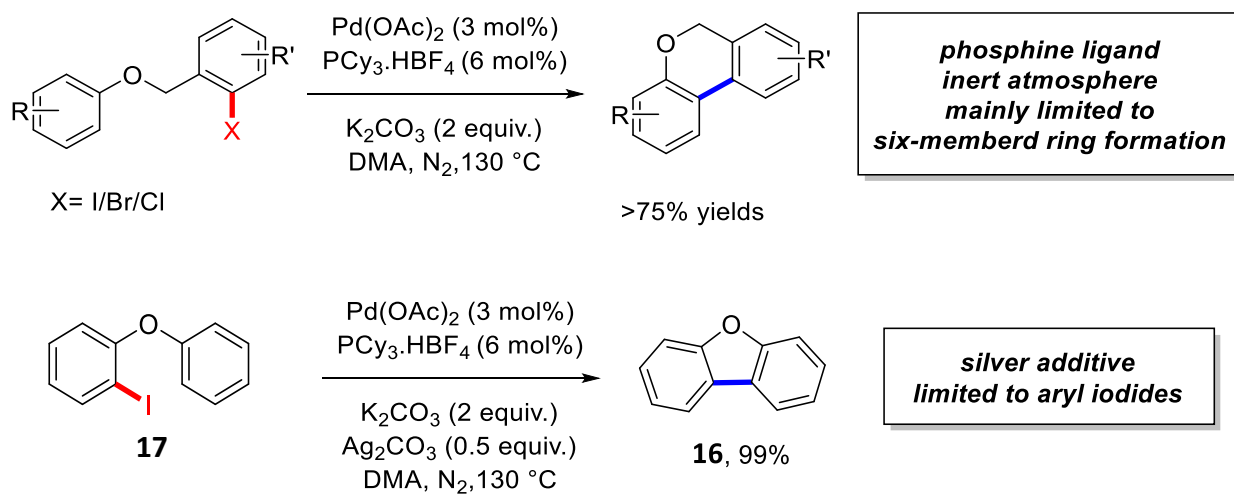
Fagnou, *Org. Lett.* 2005, 7, 1857-1860



Scheme 14. Palladium catalysed direct arylation of *ortho*-chloro diarylether.

A year later, the same group reported a phosphine ligand assisted Pd catalysed route for the intramolecular cyclisation of *ortho*-halo benzyl-oxy ethers to form six-membered rings.¹⁴ This work was extended to include the cyclisation of *ortho*-iodo diarylether (**17**) to produce dibenzofuran (**16**) (**Scheme 15**).

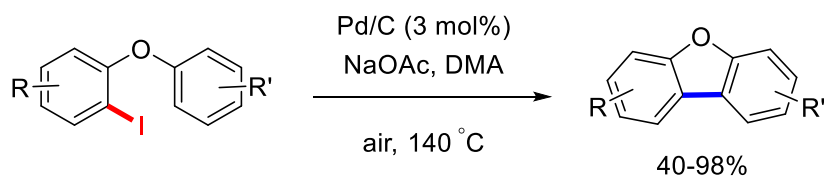
Fagnou, *J. Am. Chem. Soc.* 2006, 128, 581-590



Scheme 15. Palladium catalysed intramolecular direct arylation of *ortho*-halo benzyl-oxy ethers and *ortho*-halo diarylethers.

More recently, Panda and co-workers developed an efficient method for the synthesis of dibenzofurans from *ortho*-iodo diarylethers using a reusable Pd/C catalyst (**Scheme 16**).⁴⁸

Panda, *J. Org. Chem.* 2015, 80, 6590-6597



Scheme 16. Dibenzofuran synthesis using a reusable Pd/C catalyst.

Despite the advances made by Ames, Fagnou and others, there are a number of challenges which remain, which dissuades a broader up-take:

- 1) Very high reaction temperature (>130 °C)
- 2) Very high catalyst loading (up to 10 mol%)⁴⁶
- 3) Use of inert atmosphere
- 4) Use of phosphine ligands
- 5) Use of expensive additives
- 6) Difficulties in purification

Thus, addressing some of the above challenges would represent an important advancement in the development of a milder set of reaction conditions for the intramolecular direct arylation of *ortho*-bromo diarylethers.

1.7.3 Nitrogen based ligands in direct arylation reactions

Direct arylation protocols are often carried out in the presence of palladium complexes bearing tertiary phosphines.⁹⁻¹⁰ However, due to the high cost of phosphine ligands and also their sensitivity to oxidation in air,⁵⁶⁻⁵⁷ the development of a cheap and relatively stable phosphine free catalyst system would be an important achievement. Nitrogen based ligands offer an excellent alternative to phosphine ligands: they are cheap, readily available, easier to remove post-reaction and not as easily oxidised as phosphines. In addition, nitrogen based ligands also offer scope for electronic tuning by easy functionalisation. In contrast, the synthesis of phosphine ligands is more tedious and expensive.⁵⁷ In addition, the strong σ -donation by the nitrogen to the metal centre favours oxidative addition and allows for the formation of stable intermediates enabling C-H activation to occur.⁵⁸ This makes them suitable candidates for ligands in palladium catalysed direct arylation reactions. Among them, pyridine (**18**), 2,2'-bipyridine (**19**), 1,10-phenanthroline (**20**) and quinoline (**21**) based ligands have attracted particular attention and have frequently been utilized as ligands in palladium catalysed C-H functionalisation reactions (**Figure 8**) by the groups of Yu⁵⁹⁻⁶³ and Sanford⁶⁴⁻⁶⁶ in particular among others.⁶²⁻⁶³ In addition, our lab has recently demonstrated the viability of Pd/quinoline pre-catalysts in a one-pot tandem Suzuki-Miyaura/direct arylation reaction with di-bromo quinolines.⁶⁷ Based on these reports, we postulated that quinolines might serve as

suitable candidates for ligands in the palladium catalysed direct arylation of *o*-bromo diarylethers.

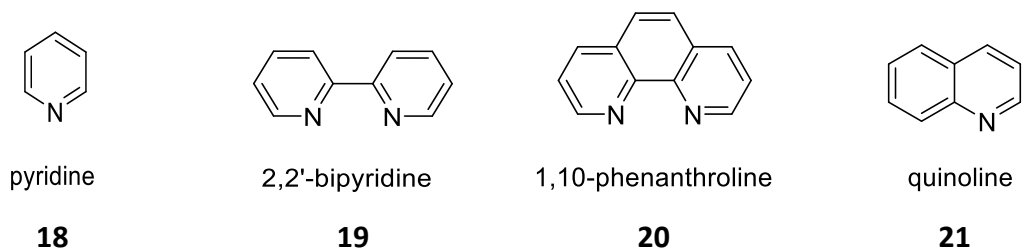


Figure 8. Heterocyclic sp^2 nitrogen donor ligands often applied in transition metal catalysed C-H activation reactions.

Following on from the McGlacken groups interest in the synthesis of heterocyclic frameworks using direct C-H activation,^{24-27, 68-71} the work outlined in **Chapter 3** addresses most of the above existing limitations discussed in this introduction (**Section 1.7.2**). *ortho*-Bromo diarylether was chosen as a suitable molecular framework for the intramolecular cyclisation. Thus, the goal of developing a new and milder set of reaction conditions aided by a cheap and bench stable nitrogen based ligand was targeted.

1.8 References

1. Anastasia, L., Negishi, E. -i in *Handbook of Organopalladium Chemistry for Organic Synthesis*, John Wiley & Sons, Weinheim, Germany, **2002**, pp. 311-334.
2. Stanforth, S. P. *Tetrahedron* **1998**, 54, 263-303.
3. Hassan, J., Sévignon, M., Gozzi, C., Schulz, E., Lemaire, M. *Chem. Rev.* **2002**, 102, 1359-1470.
4. Miyaura, N., Yanagi, T., Suzuki, A. *Synth. Commun.* **1981**, 11, 513-519.
5. McGlacken, G. P., Bateman, L. M. *Chem. Soc. Rev.* **2009**, 38, 2447-2464.
6. Hashiguchi, B. G., Bischof, S. M., Konnick, M. M., Periana, R. A. *Acc. Chem. Res.* **2012**, 45, 885-898.
7. Crabtree, R. H. *J. Am. Chem. Soc., Dalton Trans.* **2001**, 2437-2450.
8. Shilov, A. E., Shul'pin, G. B. *Chem. Rev.* **1997**, 97, 2879-2932.
9. Alberico, D., Scott, M. E., Lautens, M. *Chem. Rev.* **2007**, 107, 174-238.
10. McGlacken, G. P., Bateman, L. M. *Chem. Soc. Rev.* **2009**, 38, 2447-2464.
11. Constable, D. J., Dunn, P. J., Hayler, J. D., Humphrey, G. R., Leazer Jr, J. L., Linderman, R. J., Lorenz, K., Manley, J., Pearlman, B. A., Wells, A. *Green Chem.* **2007**, 9, 411-420.
12. Trost, B. *Science* **1991**, 254, 1471-1477.
13. Dasgupta, R., Maiti, B. R. *Ind. Eng. Chem. Process Des. Dev.* **1986**, 25, 381-386.
14. Campeau, L.-C., Parisien, M., Jean, A., Fagnou, K. *J. Am. Chem. Soc.* **2006**, 128, 581-590.
15. Li, R., Jiang, L., Lu, W. *J. Organomet. Chem.* **2006**, 25, 5973-5975.
16. Xia, J.-B., You, S.-L. *J. Organomet. Chem.* **2007**, 26, 4869-4871.
17. Stuart, D. R., Villemure, E., Fagnou, K. *J. Am. Chem. Soc.* **2007**, 129, 12072-12073.
18. Liégault, B., Lee, D., Huestis, M. P., Stuart, D. R., Fagnou, K. *J. Org. Chem.* **2008**, 73, 5022-5028.
19. Li, H., Zhu, R.-Y., Shi, W.-J., He, K.-H., Shi, Z.-J. *Org. Lett.* **2012**, 14, 4850-4853.
20. Balcells, D., Clot, E., Eisenstein, O. *Chem. Rev.* **2010**, 110, 749-823.
21. Lin, Z. *Coord. Chem. Rev.* **2007**, 251, 2280-2291.
22. David, L., Keith, F. *Chem. Lett.* **2010**, 39, 1118-1126.
23. Boutadla, Y., Davies, D. L., Macgregor, S. A., Poblador-Bahamonde, A. I. *Dalton Trans.* **2009**, 5820-5831.

24. Nolan, M.-T., Bray, J. T. W., Eccles, K., Cheung, M. S., Lin, Z., Lawrence, S. E., Whitwood, A. C., Fairlamb, I. J. S., McGlacken, G. P. *Tetrahedron* **2014**, *70*, 7120-7127.
25. Nolan, M.-T., Pardo, L. M., Prendergast, A. M., McGlacken, G. P. *J. Org. Chem.* **2015**, *80*, 10904-10913.
26. Prendergast, A. M., Pardo, L. M., Fairlamb, I. J. S., McGlacken, G. P. *Eur. J. Org. Chem.* **2017**, *2017*, 5119-5124.
27. Pardo, L. M., Prendergast, A. M., Nolan, M.-T., Ó Muimhneacháin, E., McGlacken, G. P. *Eur. J. Org. Chem.* **2015**, *2015*, 3540-3550.
28. McGlacken, G. P., Fairlamb, I. J. S. *Nat. Prod. Rep.* **2005**, *22*, 369-385.
29. Calcio Gaudino, E., Tagliapietra, S., Martina, K., Palmisano, G., Cravotto, G. *RSC Adv.* **2016**, *6*, 46394-46405.
30. Chaturvedula, V. S. P., Schilling, J. K., Kingston, D. G. I. *J. Nat. Prod.* **2002**, *65*, 965-972.
31. Oliphant, C. M., Green, G. M. *Am Fam Physician* **2002**, *65*, 455-464.
32. Heeb, S., Fletcher, M. P., Chhabra, S. R., Diggle, S. P., Williams, P., Cámara, M. *FEMS Microbiol. Rev.* **2011**, *35*, 247-274.
33. Jayashree, B., Thomas, S., Nayak, Y. *Med. Chem. Res.* **2010**, *19*, 193-209.
34. Majumdar, K. C., Pal, A. K., Taher, A., Debnath, P. *Synthesis* **2007**, *11*, 1707-1711.
35. Majumdar, K. C., Debnath, P., Taher, A., Pal, A. K. *Can. J. Chem.* **2008**, *86*, 325-332.
36. Burns, M. J., Thatcher, R. J., Taylor, R. J. K., Fairlamb, I. J. S. *Dalton Trans.* **2010**, *39*, 10391-10400.
37. Majumdar, K. C., Basu, P. K., Mukhopadhyay, P. P., Sarkar, S., Ghosh, S. K., Biswas, P. *Tetrahedron* **2003**, *59*, 2151-2157.
38. Adityachaudhury, N., Gupta, P. K. *Phytochemistry* **1973**, *12*, 425-428.
39. Horton, D. A., Bourne, G. T., Smythe, M. L. *Chem. Rev.* **2003**, *103*, 893-930.
40. Love, B. E. *Eur. J. Med. Chem.* **2015**, *97*, 377-387.
41. Sokolov, D. N., Zarubaev, V. V., Shtro, A. A., Polovinka, M. P., Luzina, O. A., Komarova, N. I., Salakhutdinov, N. F., Kiselev, O. I. *Bioorg. Med. Chem. Lett.* **2012**, *22*, 7060-7064.
42. Patpi, S., Pulipati, L., Perumal, Y., Sriram, D., Jain, N., Sridhar, B., Murthy, R., Tangutur, A., Kalivendi, S., Kantevari, S. *J. Med. Chem.* **2012**, *55*, 3911-3922.
43. Liu, J., Fitzgerald, A. E., Mani, N. S. *J. Org. Chem.* **2008**, *73*, 2951-2954.
44. Xiao, B., Gong, T.-J., Liu, Z.-J., Liu, J.-H., Luo, D.-F., Xu, J., Liu, L. *J. Am. Chem. Soc.* **2011**, *133*, 9250-9253.

45. Zhao, H., Yang, K., Zheng, H., Ding, R., Yin, F., Wang, N., Li, Y., Cheng, B., Wang, H., Zhai, H. *Org. Lett.* **2015**, *17*, 5744-5747.
46. Ames, D. E., Opalko, A. *Synthesis* **1983**, *3*, 234-235.
47. Campeau, L.-C., Thansandote, P., Fagnou, K. *Org. Lett.* **2005**, *7*, 1857-1860.
48. Panda, N., Mattan, I., Nayak, D. K. *J. Org. Chem.* **2015**, *80*, 6590-6597.
49. Lockner, J. W., Dixon, D. D., Risgaard, R., Baran, P. S. *Org. Lett.* **2011**, *13*, 5628-5631.
50. Liu, Z., Larock, R. C. *Tetrahedron* **2007**, *63*, 347-355.
51. Du, Z., Zhou, J., Si, C., Ma, W. *Synlett* **2011**, *20*, 3023-3025.
52. Wang, C., Piel, I., Glorius, F. *J. Am. Chem. Soc.* **2009**, *131*, 4194-4195.
53. Nervig, C. S., Waller, P. J., Kalyani, D. *Org. Lett.* **2012**, *14*, 4838-4841.
54. Ishida, T., Tsunoda, R., Zhang, Z., Hamasaki, A., Honma, T., Ohashi, H., Yokoyama, T., Tokunaga, M. *Appl. Catal. B Environ.* **2014**, *150*, 523-531.
55. Guo, D.-D., Li, B., Wang, D.-Y., Gao, Y.-R., Guo, S.-H., Pan, G.-F., Wang, Y.-Q. *Org. Lett.* **2017**, *19*, 798-801.
56. Iyer, S., Kulkarni, G. M., Ramesh, C. *Tetrahedron* **2004**, *60*, 2163-2172.
57. Wauters, I., Debrouwer, W., Stevens, C. V. *Beilstein J. Org. Chem.* **2014**, *10*, 1064-1096.
58. Dutta, U., Modak, A., Bhaskararao, B., Bera, M., Bag, S., Mondal, A., Lupton, D. W., Sunoj, R. B., Maiti, D. *ACS Catal.* **2017**, *7*, 3162-3168.
59. Cheng, G., Wang, P., Yu, J.-Q. *Angew. Chem. Int. Ed.* **2017**, *56*, 8183-8186.
60. Li, S., Chen, G., Feng, C.-G., Gong, W., Yu, J.-Q. *J. Am. Chem. Soc.* **2014**, *136*, 5267-5270.
61. Zhang, Y.-H., Shi, B.-F., Yu, J.-Q. *J. Am. Chem. Soc.* **2009**, *131*, 5072-5074.
62. Izawa, Y., Stahl, S. S. *Adv. Syn. Catal.* **2010**, *352*, 3223-3229.
63. Gao, G.-L., Xia, W., Jain, P., Yu, J.-Q. *Org. Lett.* **2016**, *18*, 744-747.
64. Cabrera, P. J., Lee, M., Sanford, M. S. *J. Am. Chem. Soc.* **2018**, *140*, 5599-5606.
65. Emmert, M. H., Cook, A. K., Xie, Y. J., Sanford, M. S. *Angew. Chem. Int. Ed.* **2011**, *50*, 9409-9412.
66. Kubota, A., Emmert, M. H., Sanford, M. S. *Org. Lett.* **2012**, *14*, 1760-1763.
67. Shanahan, R. M., Hickey, A., Bateman, L. M., Light, M. E., McGlacken, G. P. *J. Org. Chem.* **2020**, *85*, 2585-2596.
68. Mackey, K., Pardo, L. M., Prendergast, A. M., Nolan, M.-T., Bateman, L. M., McGlacken, G. P. *Org. Lett.* **2016**, *18*, 2540-2543.

69. Shanahan, R. M., Hickey, A., Reen, F. J., O'Gara, F., McGlacken, G. P. *Eur. J. Org. Chem.* **2018**, 2018, 6140-6149.
70. Muimhneacháin, E. Ó., Pardo, L. M., Bateman, L. M., Rao Khandavilli, U. B., Lawrence, S. E., McGlacken, G. P. *Adv. Syn. Catal.* **2017**, 359, 1529-1534.
71. Cano, R., Pérez, J. M., Ramón, D. J., McGlacken, G. P. *Tetrahedron* **2016**, 72, 1043-1050.

Chapter 2: Cyclisation of 4-phenoxy-2-pyrones, 2-coumarins and related heterocycles *via* double C-H activation

2.1 Preface

In this chapter, the synthesis of a library of 1*H*-pyrano[4,3-*c*]benzofuran-1-one and 6*H*-benzofuro[3,2-*c*]chromen-6-one analogues is described. Additionally, the methodology was extended to include a 2-quinolone analogue, as well as the synthesis of a natural product.

2.2 Background

As discussed in **Chapter 1** of this thesis, in recent years direct arylation *via* C-H functionalisation has proved a valuable alternative to traditional cross-coupling procedures.¹⁻² The ideal approach would involve the coupling of two C-H groups, representing a green route to bi(hetero)aryls.³ However, as outlined previously in **Chapter 1**, there is limited applicability of this methodology on delicate molecular frameworks. The 2-pyrone motif represents a privileged biological scaffold with broad spectrum biological activity spanning antibiotic, antifungal and cytotoxic activity.⁴ In addition, the related 2-coumarins display a remarkable impressive biological profile.⁵⁻⁷ The McGlacken group has previously utilised direct arylation methodologies for the cyclisation of 4-phenoxy-2-pyrone and 4-phenoxy-2-coumarin derivatives.⁸ However, the cyclisation of such substrates required the installation of a halogen on one coupling partner. With this in mind, we sought to gain access to tricyclic pyrones and coumarins by the coupling of phenoxy substituted substrates *via* two C-H activation events (**Figure 9**). This is a far more challenging approach as outlined (*vide supra*).

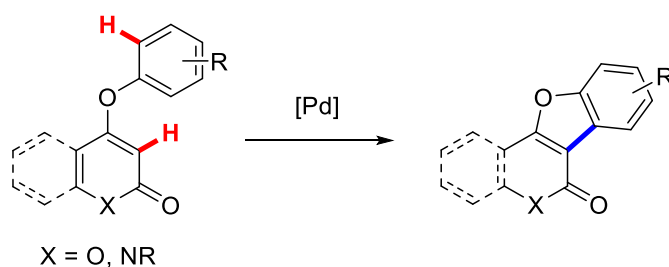
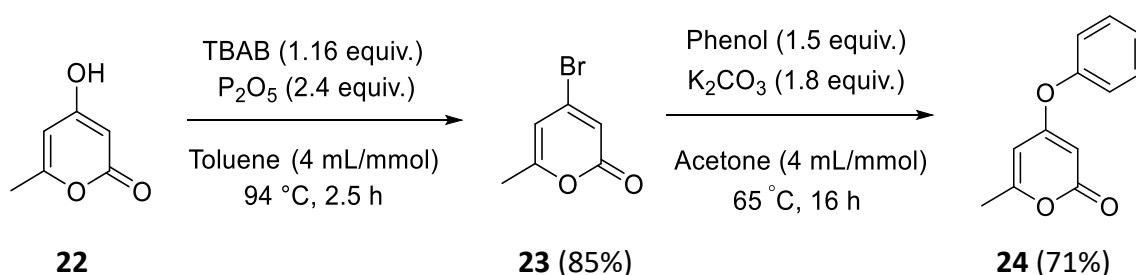


Figure 9. Objective of this research.

2.2.1 Synthesis of 4-phenoxy-2-pyrone substrate

Initially, research was focused on the double C-H activation of 4-phenoxy-2-pyrone derivatives. The first step involved synthesizing 4-phenoxy-6-methyl-2-pyrone (**24**) as this was not commercially available. To begin with, 4-bromo-6-methyl-2-pyrone (**23**) was prepared in an 85% yield using a slightly modified procedure to that described by Kato and co-workers,⁹

by reaction of 4-hydroxy-6-methyl-2-pyrone (**22**) with TBAB (tetrabutylammonium bromide) and P_2O_5 in toluene (**Scheme 17**). Multiple grams of **23** could be synthesised at a time and this methodology served as a useful precursor for many of the substrates outlined in this Chapter. 4-Phenoxy-6-methyl-2-pyrone (**24**) was then synthesized by a base mediated reaction of phenol with 4-bromo-6-methyl-2-pyrone (**23**) in acetone at reflux. The product was isolated in a 71% yield by washing the crude reaction mixture with 10% aqueous NaOH, followed by recrystallisation from hot ethanol (**Scheme 17**).

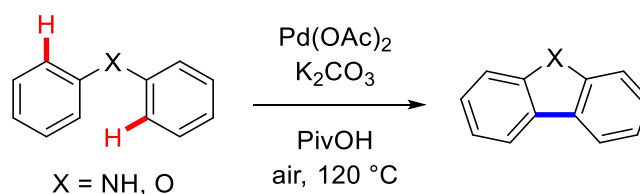


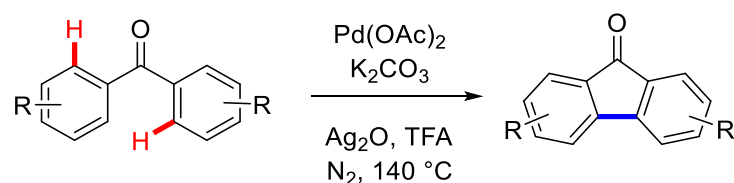
Scheme 17. Two step synthesis of 6-methyl-4-phenoxy-pyrone (**24**).

2.2.2 Optimisation of double C-H activation reaction conditions

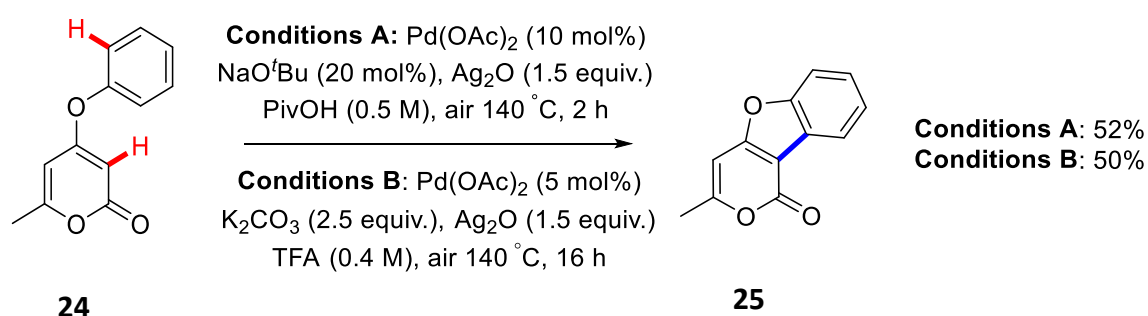
Our optimisation work began with two seminal reports by Fagnou¹⁰ and Shi¹¹ who reported the Pd catalysed intramolecular cyclisation of diphenylamine and benzophenone substrates *via* a double C-H activation. Key to the success of their reactions was the addition of pivalic acid (PivOH) and trifluoroacetic acid (TFA). In the case of Fagnou's work, the pivalate anion is proposed to play a key role in the C-H bond cleaving event,^{10, 12} allowing for increased reactivity and selectivity. This enabled the formation of the carbazole products in high yields which was in stark contrast to when acetic acid was utilised as reaction solvent.

(i) Fagnou, *J. Org. Chem.* 2008, **73**, 5022-5028



(ii) Shi, *Org. Lett.* 2012, 14, 4850-4853**Scheme 18.** Literature examples of direct arylation *via* a double C-H activation.

These two sets of reaction conditions served as key starting points for the development of our methodology towards the synthesis of 1*H*-pyrano[4,3-*c*]benzofuran-1-one and 6*H*-benzofuro[3,2-*c*]chromen-6-one analogues. Previous work from the McGlacken group by Dr. Marie-Therese Nolan identified the need for an external oxidant to help regenerate the catalyst, therefore, Ag_2O was included in the reaction conditions.¹¹ Sodium *tert*-butoxide also served as a more efficient base in comparison to K_2CO_3 . These conditions were then applied to the 4-phenoxy-2-pyrone system in air and at a higher temperature of 140 °C. Complete consumption of starting material **24** and formation of product **25** was observed after 2 hours with the product being isolated in a 52% yield (**Scheme 19, Conditions A**). Direct application of Shi's conditions on the 4-phenoxy-2-pyrone system allowed for complete consumption of starting material **24** after 16 hours and a 50% isolated yield of **25** was obtained in this case (**Scheme 19, Conditions B**).

**Scheme 19.** Double C-H activation reaction of **24**.

The low yields observed could be explained, in the case of **Conditions B**, by the presence of a large excess of trifluoroacetic acid (TFA) in the reaction media. TFA is one of the strongest organic acids (pK_a : -0.25 (H_2O)). This strongly acidic reaction medium may cause degradation

of the delicate 2-pyrone motif. Pivalic acid is also quite a strong acid (pKa: 4.04) and again the large excess of pivalic in the reaction media acid may lead to degradation of the 2-pyrone framework. It may also be possible that the high temperature required (140 °C) could degrade the 2-pyrone. Decomposition pathways will be discussed below.

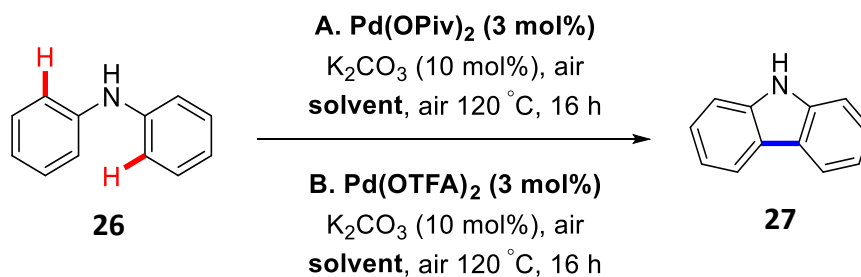
2.2.3 Optimisation of reaction conditions performed on diphenylamine and benzophenone

With the above considerations in mind, we decided to perform an optimisation screen with the aim of establishing a milder set of reaction conditions. A comprehensive screen of solvents and catalysts was performed on diphenylamine (**26**) and benzophenone (**28**). These two substrates were first chosen because of their more robust structure in comparison to the 2-pyrone scaffold. It must be noted that Fagnou¹⁰ and Shi¹¹ had previously utilised such substrates in their work. If our optimization screen produced any promising results using these substrates, we could then apply these results to the 2-pyrone system. The results are summarised in **Table 1** and **Table 2** below. Both diphenylamine and benzophenone were purchased from a commercial supplier.

To avoid using a large excess of acid as reaction solvent but also keeping in mind that both the TFA and PivOH are proposed to play key roles in the reaction, it was decided that we would incorporate both TFA and PivOH into the catalyst to avoid the presumable degradation of our 2-pyrone system. Therefore, Pd(OPiv)₂ and Pd(OTFA)₂ were chosen as the catalysts of choice for the reaction. Polar aprotic solvents are generally the solvent of choice for Pd catalysed direct arylation reactions. With this in mind, six different solvents were chosen: *N,N*-dimethyl formamide (DMF), *N,N*-dimethyl acetamide (DMA), *N*-methyl pyrrolidone (NMP), dimethyl sulfoxide (DMSO), tetrahydrofuran (THF) and one polar protic solvent, ethanol (EtOH). DMF, DMA and NMP are all high boiling point amide solvents, and thus would be suitable solvents of choice due to the high temperatures usually required for C-H activation reactions.² In addition, they can act as coordinating solvents and help stabilise organometallic intermediates as well as playing a direct role in the formation of the active catalyst.¹³ THF is a polar coordinating solvent (hydrogen bond acceptor) which could potentially facilitate catalysis.¹³ Two environmentally green solvents were additionally examined, EtOH a polar protic solvent and DMSO.¹⁴⁻¹⁵ For the diphenylamine substrate **26**, formation of product **27** was observed when DMF, DMA and THF were used as the reaction solvents. However, a

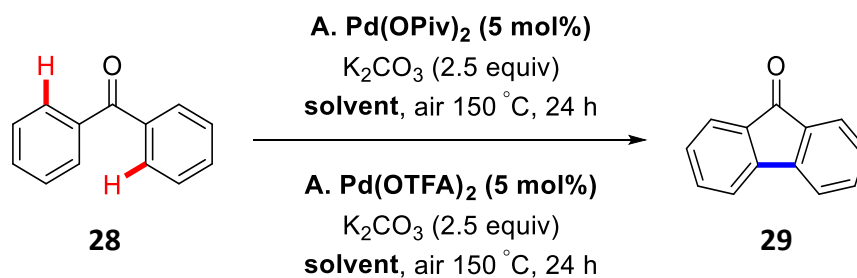
conversion of less than 10% was determined by ^1H NMR Spectroscopy (**Table 1 entries 1, 3 and 8**). In contrast, employing benzophenone (**28**) as starting material, no cyclised product **29** was detected by TLC and only starting material was visible by ^1H NMR Spectroscopy.

Table 1. Optimization of reaction conditions performed on diphenylamine (**26**).



Entry	Conditions	[Pd]	Solvent	Conversion (%) ^a
1	A	Pd(OPiv)_2	DMF	5
2	A	Pd(OPiv)_2	THF	0
3	A	Pd(OPiv)_2	DMA	2
4	A	Pd(OPiv)_2	NMP	0
5	A	Pd(OPiv)_2	EtOH	0
6	A	Pd(OPiv)_2	DMSO	0
7	B	Pd(OTFA)_2	DMF	0
8	B	Pd(OTFA)_2	THF	3
9	B	Pd(OTFA)_2	DMA	0
10	B	Pd(OTFA)_2	NMP	0
11	B	Pd(OTFA)_2	EtOH	0
12	B	Pd(OTFA)_2	DMSO	0

^aConversion calculated from ratio of starting material **26** (2H, m at 6.87-6.91 ppm) to product **27** (2H, m at 7.23-7.26 ppm) in ^1H NMR spectrum of the crude reaction mixture.

Table 2. Optimization of reaction conditions performed on benzophenone (**28**).

Entry	Conditions	[Pd]	Solvent	Conversion (%) ^a
1	A	Pd(OPiv) ₂	DMF	0
2	A	Pd(OPiv) ₂	THF	0
3	A	Pd(OPiv) ₂	DMA	0
4	A	Pd(OPiv) ₂	NMP	0
5	A	Pd(OPiv) ₂	EtOH	0
6	A	Pd(OPiv) ₂	DMSO	0
7	B	Pd(OTFA) ₂	DMF	0
8	B	Pd(OTFA) ₂	THF	0
9	B	Pd(OTFA) ₂	DMA	0
10	B	Pd(OTFA) ₂	NMP	0
11	B	Pd(OTFA) ₂	EtOH	0
12	B	Pd(OTFA) ₂	DMSO	0

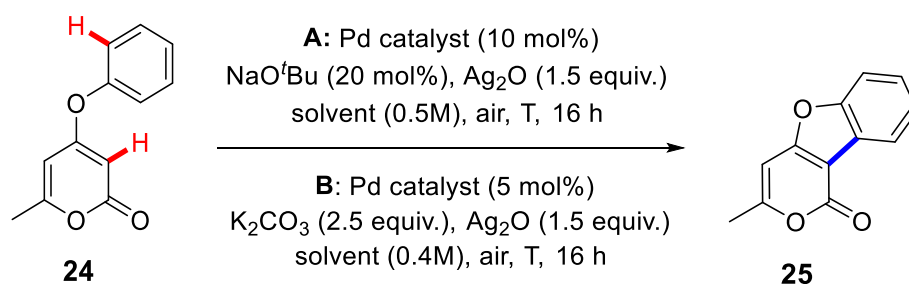
^aConversion calculated from ratio of starting material **28** (4H, m at 7.80 ppm) to product **29** (2H, m at 7.27-7.29 ppm) in ¹H NMR spectrum of the crude reaction mixture.

2.2.4 Optimisation of reaction conditions performed on 4-phenoxy-2-pyrone

Considering the results obtained in the optimisation screen, we then decided to carry out a brief optimization on the 4-phenoxy-2-pyrone substrate **24**. Again, Pd(OPiv)₂ and Pd(OTFA)₂ were chosen as the catalysts and DMF and THF were chosen as the reaction solvents due to the fact that these two particular solvents led to the highest conversions to product for the

diphenylamine (**26**) substrate (albeit marginal). The highest conversion to product **25** was 9% (Table 3, entry 1) and this was obtained with Pd(OPiv)₂ as catalyst, 30 mol% PivOH as an additive and THF as solvent at 70 °C. All other reaction conditions investigated failed to provide any satisfactory conversion to product. This result would indicate that pivalic acid plays a key role in the reaction and also implies that a higher temperature is required for the reaction to proceed.

Table 3. Optimization of reaction conditions performed on the phenoxy pyrone **24**.



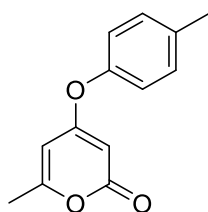
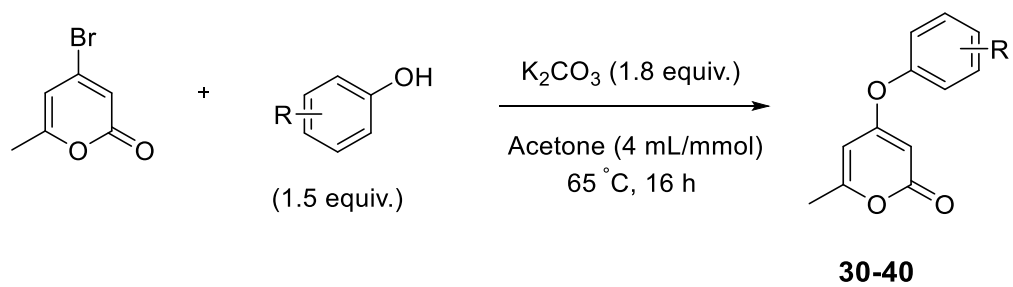
Entry	Conditions	[Pd]	Solvent	Additive (30 mol%)	Temp. (°C)	Time (h)	Conversion ^a (%)
1	A	Pd(OPiv) ₂	THF	PivOH	70	20	9
2	A	Pd(OPiv) ₂	THF	-	70	20	3
3	A	Pd(OTFA) ₂	THF	PivOH	70	16	2
4	A	Pd(OTFA) ₂	THF	-	70	17	0
5	B	Pd(OPiv) ₂	THF	-	70	16	2
6	B	Pd(OPiv) ₂	DMF	-	100	17	0
7	B	Pd(OTFA) ₂	THF	-	70	16	0
8	B	Pd(OTFA) ₂	DMF	-	100	17	0

^aConversion calculated from ratio of starting material **24** (C3-H at 5.21 ppm) to product **25** (C5-H at 6.54 ppm) in ¹H NMR spectrum of the crude reaction mixture.

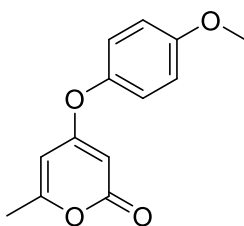
2.3.1 Synthesis of substrates

2-Pyrones

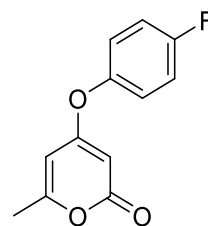
Due to the poor results obtained from our optimization screen, it was decided to continue our work using the original optimized reaction conditions (**Scheme 19, Conditions A** and **Conditions B**). An examination of the functional group tolerance was then planned. For this investigation, a range of 4-phenoxy-6-methyl-2-pyrone analogues (**30-40**) was synthesised using the same method as described for **24** (**Scheme 20**).



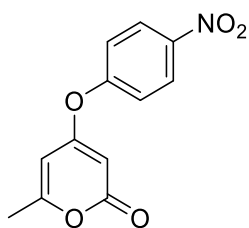
30, 44%



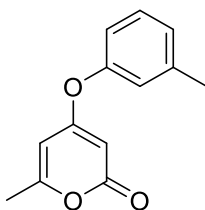
31, 55%



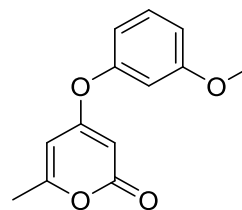
32, 64%



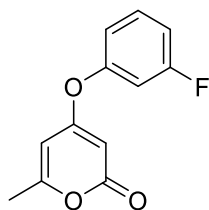
33, 50%



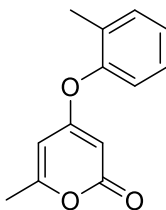
34, 73%



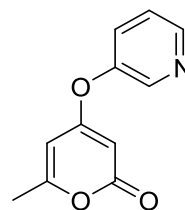
35, 58%



36, 21%



37, 87%



38, 67%

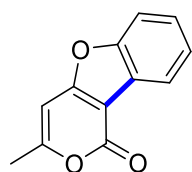
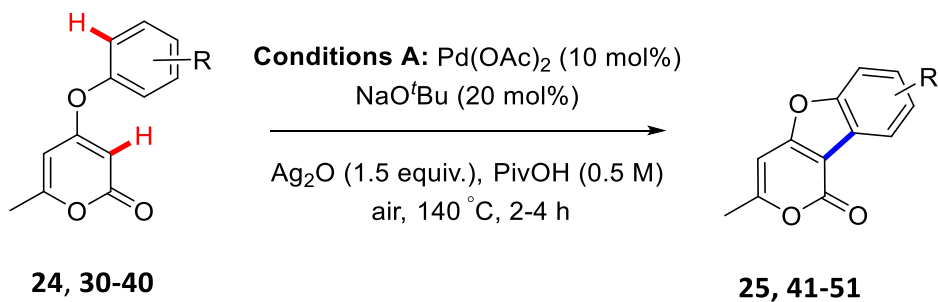
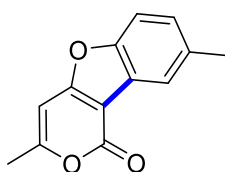
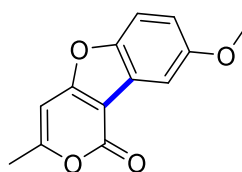
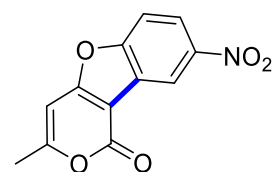
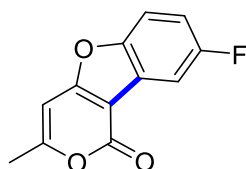
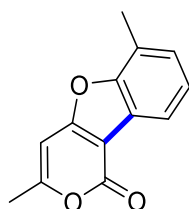
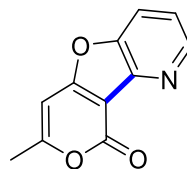
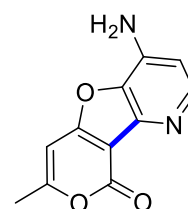


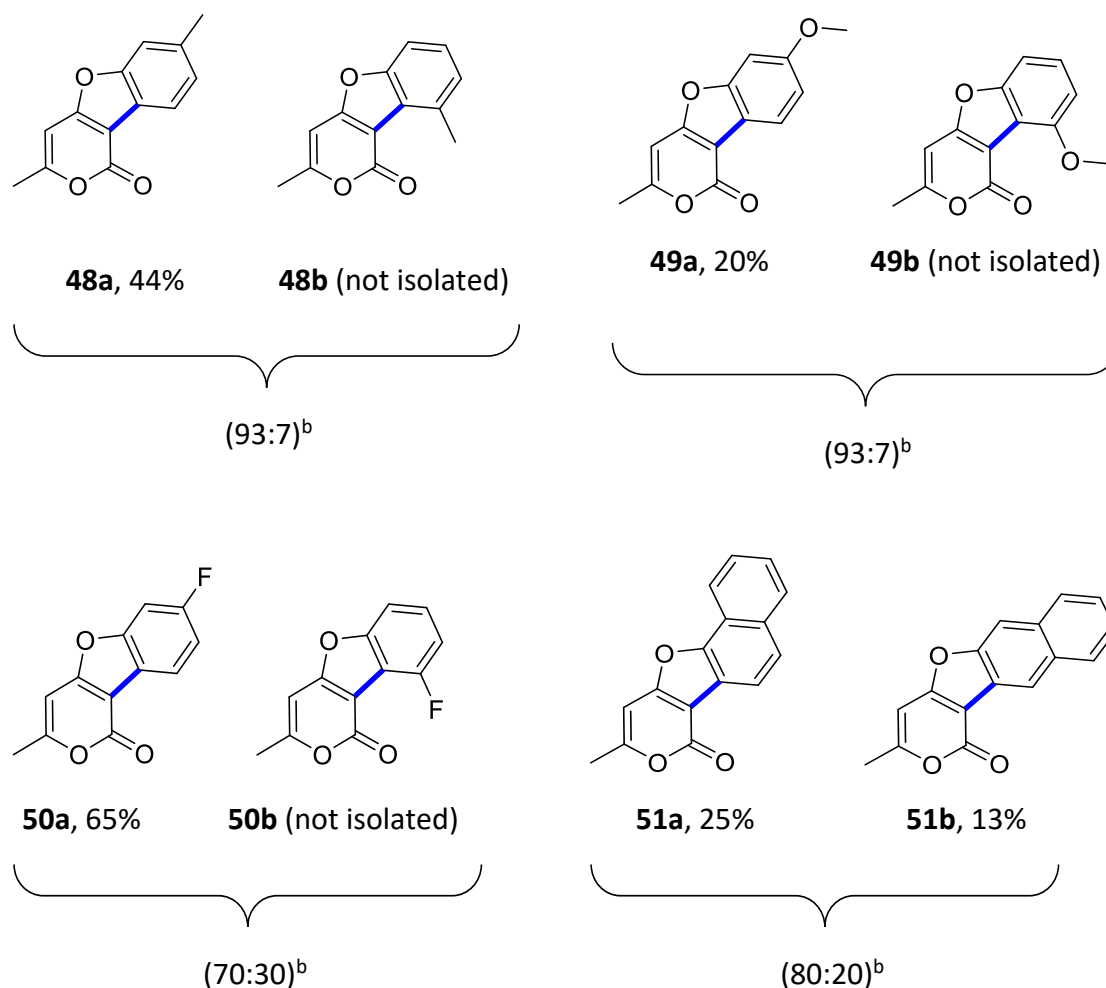
Scheme 20. Synthesis of 4-phenoxy-2-pyrone substrates.

2.3.2 Demonstration of substrate scope for double C-H activation of 2-Pyrones

Next, each of the substrates were subjected to the two sets of optimised reaction conditions. Overall, **Conditions A** employing pivalic acid as reaction solvent (**Scheme 21**) were much more successful than **Conditions B**. Complete consumption of starting material was seen after 2-4 hours for **Conditions A**. Moderate to good yields were observed for substrates bearing electron donating groups at the *para*-position **41** and **42** (42%). The substrate bearing a *para*-methyl group gave the cyclised product **41** in a 56% yield, this was the highest yield obtained overall. In contrast, an electron withdrawing group at the *para*-position did not work well, the presence of a fluoro group **44** completely inhibited the reaction. A *ca.* 31% yield was obtained for the *para*-nitro product **43**, however a number of impurities were still present despite numerous purification attempts. Interestingly, the reaction of **37** bearing a methyl group at the *ortho*-position failed to undergo cyclisation. Steric hindrance is the most plausible explanation for why the reaction failed to proceed. The *meta*-substituted phenoxy substrates gave the cyclised products **48-50** in moderate yields. For these particular substrates, some good regioselectivity toward the least hindered position was observed. For example, the reaction of **34** gave **48a:48b** in a regioisomeric ratio of 97:3 in favour of the least hindered regioisomer. A similar result was obtained for the *meta*-methoxy substituted product **49a:49b**. The reaction of **36** gave a mixture of regioisomers **50a:50b** in a 70:30 ratio, again the least hindered regioisomer was favoured under the optimised reaction conditions. Pleasingly, under our conditions a naphthyl group was well tolerated and a mixture of regioisomers was obtained (**51a:51b**) in an 80:20 ratio in favour of the least hindered product. Substrates such as pyridine (**38**) and that contained a primary amine group (**39**) did not work well. Only starting material was observed in the ^1H NMR spectrum of the crude reaction mixture for

these two particular compounds. Ligation of the pyridyl nitrogen or amine to Pd could have the potential to inhibit catalysis and would offer an explanation for the poor result obtained for such substrates.¹⁶

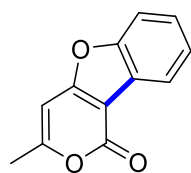
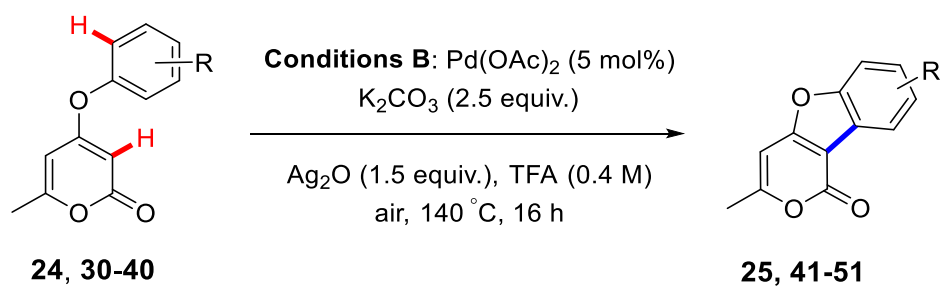
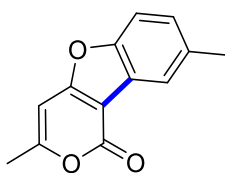
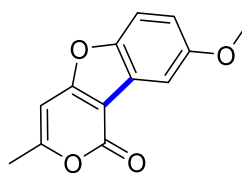
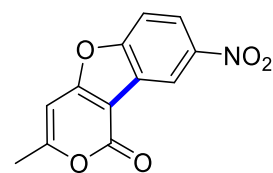
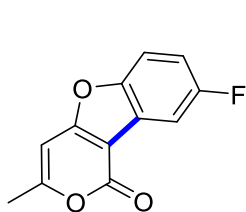
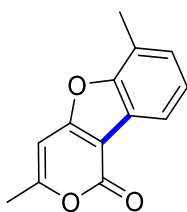
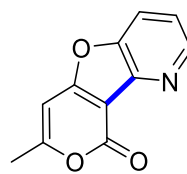
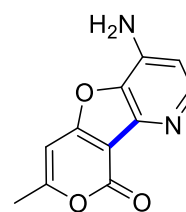
**25**, 52%**41**, 56%**42**, 42%**43**, 31%^a**44**, 0%**45**, 0%**46**, 0%**47**, 0%

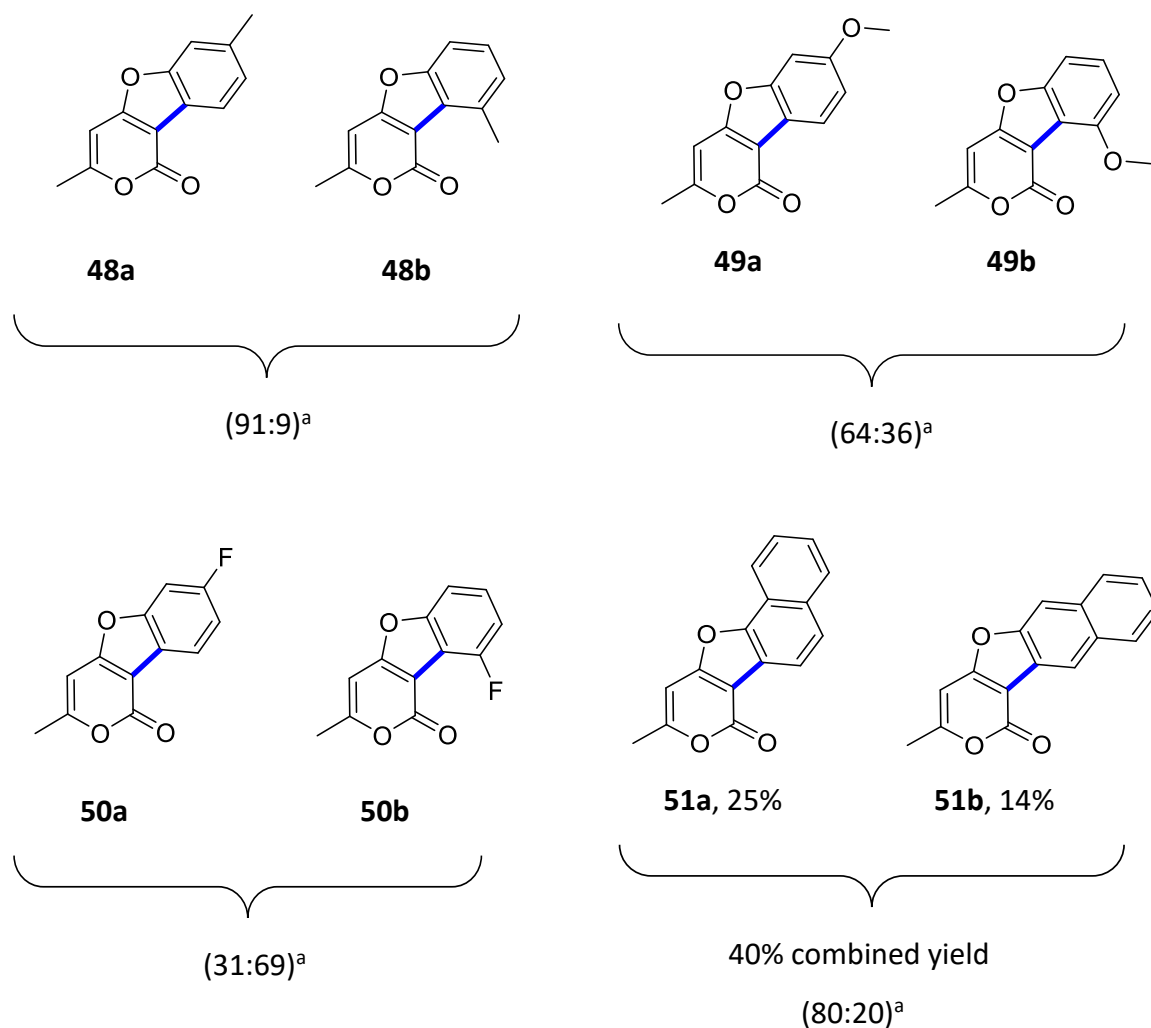


Scheme 21. Isolated yields of substituted 1*H*-pyrano [4,3-*b*] benzofuran-1-ones. ^a*ca.* 31% yield, this compound still contained a number of impurities despite numerous purification attempts. ^b Regioisomeric ratios determined from the ¹H NMR spectrum of the crude reaction mixture.

Longer reaction times were required for **Conditions B (Scheme 22)**. Complete consumption of starting material was observed after 24-48 hours. However, a significant number of the phenoxy 2-pyrone substrates failed to cyclise and were also subject to degradation under the reaction conditions. Only small amounts of products **41-50** could be detected in the ¹H NMR of the crude reaction mixtures along with unreacted starting material and degradation of starting material (which will be discussed below). In addition, the mass recovery of the reaction was very poor in most cases. It was therefore not possible to isolate the compounds from the reaction mixtures (hence regioisomeric ratios are only given in **Scheme 22**). A similar trend in terms of regioselectivity was observed for the *meta*-methyl and *meta*-methoxy substituted phenoxy-2-pyrone, seen for **Conditions A**. Reaction occurred at the least

hindered site for compounds **48-49**. Interestingly, the *meta*-fluoro substrate **50** showed a switch in regioselectivity, in this case reaction occurred at the most acidic site (39:61). This may offer some insight into the mechanism of the reaction. Pleasingly, the unsubstituted phenoxy pyrone **24** successfully underwent reaction to afford the cyclised product **25** in a 50% isolated yield. Similarly, the naphthyl group was compatible under the reaction conditions and a mixture of regioisomers **51a:51b** was obtained in an 85:15 ratio. Again, the least hindered regioisomer was favoured.

**25**, 50%**41** and degradation products**42** and degradation products**43** (trace) and degradation products**44**, unreacted starting material and degradation products**45** and unreacted starting material**46** and unreacted starting material**47**, unreacted starting material and degradation products

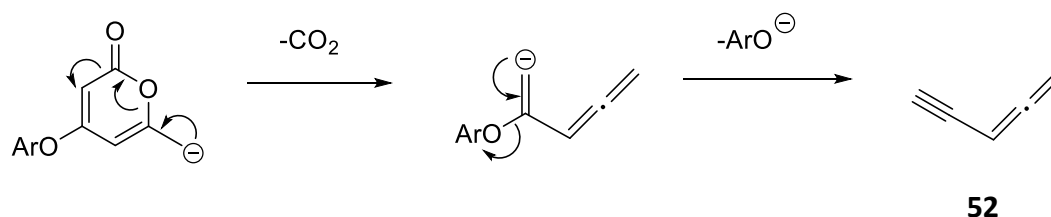


Scheme 22. Attempted double C-H activation of phenoxy pyrone substrates employing **Conditions B**.

^aRegioisomeric ratios determined from the ¹H NMR spectrum of the crude reaction mixture.

An explanation for the poor yields obtained could be the decomposition of the 2-pyrone motif under the reaction conditions. Degradation pathways are an important limitation for intramolecular arylation reactions, as reported by Fairlamb and co-workers.¹⁷ The pyrone unit itself is susceptible to ring opening and this has been documented in the literature by Fairlamb among others.¹⁸⁻¹⁹ Generally, substrates with electron withdrawing groups on the phenoxy ring of the 2-pyrone are more prone to decomposition.²⁰ Burns and co-workers proposed that following deprotonation at C-7 (methyl group) of the 2-pyrone, CO₂ is subsequently lost which in turn enables loss of the aryloxy group and this may be a major step in the degradation pathway (**Scheme 23**).²¹ The product **52** generated could be lost as a gas or undergo polymerisation under the reaction conditions. The poor yield and mass recovery observed for

the substrates possessing *para*-NO₂ and *para*-F substituents could be attributed to this process.



Scheme 23. Possible degradation pathway for phenoxy 2-pyrones.

To test whether the reactions conditions were affecting our 2-pyrone framework, four test reactions were carried out (**Table 4**). The percentage mass recovery of 4-phenoxy-2-pyrone **24** was 55% when it was simply heated at 140 °C for 2 hours (**Table 4, entry 1**). Interestingly, when 4-phenoxy-2-pyrone **24** was heated at 140 °C for 2 hours in the presence of Ag₂O or TFA (**Table 4, entries 2 and 4**), the mass recovery decreased even further to 42%. In contrast, heating 4-phenoxy-2-pyrone **24** at 140 °C in the presence of PivOH led to a mass recovery of 73% which is significantly higher (**Table 4, entry 3**). This would explain why the mass recovery and thus the yields were substantially higher using **Conditions A**. These results would indicate that degradation of the 2-pyrone framework does occur under our reaction conditions particularly when TFA and Ag₂O are present and also at the high temperature required (140 °C). **Table 4.** Test reactions carried out on the 4-phenoxy-2-pyrone (**24**).

Entry	Time (h)	Temp. (°C)	Conditions	% Pyrone remaining ^a
1	2	140	4-Phenoxy-2-pyrone 24	55
2	2	140	4-Phenoxy-2-pyrone 24 + Ag ₂ O	42
3	2	140	4-Phenoxy-2-pyrone 24 + PivOH	73
4	2	140	4-Phenoxy-2-pyrone 24 + TFA	42

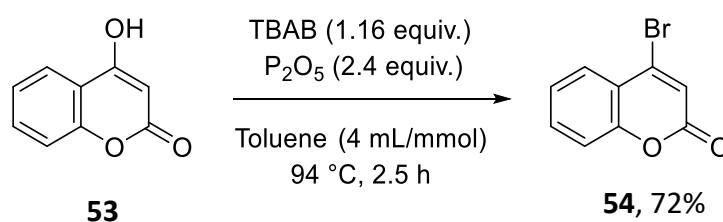
^aPercentage pyrone remaining determined using ¹H NMR Spectroscopy with 1,3,5-trimethoxybenzene as the internal standard for quantification.

2.3.3 Synthesis of substrates

2-Coumarins

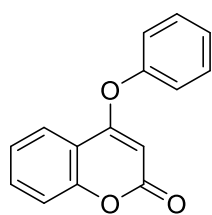
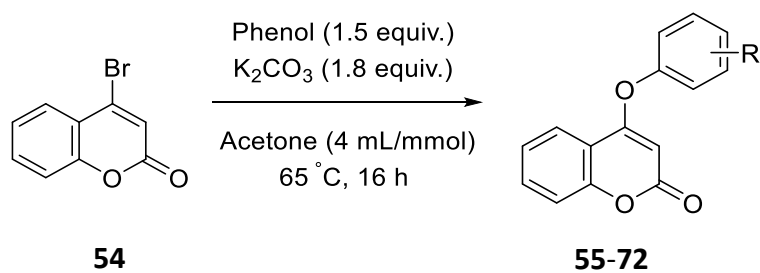
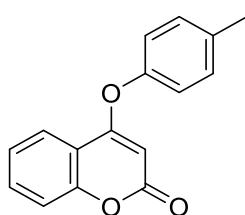
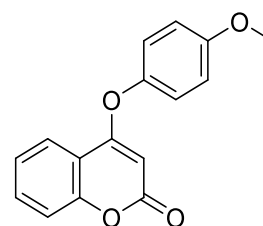
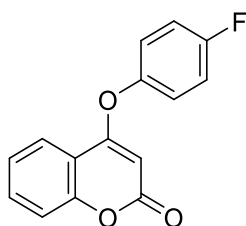
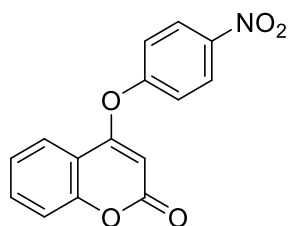
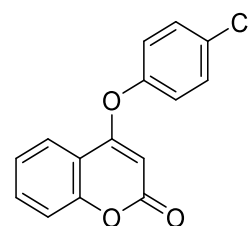
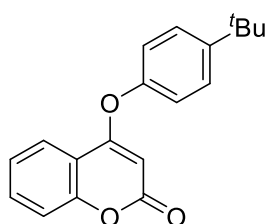
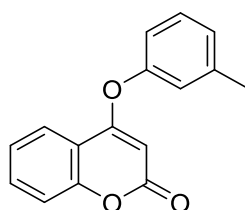
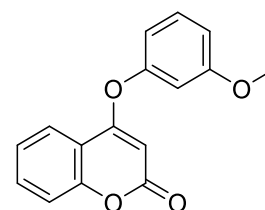
Having achieved success with a range of 2-pyrone substrates, we turned our attention towards the 2-coumarin framework. We were curious to see whether our optimised reaction conditions would facilitate the intramolecular double C-H activation of 4-phenoxy-2-coumarins. The coumarin motif is a much more robust structure than the 2-pyrone motif due to increased overall aromaticity (as well as no longer having a methyl group which is prone to deprotonation).²¹ Therefore, the coumarin scaffold is theoretically less susceptible to degradation under the harsh reaction conditions.

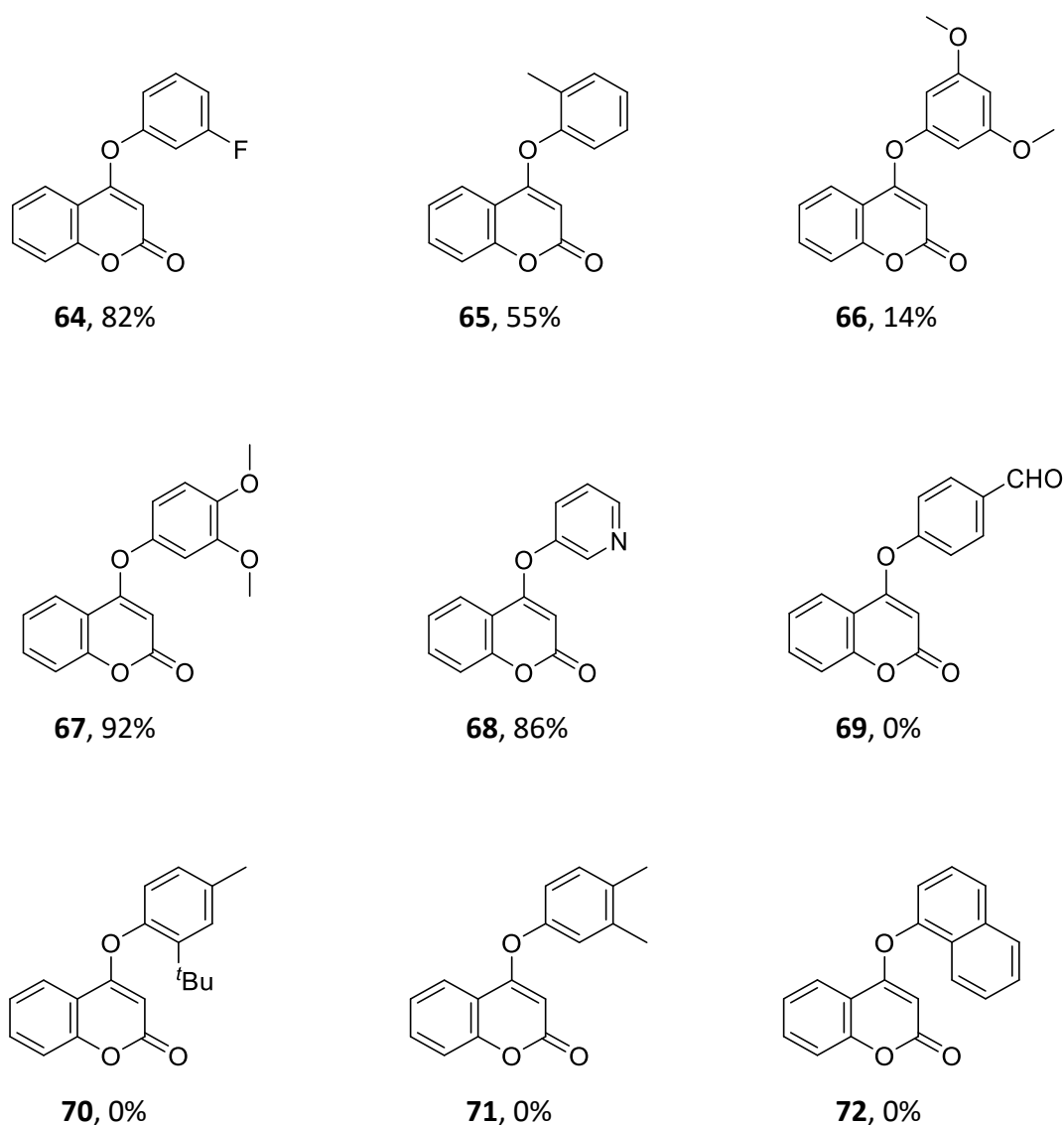
To begin with, 4-bromo-2-coumarin (**54**) was prepared in a 72% yield from the corresponding 4-hydroxy-2-coumarin (**53**) using the same procedure described in **Section 2.3.1**.⁹ 4-Hydroxy-2-coumarin (**53**) was commercially available.



Scheme 24. Synthesis of 4-bromo-2-coumarin (**54**).

Next, a variety of 4-phenoxy-2-coumarin substrates (**55-72**) were synthesised in a similar fashion to the 4-phenoxy-2-pyrone substrates (**24, 30-40**), by a base mediated reaction of the substituted phenol with 4-bromo-2-coumarin (**54**). A range of sterically and electronically different phenols were chosen. The crude products were isolated by washing with 10% aqueous NaOH, followed by a recrystallisation from EtOH. Moderate to excellent yields were achieved for compounds **55-68** (**Scheme 25**). The synthesis of a number of substrates proved unsuccessful such as **69** bearing an aldehydic group at the *para*-position. Substrate **71** with a 3,4-dimethyl group also did not progress well under the reaction conditions. Additionally, **72** containing a sterically encumbered naphthyl group and **70** with a bulky 2-*tert*-butyl-4-methyl group did not work well.

**55**, 68%**56**, 48%**57**, 84%**58**, 49%**59**, 58%**60**, 79%**61**, 71%**62**, 28%**63**, 75%

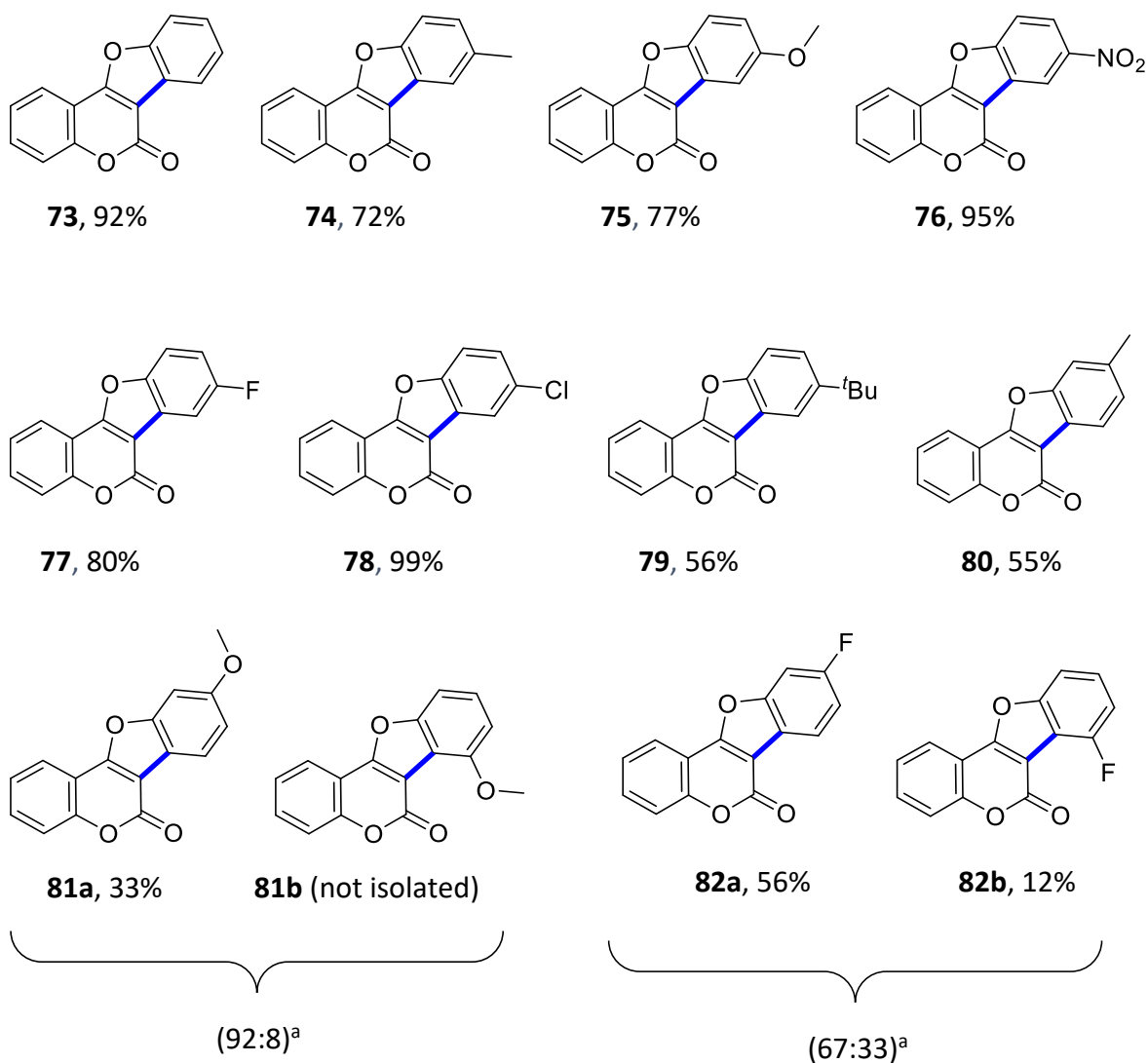
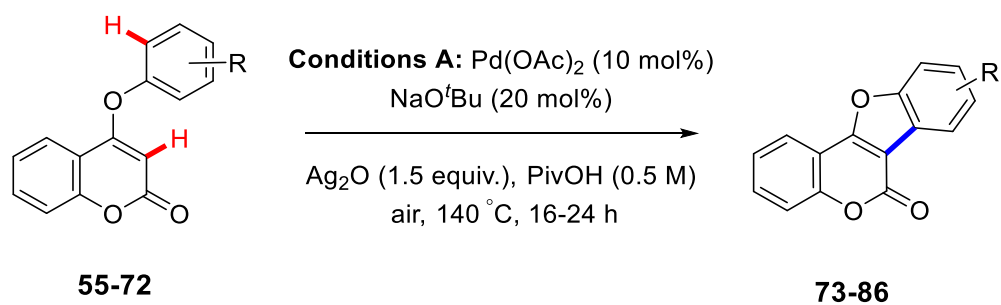


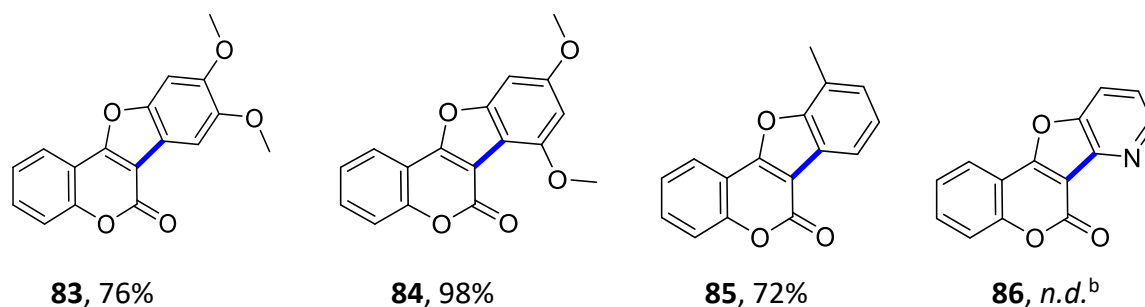
Scheme 25. Synthesis of 4-phenoxy-2-coumarin substrates.

2.3.4 Demonstration of substrate scope for double C-H activation of 2-coumarins

With a wide range of 4-phenoxy-2-coumarins synthesised, bearing diverse electronic and steric substituents on the phenoxy ring, the scope of the reaction was demonstrated (**Scheme 26**). Similar reaction conditions which worked for the 2-pyrones, using PivOH as solvent, was utilised for the substrate scope. Overall, it was observed that the reaction allowed for a variety of functional groups on the phenoxy ring. Firstly, the unsubstituted analogue **73** was isolated in an excellent yield of 92%. Electron donating groups at the *para*-position of the phenoxy ring provided the corresponding products **74-75** in good yields (72 and 77%). However, in the case of the *tert*-butyl analogue **79**, the desired product could only be obtained in 56% isolated

yield, possibly due to the steric bulk of the *tert*-butyl group. Pleasingly, substrates bearing electron withdrawing substituents on the phenoxy ring were also well tolerated with these substrates providing the highest yields overall, **76-78** (80-99%). Notably, a 95% yield was obtained for the nitro containing analogue **76**, whereas the nitro substituted pyrone analogue proved difficult to cyclise. The *meta*-substituted cyclised products gave excellent regioselectivity, with reaction occurring at the least sterically hindered site. For example, substrate **81** containing a *meta*-methoxy substituent gave a regioisomeric ratio of 92:8 (**81a:81b**). A pure sample of **81b** could not be obtained following the purification of the crude reaction material by column chromatography. This was due to the fact that **81b** was formed in a very small quantity relative to **81a**. In addition, both regioisomers **81a** and **81b** had very similar R_f values. On the contrary, the regioselectivity was lower when a fluoro group was present at the *meta*-position (67:33 for **82**). The fluorine atom may be exerting a secondary directing effect, hence directing Pd to the more sterically hindered position. This may account for the decrease in regioselectivity. Gratifyingly however, when the methyl substituent was located at the *meta*-position, only one regioisomer, **80**, was observed in the ^1H NMR spectrum of the crude reaction mixture. Surprisingly, product **80** was isolated in a moderate yield of 55%. In this case, again the least sterically hindered regioisomer was preferentially formed under the reaction conditions. Pleasingly, the *ortho*-substituted substrate **85** was isolated in 72% yield and the methyl group did not overly affect the reaction progress. Finally, when the phenoxy ring was substituted with two methoxy groups, which is common in many natural products, the reaction worked very well, with a 72% yield obtained for **83** and a 98% yield obtained for **84**. Also, only one regioisomer was observed in the ^1H NMR spectrum of the crude reaction mixture for the 3,4-dimethoxy analogue **83**. Disappointingly, the pyridyl substrate **68** failed to give satisfactory conversion to product **86** with the majority of the crude mass attributed to unreacted starting material **68**.

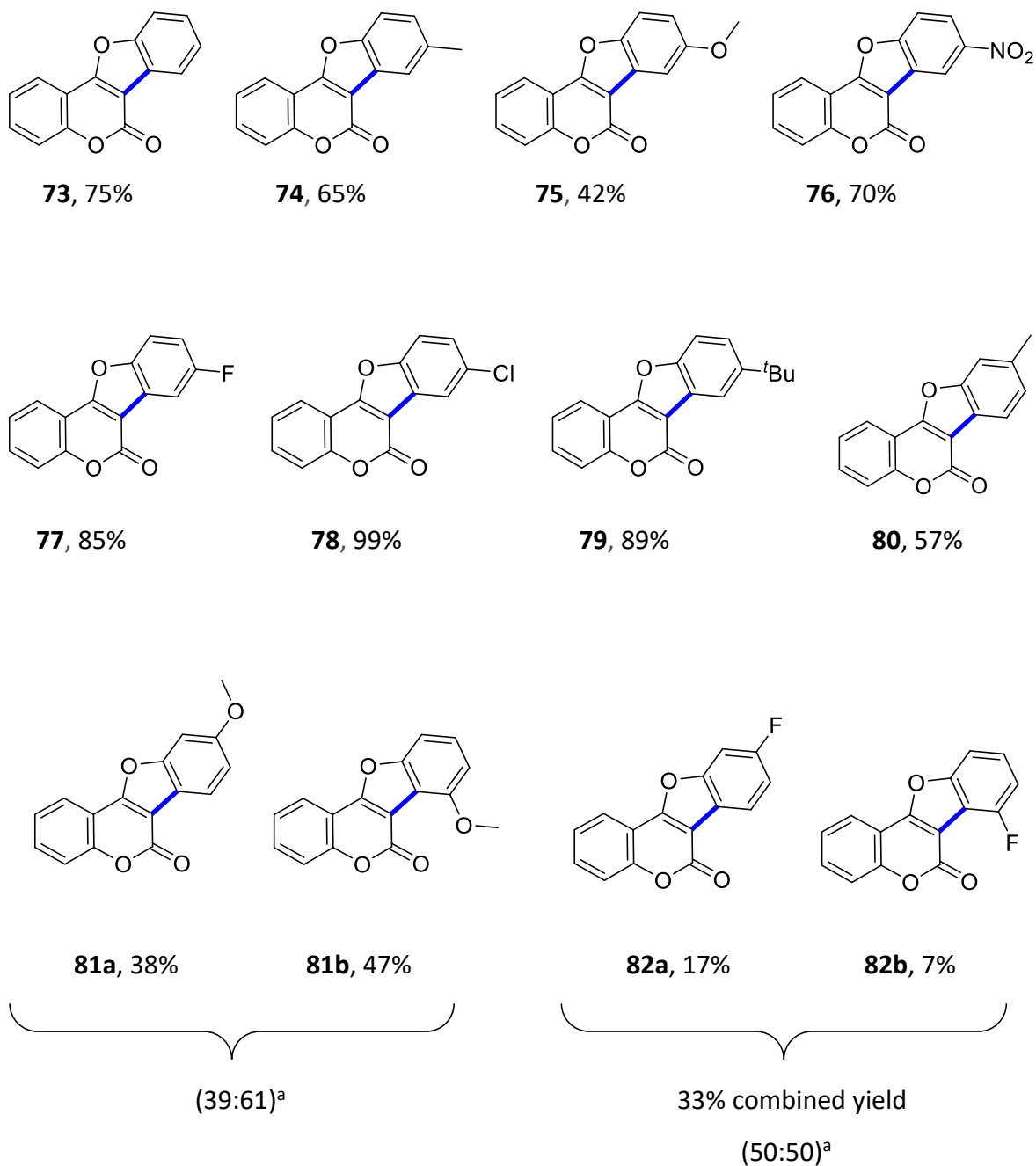
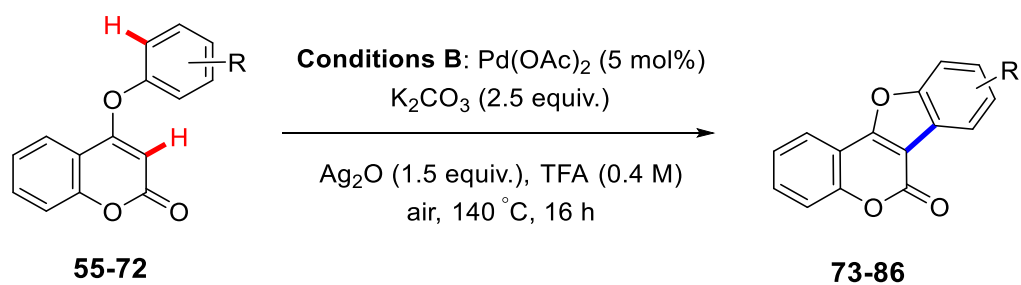


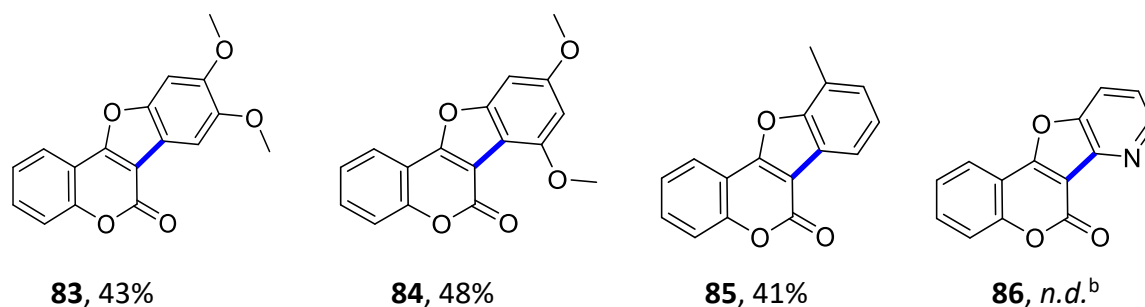


Scheme 26. 2-Coumarin scaffold scope employing **Conditions A**. ^aRegioisomeric ratio determined from the ¹H NMR spectrum of the crude reaction mixture. ^bYield not determined (*n.d.*) due to low conversion to product.

Additionally, our range of substituted 4-phenoxy-2-coumarin substrates were subjected to **Conditions B**, where TFA is used as the reaction solvent. This was carried out in order to get a direct comparison of results between both sets of conditions in terms of yield and selectivity. Pleasingly, the 2-coumarin scaffold was well tolerated under the reaction conditions. This is in stark contrast to the 2-pyrone substrates where the mass recovery and yields were very poor due to degradation and incomplete consumption of starting material. Overall, good to excellent yields were achieved for **73-85** (41-99%) and a wide range of functional group tolerance was observed (**Scheme 27**). In some cases, the isolated yields were directly comparable to the yields obtained when **Conditions A** were employed. For example, the *para*-fluoro **77** and *para*-chloro **78** analogues gave an 85% and 99% yield respectively. Satisfyingly, an increase in yield was obtained for **79** bearing a *para-tert* butyl substituent (89% for **Conditions B** versus 56% for **Conditions A**). For the *meta*-methyl substituted starting material **62**, complete regioselectivity (toward the least hindered regioisomer) was observed in the ¹H NMR spectrum of the crude reaction mixture and the corresponding product was isolated in a moderate yield of 57%. The yield and regioselectivity for **62** was directly comparable to **Conditions A**. In contrast, a decrease in selectivity was observed when a fluoro and methoxy substituent was present at the *meta*-position (39:61 for **81a:81b**, 50:50 for **82a:82b**). Notably, **82a:82b** could only be isolated in very low yields due to significant purification difficulties. Notably, a switch in regioselectivity was observed for the *meta*-methoxy substrate between **Conditions A** and **Conditions B**. **Conditions B** showed a greater preference for reaction at the more sterically hindered site (reaction occurred at the more

electron rich site). Compound **63** containing a *meta*-methoxy substituent was also subjected to **Conditions B** but at lower temperature of 120 °C. However, no improvement in regioselectivity was observed. As was observed for the reaction carried out using **Conditions A**, the pyridyl substrate **68** did not work well. Significant degradation of starting material **68** was noted, as judged by the ¹H NMR spectrum of the crude reaction mixture, with the reaction failing to give any conversion to product **86**.





Scheme 27. 2-Coumarin scaffold scope employing **Conditions B**. ^aRegioisomeric ratios determined from the ¹H NMR spectrum of the crude reaction mixture. ^bYield and regioisomeric ratio not determined due to low conversion to product.

2.3.5 Structure elucidation of the major and minor *meta*-fluoro benzofuro-chromenone regioisomers

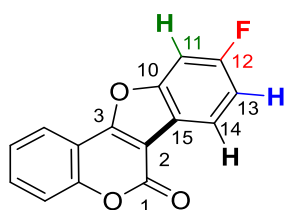
Extensive analysis using 1D and 2D NMR spectroscopy, as well as evaluation of J_{C-F} values for each carbon allowed us to identify the structures of the major and minor regioisomers, **82a** and **82b**.

Firstly, in the ¹³C NMR spectra of **82a** and **82b**, the resonances of the carbons in close proximity to the fluorine substituent on the aryl ring appeared as doublets. This allowed us to first determine which proton and carbon signals corresponded to the coumarin core structure and which corresponded to the aryloxy ring. Next, evaluation of the J_{C-F} values provided useful information as to the position of the fluorine on each aryl ring (**Table 5**). Coupling between carbon and fluorine is very strong and J_{C-F} couplings follow the trend $^1J_{C-F} > ^2J_{C-F} > ^3J_{C-F}$ (the carbon-fluorine coupling constants in fluorobenzene are $^1J_{C-F} = 245$ Hz, $^2J_{C-F} = 21$ Hz and $^3J_{C-F} = 8$ Hz).²²⁻²³ In the ¹³C NMR spectra of **82a**, the resonances of C-10, C-11, C-12, C-13, C-14 and C-15 appeared as doublets while the resonance of C-2 was not split. In addition, C-12 appeared as a quaternary carbon in the ¹³C NMR spectra with a large $^1J_{C-F}$ value of 249 Hz. Coupling was also observed for C-11 and C-13, with $^2J_{C-F}$ values of 26 and 25 Hz respectively. Additionally, coupling was observed for C-10 and C-14, with $^3J_{C-F}$ values of 14 and 10 Hz respectively. Also of note, the CH signal at 122.4 ppm corresponded to C-14. Small $^4J_{C-F}$ coupling (2 Hz) was observed for C-15.

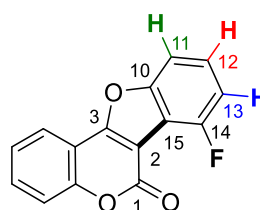
In comparison, analysis of the ¹³C NMR spectra of **82b**, C-1, C-2, C-10, C-11, C-12, C-13, C-14 and C-15 appeared as doublets. Notably, C-14 appeared as a quaternary carbon in the ¹³C

NMR spectra with a large $^1J_{\text{C-F}}$ value of 257 Hz. $^2J_{\text{C-F}}$ was observed for C-13 and C-15, with $^2J_{\text{C-F}}$ values of 20 and 22 Hz respectively. $^3J_{\text{C-F}}$ coupling was observed for C-10, C-12 and C-2 ($^3J_{\text{C-F}}$ values of 9 Hz, 8 Hz and 4 Hz respectively). Also, the CH signal at 127.8 ppm corresponded to C-12. This is in contrast to C-12 in **82a** which appeared as a quaternary carbon. Small $^4J_{\text{C-F}}$ coupling was observed for C-11 and C-1 corresponding to the carbonyl carbon of the coumarin ring. The signal corresponding to C-11 appeared as a doublet with a $^4J_{\text{C-F}}$ value of 5 Hz whilst C-1 showed as a doublet with a very small $^4J_{\text{C-F}}$ value of 1 Hz. Overall, analysis of $J_{\text{C-F}}$ coupling constants allowed us to determine that the fluorine is located at C-12 for **82a** and C-14 for **82b**

Table 5. Chemical shift data and $J_{\text{C-F}}$ values for the major **82a** and minor **82b** regioisomers.



82a



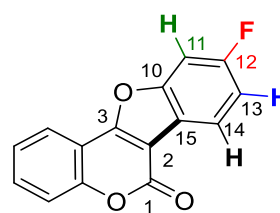
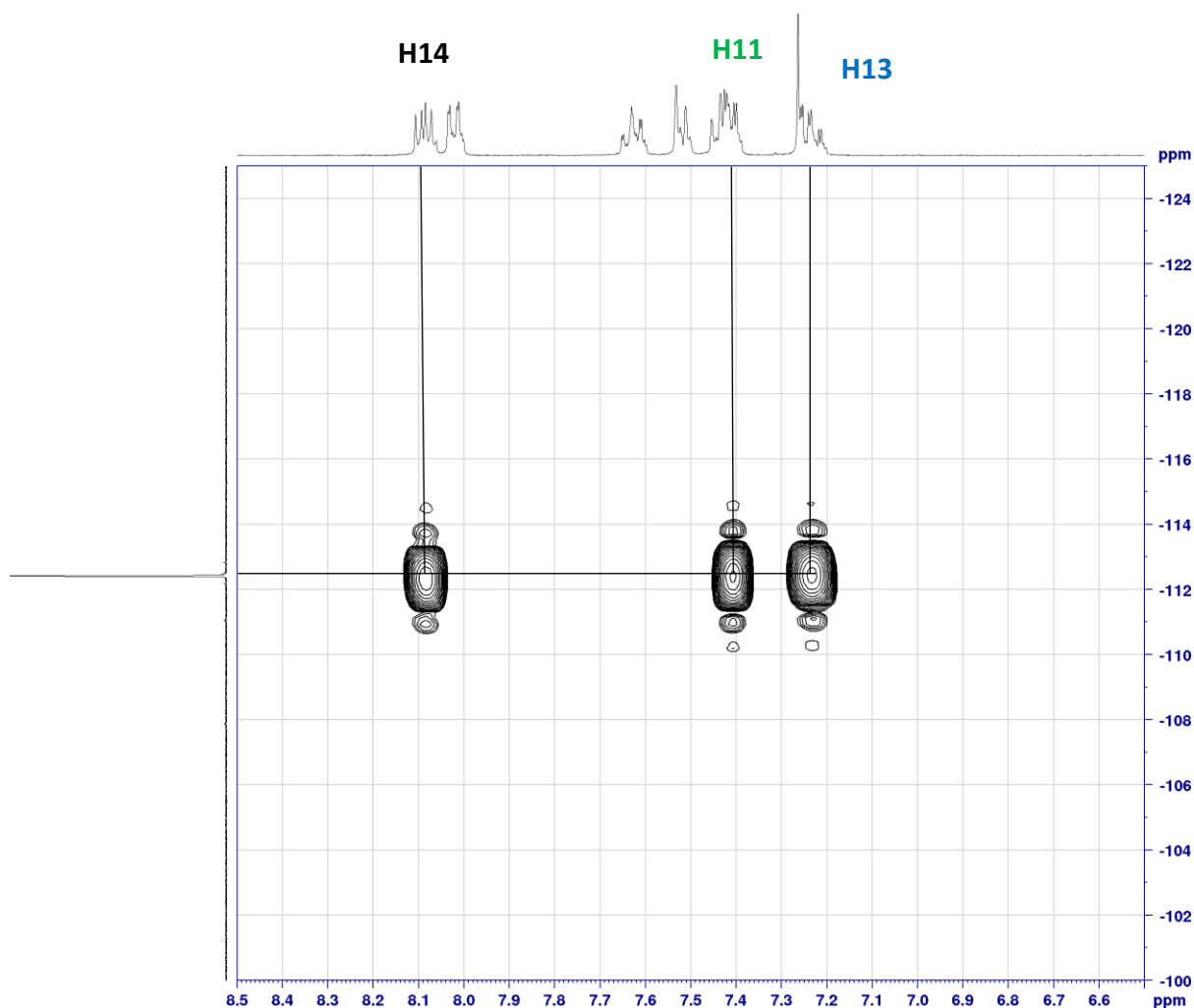
82b

Carbon	δ_{C} (ppm)	$J_{\text{C-F}}$ (Hz)
C-10	155.6	14
C-11	100.0	26
C-12	163.6	249
C-13	113.5	25
C-14	122.4	10
C-15	119.7	2

Carbon	δ_{C} (ppm)	$J_{\text{C-F}}$ (Hz)
C-10	157.0	9
C-11	108.0	5
C-12	127.8	8
C-13	111.9	20
C-14	156.3	257
C-15	112.6	22
C-1	160.2	1
C-2	104.7	4

HMBC (heteronuclear multiple bond correlation) spectroscopy detects heteronuclear correlations of protons and attached carbons over long ranges of about 2-4 bonds, with one

bond correlations being suppressed.²³⁻²⁴ In the ^{19}F - ^1H HMBC spectrum of **82a**, the fluorine resonance at -112.5 ppm showed an intense correlation to H-11, H-13 and H-14. No correlation to H-12 was detected (**Figure 10**). The ^1H NMR signals corresponding to H-11, H-13 and H-14 were determined from the ^1H - ^{13}C HSQC (heteronuclear single quantum correlation) spectra. ^1H - ^{13}C HSQC spectroscopy is used to correlate the chemical shift of protons to the chemical shift of their directly attached carbons.²⁴

**82a****Figure 10.** ^{19}F - ^1H HMBC of the major regioisomer **82a**.

In contrast, in the ^{19}F - ^1H HMBC spectrum of **82b**, the fluorine resonance at -111 ppm showed an intense correlation to H-13. There was also a strong correlation to H-12 observed. However, no correlation to H-11 was evident (**Figure 11**). The ^1H NMR signals corresponding to H-11, H-12 and H-13 were determined from the ^1H - ^{13}C HSQC spectra recorded for **82b**. A small amount of the major regioisomer was still present in the fraction containing the minor regioisomer isolated after column chromatography. This was due to significant difficulties in

separating the major and minor regioisomers. Hence, a correlation corresponding to the major regioisomer is visible in the ^{19}F - ^1H HMBC spectrum of **82b** (Figure 11).

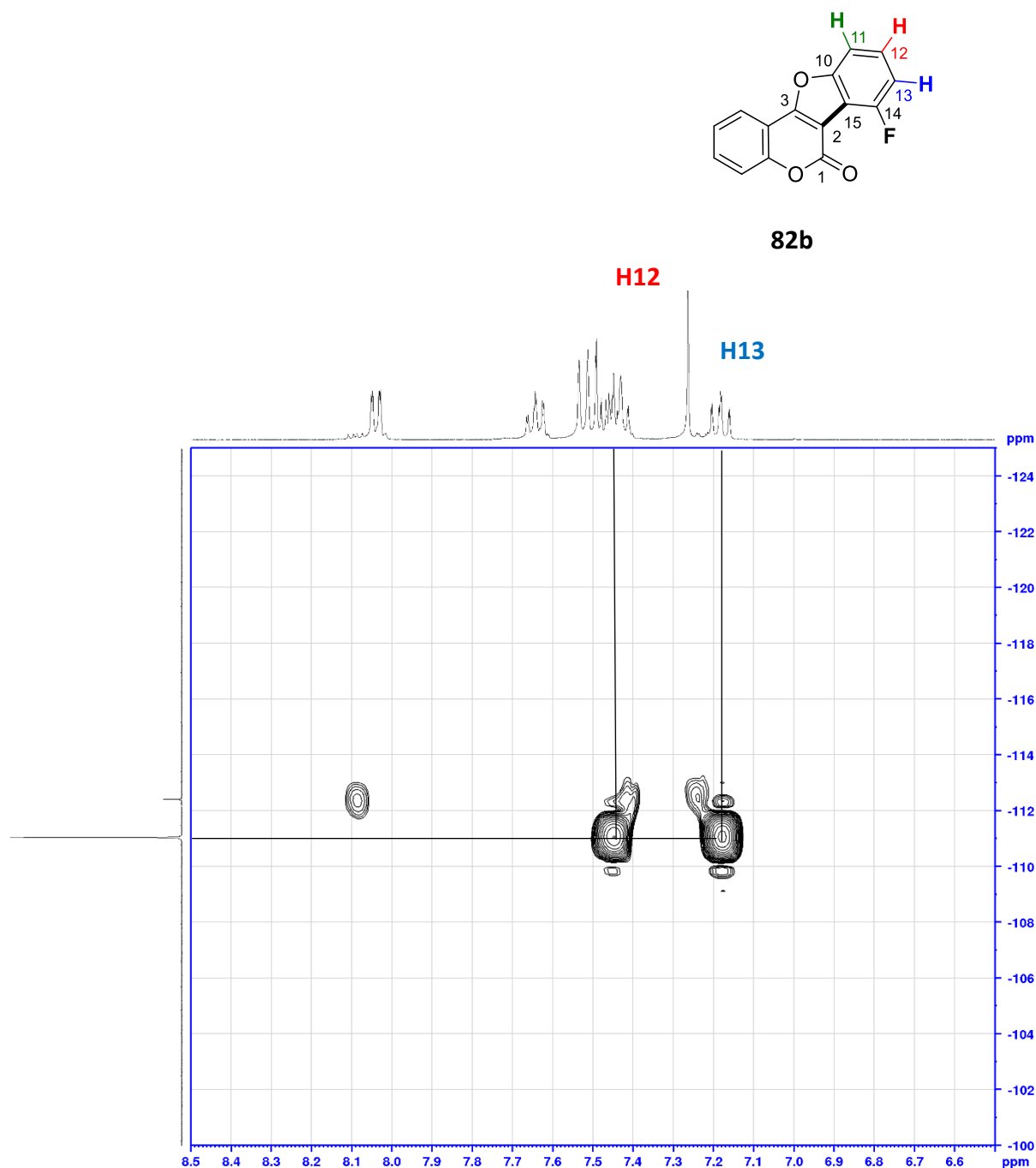


Figure 11. ^{19}F - ^1H HMBC of the minor regioisomer **82b**.

Finally, ^{19}F - ^1H HOESY (Heteronuclear Overhauser Enhancement Spectroscopy) spectra were recorded for both regioisomers **82a** and **82b**. ^{19}F - ^1H HOESY spectra provide information about through space interactions between fluorine and proton nuclei.²³ The data can then be interpreted and used to determine the position of the fluorine on the aryl ring.

Analysis of the ^{19}F - ^1H HOESY spectra for **82a**, clearly shows that the fluorine resonating at -112.5 ppm is in close proximity to H-13 and H-11 (Figure 12).

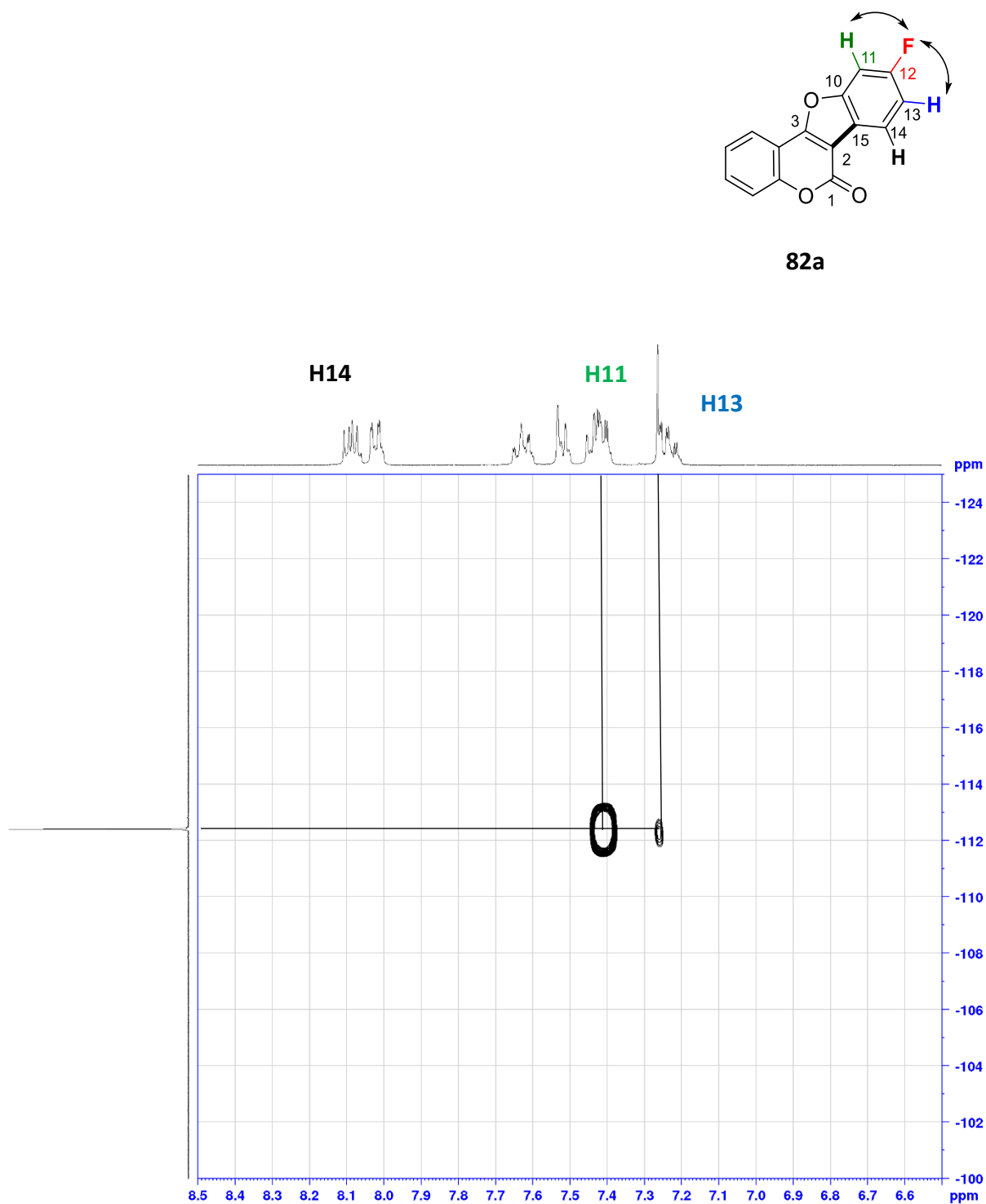


Figure 12. ^{19}F - ^1H HOESY of the major regioisomer **82a**.

For comparison, in the ^{19}F - ^1H HOESY spectra of **82b**, the fluorine resonating at -111 ppm is in close proximity to only one proton, H-13 (**Figure 13**). The lack of an NOE to H-12 or H-11 is consistent with the fluorine positioned at C-14 which correlates with previous data.

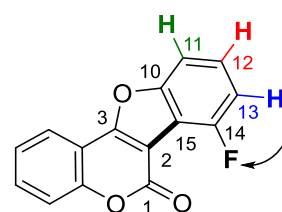
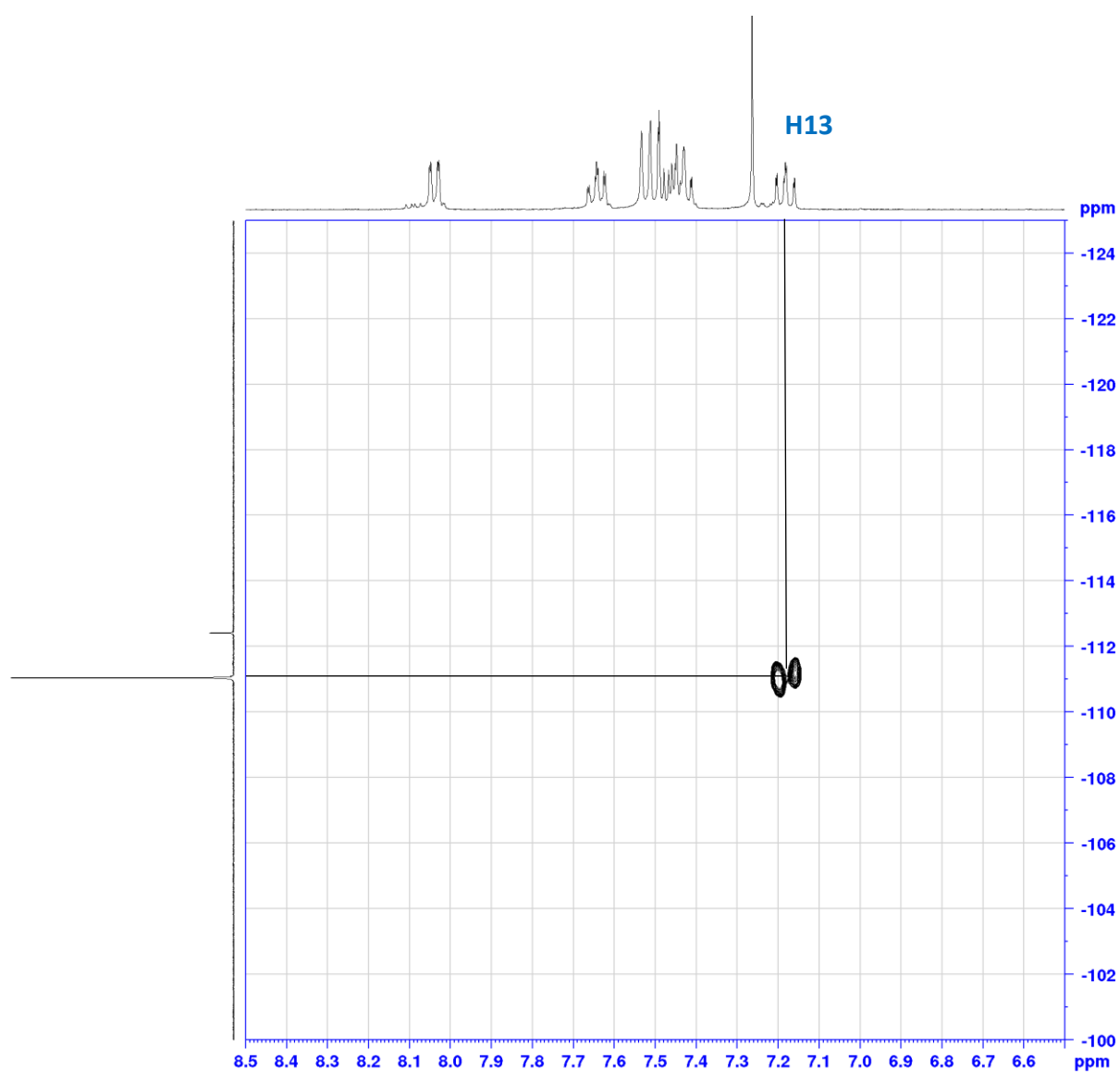
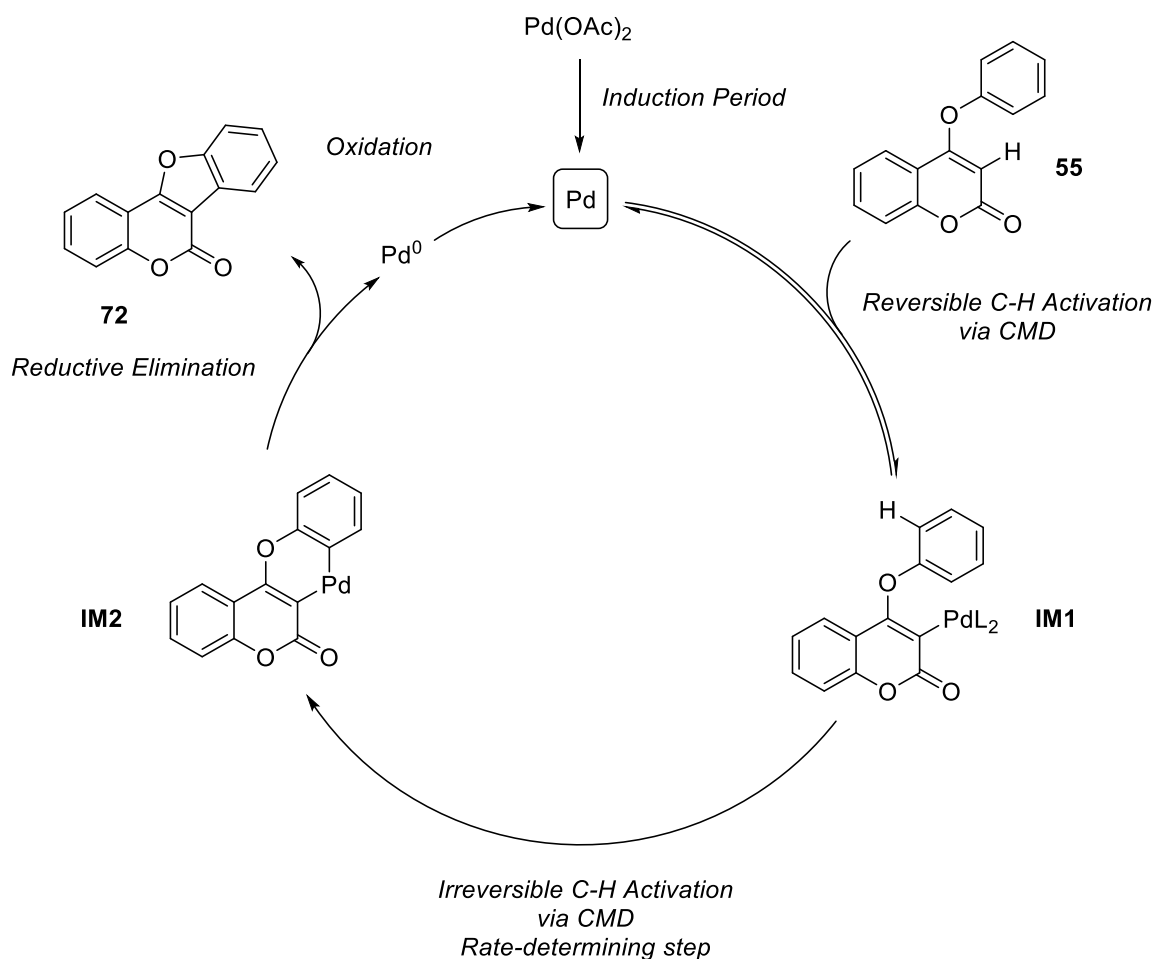
**82b**

Figure 13. ^{19}F - ^1H HOESY of the minor regioisomer **82b**.

Thus, the information provided from the 2D NMR spectra in combination with J_{C-F} values allowed us to establish that the fluorine is located at C-12 for **82a**, which was the major regioisomer. In contrast, the fluorine in **82b** (minor regioisomer) is located at C-14. The complete signal assignment is given in **Chapter 6** (Experimental Chapter).

2.4.1 Proposed reaction mechanism for Conditions A

A proposed reaction mechanism for when **Conditions A** are employed is outlined in **Scheme 28**. Based on mechanistic work involving KIE studies carried out by Dr. Aisling Prendergast and computational work involving DFT calculations conducted by the Lin group, an initial reversible CMD of the C-3-H bond of **55** to give **IM1** is proposed as the first step. This is followed by irreversible CMD of the aryl C-H bond which is proposed to be involved in the rate determining step of the reaction. Deprotonation (to give **IM2**) and reductive elimination of Pd^0 gives the product **73**. Re-oxidation of Pd^0 back to the active catalyst Pd^{II} completes the catalytic cycle.²⁵



Scheme 28. Proposed catalytic cycle.

2.4.2 Monitoring of double C-H activation by NMR Spectroscopy for Conditions B

Mechanistic studies carried out within the group by Dr. Aisling Prendergast allowed us to propose a rational reaction mechanism (outlined in (**Scheme 28**)) for when **Conditions A** with PivOH as reaction solvent are employed. However, no such mechanistic work was conducted for **Conditions B** which employ TFA as reaction solvent. Differences in yields and regioselectivities obtained for a few of the *meta*-substituted compounds (**81a:81b** and **82a:82b**) prompted our interest in probing the details of the reaction mechanism for **Conditions B**. Thus, we planned to monitor the progress of the double C-H activation reaction by NMR Spectroscopy. This was done with the assistance of UCC NMR spectroscopist Dr. Lorraine Bateman. Initially our plan was to carry out the reaction in an NMR tube in the spectrometer and monitor the reaction *in situ* by recording spectra as the reaction was proceeding. However, the probe on the 500 MHz spectrometer can only be heated to a maximum of 80 °C. Hence, it was decided to conduct the double C-H activation reaction in a

sealed reaction tube at 120 °C. It was postulated that the lower reaction temperature of 120 °C would slow down the reaction, which would facilitate NMR monitoring and also possibly allow the observation of reaction intermediates such as those involving Pd-C bonds. After a certain period of time, a small sample of the reaction mixture would be transferred to an NMR tube and the spectra recorded on the 500 MHz instrument.

First, the reaction was conducted in a sealed reaction tube with stirring at 120 °C using a stoichiometric amount of Pd (**Table 6, entry 1**). Using a stoichiometric amount of Pd might allow us to observe a palladated intermediate in the catalytic cycle. The reaction was conducted in deuterated TFA (TFA-d₁). The ¹H NMR signal arising from TFA-d₁ appears as a singlet at 11.5 ppm and shows up as a quartet 116 ppm and a quartet at 162 ppm in the ¹³C NMR spectrum. After 1 hour of heating at 120 °C, a small sample of the reaction mixture was filtered through a pipette of Celite® into an NMR tube and ran on a 500 MHz spectrometer (**Figure 14**). No starting material **67** was observed in the recorded ¹H NMR spectra. There was evidence of product **83** formation in addition to new peaks being identified. Notably, the signal corresponding to the C-3-H of the starting material at 5.7 ppm was absent in the new set of signals observed. Due to difficulties in accurate integration of the ¹H NMR signals as a result of overlapping signals between the product **83** and new species, it was difficult to determine the number of protons associated with the new species observed. It was determined to be 6/7 protons. While this information is not conclusive, it does suggest that the C-3-H of the coumarin ring is broken first possibly leading to a palladated intermediate of which the exact structure is undetermined. Also of note, no Pd hydride resonance was detected in the ¹H NMR spectra.

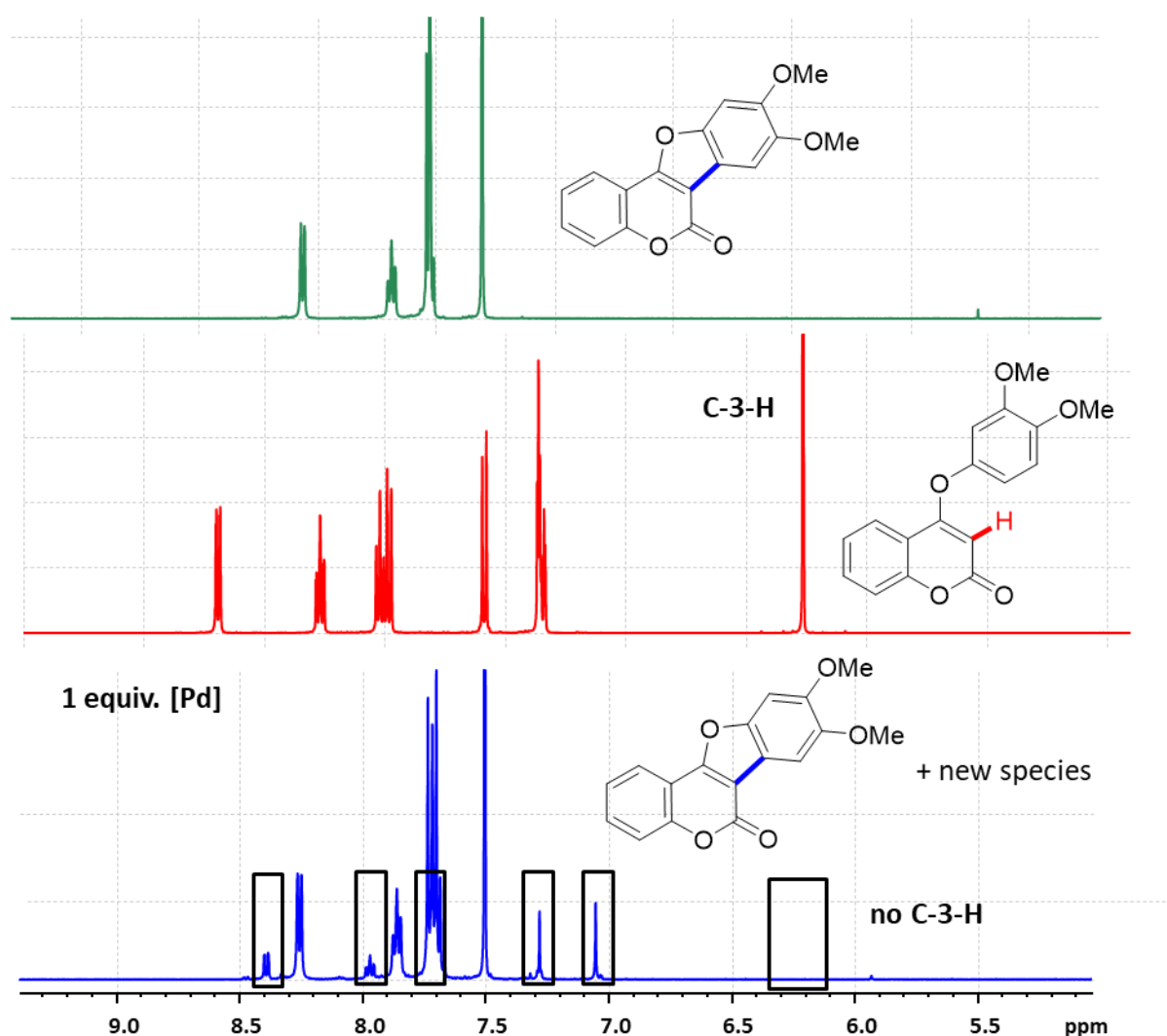


Figure 14. Stacked ^1H NMR spectra of starting material **67**, product **83** and crude reaction mixture after 1 hour at 120 °C.

Next, the effect of excluding the Pd catalyst was investigated (**Table 6, entry 2**). This time, the reaction was stopped after 15 minutes, a small sample was transferred to an NMR tube and the spectra was recorded on the 500 MHz spectrometer. The reaction failed to progress and no product **83** was observed. Only starting material **67** was visible in the ^1H NMR spectrum (**Figure 15**). Interestingly, the ^1H NMR spectrum of the reaction showed deuterium incorporation at the C-3 position (the C-3-H at 5.7 ppm now integrated for 0.20H). This is not completely unexpected however, as K_2CO_3 could be expected to deprotonate the acidic C-3-H of the 2-coumarin. This result would indicate that the C-3-H of the coumarin is likely to be activated first in the catalytic cycle and is indicative of a reversible process.

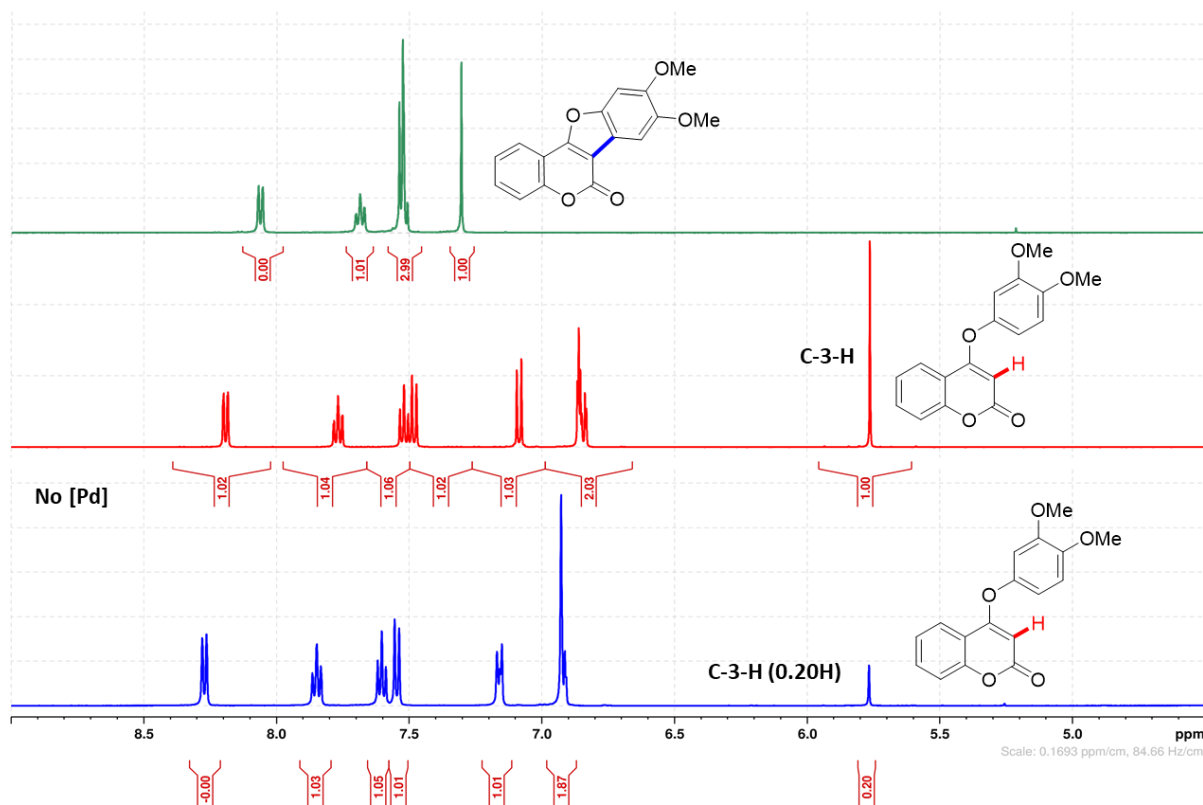


Figure 15. Stacked ^1H NMR spectra of starting material **67**, product **83** and crude reaction mixture after 15 minutes at 120 °C with no [Pd].

Thirdly, the effect of excluding Ag_2O from the reaction mixture was evaluated (**Table 6, entry 3**). A stoichiometric amount of Pd was again used in this case. It was found that the reaction did proceed in the absence of Ag_2O with signals corresponding to product **83** observed in the ^1H NMR spectrum (**Figure 16**). This result shows that at least some of the catalyst is oxidised back to Pd^{II} by air or some other oxidant. No starting material **67** was visible in the ^1H NMR spectrum. Also evident was new signals which did not, correspond to starting material **67** or product **83**. Again, due to overlapping signals it was difficult to accurately determine how many new signals were present. It was estimated at 7 H. The set of new signals was very similar to the signals observed for the new species identified when the reaction was conducted at 120 °C for 1 hour (**Table 6, entry 1**). However, an extra singlet and triplet was also observed. Again, the signal corresponding to the C-3-H of the coumarin ring at 5.7 ppm was absent. In the ^{13}C NMR spectra, 7 new CH signals were identified along with 8 new quaternary signals. The ^{13}C NMR spectra also showed no signal at 90 ppm which would correspond to the C-3-H carbon of the coumarin ring. Present in the ^{13}C NMR spectra was a

new quaternary carbon signal at 112 ppm corresponding to the C-3 carbon of a coumarin ring. There is evidence in the literature which suggests that upon coordination of Pd to carbon, the ^{13}C NMR shift for the corresponding carbon would be shifted approximately 20 ppm downfield with respect to free starting material/non-coordinated complex.²⁶ Also, a CH signal at 105 ppm was visible in the ^{13}C NMR spectrum and this was part of the new set of peaks identified. The ^{13}C NMR spectrum of product **83** shows a quaternary carbon signal at 105 ppm and the ^{13}C NMR spectrum of the starting material **67** shows a CH signal at 105 ppm which correlates to C-15 of the aryloxy ring. Taking this data together, it is likely that cleavage of the C-3-H occurs first (in preference to the aryl ring). The new species observed in the ^1H and ^{13}C NMR spectra is suggestive of a palladated intermediate, of which the exact structure is not determined.

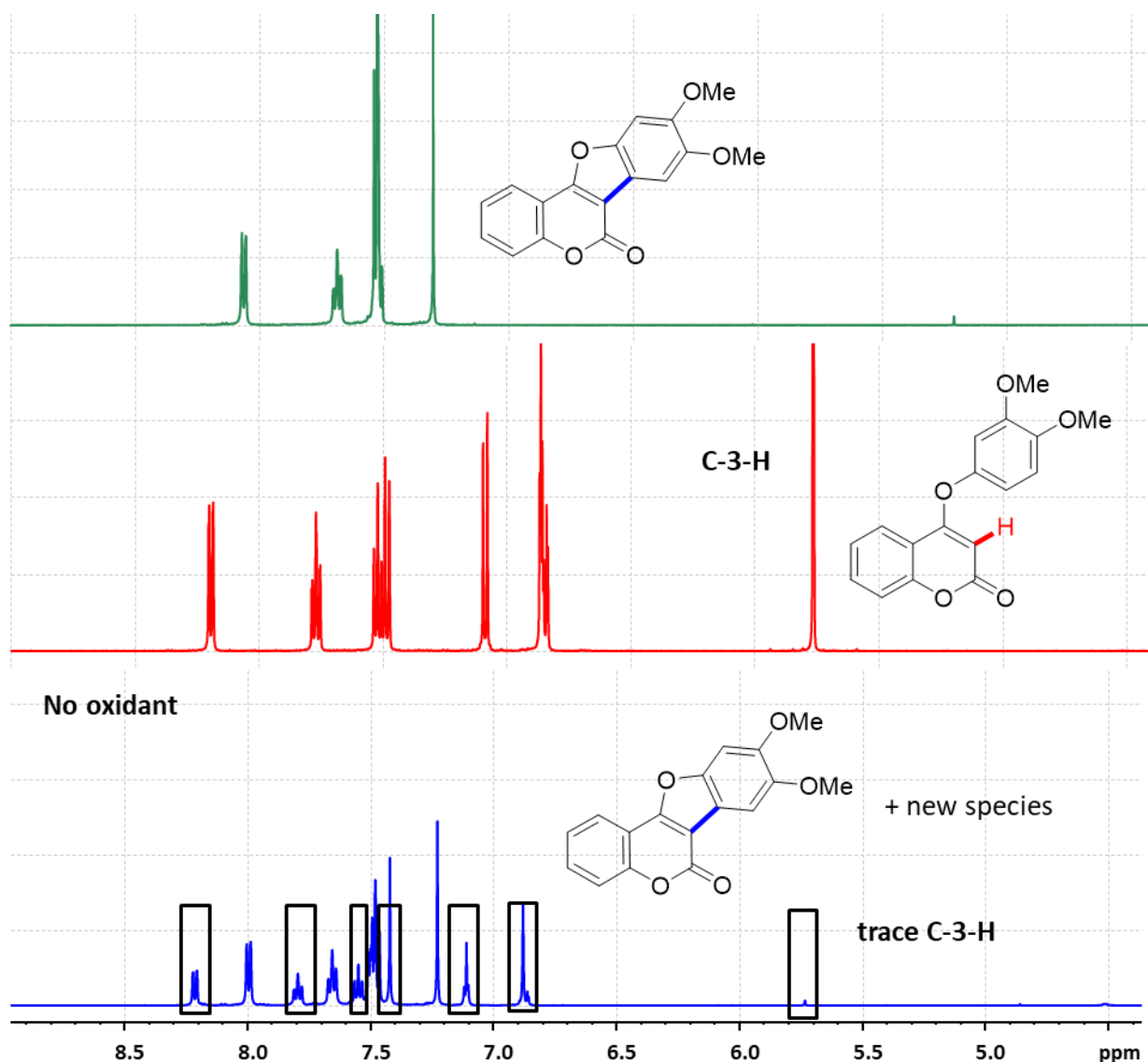


Figure 16. Stacked ^1H NMR spectra of starting material **67**, product **83** and crude reaction mixture after 15 minutes at 120 °C without added oxidant.

Finally, the reaction was carried out in the absence of base (**Table 6, entry 4**). The ^1H NMR spectra recorded after 15 minutes showed a complex mixture (**Figure 17**). The peaks corresponding to starting material **67** were absent in the ^1H NMR spectra and also the ^{13}C NMR spectra. However, the spectra indicated a complex mixture so it was difficult to determine what species were present. It is difficult to know the exact role of the base in the reaction; it may play a role in activating the catalyst, along with facilitating proton abstraction. Carbonate bases are also known to act as insoluble proton sinks during the catalytic cycles responsible for sequestration of H^+ and carboxylate regeneration.^{12, 27-28}

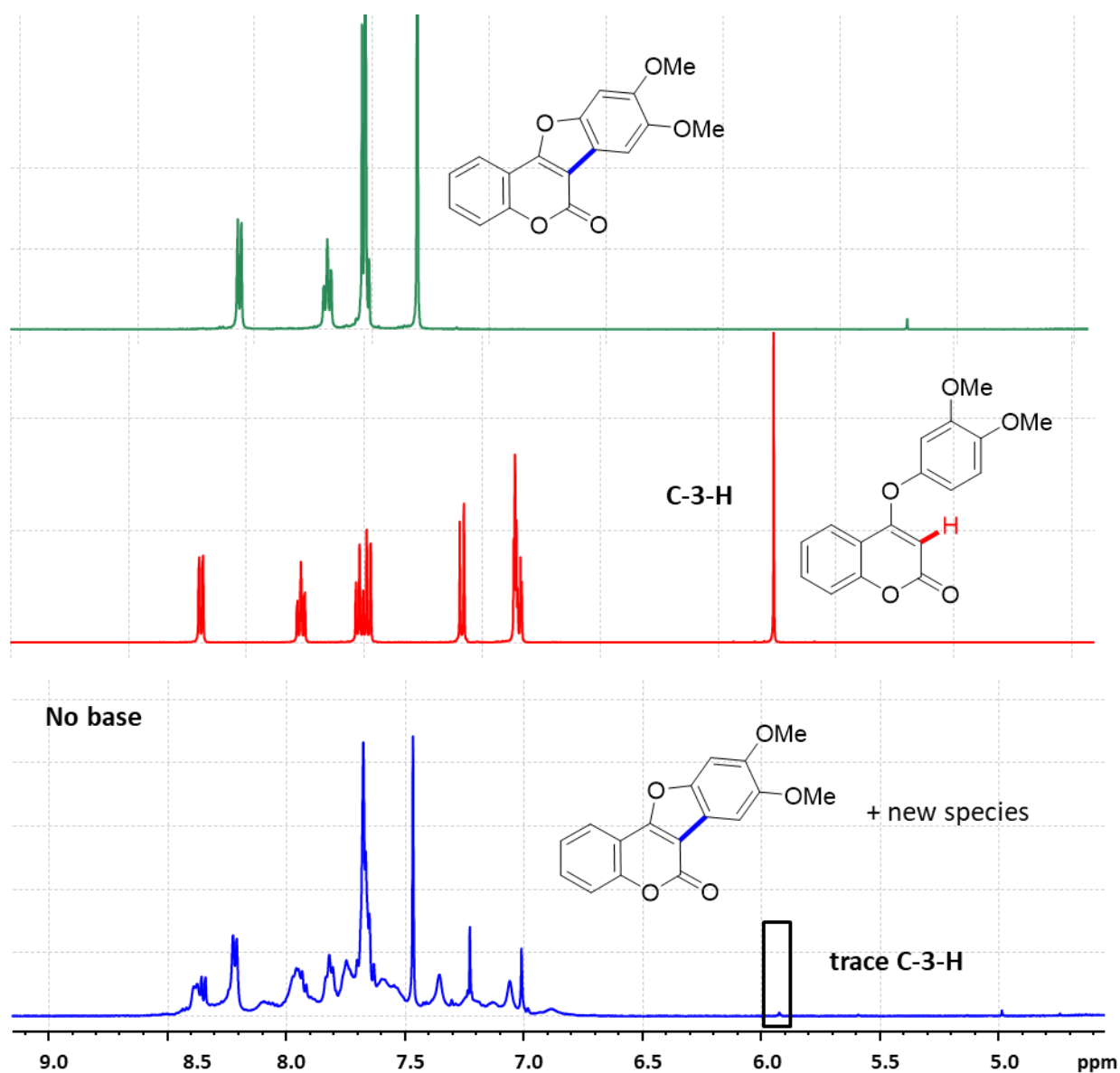
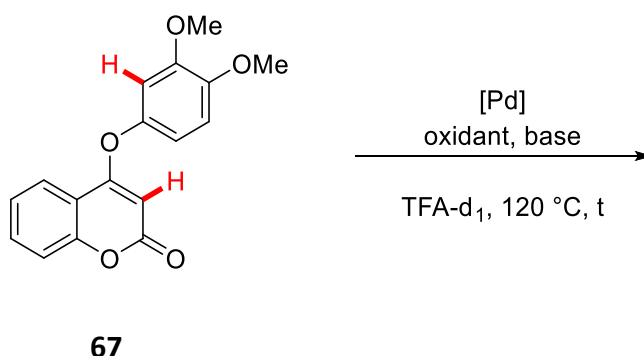


Figure 17 Stacked ^1H NMR spectra of starting material **67**, product **83** and crude reaction mixture after 15 minutes at 120 °C with no added base.

Table 6. Mechanistic work carried out on **67**.

Entry	Catalyst (1 equiv.)	Base (2.5 equiv.)	Oxidant (1.5 equiv.)	Time (mins)	Result
1	Pd(OAc) ₂	K ₂ CO ₃	Ag ₂ O	60	Product 83 and intermediate
2	-	K ₂ CO ₃	Ag ₂ O	15	Starting material 67
3	Pd(OAc) ₂	K ₂ CO ₃	-	15	Product 83 and intermediate
4	Pd(OAc) ₂	-	Ag ₂ O	15	Complex mixture

In conclusion, results from the reaction monitoring experiments:

- Indicate that activation of the C-3-H bond of the coumarin ring is likely be the first mechanistic step and is likely to be reversible.
- New peaks were identified which could correspond to a palladated intermediate. However, the structure of this species is unknown.

Due to time constraints, no further work was carried out. Future work would involve determining the structures of the key intermediates involved in the catalytic cycle and determining the rate-determining step in the reaction. KIE studies would be useful in determining whether C-H activation is involved in the rate-determining step. Also, we do not know the exact role of K₂CO₃, Ag₂O and TFA, hence, further study will be required to elucidate their roles. The combination of Pd(OAc)₂ and TFA is likely to be forming a highly electrophilic

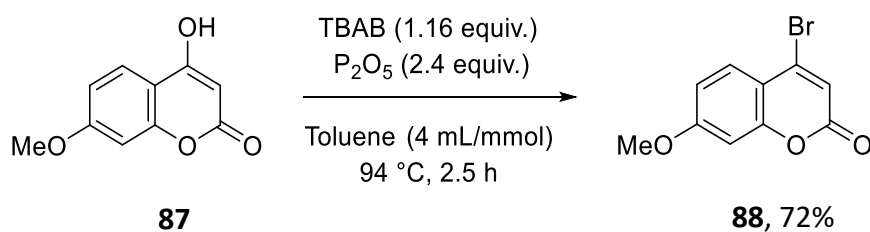
Pd catalyst, which has been shown to exhibit enhanced reactivity and greatly lower the activation barrier for C-H bond metalation.²⁹⁻³⁰ Thus, the first mechanistic step may involve electrophilic palladation involving Pd(OTFA)₂ to generate a palladacycle intermediate. The next step may involve intramolecular C-H bond cleavage *via* a CMD type mechanism. This was proposed by Shi and co-workers in their paper on the synthesis of fluorenone derivatives *via* a Pd catalysed double C-H activation.¹¹

However, the same mechanism may not be in operation for our system. For example, it was observed that the yields were higher for *meta*-substituted substrates possessing electron donating substituents over *meta*-substituted substrates possessing electron withdrawing substituents, suggesting an electrophilic aromatic substitution mechanism may be operative. Electron poor catalysts such as Pd(OTFA)₂ have been shown to be effective in these instances.³¹ However, the exact mechanistic details are not fully understood and would require further investigation. A key question to be answered is what exactly the structure of active catalytic species is. Vana and co-workers published an insightful paper in 2017 on the role of trinuclear species in a Pd(OAc)₂/TFA catalytic system.³² Their work proved that TFA plays a key role in the C-H activation of acetanilides. They showed that the key catalytic species are cyclic trinuclear complexes formed by a sequential ligand exchange from [Pd₃(OAc)₆]. Moreover, they showed that in the absence of TFA the reaction failed to proceed. This was similar to what we observed when the reaction was carried out in the absence of TFA. This seminal report provides useful information on C-H activation reactions involving Pd(OAc)₂/TFA systems which was previously lacking in publications to date.

2.5 Three step synthesis of flemichapparin C

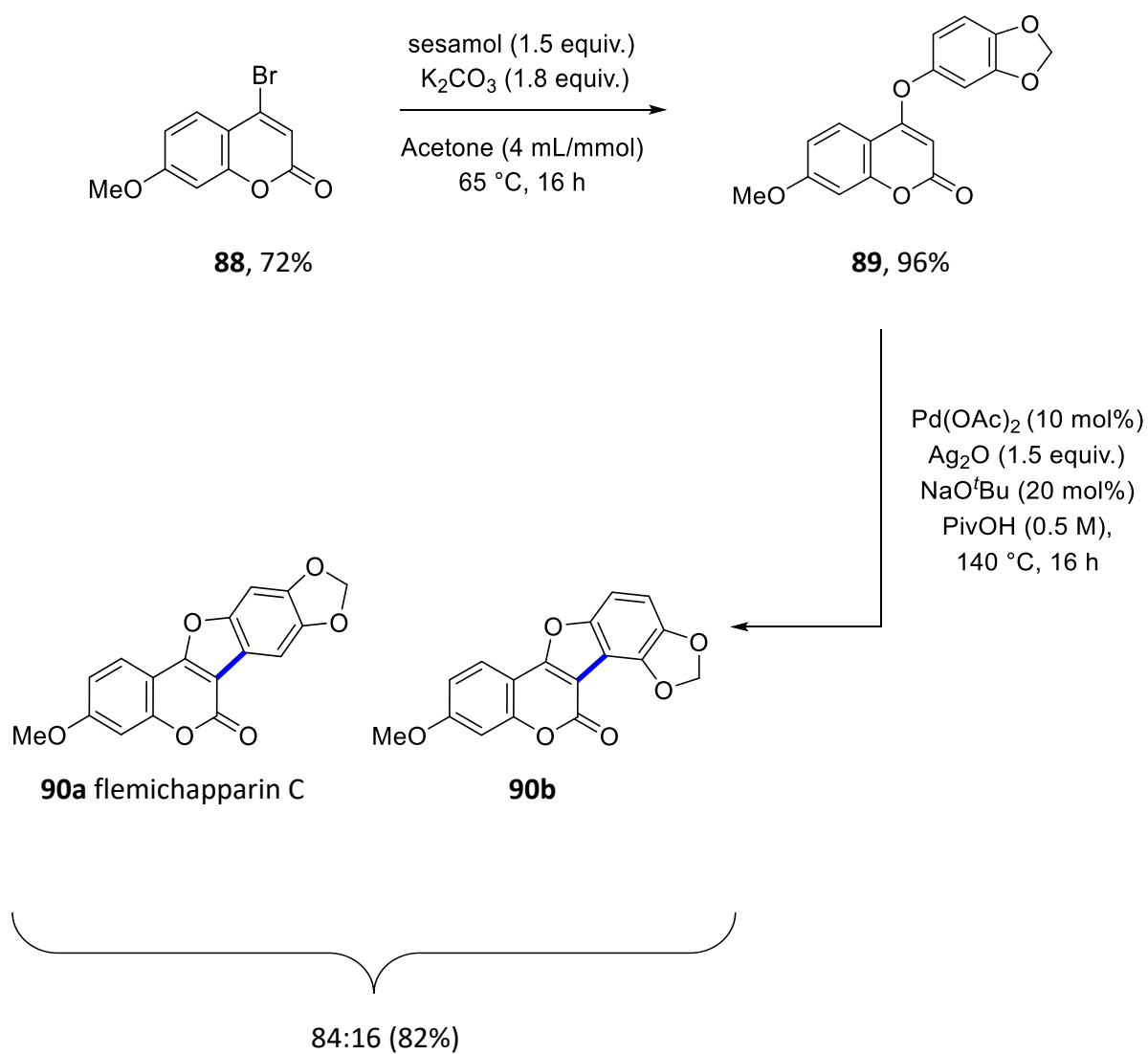
The good yield and regioselectivity observed with coumarin **67** prompted us to attempt to access the coumestan group of natural products which are characterised by a 6*H*-benzofuro[3,2-*c*]chromen-6-one skeleton. This group of natural products exhibit a number of interesting biological activities.⁵⁻⁷ We envisioned that our methodology could facilitate a short three step synthesis of flemichapparin C in comparison to previous more complex chemical³³ and enzyme mediated routes.³⁴

The first step involved bromination of commercially available 4-hydroxy-7-methoxy-2-coumarin **88** to give in a good yield of 72% (**Scheme 29**).



Scheme 29. Synthesis of 4-bromo-7-methoxy-2-coumarin (**88**).

4-Bromo-7-methoxy-2-coumarin was then coupled with sesamol and the resulting 4-phenoxy product **89** was isolated in 96% yield. Application of our **Conditions A** gave flemichapparin C (**90a**) as the major regioisomer and a minor regioisomer **90b**. The regioisomeric ratio was determined to be 84:16 (**90a:90b**) from the ¹H NMR spectrum of the crude reaction mixture (**Figure 18**). A combined yield of 82% was obtained (**Scheme 30**). Due to significant difficulties in separating the major and minor regioisomers, flemichaparrin C (**90a**) could only be isolated in 23% yield after column chromatography.

**Scheme 30.** Synthesis of flemichapparin C in three steps.

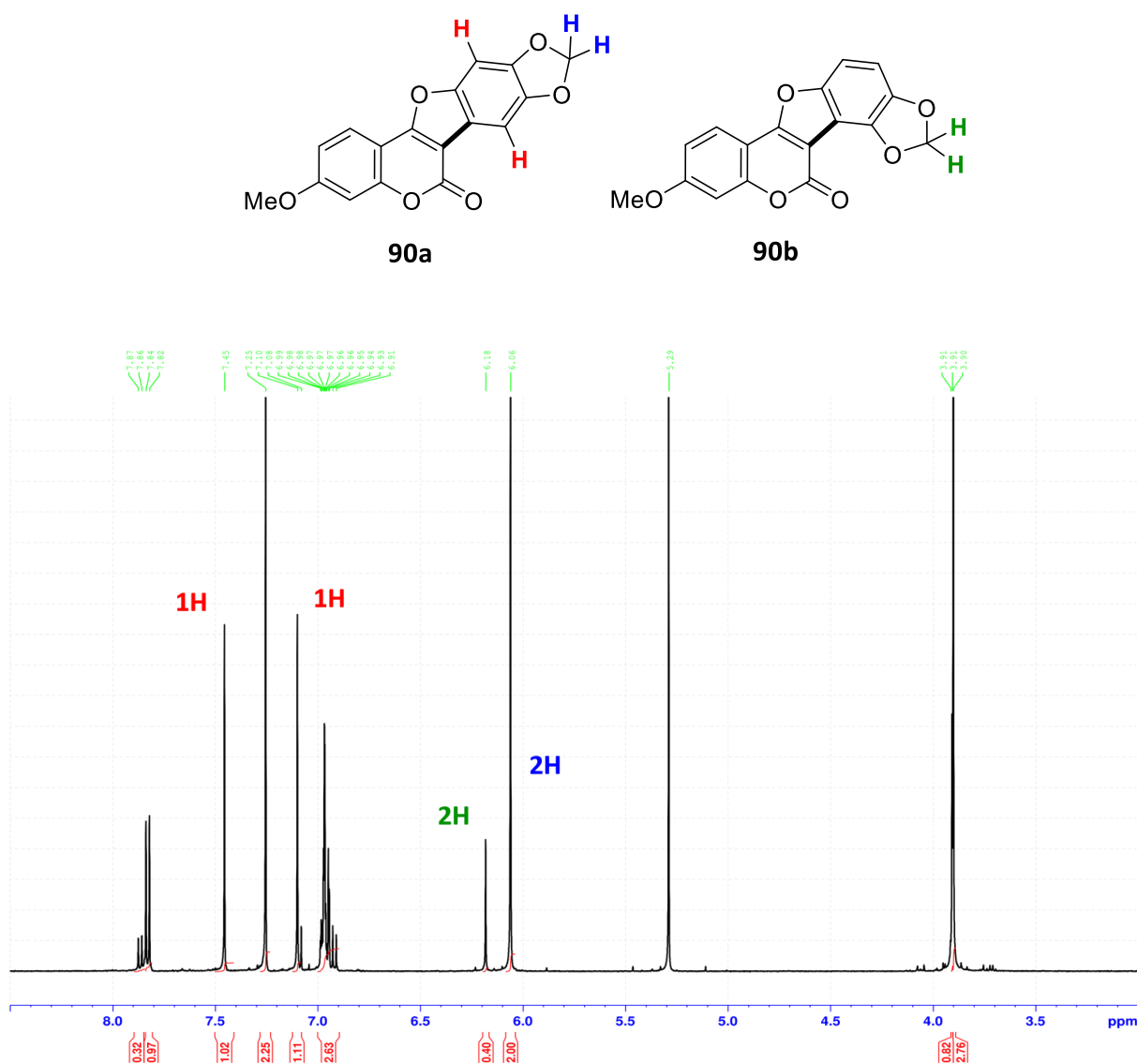
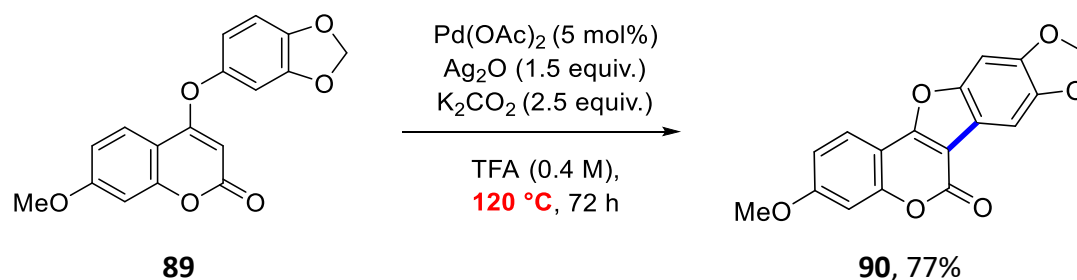


Figure 18. ^1H NMR spectrum of crude reaction mixture containing a mixture of regioisomers **90a** and **90b**.

Notably, complete regioselectivity in favour of flemichapparrin C **90a** was achieved when **Conditions B** were employed at a lower temperature of 120 °C. The desired product could be isolated in 77% yield (**Scheme 31**). However, we found that this result was highly dependent on the quality of TFA employed in the reaction (larger amounts of degradation was observed when using a newly opened bottle of TFA).



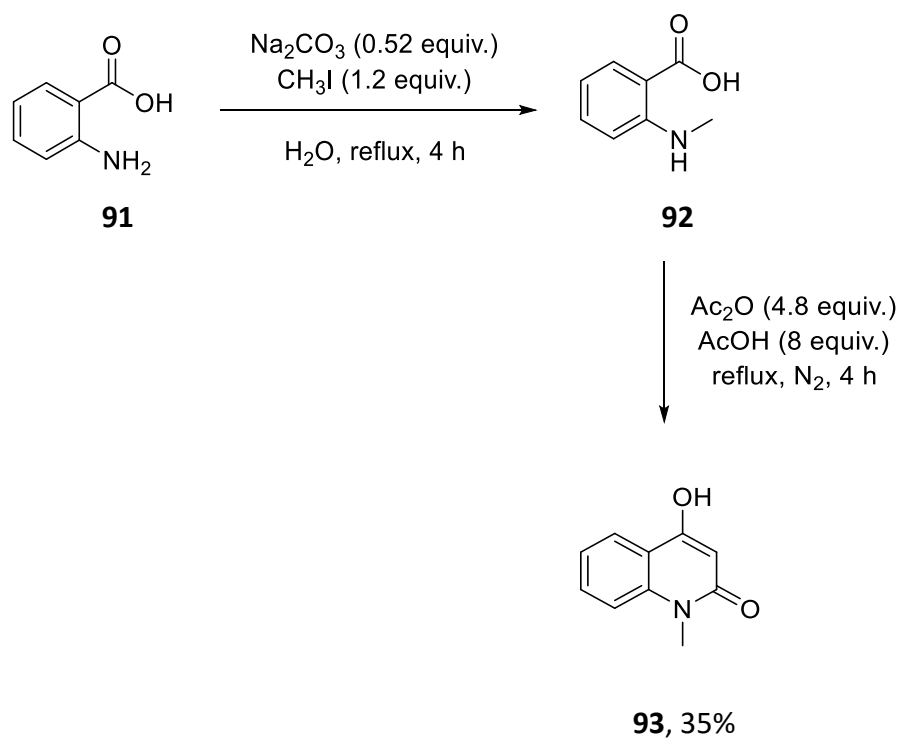
Scheme 31. Regioselective synthesis of flemichapparin C employing **Conditions B**.

2.6 Double C-H activation of 2(1*H*)-quinolone analogue

The structurally similar 2(1*H*)-quinolones are very prevalent structural motifs in many natural products and pharmaceutical drugs, as previously discussed in **Chapter 1**.³⁵⁻³⁷ Thus, we sought to expand our methodology to the quinolone class of compounds.

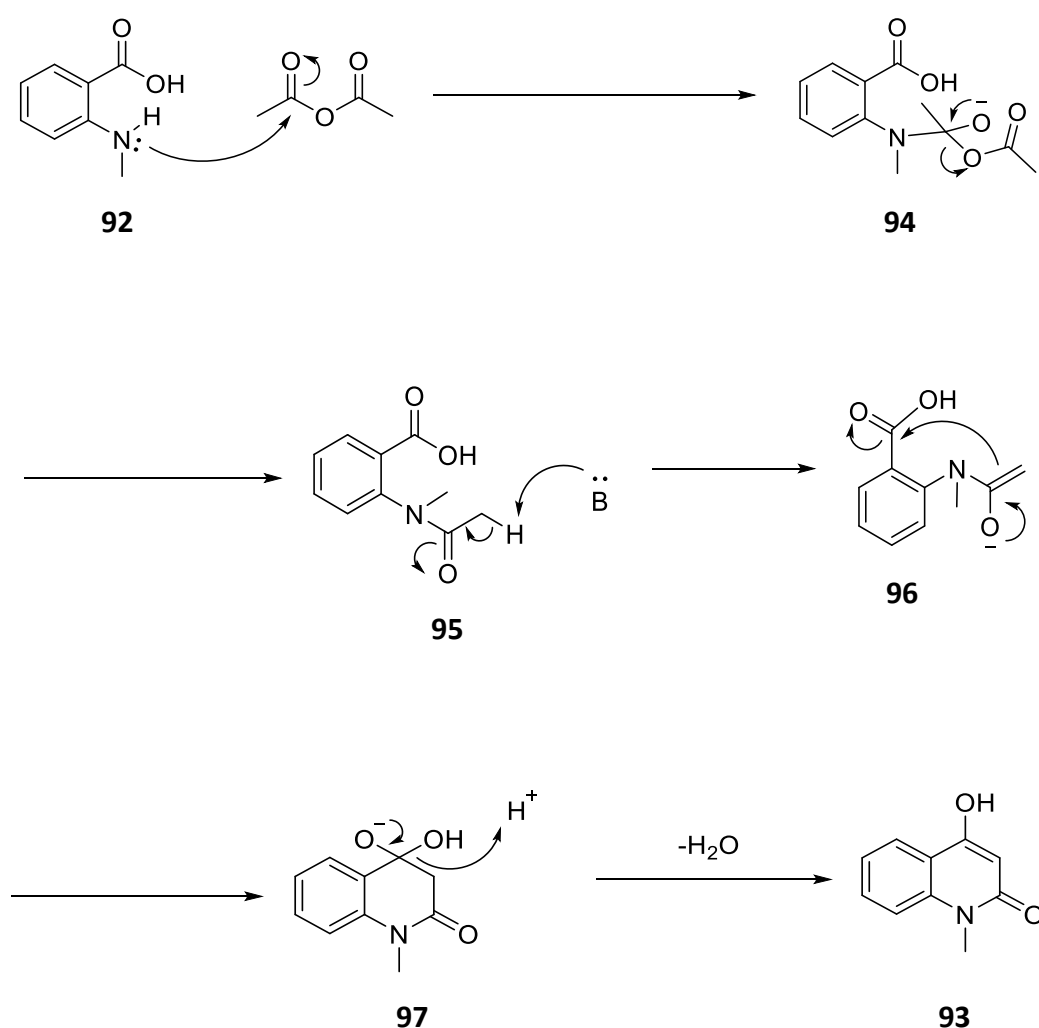
2.6.1 Synthesis of starting material

The first step involved preparation of 4-hydroxy-*N*-methyl-2-quinolone (**93**), as this was not commercially available. This was achieved using a procedure detailed by Lutz and co-workers.³⁸ *N*-Methylation of anthranilic acid (**91**) was accomplished using CH_3I as the alkylating agent in the presence of Na_2CO_3 (**Scheme 32**) using a procedure optimised by a previous member of the McGlacken group. The methylated product **92** was brought forward to the next step without purification. Compound **92** was reacted with acetic anhydride in refluxing acetic acid to give the corresponding 4-hydroxy-*N*-methyl quinolone (**93**) in 35% isolated yield. A proposed mechanism is outlined below (**Scheme 33**).



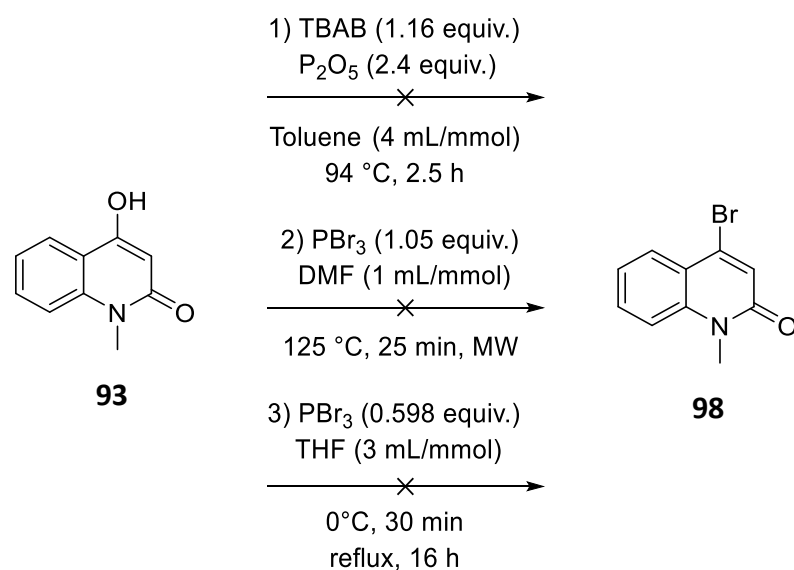
Scheme 32. Synthesis of 4-hydroxy-*N*-methyl-2-quinolone (**93**) from anthranilic acid (**91**).

The first step of the process appears to involve acylation of *N*-methyl anthranilic acid (**92**) by reaction with acetic anhydride (**92-93**) and this is followed by an intramolecular cyclisation (**95-97**) ultimately involving loss of water to give the final 4-hydroxy-*N*-methyl-2-quinolone (**93**).



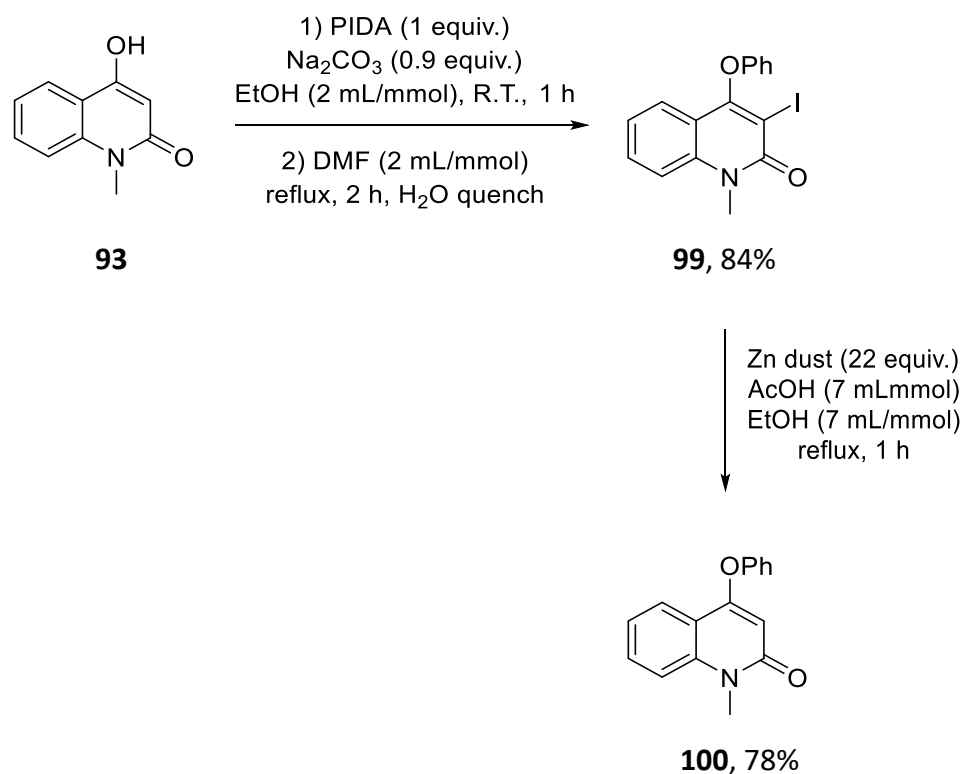
Scheme 33. Proposed mechanism of *N*-acylation and cyclisation of *N*-methyl anthranilic acid (**92**) to give *N*-methyl-4-hydroxy-2-quinolone (**93**).

We then sought to employ the same strategy used for the synthesis of our 4-phenoxy-2-pyrone and 4-phenoxy-2-coumarin substrates (**Scheme 17**). This first involved bromination of 4-hydroxy-2-quinolone **93** with TBAB in the presence of P_2O_5 (**Scheme 34, 1**). The product from this reaction would then be coupled with phenol. However, bromination of the hydroxy quinolone **93** proved unsuccessful. Next, we looked at treating **93** with PBr_3 . Here, two slightly different procedures were investigated. The first procedure which employed DMF as reaction solvent and was carried out under MW conditions at 125°C (**Scheme 34, 2**). The second procedure involved reacting **93** with PBr_3 in refluxing THF (**Scheme 34, 3**). Disappointingly, neither of these two protocols proved successful.



Scheme 34. Attempted bromination of **93**.

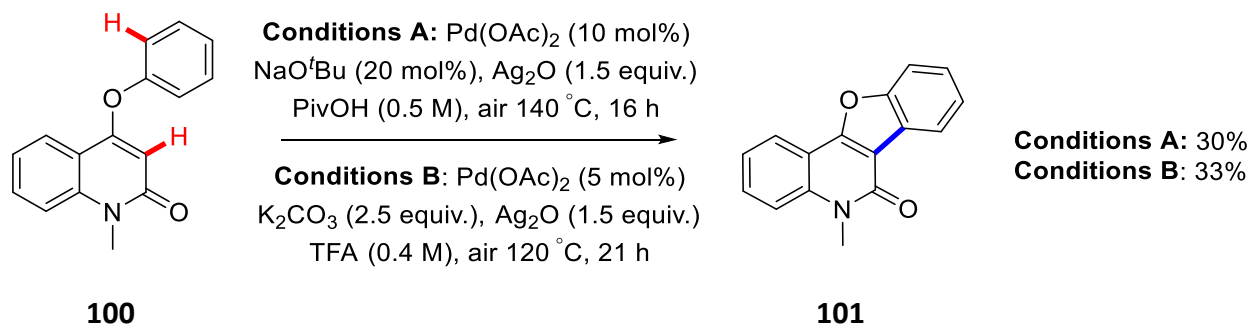
Finally, after attempts at brominating **93** failed, we then looked at preparing 4-phenoxy quinolone (**100**) *via* an alternative route. Pleasingly, a procedure described by Kappe and co-workers³⁹ allowed us to gain access to the desired phenoxy quinolone **100** in two synthetic steps, although the overall atom economy of the process was not very appealing (**Scheme 35**). Initially, 3-iodo-4-phenoxy-*N*-methyl quinolone (**99**) was prepared by treatment of **93** with phenyliodo(III)diacetate (PIDA) and Na₂CO₃ in refluxing EtOH giving a zwitterion, which was subsequently refluxed in DMF. This initiated thermal migration of the aryl group from the iodide to the oxygen affording **99** after a H₂O quench in 84% yield. Finally, reductive deiodination of 3-iodo-4-phenoxy-*N*-methyl quinolone (**99**) with Zn dust in acetic acid and EtOH gave the desired 4-phenoxy-*N*-methyl 2-quinolone (**100**) in 78% yield.



Scheme 35. Two step synthesis of 4-phenoxy-*N*-methyl-2-quinolone (**100**).

2.6.2. Cyclisation of the 4-phenoxy-2-quinolone substrate

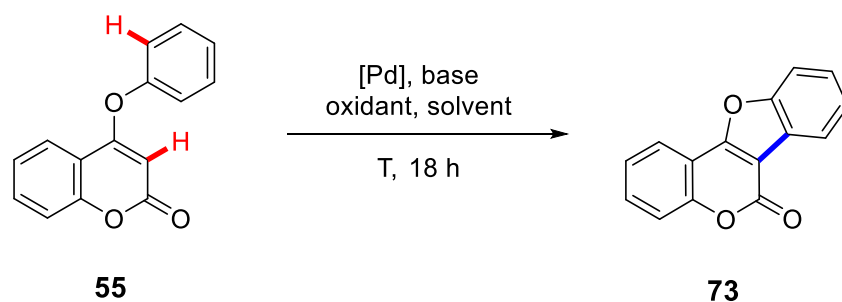
Once synthesised, 4-phenoxy-*N*-methyl-2-quinolone **100** was subjected to our two sets of optimised conditions (**Scheme 36**). Disappointingly, 2-quinolone **96** did not work as well as the 2-coumarin substrates, however, product **101** was isolated in 30% yield with **Conditions A**. A slightly higher yield of 33% was obtained when **Conditions B** were employed.



Scheme 36. Double C-H activation of 2-quinolone analogue **100**.

2.7.1 Alternative solvent investigation

In recent years, there has been much attention drawn to certain solvents due to their undesirable health, safety and environmental problems. Thus, there has been a push towards establishing greener solvents for reactions, separations and extractions.¹⁴ With this in mind, the final part of the project was aimed at establishing more environmentally friendly reaction conditions which align to the principles of green chemistry. Several general purpose solvent selection guides have been published over the last number of years. Thus, solvents we chose based on criteria as outlined in these solvent selection guides^{14-15, 40} and also precedence for their use in direct arylation reactions.^{29, 41-43} Several green solvent candidates were tested for their feasibility to replace PivOH and TFA as reaction solvent (**Table 7**). Of the solvents tested, the combination of *i*PrOH and AcOH (4:1) gave the best result (**Table 7, entry 3**), facilitating 55% conversion to product **73** and an isolated yield of 41% yield. No other solvent tested gave any conversion to product **73** (**Table 7, entry 1-2, 4-7**).

Table 7. Investigation of green reaction solvents.

Entry	Catalyst (5 mol%)	Base (2.5 equiv.)	Oxidant (1.5 equiv.)	Additive (30 mol%)	Solvent (0.4 M)	Temp. (°C)	Conv. (%)
1	Pd(OAc) ₂	K ₂ CO ₃	Ag ₂ O	TFA	MeOH	65	0
2	Pd(OAc) ₂	K ₂ CO ₃	Ag ₂ O	TFA	MeCN	80	0
3	Pd(OAc)₂	K₂CO₃	Ag₂O	TFA	<i>i</i>PrOH/AcOH (4:1)	100	55 (41)^a
4	Pd(OAc) ₂	K ₂ CO ₃	Ag ₂ O	TFA	Dioxane/H ₂ O (1:1)	100	0
5	Pd(OAc) ₂	K ₂ CO ₃	Ag ₂ O	TFA	EtOAc/H ₂ O (2.5:1)	100	0
6^b	Pd(OAc) ₂	NaO ^{<i>t</i>} Bu	Ag ₂ O	-	MeOH	65	0
7^b	Pd(OAc) ₂	NaO ^{<i>t</i>} Bu	Ag ₂ O	-	MeCN	80	0

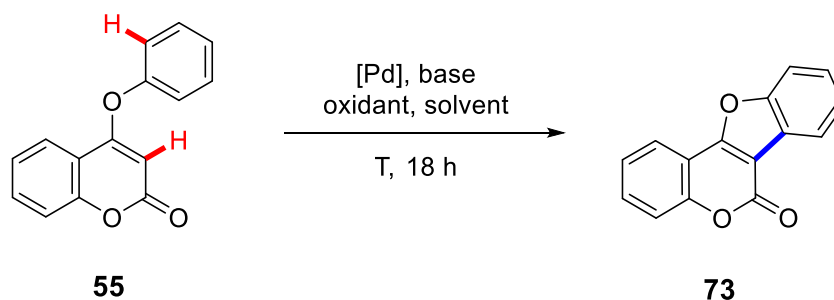
^aIsolated yield in parenthesis. Yield determined by ¹H NMR Spectroscopy using 1,3,5-trimethoxy benzene as an internal standard for quantification. ^bEntries 6-7: 10 mol% [Pd], 20 mol% base.

2.7.2 Alternative oxidant investigation

We also briefly examined a few non-metal based oxidants.^{29, 44} Disappointingly, benzoquinone and *tert*-butyl hydroperoxide (TBHP) did not provide any conversion to desired product **73** (**Table 8, entry 1-2**). In the last 20 years, hypervalent iodine reagents have been used as oxidants in high valent transition metal chemistry. From a green chemistry perspective, they can be considered environmentally benign, non-toxic and relatively inexpensive reagents compared to other inorganic oxidants.⁴⁴ Thus, two hypervalent iodine reagents, diacetoxyiodobenzene (PIDA) and bis(trifluoroacetoxy)iodo benzene (PIFA) were

tested (**Table 8, entry 3-4**). Unfortunately, PIDA only allowed for a 16% conversion to product **73**. The more electron withdrawing analogue PIFA, gave a 35% conversion to desired product **73**. It is important to note that O₂ was also examined as a possible oxidant for this transformation by a previous member of the McGlacken group. However, no appreciable conversion to product was observed.

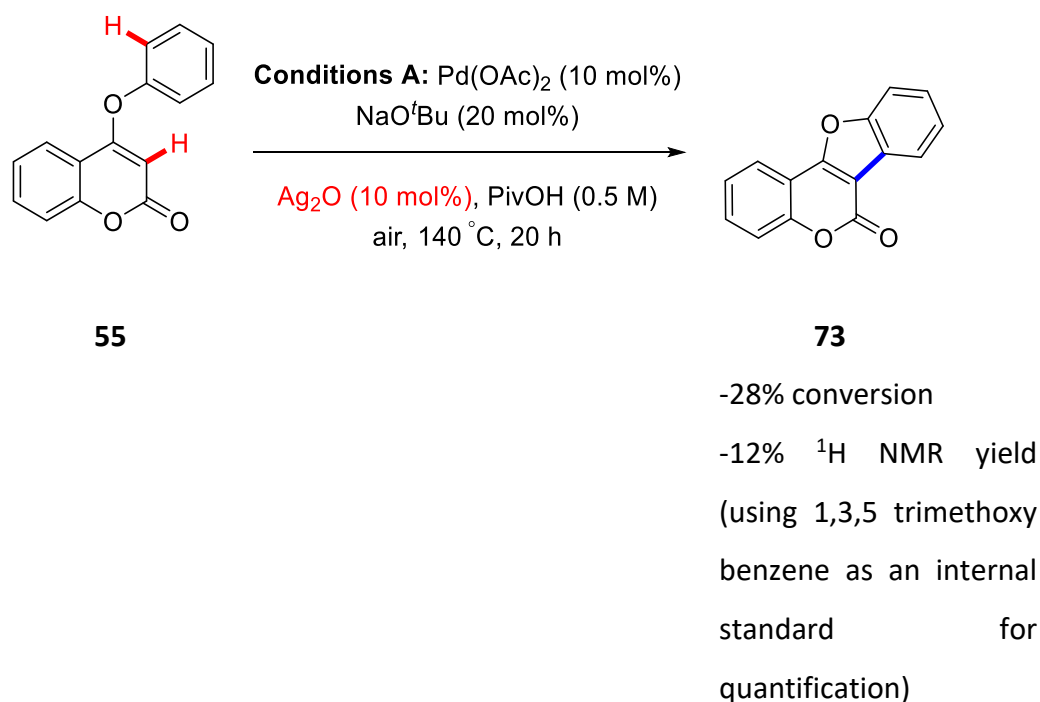
Table 8. Investigation of non-metal based oxidants.



Entry	Catalyst (5 mol%)	Base (2.5 equiv.)	Oxidant (1.5 equiv.)	Solvent (0.4 M)	Temp. (°C)	Conv. (%) ^a
1	Pd(OAc) ₂	K ₂ CO ₃	Benzoquinone	TFA	140	0
2	Pd(OAc) ₂	K ₂ CO ₃	TBHP	TFA	140	0
3	Pd(OAc) ₂	K ₂ CO ₃	PIDA	TFA	140	16
4	Pd(OAc) ₂	K ₂ CO ₃	PIFA	TFA	140	35

^aConversion calculated from ratio of starting material **55** to product **73** in the ¹H NMR spectrum of the crude reaction mixture.

Lastly, we also examined carrying out the reaction with a catalytic amount of Ag₂O to investigate if it was possible to reduce the amount of oxidant required (**Scheme 37**). Unfortunately, using 10 mol% of Ag₂O only allowed for a 28% conversion to product (which is 2-3 turnovers of the catalyst). The true role of Ag₂O in the catalytic cycle is not fully understood. Ag₂O may be acting as an oxidant, as well as participating in other steps of the catalytic cycle.²⁵



Scheme 37. Investigation into using a catalytic amount of silver oxidant.

2.8 Conclusion

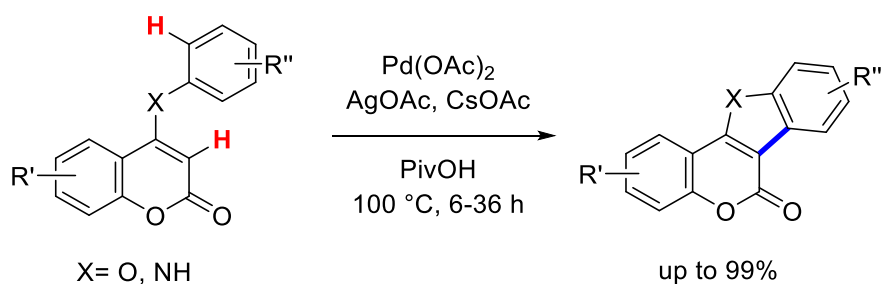
In conclusion, a double C-H activation protocol was applied to 2-pyrones and 2-coumarins giving quick access to the cyclised products. Good to excellent yields were obtained for the 6*H*-benzofuro[3,2-*c*]chromen-6-one analogues with both sets of conditions, whilst moderate yields were achieved for the 1*H*-pyrano[4,3-*c*]benzofuran-1-one products employing **Conditions A**. Substitution patterns (on the phenoxy ring), which would be difficult to access *via* other routes, are available with this methodology. The methodology was also extended to include a 2-quinolone analogue, albeit the yield was reduced. Overall, this is one of the most delicate molecular frameworks to have been reported for this type of transformation. This approach also facilitated a short three step synthesis of flemichapparin C.

2.9 Expansion of double C-H activation methodology in the literature

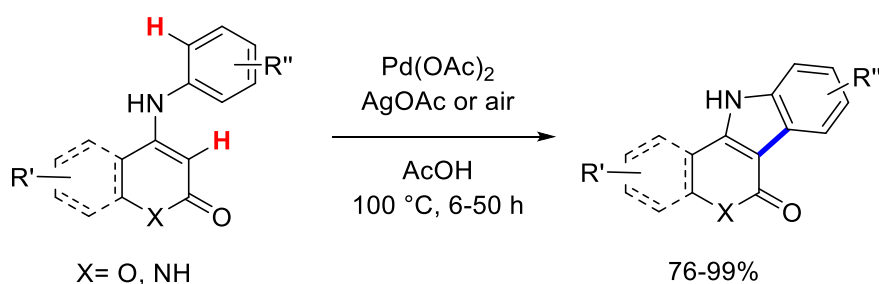
Finally, two separate groups also published work on systems similar to the McGlacken group in 2016 and 2017, with PivOH again and AcOH serving as key reaction components enabling facile syntheses of fused polyheterocyclic analogues (**Scheme 38**). In 2016, Cheng and co-workers developed a highly efficient palladium catalysed intramolecular cross dehydrogenative protocol for the synthesis of coumestans and indole[3, 2-*c*]coumarins in

yields of up to 99%.⁴⁵ The same group subsequently improved on these reaction conditions for the synthesis of indolo[3,2-*c*]coumarins, pyrones and quinolones, with the optimised conditions requiring no additional base or oxidant.⁴⁶ Following on from this, in 2017 Litinas published a palladium catalysed oxidative coupling of 4(-arylamino)coumarins in the presence of $\text{Cu}(\text{OAc})_2$ under microwave irradiation.⁴⁷

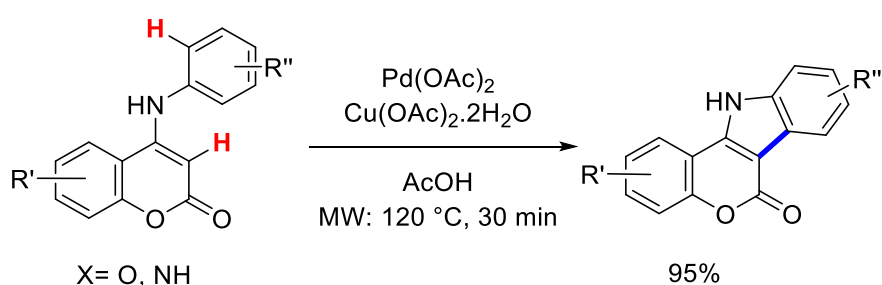
(i) Cheng, *Org. Chem. Front*, 2016, 3, 1111-1115



(ii) Cheng, *J. Org. Chem.*, 2016, 81, 11501-11507



(iii) Litinas, *Synthesis*, 2017, 49, 2575-2583



Scheme 38. Palladium catalysed intramolecular cross dehydrogenative coupling toward the synthesis of fused polyheterocycles.

2.10 Background (dibenzofurans)

As discussed in **Chapter 1** of this thesis, dibenzofuran derivatives are an important class of structural motifs and are found in many natural products, bioactive molecules and pharmaceuticals. Significant biological activity has been exhibited by many members of this class of compounds and a large number of naturally occurring dibenzofurans possess anti-cancer, anti-inflammatory, anti-bacterial, anti-malarial and anti-oxidant properties.⁴⁸⁻⁵¹ As previously mentioned, many of the current methods to synthesise dibenzofurans suffer from a number of drawbacks.⁵²⁻⁵⁵ Thus, we were interested to see if the double C-H activation conditions which were applied in the synthesis of 1*H*-pyrano[4,3-*c*]benzofuran-1-one and 6*H*-benzofuro[3,2-*c*]chromen-6-one analogues would be suitable for the double C-H activation of diarylethers. Due to good regioselectivity observed for the *meta*-substituted 2-pyrone and 2-coumarin analogues, particularly when **Conditions A** were applied, it was decided to focus only on the synthesis of *meta*-substituted dibenzofurans and to investigate using our optimised double C-H activation conditions.

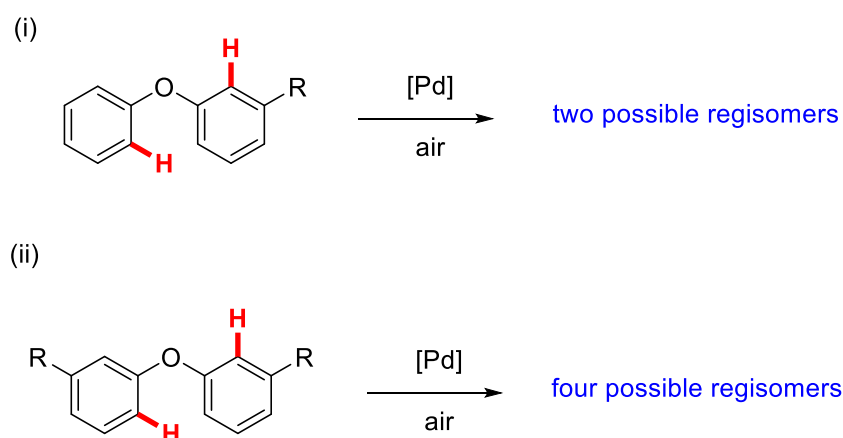
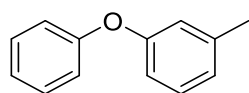
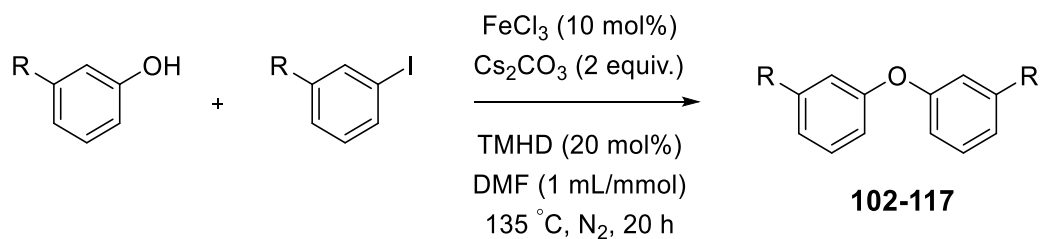
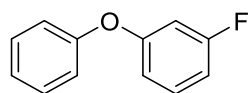
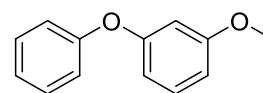
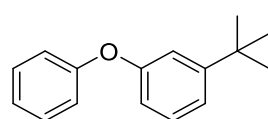
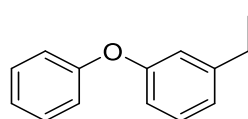
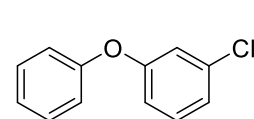
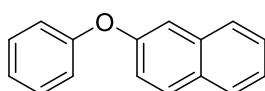
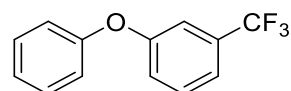
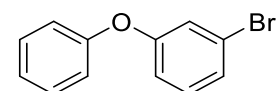
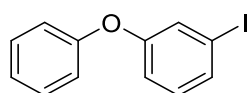
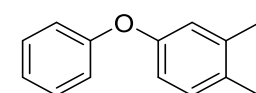
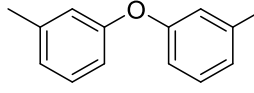
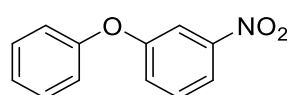
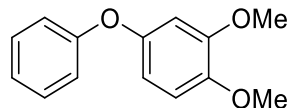
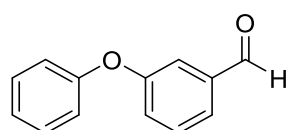
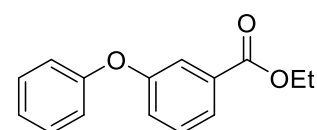


Figure 19. Targeted objective.

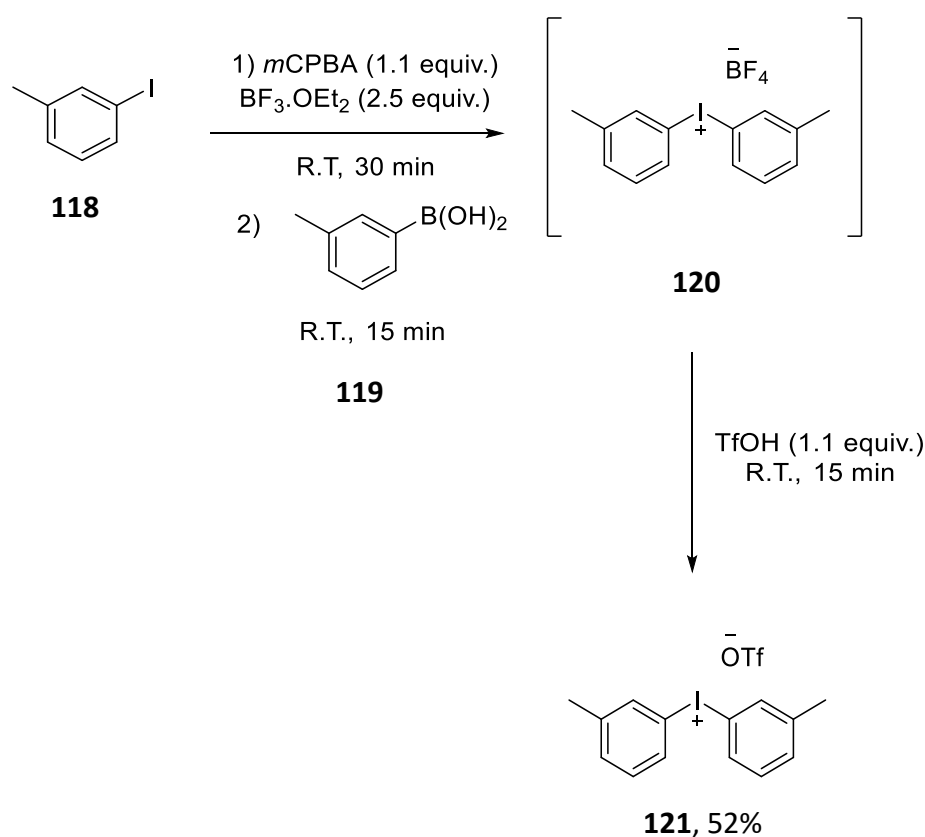
2.11 Synthesis of diarylether substrates

Iron catalysed cross-coupling reactions offer an attractive alternative to other transition metal catalysed cross-coupling protocols due to the low price and environmentally benign features of iron.⁵⁶⁻⁵⁷ Thus, an iron catalysed *O*-arylation reaction demonstrated by Bolm and co-workers in 2008 was chosen as the method for the synthesis of diarylether starting materials.⁵⁸ This versatile and convenient protocol uses readily available aryl iodides as arylating agents and phenols. The success of this protocol is dependent on the employment

of 10 mol% FeCl_3 together with 2,2,6,6-tetramethyl-3,5-heptadione (TMHD) as the chelating ligand, in DMF at 135 °C. A range of substituted analogues were synthesised and purified *via* silica gel column chromatography with yields ranging from 23-78%. Compound **114** with a nitro substituent, compound **115** with two methoxy substituents and compounds **116** and **117** with an aldehyde group and ester group respectively, failed to give any conversion to product. This was the case when the phenol was substituted at the *meta* position and subsequently reacted with aryl iodide and *vice versa*.

**102**, 52%**103**, 52%**104**, 78%**105**, 44%**106**, 78%**107**, 51%**108**, 71%**109**, 64%**110**, 51%**111**, 23%**112**, 51%**113**, 51%**114**, 0%**115**, 0%**116**, 0%**117**, 0%**Scheme 39.** Synthesis of diarylethers *via* iron catalysed *O*-arylation.

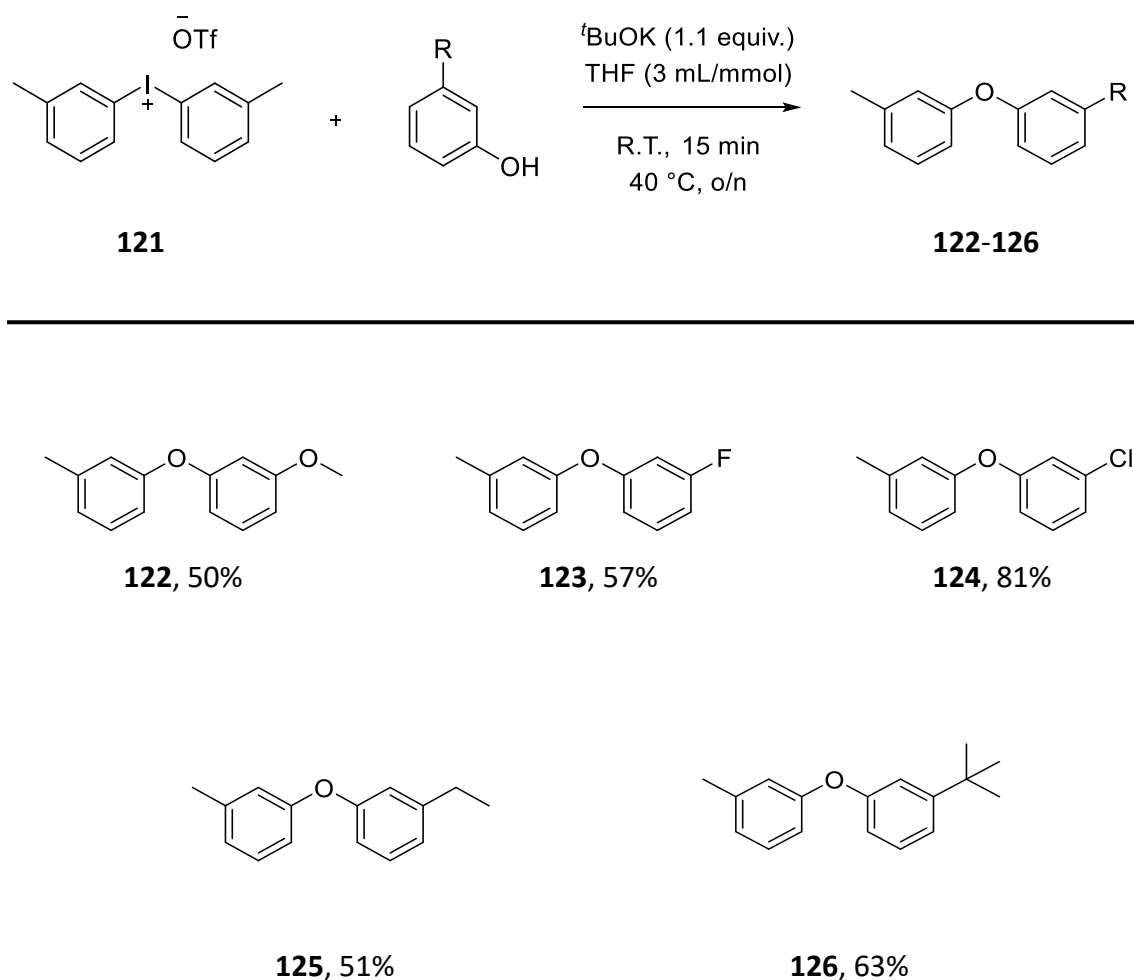
The synthesis of a number of disubstituted diarylethers was carried out *via* a two step protocol developed by Olofsson and co-workers (**Scheme 40**).⁵⁹⁻⁶⁰ This mild and convenient synthesis of diarylethers avoids the use of transition metals, additives or excess reagents. Also, precautions to avoid air or moisture are not needed. The first step involved synthesis of bis(3-methylphenyl)iodonium triflate **121** which was isolated in 52% yield following initial formation of the tetrafluoroborate salt **120** by reaction of 3-iodo toluene **118** and 3-methyl phenyl boronic acid **119** in the presence of *m*CPBA and boron trifluoride. The tetrafluoroborate salt **120** was then converted to the triflate salt by an *in-situ* anion exchange with triflic acid to yield **121**.⁶⁰



Scheme 40. Synthesis of Iodonium triflate salt **121**.

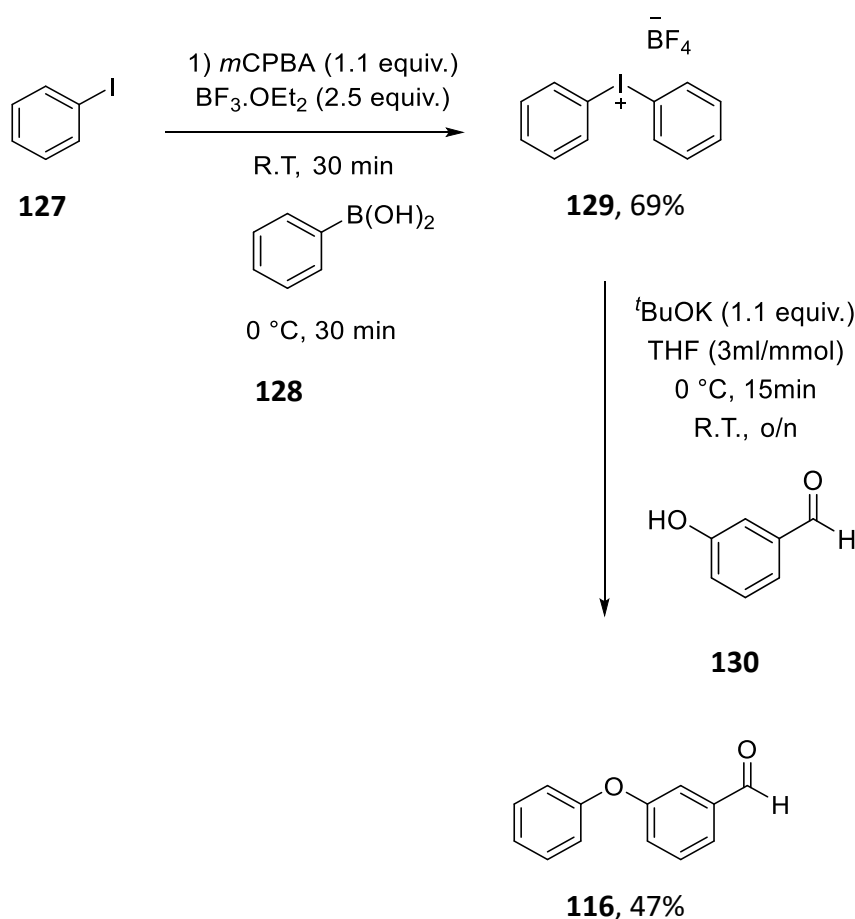
The second step involved reaction of the diaryliodonium triflate salt **121** with the corresponding substituted phenol to yield the disubstituted diarylethers **122-126** in moderate to good yields (**Scheme 41**).⁵⁹ The lower yields observed for the fluoro **123**, ethyl **125** and *tert*-butyl **126** derivatives was primarily due to difficulties in purification. One of the main drawbacks of the reaction is the use of the stoichiometric iodonium salt which resulted in one

equivalent of 3-methyl iodobenzene as the by-product. This by-product proved particularly problematic during purification and often co-eluted with the desired products, hence a reduction in yield was observed for a number of products.



Scheme 41. Diarylether synthesis *via* diaryl iodonium triflate salt **121**.

Finally, to expand the scope of the double C-H activation reaction to include more functionalities, the two step iodonium salt protocol was adopted for the synthesis of an aldehyde variant (**Scheme 42**). Firstly, the diaryliodonium tetrafluoroborate salt **129** was synthesised in 69% yield by treating iodobenzene (**127**) with *m*CPBA and $\text{BF}_3 \cdot \text{OEt}_2$ followed by addition of phenyl boronic acid (**128**). The second step involved reaction of the iodonium salt **129** with **130** in the presence of $t\text{BuOK}$ to give the corresponding diarylether product **116** in 47% isolated yield, following purification by column chromatography.



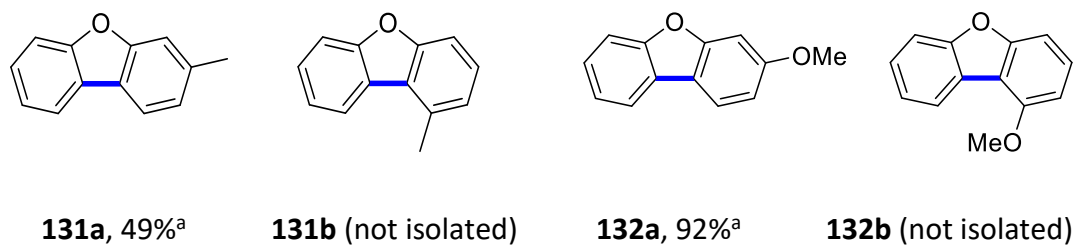
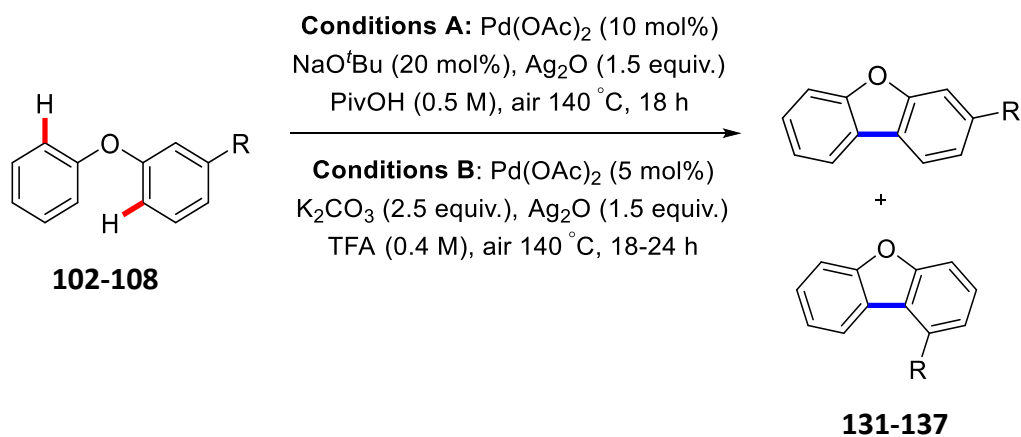
Scheme 42. Synthesis of aldehyde starting material **116**.

2.12.1 Demonstration of substrate scope for double C-H activation of mono-substituted diarylethers

Once synthesised, the diarylether substrates were subjected to our optimised double C-H activation reaction conditions (**Scheme 43**). Cyclisation of the mono-substituted diarylethers under the reaction conditions could lead to two possible regioisomers being formed. Not surprisingly, it was observed that **Conditions A** produced higher yields than **Conditions B**. This was a similar trend to that observed for the 2-pyrone and 2-coumarin substrates. Good to excellent yields were obtained for **131-137** (49-99%) using **Conditions A**. This was applicable to both substrates bearing electron donating substituents and electron withdrawing substituents. A decrease in yield was observed for the naphthyl analogue **135** and the cyclised products **135a:135b** were isolated in a combined 58% yield. This is probably due to the steric bulk of the naphthyl group hindering access to the coupling site. In terms of regioselectivity, good regioselectivity was observed for substrates bearing electron donating substituents (**131**, **136** and **137**). For these particular substrates, one regioisomer was exclusively formed.

A slight decrease in regioselectivity was observed for the methoxy analogue **132**, 94:6 in favour of the less sterically hindered regioisomer. In the case of substrates with electron withdrawing substituents, good to excellent regioselectivity was observed. For example, the regioisomeric ratio for the chloro analogue was determined to be 97:3 in favour of **134a** and this was isolated in 90% yield. Additionally, the chloride in **134a** was retained as a synthetic handle for further cross-coupling. However, for the fluoro analogue a mixture of regioisomers was obtained **133a:133b** and the regioisomeric ratio was determined to be 88:12.

In contrast, moderate to good yields were observed when **Conditions B** were employed. Yields ranged from 31-72%. In two cases, only one regioisomer was formed exclusively. This was for substrates with sterically bulky electron donating substituents (**136-137**). However, for the majority of substrates, a decrease in regioselectivity was observed (**131-134**).

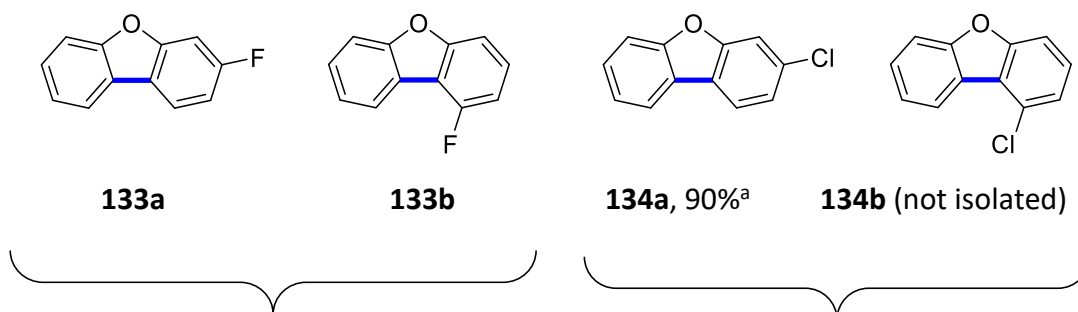


A: (99:1)^b

B: 38% (93:7)^{b,c}

A: (94:6)^b

B: 62% (72:28)^{b,c}

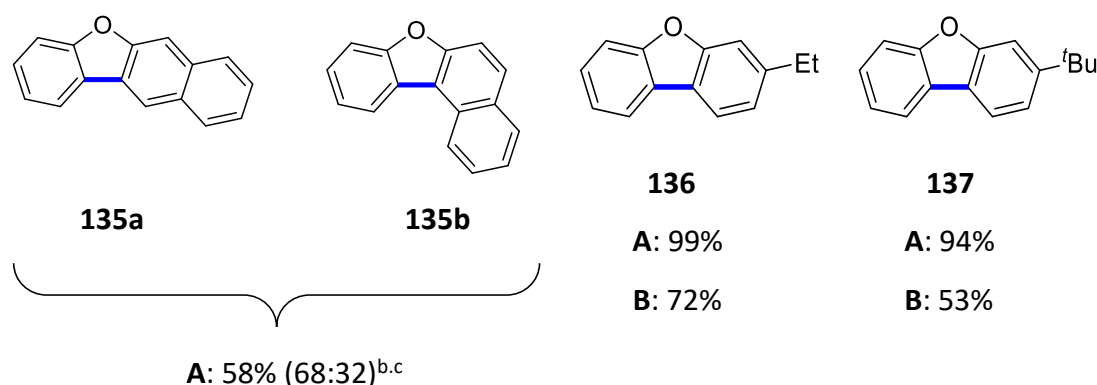


A: 84% (88:12)^{b,c}

B: 46% (65:35)^{b,c}

A: (97:3)^b

B: 31% (87:13)^{b,c}

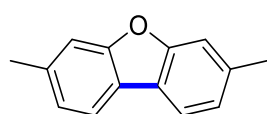
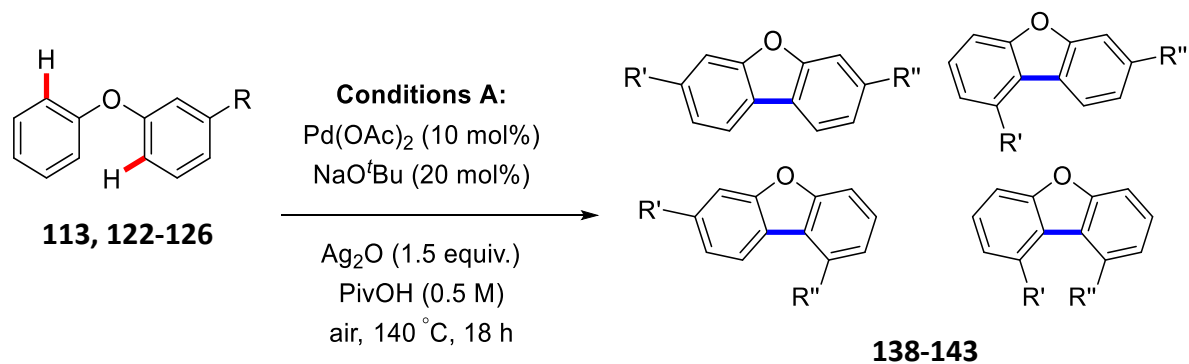
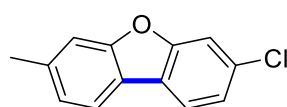
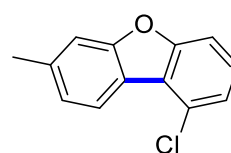
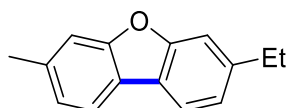


Scheme 43. Substrate scope for mono-substituted dibenzofurans. ^aIsolated yield using **Conditions A**.

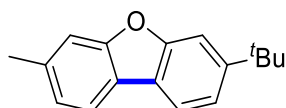
^bRegioisomeric ratios determined from the ¹H NMR spectrum of the crude reaction mixtures. ^c Combined yield of both regioisomers isomers.

2.12.2 Demonstration of substrate scope for double C-H activation of di-substituted diarylethers

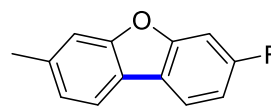
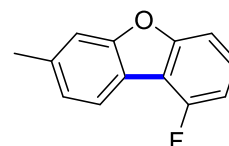
Since **Conditions A** allowed us to achieve better results both in terms of yield and regioselectivity, it was decided that going forward these would be the reaction conditions of choice. The di-substituted diarylethers were then examined (**Scheme 44**). These substrates presented an additional challenge as three or four regioisomers could be possibly formed. All of the di-substituted substrates synthesised contained a methyl substituent and an additional electron donating or electron withdrawing substituent. This was primarily due to cost and availability of starting materials in-house. Overall, good to excellent yields were achieved for the di-substituted analogues **138-143** (50-81%). Excellent regioselectivity was observed compounds with two electron donating substituents (**138, 140-141**) as well as compound **139** containing a methyl and a chloro substituent. In these four cases, only one regioisomer was exclusively formed. A slight decrease in regioselectivity was observed for substrates with an electron donating substituent and an electron withdrawing substituent (**142**), as well as compound **143** with a methyl and a methoxy substituent. However, excellent regioselectivity was achieved overall for the di-substituted analogues.

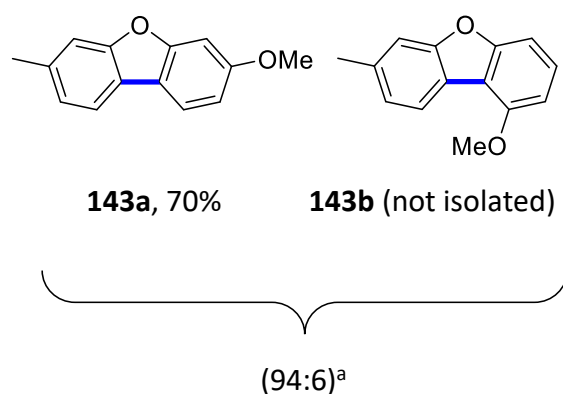
**138**, 81% (98:1:1)**139a**, 50%**139b** (not isolated)(97:3)^a**140**, 77%

(97:1:1:1)

**141**, 76%

(97:1:1:1)

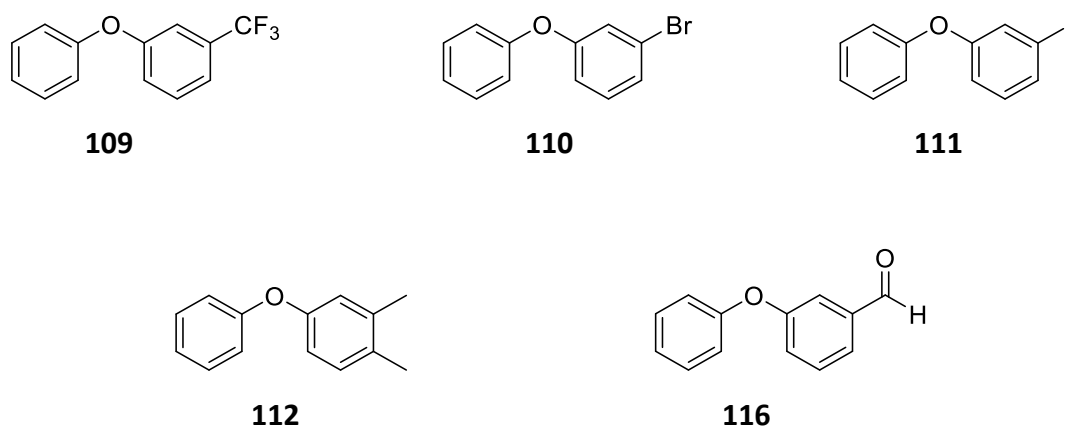
**142a****142b**70% (84:16)^a



Scheme 44. Substrate scope for di-substituted dibenzofurans. ^aRegioisomeric ratios determined from the ¹H NMR spectrum of the crude reaction mixtures.

2.12.3 Substrates which proved difficult to cyclise

Some functional groups were incompatible with the optimised double C-H activation conditions. Five of the substrates (**109**, **110**, **111**, **112**, **116**) resulted in very low conversion to cyclised products, in addition to numerous side-products being formed during the course of the reaction. This may be attributed to the steric **112** and electronic properties (**109**, **116**) of the substituents which may be incompatible with the reaction conditions. Compound **116** bearing an aldehydic functionality did allow for 50% conversion to product after 60 hours. A mixture of regioisomers was formed. However, separation of the starting material **116** from the cyclised products by silica gel column chromatography (hexanes) proved extremely difficult owing to the similar polarities of both the starting material **116** and cyclised products. Numerous recrystallisation attempts also failed to separate the starting material **116** from the product. A reduction in catalyst loading to 2 mol% Pd(OAc)₂ was also investigated using **116**, however this failed to provide any significant improvement. Presumably for **110** and **111**. (bearing a bromo and iodo substituent respectively), competing oxidative addition of the palladium catalyst into the C-Br and C-I bonds led to poor conversion to the desired cyclised products and resulted in by-product formation.



Scheme 45. Substrates which proved problematic.

2.13 Investigation of *N*-linker for double C-H activation

Following on from our work on the synthesis of a range of *meta*-substituted dibenzofurans, we were interested to see if our methodology could be expanded to include different heteroatom linkers, to form carbazoles for example (**Figure 20**). A previous publication by Fagnou and co-workers demonstrated the viability of such a transformation on diphenylamine substrates.¹⁰ However, their scope was mainly limited to substrates possessing *para* substituents. Focus was again directed towards synthesising *meta*-substituted compounds. In addition, we were interested to see if our conditions were applicable to the *N*-methyl analogues.

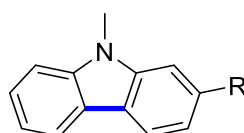
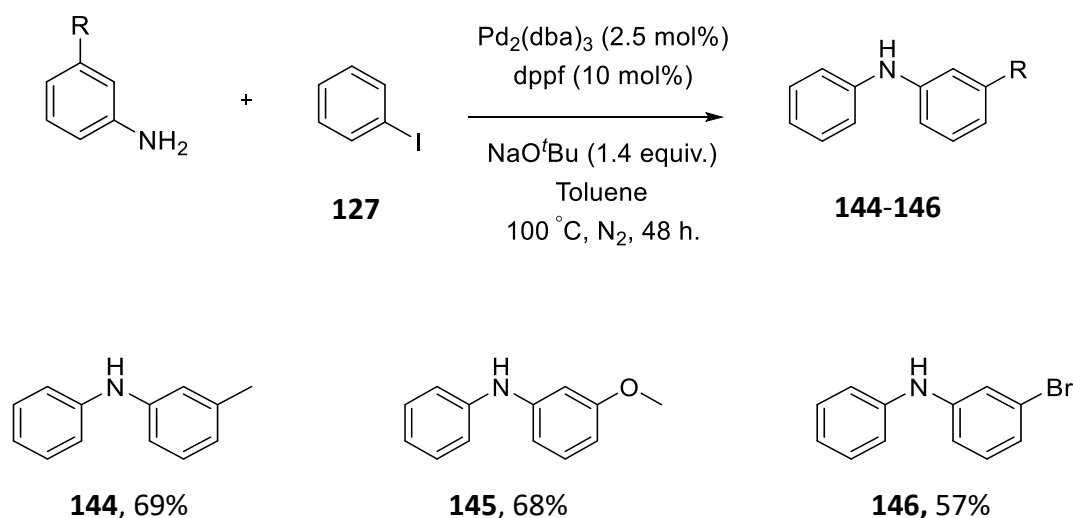


Figure 20. Carbazole product.

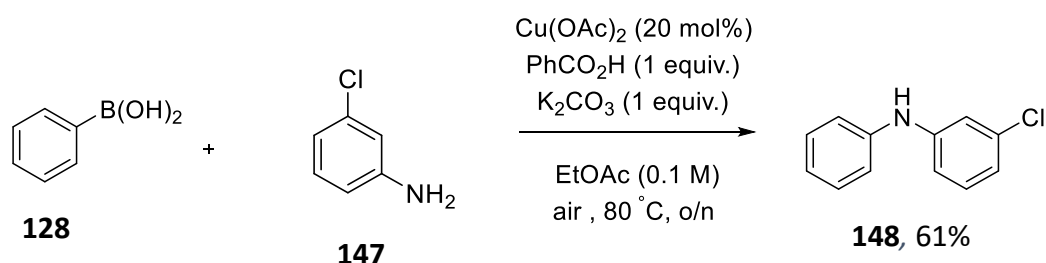
2.14 Synthesis of starting materials

The synthesis of the diphenylamine substrates was achieved *via* a Buchwald-Hartwig cross-coupling of iodobenzene and the *meta*-substituted aniline in the presence of $\text{Pd}_2(\text{dba})_3$, dppf as ligand and sodium *tert*-butoxide as base.⁶¹ The corresponding diphenylamine products **144-146** were isolated in moderate yields of 57-69% (**Scheme 46**).



Scheme 46. Diphenylamine synthesis *via* Buchwald-Hartwig coupling.

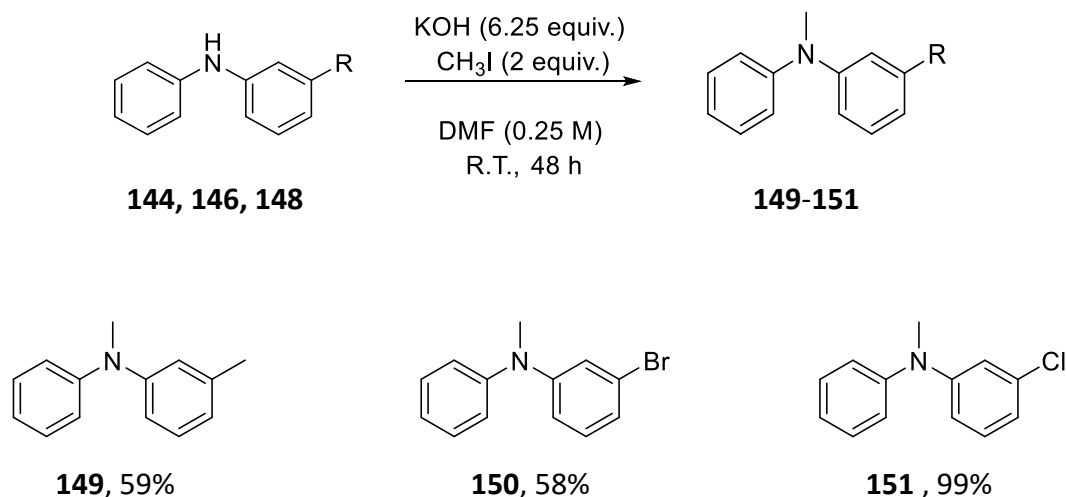
The synthesis of the chloro analogue **148** involved a copper catalysed Chan-Lam-Evans coupling of phenyl boronic acid **128** and 3-chloro aniline **147** using reaction conditions reported by Wang and co-workers.⁶² This reaction was conveniently carried out in air at 80°C with K_2CO_3 as base, benzoic acid as an acid additive and ethyl acetate as solvent. The corresponding product **148** was isolated in 61% yield.



Scheme 47. Synthesis of 3-chloro diphenylamine (**148**) *via* Chan-Lam-Evans coupling.

Methylation of the diphenylamine substrates was achieved under standard methylation conditions by treating **144**, **146** and **148** with KOH in anhydrous DMF followed by slow addition of the methylating agent, CH_3I . The resulting mixture was stirred at ambient temperature for 48 hours and the corresponding *N*-methylated products **149-151** were isolated in 58-99% yield following purification by silica gel column chromatography. The characteristic methyl 3H singlet at 3.3 ppm in the ^1H NMR spectrum and at 40 ppm in the ^{13}C

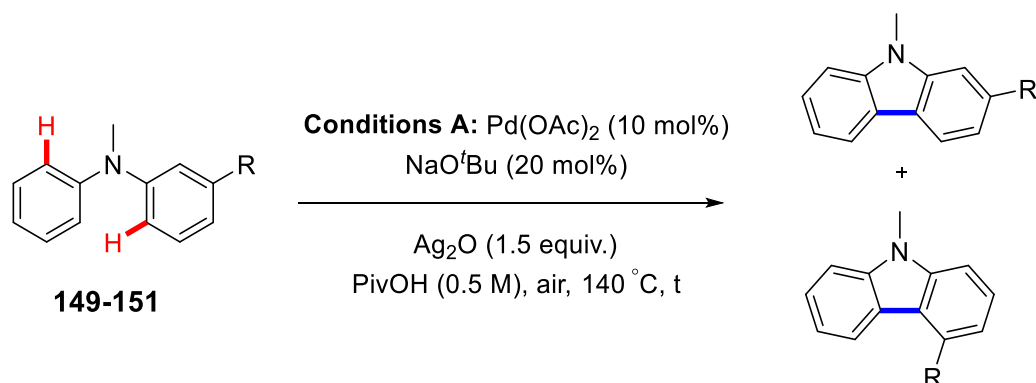
NMR spectrum observed in the crude NMR spectra for **149-151** initially indicated the success of the transformation.



Scheme 48. N-Methylation of diphenylamines.

2.15.1 Double C-H activation of N-methyl diphenylamine substrates

Application of **Conditions A** to substrates **149-151** failed to give in each case full consumption of starting material (**Table 9**). The reactions proceeded sluggishly and attempts to drive the reactions to completion proved unsuccessful. For example, after 50 hours, the ¹H NMR spectra of the crude reaction mixtures showed low conversion to cyclised product and a number of side products were also evident. For compound **150** with a *meta*-bromo substituent, it was evident that numerous side products were present in the crude reaction mixture. The poor reactivity may be due to hydrodebromination. Competing oxidative addition of the palladium catalyst into the C-Br bond may be inhibiting formation of the desired cyclised product. Furthermore, two possible regioisomers could be possibly formed for each substrate tested. However, the regioisomeric ratios could not be determined for the methyl and bromo substrates (**Table 9, entries 1 and 2**). This was due to the complexity of the ¹H NMR spectra of the crude reaction mixtures for both of these compounds. The regioisomeric ratio for the chloro analogue was determined to be 95:5 in favour of the less sterically hindered regioisomer (**Table 9, entry 3**). Furthermore, it was decided not to isolate the compounds from the complex mixtures due to the above reasons.

Table 9. Attempted double C-H activation of *N*-methyl diphenylamines.

Entry	R	Time (h)	Result ^a
1	Me	50	Complex mixture
2	Br	50	Complex mixture
3	Cl	50	Complex mixture

Reactions were monitored by TLC and ¹H NMR spectroscopy. ^aCrude reaction material contained a complex mixture of starting material, cyclised product (two regioisomers) and side products.

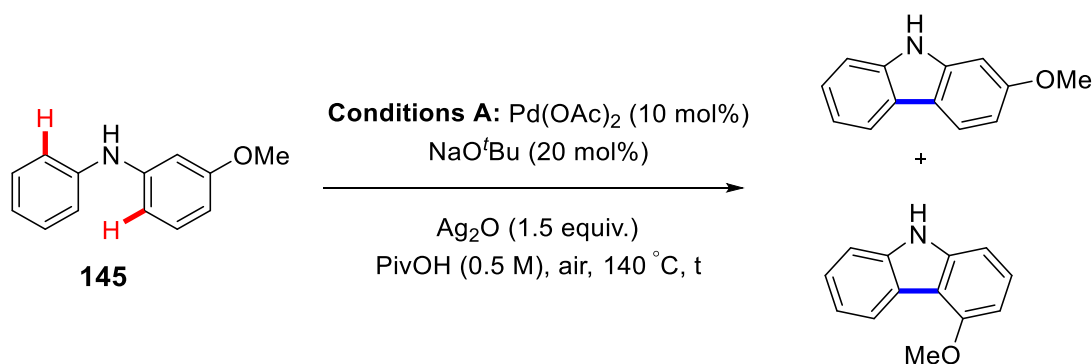
2.15.2 Double C-H activation of 3-methoxy diphenylamine

Finally, it was decided to go back and examine diphenylamine bearing a free N-H. A test reaction was carried out on the methoxy substrate **145** (Table 10). Fagnou and co-workers had previously demonstrated that this particular substrate could be effectively cyclised under their optimised reaction conditions to give a mixture of regioisomers in a ratio of 95:5 in favour of the less sterically hindered regioisomer.¹⁰ In contrast, direct application of **Conditions A** on **145** resulted in only very low conversion to the desired carbazole product and it was clear from the ¹H NMR spectrum of the crude reaction mixture that decomposition of **145** had occurred and that other by-products were being formed. Fagnou and co-workers had noted the presence of various by-products during the course of their investigations on diphenylamine substrates. However, the use of pivalic acid as reaction solvent had a significant effect on suppressing by-product formation, although the authors did isolate a side product involving the formation of a new C-O bond even when PivOH was substituted for acetic acid.¹⁰ In comparison to Fagnou's system, our optimised conditions employ

stoichiometric quantities of Ag₂O as oxidant and sodium *tert*-butoxide as base. Both of these reagents may contribute to increased formation of unwanted by-products.

Some undesirable products which may be formed during the course of the reaction are shown in **Figure 21**. These include **153**, which results from the formation of a new C-O bond. Product **152** could arise following fragmentation of the starting material **145**, followed by recombination with another molecule of starting material or product. Finally, dimer **155** and product **154** resulting from oxidative C-N bond formation are also possibilities. Other side reactions may also be possible. The by-products formed would explain the low mass recovery observed for this reaction.

Table 10. Double C-H activation reaction of 3-methoxy diphenylamine.



Entry	Starting material	Time (h)	Result
1	145	50	Complex mixture ^a

^aCrude reaction mixture contained a complex mixture of starting material **145**, a mixture of both regioisomers (the regioisomeric ratio could not be determined due to the complexity of the ¹H NMR spectrum) and by-products.

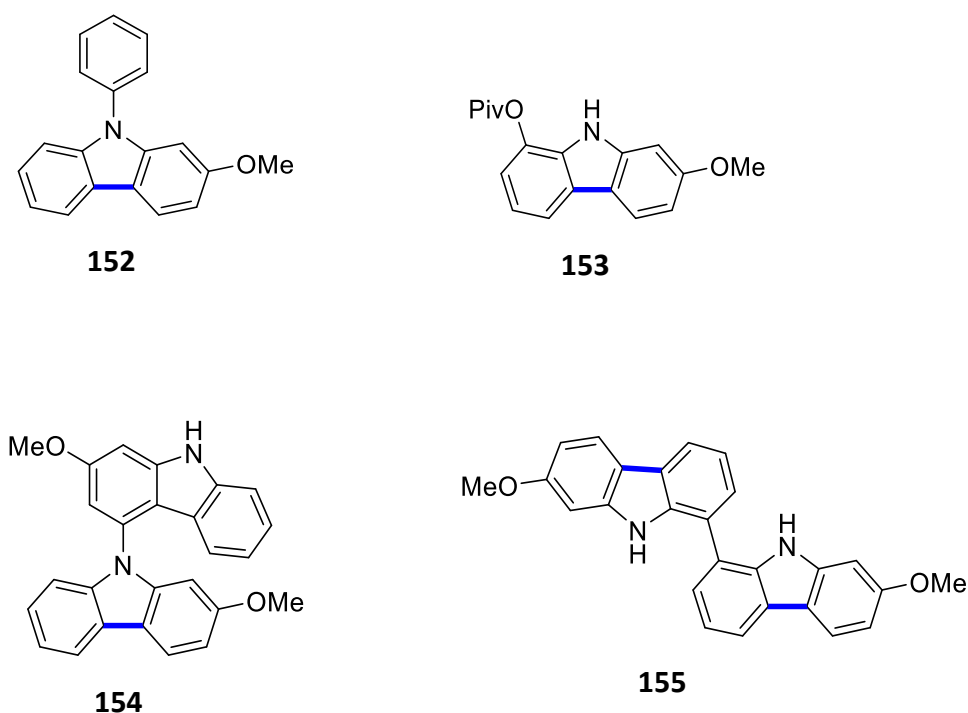


Figure 21. Potential by-products formed under reaction conditions **A**.

Due to poor results obtained both for the *N*-methyl substrates and *N*-H substrate **145**, this line of investigation was not pursued any further.

2.16 Conclusion

The application of our double C-H activation methodology towards the synthesis of *meta*-substituted dibenzofurans was demonstrated. Application of **Conditions A** on the mono-substituted diarylethers allowed for efficient conversion to cyclised products and good to excellent yields were achieved (**Scheme 43**). The reaction proceeded particularly smoothly for substrates possessing sterically bulky alkyl groups (**136** and **137**) with yields of up to 99% being obtained. Overall, excellent regioselectivity was observed for the majority of substrates. A slight decrease in regioselectivity was observed for the *meta*-fluoro analogue **133** and a mixture of regioisomers was obtained for the naphthyl analogue **135**. On the contrary, **Conditions B** employing TFA as reaction solvent, resulted in diminished yields and regioselectivities (**Scheme 43**). Pleasingly, the di-substituted diarylethers were cyclised in excellent yields and with excellent regioselectivity (**Scheme 44**). Overall, reaction at the least sterically hindered site was favoured when **Conditions A** were employed, whereas when

Conditions B were employed a less selective process was observed. Due to difficulties in preparing a number of diarylether substrates, the substrate scope was somewhat limited. In addition, a few substrates failed to undergo efficient cyclisation which again narrowed the scope of the reaction (**Scheme 45**). Finally, the *N*-methyl diphenylamine substrates (**149-151**) did not participate well in the reaction. Unfortunately, the reaction was extremely sluggish for these particular substrates and complete consumption of starting material could not be achieved for any of the substrates tested. A similar result was obtained for **145** bearing a free N-H group.

2.17 References

1. Alberico, D., Scott, M. E., Lautens, M. *Chem. Rev.* **2007**, *107*, 174-238.
2. McGlacken, G. P., Bateman, L. M. *Chem. Soc. Rev.* **2009**, *38*, 2447-2464.
3. Constable, D. J., Dunn, P. J., Hayler, J. D., Humphrey, G. R., Leazer Jr, J. L., Linderman, R. J., Lorenz, K., Manley, J., Pearlman, B. A., Wells, A. *Green Chem.* **2007**, *9*, 411-420.
4. McGlacken, G. P., Fairlamb, I. J. S. *Nat. Prod. Rep.* **2005**, *22*, 369-385.
5. Tuskaev, V. A. *Pharm. Chem. J.* **2013**, *47*, 1-11.
6. Xu, M.-Y., Kim, Y. S. *Food Chem. Toxicol.* **2014**, *74*, 311-319.
7. Nehybova, T., Smarda, J., Daniel, L., Brezovsky, J., Benes, P. J. *Steroid Chem.* **2015**, *152*, 76-83.
8. Nolan, M.-T., Pardo, L. M., Prendergast, A. M., McGlacken, G. P. *J. Org. Chem.* **2015**, *80*, 10904-10913.
9. Kato, Y., Okada, S., Tomimoto, K., Mase, T. *Tetrahedron Lett.* **2001**, *42*, 4849-4851.
10. Liégault, B., Lee, D., Huestis, M. P., Stuart, D. R., Fagnou, K. *J. Org. Chem.* **2008**, *73*, 5022-5028.
11. Li, H., Zhu, R.-Y., Shi, W.-J., He, K.-H., Shi, Z.-J. *Org. Lett.* **2012**, *14*, 4850-4853.
12. Lafrance, M., Fagnou, K. *J. Am. Chem. Soc.* **2006**, *128*, 16496-16497.
13. Sherwood, J., Clark, J. H., Fairlamb, I. J. S., Slattery, J. M. *Green Chem.* **2019**, *21*, 2164-2213.
14. Byrne, F. P., Jin, S., Paggiola, G., Petchey, T. H. M., Clark, J. H., Farmer, T. J., Hunt, A. J., Robert McElroy, C., Sherwood, J. *Sustain. Chem. Process* **2016**, *4*:7.
15. Henderson, R. K., Jiménez-González, C., Constable, D. J. C., Alston, S. R., Inglis, G. G. A., Fisher, G., Sherwood, J., Binks, S. P., Curzons, A. D. *Green Chem.* **2011**, *13*, 854-862.
16. Zheng, T., Liao, H., Gao, J., Zhong, L., Gao, H., Wu, Q. *Polym. Chem.* **2018**, *9*, 3088-3097.
17. Burns, M. J., Thatcher, R. J., Taylor, R. J. K., Fairlamb, I. J. S. *Dalton Trans.* **2010**, *39*, 10391-10400.
18. Sun, C.-L., Fürstner, A. *Angew. Chem. Int. Ed.* **2013**, *52*, 13071-13075.
19. Chia, M., Haider, M. A., Pollock, G., Kraus, G. A., Neurock, M., Dumesic, J. A. *J. Am. Chem. Soc.* **2013**, *135*, 5699-5708.
20. Burns, M. J., Thatcher, R. J., Taylor, R. J. K., Fairlamb, I. J. S. *Dalton Trans.* **2010**, *39*, 10391-10400.

21. Burns, M. J. *Ph.D thesis*, York, **2010**.
22. Roberts, J. D., Weigert, F. J. *J. Am. Chem. Soc.* **1971**, *93*, 2361-2369.
23. Dolbier Jr., W.R. *Guide to Fluorine NMR for Organic Chemists*, John Wiley & Sons, New Jersey, USA, **2016**, pp. 35.
24. Field, L. D., Li, H. L., Magill, A. M. *Organic Structures from 2D NMR Spectra*, John Wiley & Sons, USA, **2015**, pp. 25-38.
25. Prendergast, A. M., Zhang, Z., Lin, Z., McGlacken, G. P. *Dalton Trans.* **2018**, *47*, 6049-6053.
26. Martinez-Viviente, E., Pregosin, P. S., Tschoerner, M. *Magn. Reson. Chem.* **2000**, *38*, 23-28.
27. Lapointe, D., Fagnou, K., *Chem. Lett.* **2010**, *39*, 1118-1126.
28. Rousseaux, S., Gorelsky, S. I., Chung, B. K. W., Fagnou, K. *J. Am. Chem. Soc.* **2010**, *132*, 10692-10705.
29. Wencel-Delord, J., Dröge, T., Liu, F., Glorius, F. *Chem. Soc. Rev.* **2011**, *40*, 4740-4761.
30. Váňa, J., Bartáček, J., Hanusek, J., Roithová, J., Sedlák, M. *J. Org. Chem.* **2019**, *84*, 12746-12754.
31. Nishikata, T., Abela, A. R., Huang, S., Lipshutz, B. H. *Beilstein J. Org. Chem.* **2016**, *12*, 1040-1064.
32. Váňa, J., Lang, J., Šoltésová, M., Hanusek, J., Růžička, A., Sedlák, M., Roithová, J. *Dalton Trans.* **2017**, *46*, 16269-16275.
33. Kamara, B. I., Brandt, E. V., Ferreira, D. *Tetrahedron* **1999**, *55*, 861-868.
34. Leutbecher, H., Conrad, J., Klaiber, I., Beifuss, U. *Synlett* **2005**, *20*, 3126-3130.
35. Oliphant, C. M., Green, G. M. *Am. Fam. Physician* **2002**, *65*, 455-464.
36. Heeb, S., Fletcher, M. P., Chhabra, S. R., Diggle, S. P., Williams, P., Cámara, M. *FEMS Microbiol. Rev.* **2011**, *35*, 247-274.
37. Jayashree, B., Thomas, S., Nayak, Y. *Med. Chem. Res.* **2010**, *19*, 193-209.
38. Lutz, R. E., Codington, J. F., Rowlett, R. J., Deinet, A. J., Bailey, P. S. *J. Am. Chem. Soc.* **1946**, *68*, 1810-1812.
39. Kappe, T., Korbuly, G., Stadlbauer, W. *Chem. Ber.* **1978**, *111*, 3857-3866.
40. Cue, B. W., Zhang, J. *Green Chem. Lett. Rev.* **2009**, *2*, 193-211.

41. Campeau, L.-C., Stuart, D. R., Leclerc, J.-P., Bertrand-Laperle, M., Villemure, E., Sun, H.-Y., Lasserre, S., Guimond, N., Lecavallier, M., Fagnou, K. *J. Am. Chem. Soc.* **2009**, *131*, 3291-3306.
42. René, O., Fagnou, K. *Org. Lett.* **2010**, *12*, 2116-2119.
43. Giri, R., Chen, X., Yu, J.-Q. *Angew. Chem. Int. Ed.* **2005**, *44*, 2112-2115.
44. Sousa e Silva, F. C., Tierno, A. F., Wengryniuk, S. E. *Molecules* **2017**, *22*, 1-54.
45. Cheng, C., Chen, W.-W., Xu, B., Xu, M.-H. *Org. Chem. Front.* **2016**, *3*, 1111-1115.
46. Cheng, C., Chen, W.-W., Xu, B., Xu, M.-H. *J. Org. Chem.* **2016**, *81*, 11501-11507.
47. Balalas, T., Abdul-Sada, A., Hadjipavlou-Litina, D. J., Litinas, K. E. *Synthesis* **2017**, *49*, 2575-2583.
48. Love, B. E., *Eur. J. Med. Chem.* **2015**, *97*, 377-387.
49. Sokolov, D. N., Zarubae, V. V., Shtro, A. A., Polovinka, M. P., Luzina, O. A., Komarova, N. I., Salakhutdinov, N. F., Kiselev, O. I. *Bioorg. Med. Chem. Lett.* **2012**, *22*, 7060-7064.
50. Patpi, S., Pulipati, L., Perumal, Y., Sriram, D., Jain, N., Sridhar, B., Murthy, R., Tangutur, A., Kalivendi, S., Kantevari, S. *J. Med. Chem.* **2012**, *55*, 3911-3922.
51. Liu, J., Fitzgerald, A. E., Mani, N. S. *J. Org. Chem.* **2008**, *73*, 2951-2954.
52. Xiao, B., Gong, T.-J., Liu, Z.-J., Liu, J.-H., Luo, D.-F., Xu, J., Liu, L. *J. Am. Chem. Soc.* **2011**, *133*, 9250-9253.
53. Lockner, J. W., Dixon, D. D., Risgaard, R., Baran, P. S. *Org. Lett.* **2011**, *13*, 5628-5631.
54. Du, Z., Zhou, J., Si, C., Ma, W. *Synlett* **2011**, *20*, 3023-3025.
55. Wang, C., Piel, I., Glorius, F. *J. Am. Chem. Soc.* **2009**, *131*, 4194-4195.
56. Fürstner, A. *ACS Cent. Sci.* **2016**, *2*, 778-789.
57. Egorova, K. S., Ananikov, V. P. *Angew. Chem. Int. Ed.* **2016**, *55*, 12150-12162.
58. Bistri, O., Correa, A., Bolm, C. *Angew. Chem. Int. Ed.* **2008**, *47*, 586-588.
59. Jalalian, N., Ishikawa, E. E., Silva, L. F., Olofsson, B. *Org. Lett.* **2011**, *13*, 1552-1555.
60. Bielawski, M., Aili, D., Olofsson, B. *J. Org. Chem.* **2008**, *73*, 4602-4607.
61. Ali, M. H., Buchwald, S. L. *J. Org. Chem.* **2001**, *66*, 2560-2565.
62. Wang, X., Jang, H.-Y. *Bull. Korean Chem. Soc.* **2012**, *33*, 1785-1787.

Chapter 3: Synthesis of
dibenzofurans *via*
intramolecular direct
arylation of *ortho*-bromo
diarylethers

3.1 Preface

An efficient construction of dibenzofuran motifs through a ligand enhanced palladium catalysed direct arylation of *ortho*-bromo diarylethers is described in this **Chapter**. Furthermore, the scope and limitations of this reaction will be discussed.

3.2 Background

As discussed in **Chapter 1** of this thesis, a number of useful methods have emerged for the synthesis of dibenzofurans. Considering the problems associated with traditional and dehydrogenative coupling reactions (as previously outlined in **Chapter 1**), the transition metal catalysed cyclisation of mono-halogenated diarylethers *via* C-H activation is a particularly attractive route and is relatively less explored. Led by Ames and co-workers¹ in the 1980s and subsequent work by a number of different groups²⁻⁴, this would seem like a go to method for the synthesis of dibenzofurans. However, a number of challenges still remain as previously discussed in **Chapter 1**. Thus, the main focus of this **Chapter** was focused on addressing some of these challenges. Moreover, the following **Chapter** describes the optimisation and development of an efficient set of reaction conditions enhanced by a cheap, bench stable and commercially available quinoline ligand for the intramolecular cyclisation of *ortho*-bromo diarylethers (**Figure 22**).

This work

Dibenzofuran synthesis

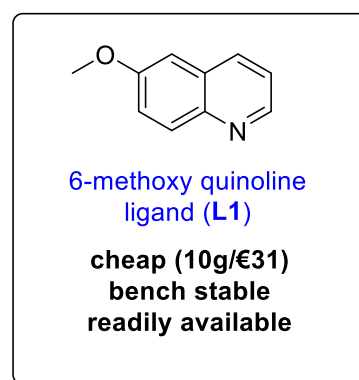
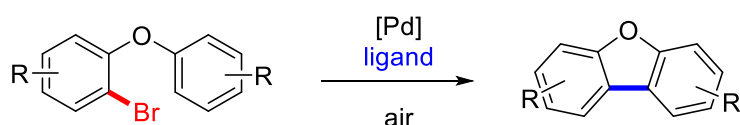
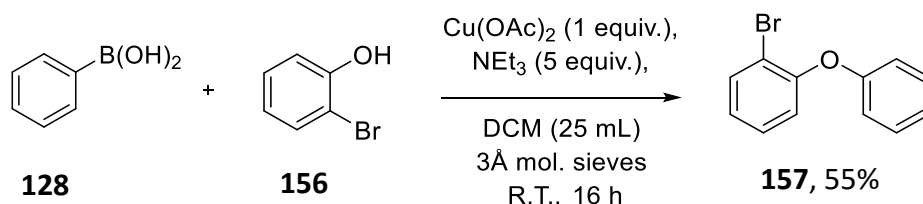


Figure 22. Focus of this research.

A detailed review by Yu and Engle⁵ in 2013 described that in order for novel C-H activation reactions to be developed, '*the reactions must be operationally simple and robust*'. They further noted that reactions with '*substrates, coupling partners, catalysts and ligands that are*

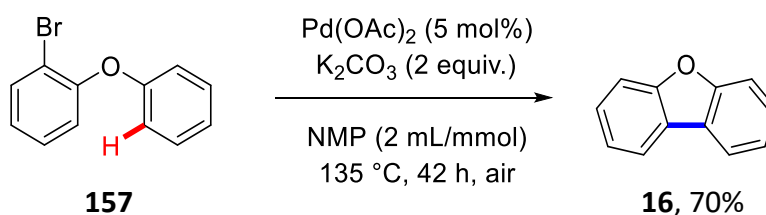
commercially available or easily accessible are preferable. In addition, *reactions that do not require special equipment and can be set up on the benchtop without rigorous exclusion of air or moisture are desirable.* Thus, some of these aspects were taken into consideration during the course of the work described in this **Chapter**.

To begin, *ortho*-bromo diarylether was chosen as the model substrate. Substrate **157** was synthesised *via* a copper mediated Chan-Lam-Evans coupling of phenyl boronic acid (**128**) 2-bromo phenol (**156**) in the presence of triethylamine as base. Purification by column chromatography provided the product **157** in 55% yield (**Scheme 49**).



Scheme 49. Synthesis of *o*-bromo diarylether (**157**).

To achieve the intramolecular cyclisation of **157**, conditions previously optimised by Dr. Rachel Shanahan for the intramolecular cyclisation of 4-(2-bromophenoxy)quinoline substrates were adopted.⁶ Direct application of these reaction conditions allowed formation of the fused dibenzofuran product **16** in 70% yield, as determined by ^1H NMR spectroscopy using 1,3,5-trimethoxybenzene as internal standard (**Scheme 50**). Attempts to drive the reaction to completion failed. After 42 hours, complete consumption of starting material **157** could not be achieved. Furthermore, separation of product **16** from starting material **157** by column chromatography in 100% hexanes proved difficult owing to similar polarities of **16** and **157**. Hence, it was decided that further optimisation of the reaction conditions was necessary.

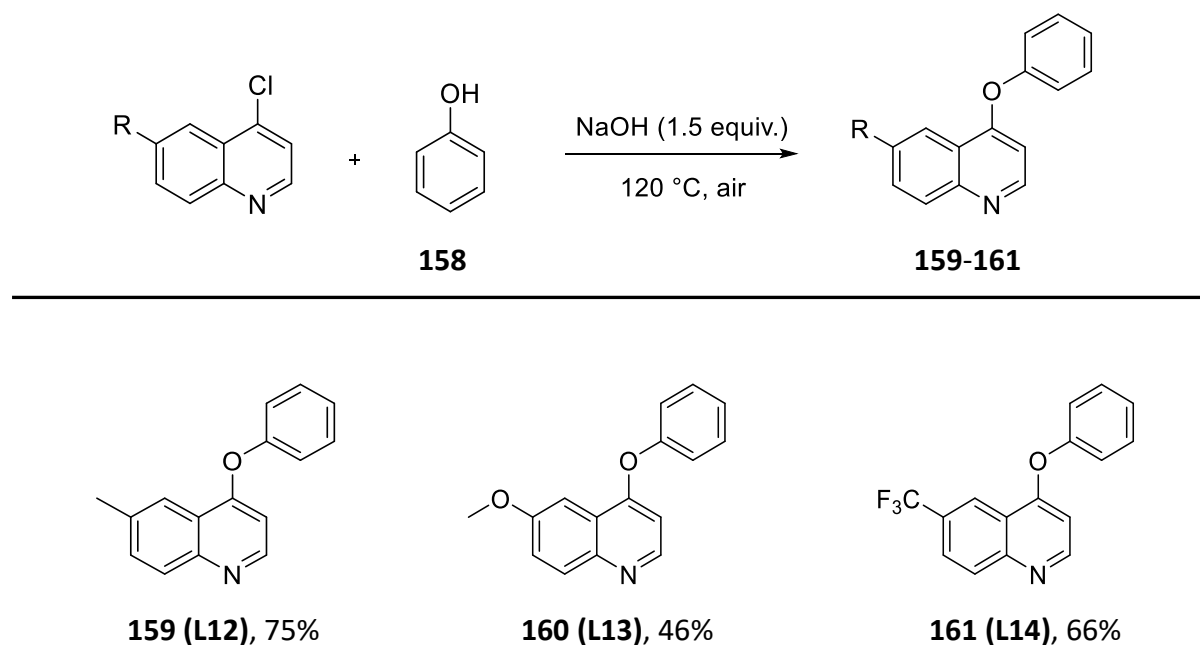


Scheme 50. Initial reaction conditions for the direct arylation of **157**.

3.3 Ligand Identification

It was decided to test a number of quinoline and pyridine additives with a view towards addressing some of the limitations discussed above and in **Chapter 1** of this thesis in the classic intramolecular direct arylation of *ortho*-bromo diarylethers. This was based on previous reports on the use pyridine and quinoline ligands in Pd catalysed C-H activation reactions, particularly by the groups of Yu and Sanford.⁷⁻¹⁵ Additionally, our group had recently discovered that simple quinolines can act as both a substrate and ligand in the arylation of quinolines.¹⁶

The majority of pyridine and quinoline ligands examined in the direct arylation of *o*-bromo diarylether were purchased from a commercial supplier. Benzofuroquinoline (**L15**) and phenoxy quinoline (**L11**) were synthesised by another member of the McGlacken group. Phenoxy quinolines **L12**, **L13** and **L14** were easily prepared in moderate yields (46-75%) by reaction of the corresponding 6-substituted-4-chloroquinoline with phenol (**158**) in the presence of sodium hydroxide. This transformation proceeds *via* nucleophilic attack of the phenoxide anion (generated *in situ*) on the 4-position of the quinoline (**Scheme 51**).

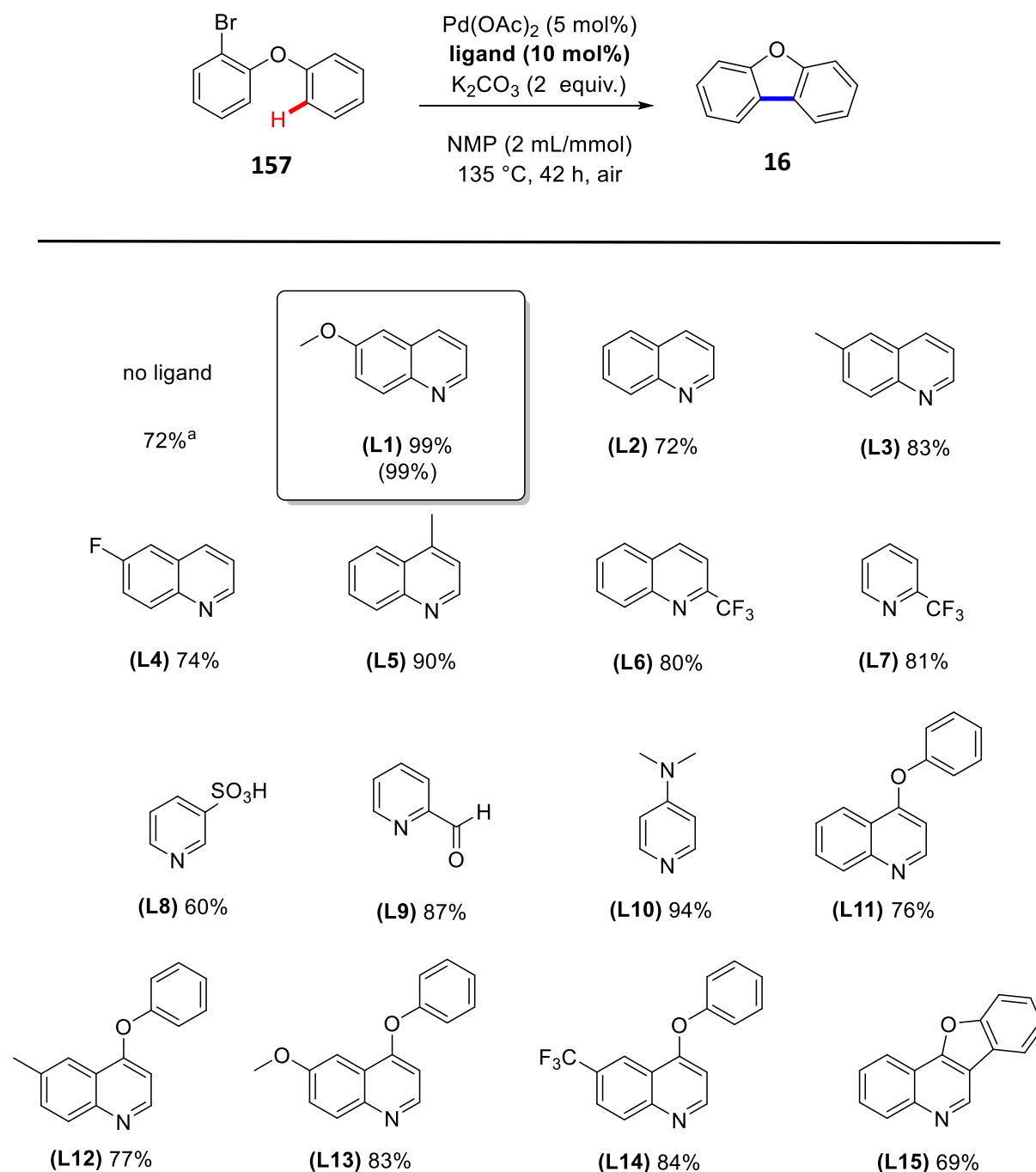


Scheme 51. Synthesis of 4-phenoxy quinolines **159-161**.

A series of monodentate pyridine and quinoline type ligands varying in electronic and steric character were evaluated (**Scheme 52**). The addition of 10 mol% quinoline (**L2**) resulted in no improvement in the yield of **16** compared to the no added ligand reaction. Both of these reactions only reached *ca.* 70% conversion to **16**. Yu had previously utilised quinoline as a ligand in the Pd catalysed *meta*-C-H arylation and alkylation of benzylsulfonamides.⁸ Three quinoline based ligands with substituents at C-6 on the quinoline ring were investigated (**L1**, **L3** and **L4**). Pleasingly, incorporation of electron donating groups at C-6 allowed for $\geq 90\%$ consumption of starting material **157**. Satisfyingly, **L1** containing a methoxy group facilitated complete consumption of starting material **157** and afforded **16** in a 99% isolated yield. Use of **L3** (containing a methyl group at C-6) allowed for 90% consumption of starting material **157** and a yield of 83%. Notably, addition of a fluoro group at C-6 (**L4**) only had a minimal impact on the yield of **16** in comparison to the no added ligand reaction (74% versus 72% respectively). The yield of **16** was also improved to 90% when a methyl group was positioned at C-4 in **L5**. Incorporation of a strongly electron withdrawing group at the C-2 position of quinoline and pyridine surprisingly did lead to an increase in yield of **16** (**L6**, 80% and **L7**, 81% respectively). Yu, Stoltz, Fagnou and Stahl previously had demonstrated the applicability of electron deficient pyridine and pyridone ligands in Pd catalysed C-H functionalisation reactions, suggesting that they either act to stabilise Pd⁰ before re-oxidation or they can facilitate the formation of a more electrophilic and therefore more reactive Pd catalyst.^{7, 17-19} An electron deficient metal center could be beneficial in accelerating key steps in the catalytic cycle such as reductive elimination or C-H bond cleavage *via* a CMD type mechanism. In addition, strong non-covalent F $\cdots \pi$ interactions (dispersion forces) between the aryl ring of the substrate and the fluoro/trifluoromethyl substituent on the pyridine ligand, could result in increased stability of a Pd-aryl intermediate species during the catalytic cycle. This type of interaction has been documented in electron poor Pd phosphine systems resulting in increased stability of the Pd complex.²⁰ Finally, an electron deficient trifluoromethyl pyridine/quinoline ligand could equally facilitate substrate binding by providing a vacant site on Pd by undergoing a more facile displacement from the metal center.²¹

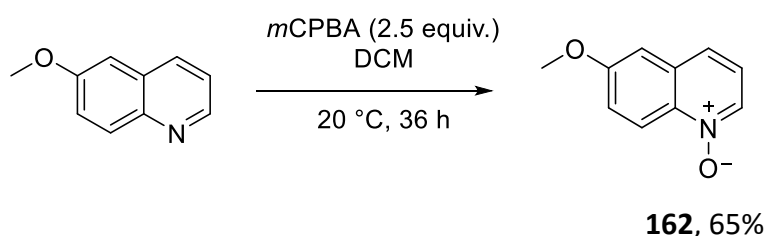
DMAP (**L10**) also performed excellently providing **16** in a yield of 94%. Likewise, use of pyridine carboxaldehyde (**L9**) gave a yield of 87% for the cyclized product. Overall, the more sterically bulky phenoxy quinoline ligands (**L11-L14**) performed less well with yields ranging from 76-

84%. Changing to 3-pyridine sulfonic acid as ligand (**L8**),²² led to a significant decrease in yield (60%). Finally, the sterically encumbered benzofuroquinoline (**L15**) was less effective and did not appear to enhance the reaction, giving the cyclised product **16** a yield of 69%.



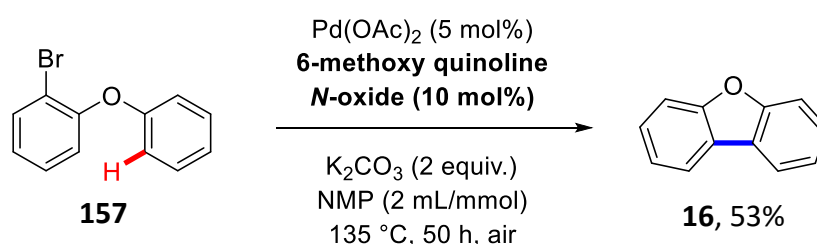
Scheme 52. Ligand evaluation for Pd catalysed direct arylation of *ortho*-bromo diarylether (**157**). Yields were determined using ¹H NMR spectroscopy with 1,3,5-trimethoxybenzene as the internal standard. Isolated yields in parenthesis. ^aAverage of three reactions.

6-Methoxy quinoline *N*-oxide (**162**) was also examined in the direct arylation of *ortho*-bromo diarylether. Firstly, 6-Methoxy quinoline (**L1**) was readily oxidised to the corresponding *N*-oxide using *m*CPBA to yield the product **162** in 65% yield following purification by flushing the crude compound through a plug of silica using DCM/MeOH (**Scheme 53**).



Scheme 53. Synthesis of 6-methoxy-quinoline *N*-oxide (**162**).

Addition of 10 mol% 6-methoxy quinoline *N*-oxide (**162**) to the reaction only led to a 53% yield after 50 hours (**Scheme 54**). This was in contrast to the no added ligand reaction, which allowed for a 72% yield and was in stark contrast to the reaction carried out with 10 mol% 6-methoxy quinoline (**L1**), which allowed for full consumption of starting material **157** and a 99% yield of product **16**. This would indicate that the *N*-oxide additive is inhibiting catalysis and may provide some evidence of coordination of the quinoline nitrogen to the Pd, which may be facilitating the direct arylation reaction.

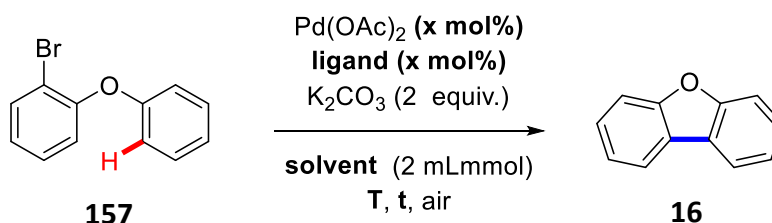


Scheme 54. Direct arylation with 6-methoxy quinoline *N*-oxide (**162**).

3.4 Optimisation of reaction conditions

We next sought to improve the reaction conditions with the optimal ligand (**Table 11, L1**). Hence, a variety of reaction parameters were assessed. These included examining different catalyst loadings, as well as investigating the affect different catalyst:ligand ratios had on the outcome of the reaction. A number of greener solvents were additionally investigated.

As shown in **Table 11**, decreasing the catalyst loading to 2 mol% Pd(OAc)₂ and 4 mol% **L1** led to a decrease in yield of **16** (**Table 11, entry 1**). This was in comparison to when 5 mol% Pd(OAc)₂ and 10 mol% **L1** were employed (81% versus 99% respectively). Employing 2 mol% Pd(OAc)₂ and 4 mol% DMAP (**L10**), allowed **16** to be obtained in 70% yield (**Table 11, entry 2**). Decreasing the catalyst loading even further to 1 mol% Pd(OAc)₂ and 3 mol% **L1** lead to a dramatic decrease in yield of **16**, 58% (**Table 11, entry 3**). Pleasingly, the combination of 2.5 mol% Pd(OAc)₂ and 7.5 mol% of **L1** (**Table 11, entry 4**) allowed for full consumption of starting material **157** and provided **16** in an isolated yield of 99%. As a control, the reaction was carried out without any added ligand each time the catalyst loading was reduced (**Table 11, entries 3, 5 and 8**) and importantly, no increase in conversion and yield of **16** was achieved. Further tuning of the reaction conditions by changing the solvent failed to improve results (**Table 11, entries 9-11**). The reaction carried out in 1,4-dioxane only allowed for a 50% yield of **16**, after 63 hours (**Table 11, entry 11**). The greater reaction efficiency observed with NMP, may suggest that NMP may be involved in the stabilisation of charged intermediates during the catalytic cycle, as well as facilitating catalyst activation.^{18, 23-24} The stabilisation of Pd⁰ nanoparticles by NMP is also well established in the literature.²⁵⁻²⁶ It is possible that NMP may be providing a similar stabilising effect in our case. Finally, the reaction time could be reduced to 22 hours (**Table 11, entries 4 and 7**).

Table 11. Optimisation of direct arylation conditions for *ortho*-bromo diarylether (**157**).

Entry	Pd(OAc) ₂ (mol %)	Ligand (L1) (mol %)	Solvent	Temperature (°C)	Time (h)	Yield ^a (%)
1	2	4	NMP	135	42	81
2	2	4 ^b	NMP	135	42	70
3	2	-	NMP	135	42	58
4	2.5	7.5	NMP	135	22	100 (99)
5	2.5	-	NMP	135	42	59
6	1	3	NMP	135	22	44
7	5	10	NMP	135	22	100 (99)
8	5	-	NMP	135	42	72
9	5	10	DMSO	135	36	0
10	5	10	Ethylene carbonate	135	42	8
11	5	10	1,4-dioxane	110	63	50

^aYields were determined using ¹H NMR spectroscopy with 1,3,5-trimethoxybenzene as the internal standard. Isolated yields in parenthesis. ^bDMAP was used as the added ligand.

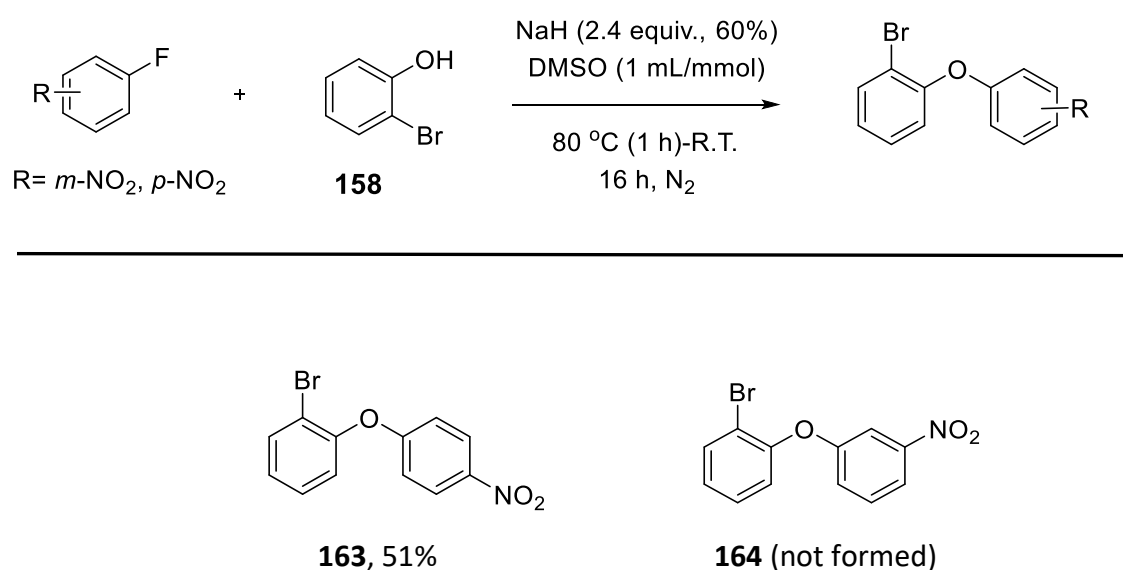
Thus, the optimised conditions established for the direct arylation reaction were 5 mol% Pd(OAc)₂, 10 mol% 6-methoxy quinoline (**L1**), 2 equivalents of K₂CO₃ in NMP (2 mL/mmol) at 135 °C for 22 hours. It is worth noting the cheap cost of 6-methoxy quinoline. 10g are available for €31.²⁷

3.5 Synthesis of *ortho*-bromo diarylether starting materials

With the optimised conditions in hand, an examination of the functional group tolerance was undertaken. For this investigation, a range of substituted analogues with electron rich and electron poor substituents were synthesised. Three separate protocols were adopted for the synthesis of the starting materials. This was in part due to the difficulties encountered in the applicability of a general procedure for the synthesis of a diverse range of *ortho*-bromo substituted diarylethers.

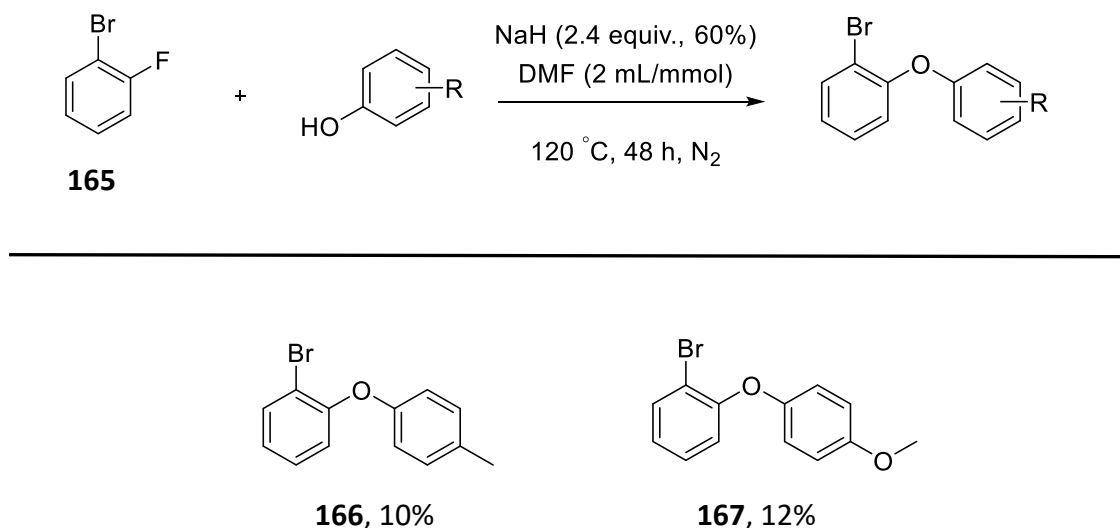
3.5.1 Starting material synthesis *via* nucleophilic aromatic substitution

The synthesis of two nitro substituted *ortho*-bromo diarylethers were attempted by coupling of the appropriately substituted fluorobenzene and 2-bromo phenol (**156**). This procedure was adopted from Ames 1983 paper on the direct arylation of *ortho*-bromo diarylethers.¹ The reaction proceeds *via* nucleophilic attack of the phenoxide anion generated *in situ* on the fluorobenzene in a straightforward nucleophilic aromatic substitution. In the case of the highly activated *para*-nitro fluorobenzene, the reaction occurred at room temperature. Precipitation of the solid after addition of water followed by recrystallisation from ethanol provided the product **163**, in 51% yield. Reaction of 2-bromo phenol (**156**) with *meta*-nitro fluorobenzene failed to allow for satisfactory conversion to desired product (**Scheme 55**).



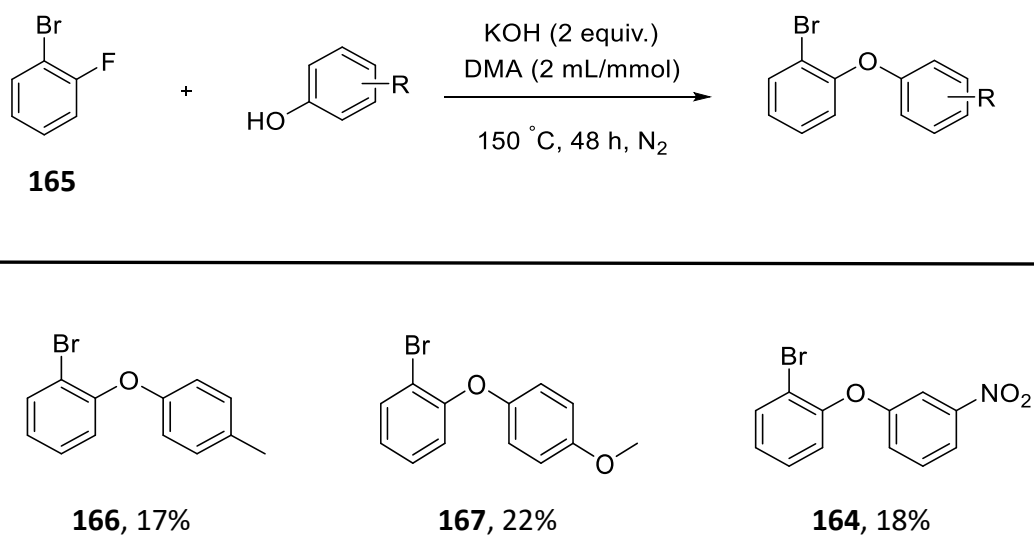
Scheme 55. Synthesis of nitro substituted diarylethers.

Further substrates were prepared in a similar fashion to **163** using the appropriately substituted fluorobenzene as the electrophile and the corresponding substituted phenols (**Scheme 56**). The desired products were prepared albeit in poor yields (10% and 12%) for the two electron donating substrates **166** and **167** respectively.



Scheme 56. Synthesis of compounds **166** and **167**.

Modification of the reaction conditions allowed for slightly higher yields of **166** and **167** to be achieved. Upon switching the base to KOH and solvent to DMA, as well as increasing the temperature to 150 °C, **166** and **167** were furnished in 17% and 22% yield respectively following isolation by silica gel column chromatography (**Scheme 57**). In addition, modification of the reaction conditions allowed the *meta*-nitro analogue **164** to be prepared in a synthetically useful yield of 18%.



Scheme 57. Improved yields of **164**, **166** and **167** using above modified conditions.

Unfortunately, a number of reactions resulted in very poor conversion to product. Instead, a complex mixture of degradation products, in addition to trace amounts of products were observed. Access to a number of these substrates were accomplished *via* alternative routes which will be discussed later in this chapter (**Figure 23**).

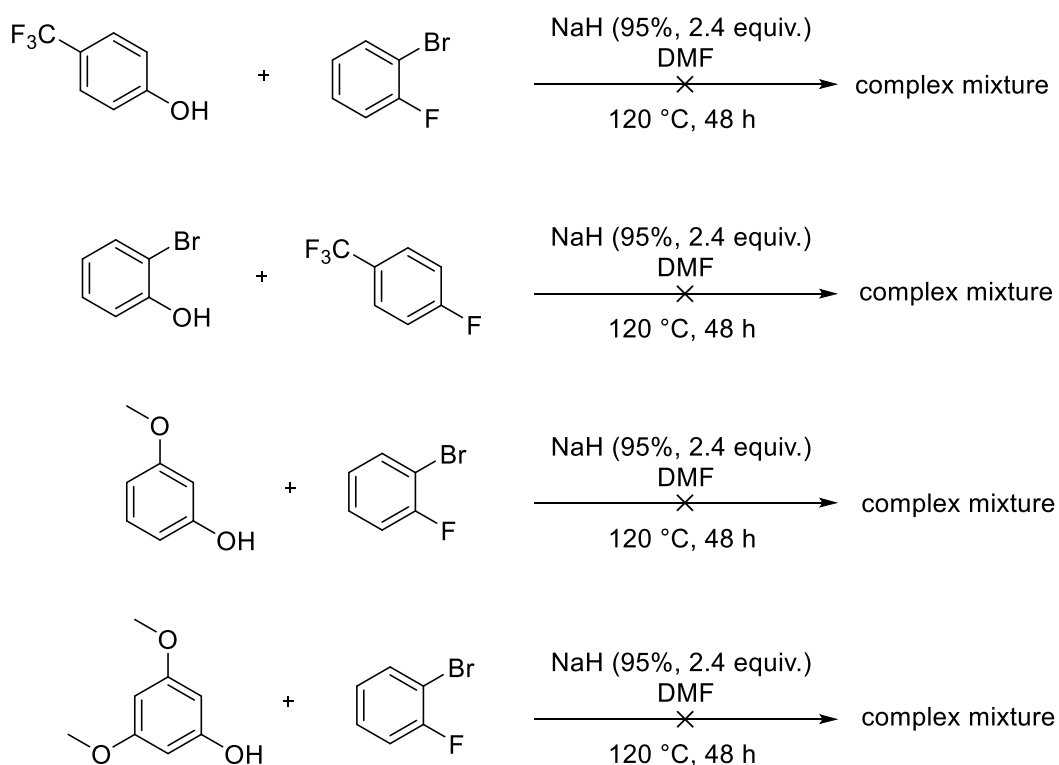
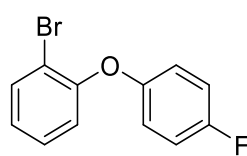
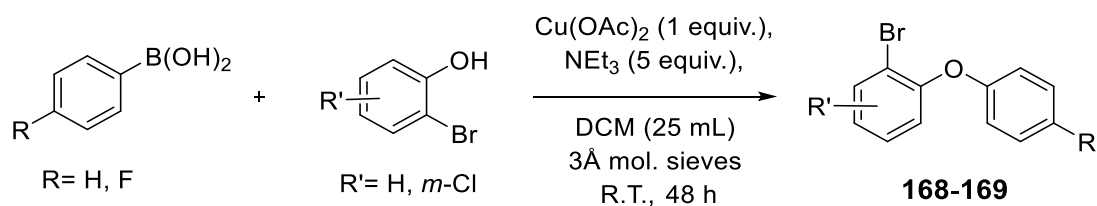
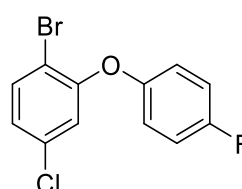


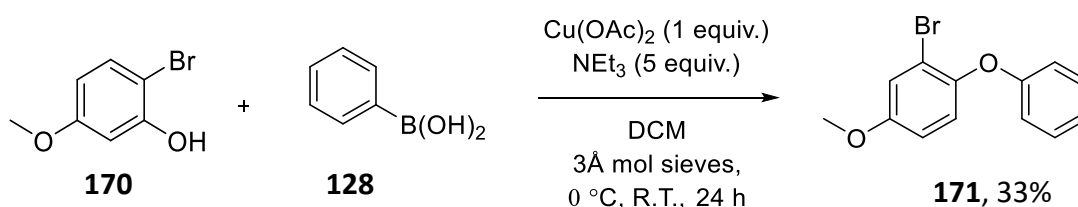
Figure 23. Substrates which resulted in poor conversions to products.

3.5.2 Starting material synthesis *via* Chan-Lam-Evens arylation of phenols and phenyl boronic acids

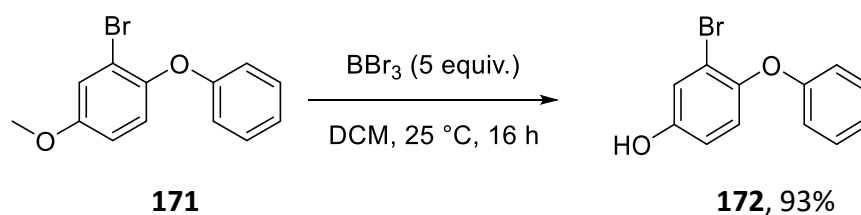
Compounds **168-169** were synthesised using Chan-Lam-Evens copper mediated coupling of phenyl boronic acids and *ortho*-bromo substituted phenols (**Scheme 58**).²⁸⁻³⁰ Purification *via* silica gel column chromatography yielded the products in yields ranging from 31-72%. It should be noted that the yields obtained for this type of reaction are extremely dependent on the nature of the substrate and also the substitution on the phenyl boronic acid. This is well documented in the literature.³⁰

**168**, 72%**169**, 31%**Scheme 58.** Synthesis of *ortho*-bromo diarylethers **168-169** via Chan-Lam-Evans coupling.

Two substrates with electron donating substituents were also synthesised through the copper promoted Chan-Lam-Evans arylation of phenols with aryl boronic acids. Reaction of 2-bromo-4-methoxy phenol (**171**) (synthesised by Dr. David Jones) with phenyl boronic acid (**128**) yielded **172**, albeit in low yield of 33% following isolation by silica gel column chromatography.

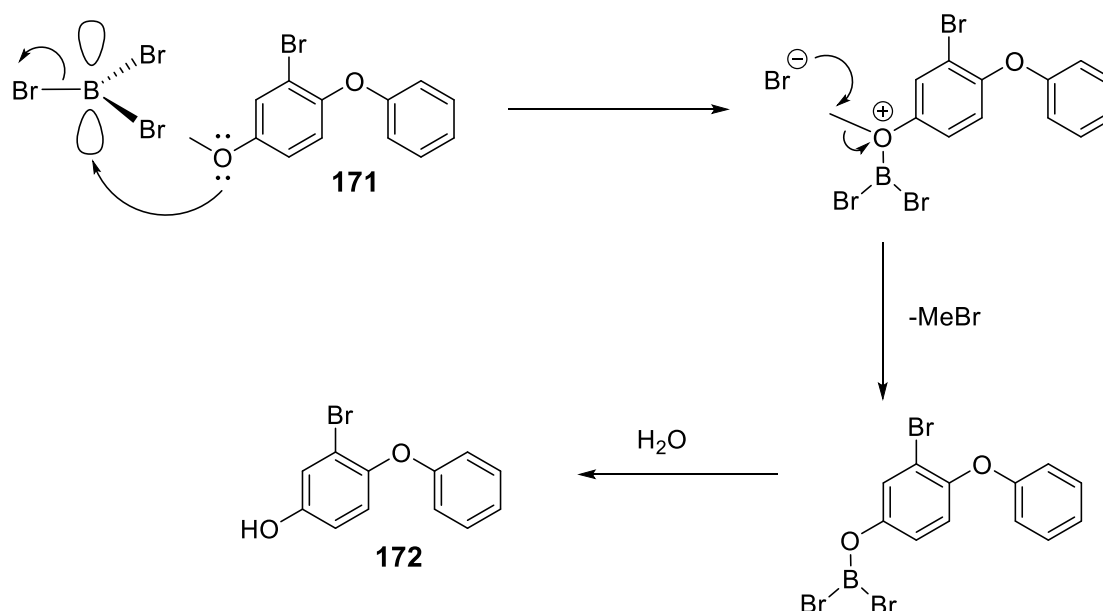
**Scheme 59.** Synthesis of diarylether **171** via Chan-Lam-Evans coupling.

To further expand the substrates scope, diarylether **171** was conveniently converted to the hydroxylated product **172** based on a procedure by Wiegrebé.³¹ The methyl ether was successfully cleaved by treating **171** with 5 equivalents of BBr₃ in DCM. Pleasingly, the reaction went to completion after 16 hours to give the hydroxylated product **173** in 93% yield.



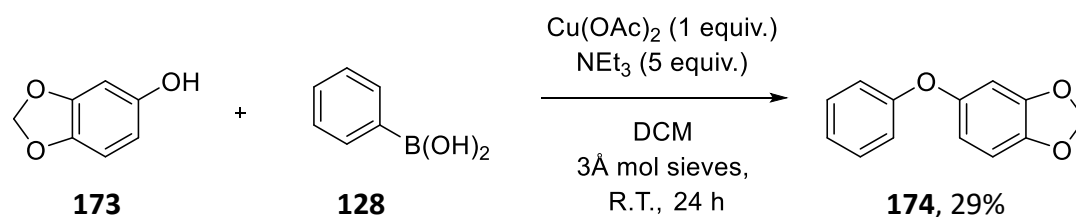
Scheme 60. Cleavage of the methyl ether group **171**.

A potential mechanism for the demethylation reaction is provided in **Scheme 61**, which involves the generation of a cation on the oxygen of the methoxy group and loss of a bromide anion. Nucleophilic attack of the bromide anion on the methyl group of the cationic intermediate cleaves the C-O bond, with loss of MeBr. Finally, aqueous hydrolysis gives the final product **172**.



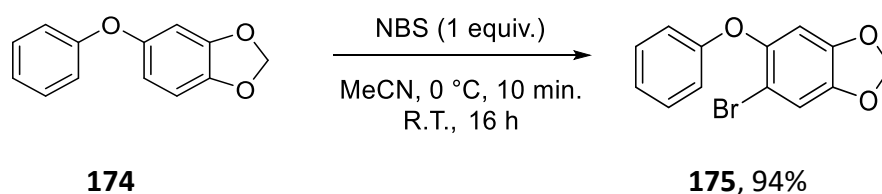
Scheme 61. Potential mechanism for demethylation of **171**.

The benzo[1,3]dioxole ring system is found in many drug molecules and is an important intermediate in the synthesis of many natural products.³²⁻³⁴ Hence, synthesis of a benzo[1,3]dioxole analogue was of interest. Dioxole analogue **174** was synthesised *via* coupling of sesamol (**173**) with phenyl boronic acid (**128**) to yield the product in 29% yield (**Scheme 62**). Previous attempts to couple 2-bromo sesamol with phenyl boronic acid (**128**) proved unsuccessful. Therefore, a new strategy had to be adopted whereby the non-brominated analogue **174** was synthesised initially, prior to bromination of the sesamol ring.



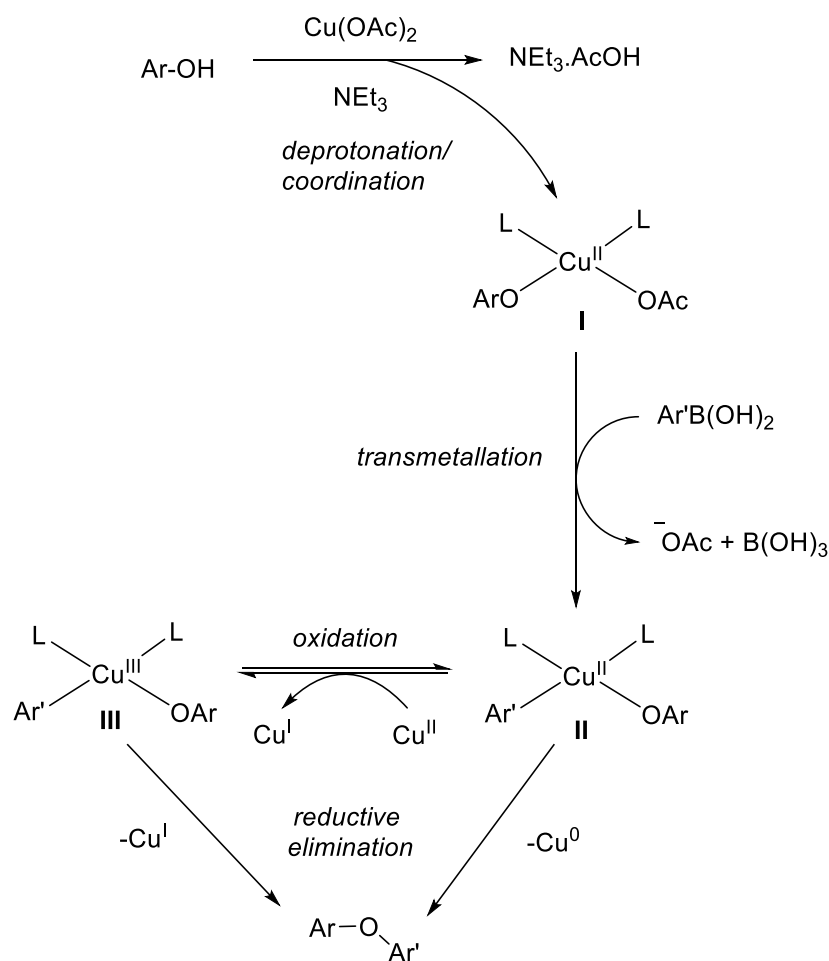
Scheme 62. Synthesis of diarylether **174**.

Compound **174** was brominated in a facile manner using 1 equivalent of NBS in acetonitrile.³⁵ The reaction was stirred at 0 °C for 10 minutes and warmed to room temperature overnight. Following column chromatography on silica gel using hexane as eluent, the desired product **175** was isolated in 94% yield (**Scheme 63**).



Scheme 63. Bromination of compound **174**.

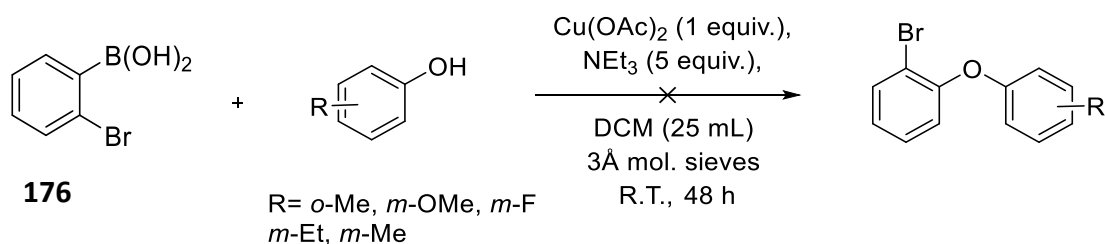
A general mechanism for the Chan-Lam-Evans arylation of phenols with phenyl boronic acids is outlined in **Scheme 64**. The first step involves initial deprotonation of the phenol followed by coordination of the phenoxide anion to a Cu(II) species to give **I**. Transmetalation of the organoboron species with the Cu(II) species (**I**) gives an aryl Cu(II) phenoxide intermediate (**II**) bearing the two coupling partners and this is believed to be the turnover limiting step. This intermediate can then undergo reductive elimination or could be oxidised to Cu(III) *via* disproportionation with a second equivalent of Cu(OAc)_2 to give **III** (and a Cu(I) complex). The latter is more likely to occur.³⁶ This is followed by reductive elimination to yield the diarylether product. Reductive elimination from a Cu(III) species is proposed to proceed faster than from a Cu(II) species. Completion of the catalytic cycle is achieved *via* oxidation to Cu(II) and this is proposed to be facilitated by O_2 , $\text{NEt}_3\cdot\text{AcOH}$ and BX(OH)_2 . This is based on seminal studies by Stahl³⁵ who provided key insights into the mechanism of the Chan-Lam-Evans coupling reaction, and subsequent investigations by Watson and co-workers.³⁷



Scheme 64. General mechanism of the Chan-Lam-Evans coupling reaction.

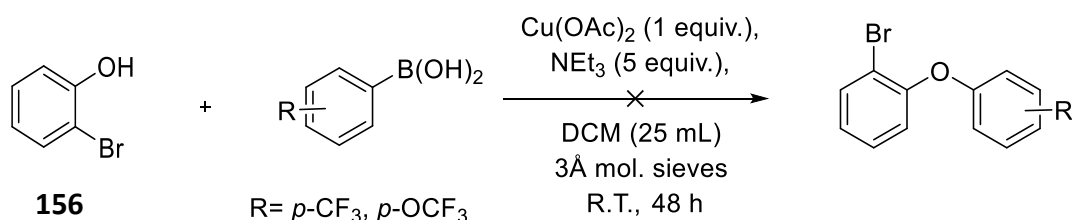
A number of reactions proved unsuccessful using the Chan-Lam-Evans protocol and will be discussed below (**Scheme 65** and **Scheme 66**). Hence, alternative protocols had to be adopted in order to gain access to a more diverse range of substituted *ortho*-bromo diarylethers, to further examine the scope of the direct arylation reaction.

A diverse range of substituted phenols were easily available. As a result, 2-bromo benzene boronic acid (**176**) was chosen as the common boronic acid. Access to substituted phenyl boronic acids was less convenient and would be a more expensive approach. Unfortunately, the reaction proceeded much more sluggishly when **176** was used as the boronic acid coupling partner. Moreover, conversions to diarylether products were very low (**Scheme 65**). This in part may be due to the low nucleophilicity of **176** which would result in slower transmetallation and thus would inhibit the desired C-O bond forming reaction.³⁸



Scheme 65. Unsuccessful substrates employing **176** as the boronic acid coupling partner.

Similarly, the electron poor *para*-trifluoromethylphenyl boronic acid and *para*-trifluoromethoxyphenyl boronic acid were not well tolerated in the reaction (**Scheme 66**). Again, this may be due to the low nucleophilicity of the *para*-CF₃ and *para*-OCF₃ phenyl boronic acids.



Scheme 66. Unsuccessful diarylether substrates employing electron poor phenyl boronic acids.

The Chan-Lam-Evans reaction offers a number of advantages over other transition metal mediated C-O bond formation processes. Traditional processes such as the Ullman reaction requires very high temperatures and often gives variable yields. In contrast, the Chan-Lam-Evans reaction is conducted under much milder oxidative conditions (air or O₂). On the other hand, there are a number of limitations associated with the Chan-Lam-Evans reaction. The yields of the reaction are very much dependent on the nature of the substrate and also the substituents on the boronic acid, for instance, *ortho* substituted and electron poor boronic acids performed poorly, as outlined above. In addition, the Chan-Lam-Evans reaction is significantly hampered by problems with by-product formation. As a consequence, this can lead to variable and diminished yields depending on the substrate. By-products which were identified in the ¹H NMR spectrum of the crude reaction mixtures for several substrates and are well documented in the literature are outlined in **Figure 24**.^{28-29, 37} These by-products arise from oxidation of the phenyl boronic acid due to competitive arylation of water, with oxidative homocoupling of the generated phenol giving rise to diphenylether as a second by-

product. Evans remarked in his original paper that water is generated from the phenyl boronic acid, through triphenylboroxine formation.²⁹ Evans²⁹ and Watson³⁷ noted that conducting the reaction under strictly anhydrous conditions failed to completely suppress the formation of these by-products, although addition of molecular sieves to the reaction mixture is beneficial in lowering production of the oxidation product. Protodeboronation is also a major by-product of the Chan-Lam-Evans coupling reaction. In addition, Watson and co-workers also observed the homocoupling (resulting from coupling of the protodeboronation product) under strictly anhydrous reaction conditions.³⁷ Re-oxidation of Cu(I) to Cu(II) is proposed to have significant implications on the *O*-arylation reaction particularly with respect to by-product formation, with the oxidation of phenyl boronic acid and protodeboronation known to be favoured more by Cu(I) over Cu(II). Therefore, slow Cu(I) to Cu(II) oxidation will consequently lead to increased side reactions occurring. It must be noted that a test reaction of phenyl boronic acid (**128**) and 2-bromo phenol (**156**) was carried out using molecular oxygen as the external oxidant. However, no increase in conversion to product **157** was observed.²⁸

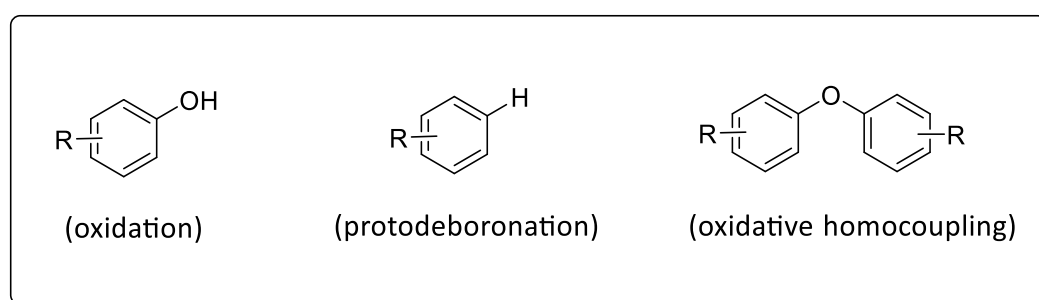
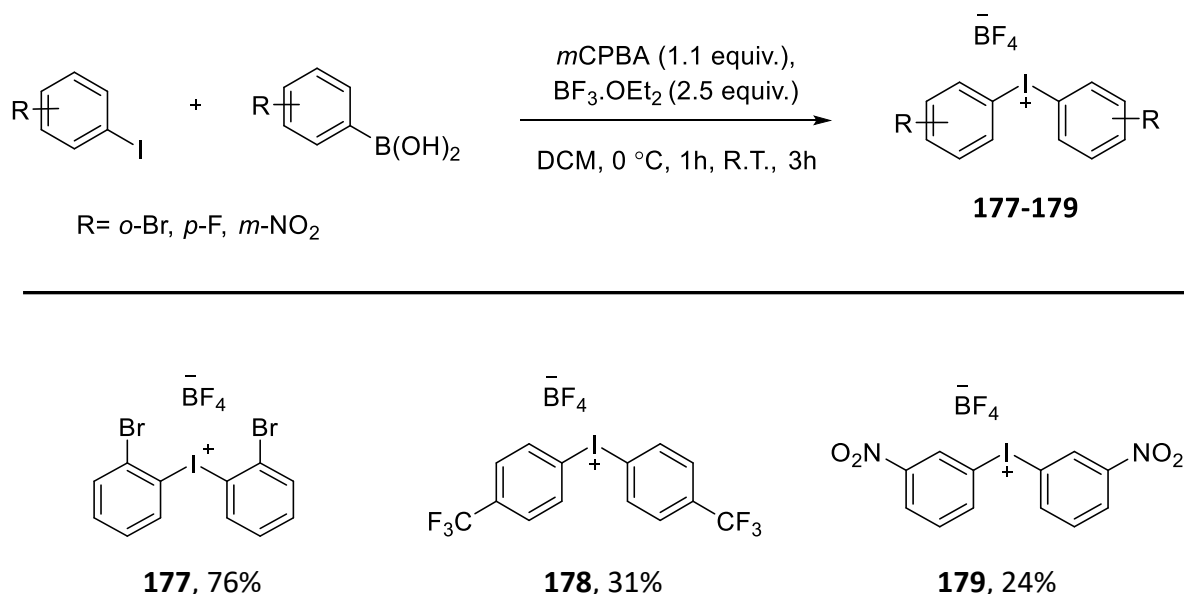


Figure 24. Products from side reactions.

3.5.3 Synthesis of starting materials using iodonium salts

It was of interest to expand the variety of substrates bearing both electron donating and electron withdrawing groups. Hence, an alternative method was employed using tetrafluoroborate iodonium salts in a similar manner to that described in **Section 2.11** using the procedure adopted from Olofsson and co-workers.³⁹⁻⁴⁰ This involved initial preparation of the bis-substituted phenyl iodonium tetrafluoroborate salts by reaction of the relevant substituted iodobenzene and corresponding substituted phenyl boronic acid in the presence of *m*CPBA and boron trifluoride diethyl etherate. The salts were obtained by passing the crude product through a short plug of silica using DCM/MeOH (20:1). Precipitation of the

concentrated filtrate with Et₂O afforded products **177-179** in moderate to good yields (Scheme 67).



Scheme 67. Synthesis of tetrafluoroborate iodonium salts **177-179**.

Bis-(4-trifluoromethoxyphenyl)iodoniumtetrafluoroborate (**180**), bis-(4-fluorophenyl)iodonium tetrafluoroborate (**181**) and bis-(3-trifluoromethylphenyl)iodonium tetrafluoroborate (**182**) were obtained by other members of the McGlacken group (Figure 25).

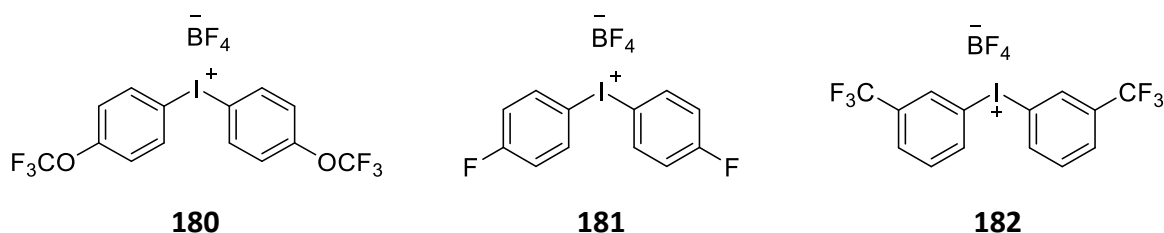
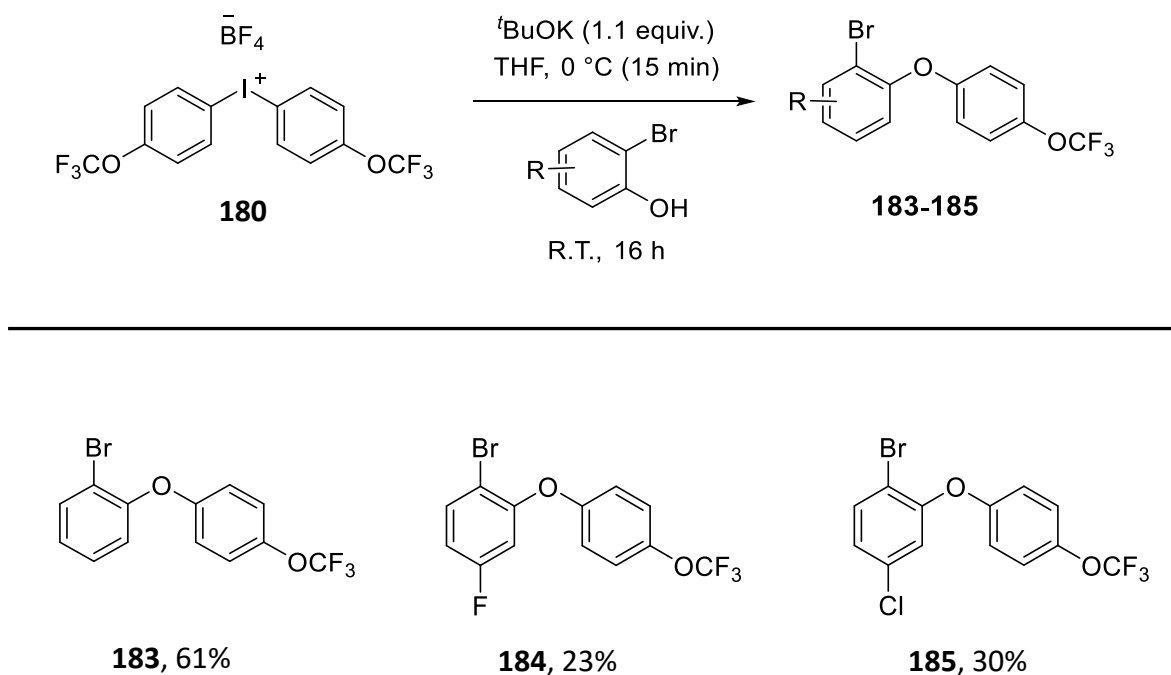


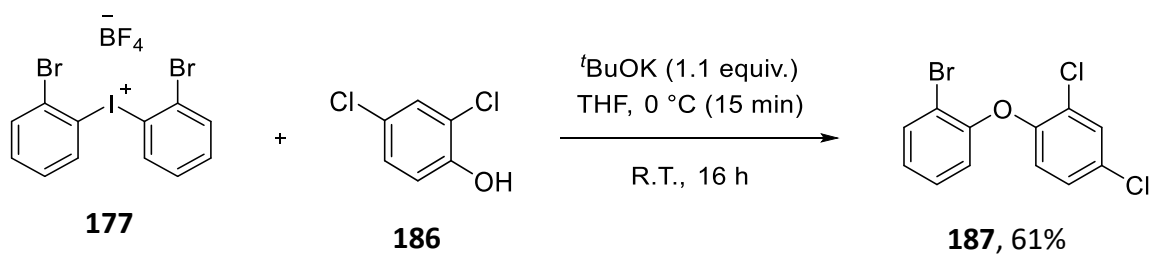
Figure 25. Diaryliodonium salts synthesised in the McGlacken group.

Reaction of iodonium salt **180** with a number of substituted 2-bromo phenols in the presence of ^tBuOK afforded products **183-185**, in yields ranging from 23-61% following purification by column chromatography (Scheme 68). Difficulties were encountered in the purification of the products due to the presence *para*-trifluoromethoxy iodobenzene as a by-product of the reaction in a similar manner to that discussed in Section 2.11.



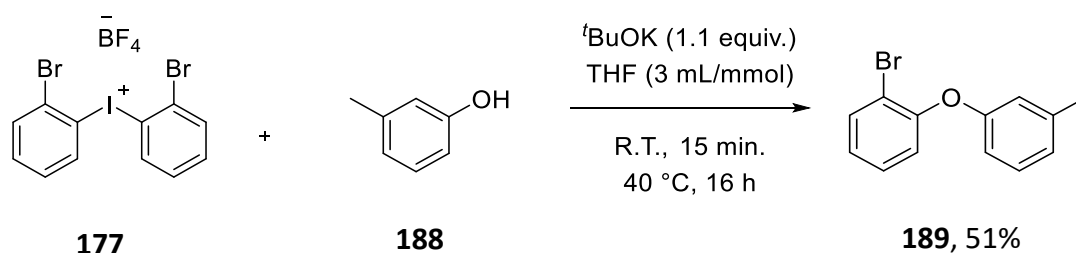
Scheme 68. Synthesis of *para*-trifluoromethoxy substrates **183-185**.

Similarly, reaction of bis-(2-bromophenyl)iodonium tetrafluoroborate (**177**) with **186** provided the di-chloro analogue **187** in 61% yield after purification *via* column chromatography (**Scheme 69**).



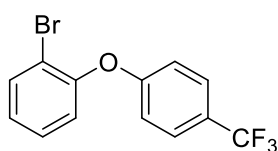
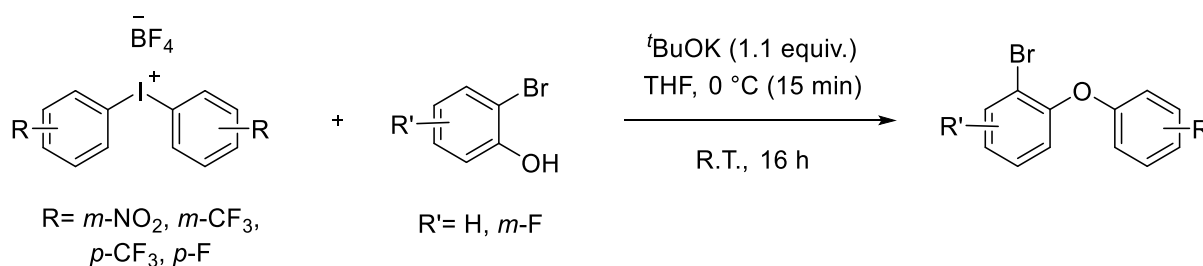
Scheme 69. Synthesis of di-chloro analogue **187**.

Substrate **189** was prepared in 51% yield from **177** and *m*-cresol (**188**) (**Scheme 70**).

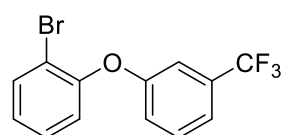


Scheme 70. Synthesis of compound **189**.

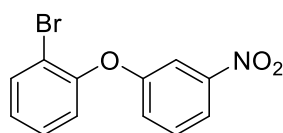
Compounds **190-192** were synthesised in the same manner as described above in yields of 65-80%. Attempts to improve the yield of **164** proved unsuccessful and this product could only be isolated in 15% yield. The presence of a number of by-products as well as difficulties during purification being attributed to the poor yield obtained (**Scheme 71**).



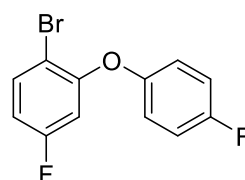
190, 65%



191, 80%



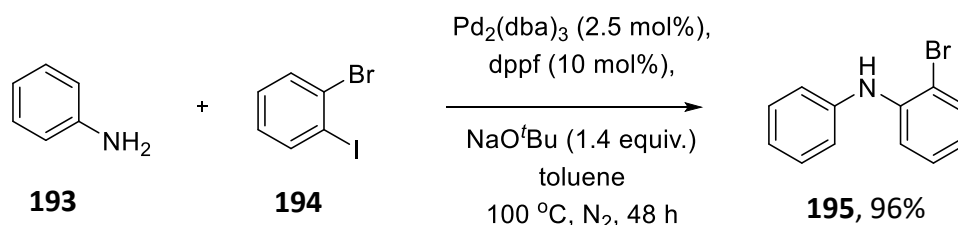
164, 15%



192, 65%

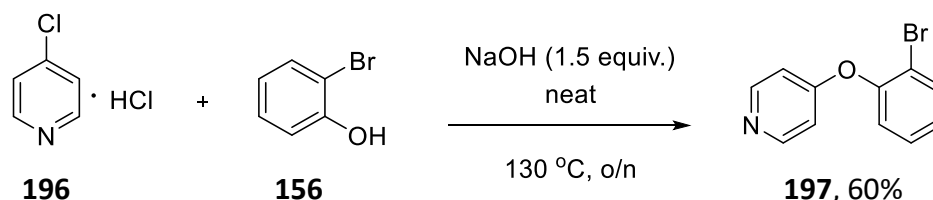
Scheme 71. Synthesis of diarylethers **164, 190-192** via tetrafluoroborate salts.

In an effort to expand the substrate scope beyond dibenzofurans, the ether linker was replaced with an amine. This would allow access to carbazoles which are known to possess a number of important medicinal properties.^{34, 41-44} The amine linked substrate was accessed by performing a Buchwald-Hartwig coupling reaction of aniline (**193**) and 2-bromoiodobenzene (**194**) to afford **195** 96% yield (**Scheme 72**).



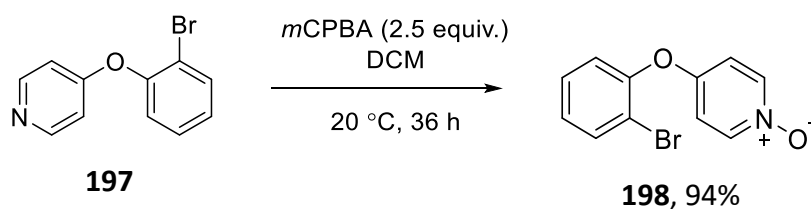
Scheme 72. Synthesis of 2-bromo diphenylamine (**195**).

Like carbazoles, pyridine based compounds are present in many biologically active and pharmaceutically relevant compounds.⁴⁵ Pyridine is the 2nd most frequent occurring ring system in FDA approved drugs.⁴⁶ Reaction of 4-chloro pyridine hydrochloride (**196**) and 2-bromo phenol (**156**) in the presence of NaOH gave **197** in 60% yield (**Scheme 73**).



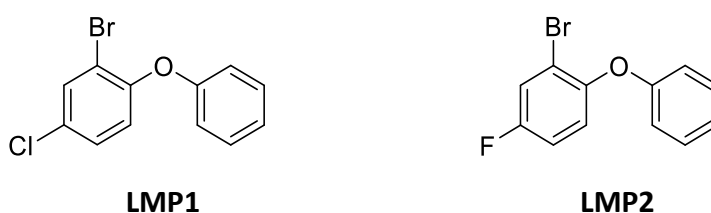
Scheme 73. Synthesis of 4-(2-Bromophenoxy)pyridine (**197**).

Synthesis of the *N*-oxide derivative was undertaken in an attempt to test the efficacy of our reactions conditions to substrates beyond *o*-bromo diarylethers. 4-(2-Bromophenoxy)pyridine (**197**) was subsequently oxidised in a facile manner using 2.5 equivalents of *m*CPBA in DCM to give **198** in 94% yield (**Scheme 74**).



Scheme 74. Synthesis of *N*-oxide derivative (**198**).

Two substrates were synthesised by Dr. Leticia Pardo, a *para*-fluoro and *para*-chloro analogue (**Scheme 75**).



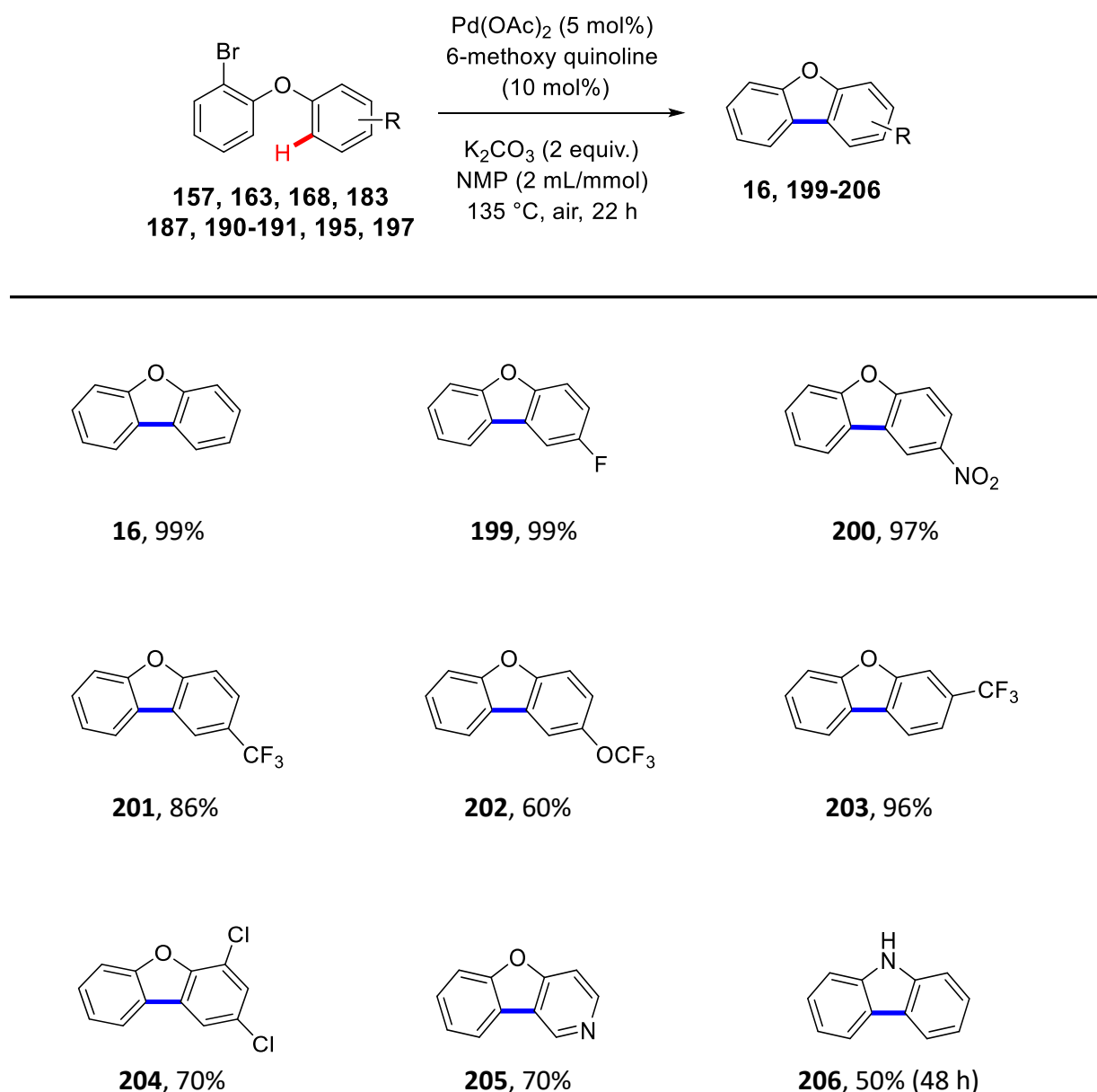
Scheme 75. Substrates synthesised by Dr. Leticia Pardo.

3.6.1 Demonstration of substrate scope for direct arylation of *ortho*-bromo diarylethers

With the optimal conditions in hand, the substrate scope of the reaction was evaluated. Due to the small scale on which the products were synthesised (approx. 0.1 mmol), the physical amount of Pd(OAc)₂ required for a 2.5 mol% loading (<1 mg) was too small to be consistently weighed out. Therefore, to ensure reproducibility, the catalytic loading was increased to 5 mol% Pd(OAc)₂ and 10 mol% **L1** for the substrate scope investigation.

Overall, the optimised direct arylation conditions facilitated smooth cyclisation and substrates bearing electron withdrawing substituents were very well tolerated (**Scheme 76**). This was applicable to both weakly and strongly electron withdrawing substituents (**16**, **199-206**). Compound **199** bearing a valuable fluoride group was obtained in an excellent yield of 99%. Other substrates with more strongly electron withdrawing substituents such as **200** (*para*-nitro) and **201** (*para*-trifluoromethyl) were cyclised in excellent yields of 97% and 86% respectively. In the case of the trifluoromethoxy analogue **202**, a reduction in isolated yield was observed and the fused product was isolated in a 60% yield.

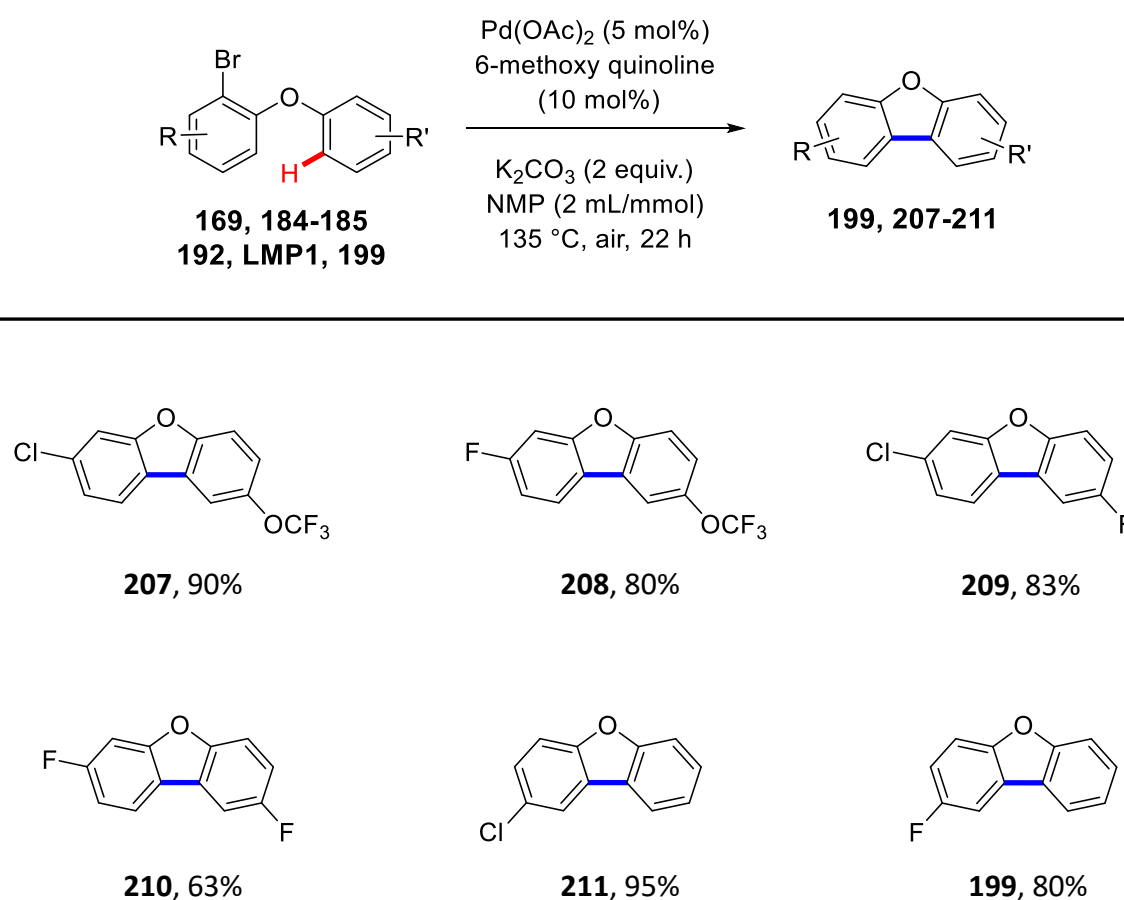
Complete regioselectivity toward the least sterically hindered position was observed for **203** (with a trifluoromethyl substituent) and a single regioisomer was isolated in 96% yield. Additionally, the reaction of a 2,4-dichloro substituted diarylether **187** afforded a 70% yield of **204**. It is noteworthy that whilst complete consumption of **187** was observed in the ^1H NMR spectrum of the crude reaction mixture, a number of extra signals were also apparent. Due to overlapping signals, it was difficult to accurately identify the products corresponding to the extra signals. However, hydrodehalogenation and homo coupling products are the most likely causes of the reduction in yield for **204**. Pleasingly, compound **205** incorporating a potentially problematic pyridine moiety was obtained in a good yield of 70%. Carbazole containing molecules have garnered much interest owing to their diverse biological profiles, hence, synthesis of a carbazole derivative provoked our interests.^{34, 42-44, 47} Pleasingly, application of our optimised direct arylation conditions on the diphenylamine precursor **195**, furnished 9*H*-carbazole **206** in 50% yield. Interestingly, in the absence of **L1**, **206** could only be obtained in 27% yield after 48 hours.



Scheme 76. Demonstration of substrate scope.

Gratifyingly, a number of substrates with electron withdrawing substituents on both aryl rings could be efficiently synthesised in good to excellent yields, allowing access to a number of novel dibenzofurans (**Scheme 77**, **207-210**). Notably, all of these cyclised products feature a fluoro substituent, with some products possessing two fluoro substituents (**208** and **210**). Fluorine containing compounds play a very important role in pharmaceuticals with up to 20% of pharmaceuticals on the market or in clinical development possessing a fluorine atom.

Furthermore, over 50% of blockbuster drugs contain a fluorine atom.⁴⁸⁻⁴⁹ In addition, a number of newly approved pharmaceuticals feature several types of aromatic rings substituted with F and CF₃.⁵⁰ In the case of the *para*-chloro analogue **211** where the chloride was located on the same aryl ring bearing the bromide, the cyclised product was obtained in an excellent yield of 95%. A decrease in isolated yield was obtained for **199** when the fluoro substituent was positioned on the aryl ring bearing the bromide at the *ortho* position (**Scheme 77**, **199**, 80%). This was in contrast to compound **168** where the bromide was located on the adjacent aryl ring to the fluoro substituent. In this case, cyclisation of **168** under the reaction conditions provided **199** in a 99% yield (**Scheme 76**, **50**).



Scheme 77. Demonstration of substrate scope.

3.6.2 Substrates that proved difficult to cyclise

A number of substrates proved difficult to cyclise (**Figure 26**). For example, this was the case for **164** containing a *meta*-nitro substituent and the *N*-oxide compound **198** and may be

attributed to the electronic properties of the substrates proving incompatible with the reaction conditions. Fagnou had previously reported the Pd catalysed direct arylation of pyridine and quinoline *N*-oxides using a Pd/phosphine catalytic system.⁵⁰⁻⁵² In theory, the *N*-oxide moiety should prevent non-productive binding of Pd to the *N*-lone pair, as well as favouring π -binding interactions resulting in a more facile pyridine metalation.⁵¹ In addition, the *N*-oxide should increase the acidity of the adjacent pyridyl C-H bonds and thus facilitate cyclisation. However, in our case, cyclisation of **198** under our optimised reaction conditions resulted in very low yield of desired product. In addition, a number of impurities were still present despite many attempts to obtain pure samples of the dibenzofuran product. Pyridine *N*-oxides are known to undergo decomposition at high temperatures⁵² and this could be a contributing factor to the low yield obtained for the cyclised product. A similar low yield of cyclised product was obtained when the *meta*-nitro analogue **164** was subjected to our optimised reaction conditions. In contrast, an excellent yield was achieved with the *para*-nitro analogue **200** (97%). This would indicate that the position of the nitro group on the aryl ring has a significant effect on the electronics of the reaction.



Figure 26. Compounds which resulted in poor yields.

3.7.1 Investigation into electron rich substrates

Next, a substrate scope involving electron rich substrates was investigated. Additionally, an alcohol and acetate derivative were examined. **LMP3** and **LMP4** were obtained from another member of the McGlacken group (**Figure 27**). It was envisioned that the successful cyclisation of the ester substrate **LMP4** would allow the direct application of our methodology in the short three to four-step synthesis of ruscodibenzofuran, which is a naturally occurring dibenzofuran isolated from the roots of *Ruscus aculeatus* L. (Liliaceae) (**Figure 28**).⁵³ Ruscodibenzofuran had previously been synthesised by Stevenson and co-workers in a seven-step synthesis.⁵⁴



Figure 27. Alcohol and acetate derivative synthesised within the McGlacken group.

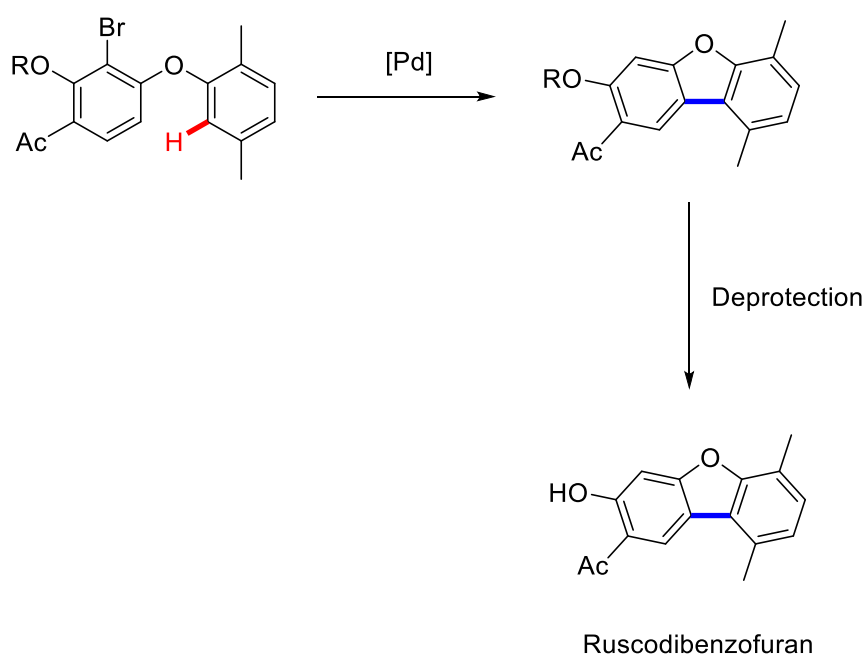
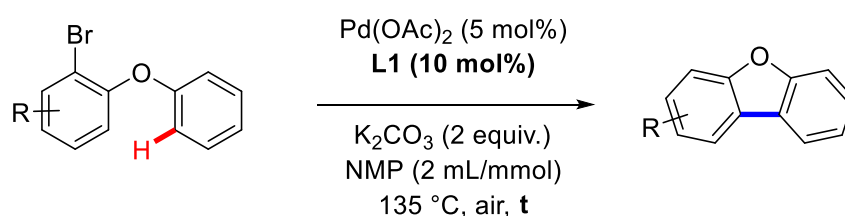


Figure 28. Proposed synthesis of Ruscodibenzofuran.

Firstly, a number of substrates possessing electron donating groups on the aryl ring bearing the bromide were examined (**Table 12**). These two functionalities proved to be incompatible with the reaction conditions, as after 22 hours significant degradation of both starting materials (**LMP3** and **LMP4**) was evident in the ^1H NMR spectrum of the crude reaction mixture (**Table 12**, **entry 1** and **2**). For substrate **171** with a *para*-methoxy substituent, after 48 hours, the reaction conditions failed to allow complete consumption of starting material (**Table 12**, **entry 3**). Similarly, for the sesamol-type substrate **175**, only 30% conversion to product was observed (**Table 12**, **entry 4**). It is postulated that oxidative addition into the C-Br bond for substrates **171** and **175** would be particularly sluggish due to the electron rich

nature of the aryl rings. It is well established that electron poor aryl halides oxidatively add to Pd more readily than the corresponding electron rich aryl halides.⁵⁵ Thus, unfavourable oxidation addition is more than likely a contributing factor in the poor conversions observed for **171** and **175**.

Table 12. Attempted direct arylation of electron rich, hydroxy and acetate substrates.



Entry	Compound	R	Ligand	t (h)	Result ^a
1	LMP3	<i>p</i> -OH	L1	22	Degradation products
2	LMP4	<i>p</i> -OAc	L1	22	Degradation products
3	171	<i>p</i> -OMe	L1	48	62%
4	175	-OCH ₂ O-	L1	24	30%

^aConversion calculated from the percentage of starting material to product in the ¹H NMR spectrum of the crude reaction mixture.

It was then decided to investigate substrates which contained electron donating groups on the aryl ring which was adjacent to the aryl ring bearing the bromide. It was postulated that oxidative addition for such substrates may be more favourable and would allow for improvements in conversions. Substrate **DJ2** was synthesised by Dr. David Jones (**Figure 29**).

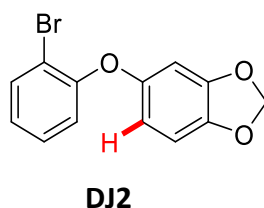
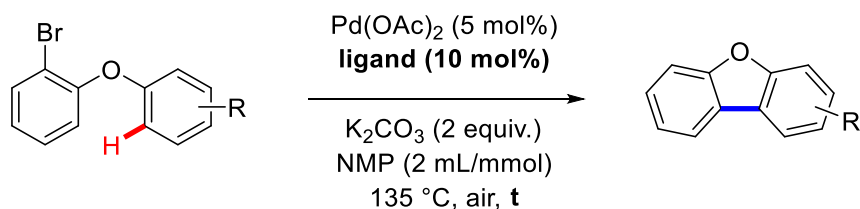


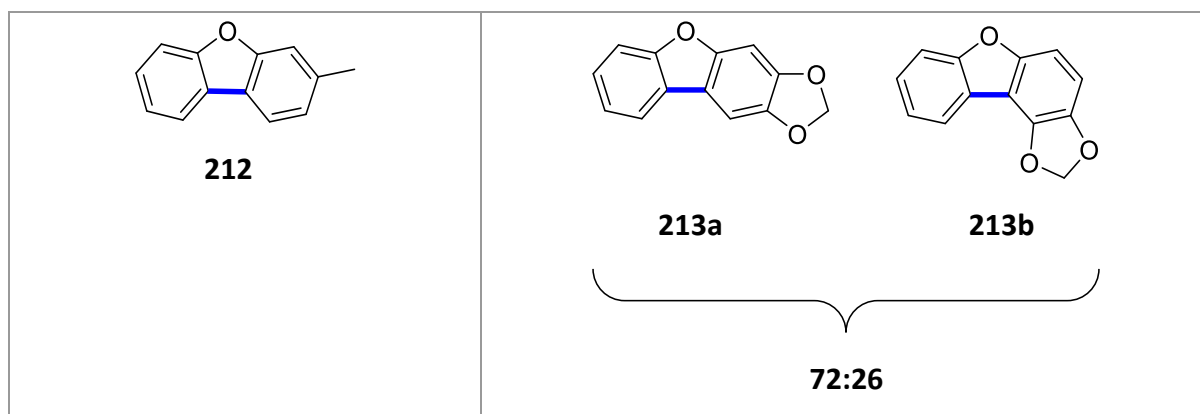
Figure 29. Sesamol derivative **DJ2** synthesised within the group.

Unfortunately, attempts to cyclise **166**, **167**, **189** and **DJ2** using the optimised conditions also proved difficult and disappointingly no substrate underwent complete conversion to product (**Table 13**, entries 1-4). Pleasingly though, the reaction conditions did allow for the selective formation of the least hindered regioisomer **212** for the *meta*-methyl substrate **189**. On the contrary, substrate **DJ2** provided a mixture of regioisomers **213a** and **213b** in a ratio of 72:28, again with reaction preferentially occurring at the least sterically hindered site (**Table 13**). The major regioisomer **213a** was identifiable by a singlet at 7.07 ppm in the ^1H NMR spectrum of the crude reaction mixture, which is distinct from the minor regioisomer **213b**.

Table 13. Attempted direct arylation of electron rich substrates.



Entry	Compound	R	Ligand	t (h)	Conversion (%) ^a
1	166	<i>p</i> -Me	L1	48	60% (42%)
2	167	<i>p</i> -OMe	L1	48	68%
3	189	<i>m</i> -Me	L1	48	64%
4	DJ2	-OCH ₂ O-	L1	48	Mixture of SM DJ2 and regioisomers ^b

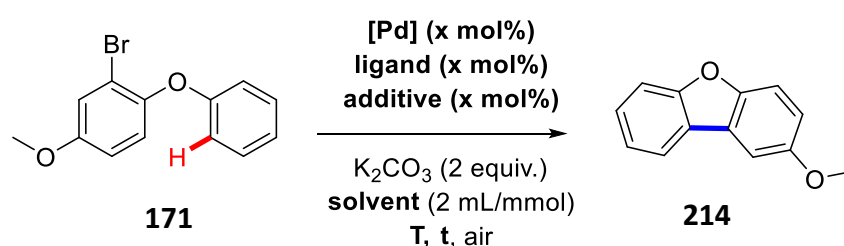


Isolated yield in parenthesis. ^aConversion calculated from the percentage of starting material to product in the ¹H NMR spectrum of the crude reaction mixture. ^bRatio of **DJ2**: **213a**: **213b** determined as 50: 35: 15 from the ¹H NMR spectrum of the crude reaction mixture.

3.7.2 Re-optimisation of direct arylation conditions for electron rich substrates

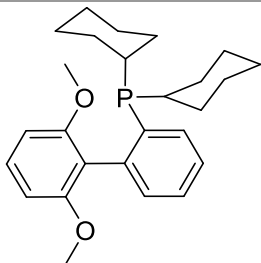
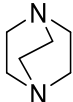
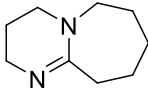
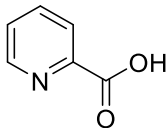
The initially optimised reaction conditions which produced excellent yields for the electron poor substrates failed to induce complete conversion to arylated product when electron rich substrates were employed. This prompted us to reinvestigate the reaction conditions for electron rich substrates. Thus, a brief optimisation screen was carried out on substrates **171** (Table 14), **166** (Table 15) and **167** (Table 16).

Table 14. Optimisation of reaction conditions for direct arylation of **171**.



Entry	[Pd] (5 mol%)	Ligand (10 mol%)	Additive (mol%)	Temp. (°C)	Time (h)	Conv. (%) ^a
1	Pd(OAc) ₂	L1	-	135	48	62
2	Pd(OAc) ₂	-	-	135	48	26

3^b	Pd(OAc) ₂	L1		135	48	50
4	Pd(OAc) ₂	L1	Ag ₂ CO ₃ (50 mol%)	135	24	10
5	Pd(OAc) ₂	L10	-	135	50	66
6	Pd(OAc) ₂	L1	PivOH (30 mol%)	135	48	40
7	Pd ₂ (dba) ₃	L1	PivOH (30 mol%)	135	48	18
8	Pd(OAc) ₂	-	DABCO (10 mol%)	135	48	76
9	Pd(OAc) ₂	-	DBU (10 mol%)	135	48	68
10	Pd(OAc) ₂	Picolinic acid	-	135	48	43
11	Pd(OAc) ₂	SPhos	-	135	48	67
12	Pd(OAc) ₂	L1	-	150 (MW)	1.5	25

			
SPhos	DABCO	DBU	picolinic acid

Results based on one run. ^aConversion calculated from the percentage of starting material to product in the ¹H NMR spectrum of the crude reaction mixture. ^b5 mol% Pd(OAc)₂ and 15 mol% **L1** were used.

The previously optimised direct arylation conditions resulted in 62% conversion to product **214** (Table 14, entry 1). In the absence of **L1** (Table 14, entry 2), a significant reduction in

conversion was observed. Reduced Pd loading (but an increase in Pd:ligand ratio (1:3)) did not allow for an improvement in conversion. In fact, a decrease in conversion to **214** (50%) was observed (**Table 14, entry 3**). A range of additional ligands and additives were screened. Switching the ligand to the more electron rich DMAP **L10** resulted in no significant increase in conversion (**Table 14, entry 5**). Picolinic acid resulted in diminished conversion (**Table 14, entry 10**).

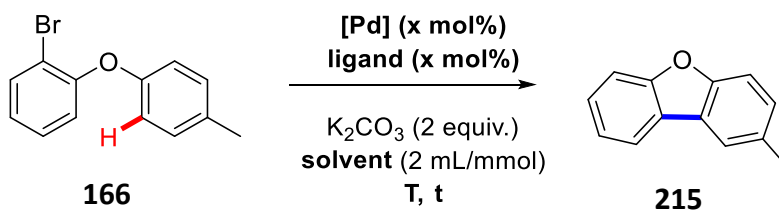
Bulky electron rich phosphine ligands are known to facilitate oxidation addition by donating electron density to the Pd⁰ center, thereby increasing the nucleophilicity of Pd and lowering the activation barrier for oxidative addition.⁵⁶⁻⁵⁷ In addition, SPhos has the ability to stabilise a monoligated Pd⁰ center by interaction between the *ipso*-carbon of the lower biaryl ring and Pd, as well as having the capacity to stabilise a Pd^{II} center by coordination of the methoxy group to Pd. The stabilisation provided by SPhos could allow for the formation of a highly active yet stable monophosphine Pd complex. The ability of bulky electron rich monophosphine ligands to promote the formation of highly reactive monophine Pd complexes is well documented in the literature.^{56, 58-61} It was thought that perhaps oxidative addition into the C-Br bond on the electron rich aryl ring of **171** may be sluggish. However, the employment of SPhos failed to provide an improvement on results (**Table 14, entry 11**).

Attempts to improve conversion by addition of an external oxidant proved detrimental to the reaction and only allowed for 10% conversion to **214** (**Table 14, entry 4**). Addition of 30 mol% PivOH as an additive led to a reduction in conversion (**Table 14, entry 6**). Changing to a Pd⁰ source in combination with PivOH completely hindered the reaction and led to only 14% conversion to **214** (**Table 14, entry 7**).

Two organic bases were examined in the absence of **L1**. This was on the basis that simple primary and secondary amine bases are often used in cross-coupling reactions and display some properties as ligands along with acting as bases, to stabilise reactive intermediates.⁶² For example, in 2004, Li and co-workers demonstrated the utility of a Pd(OAc)₂/DABCO (1,4-diazabicyclo[2.2.2]octane) catalytic system for the Suzuki-Miyaura coupling of deactivated aryl bromides and phenyl boronic acids.⁶³ This initiated an investigation to determine if DABCO could facilitate the reaction of the deactivated aryl bromide **171**. Pleasingly, DABCO did allow for an increase in conversion to 76%. On the contrary, the addition of 1,8-diazabicyclo[5.4.0]undec-7-ene (DBU) gave 68% conversion to **214** (**Table 14, entries 8-9**).

Finally, substrate **214** was subjected to microwave conditions at 150 °C. Disappointingly, in this case the reaction conditions only allowed for 25% conversion to product after 1.5 hours. (**Table 14, entry 10**).

As mentioned above, an optimisation study was also conducted on substrate **166**. A variety of reaction parameters were evaluated (**Table 15**).

Table 15. Optimisation of reaction conditions for direct arylation of **166**.

Entry	Pd(OAc) ₂ (mol%)	Ligand (mol%)	Solvent	Atmosphere	Temp. (°C)	Time (h)	Conv. (%) ^a
1	5	L1 (10 mol%)	NMP	Air	135	48	60 (42)
2	2.5	L1 (7.5 mol%)	NMP	Air	135	48	50
3	5	-	NMP	Air	135	48	60
4^b	5	-	NMP	Air	135	48	0
5	3	PCy ₃ .HBF ₄ (6 mol%)	DMA	N ₂	140	44	43
6^c	10	-	NMP	Air	135	48	0
7	5	-	NMP	Air	200 (MW)	1	(23) ^d
8	5	-	NMP	Air	170 (MW)	1.5	30 (27) ^d

Results based on average of two runs excluding entries 7 and 8. ^aConversion calculated from the percentage of starting material to product in the ¹H NMR spectrum of the crude reaction mixture. Isolated yield in parenthesis. ^b30 mol% TFA added as an additive to form Pd(TFA)₂ *in situ*. ^cPd/C (10 wt. %) was used as catalyst. ^dYield determined using ¹H NMR spectroscopy with 1,3,5-trimethoxybenzene as the internal standard.

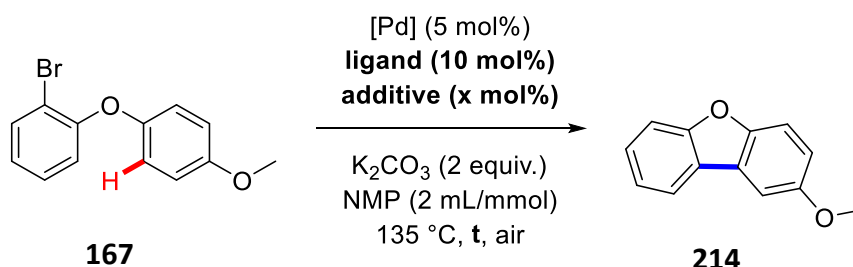
As previously demonstrated, application of the optimal conditions on **166** allowed for 60% conversion to product **215** (Table 15, entry 1). The product **215** was subsequently isolated in 42% yield *via* preparative TLC (hexanes). Decreasing the catalyst loading to 2.5 mol% (whilst

increasing the catalyst:ligand ratio to 1:3) resulted in slightly diminished conversion to product (**Table 15, entry 2**). In the absence of **L1**, the conversion remained the same as was observed for when the reaction was carried out in the presence of **L1** (both 60%). (**Table 15, entry 3**). Due to the poor to moderate conversions observed, it was postulated that the current optimised reaction conditions may not be suited to electron rich substrates and that it may be possible to bias the C-H bond cleavage step toward an electrophilic aromatic substitution type mechanism by modification of the reaction conditions. An electrophilic aromatic substitution (S_EAr) type mechanism is often suggested as the mode of C-H bond cleavage for electron rich aromatic substrates.⁶⁴⁻⁶⁵ An S_EAr type pathway would favour electron rich over electron poor substrates due to their enhanced nucleophilicity. Electron poor catalysts such as $Pd(OTFA)_2$ have been shown to be effective in these instances.⁶⁶ To further probe this hypothesis, the reaction was carried out in the absence of 6-methoxy quinoline **L1**. Instead, 30 mol% TFA was added to the reaction mixture to potentially form a more electrophilic Pd(II) catalyst *in situ*, $Pd(TFA)_2$. Disappointingly however, no discernible product **215** was identified in the 1H NMR spectrum of the crude reaction mixture (**Table 15, entry 4**).

Conditions adopted from Fagnou and co-workers for the intramolecular direct arylation with aryl bromides, aryl chlorides and aryl iodides were also examined.² Under inert conditions, the reaction did proceed in the presence of $PCy_3.HBF_4$ but once again not to full conversion, even after prolonged reaction time (**Table 15, entry 5**). When the heterogeneous palladium catalyst Pd/C (10 wt. %) was employed instead of $Pd(OAc)_2$, no evidence for the formation of product **215** was observed. In this instance only starting material **166** was recovered from the crude reaction mixture (**Table 15, entry 6**). Finally, microwave conditions were investigated. At 200 °C for 1 hour, a 23% yield of **215** was obtained. In this case, the starting material **166** was completely consumed, however this was accompanied by a number of unidentifiable side products, possibly due to dehalogenation and homo-coupling of the substrate (**Table 15, entry 7**). A reduction in temperature to 170 °C failed to provide any improvement (**Table 15, entry 8**). At this temperature, the starting material **166** was not completely consumed and numerous side products were present in the 1H NMR spectrum of the crude reaction mixture.

A further optimisation screen was carried out on **167** in an effort to drive the reaction to completion which would alleviate difficulties with purification, as discussed previously (**Table 16**).

Table 16. Optimisation of reaction conditions for direct arylation of **167**.



Entry	[Pd] (5 mol%)	Ligand (10 mol%)	Additive (mol%)	Time (h)	Conversion (%) ^a
1	Pd(OAc) ₂	L1	-	48	(62)
2	Pd(OAc) ₂	-	-	48	(41)
3	Pd(OAc) ₂	SPhos	-	48	(78)
4	Pd(OAc) ₂	-	DBU (10 mol%)	48	85
5	Pd(OAc) ₂	-	DBU (15 mol%)	48	56
6	Pd(OAc) ₂	picolinic acid	-	48	50
7	Pd(OAc) ₂	-	DABCO (10 mol%)	48	68

Results based one run. Yield in parenthesis. Yield determined using ¹H NMR spectroscopy with 1,3,5-trimethoxybenzene as the internal standard. ^aConversion calculated from the percentage of starting material to product in the ¹H NMR spectrum of the crude reaction mixture.

In the presence of 5 mol% Pd(OAc)₂, 10 mol% **L1** and 2.5 equiv. K₂CO₃, a 62% yield of **214** was obtained (**Table 16, entry 1**). The absence of **L1** gave inferior results (**Table 16, entry 2**). Various additives and ligands were also examined. Best results were obtained with SPhos and DBU (**Table 16, entry 3 and 4**). SPhos gave a 78% yield of **214** (**Table 16, entry 3**). The best

result was obtained when 10 mol% DBU was employed (**Table 16, entry 4**). This allowed for an 85% conversion to product (**214**) after 48 hours. DBU can act as a ligand and coordinate to transition metal complexes, however, this can be inhibitory in a lot of cases, rendering the catalyst ineffective for the desired catalytic reaction. This has been shown to be the case in C-N bond forming reactions, whereby the use of DBU as base can lead to catalyst deactivation.⁶⁷⁻⁶⁸ On the contrary, DBU, may in this case be acting as a ligand for Pd. In 2019, Khan and co-workers disclosed a mild and efficient synthesis of carbazoles *via* a Pd catalysed intramolecular direct arylation of *o*-iodo diphenylamines assisted by DBU.⁴¹ The authors propose that DBU participates at various stages of the catalytic cycle acting as both a mild organic base and ligand for Pd. First, DBU is suggested to act as a reducing agent to generate the active catalytic Pd⁰ species. It may then be acting as a σ -donating ligand for Pd, which may accelerate both the oxidative addition step as well as the reductive elimination step. In addition, DBU is critical for the C-H activation step, which the authors propose to be a CMD type mechanism for electron poor substrates and an S_EAr type mechanism for electron rich substrates, with DBU promoted deprotonation resulting in a six-membered palladacycle. The authors report that the use of DBU resulted in improved functional group tolerance and higher yields relative to those observed with inorganic bases. It is plausible that DBU may be exerting a similar effect in the case of the *o*-bromo diarylethers. However, at this time further mechanistic work is required to fully elucidate the mechanism of action for our substrates. Increasing the DBU loading to 15 mol% resulted in a decrease in conversion (**Table 16, entry 5**). Additional additives screened did not allow for any significant increase in conversion to product. Employment of picolinic acid as a ligand only allowed partial conversion to product (**Table 16, entry 6**). Finally, DABCO performed moderately well giving a 68% conversion to **214** (**Table 16, entry 7**).

3.7.3 Difficulties encountered during the purification of crude material

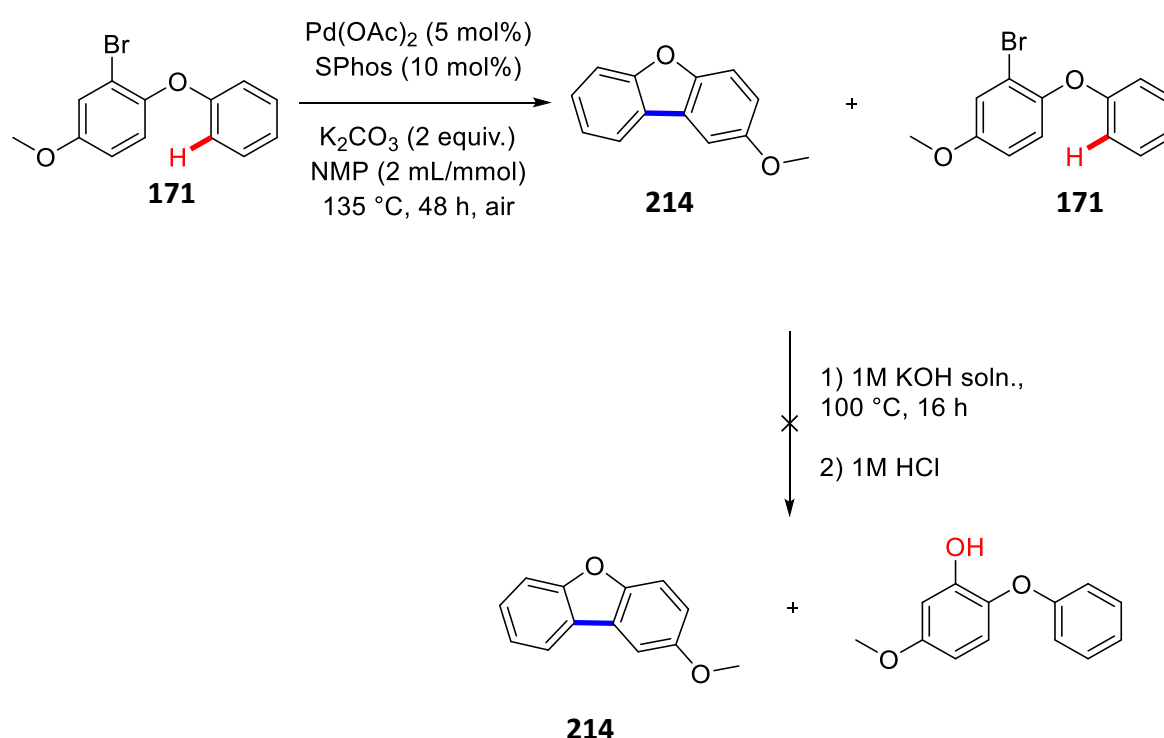
A significant challenge was encountered during the isolation of the cyclised product for the electron rich substrates, for which no reaction ran to completion. Recovering a clean sample of the dibenzofuran product was a major challenge as separation of starting material and product proved particularly problematic. As noted by Studer in *Science*⁶⁹ in 1997 '*The practical synthesis of organic compounds is limited not only by the yield of specific reactions but also by the ability to recover the desired product in pure form.....recovering and purification*

difficulties can limit the yield and utility of otherwise successful organic synthesis strategies.'

Given the similar polarity of the halide starting material and the cyclised product, isolation of the desired dibenzofuran product often proved impossible. As was detailed in the previous section driving these reactions to completion proved difficult, even at high catalyst loading, elevated temperatures, under inert conditions in the presence of phosphine ligands. The highest conversion to product was achieved with substrate **167** using DBU as an additive, which afforded an 85% conversion to product **214**. Initial attempts to purify the crude reaction material by silica gel column chromatography with hexanes or cyclohexane as eluent failed to allow separation of starting material from product. Analogous preparative TLC afforded the same result. Additionally, no increase in separation could be observed on alumina (neutral or basic) TLC plates. Chromatography with silver nitrate is a well known and established methodology for the separation of non-polar compounds with similar polarities. The silver ions reversibly interact with π -systems to form polar complexes. The silver nitrate is typically impregnated on silica gel or alumina for separation.⁷⁰⁻⁷¹ Thus, the silica gel coated plates were impregnated with an aqueous AgNO₃ solution 5% (w/v), dried and heat activated for two minutes. Next, the crude reaction material was spotted on the AgNO₃ impregnated TLC plate. Disappointingly, after running the TLC plate in hexane and examining it under a UV lamp, no distinct separation between the starting material **167** and product **214** was observed. Finally, Florisil[®], which is a hard powdered gel of magnesium silicate, is a less polar and less acidic adsorbent in comparison to silica gel.⁷⁰ Thus, it was postulated that this might enable improved separation between the non-polar starting material **167** and product **214**. Unfortunately, Florisil[®] did not provide any improvement in separation, with both compounds (**167** and **214**) eluting off the column at the same rate. It is worth noting that numerous recrystallisation efforts with a number of different solvent systems also failed to induce precipitation of the solid dibenzofuran product **214**.

Additionally, we attempted to exploit the inherent differences in reactivity between the aryl bromide starting material and dibenzofuran product. In 2006, Buchwald and co-workers developed an elegant system for the Pd catalysed synthesis of phenols from aryl halides using KOH as the nucleophilic source in the presence of bulky monodentate phosphine ligands.⁷² Thus, it was hypothesised that conversion of the remaining aryl bromide (once the reaction had reached maximum conversion) to the corresponding phenol using KOH may be possible.

The formed phenol could potentially be extracted into the aqueous layer afterwards, allowing a pure sample of the dibenzofuran product to be obtained. A mixture of **214** and **171** was obtained (in a ratio of 67:33) following reaction of **171** in the presence of 5 mol% Pd(OAc)₂, 10 mol% SPhos and 2 equivalents of K₂CO₃ in NMP. A few drops of a 1M solution of KOH was then added to the reaction vial and the resulting mixture was stirred at 100 °C for 16 hours. The reaction mixture was then cooled to room temperature and acidified with dilute aqueous 1M HCl (**Scheme 78**). Disappointingly, analysis of the ¹H NMR spectrum of the crude reaction mixture only showed a mixture of aryl bromide starting material **171** and dibenzofuran product **214**. No evidence for the formation of the desired phenol product **171** was visible.

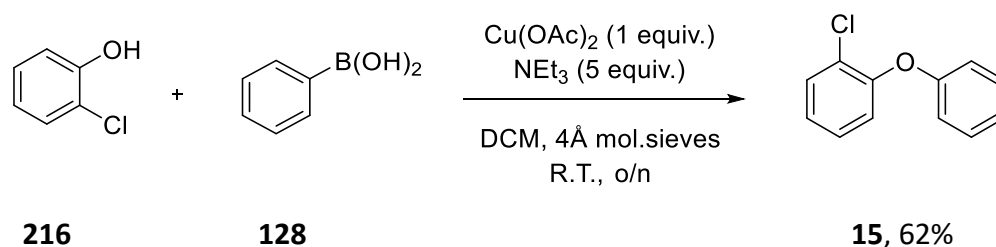


Scheme 78. Attempted interconversion of aryl bromide starting material to phenolic product.

Pleasingly, the *para*-methyl product **215** could be isolated in 42% by preparative TLC (**Table 15, entry 3**). Slight separation of the bands corresponding to the starting material and product on the TLC plate allowed a clean sample of both the starting material **166** and product **215** to be obtained.

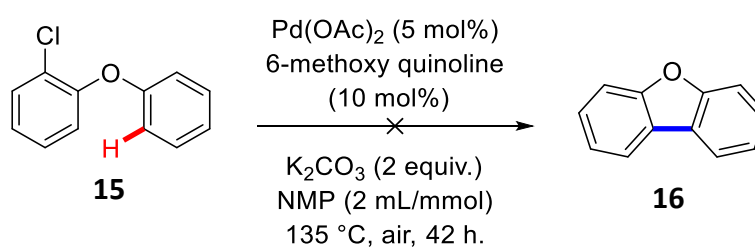
3.8 Additional substrates examined under the reaction conditions

Attention was then turned to the more challenging aryl chloride substrates. Aryl chlorides are more readily available and less expensive than aryl bromides and iodides.^{2, 64-65, 73} However, cleavage of a C-Cl bond is inherently more difficult than a C-Br or C-I bond.⁷⁴ As a consequence, direct arylation reactions more commonly employ aryl bromide or aryl iodide substrates.^{1, 4} In a seminal report in 2006, Fagnou and co-workers developed a broadly applicable catalytic system for the intramolecular direct arylation to aryl chlorides, bromides and iodides, with aryl iodides surprisingly exhibiting inferior reactivity relative to aryl chlorides and bromides.² The optimum catalytic system of a 1:1 ratio of Pd to P^tBu₃.HBF₄ at a Pd loading of 1 mol% allowed for a broad range of five, six and even seven membered oxygen and nitrogen ring systems to be synthesised. Thus, we were interested if our methodology would be applicable to the analogous aryl chloride substrate. The first step involved preparation of 2-chloro diphenyl ether (**217**) which was achieved in a similar manner to that described in **Section 3.5.2**. Reaction of 2-chloro phenol (**216**) and phenyl boronic acid (**128**) in the presence of a copper catalyst and NEt₃ afforded **217** in 62% yield (**Scheme 79**).



Scheme 79. Synthesis of 2-chloro diarylether **15**.

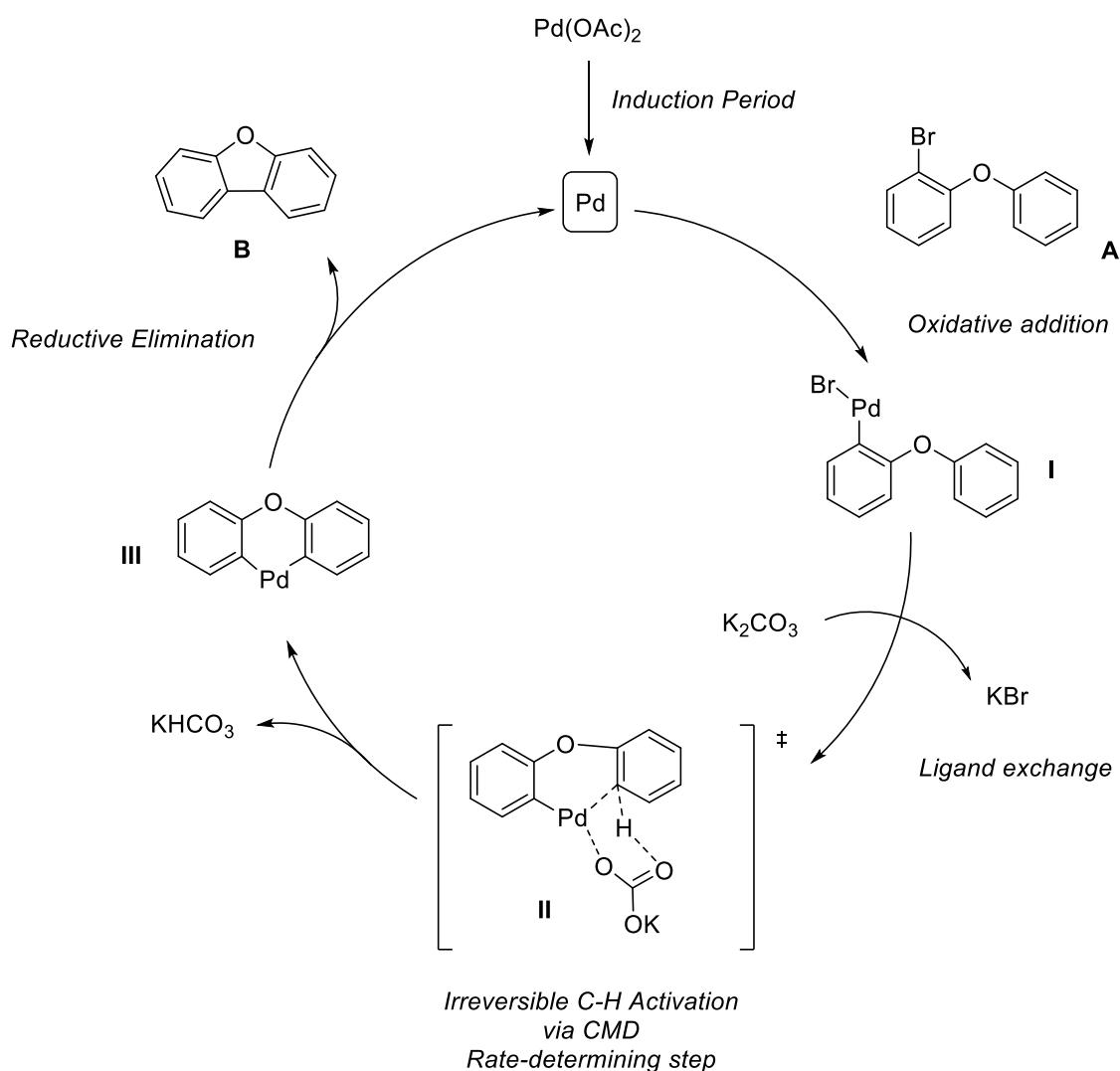
Disappointingly, attempts to cyclise **15** under the optimised reaction conditions failed to provide any of the desired product **16**. Consequently, only starting material **15** was identified in the ¹H NMR spectrum of the crude reaction mixture (**Scheme 80**).



Scheme 80. Attempted direct arylation of **15**.

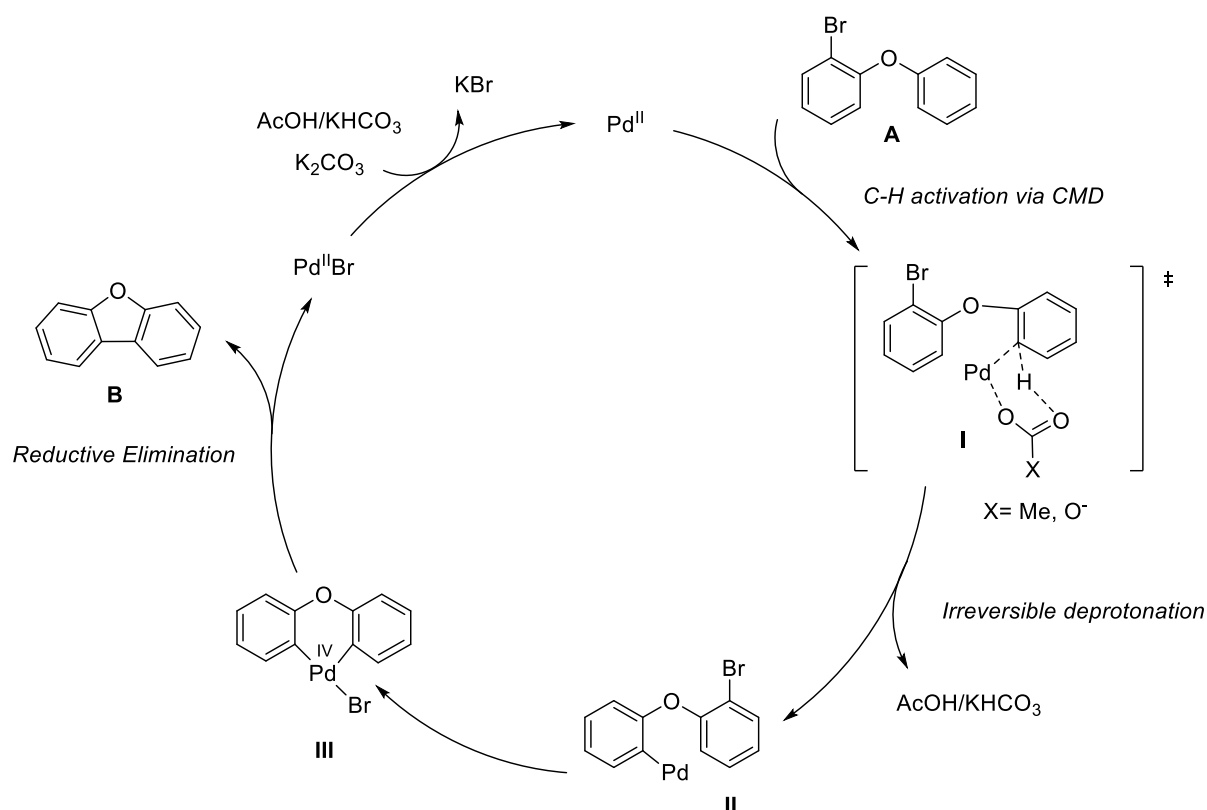
3.9 Mechanism for the direct arylation of *ortho*-bromo diarylethers

The high reactivity and excellent yields achieved with electron poor substrates in our system is consistent with a CMD mechanism for the C-H bond cleavage step rather than an electrophilic aromatic substitution or a Heck type mechanism which show strong preference for more electron rich substrates. This is consistent with Fagnou's observations regarding the importance of C-H bond acidity in the CMD pathway.⁷⁵ A possible mechanism for the reaction is outlined below in **Scheme 81**. Initial oxidative addition of Pd into the C-Br bond of **A** generates **I**. The resulting Pd^{II} complex is anticipated to undergo ligand exchange to form the key CMD transition state **II**. An irreversible deprotonation (by an acetate or carbonate base), as suggested by Fagnou⁷⁵⁻⁷⁶, Echavarren⁷⁷⁻⁷⁸ and Davies/MacGregor⁷⁹⁻⁸⁰ would generate **III**, with reductive elimination giving the cyclised product **B** and regeneration of the active catalyst.



Scheme 81. Possible catalytic cycle for the direct arylation of *o*-bromo diarylethers (ligands omitted for clarity).

However, it is important to note that there may be other potential mechanisms at play. For example, a Pd^{II}/Pd^{IV} catalytic cycle may also be operating, which has recently been proposed by Yu and Morokuma.⁸¹⁻⁸² Such a mechanism could involve C-H activation of **A** as the first step followed by oxidative addition. C-H bond cleavage *via* a CMD type mechanism (**I**) would give intermediate **II**. Oxidative addition of Pd^{II} into the C-Br bond would generate a Pd^{IV} species **III**, with reductive elimination and ligand association giving the product **B** and regenerating the active catalyst (**Scheme 82**).



Scheme 82. Possible Pd^{II}/Pd^{IV} catalytic cycle for the direct arylation of *o*-bromo diarylethers (ligands omitted for clarity).

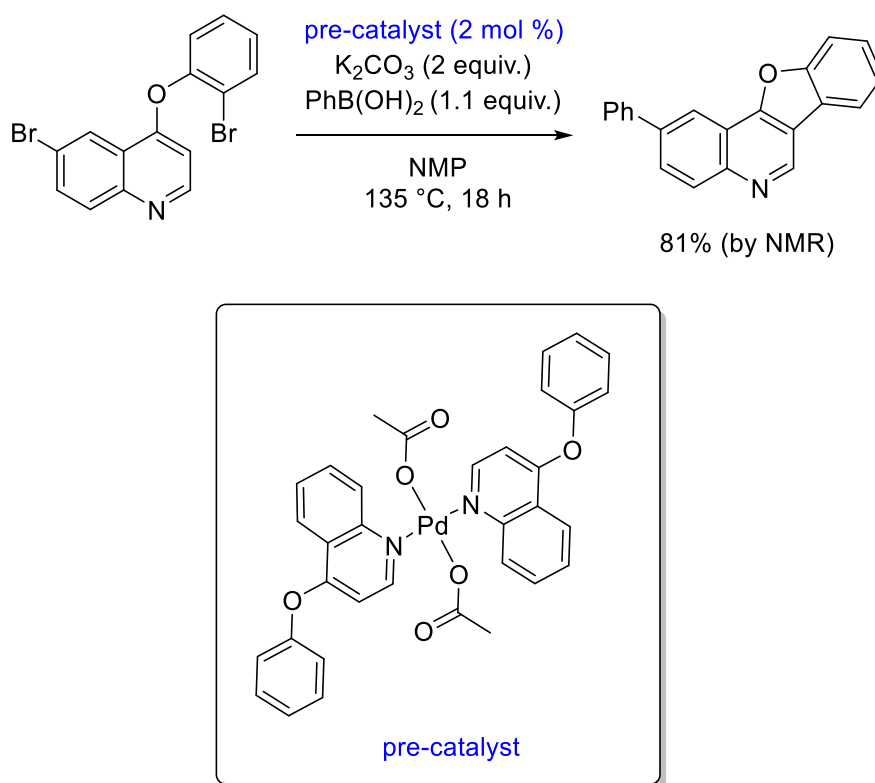
The nature and composition of the active catalytic species remains unclear. The extent to which the quinoline (**L1**) is participating in the transformation is also undetermined. However, based on a number publications, there are many possible roles:

1) The ligand may facilitate a slow step in the catalytic cycle (e.g. C-H activation). The quinoline may act as a σ -donor ligand and could potentially play a role in the C-H activation step by making the Pd center more nucleophilic which may be more desirable for a CMD mechanism.⁵ Ess and co-workers noted that a correlation exists between the energy of the CMD transition state and the thermodynamic stability of the developing Pd-Ar bond.⁸³ Thus, it may be reasonable to postulate that **L1** may exert a stabilising effect on Pd which would lead to a more stable Pd-aryl intermediate complex. The increase in nucleophilicity of the Pd center by strong σ -donation from the quinoline, as well as an increase in the steric bulk around Pd, may also accelerate the oxidative addition and reductive elimination steps in a similar manner to electron rich phosphine ligands⁵⁶, although, the former is unlikely as reaction of the electron

rich substrate **172**, in the presence of 6-methoxy quinoline (**L1**) failed to allow full consumption of starting material (**Table 14, entry 1**).

2) The ligand could also be playing a role outside the primary catalytic cycle. For example, prolonging the lifetime of the catalyst by preventing or slowing catalyst decomposition or by recovering Pd catalyst that is sequestered off-cycle, as well as intercepting and stabilising unligated Pd⁰ before the formation of Pd black and thus facilitating re-oxidation and regeneration of the active catalyst. There is precedence in the literature for all of these scenarios in other Pd catalysed transformations as well as other related reactions, primarily by Sanford, Yu and Fagnou.^{3, 5, 9, 12, 18-19, 59, 81, 84} For example, Sanford demonstrated the key role a quinoline carboxylate ligand played in rescuing off-cycle Pd species from a precipitate that was formed during the course of the reaction. This catalyst system was exploited to achieve the C-H arylation of azabicycloalkanes.¹²

3) The ligand may also have other beneficial roles in the catalytic cycle such as facilitating in stabilising high energy Pd^{IV} intermediates in the direct arylation reaction.^{5, 81} Conversely, the quinoline ligand may play a role in the formation of the active catalyst i.e. with the quinoline aiding precatalyst-to-catalyst transformation. Pd(OAc)₂ exists in the trimeric form in the solid state²³ and in some solvents such as chloroform, benzene, acetic acid and methanol at room temperature.⁸⁴ Quinoline (**L1**) may facilitate deaggregation of trimeric or polymeric Pd(OAc)₂ and allow the formation of a more reactive PdL_n(OAc)₂ species, a role for which Sanford had previously demonstrated for pyridine ligands.¹⁰ Our lab has recently shown that Pd(OAc)₂/quinoline complexes can act as competent pre-catalysts in a one-pot tandem Suzuki Miyaura/direct arylation (SM/DA) reaction with di-bromo quinolines (**Scheme 83**).¹⁶



Scheme 83. $Pd(OAc)_2$ /quinoline pre-catalyst for SM/DA reaction of di-bromo quinolones.

3.10 Conclusion and Future Work

In summary, an efficient catalytic protocol aided by a cheap and commercially available quinoline ligand for the construction of dibenzofuran motifs has been developed. Gratifyingly, a number of challenges with existing protocols for the classic intramolecular C-H activation of diarylethers, which were discussed in **Chapter 1** of this thesis, have been addressed (**Table 17**). Crucially, the reactions take place in air, without added phosphine or *tert*-alkyl ammonium salt. Importantly, the newly developed reaction conditions allowed for complete consumption of diarylether starting material, as in the absence of added quinoline ligand, attempts at separating the product from the unreacted starting material proved challenging. In particular, column chromatography on conventional silica gel was found to be unsuitable as both the diarylether starting material and dibenzofuran product are very non-polar. The optimised reaction conditions also allowed for a reduction in temperature below $170^\circ C$ (as was previously reported in Ames early report on the intramolecular arylation of diaryl ethers). Overall, substrates bearing electron withdrawing groups were particularly well tolerated and yields of up to 99% were observed. Notably, the optimised conditions allow for the use of a

pyridyl moiety and an N-H linker. On the contrary, substrates with strongly electron donating substituents did not progress as well.

Table 17. Challenges addressed by this work.

Current challenges	This work
very high temperature (<170 °C)	✓
very high catalyst loading	✓
inert atmosphere	✓
phosphine ligands	✓
expensive additives	✓
product isolation problems	✓

Current work within the group is focused on probing the mechanistic details of the reaction, with future work targeted at broadening the scope of the current transformation as well as exploiting this catalytic system for other synthetically useful C-H activation reactions. The exact role of the quinoline has yet to be discerned. However, it is suspected that it acts as either a discrete ligand to the palladium during the catalytic cycle¹⁶ or as a vehicle to dissolve palladium aggregates as recently report by Sanford.¹² Further study is required to fully elucidate the role of the quinoline and related species in the reaction.

3.11 References

1. Ames, D. E., Opalko, A. *Synthesis* **1983**, 234-235.
2. Campeau, L.-C., Parisien, M., Jean, A., Fagnou, K. *J. Am. Chem. Soc.* **2006**, *128*, 581-590.
3. Campeau, L.-C., Thansandote, P., Fagnou, K. *Org. Lett.* **2005**, *7*, 1857-1860.
4. Panda, N., Mattan, I., Nayak, D. K. *J. Org. Chem.* **2015**, *80*, 6590-6597.
5. Engle, K. M., Yu, J.-Q. *J. Org. Chem.* **2013**, *78*, 8927-8955.
6. Shanahan, R. M., Hickey, A., Reen, F. J., O'Gara, F., McGlacken, G. P. *Eur. J. Org. Chem.* **2018**, *2018*, 6140-6149.
7. Izawa, Y., Stahl, S. S. *Adv. Syn. Catal.* **2010**, *352*, 3223-3229.
8. Cheng, G., Wang, P., Yu, J.-Q. *Angew. Chem. Int. Ed.* **2017**, *56*, 8183-8186.
9. Zhang, Y.-H., Shi, B.-F., Yu, J.-Q. *J. Am. Chem. Soc.* **2009**, *131*, 5072-5074.
10. Emmert, M. H., Cook, A. K., Xie, Y. J., Sanford, M. S. *Angew. Chem. Int. Ed.* **2011**, *50*, 9409-9412.
11. Gary, J. B., Cook, A. K., Sanford, M. S. *ACS Catal.* **2013**, *3*, 700-703.
12. Cabrera, P. J., Lee, M., Sanford, M. S. *J. Am. Chem. Soc.* **2018**, *140*, 5599-5606.
13. Zhang, S., Shi, L., Ding, Y. *J. Am. Chem. Soc.* **2011**, *133*, 20218-20229.
14. Li, S., Chen, G., Feng, C.-G., Gong, W., Yu, J.-Q. *J. Am. Chem. Soc.* **2014**, *136*, 5267-5270.
15. Izawa, Y., Pun, D., Stahl, S. S. *Science* **2011**, *333*, 209-213.
16. Shanahan, R. M., Hickey, A., Bateman, L. M., Light, M. E., McGlacken, G. P. *J. Org. Chem.* **2020**, *85*, 2585-2597.
17. Liu, L. Y., Yeung, K. S., Yu, J. Q. *Chem. Eur. J.* **2019**, *25*, 2199-2202.
18. Ferreira, E. M., Stoltz, B. M. *J. Am. Chem. Soc.* **2003**, *125*, 9578-9579.
19. Stuart, D. R., Fagnou, K. *Science* **2007**, *316*, 1172-1175.
20. Jakab, A., Dalicsek, Z., Holczbauer, T., Hamza, A., Pápai, I., Finta, Z., Timári, G., Soós, T. *Eur. J. Org. Chem.* **2015**, *2015*, 60-66.
21. Lafrance, M., Lapointe, D., Fagnou, K. *Tetrahedron* **2008**, *64*, 6015-6020.
22. Park, H., Chekshin, N., Shen, P.-X., Yu, J.-Q. *ACS Catal.* **2018**, *8*, 9292-9297.
23. Sherwood, J., Clark, J. H., Fairlamb, I. J. S., Slattery, J. M. *Green Chem.* **2019**, *21*, 2164-2213.
24. Carole, W. A., Colacot, T. J. *Chem. Eur. J.* **2016**, *22*, 7686-7695.

25. Reetz, M. T., de Vries, J. G. *Chem. Commun.* **2004**, 1559-1563.
26. Reetz, M. T., Westermann, E., Lohmer, R., Lohmer, G. *Tetrahedron Lett.* **1998**, 39, 8449-8452.
27. <http://www.fluorochem.co.uk/Products/Search?searchType=C&searchText=5263-87-6>, accessed 8th October 2019.
28. Lam, P. Y., Clark, C. G., Saubern, S., Adams, J., Winters, M. P., Chan, D. M., Combs, A. *Tetrahedron Lett.* **1998**, 39, 2941-2944.
29. Evans, D. A., Katz, J. L., West, T. R. *Tetrahedron Lett.* **1998**, 39, 2937-2940.
30. Chan, D. M., Monaco, K. L., Wang, R.-P., Winters, M. P. *Tetrahedron Lett.* **1998**, 39, 2933-2936.
31. Kammermeier, T., Kaiser, A., Lee, G. S., Burgemeister, T., Wiegrebbe, W. *Arch. Pharm.* **1994**, 327, 207-210.
32. da Silva, L. M. M. G., de Oliveira, J. F., Silva, W. L., da Silva, A. L., de Almeida Junior, A. S. A., Barbosa dos Santos, V. H., Alves, L. C., Brayner dos Santos, F. A., Costa, V. M. A., Aires, A. d. L., de Lima, M. d. C. A., Albuquerque, M. C. P. d. A. *Chem-Biol. Interact.* **2018**, 283, 20-29.
33. Chen, Z., Pitchakuntla, M., Jia, Y. *Nat. Prod. Rep.* **2019**, 36, 666-690.
34. Baumann, M., Baxendale, I. R., Ley, S. V., Nikbin, N. *Beilstein J. Org. Chem.* **2011**, 7, 442-495.
35. Colman, E. Z., Arias, K., Siegel, J. S., *Can. J. Chem.* **2009**, 87, 440-447.
36. King, A. E., Brunold, T. C., Stahl, S. S. *J. Am. Chem. Soc.* **2009**, 131, 5044-5045.
37. Vantourout, J. C., Miras, H. N., Isidro-Llobet, A., Sproules, S., Watson, A. J. B. *J. Am. Chem. Soc.* **2017**, 139, 4769-4779.
38. Chen, W.-B., Xing, C.-H., Dong, J., Hu, Q.-S. *Adv. Syn. Catal.* **2016**, 358, 2072-2076.
39. Bielawski, M., Aili, D., Olofsson, B. *J. Org. Chem.* **2008**, 73, 4602-4607.
40. Jalalian, N., Ishikawa, E. E., Silva, L. F., Olofsson, B. *Org. Lett.* **2011**, 13, 1552-1555.
41. Khan, A., Karim, R., Dhimane, H., Alam, S. *ChemistrySelect* **2019**, 4, 6598-6605.
42. Lissa, S. T., Daniela, G., Dianqing, S. *Curr. Top. Med. Chem.* **2016**, 16, 1290-1313.
43. Knölker, H.-J., Reddy, K. R. *Chem. Rev.* **2002**, 102, 4303-4428.
44. Głuszyńska, A. *Eur. J. Med. Chem.* **2015**, 94, 405-426.
45. A. A. Altaf, A. S., Z Gul, N Rasool, A. Badshah, B. Lal, E. Khan *J. Drug Des. Med. Chem.* **2015**, 1, 1-11.

46. Taylor, R. D., MacCoss, M., Lawson, A. D. G. *J. Med. Chem.* **2017**, *60*, 1638-1647.
47. Sánchez, C., Méndez, C., Salas, J. A. *Nat. Prod. Rep.* **2006**, *23*, 1007-1045.
48. O'Hagan, D. *J. Fluor. Chem.* **2010**, *131*, 1071-1081.
49. Mei, H., Han, J., Fustero, S., Medio-Simon, M., Sedgwick, D. M., Santi, C., Ruzziconi, R., Soloshonok, V. A. *Chem. Eur. J.* **2019**, *25*, 11797-11819.
50. Leclerc, J.-P., Fagnou, K. *Angew. Chem. Int. Ed.* **2006**, *45*, 7781-7786.
51. Campeau, L.-C., Stuart, D. R., Leclerc, J.-P., Bertrand-Laperle, M., Villemure, E., Sun, H.-Y., Lasserre, S., Guimond, N., Lecavallier, M., Fagnou, K. *J. Am. Chem. Soc.* **2009**, *131*, 3291-3306.
52. Campeau, L.-C., Rousseaux, S., Fagnou, K. *J. Am. Chem. Soc.* **2005**, *127*, 18020-18021.
53. Elsohly, M. A., Slatkin, D. J., Knapp, J. E., Doorenbos, N. J., Quimby, M. W., Schiff, P. L., Gopalakrishna, E. M., Watson, W. H. *Tetrahedron* **1977**, *33*, 1711-1715.
54. Scannell, R. T., Stevenson, R. *J. Am. Chem. Soc., Perkin Trans. 1* **1983**, 2927-2931.
55. Amatore, C., Pfluger, F. *Organometallics* **1990**, *9*, 2276-2282.
56. Martin, R., Buchwald, S. L. *Acc. Chem. Res.* **2008**, *41*, 1461-1473.
57. Surry, D. S., Buchwald, S. L. *Angew. Chem. Int. Ed.* **2008**, *47*, 6338-6361.
58. Ross, A. J., Lang, H. L., Jackson, R. F. W. *J. Org. Chem.* **2010**, *75*, 245-248.
59. Baxter, R. D., Sale, D., Engle, K. M., Yu, J.-Q., Blackmond, D. G. *J. Am. Chem. Soc.* **2012**, *134*, 4600-4606.
60. Hartwig, J. F., Paul, F. *J. Am. Chem. Soc.* **1995**, *117*, 5373-5374.
61. Galardon, E., Ramdeehul, S., Brown, J. M., Cowley, A., Hii, K. K., Jutand, A. *Angew. Chem. Int. Ed.* **2002**, *41*, 1760-1763.
62. Overman, L. E. *Organic Reactions*, John Wiley & Sons, New York, USA, **2002**, pp. 576.
63. Li, J.-H., Liu, W.-J. *Org. Lett.* **2004**, *6*, 2809-2811.
64. McGlacken, G. P., Bateman, L. M. *Chem. Soc. Rev.* **2009**, *38*, 2447-2464.
65. Alberico, D., Scott, M. E., Lautens, M. *Chem. Rev.* **2007**, *107*, 174-238.
66. Nishikata, T., Abela, A. R., Huang, S., Lipshutz, B. H. *Beilstein J. Org. Chem.* **2016**, *12*, 1040-1064.
67. Kim, S.-T., Pudasaini, B., Baik, M.-H. *ACS Catal.* **2019**, *9*, 6851-6856.
68. Sunesson, Y., Limé, E., Nilsson Lill, S. O., Meadows, R. E., Norrby, P.-O. *J. Org. Chem.* **2014**, *79*, 11961-11969.

69. Studer, A., Hadida, S., Ferritto, R., Kim, S.-Y., Jeger, P., Wipf, P., Curran, D. P. *Science* **1997**, 275, 823-826.
70. Gocan, S. *J. Chromatogr. Sci.* **2002**, 40, 538-549.
71. Zhang, Q.-W., Lin, L.-G., Ye, W.-C. *Chin. Med.* **2018**, 13, 20.
72. Anderson, K. W., Ikawa, T., Tundel, R. E., Buchwald, S. L. *J. Am. Chem. Soc.* **2006**, 128, 10694-10695.
73. Littke, A. F., Fu, G. C. *J. Org. Chem.* **1999**, 64, 10-11.
74. Jin, M. J., Lee, D. H. *Angew. Chem. Int. Ed.* **2010**, 49, 1119-1122.
75. Lafrance, M., Fagnou, K. *J. Am. Chem. Soc.* **2006**, 128, 16496-16497.
76. David, L., Keith, F. *Chem. Lett.* **2010**, 39, 1118-1126.
77. García-Cuadrado, D., de Mendoza, P., Braga, A. A. C., Maseras, F., Echavarren, A. M. *J. Am. Chem. Soc.* **2007**, 129, 6880-6886.
78. García-Cuadrado, D., Braga, A. A. C., Maseras, F., Echavarren, A. M. *J. Am. Chem. Soc.* **2006**, 128, 1066-1067.
79. Boutadla, Y., Davies, D. L., Macgregor, S. A., Poblador-Bahamonde, A. I. *Dalton Trans.* **2009**, 5820-5831.
80. Davies, D. L., Macgregor, S. A., McMullin, C. L. *Chem. Rev.* **2017**, 117, 8649-8709.
81. Ye, M., Gao, G.-L., Edmunds, A. J. F., Worthington, P. A., Morris, J. A., Yu, J.-Q. *J. Am. Chem. Soc.* **2011**, 133, 19090-19093.
82. Jiang, J., Yu, J.-Q., Morokuma, K. *ACS Catal.* **2015**, 5, 3648-3661.
83. Petit, A., Flygare, J., Miller, A. T., Winkel, G., Ess, D. H. *Org. Lett.* **2012**, 14, 3680-3683.
84. Nishimura, T., Onoue, T., Ohe, K., Uemura, S. *J. Org. Chem.* **1999**, 64, 6750-6755.
85. Stephens, D. E., Lakey-Beitia, J., Atesin, A. C., Ateşin, T. A., Chavez, G., Arman, H. D., Larionov, O. V. *ACS Catal.* **2015**, 5, 167-175.

Chapter 4: Introduction

4.1 Manganese catalysed C-H activation

The formation of carbon-carbon bonds in an efficient manner is a key goal for organic chemists. So-called 'C-H activation' protocols¹⁻³ (previously discussed in **Chapter 1** of this thesis) have emerged as an increasingly viable alternative to traditional cross-coupling methods (Suzuki-Miyaura, Stille, Negishi) with applications in natural product synthesis⁴, pharmaceuticals⁵ and material sciences.⁶⁻⁷ The vast majority of these processes however have been accomplished by using Pd, which is rare in the Earth's crust (0.89 ppm)³ and its cost is steadily increasing.⁴ Clearly, there is an urgent need to alleviate the worldwide reliance on platinum group metals, and Pd in particular.

One potential solution is to develop chemistry using Earth Abundant Metals (EAM).⁵ Use of 3d transition metals is commonly reported now, with complexes derived from iron and nickel (and cobalt to a certain extent) proving the most useful. In recent years, manganese (Mn) catalysed C-H activation has emerged as a promising alternative to the well-established precious-metal-mediated processes.⁸⁻¹⁰ Mn is the 12th most abundant element on the earth's crust (Pd is 74th, for example).¹¹ The low toxicity, which matches with principles of green chemistry,¹² and low cost (**Figure 30**) of Mn render it a particularly attractive alternative to typically used transition metal based catalysts.¹³

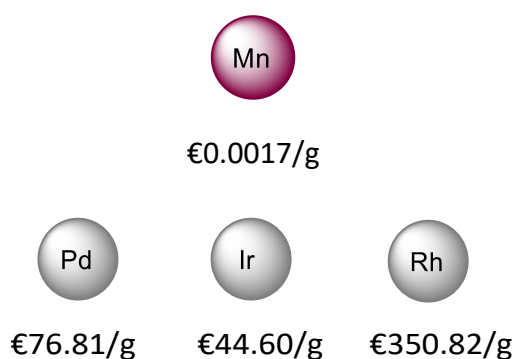
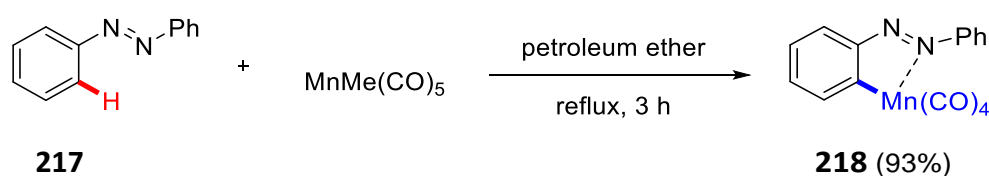


Figure 30. Price of precious metals.¹⁴⁻¹⁵

In general, first row transition metal based catalysts usually display different and complementary catalytic activities to second and third row transition metals.¹⁶ Mn exhibits the widest range of oxidation states of any of the first row d-block metals (-3 to +7) and has the ability to form compounds with a coordination number of up to seven. Many of the difficulties surrounding the use of Mn in classical organometallic reactions stems from the lack of well-characterised examples of organomanganese complexes in oxidation states other

than +1. Although manganese is most frequently encountered in the +2 state, the majority of its organometallic chemistry concerns the univalent state. These Mn(I) compounds exhibit almost exclusively low-spin d^6 configurations and typically feature very strong crystal field ligands such as carbonyl.¹⁷ This is not surprising as, in general, transition metal complexes in low oxidation states are almost always stabilized by π -acceptor ligands such as CO, NO or PR_3 . However, only a limited number of Mn catalysed C-H bond activation protocols have been reported to operate by an organometallic mode of action and they normally utilise the Mn(I) catalysts: $Mn(CO)_5Br$ and $Mn_2(CO)_{10}$.

On the other hand, Mn catalysed C-H oxygenations,¹⁸⁻²² nitrogenations²³⁻²⁶ and halogenations²⁷⁻³² catalysed by high valent manganese species, proceeding *via* a radical mechanism have been well developed. These methods lead to functionalisation at the weakest C-H bond in the substrates, typically at the benzylic position. Recently however, Mn catalysed organometallic C-H activation at thermodynamically more stable aryl or alkenyl C-H bonds has gained considerable momentum. Since the seminal report by Stone, Bruce and co-workers detailing the first stoichiometric Mn mediated C-H activation of azobenzene (**217**) to give the corresponding five membered manganacycle **218** (Scheme 84),³³ and subsequent stoichiometric transformations by Liebeskind,³⁴ Nicholson and Main,³⁵⁻³⁷ and Woodgate,³⁸⁻⁴⁰ key contributions from a number of groups in recent years have changed the landscape of Mn catalysis, which will be discussed in this introduction.

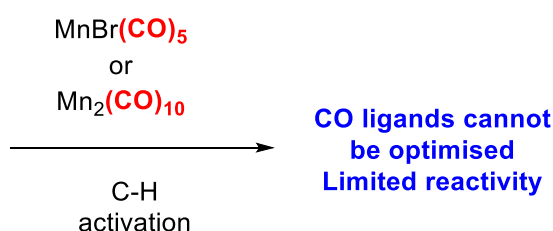


Scheme 84. The first Mn promoted C-H activation.

4.2 Aims and Objectives

The aim of **Chapter 4** of this thesis will be focused on addressing some of the current limitations underpinning Mn catalysed C-H activation with a particular focus on ligand design and development (**Figure 31**). Of the *ca.* 100 reports on Mn catalysed C-H activation, almost all use the commercially available $\text{MnBr}(\text{CO})_5$ or $\text{Mn}_2(\text{CO})_{10}$ precatalysts.⁸⁻⁹ These catalytic systems cannot be optimised, as the CO ligands do not possess the required complexity. To date, there has been no study on the ligand effects in Mn catalysed C-H activation. Given that Pd catalysis is generally underpinned by the features of associated ligands, and that ligand design and development has driven the development of almost all transition metal mediated processes, it seems imperative that ligand design will be crucial in future Mn catalysed C-H activation reactions. Hence, the work in this Chapter outlines the development of new Mn/L complexes and their application in C-H activation reactions.

(i) Previous work



(ii) This work

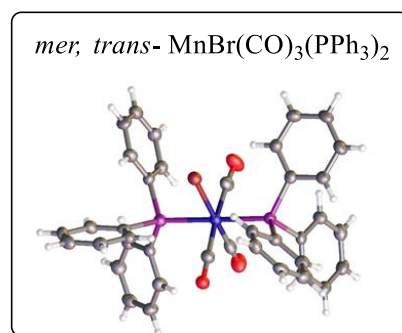
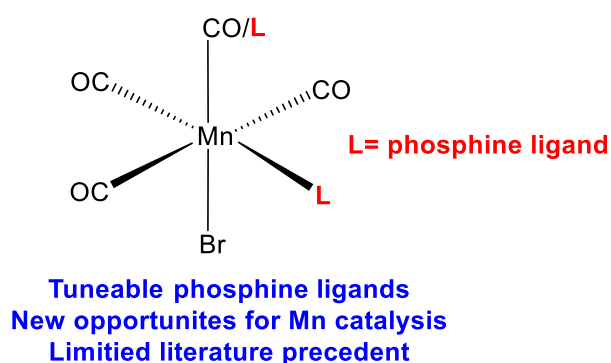
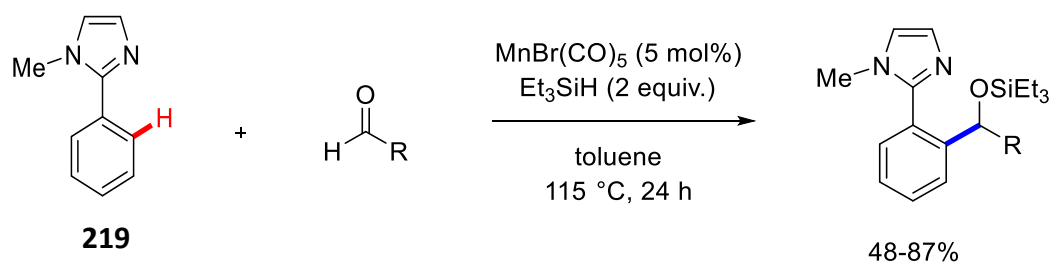


Figure 31. (i) Commercially available Mn(I) catalysts *versus* (ii) tuneable Mn(I) phosphine catalysts.

4.3.1 Literature examples of manganese catalysed C-H activation reactions: addition to aldehydes

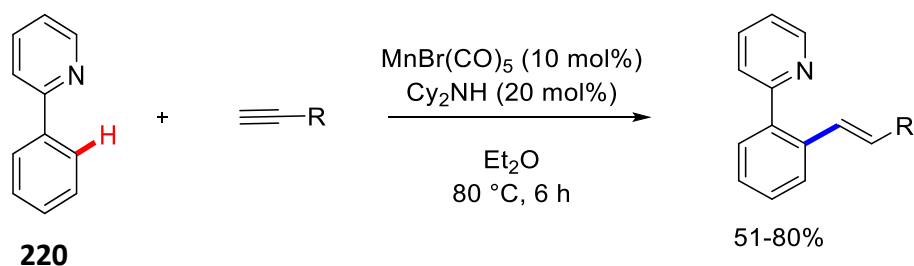
In the following 40 years since the first stoichiometric Mn mediated C-H activation of azobenzene was disclosed by Stone and Bruce³³ (**Scheme 84**), the development of Mn catalysed C-H activation remained dormant until 2007 when Kuninobu and Takai reported the first example of Mn catalysed C-H activation for carbon-carbon bond formation.⁴¹ They described the Mn catalysed imidazole (**219**) directed aromatic C-H bond addition to aldehydes (**Scheme 85**). Notably, triethyl silane proved to be a crucial additive, allowing for catalyst turnover. The silyl protected benzylic alcohols were synthesised in moderate to good yields. The authors state that in the presence of various other metal complexes (Rh, Re, Ru, Ir, Mn complexes), the reaction failed to proceed. The reaction was also extended to a diastereoselective transformation using an aromatic compound with a chiral substituent. Good yields of the silyl ether products were obtained in moderate diastereomeric excess.



Scheme 85. Mn(I) catalysed C-H addition to aldehydes.

4.3.2 Literature examples of manganese/base system for C-H activation reactions: alkyne coupling partners

Following on from this, a paper by Wang and co-workers in 2013 reported the first Mn catalysed aromatic C-H alkenylation of phenyl pyridine (**220**) with terminal alkynes (**Scheme 86**).⁴² Key to the success of the reaction was the addition of dicyclohexylamine, which the authors claim facilitates the C-H activation step by cooperation with the manganese catalyst (**Figure 32**). A broad substrate scope was demonstrated that included carbon-halogen bonds and the reaction proceeded with high levels of control in chemo-, regio- and stereoselectivity. This seminal report paved the way for a flurry of scientific publications in Mn catalysed C-H activation over the next number of years.



Scheme 86. Mn catalysed alkenylation.

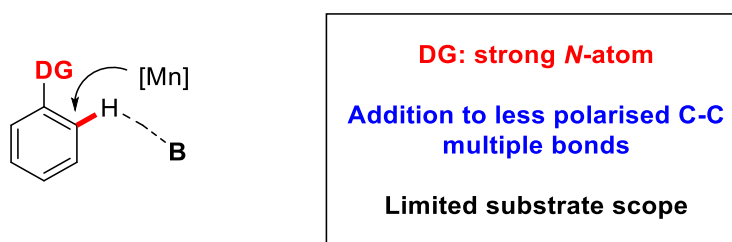
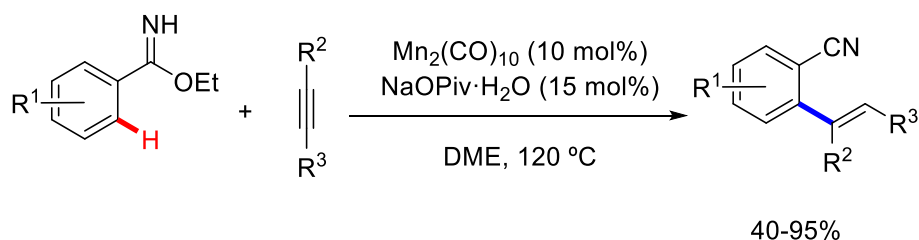


Figure 32. Mn/base system for manganese catalysed C-H activation.

The C-H alkenylation of aromatic N-H imidates with alkynes was developed by the Wang group in 2016 (**Scheme 87**).⁴³ This is a useful strategy, providing access to *ortho*-functionalised aromatic nitriles. The authors report that electron donating and electron withdrawing groups on the aromatic ring of the alkyne were compatible, and halogens (Cl, Br) which are potentially susceptible to further functionalisation, were well tolerated. Notably however, the yields were decreased when internal alkynes were used.

Wang, *Adv. Synth. Catal.* 2016, 358, 2436-2442.

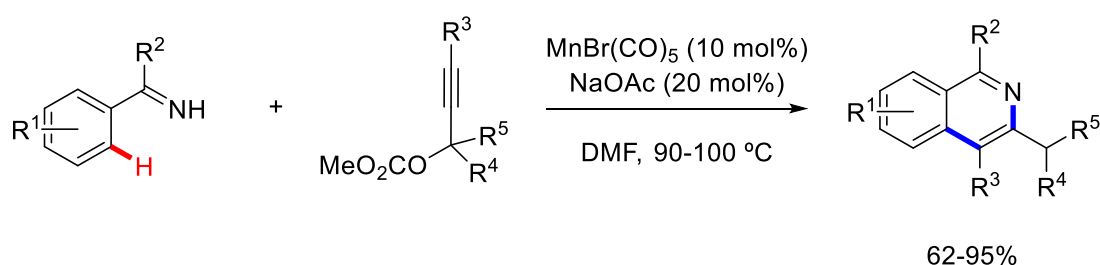


Scheme 87. Mn catalysed *ortho*-C-H alkenylation of aromatic imidates with alkynes.

A new strategy to prepare isoquinolines and isoquinolones was then reported by the Glorius group (**Scheme 88**).⁴⁴ This clever and efficient strategy solved the ever-present limitation of controlling stereoselectivity in C-H activation with unsymmetrical alkynes, with the

introduction of a traceless directing group. The introduction of this directing group (which serves as both **chelator** and **internal oxidant**), offers control of the regioselectivity. This system is also applicable to other heterocycles such as thiophene and benzothiophene-based moieties. An array of isoquinolines with switchable regioselectivity were prepared *via* this methodology. It is noteworthy that many of these substrates had previously not been successfully prepared as a single isomer using C-H activation methods.

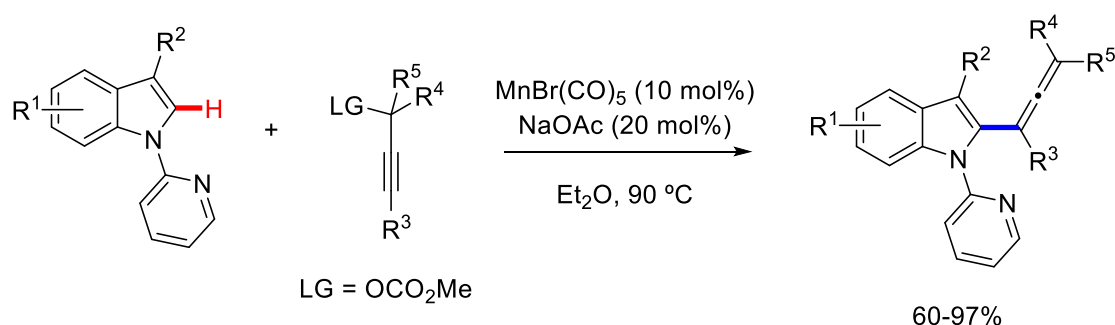
Glorius, *Angew. Chem. Int. Ed.* 2017, 56, 12778-12782.



Scheme 88. Mn catalysed regioselective synthesis of isoquinolines.

In another report by the Glorius group, 2-allenylindoles could be prepared *via* sequential C-H activation of indoles and internal alkynes (**Scheme 89**).⁴⁵ The authors state that the regioselectivity of the alkyne insertion was perfectly controlled, and further reaction of the obtained 2-allenylindoles, such as cyclisations or polymerisations were avoided. Remarkably 2-allenylindoles containing strong electron withdrawing groups were prepared in excellent yields. Unfortunately, this protocol could not be applied widely to other heterocycles, but could be scaled up to gram quantities with high efficiency.

Glorius, *Angew. Chem. Int. Ed.* 2017, 56, 6660-6664.



Scheme 89. Mn catalysed regioselective C-H allenylation.

In 2014, Wang and colleagues disclosed the first one-step Mn catalysed aromatic conjugate addition to unsaturated carbonyls. The reaction is accelerated by a catalytic amount of

dicyclohexylamine (Cy₂NH) (**Scheme 90, a**).⁴⁶ Since this report, there have been a wide range of Mn catalysed C-H activation reactions with olefin substrates (**Scheme 90** and **Scheme 91**). The groups of Glorius and Ackermann concurrently reported the Mn catalysed C-H/C-C activation reaction of indoles with challenging vinylcyclopropanes.⁴⁷⁻⁴⁸ Slightly different reaction conditions were disclosed by both groups and comparable yields were obtained with both methodologies (**Scheme 90, b**). The Mn catalysed C-H hydroarylation of allenes has been described by Rueping and co-workers, providing access to various alkenylated indoles in excellent yields with a good functional group tolerance (**Scheme 90, c**).⁴⁹ Moreover, an interesting cascade reaction involving a Smiles rearrangement was observed when tri-substituted allenes were employed to afford substituted pyrroloindolone products (**Scheme 90, d**).⁴⁹ At the same time, very similar work was also disclosed by Wang and colleagues (**Scheme 90, d**).⁵⁰ Subsequently, Wang extended this methodology to di-substituted allenes to give the corresponding allylated arenes along with heteroarenes (**Scheme 90, e**).⁵¹ Glorius and Ackermann independently published work on the Mn catalysed C-H activation of indoles with vinyl-1,3-dioxolan-2-ones (**Scheme 90, f**).^{47, 52} Both groups propose that the solvent has a strong influence on the *E/Z* selectivity of the transformation. Glorius and co-workers also extended the scope of the allylation reaction to include 2-vinyloxiranes.

**f) Glorius, *Chem. Sci.* 2017, 8, 3379-3383
Ackermann, *Angew. Chem. Int. Ed.* 2017, 56, 6339-6342**

a) Wang, *Chem. Commun.* 2014, 50, 14558-14561

**b) Glorius, *Chem. Sci.* 2017, 8, 3379-3383
Ackermann, *Chem. Eur. J.* 2017, 23, 5443-5447**

c) Rueping, *Angew. Chem. Int. Ed.* 2017, 56, 9935-9938

e) Wang, *J. Org. Chem.* 2017, 82, 11173-11181

**d) Rueping, *Angew. Chem. Int. Ed.* 2017, 56, 9935-9938
Wang, *Angew. Chem. Int. Ed.* 2017, 56, 9939-9943**

Chemical reaction scheme showing the cross-coupling of a substituted arene (Ar-DG-H) with various functional groups using a [Mn] catalyst and base. The central arene has a DG group (pyridyl or pyrimidine) and a hydrogen atom. Eight different reaction pathways are shown, each leading to a specific product. The pathways are:

- Top-left: Reaction with an allylic alcohol derivative to form a propenyl-substituted arene.
- Top: Reaction with an α,β -unsaturated ketone to form a propenyl-substituted arene.
- Top-right: Reaction with an allylic ether derivative to form a propenyl-substituted arene.
- Right: Reaction with an α,β -unsaturated ester to form a propenyl-substituted arene.
- Bottom-right: Reaction with an α,β -unsaturated ester to form a propenyl-substituted arene.
- Bottom: Reaction with an α,β -unsaturated ester to form a propenyl-substituted arene.
- Bottom-left: Reaction with an α,β -unsaturated ester to form a propenyl-substituted arene.
- Left: Reaction with an α,β -unsaturated ester to form a propenyl-substituted arene.

DG = pyridyl, pyrimidine

Central arene: Ar-DG-H

[Mn] catalyst, cat. base

Products and reagents:

- Top-left: $\text{Ar-DG-CH=CH-CH(R')OH}$
- Top: $\text{Ar-DG-CH=CH-C(=O)R}$
- Top-right: $\text{Ar-DG-CH=CH-CH(E)E}$
- Right: $\text{Ar-DG-CH=CH-CO}_2\text{R}^2$
- Bottom-right: $\text{Ar-DG-CH=CH-CO}_2\text{R}^2$
- Bottom: $\text{Ar-DG-CH=CH-CO}_2\text{R}^2$
- Bottom-left: $\text{Ar-DG-CH=CH-CO}_2\text{R}^2$
- Left: $\text{Ar-DG-CH=CH-CO}_2\text{R}^2$

Reagents and conditions for the products:

- Top-left: R^1/H , R/H
- Top: R
- Top-right: E , E
- Right: CO_2R^2 , R^1
- Bottom-right: CO_2R^2 , R^1
- Bottom: R^1 , CO_2R^4 , R^2 , R^3
- Bottom-left: R^1 , CO_2R^4 , R^2 , R^3
- Left: R^1/H

Additional reagents and conditions:

- Top-left: $\text{DG} = \text{pyridyl, pyrimidine}$
- Top: $\text{DG} = \text{pyridyl, pyrimidine}$
- Top-right: $\text{DG} = \text{pyridyl, pyrimidine}$
- Right: $\text{DG} = \text{pyridyl, pyrimidine}$
- Bottom-right: $\text{DG} = \text{pyridyl, pyrimidine}$
- Bottom: $\text{DG} = \text{pyridyl, pyrimidine}$
- Bottom-left: $\text{DG} = \text{pyridyl, pyrimidine}$
- Left: $\text{DG} = \text{pyridyl, pyrimidine}$

Additional reagents and conditions:

- Top-left: R^1/H , R/H
- Top: R
- Top-right: E , E
- Right: CO_2R^2 , R^1
- Bottom-right: CO_2R^2 , R^1
- Bottom: R^1 , CO_2R^4 , R^2 , R^3
- Bottom-left: R^1 , CO_2R^4 , R^2 , R^3
- Left: R^1/H

Additional reagents and conditions:

- Top-left: $\text{DG} = \text{pyridyl, pyrimidine}$
- Top: $\text{DG} = \text{pyridyl, pyrimidine}$
- Top-right: $\text{DG} = \text{pyridyl, pyrimidine}$
- Right: $\text{DG} = \text{pyridyl, pyrimidine}$
- Bottom-right: $\text{DG} = \text{pyridyl, pyrimidine}$
- Bottom: $\text{DG} = \text{pyridyl, pyrimidine}$
- Bottom-left: $\text{DG} = \text{pyridyl, pyrimidine}$
- Left: $\text{DG} = \text{pyridyl, pyrimidine}$

Additional reagents and conditions:

- Top-left: R^1/H , R/H
- Top: R
- Top-right: E , E
- Right: CO_2R^2 , R^1
- Bottom-right: CO_2R^2 , R^1
- Bottom: R^1 , CO_2R^4 , R^2 , R^3
- Bottom-left: R^1 , CO_2R^4 , R^2 , R^3
- Left: R^1/H

Additional reagents and conditions:

- Top-left: $\text{DG} = \text{pyridyl, pyrimidine}$
- Top: $\text{DG} = \text{pyridyl, pyrimidine}$
- Top-right: $\text{DG} = \text{pyridyl, pyrimidine}$
- Right: $\text{DG} = \text{pyridyl, pyrimidine}$
- Bottom-right: $\text{DG} = \text{pyridyl, pyrimidine}$
- Bottom: $\text{DG} = \text{pyridyl, pyrimidine}$
- Bottom-left: $\text{DG} = \text{pyridyl, pyrimidine}$
- Left: $\text{DG} = \text{pyridyl, pyrimidine}$

Additional reagents and conditions:

- Top-left: R^1/H , R/H
- Top: R
- Top-right: E , E
- Right: CO_2R^2 , R^1
- Bottom-right: CO_2R^2 , R^1
- Bottom: R^1 , CO_2R^4 , R^2 , R^3
- Bottom-left: R^1 , CO_2R^4 , R^2 , R^3
- Left: R^1/H

Additional reagents and conditions:

- Top-left: $\text{DG} = \text{pyridyl, pyrimidine}$
- Top: $\text{DG} = \text{pyridyl, pyrimidine}$
- Top-right: $\text{DG} = \text{pyridyl, pyrimidine}$
- Right: $\text{DG} = \text{pyridyl, pyrimidine}$
- Bottom-right: $\text{DG} = \text{pyridyl, pyrimidine}$
- Bottom: $\text{DG} = \text{pyridyl, pyrimidine}$
- Bottom-left: $\text{DG} = \text{pyridyl, pyrimidine}$
- Left: $\text{DG} = \text{pyridyl, pyrimidine}$

Additional reagents and conditions:

- Top-left: R^1/H , R/H
- Top: R
- Top-right: E , E
- Right: CO_2R^2 , R^1
- Bottom-right: CO_2R^2 , R^1
- Bottom: R^1 , CO_2R^4 , R^2 , R^3
- Bottom-left: R^1 , CO_2R^4 , R^2 , R^3
- Left: R^1/H

Additional reagents and conditions:

- Top-left: $\text{DG} = \text{pyridyl, pyrimidine}$
- Top: $\text{DG} = \text{pyridyl, pyrimidine}$
- Top-right: $\text{DG} = \text{pyridyl, pyrimidine}$
- Right: $\text{DG} = \text{pyridyl, pyrimidine}$
- Bottom-right: $\text{DG} = \text{pyridyl, pyrimidine}$
- Bottom: $\text{DG} = \text{pyridyl, pyrimidine}$
- Bottom-left: $\text{DG} = \text{pyridyl, pyrimidine}$
- Left: $\text{DG} = \text{pyridyl, pyrimidine}$

Additional reagents and conditions:

- Top-left: R^1/H , R/H

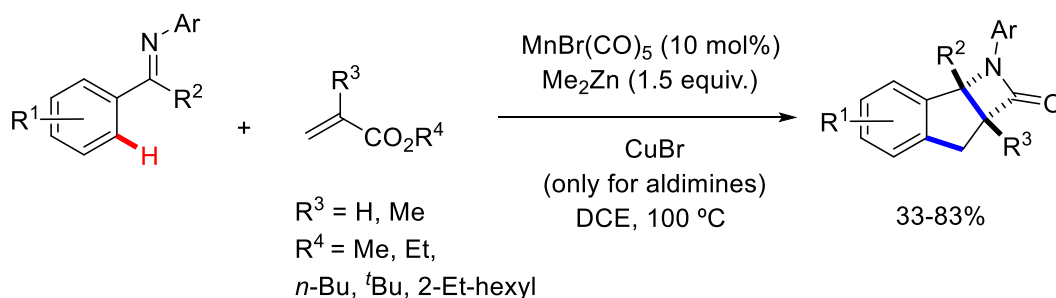
Three groups have independently reported methods for the fluoroalkenylation and fluoroallylation of arenes and heteroarenes (**Scheme 91**). The Ackermann group developed a strategy for the (per)fluoro allylation of indoles and ketimines *via* Mn catalysis in a highly chemo-, regio- and stereoselective process (**Scheme 91, a**).⁵³ The methodology was also expanded to include the Mn catalysed C-F/C-H alkenylation with difluoroalkenes and alkenylation with perfluoroalkenes (**Scheme 91, b**).⁵³ At the same time, a second method was disclosed by Zhang for the Mn catalysed difluoroallylation of indoles and pyridines. In contrast to Ackermann's work, this protocol avoided the *E/Z* selectivity problem by using 3-bromo-3,3-difluoropropene as the fluoroallylation source (**Scheme 91, a**).⁵⁴ Loh and co-workers reported an alternative method for the Mn catalysed fluoroalkenylation of indoles using *gem*-

91, f)).⁵⁸



In 2016, Wang and co-workers published an interesting paper on the bicyclic annulation of imines and unsaturated esters *via* Mn catalysed C-H activation (**Scheme 92**).⁵⁹ The methodology combines both Mn and Zn catalysis to give the fused β -lactam products. This was based on previous work carried out by the Ackermann group on the Mn catalysed synthesis of cis- β -amino acid esters from ketimines and α , β -unsaturated esters.⁶⁰

Wang, *Sci. China Chem.* 2016, 59, 1301-1305.



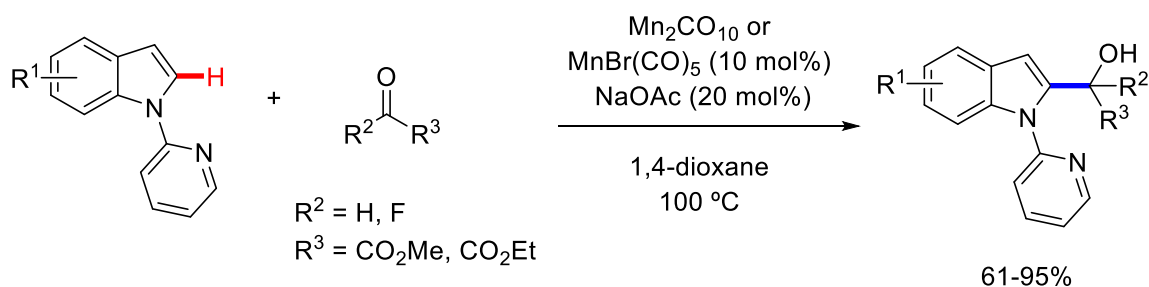
Scheme 92. Mn catalysed bicyclic annulation of imines with α , β -unsaturated esters.

4.3.4 Manganese hydroarylation reactions of aldehydes, ketones and imines

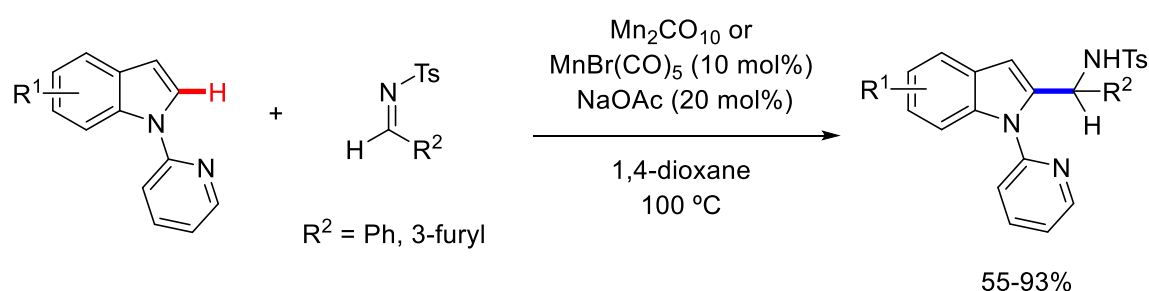
In 2016, Ackermann and co-workers reported a Mn catalysed hydroarylation of carbon-heteroatom multiple bonds (**Scheme 93**).⁶¹ Remarkably, the Mn(I) catalysts allowed for an unprecedented C-2 selective hydroarylation of indoles with aldehydes and ketones (**Scheme 93, a**). Other transition metals tested exclusively gave only the C-3 substituted product. The Mn catalysed C-H functionalisation of imines was also reported in the same paper (**Scheme 93, b**).

Ackermann, *Chem. Eur. J.* 2016, 22, 14856-14859.

a)



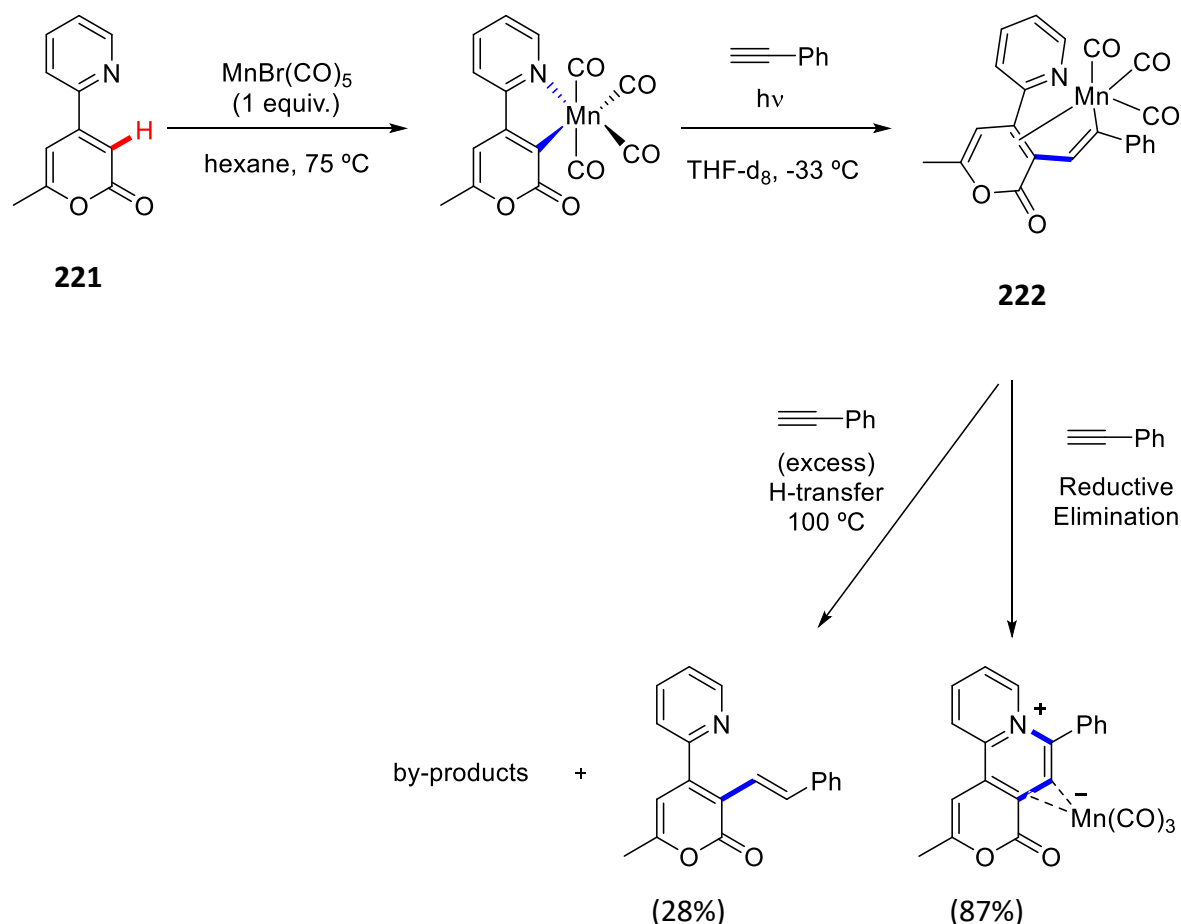
b)



Scheme 93. Mn catalysed C-H hydroarylation of carbon-heteroatom multiple bonds.

4.4 Mechanistic papers on manganese catalysed C-H activation

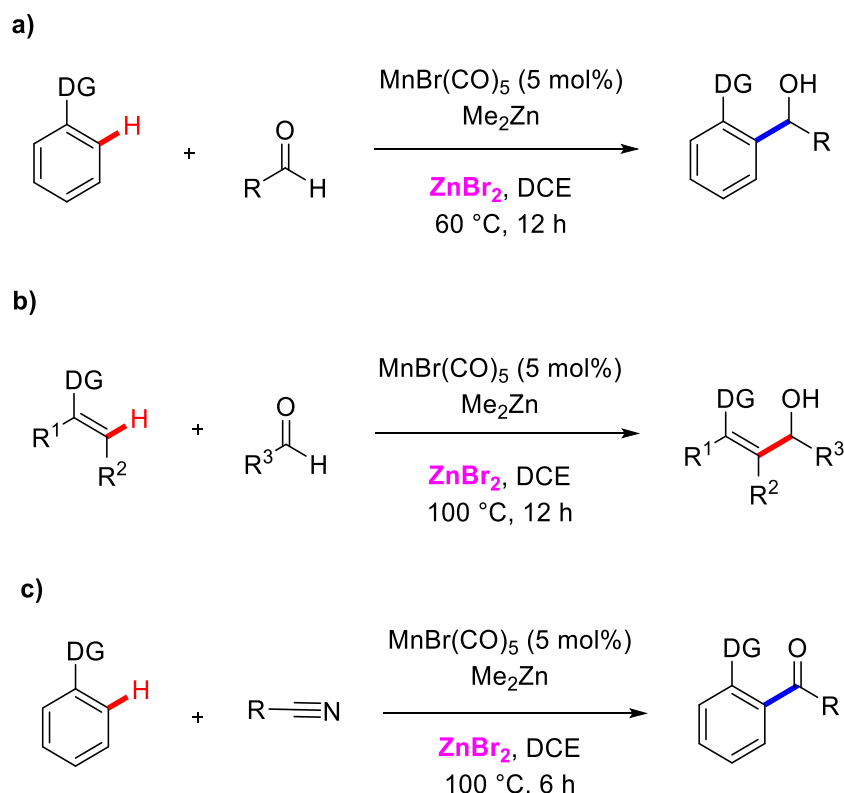
A few very interesting and important papers have been published by Fairlamb and co-workers in the last three years concerning the mechanistic details of Mn catalysed C-H activation reactions. In 2016, they reported a very insightful study on the C-H activation of 2-pyrone **221** and phenylacetylene (**Scheme 94**).⁶² Their work provided key information on the mechanism of some Mn catalysed C-H activation reactions. This involved detection and characterisation of a 7-membered manganacycle (**222**) proposed to play a key role in proton transfer and reductive elimination process and how different reaction conditions favour the formation of different products. Three more recent publications by Fairlamb and Lynam and co-workers involved real time infrared spectroscopic analysis for studying transient manganese carbonyl species formed during C-H bond activation reactions.⁶³⁻⁶⁵ This method enabled changes in metal carbonyl absorbances to be monitored (both qualitatively and quantitatively), and thus observation of the dynamic processes occurring at the manganese centre. Their work also provided an important insight into the key role of acid additives in Mn catalysed C-H activation reactions.



Scheme 94. Fairlamb's study of Mn catalysed C-H activation of 2-pyrone.

4.5 Literature examples of manganese/acid systems for C-H activation reactions

The nucleophilic reaction of inert carbon bonds to aldehydes is highly desirable for the synthesis of alcohols.⁶⁶ Previously, Kuninobu and co-workers used silanes as trapping agents providing silyl ether products (**Scheme 85**). However, the direct formation of alcohols is much less explored. An important advancement was made by the Wang group in 2015.⁶⁶ The Mn catalysed nucleophilic addition to aldehydes and nitriles was disclosed by using a dual activation strategy (**Scheme 95**). This clever protocol merged both Mn catalysed C-H activation and aldehyde (**Scheme 95, a**) and **b**) and nitrile (**Scheme 95, c**) activation by a **Lewis acid** (ZnBr₂). This seminal work found that the synergistic use of Me₂Zn and ZnBr₂ proved crucial in accessing the desired products. The methodology employs relatively mild reaction conditions, has a broad substrate scope and demonstrates excellent regio- and stereoselectivity.



Scheme 95. Mn catalysed direct nucleophilic addition to aldehydes and nitriles.

This Mn/acid cooperation strategy developed by Wang has allowed for the expansion of the substrate scope for Mn catalysed C-H activation to include more polarised C=X/C≡X systems. Also, the scope with respect to the arenes was extended to those with weakly coordinating directing groups (**Figure 33**). Representative examples are discussed below.

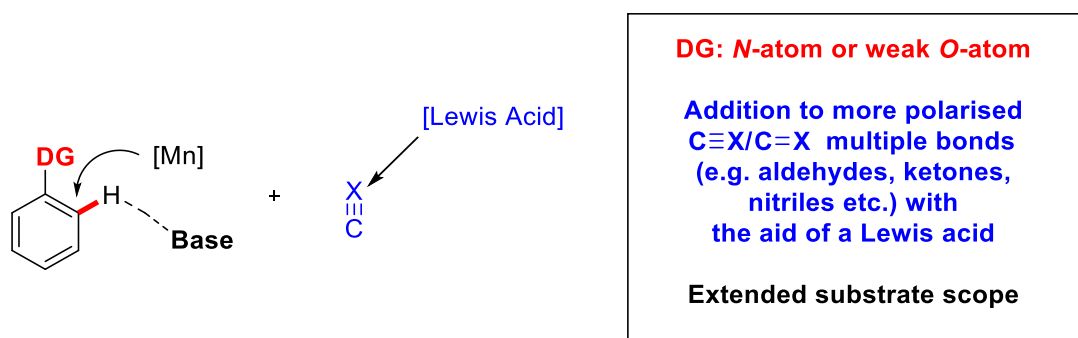
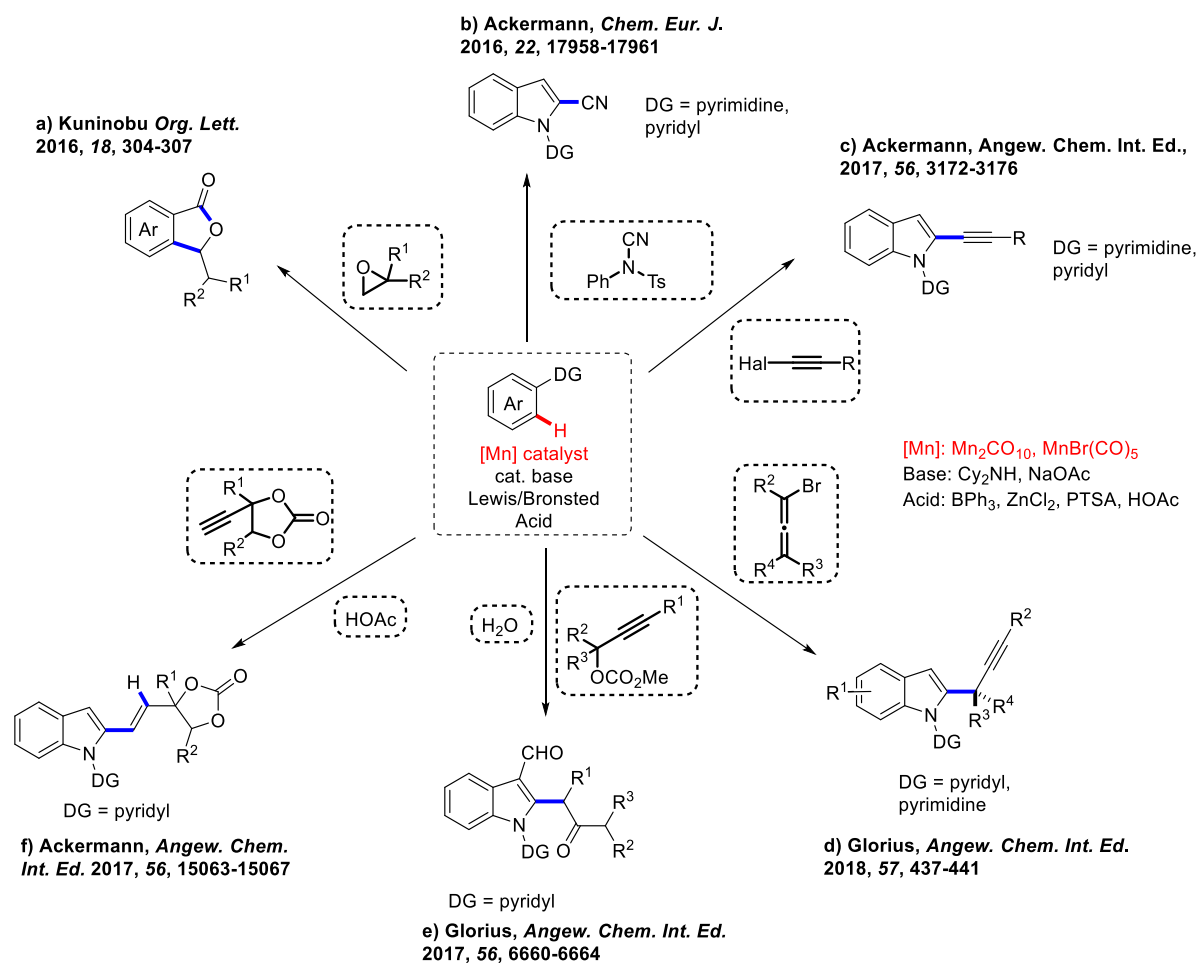


Figure 33. Mn/acid system for manganese catalysed C-H activation.

In 2016, Kuninobu and co-workers developed a Mn catalysed annulation of esters and oxiranes in the presence of a Lewis acid, triphenylborane (BPh₃) (**Scheme 96, a**).⁶⁷ This was the first example of a Mn catalysed C-H transformation using an oxygen directing group. The isobenzofuranone products were synthesised in moderate to good yields with high functional

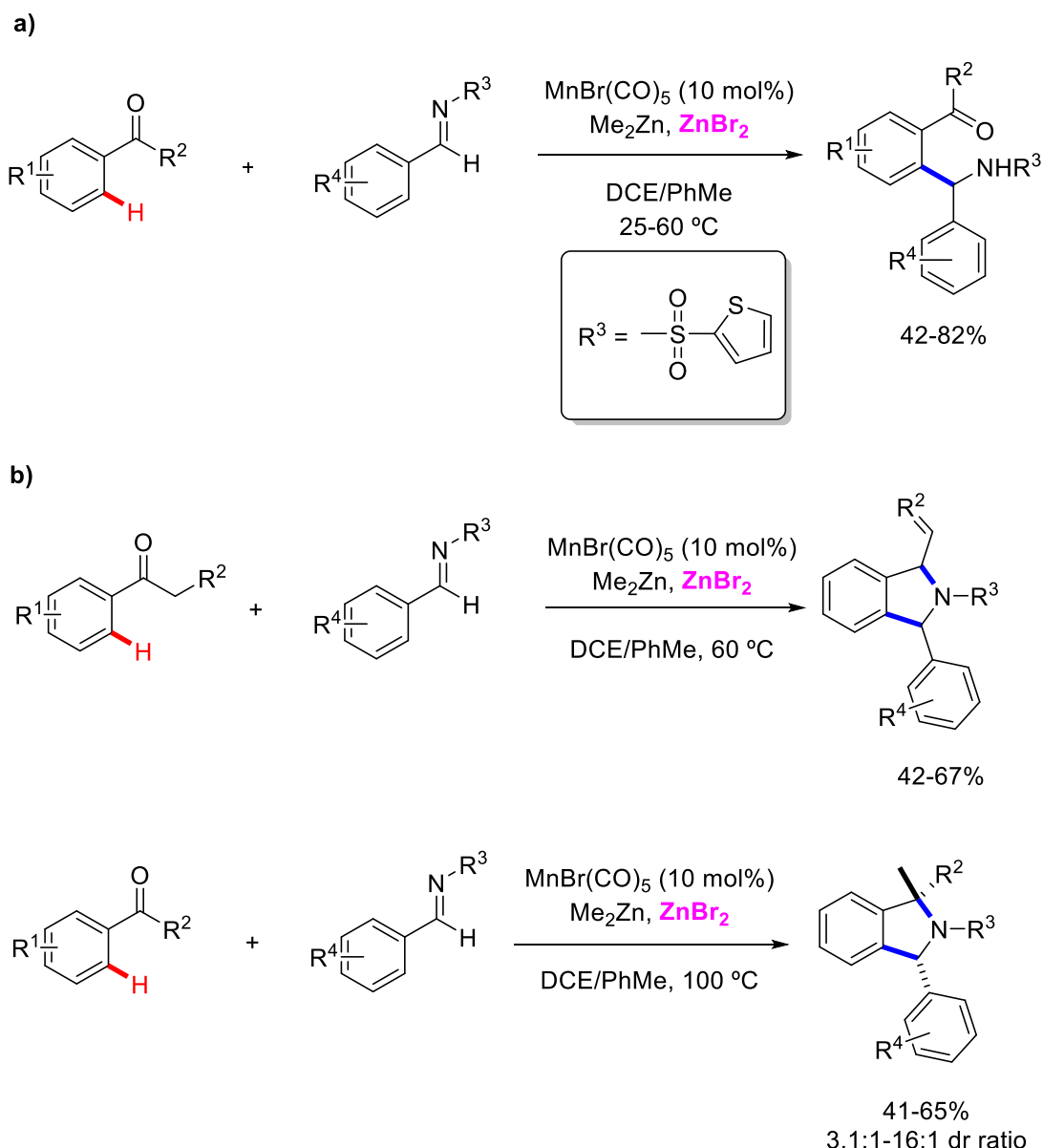
group tolerance. The authors claim that the Lewis acid, BPh_3 , is essential in promoting the reaction by cooperating with the Mn catalyst. The Mn catalysed C-H cyanation of heterocycles was developed by the Ackermann group by means of synergistic heterobimetallic catalysis (**Scheme 96, b**).⁶⁸ A large substrate scope and high functional group tolerance was reported. The Mn(I) catalyst in combination with a catalytic amount of ZnCl_2 allowed the cyanation of various heterocycles including indoles, pyrroles, thiophenes and even tryptophans. Ackermann and co-workers recently disclosed the C-H alkynylation of indoles and pyrroles in the presence of $\text{MnBr}(\text{CO})_5$ (**Scheme 96, c**).⁶⁹ Silyl haloalkynes were employed with good results. A significant substrate scope was reported. Moreover, it was possible to extend the methodology to non-activated aryl, alkenyl and alkyl haloalkynes under the same conditions by the addition of BPh_3 . As usual in Mn catalysis, the protocol was fully tolerant of valuable functionalities, including halogen, ester, cyano and nitro groups. The practical utility of this approach was further demonstrated in this remarkably dense and expansive report, by successful reactions on substrates bearing a fluorescent tag, a complex steroid motif and an enantiomerically pure amino acid. It could also be applied to peptides. Recently, the Glorius group developed a novel Mn/Lewis acid co-catalysed direct propargylation reaction utilising BPh_3 as the Lewis acid (**Scheme 96, d**).⁷⁰ The authors propose that the BPh_3 Lewis acid plays a significant role in enhancing the electrophilicity of the bromoallene, thereby promoting both the reactivity and selectivity. It is noteworthy that both terminal and internal alkynes can be obtained by this methodology as this has not been achieved in previous studies.

As well as Lewis acids, Brønsted acids can also be combined with manganese catalysts and this has allowed new reactivity in many cases (**Scheme 96, e**).⁷¹ This strategy was adopted by Glorius and co-workers in 2017. They developed an efficient strategy to synthesise 2-allenylindoles and this methodology was extended enabling the preparation of ketone products by the addition of a Brønsted acid, *p*-toluenesulfonic acid (PTSA). In addition, the Ackermann group demonstrated a chemo- and regioselective hydroarylation of alkynes with indoles by synergistic Brønsted acid/Mn catalysis and flow chemistry (**Scheme 96, f**).⁷² The corresponding products could easily be prepared in less than 20 minutes.



Scheme 96. Selected examples of Mn catalysed C-H activation reactions aided by Lewis/Brønsted Acids.

A very interesting piece of work was described by the Wang group in 2017. The Mn catalysed addition of ketones to imines was disclosed by the combination of Mn and Zn catalysis (**Scheme 97, a) and b)**).⁷³ Remarkably, the classic Mannich reaction was suppressed with the aid of Mn and at the same time the less reactive C-H bond of the aromatic ring of the ketone was activated. Interestingly, cyclised *exo*-olefinic isoindoline and three-component methylated isoindoline derivatives (**Scheme 97, b) and c)**) could be selectively obtained by slight tuning of the reaction conditions.

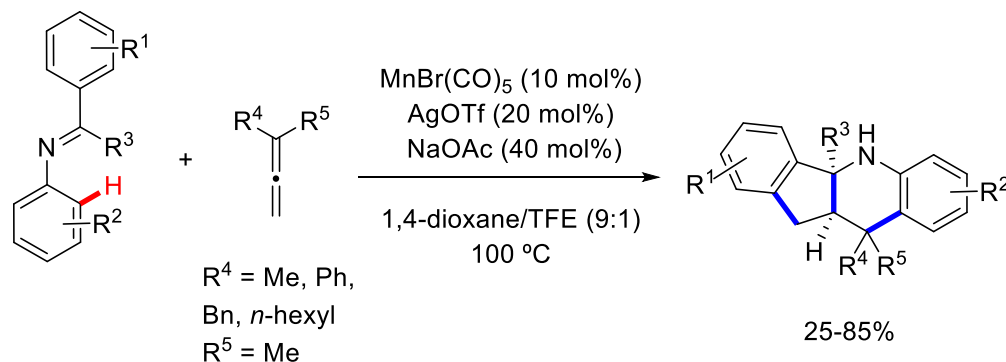


Scheme 97. a) Mn catalysed addition of ketones to imines b) Mn catalysed C-H activation for the selective preparation of *exo*-olefinic isoindoline and three component methylated isoindolines.

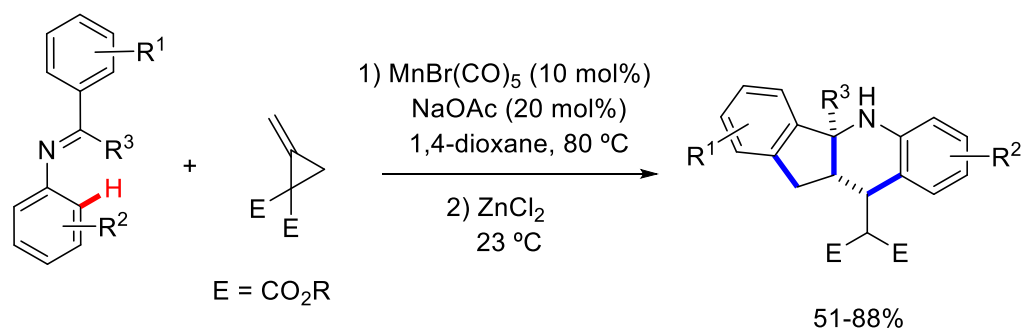
Further examples of bimetallic catalysis enabled by a cooperative Mn/Lewis acid system have been reported by the groups of Wang and Ackermann (**Scheme 98**). However, unlike the previous examples described above (**Scheme 96** and **Scheme 97**), whereby the acid is involved in the Mn catalytic cycle, these two reports describe a tandem catalysis in which the acid is not involved in the Mn catalytic cycle. Wang and co-workers reported a one-pot Mn catalysed C-H allylation and Ag catalysed Povarov cyclisation (**Scheme 98, (i)**). Three new carbon-carbon bonds are formed and two quaternary carbons are generated with yields of up to 85% being reported.⁷⁴ A similar methodology was developed by the Ackermann group (**Scheme 98, (ii)**).

In this work, similar products could be prepared substituting methylenecyclopropanes instead of allenes by using a combination of Mn and Zn catalysis.⁷⁵

(i) Wang, *ChemSusChem*, 2017, 10, 2360-2364.



(ii) Ackermann, *Angew. Chem. Int. Ed.* 2017, 29, 9543-9547.



Scheme 98. Selected examples of tandem catalysis involving a Mn/Lewis acid system.

An array of other Mn catalysed C-H activation reactions with various different coupling partners have been reported by numerous groups in the last few years, such as Ackermann's aminocarbonylation of heteroarenes using isocyanates as the coupling partner.⁷⁶ In 2014, the Wang group described a highly atom economical reaction for the synthesis of isoquinolines by means of a Mn catalysed C-H/C-N activation.⁷⁷ Interestingly, the transformation produced H₂ as the sole by-product without the need for any oxidant which is in contrast to previously established methods for the synthesis of isoquinolines by transition metal catalysed C-H activation.⁸ In addition, the Glorius group recently disclosed a Mn catalysed (2-indolyl)methylation of heteroarenes, which describes access to challenging unsymmetrical diheteroarylmethanes.⁷⁸ In 2019, Ackermann and co-workers developed an unprecedented Mn catalysed domino reaction consisting of a C-H activation, Diels-Alder reaction and a retro Diels-Alder reaction which provided access to invaluable indolone alkaloid derivatives.⁷⁹

Additionally, a few Mn catalysed C-H alkylation reactions have been published by different groups in the previous few years with alkyl halides⁸⁰, Grignard reagents⁸¹ and diazo malonates⁸² being successfully utilised as the coupling partners. Glorius and colleagues have also exploited diazo compounds as coupling partners for the β -functionalisation of α -diazo ketones through Mn(I)/Ag(I) relay catalysis. This approach allowed efficient access to β -(hetero)aryl ketones.⁸³

Mn catalysed C-H activation is a quickly emerging area in the field of organic synthesis and great strides have been made by various groups in recent years as discussed above. However, many limitations remain:

- 1) The substrate scope is sometimes limited
- 2) Rather harsh reaction conditions are required
- 3) Reliance on directing groups in the majority of cases
- 4) Reliance on $\text{MnBr}(\text{CO})_5$ and $\text{Mn}_2\text{CO}_{10}$ as the pre-catalytic species**
- 5) High catalyst loading (typically 10 mol%)
- 6) Relatively little information is known about the catalytic cycles

Thus, the aim of **Chapter 5** will be focused on addressing some of these limitations, in particular investigating the effect of other **ligands** (besides CO ligands) on Mn.

4.6 References

1. Bergman, R. G. *Nature* **2007**, *446*, 391.
2. Alberico, D., Scott, M. E., Lautens, M. *Chem. Rev.* **2007**, *107*, 174-238.
3. McGlacken, G. P., Bateman, L. M. *Chem. Soc. Rev.* **2009**, *38*, 2447-2464.
4. Yamaguchi, J., Yamaguchi, A. D., Itami, K. *Angew. Chem. Int. Ed.* **2012**, *51*, 8960-9009.
5. Ackermann, L. *Org. Process Res. Dev.* **2015**, *19*, 260-269.
6. Schipper, D. J., Fagnou, K. *Chem. Mater.* **2011**, *23*, 1594-1600.
7. Kuninobu, Y., Sueki, S. *Synthesis* **2015**, *47*, 3823-3845.
8. Liu, W., Ackermann, L. *ACS Catal.* **2016**, *6*, 3743-3752.
9. Cano, R., Mackey, K., McGlacken, G. P. *Catal. Sci. Tech.* **2018**, *8*, 1251-1266.
10. Hu, Y., Zhou, B., Wang, C. *Acc. Chem. Res.* **2018**, *51*, 816-827.
11. Morgan, J. W., Anders, E. *Proc. Natl. Acad. Sci.* **1980**, *77*, 6973-6977.
12. Erythropel, H. C., Zimmerman, J. B., de Winter, T. M., Petitjean, L., Melnikov, F., Lam, C. H., Lounsbury, A. W., Mellor, K. E., Janković, N. Z., Tu, Q., Pincus, L. N., Falinski, M. M., Shi, W., Coish, P., Plata, D. L., Anastas, P. T. *Green Chem.* **2018**, *20*, 1929-1961.
13. Gandeepan, P., Müller, T., Zell, D., Cera, G., Warratz, S., Ackermann, L. *Chem. Rev.* **2019**, *119*, 2192-2452.
14. <http://www.infomine.com/investment/steel/>, accessed 18th February 2020.
15. Bastian, D., *Preismonitor*, Federal Institute for Geosciences and Natural Resources, Germany, **2019**. Available at: https://www.bgr.bund.de/DE/Themen/Min_rohstoffe/Produkte/Preisliste/pm_19_12.pdf.
16. Su, B., Cao, Z.-C., Shi, Z.-J. *Acc. Chem. Res.* **2015**, *48*, 886-896.
17. Al-Afyouni, M. H., Krishnan, V. M., Arman, H. D., Tonzetich, Z. J. *Organometallics* **2015**, *34*, 5088-5094.
18. Breslow, R., Zhang, X., Huang, Y. *J. Am. Chem. Soc.* **1997**, *119*, 4535-4536.
19. Das, S., Incarvito, C. D., Crabtree, R. H., Brudvig, G. W. *Science* **2006**, *312*, 1941-1943.

20. Ottenbacher, R. V., Samsonenko, D. G., Talsi, E. P., Bryliakov, K. P. *ACS Catal.* **2014**, *4*, 1599-1606.
21. Shen, D., Miao, C., Wang, S., Xia, C., Sun, W. *Org. Lett.* **2014**, *16*, 1108-1111.
22. Adams, A. M., Du Bois, J., Malik, H. A. *Org. Lett.* **2015**, *17*, 6066-6069.
23. Yu, X.-Q., Huang, J.-S., Zhou, X.-G., Che, C.-M. *Org. Lett.* **2000**, *2*, 2233-2236.
24. Liang, J.-L., Huang, J.-S., Yu, X.-Q., Zhu, N., Che, C.-M. *Chem. Eur. J.* **2002**, *8*, 1563-1572.
25. Kim, J. Y., Cho, S. H., Joseph, J., Chang, S. *Angew. Chem. Int. Ed.* **2010**, *49*, 9899-9903.
26. Huang, X., Bergsten, T. M., Groves, J. T. *J. Am. Chem. Soc.* **2015**, *137*, 5300-5303.
27. Liu, W., Groves, J. T. *J. Am. Chem. Soc.* **2010**, *132*, 12847-12849.
28. Liu, W., Huang, X., Cheng, M.-J., Nielsen, R. J., Goddard, W. A., Groves, J. T. *Science* **2012**, *337*, 1322-1325.
29. Liu, W., Groves, J. T. *Angew. Chem. Int. Ed.* **2013**, *52*, 6024-6027.
30. Liu, W., Huang, X., Groves, J. T. *Nat. Protoc.* **2013**, *8*, 2348.
31. Huang, X., Liu, W., Ren, H., Neelamegam, R., Hooker, J. M., Groves, J. T. *J. Am. Chem. Soc.* **2014**, *136*, 6842-6845.
32. Liu, W., Groves, J. T. *Acc. Chem. Res.* **2015**, *48*, 1727-1735.
33. Bruce, M. I., Iqbal, M. Z., Stone, F. G. A. *J. Chem. Soc. A* **1970**, 3204-3209.
34. Liebeskind, L. S., Gasdaska, J. R., McCallum, J. S., Tremont, S. J. *J. Org. Chem.* **1989**, *54*, 669-677.
35. Gommans, L. H., Main, L., Nicholson, B. K. *J. Am. Chem. Soc. Chem. Commun.* **1987**, 761-762.
36. Robinson, N. P., Main, L., Nicholson, B. K. *J. Organomet. Chem.* **1989**, *364*, C37-C39.
37. Depree, G. J., Main, L., Nicholson, B. K. *J. Organomet. Chem.* **1998**, *551*, 281-291.
38. Cambie, R. C., Metzler, M. R., Rutledge, P. S., Woodgate, P. D. *J. Organomet. Chem.* **1990**, *381*, C26-C30.
39. Cambie, R. C., Metzler, M. R., Rutledge, P. S., Woodgate, P. D. *J. Organomet. Chem.* **1990**, *398*, C22-C24.

40. Cambie, R. C., Metzler, M. R., Rutledge, P. S., Woodgate, P. D. *J. Organomet. Chem.* **1992**, 429, 41-57.
41. Kuninobu, Y., Nishina, Y., Takeuchi, T., Takai, K. *Angew. Chem. Int. Ed.* **2007**, 46, 6518-6520.
42. Zhou, B., Chen, H., Wang, C. *J. Am. Chem. Soc.* **2013**, 135, 1264-1267.
43. Yang, X., Jin, X., Wang, C. *Adv. Syn. Catal.* **2016**, 358, 2436-2442.
44. Lu, Q., Greßies, S., Cembellín, S., Klauck, F. J., Daniliuc, C. G., Glorius, F. *Angew. Chem. Int. Ed.* **2017**, 56, 12778-12782.
45. Lu, Q., Greßies, S., Klauck, F. J., Glorius, F. *Angew. Chem. Int. Ed.* **2017**, 56, 6660-6664.
46. Zhou, B., Ma, P., Chen, H., Wang, C. *Chem. Commun.* **2014**, 50, 14558-14561.
47. Lu, Q., Klauck, F. J. R., Glorius, F. *Chem. Sci.* **2017**, 8, 3379-3383.
48. Meyer, T. H., Liu, W., Feldt, M., Wuttke, A., Mata, R. A., Ackermann, L. *Chem. Eur. J.* **2017**, 23, 5443-5447.
49. Wang, C., Wang, A., Rueping, M. *Angew. Chem. Int. Ed.* **2017**, 56, 9935-9938.
50. Chen, S.-Y., Han, X.-L., Wu, J.-Q., Li, Q., Chen, Y., Wang, H. *Angew. Chem. Int. Ed.* **2017**, 56, 9939-9943.
51. Chen, S.-Y., Li, Q., Wang, H. *J. Org. Chem.* **2017**, 82, 11173-11181.
52. Wang, H., Lorion, M. M., Ackermann, L. *Angew. Chem. Int. Ed.* **2017**, 56, 6339-6342.
53. Zell, D., Dhawa, U., Müller, V., Bursch, M., Grimme, S., Ackermann, L. *ACS Catal.* **2017**, 7, 4209-4213.
54. Ni, J., Zhao, H., Zhang, A. *Org. Lett.* **2017**, 19, 3159-3162.
55. Cai, S.-H., Ye, L., Wang, D.-X., Wang, Y.-Q., Lai, L.-J., Zhu, C., Feng, C., Loh, T.-P. *Chem. Commun.* **2017**, 53, 8731-8734.
56. Liu, W., Richter, S. C., Zhang, Y., Ackermann, L. *Angew. Chem. Int. Ed.* **2016**, 55, 7747-7750.
57. Kaplaneris, N., Rogge, T., Yin, R., Wang, H., Sirvinskaite, G., Ackermann, L. *Angew. Chem. Int. Ed.* **2019**, 58, 3476-3480.
58. Liu, S.-L., Li, Y., Guo, J.-R., Yang, G.-C., Li, X.-H., Gong, J.-F., Song, M.-P. *Org. Lett.* **2017**, 19, 4042-4045.
59. Hu, Y., Wang, C. *Sci. China Chem.* **2016**, 59, 1301-1305.

60. Liu, W., Zell, D., John, M., Ackermann, L. *Angew. Chem. Int. Ed.* **2015**, *54*, 4092-4096.
61. Liang, Y.-F., Massignan, L., Liu, W., Ackermann, L. *Chem. Eur. J.* **2016**, *22*, 14856-14859.
62. Yahaya, N. P., Appleby, K. M., Teh, M., Wagner, C., Troschke, E., Bray, J. T. W., Duckett, S. B., Hammarback, L. A., Ward, J. S., Milani, J., Pridmore, N. E., Whitwood, A. C., Lynam, J. M., Fairlamb, I. J. S. *Angew. Chem. Int. Ed.* **2016**, *55*, 12455-12459.
63. Hammarback, L. A., Robinson, A., Lynam, J. M., Fairlamb, I. J. S. *Chem. Commun.* **2019**, *55*, 3211-3214.
64. Hammarback, L. A., Robinson, A., Lynam, J. M., Fairlamb, I. J. S. *J. Am. Chem. Soc.* **2019**, *141*, 2316-2328.
65. Hammarback, L. A., Clark, I. P., Sazanovich, I. V., Towrie, M., Robinson, A., Clarke, F., Meyer, S., Fairlamb, I. J. S., Lynam, J. M. *Nat. Catal.* **2018**, *1*, 830-840.
66. Zhou, B., Hu, Y., Wang, C. *Angew. Chem. Int. Ed.* **2015**, *54*, 13659-13663.
67. Sueki, S., Wang, Z., Kuninobu, Y. *Org. Lett.* **2016**, *18*, 304-307.
68. Liu, W., Richter, S. C., Mei, R., Feldt, M., Ackermann, L. *Chem. Eur. J.* **2016**, *22*, 17958-17961.
69. Ruan, Z., Sauermann, N., Manoni, E., Ackermann, L. *Angew. Chem. Int. Ed.* **2017**, *56*, 3172-3176.
70. Zhu, C., Schwarz, J. L., Cembellín, S., Greßies, S., Glorius, F. *Angew. Chem. Int. Ed.* **2018**, *57*, 437-441.
71. Lu, Q., Greßies, S., Klauck, F. J. R., Glorius, F. *Angew. Chem. Int. Ed.* **2017**, *56*, 6660-6664.
72. Wang, H., Pesciaioli, F., Oliveira, J. C. A., Warratz, S., Ackermann, L. *Angew. Chem. Int. Ed.* **2017**, *56*, 15063-15067.
73. Zhou, B., Hu, Y., Liu, T., Wang, C. *Nature Commun.* **2017**, *8*, 1169.
74. Chen, S.-Y., Li, Q., Liu, X.-G., Wu, J.-Q., Zhang, S.-S., Wang, H. *ChemSusChem* **2017**, *10*, 2360-2364.
75. Liang, Y.-F., Müller, V., Liu, W., Münch, A., Stalke, D., Ackermann, L. *Angew. Chem. Int. Ed.* **2017**, *129*, 9543-9547.

76. Liu, W., Bang, J., Zhang, Y., Ackermann, L. *Angew. Chem. Int. Ed.* **2015**, *54*, 14137-14140.
77. He, R., Huang, Z. T., Zheng, Q. Y., Wang, C. *Angew. Chem. Int. Ed.* **2014**, *53*, 4950-4953.
78. Lu, Q., Cembellín, S., Greßies, S., Singha, S., Daniliuc, C. G., Glorius, F. *Angew. Chem. Int. Ed.* **2018**, *57*, 1399-1403.
79. Zhu, C., Kuniyil, R., Ackermann, L. *Angew. Chem. Int. Ed.* **2019**, *58*, 5338-5342.
80. Liu, W., Cera, G., Oliveira, J. C. A., Shen, Z., Ackermann, L. *Chem. Eur. J.* **2017**, *23*, 11524-11528.
81. Sato, T., Yoshida, T., Al Mamari, H. H., Ilies, L., Nakamura, E. *Org. Lett.* **2017**, *19*, 5458-5461.
82. Wang, C., Maity, B., Cavallo, L., Rueping, M. *Org. Lett.* **2018**, *20*, 3105-3108.
83. Lu, Q., Mondal, S., Cembellín, S., Glorius, F. *Angew. Chem. Int. Ed.* **2018**, *57*, 10732-10736.

Chapter 5: Synthesis of Mn carbonyl phosphine complexes and their application in C-H activation reactions

5.1 Preface

The design, synthesis and characterisation of Mn carbonyl phosphine complexes is described in this Chapter. Their application in a number of transition metal catalysed C-H activation reactions will also be discussed.

5.2 Background

As previously discussed in **Chapter 4** of this thesis, Mn catalysis has recently emerged as an attractive alternative to Pd (as well as Ir and Rh) catalysed C-H activation processes. Although the reactions published in the literature up to now represent noteworthy advancements in the field of Mn catalysed C-H activation, several challenges remain. To date, only commercially available $\text{MnBr}(\text{CO})_5$ and $\text{Mn}_2\text{CO}_{10}$ pre-catalysts have been utilised in Mn catalysed C-H activation reactions. Importantly, these systems cannot be easily optimised as the CO ligands cannot be tailored by steric or electronic alterations.

5.3.1 Ligand design

The rational choice and design of appropriate ligands is critical for both the development and fine tuning of catalyst reactivity and selectivity (i.e. enantioselectivity, diastereoselectivity, regioselectivity and chemoselectivity) of metal complexes. Both the steric and electronic properties of the ligand can influence the bond-making and bond-breaking processes that occur about the metal centre. Thus, ligand design and an understanding of how ligands influence both the structural and reactivity properties of metal species has allowed for the development of new and improved catalytic reactions.¹ Ligand design is therefore essential in the advancement of manganese catalysis. Since ligand design and development has been crucial to the success of Pd catalysis over the last few decades, it seems imperative that the future of Mn catalysed C-H activation reactions will be dependent on the design and development of new ligands for Mn.

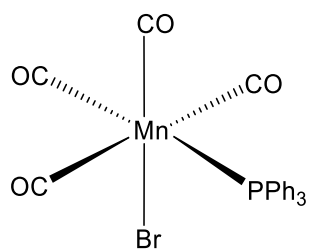
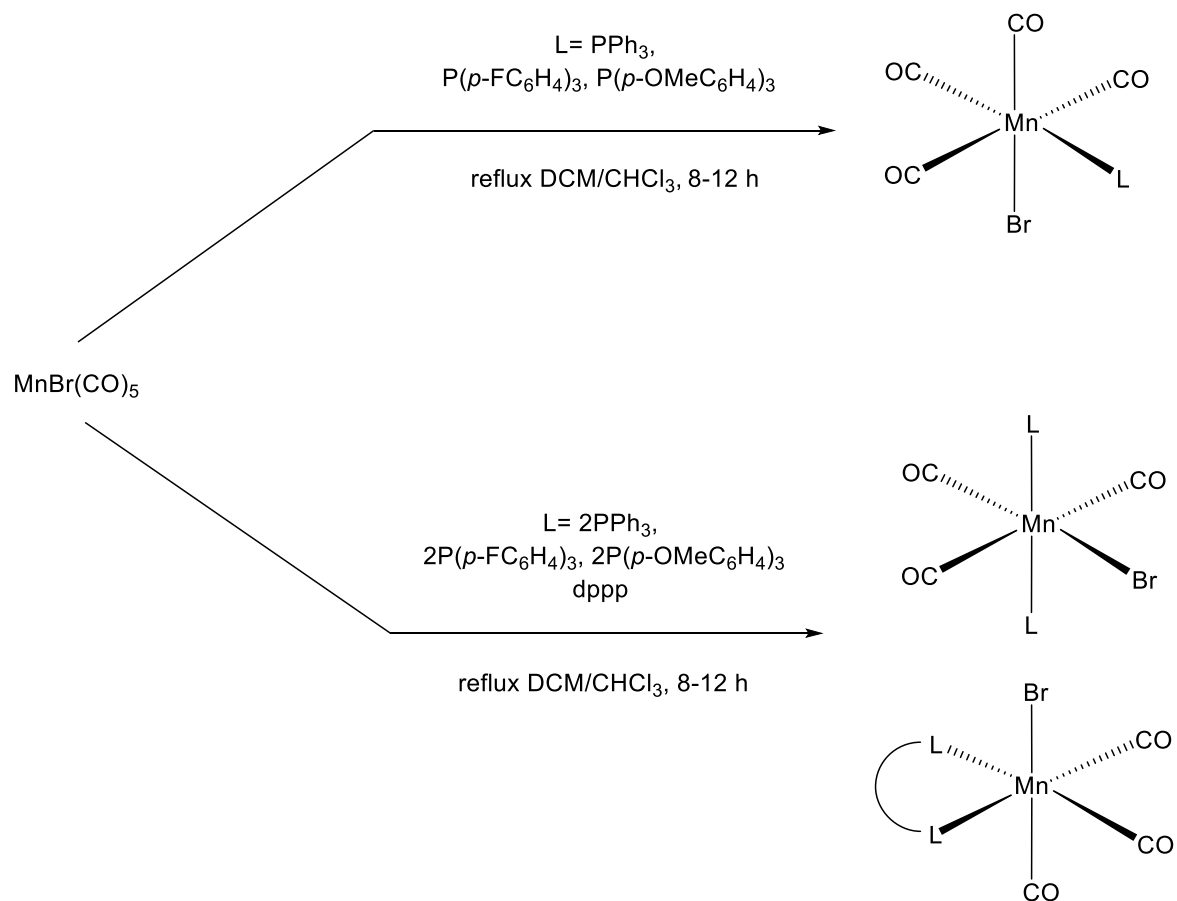
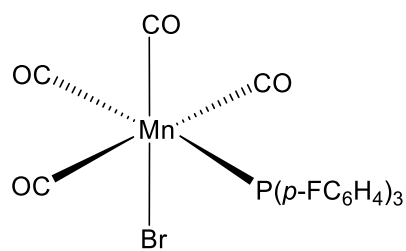
5.3.2 Choice of ligand for Mn

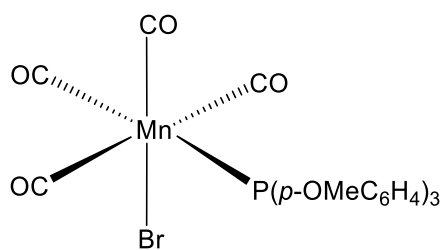
The use of phosphorus-based ligands to facilitate and tune metals centres has been well documented in the literature over the last number of decades.¹⁻² In the case of Pd-catalysed cross-coupling reactions³⁻¹⁵ and Pd-catalysed C-H activation,¹⁶ the contribution of phosphine ligands has been fundamental to selectivity and reactivity. Hence, we sought to prepare a Mn

phosphine template to allow for tuneable phosphine ligands and apply these complexes in C-H activation reactions.¹⁷

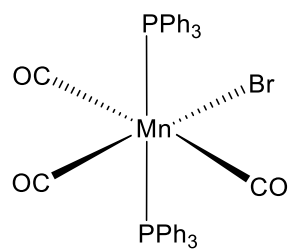
5.3.3 Synthesis of Mn carbonyl phosphine complexes

The Mn carbonyl phosphine complexes were easily prepared *via* a procedure described by Bond and co-workers from 1978.¹⁸ The complexes were prepared with a view to investigating how the steric and electronic properties of the ligand(s) could influence both the structure and reactivity at the Mn centre and how this affects the rate of reaction. Initially, we began our study by preparing four Mn carbonyl mono-phosphine complexes (tetracarbonyl Mn phosphine complexes) (**223-225**). Next, we looked at synthesising the more sterically crowded Mn carbonyl di-phosphine complexes (tricarbonyl Mn phosphine complexes) (**226-228**). Finally, one bidentate complex¹⁹ (dppp) **229** was prepared using the procedure described herein. Complexes **223-229** were prepared by reaction of commercially available $\text{MnBr}(\text{CO})_5$ with 1 or 2 equivalents of the corresponding phosphine ligand in refluxing chloroform or dichloromethane for 8 h (**Scheme 99**).¹⁸ The compounds were isolated in yields ranging from 73-99% by evaporation of the solvent and recrystallisation from a dichloromethane/hexane mixture. The resulting bright yellow complexes were fully characterised by $^1\text{H}/^{31}\text{P}/^{13}\text{C}$ NMR spectroscopy, infrared spectroscopy (IR), single crystal X-ray structure analysis and elemental analysis (see Experimental Section, **Chapter 6**). The reaction of $\text{MnBr}(\text{CO})_5$ with a number of substituted phosphine ligands failed to yield the desired Mn phosphine complex. For example, reaction of tris-(4-*tert*-butylphenyl)phosphine, tris-(3, 4-dimethylphenyl)phosphine, tris-(3,4-dimethoxyphenyl)phosphine, tris-(*o*-tolylphenyl) phosphine, tricyclohexylphosphine (previously synthesised *via* photochemical means²⁰) and tris-(pentafluorophenyl)phosphine with $\text{MnBr}(\text{CO})_5$ failed to yield the corresponding Mn phosphine complex. In the case of tris-(3,4-dimethylphenyl)phosphine, tris-(3,4-dimethoxy phenyl)phosphine, tris-(*o*-tolylphenyl)phosphine, tricyclohexylphosphine, this may be attributed to steric effects. For the penta-fluoro phosphine ligand, the phosphorus atom would lack the necessary basicity to undergo reaction. Finally, complex **DJ1** with a *para*-trifluoromethyl group was synthesised by co-worker Dr. David Jones.

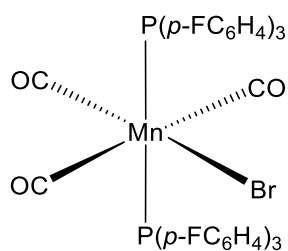
*cis*- $\text{MnBr}(\text{CO})_4(\text{PPh}_3)$ **223**, 95%*cis*- $\text{MnBr}(\text{CO})_4(\text{P}(p\text{-FC}_6\text{H}_4)_3)$ **224**, 86%



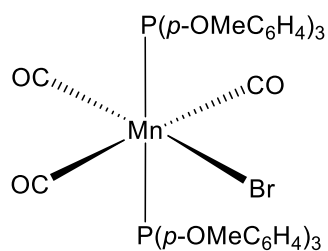
cis-MnBr(CO)₄(P(*p*-OMeC₆H₄)₃)
225, 91%



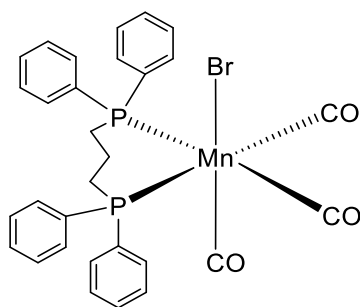
mer-trans-MnBr(CO)₃(PPh₃)₂
226, 73%



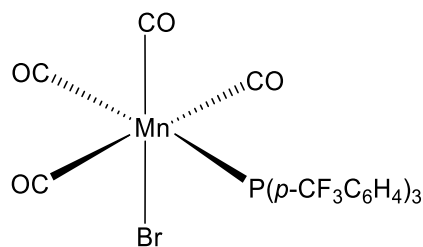
mer-trans-
MnBr(CO)₄(P(*p*-FC₆H₄)₃)₂
227, 82%



mer-trans-
MnBr(CO)₄(P(*p*-OMeC₆H₄)₃)₂
228, 88%



fac-cis-MnBr(CO)₃(dppp)
229, 81%



cis-MnBr(CO)₄(P(*p*-CF₃C₆H₄)₃)
DJ1

Scheme 99. Synthesis of Manganese phosphine complexes **223-229**.

5.3.4 Bonding in metal carbonyl phosphine complexes

The bonding in metal carbonyl phosphine complexes has important implications on the reactivity of the complex and is evident upon analysis of the spectroscopic data of the complex. This will be discussed more in detail in the following section. For complexes **223-229** and **DJ1**, the bonding between Mn and CO ligands involves both a σ component and a π component. The sigma bond is formed as a result of overlap of an sp orbital on carbon and an empty d-orbital on Mn. π -Back donation is as a result of overlap of a filled d-orbital Mn and a π^* orbital on the CO ligand.²¹ The bonding between Mn and the tertiary phosphine ligand also involves two important interactions. A sigma bond is formed by donation of a one pair of electrons in an sp^3 orbital on phosphorus into an empty d-orbital on Mn (**Figure 34, (i)**). Like CO, phosphines can also participate in backbonding to a certain degree. However, rationalisation of $M \rightarrow P$ backbonding is controversial. Previously, backbonding in metal-phosphine complexes was attributed to an interaction between a $d\pi$ -orbital on the metal and an empty 3d orbital on phosphorus. Quantum mechanical calculations have elegantly shown that P-R σ^* orbitals play a major role. Hybridisation of P 3d orbitals and P-R σ^* orbitals result in the formation of π -acceptor molecular orbitals (MOs) available for π -backbonding (**Figure 34, (ii)**).²²⁻²³

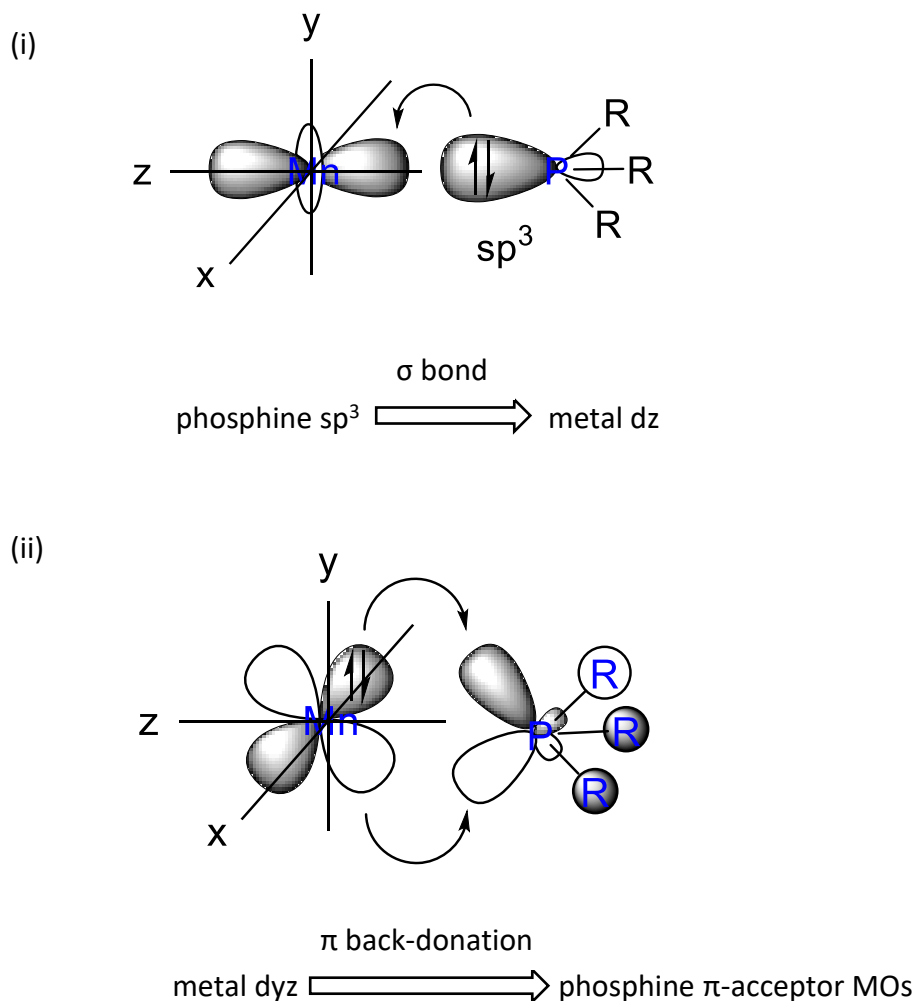


Figure 34. Description of bonding in metal carbonyl phosphine complexes.

5.3.5 Spectroscopic and single crystal X-ray results

^{31}P NMR Spectra (complexes 223-225)

The ^{31}P nucleus couples to any other nucleus with a nuclear spin (I) > 0 . Thus, coupling of the phosphorus to the NMR active isotope of Mn (^{55}Mn) was observed in the ^{31}P NMR spectra for each complex (**223-229**). The directly bonded ^{55}Mn quadrupolar nucleus ($I=5/2$) resulted in the ^{31}P NMR resonances for each complex being broadened, although coupling to ^{55}Mn was not resolved.²⁴ The ^{31}P NMR spectra of compounds **223** to **225** (mono-phosphine complexes) show a single resonance and this is consistent with only one species in solution (**Figure 35**).¹⁹ The large change in chemical shift observed in the ^{31}P NMR spectra of each of the complexes in comparison to the free phosphine ligand provides evidence for the coordinated ligand to

the Mn centre in each case. The change in chemical shift from the free ligand to the coordinated complex is represented by the coordination shift ($\Delta\delta_P$) (**Table 18**).²⁴

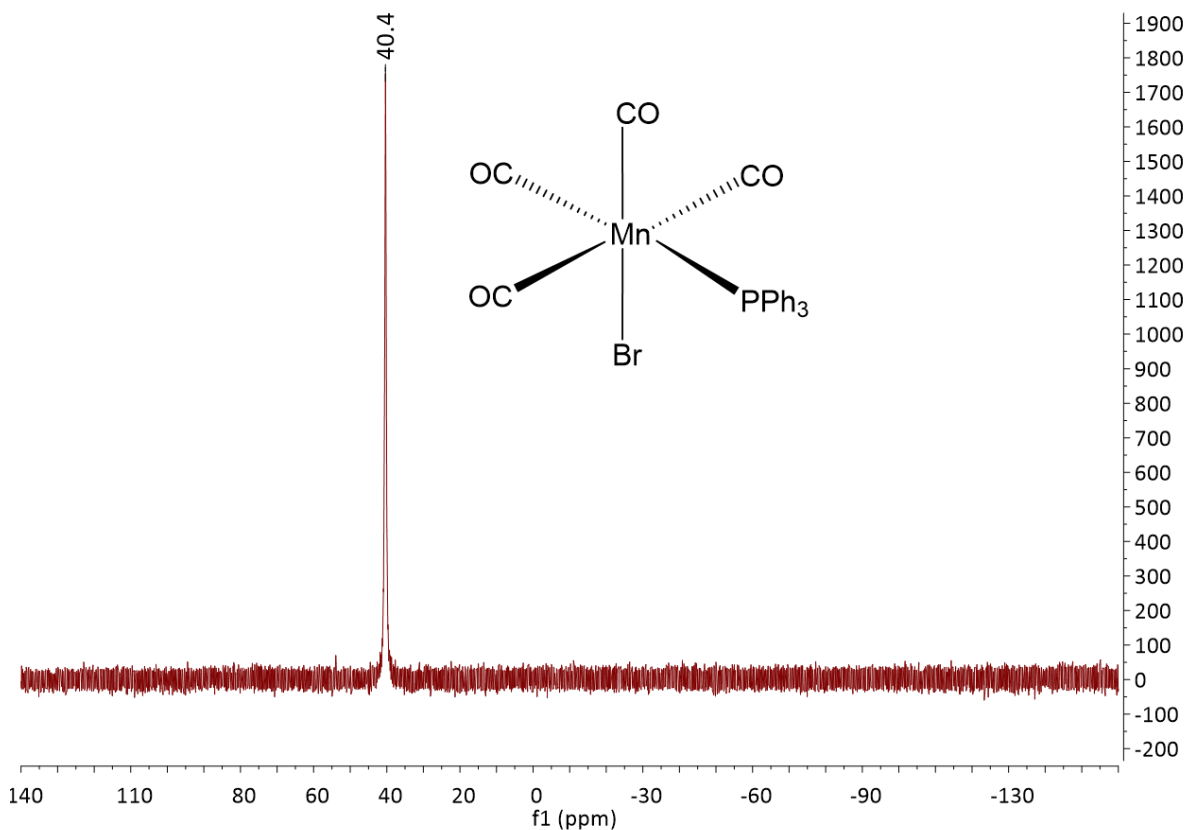


Figure 35. ^{31}P NMR spectra of Mn mono-phosphine complex **223**.

Table 18. Comparison of ^{31}P chemical shift values between Mn complexes **223-225** and the corresponding free phosphine ligand.

Entry	Mn complex	^{31}P NMR shift (ppm): Mn Complex	^{31}P NMR shift (ppm): Free phosphine ligand ²⁵	$\Delta\delta_P$ (ppm)
1	223	40.4	-6.0	46.4
2	224	39.4	-9.0	48.4
3	225	36.1	-10.8	46.9

^{31}P NMR data recorded in CDCl_3 .

X-ray crystal structure and IR spectra (tetracarbonyl Mn phosphine complexes)

The crystal structure of **223** (**Figure 36**) shows a *cis*-octahedral arrangement and this is also predicted from the spectroscopic analysis as described above. Carbonyl stretching modes in

transition metal complexes depend on the symmetry of the molecule. The number and nature of the symmetry elements of a given molecule are donated by its point group. Tetracarbonyl Mn phosphine bromide complexes belong to the C_s point group. The C_s symmetry of *cis*-complexes leads to three absorption bands ($2A' + 2A''$) in the IR spectra.²⁶ Thus, the IR spectra of complexes **223-225** show three strong CO stretching vibrations consistent again with *cis*-tetracarbonyl phosphine organomanganese complexes previously reported (**Table 19**).²⁷

These three bands correspond to the axial and radial A_1 modes. The A'' mode corresponds to the E mode of the complex.²⁶ All absorptions are of medium-high intensity as all modes involve dipole moment changes. The highest frequency $\bar{\nu}(\text{CO})$ band relates to the two CO ligands which are *trans* to each other. The middle $\bar{\nu}(\text{CO})$ band corresponds to the CO ligand *trans* to the phosphine ligand. Finally, the lowest frequency $\bar{\nu}(\text{CO})$ band corresponds to the CO ligand *trans* to Br.

The steric and electronic properties of phosphine ligands can be classified in terms of two parameters devised by Tolman.⁷⁵ Firstly, the cone angle addresses the steric bulk of phosphine ligands. Secondly, the electronic effect of various tertiary phosphine ligands can be adjusted by changing the R group. This was quantified by Tolman, who compared the $\bar{\nu}(\text{CO})$ stretching frequencies of a series of $\text{LNi}(\text{CO})_3$ complexes, where L is a tertiary phosphine ligand. Importantly, $\bar{\nu}(\text{CO})$ changes as the electron donating ability of the phosphine ligand increases. Thus, the increase in electron density at Ni from σ donation of the tertiary phosphine ligand is dispersed through the M-L ligand system *via* π -backbonding. Most of the electron density is passed onto the CO π^* orbitals. This is reflected in decreased $\bar{\nu}(\text{CO})$ stretching frequencies which corresponds to weaker C-O bonds.⁷⁵ In addition, more electron donating phosphine ligands are associated with more electron rich metals, which are better at CO π -backbonding. Thus, the greater the CO π -backbonding corresponds to lower $\bar{\nu}(\text{CO})$ due to decreased bond order. Consequently, better donor ligands translates to lower $\bar{\nu}(\text{CO})$ values. This is evident upon analysis of the IR spectra for complexes **223-225**. The $\bar{\nu}(\text{CO})$ stretching frequencies are similar for **223-225**. However, a slight reduction in the frequencies was observed as the electron donating ability of the phosphine ligand increases.²⁸ In particular, comparing the $\bar{\nu}(\text{CO})$ band corresponding to the CO ligand *trans* to the tertiary phosphine ligand, for the complex with the *para*-methoxy phosphine ligand (**225**), $\bar{\nu}(\text{CO})$ shows up at 1989 cm^{-1} . Complex **224** with a *para*-fluoro phosphine ligand (**224**), $\bar{\nu}(\text{CO})$ shows up at 1998 cm^{-1} . Finally, complex **223** with a triphenyl phosphine ligand (*para*-H), $\bar{\nu}(\text{CO})$ shows

up at 2002 cm^{-1} . Complex (**225**) can be considered the greatest electron donor and thus the electron density at the Mn is greatest for this complex. Thus, this translates into enhanced CO π -backbonding and lower $\bar{\nu}_{\text{CO}}$ values as a result. Comparing complexes **223** and **224**, **224** (*para*-F substituent on the phosphine ligand, the lone pair of electrons in the 2p orbital on the *para*-F substituent increases the electron donating ability of this phosphine ligand) can be considered a greater electron donor relative to **223** (*para*-H substituent on the phosphine ligand). Thus, $\bar{\nu}_{\text{CO}}$ shows up at 1998 cm^{-1} for **224** and 2002 cm^{-1} for **223**.

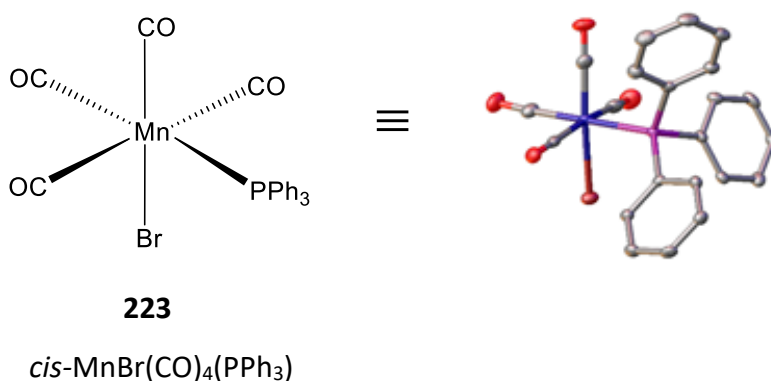


Figure 36. Molecular and crystallographic structure of complex **223**, *cis*-[MnBr(CO)₄(PPh₃)]. Thermal ellipsoids drawn at the 50% probability level. Second molecule and hydrogen atoms omitted for clarity.

Table 19. IR spectroscopic data for complexes **223-225** (CO region only).

Entry	Mn complex	IR data $\bar{\nu}_{\text{CO}}/\text{cm}^{-1}$
1	223	2086, 2002, 1956
2	224	2091, 1998, 1946
3	225	2083, 1989, 1943

³¹P NMR spectra (complexes 226-228)

The single resonance in the ³¹P NMR spectra of complexes to **226-228** is consistent with a *mer-trans* configuration (**Figure 37**) and is in accordance with previous literature reports.¹⁹ The single resonance in the ³¹P NMR spectra for each of the di-phosphine complexes (**226-228**) indicates that the two phosphine ligands are bound *trans* to each other.²⁰ Again, the significant change in chemical shift observed in the ³¹P NMR spectra of each of the complexes

(**223-228**) in comparison to the free phosphine ligand provided evidence for the coordination of the phosphine ligand to the Mn centre (**Table 20**).

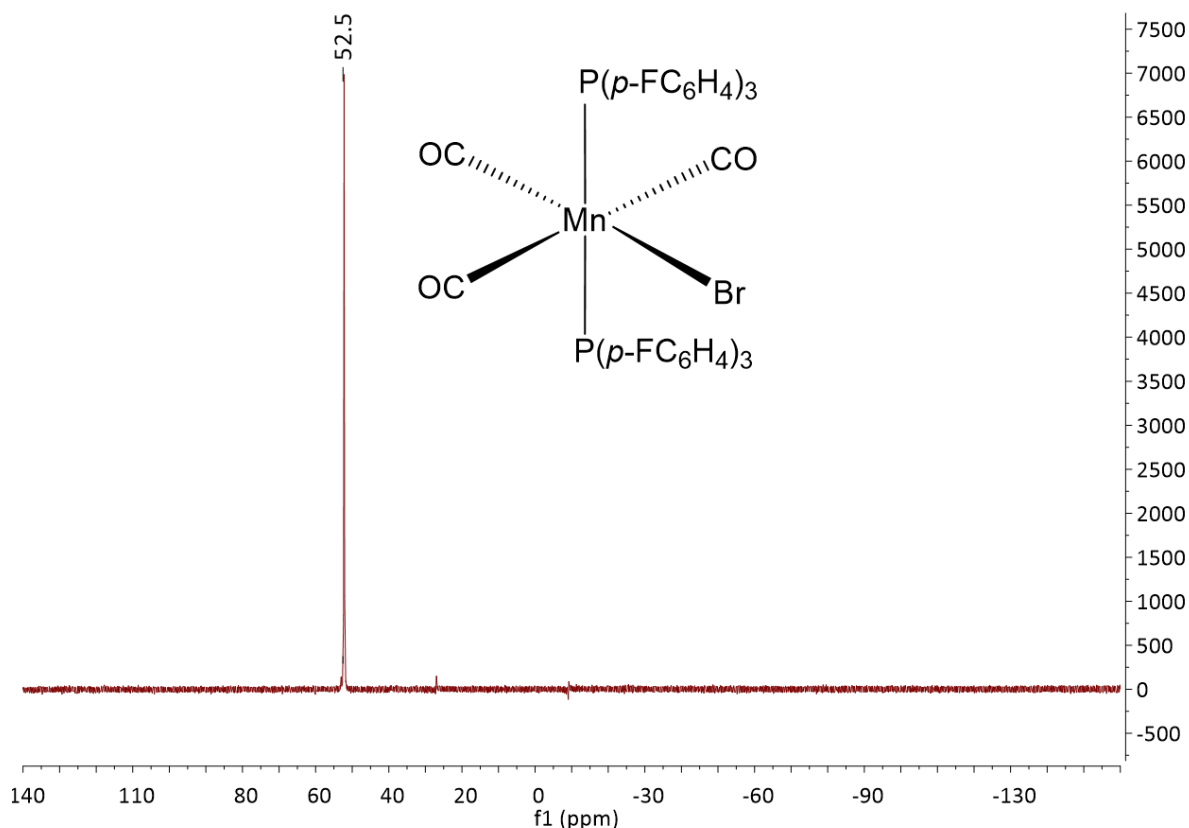


Figure 37. ^{31}P NMR spectra of Mn diphosphine complex **227**.

Table 20. Comparison of ^{31}P chemical shift values between Mn complexes **226-228** and the corresponding free phosphine ligand.

Entry	Mn complex	^{31}P NMR shift (ppm): Mn complex	^{31}P NMR shift (ppm): Free phosphine ligand ²⁵	$\Delta\delta_{\text{P}}$ (ppm)
1	226	54.0	-6.0	60.0
2	227	52.2	-9.0	61.2
3	228	49.5	-10.8	60.3

^{31}P NMR data recorded in CDCl_3 .

X-ray crystal structure and IR spectra (tricarbonyl Mn phosphine complexes)

Mer, *trans*-diphosphine complexes show C_{2v} symmetry and therefore three IR active modes ($2A_1 + B_1$).²⁶ Accordingly, three $\bar{\nu}(\text{CO})$ bands were observed in the IR spectra for each complex

which is consistent with a *mer*-CO arrangement.²⁰ The IR spectra for each of the di-phosphine complexes **226-228** show two strong and one weak CO stretching vibrations (**Table 21**).²⁶ The highest frequency $\bar{\nu}(\text{CO})$ band corresponds to the symmetric A_1 mode and is of weak intensity due to a weak dipole moment change. The lowest frequency $\bar{\nu}(\text{CO})$ band (second A_1 mode) corresponds to the CO ligand *trans* to the bromide and is of the strongest intensity. This is because the CO *trans* to Br is expected to have the greatest degree of $\text{Mn} \rightarrow \text{CO}$ π -backbonding. An intense B_1 mode relates to the two CO ligands *trans* to each other. This is consistent with previous literature reports of Mn(I) di-phosphine complexes, although it is important to note that analysis of the IR spectra alone does not easily allow one to distinguish between the *mer-trans* and *mer-cis* isomers.¹⁹

Again, analysis of the IR spectra for complexes **226-228**, lower $\bar{\nu}(\text{CO})$ values were observed as the electron donating ability of the phosphine ligand increased.²⁸ The $\bar{\nu}(\text{CO})$ stretching frequencies for complexes **226** (*para*-F substituent on the phosphine ligand) and **227** (*para*-methoxy substituent on the phosphine ligand) showed up at lower frequencies relative to complex **225** (triphenyl phosphine ligand (*para*-H)). This is as a result of greater π -backbonding in complexes **226** and **227**, which translates into lower $\bar{\nu}(\text{CO})$ as a result.

The ^{31}P NMR data and IR spectroscopic data correlate with a *mer-trans* configuration for the Mn di-phosphine complexes (**226-228**), identified by X-ray crystal structure analysis (**Figure 38**).

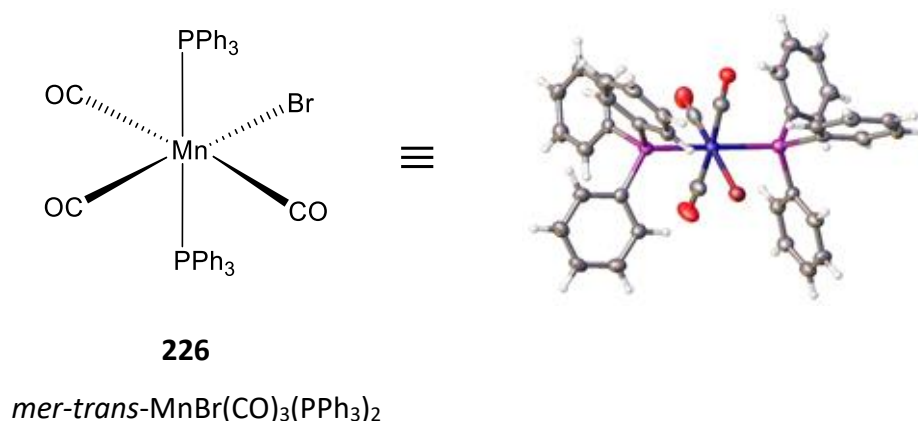


Figure 38. Molecular and crystallographic structure of complex **226**, *mer, trans*-[MnBr(CO)₃(PPh₃)₂]. Thermal ellipsoids drawn at the 50% probability level.

Table 21. IR spectroscopic data for complexes **226-228** (CO region only).

Entry	Mn complex	IR data $\bar{\nu}(\text{CO})/\text{cm}^{-1}$
1	226	2087, 2003, 1943
2	227	2036, 1931, 1902
3	228	2008, 1939, 1908

 ^{31}P NMR spectra (complex 229)

The ^{31}P NMR spectra of the bidentate complex **229** shows a singlet indicating that both of the phosphorus atoms are coordinated to the Mn and furthermore that both of the phosphorus atoms are equivalent (**Figure 39**).²⁹ In addition, the single resonance at 28.3 ppm in the ^{31}P NMR spectra is consistent with only one species being present in solution. The difference in chemical shift between complex **229** and the free phosphine is given in **Table 22** and, is in accordance to similar observations for the mono- and di-phosphine Mn complexes.

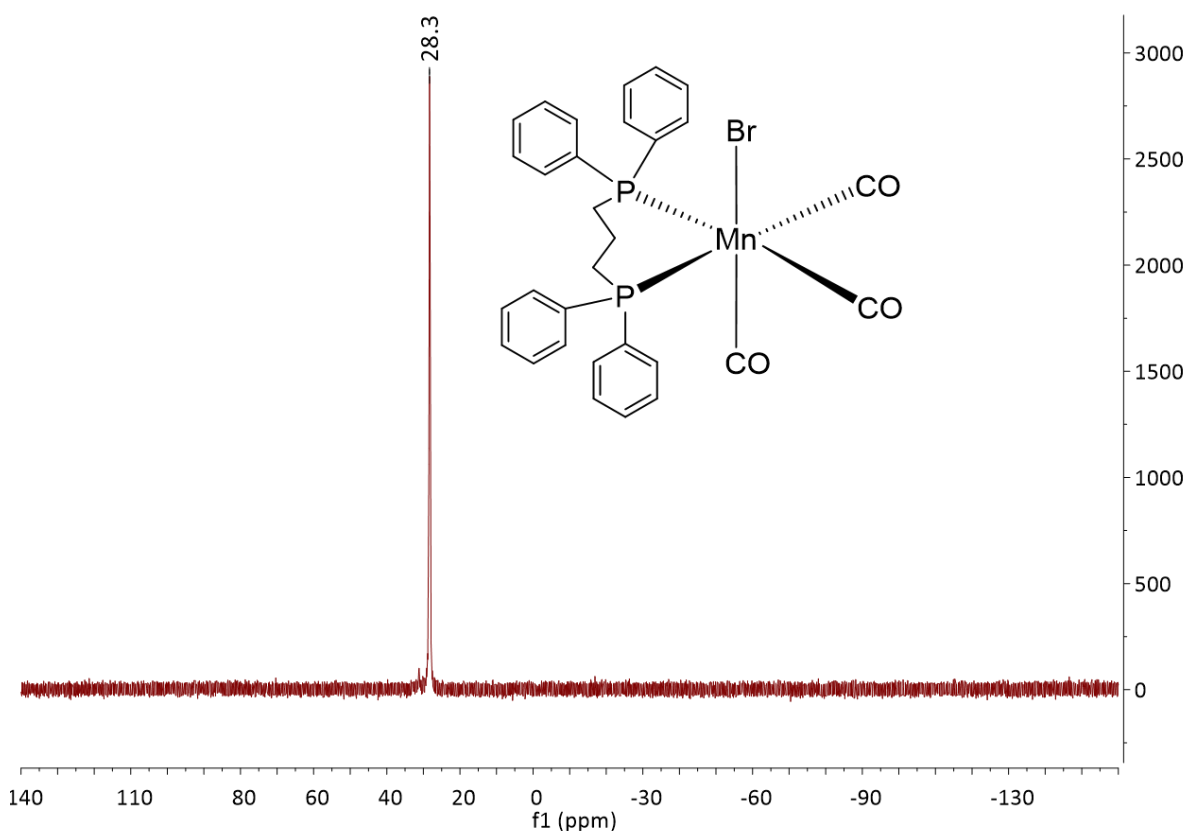
**Figure 39.** ^{31}P NMR spectra of bidentate Mn complex **229**.

Table 22. ^{31}P chemical resonances of Mn complex **229** and free phosphine ligand, and coordination chemical shift values.

Entry	Mn complex	^{31}P NMR shift (ppm): Mn complex	^{31}P NMR shift (ppm): Free phosphine ligand	$\Delta\delta_{\text{P}}$ (ppm)
1	229	28.3	-26.7 ³⁰	55

^{31}P NMR data recorded in CDCl_3 .

Complex **229** was identified as having a *fac-cis* configuration by single crystal X-ray structure and spectroscopic analysis (**Figure 40**). *Fac*-diphosphine complexes possess C_s symmetry and this would give rise to three carbonyl stretching absorptions ($2A' + A''$).²⁶ Accordingly, three strong bands were observed in the IR spectrum of complex **229** (**Table 23**). The lowest frequency $\bar{\nu}(\text{CO})$ band is due to the CO ligand which is *trans* to the bromine atom and the two higher frequency $\bar{\nu}(\text{CO})$ bands are due to the two CO ligands which are *trans* to the two phosphorus atoms. This data correlates with *fac*-di-phosphine complexes previously reported.²⁹

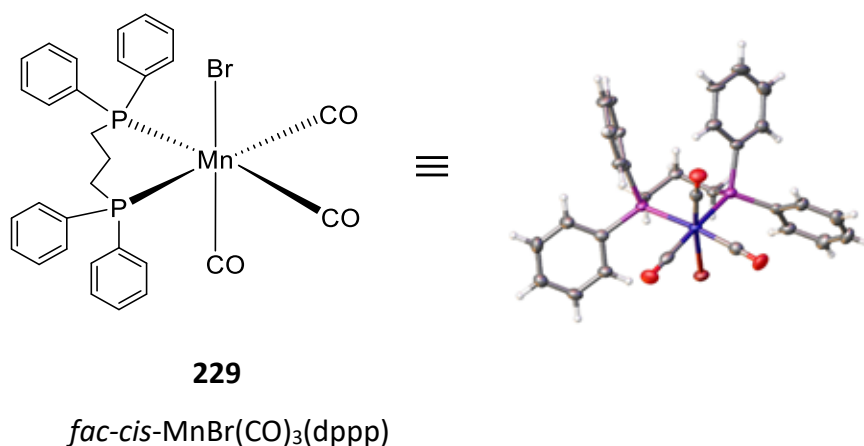


Figure 40. Molecular and crystallographic structure of **229**, *fac, cis*- $[\text{MnBr}(\text{CO})_4(\text{dppp})]$. Thermal ellipsoids drawn at the 50% probability level.

Table 23. IR spectroscopic data for complex **229** (CO region only)

Entry	Mn complex	IR data $\bar{\nu}(\text{CO})/\text{cm}^{-1}$
1	229	2019, 1953, 1905

^{13}C NMR spectra of complexes 223-229

In the ^{13}C NMR spectra of complexes **223-229**, the CO resonances are broad (spanning a few ppm) due to the effect of the directly bonded ^{55}Mn quadrupole. The di-phosphine complexes (**226-229**) all show two broad carbonyl signals of relative intensity 2:1, although this is not quantitative (the signal at higher frequency is assigned to the carbonyl *trans* to the Br and the signal at lower frequency is assigned to the mutually *trans* carbonyls),¹⁸⁻¹⁹ which proves the *mer-trans* configuration for complexes **226-228** and a *fac-cis* configuration for complex **229** (correlating with single crystal X-ray analysis for these complexes) (**Figure 41** and **Figure 42**).

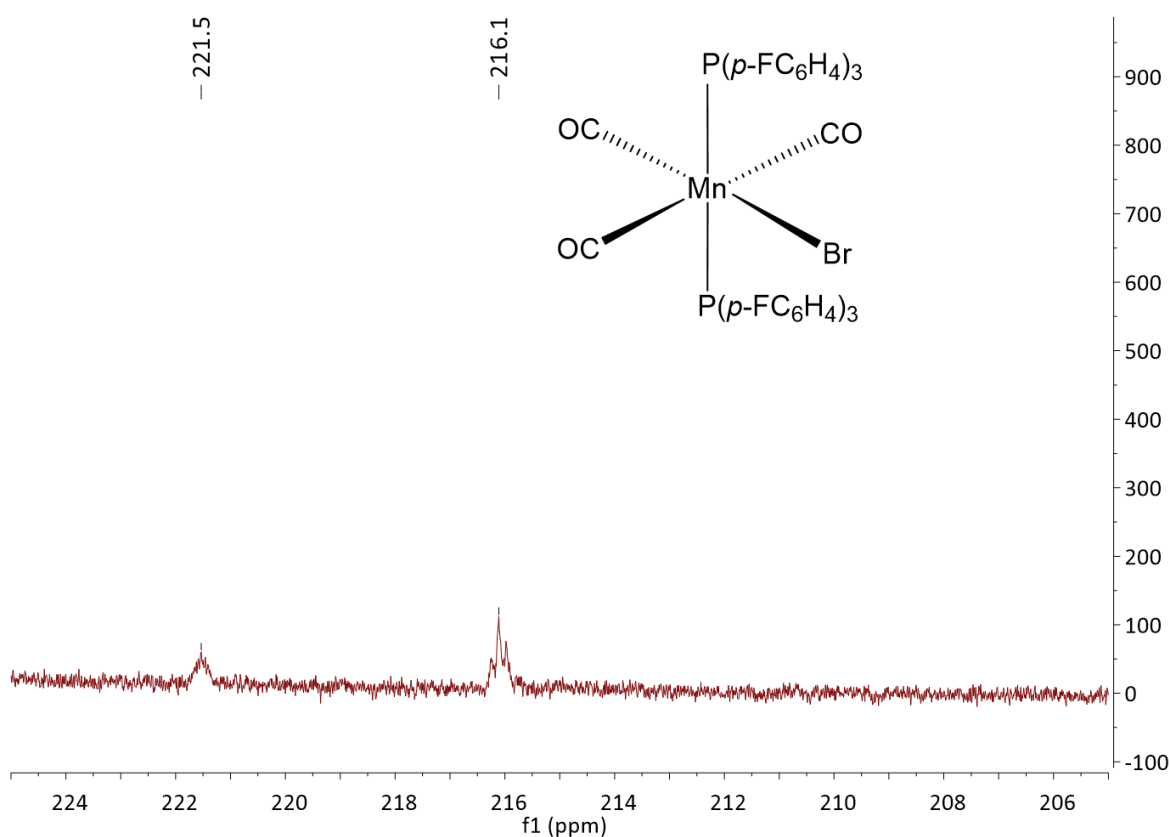


Figure 41. ^{13}C NMR spectra of complex **227** showing two broad CO signals in a relative intensity of approximately 2:1.

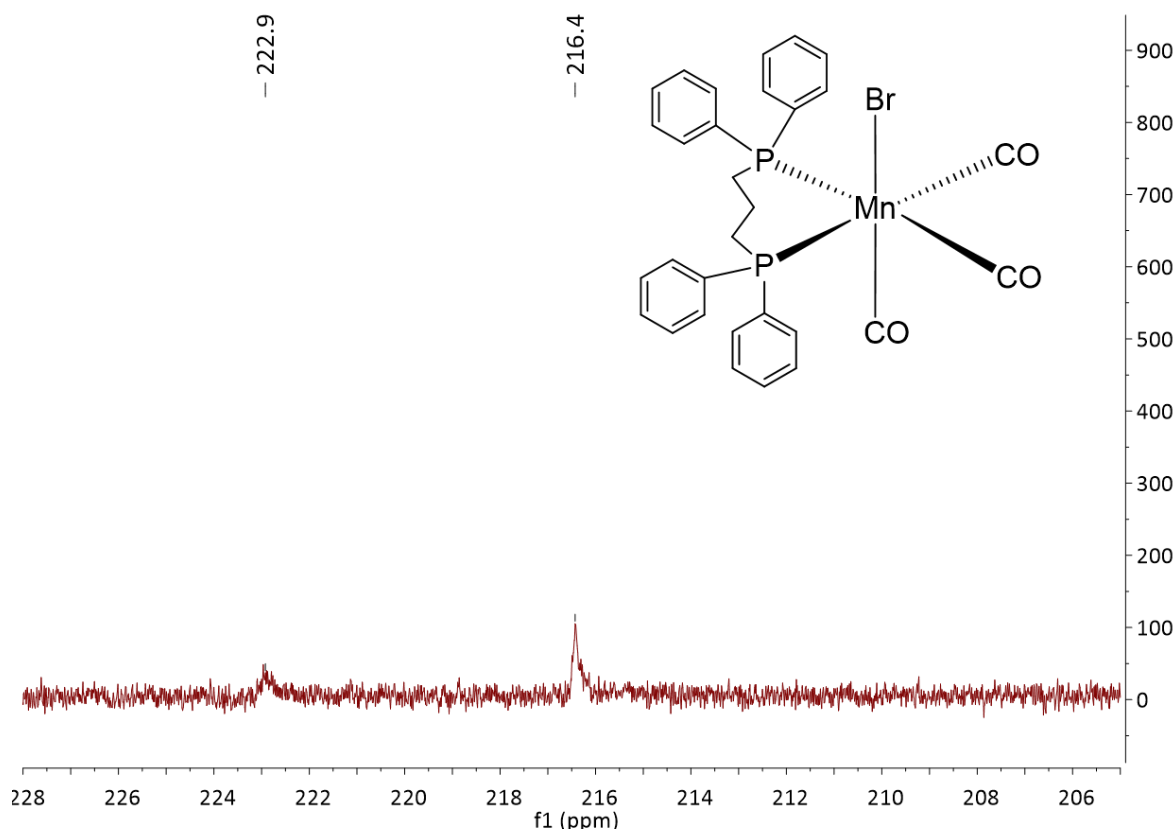


Figure 42. ^{13}C NMR spectra of complex **229** showing two broad CO signals in a relative intensity of approximately 2:1.

In the ^{13}C NMR spectra for the mono-phosphine complexes (**223-225**), three separate broad carbonyl signals (which are poorly resolved) are observed, in a ratio of approximately 2:1:1 (**Figure 43**). The relative ratios identify the first signal (most upfield shift) as that arising from the two equivalent *trans* carbonyl ligands, the second signal correlating to the carbonyl which is *trans* to the phosphorus atom (and *cis* to the Br) and finally the most downfield shift being assigned as the carbonyl *trans* to the Br (*cis* to the phosphorus atom). This coincides with literature reports of carbonyl groups *trans* to the phosphine ligand showing a larger downfield shift than *cis* carbonyl groups.³⁰

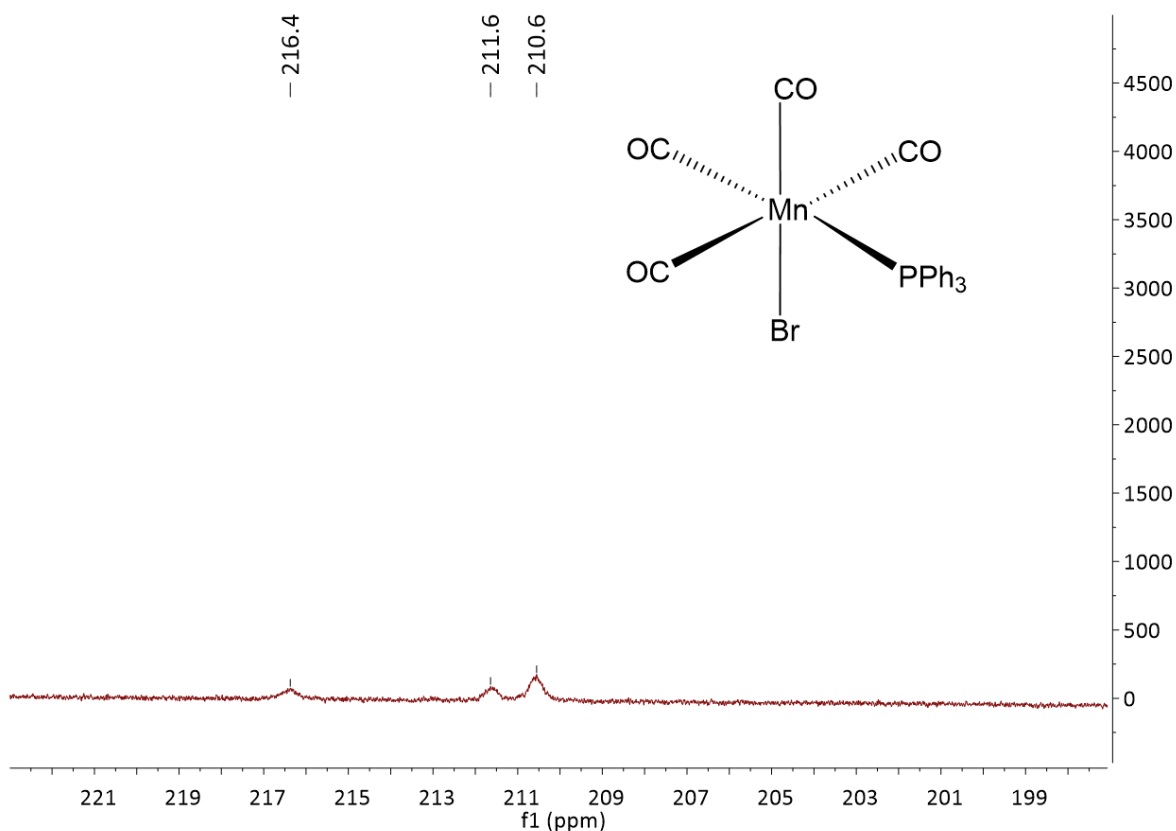


Figure 43. ^{13}C NMR spectra of complex **223** showing three broad CO signals in a relative intensity of approximately 2:1:1.

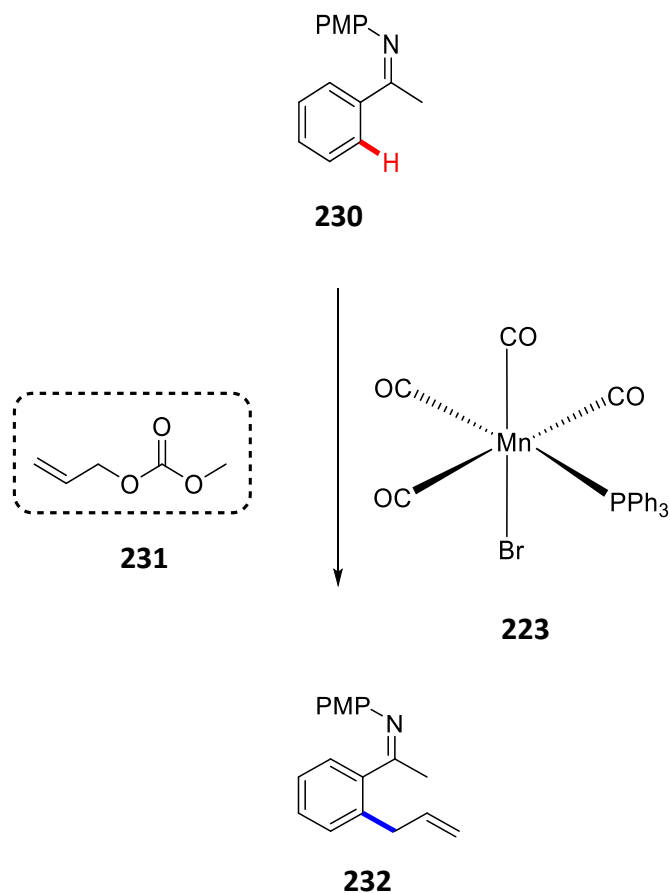
5.4.1 Investigation of Mn phosphine complexes in C-H activation reactions

In most Mn catalysed C-H activation reactions published in the literature to date, the action of a directing group such as a nitrogen containing heterocycle or an imine group is necessary.³¹⁻³³ Thus, substrates **230**, **220** and **247** were all investigated as potential substrates in Mn catalysed C-H activation reactions using the tetracarbonyl and tricarbonyl Mn phosphine complexes (**223-229**), with general reaction conditions also based on previous work published. Substrate **230** containing an imine group was obtained by another member of the McGlacken group, phenyl pyridine (**220**) was available from a commercial supplier and *N*-(2-pyridyl) indole (**247**) was synthesised *via* a procedure described by Ramon and co-workers.³⁴

1. Ketimine directing group

A variety of Mn catalysed C-H activation reaction conditions were applied to imine **230**. The reactions investigated were based on previous Mn (as well as Rh) catalysed C-H activation reactions published in the literature.

First, the mono-phosphine complex **223** was examined in the Mn catalysed C-H allylation of ketimine **230**.³⁵ Unfortunately, no encouraging results were obtained. Only *ca.* 10% conversion to product **232** could be detected in the ¹H NMR spectrum of the crude reaction mixture (**Table 24, entry 1**). The conversion to product **232** was even less when TBAB was used as an additive in the reaction (**Table 24, entry 2**). Secondly, we investigated the effect 15 mol% triphenylphosphine had on the allylation reaction when the commercial catalyst MnBr(CO)₅ was used (**Table 24, entry 3**). However, only unreacted starting material **230** was recovered from the crude reaction mixture. When 10 mol% TBAB was added to the reaction mixture in addition to 15 mol% triphenyl phosphine, only a trace of allylated product **232** was detected (**Table 24, entry 4**). The triphenyl phosphine is most likely coordinating to a vacant site on Mn (rendering the catalyst inactive), which could prevent the acrylate substrate **231** from binding to Mn, hence shutting down the catalytic cycle.

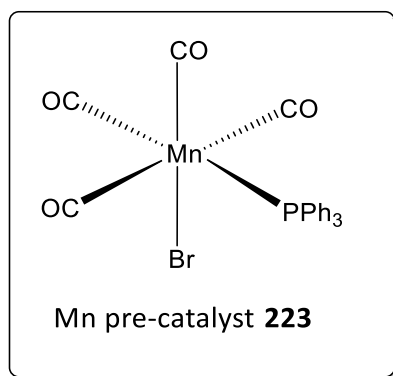
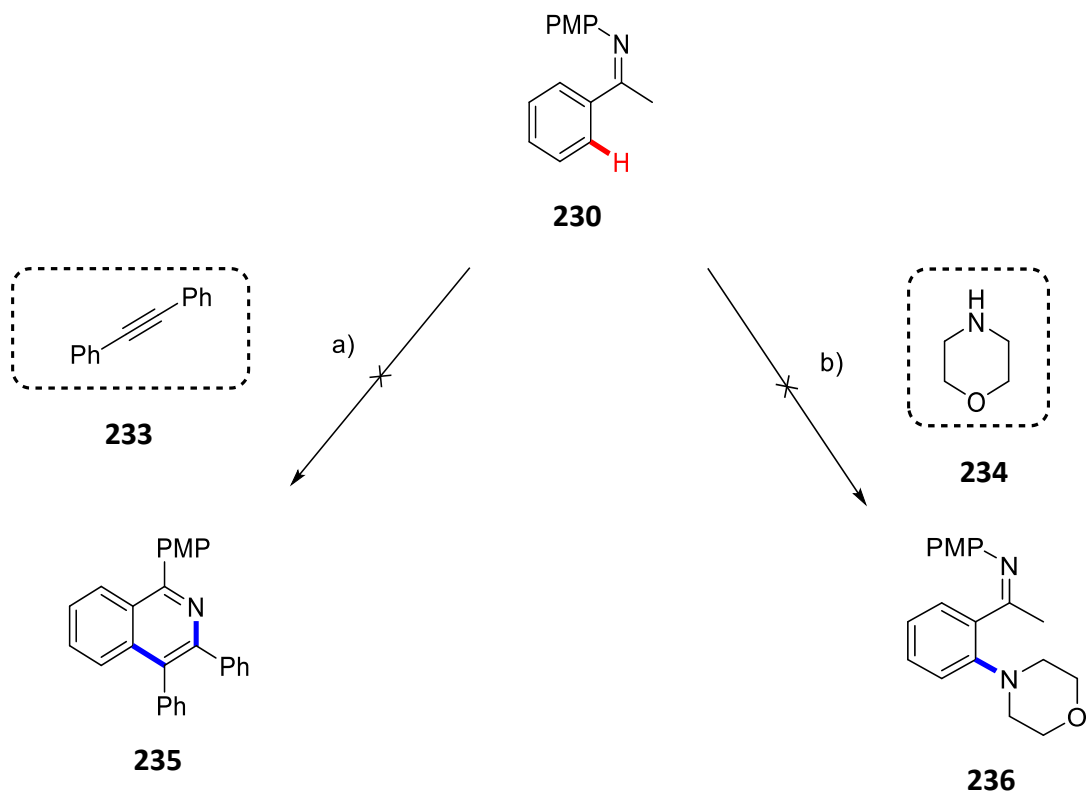
Table 24. Mn catalysed C-H allylation of ketimine **230**.

Entry	Reaction Conditions	Result
1³⁵	MnBr(CO) ₄ PPh ₃ (223), KOAc, dioxane, 100 °C	10% conversion 232
2³⁵	MnBr(CO) ₄ PPh ₃ (223), TBAB, KOAc, dioxane, 100 °C	Trace of 232
3³⁵	MnBr(CO) ₅ , KOAc, PPh ₃ , dioxane, 100 °C	Unreacted starting material 230
4³⁵	MnBr(CO) ₅ , KOAc, PPh ₃ , TBAB, dioxane, 100 °C	Trace of 232

Reaction conditions: **230** (1 equiv.), **231** 1.5 (equiv.), Mn pre-catalyst **223** (10 mol%), KOAc (20 mol%), PPh₃ (15 mol%), TBAB (10 mol%).

Two more C-H activation reactions involving ketimine **230** and MnBr(CO)₄(PPh₃) (**223**) were investigated (**Table 25**). The first reaction was based on a highly efficient protocol detailed by Wang and co-workers in 2014 for the synthesis of isoquinolines *via* Mn catalysed C-H/C-N activation of ketimines with diphenylacetylene (**233**) (**Table 25, entry 1**).³⁶ The second reaction was an amination reaction based on work reported by Yu and co-workers in 2017 on

the Rh catalysed *ortho* amination of benzamides.³⁷ For this particular reaction, morpholine (**234**) was the chosen coupling partner (**Table 25, entry 2**). However, only starting material **230** was recovered from the crude reaction mixtures for both reactions investigated and no isoquinoline **235** or amination product **236** was detected.

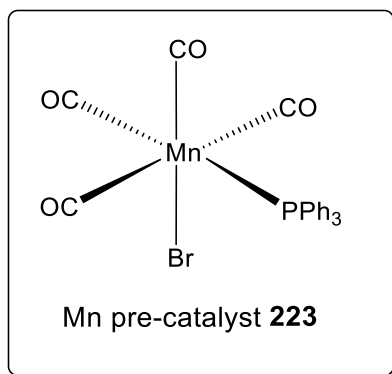
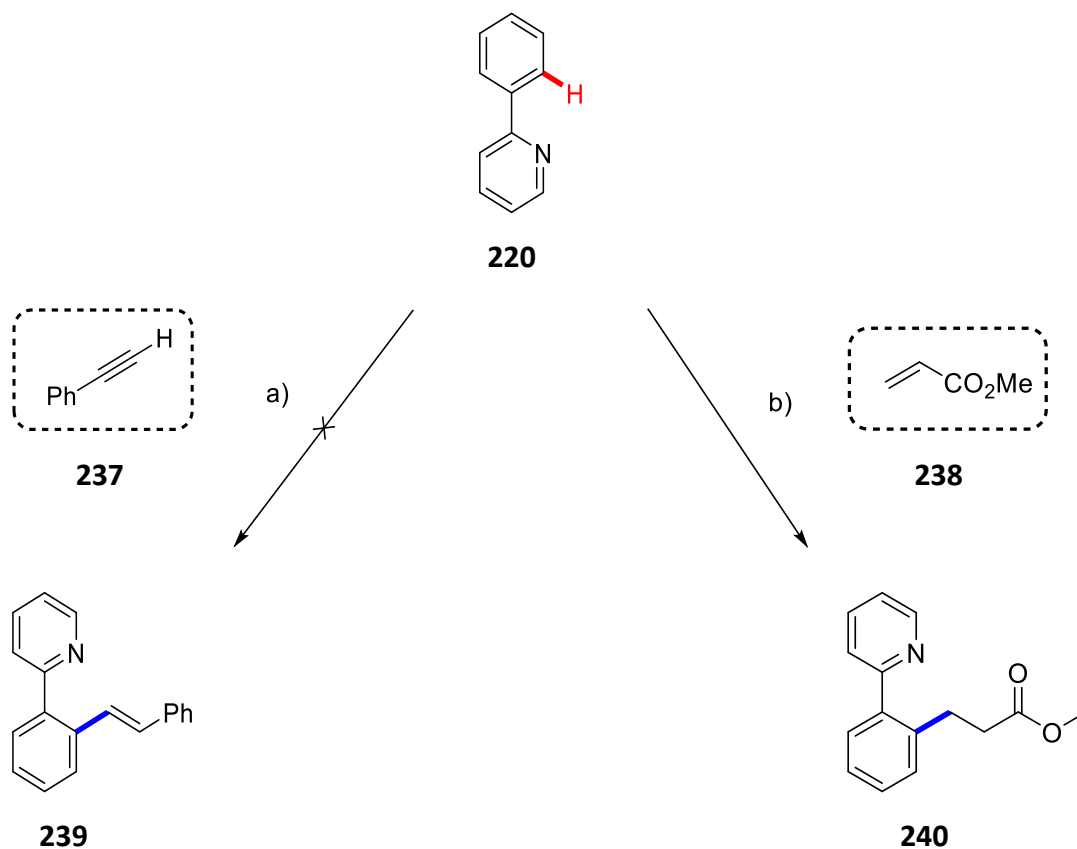
Table 25. Investigation into Mn catalysed C-H activation of ketimine **230**.

Entry	Reaction Conditions	Result
2³⁶	b) MnBr(CO) ₄ PPh ₃ (223), KOAc, dioxane, 100 °C	Unreacted starting material 230
1³⁷	a) MnBr(CO) ₄ (PPh ₃) (223), Ag ₂ CO ₃ , quinoline, sodium benzoate, toluene, 90 °C	Unreacted starting material 230

Reaction conditions: a) **230** (1 equiv.), **233** (1.5 equiv.), Mn pre-catalyst **224** (10 mol%), KOAc (20 mol%). b) **230** (1 equiv.), **234** (2 equiv.), Mn pre-catalyst **224** (5 mol%), Ag₂CO₃ (2 equiv.), quinoline (20 mol%), sodium benzoate (1.7 equiv.).

2. Pyridyl directing group

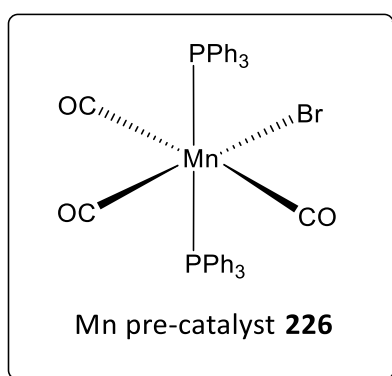
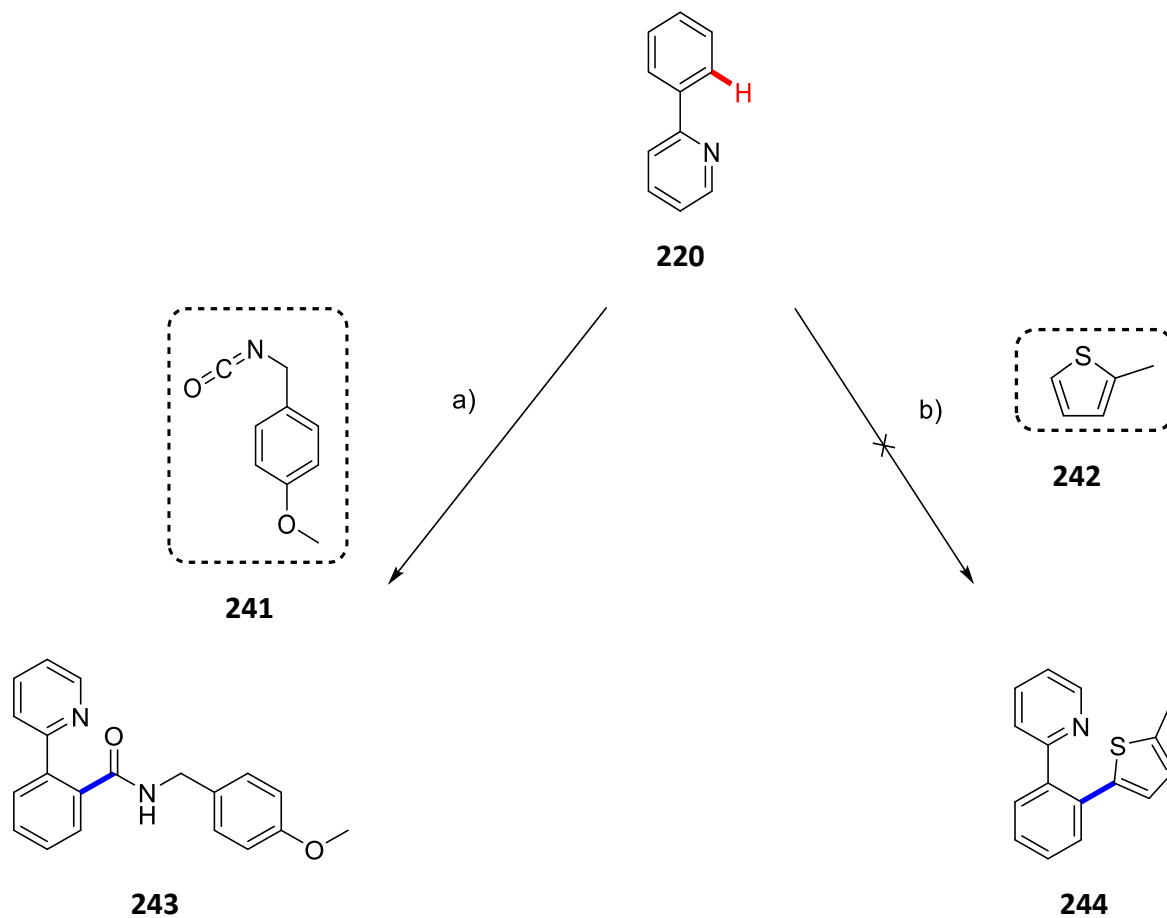
Next, two reactions reported by Wang and co-workers in 2013 and 2014 were investigated using the Mn di-phosphine complex **226** (Table 26). As with all Mn catalysed C-H activation reactions reported, a directing group to facilitate the C-H activation step is required. Hence, the substrate chosen by the authors for these two reactions was phenyl pyridine **220**. The first reaction involved a Mn catalysed C-H alkenylation reaction with terminal alkyne **237** to produce product **239** (Table 26, entry 1).³⁸ Unfortunately, substitution of the commercial $\text{MnBr}(\text{CO})_5$ pre-catalyst with our Mn di-phosphine catalyst **226**, only resulted in unreacted starting material **220** being recovered from the crude reaction mixture. A similar result was obtained for the second reaction investigated, involving the Mn catalysed addition of methyl acrylate (**238**) to phenyl pyridine (**220**) to give the hydroarylated product **240** (Table 26, entry 2).³⁹ Only a trace of product **240** was detected for this particular reaction with the majority of mass recovered attributed to unreacted starting material **220**.

Table 26. Investigation into Mn catalysed C-H activation of phenyl pyridine (**220**).

Entry	Reaction Conditions	Result
1³⁸	a) MnBr(CO) ₃ (PPh ₃) ₂ (226) Cy ₂ NH, Et ₂ O, 80 °C	Unreacted starting material 220
2³⁹	b) MnBr(CO) ₃ (PPh ₃) ₂ (226), Cy ₂ NH, Et ₂ O, 100 °C	Trace of 240 and unreacted starting material 220

Reaction conditions: a) **220** (2 equiv.), **237** (1 equiv.), Mn pre-catalyst **226** (10 mol%), Cy₂NH (10 mol%)
 (b) **220** (1.5 equiv.), **238** (1 equiv.), Mn pre-catalyst **226** (10 mol%), Cy₂NH (13 mol%).

MnBr(CO)₃(PPh₃)₂ (**226**) was also tested in a C-H bond amidation reaction of phenyl pyridine (**220**) with isocyanate **241** (Table 27, entry 1). This reaction was previously demonstrated by Ackermann in 2015⁴⁰ using MnBr(CO)₅ as the pre-catalyst and also by Ellman and co-workers in 2015 utilising Co catalysis.⁴¹ However, only a trace of product **243** could be detected in the ¹H NMR spectrum of the crude reaction mixture (and by mass spectrometry). MnCp(CO)₃ was also investigated as a possible catalyst for the amidation reaction. MnCp(CO)₃ was purchased from a commercial supplier. However, this failed to provide any improvement on results (Table 27, entry 2). MnBr(CO)₃(PPh₃)₂ (**226**) was also examined in the oxidative cross coupling reaction of phenyl pyridine (**220**) and 2-methyl thiophene (**242**) (Table 27, entry 3). This reaction was based on a Rh catalysed oxidative cross coupling reaction of (hetero)arenes with chalcogenophenes reported by Kambe and co-workers.⁴² Unfortunately, no conversion to product **244** was observed.

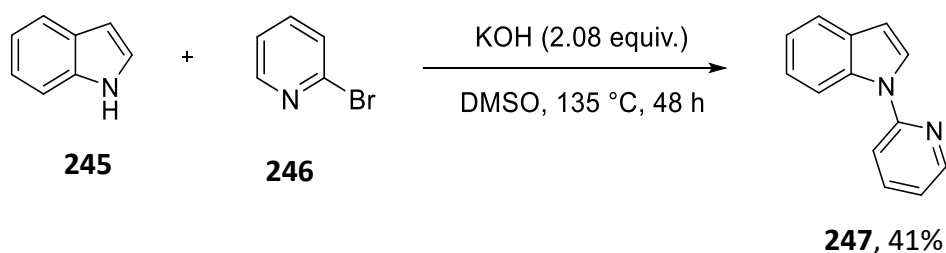
Table 27. Attempted Mn catalysed C-H reactions of phenyl pyridine (**220**).

Entry	Reaction Conditions	Result
1 ⁴⁰⁻⁴¹	a) MnBr(CO) ₃ (PPh ₃) ₂ (226), KOAc, 1,4-dioxane, 120 °C	Trace of 243 and unreacted starting material 220
2 ⁴⁰⁻⁴¹	a) MnCp(CO) ₃ , KOAc, 1,4-dioxane, 120 °C	Unreacted starting material 220
3 ⁴³	b) MnBr(CO) ₃ (PPh ₃) ₂ (226), CuOAc, AgOAc, DMA, 140 °C	Unreacted starting material 220

Reaction conditions: a) **220** (2 equiv.), **241** (1 equiv.), Mn pre-catalyst **226** (10 mol%), KOAc (20 mol%)
 (b) **220** (1 equiv.), **242** (3 equiv.), Mn pre-catalyst **226** (10 mol%), CuOAc (2.8 mol%), AgOAc (10 mol%), N₂.

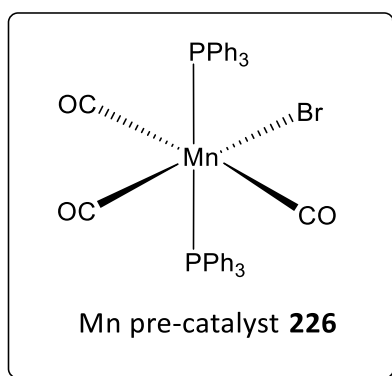
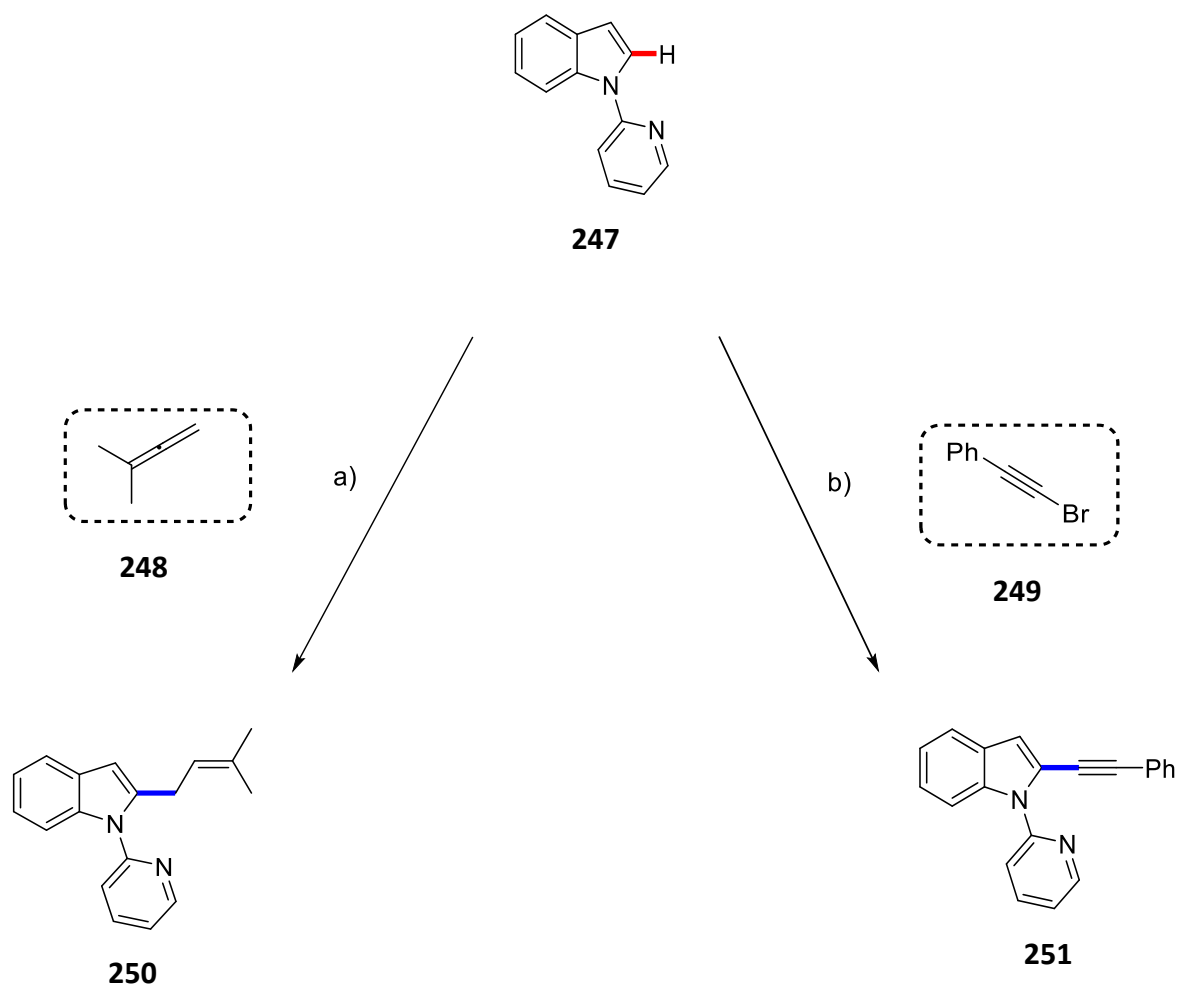
5.4.2 Synthesis of *N*-(2-pyridyl) indole

A number of C-H activation reactions involving *N*-(2-pyridyl) indole (**247**) were also investigated. Firstly, **247** was prepared in 41% yield by initially treating indole **245** with KOH in DMSO and stirring at 135 °C for 1 hour. Subsequent reaction with 2-bromo pyridine (**246**) and stirring at 135 °C for 48 hours yielded *N*-(2-pyridyl) indole (**247**) as a colourless oil after column chromatography on silica gel (**Scheme 100**).³⁴



Scheme 100. Synthesis of *N*-(2-pyridyl)-indole (**247**).

MnBr(CO)₃(PPh₃)₂ (**226**) was investigated in a Mn catalysed allylation and alkylation reaction previously reported by Wang⁴³ and Ackermann⁴⁴ respectively (**Table 28**). Unfortunately, reaction of **247** with allene **248** only resulted in a trace amount of product **250** detected. (**Table 28, entry 1**). Similarly, the Mn catalysed C-H alkylation reaction of *N*-(2-pyridyl) indole (**247**) with bromo phenyl acetylene (**249**) only resulted in a trace amount of product **251** observed in the ¹H NMR spectrum of the crude reaction mixture (**Table 28, entry 2**).

Table 28. Attempted Mn catalysed C-H activation of *N*-(2-pyridyl) indole (**247**).

Entry	Reaction Conditions	Result
1⁴³	a) MnBr(CO) ₃ (PPh ₃) ₂ (226), NaOAc, 1,4-dioxane, 100 °C	Trace of 250 and unreacted starting material 247
2⁴⁴	b) MnBr(CO) ₃ (PPh ₃) ₂ (226), BPh ₃ , DCE, 80 °C	Trace of 251 and unreacted starting material 247

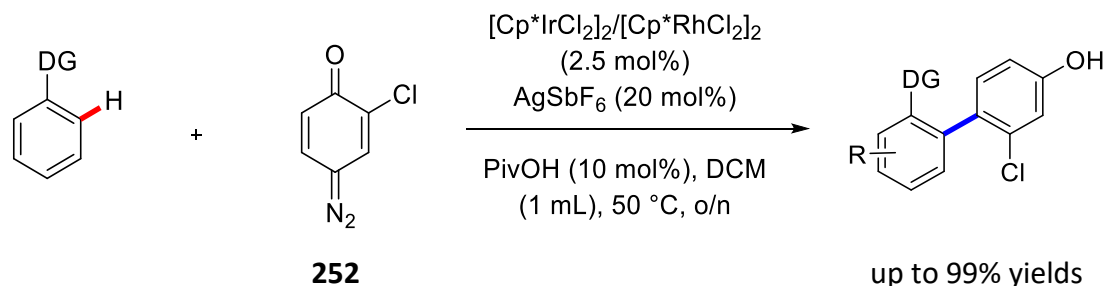
Reaction conditions: a) **247** (1 equiv), **248** (1 equiv.), Mn pre-catalyst **226** (10 mol%), NaOAc (20 mol%)
 (b) **247** (1 equiv.), **249** (1 equiv.), Mn pre-catalyst **226** (10 mol%), BPh₃ (5 mol%).

5.4.3 Investigation into alternative coupling partners for Mn catalysis

Various Mn catalysed C-H allylations, C-H alkenylations, C-H alkynylations, C-H hydroarylations and C-H halogenations have been successfully achieved over the last number of years.³¹⁻³³ Several arenes and heteroarenes have been coupled with aldehydes, ketones, alkenes, terminal and internal alkynes, isocyanates, nitriles, oxiranes etc. As mentioned previously, in all these examples the requirement of a directing group such as a nitrogen containing heterocycle or an imine group is necessary. We sought to investigate new coupling partners for Mn that had not been previously reported. A number of Mn catalysed C-H activation reactions employing diazo compounds as coupling partners were examined as it was postulated that the reactive nature of diazo compounds would render them suitable coupling partners.

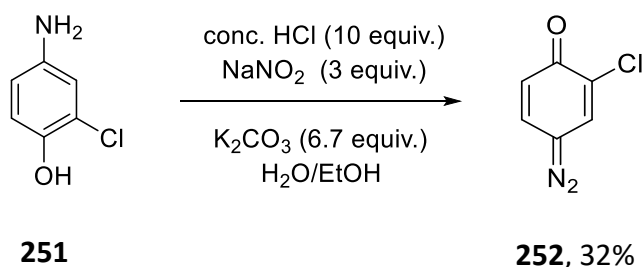
1. Quinone diazides as coupling partners

The first reaction investigated was based on impactful work described by Wang and co-workers in 2015, whereby they reported a Cp*Rh(III) and Cp*Ir(III) catalysed redox neutral C-H arylation with quinone diazides to furnish arylated phenols (**Scheme 101**).⁴⁴



Scheme 101. Rh/Ir catalysed C-H arylation with quinone diazides.

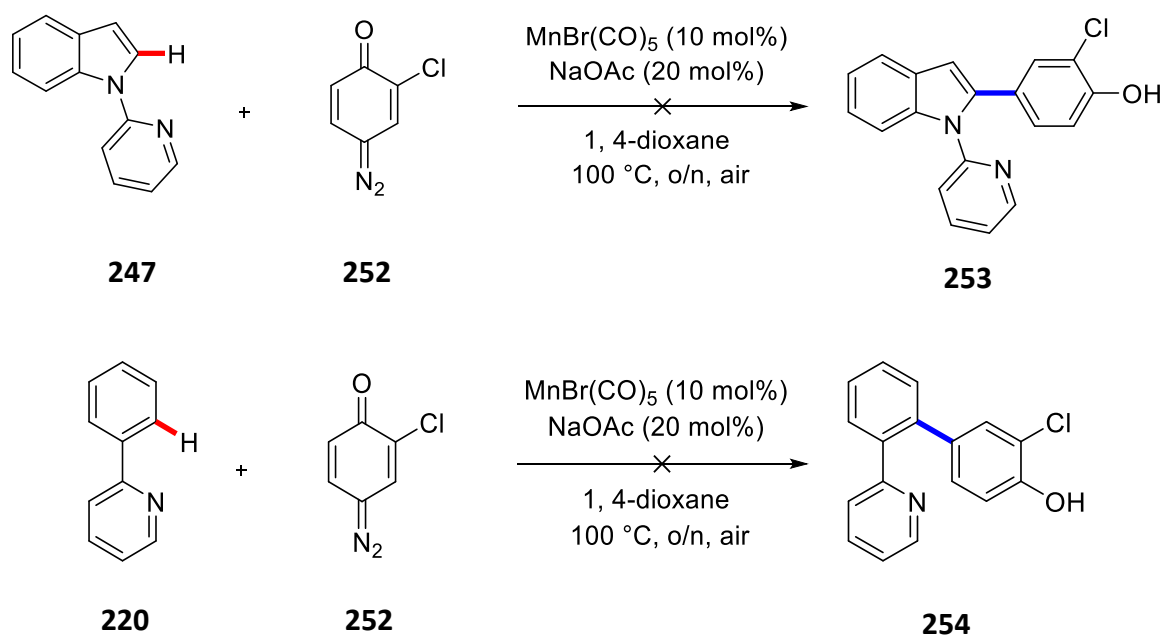
The first step in the reaction involved preparation of the diazo precursor. Quinone diazide **252** was readily synthesised by the diazotisation of 2-chloro-amino phenol (**251**) with conc. HCl and NaNO₂ (**Scheme 102**). A ¹H NMR spectrum of compound **252** was obtained following work-up and evaporation of the solvent, which was comparable to literature reports.⁴⁵ Quinone diazide **252** was subsequently kept under a nitrogen atmosphere and applied in two reactions without further purification within 15 minutes.



Scheme 102. Preparation of quinone diazide **252**.

The reaction of 2-chloro-quinone diazide (**252**) with substrates **220** and **247** was first attempted with the commercial MnBr(CO)₅ pre-catalyst, as this particular reaction had not been previously reported using Mn catalysis. *N*-(2-Pyridyl) indole (**247**) and phenyl pyridine (**220**) were chosen as model substrates for the arylation reaction as they are commonly used substrates utilized in manganese catalysed C-H activation reactions. It was decided to modify the original reaction conditions reported by Wang and co-workers to conditions more commonly suited to manganese catalysis. Hence, NaOAc was the chosen base for the reaction, with 1,4-dioxane as solvent. Difficulties were encountered upon transfer of the diazo compound to the Schlenk tubes, this was in part due to the low solubility of the diazo compound **252** in 1,4-dioxane. It must be noted that Wang and co-workers had previously

used dichloromethane as reaction solvent. Finally, the reaction was carried out at the higher temperature of 100 °C.⁴⁵ However, application of these reaction conditions on both *N*-(2-pyridyl) indole (**247**) and phenyl pyridine (**220**) failed to provide any conversion to arylated products **253** and **254**, with only unreacted starting materials recovered from the crude reaction mixtures (**Scheme 103**).



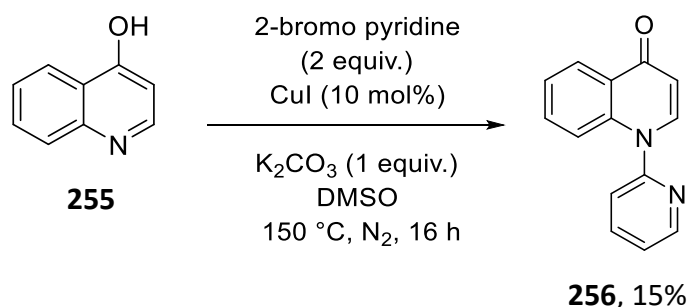
Scheme 103. Attempted C-H arylation of *N*-(2-pyridyl) indole **247** and phenyl pyridine **220**.

Due to the presence of the quinolone structure in many pharmaceutical and biologically active natural products,⁴⁶⁻⁴⁷ regioselective functionalisation of the quinolone motif is of particular interest to the McGlacken group, with previous research in the group demonstrating the application of quinolones in various Pd catalysed transformations.⁴⁸⁻⁵⁰

Thus, one last reaction was attempted with the quinone diazide substrate **252**. The reaction of *N*-(pyridyl) quinolone (**256**) and quinone diazide **252** in the presence of MnBr(CO)₅ was examined. *N*-(pyridyl) quinolone (**256**) is a challenging substrate and often difficult to functionalise. Samanta and co-workers had previously reported the regioselective C-2 arylation of *N*-pyridyl-4-quinolone with quinone diazide, which was achieved using Rh catalysis.⁵¹ Thus, we sought to investigate this reaction using Mn catalysis.

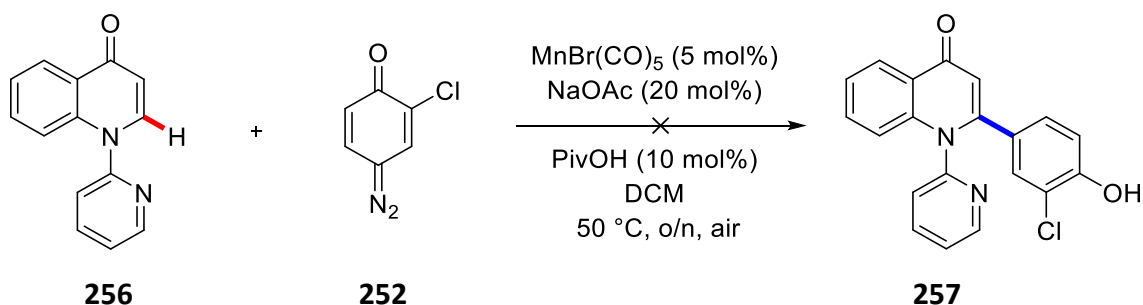
The preparation of *N*-pyridyl-4-quinolone (**256**) involved treatment of 4-quinolinol (**255**) and 2-bromo pyridine (**246**) with copper iodide in the presence of a base.⁵¹⁻⁵² The resulting

reaction mixture was refluxed in DMSO for 16 hours to yield the resulting product in a low yield of 15% (**Scheme 104**).



Scheme 104. Synthesis of *N*-(pyridyl)-4-quinolone (**256**).

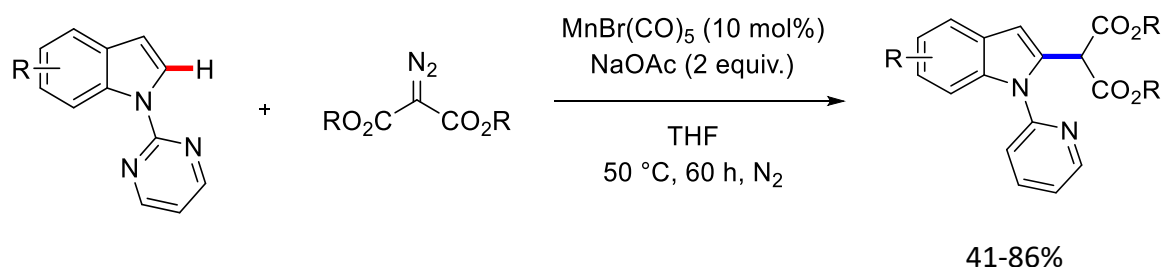
Next, the arylation of *N*-pyridyl-4-quinolone (**256**) with quinone diazide **252** was attempted. For this particular reaction, the azide **252** was added to the reaction mixture at 50 °C (hot plunge). Application of the reaction conditions (i.e. PivOH in DCM at 50 °C) reported by Samanta and co-workers on **256**, failed however to provide any of the desired C-H arylated product **257** (**Scheme 105**).



Scheme 105. Attempted C-H arylation of *N*-pyridyl-4-quinolone (**256**) with quinone diazide **252**.

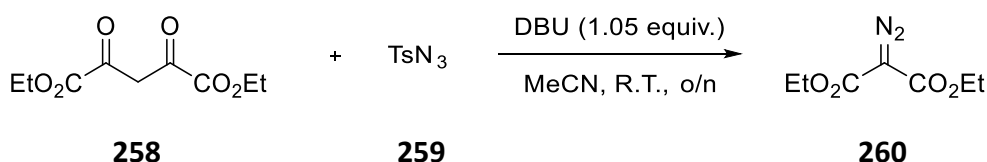
2. Diazo malonate as a coupling partner

Finally, we investigated the possibility of carrying out a Mn catalysed regioselective C-H alkylation of *N*-pyridyl-4-quinolone (**256**) again using diazo compounds. Rueping and co-workers had successfully carried out the regioselective C-2 alkylation of *N*-pyrimidinyl indoles using diazo malonates as alkylating agents *via* Mn catalysis (**Scheme 106**).⁵³ Prior to this, Samanta and co-workers had achieved a Rh catalysed C-2 alkylation of *N*-pyridyl-4-quinolone (**256**) using dimethyl diazo malonate.⁵⁴ α -Diazo carbonyl compounds are versatile intermediates due to their inherent ability to form carbenoids, carbenes, ketenes and other intermediate species and hence serve as attractive coupling partners for Mn catalysis.⁵⁵



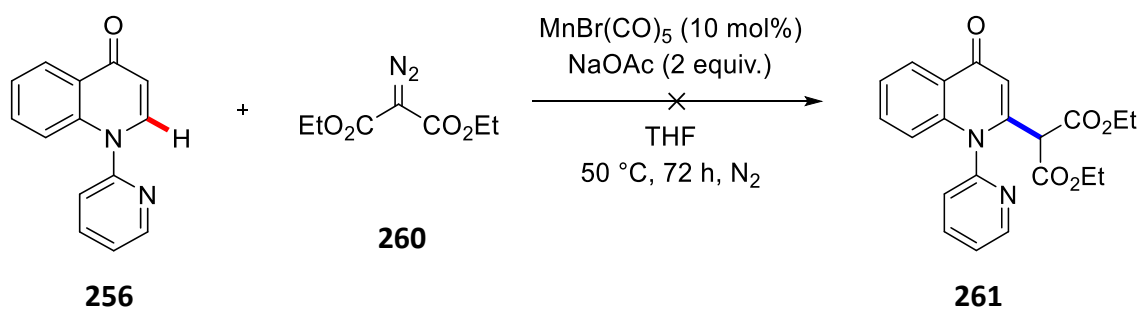
Scheme 106. Mn catalyzed C-2 alkylation of *N*-pyrimidinyl indoles.

Diethyl diazo malonate (**260**) was prepared *via* a diazo transfer process by reaction of diethyl malonate (**258**) with DBU followed by slow addition of tosyl azide (**259**) (obtained from another research group in UCC) in acetonitrile (**Scheme 107**).⁵⁵ The subsequent reaction mixture was stirred at room temperature overnight to give diazo malonate (**260**). This was followed by a quench with NaNO_2 and H_2SO_4 to remove any TsN_3 and other diazo compounds formed during the course of the reaction and subsequent extraction of the product **260** with Et_2O . Analysis of the IR spectra of the crude product indicated the presence of diethyl diazo malonate (**260**). The IR data obtained matched previous literature IR data for diethyl diazo malonate (**260**).⁵⁵ The crude material obtained was subsequently used without further purification.



Scheme 107. Preparation of ethyl diazo malonate (**259**).

Unfortunately, direct application of Rueping's reaction conditions on **256** did not allow for any conversion to alkylated product **261** (**Scheme 108**). It was clear that only unreacted starting materials (**256** and **260**) could be observed in the ^1H NMR spectrum of the crude reaction mixture, even after stirring for three days at $50\text{ }^\circ\text{C}$.

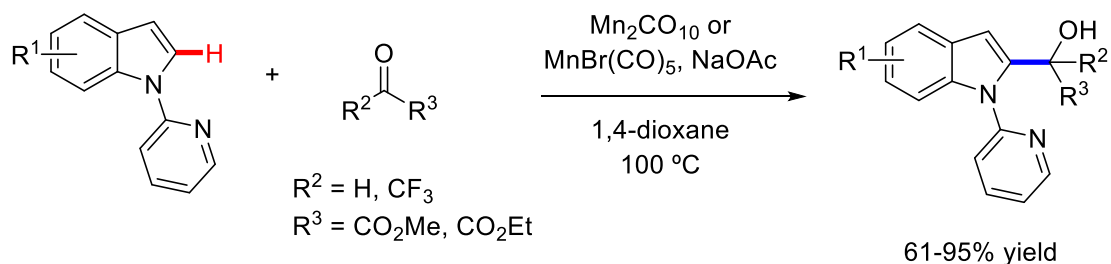


Scheme 108. Attempted Mn catalysed C-2 alkylation of *N*-pyridyl-4-quinolone (**256**).

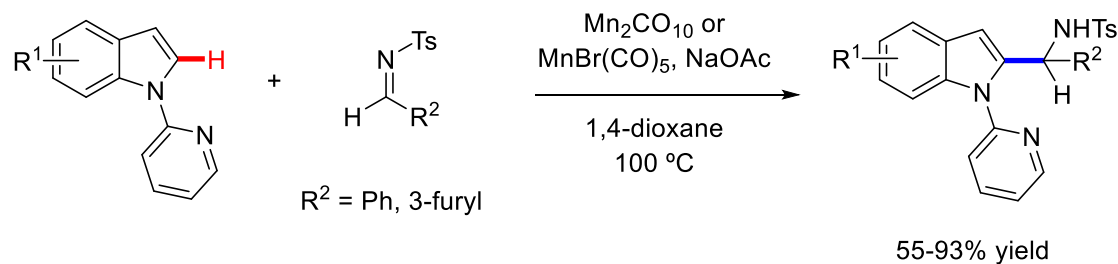
5.5.1 Mn catalysed hydroarylation of ketones

In 2016, Ackermann and co-workers developed a highly versatile Mn(I) catalytic system that allowed for the efficient and C-2 selective hydroarylation of ketones and aldehydes with *N*-(2-pyridyl) indoles.¹⁷ Remarkably, their Mn catalytic system overrode the innate C-3 selectivity of indole and enabled an unprecedented C-2 hydroarylation of ketones, aldehydes as well as imines with *N*-(2-pyridyl) indoles (**Scheme 109**). This was in contrast to other transition metal complexes, which followed the classical electrophilic indole functionalisation at the C-3 position.

a)



b)



Scheme 109. Mn catalysed C-H hydroarylation of carbon-heteroatom multiple bonds.

Having synthesised a range manganese phosphine complexes differing in sterics and electronics, it was decided to investigate their behaviour as catalysts in the Mn catalysed hydroarylation of ketones with *N*-(2-pyridyl) indole (**247**). The pure Mn(I) phosphine complexes (**223-229**) were evaluated in terms of selectivity and yield against the commercially available MnBr(CO)₅ catalyst (**Table 29**). The reaction was carried out in 1,4-dioxane at 100 °C in the presence of 10 mol% Mn catalyst and two equivalents of base.

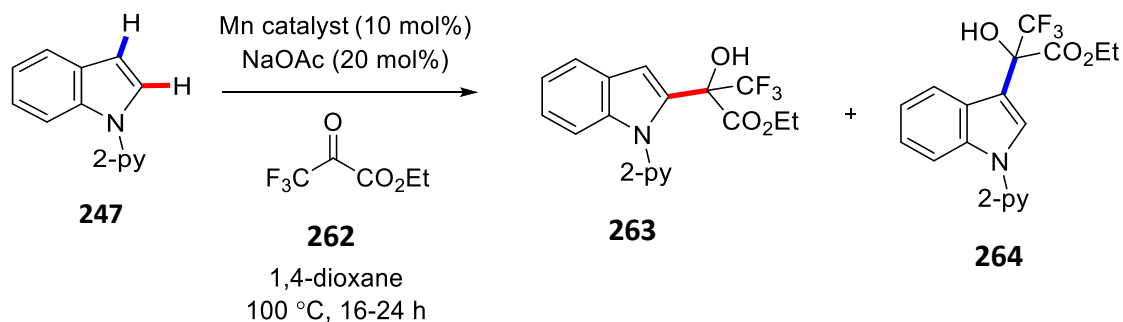
5.5.2 Results and Discussion

The results shown in **Table 29** indicate that overall the less sterically crowded mono-phosphine complexes (**223-225**, **DJ1**) gave rise to the highest yields for the C-2 product (**263**) (**Table 29**, **entries 3-7**). The sterically encumbered dppp complex **229**, (**Table 29**, **entry 8**) resulted in the poorest performance relative to MnBr(CO)₅. No C-2 product, **263**, was observed in the ¹H NMR spectrum of the crude reaction mixture for this complex. In comparison, complex **223** with a triphenylphosphine group, was the most reactive complex. A 51% isolated yield of C-2 product, **263** was obtained (**Table 29**, **entry 3**). For the methoxy derivative **225**, a 26% isolated yield of **263** was achieved (**Table 29**, **entry 7**). Two derivatives with electron withdrawing groups on the phosphine ligand backbone were investigated in the model reaction, complex **224**, bearing a *para*-fluoro substituent on the phosphine ligand and complex **DJ1**, bearing a stronger, *para*-trifluoromethyl substituent on the phosphine ligand. Interestingly, little difference in isolated yield was observed between both of these complexes, with a 30% yield of C-2 product, **263**, obtained for complex **224** and **DJ1** (**Table 29**, **entries 2-3**). Notably, the ratio of C-2:C-3 (**263:264**) for the mono-phosphine complexes evaluated were in general comparable to the C-2:C-3 ratio obtained for the commercially available MnBr(CO)₅ catalyst (**Table 29**, **entry 2**). Due to the complexity of the ¹H NMR spectrum of the crude reaction mixture, the C-2:C-3 ratio could not be determined accurately using the pre-catalyst **225**, with a *para*-methoxy group on the phosphine ligand (**Table 29**, **entry 7**).

Relative to the mono-phosphine complexes (**223-225**, **DJ1**) examined, the Mn di-phosphine complexes (**226-229**) all performed poorly (**Table 29**, **entries 8-11**). Interestingly, complex **228** with a *para*-methoxy group on the phosphine ligand (**Table 29**, **entry 7**), was the best performing di-phosphine complex, providing a 24% yield of **263**. Complex, **226** with a triphenylphosphine group, gave an 11% yield of the C-2 product (**263**) (**Table 29**, **entry 5**).

Complex **227**, with with a *para*-fluoro group on the phosphine ligand, provided an 18% yield of the C-2 product (**Table 29, entry 6**).

Additionally, the hydroarylation reaction was also investigated in DCE and benzonitrile as solvent using complex **223** as the Mn catalyst. DCE was chosen as it has previously being used as a reaction solvent in Mn catalysis.^{31, 33, 56} Notably, when the reaction was carried out in DCE, a decrease in selectivity for C-2 was observed (**Table 29, entry 12**). Although, the starting material **247** was fully consumed, the ratio of C-2:C-3 (52:48) was significantly lower in comparison to when the reaction was carried out in 1,4-dioxane. Some nitrile ligands can act as weakly coordinating ligands.⁵⁷ Thus, benzonitrile was considered as a good choice of solvent as coordination of the nitrile group to the Mn centre may tune the activity and selectivity of the catalyst in a positive manner. However, the use of benzonitrile as solvent afforded no C-2 product (**Table 29, entry 13**). Lastly, MnCp(CO)₃ was investigated as a possible catalyst for the hydroarylation reaction (**Table 29, entry 14**). However, only a trace amount of C-2 product was detected. The remaining mass was attributed to unreacted starting material **247** and C-3 substituted product **264**.

Table 29. Mn catalysed hydroarylation of *N*-(2-pyridyl) indole (**247**) with ketone **262**.

Entry	Complex	Solvent	Ratio (C-2:C-3) ^a (263 : 264)	Yield of 263 (%) ^b
1	-	1,4-dioxane	0:100	0
2	MnBr(CO) ₅	1,4-dioxane	88:12	88
3	223	1,4-dioxane	82:18	51
5	224	1,4-dioxane	72:28	30
6	DJ1	1,4-dioxane	78:22	30
7	225	1,4-dioxane	-	26
8	226	1,4-dioxane	76:24	11
9	227	1,4-dioxane	74:26	18
10	228	1,4-dioxane	82:18	24
11	229	1,4-dioxane	0:100	0
12	223	DCE	48:52	-
13	223	benzonitrile ^c	-	-
14	MnCp(CO) ₃	1,4-dioxane	-	Trace ^d

^aRatio determined from the ¹H NMR spectrum of the crude reaction mixture. ^bYields of isolated C-2 product shown. ^cNo C-2 product observed in the ¹H NMR spectrum of the crude reaction mixture when benzonitrile was used as the reaction solvent (complex mixture of C-3 product and a number of unidentifiable products). ^dOnly a trace amount of C-2 product was detected in the ¹H NMR spectrum of the crude reaction mixture.

5.5.3 Reaction monitoring

Focus was then turned to investigating the kinetics of the hydroarylation reaction with respect to each of the pre-catalysts (**223-229**, **DJ1**). Thus, it was decided to monitor the reaction over time and to determine if a rate difference was observed between each of the pre-catalysts (**223-229**, **DJ1**), and also if a trend could be established depending on whether the phosphine ligand coordinated to the Mn centre contained an electron withdrawing substituent or an electron donating substituent. For the purposes of this work, a control reaction was also ran

in parallel with the reaction mixture which was sampled. The control reaction involving each pre-catalyst was stirred at 100 °C for 26 hours. The ratio of starting material:C-2 product (**247:263**) and C-2:C-3 product (**263:264**) was then determined from the crude reaction mixtures after 26 hours.

5.5.4 Reaction sampling

During the course of the reaction, aliquots of the reaction mixture were taken at regular intervals and the progress of the reaction was monitored by ^1H NMR spectroscopy. Initially, aliquots of the reaction mixture for each pre-catalyst were taken after 4 hours, 8 hours, 16 hours and 24-26 hours. The ratio of *N*-(2-pyridyl) indole:C-2 product (**247:263**) was examined over time for each pre-catalyst, as well as the ratio of C-2:C-3 product (**263:264**). However, presumably due to the heterogeneous nature of the reaction mixture, inconsistent results were obtained between the control reaction which was not sampled and the sampled reaction mixture. There were clear discrepancies between the sampled reaction mixture and the control reaction in terms of ratios of starting material: C-2 product and C-2:C-3 product ratios. Therefore, it was deemed that removal of aliquots from the reaction mixture and monitoring by ^1H NMR spectroscopy was not an accurate way of monitoring the progress of the reaction.

5.5.5 Analysis of the ^1H NMR spectra of the crude reaction mixtures

Figure 44 shows a comparison of the ^1H NMR spectra between *N*-(2-pyridyl) indole (**247**), C-2 product **263** and C-3 product **264**. In the reaction of *N*-(2-pyridyl) indole (**247**) with ketone **262** using the commercial pre-catalyst $\text{MnBr}(\text{CO})_5$, full consumption of starting material **247** was observed. In addition, the major product formed was the C-2 substituted product (**263**). Conversely, a less clean reaction mixture was obtained for the tetracarbonyl Mn phosphine complexes **223-225**, **DJ1** as well as the tricarbonyl Mn phosphine complexes **226-229** (**Figure 45** and **Figure 46**).

The following observations were made after analysis of the ^1H NMR spectra of the crude reaction mixtures for the tetracarbonyl Mn phosphine complexes (**223-225**, **DJ1**). For pre-catalyst (**224**) containing a *para*-fluoro substituent on the phosphine ligand, the *N*-(2-pyridyl) indole **247** was completely consumed after 24 hours. For pre-catalyst (**223**), <10% of the indole starting material **247** remained after 24 hours. In contrast, pre-catalyst complexes **DJ1**

(with a *para*-trifluoromethyl group on the phosphine ligand) and, **225** (with a *para*-methoxy group on the phosphine ligand) did not allow for full consumption of starting material **247** after 24 hours (**Figure 45**). Furthermore, it was apparent that extra signals were visible in each of the ^1H NMR spectra of the crude reaction mixtures when the tetracarbonyl Mn phosphine complexes were used, which did not correspond to **247**, **263** or **264**. Moreover, the poor yields observed may be attributed to unproductive pathways (polymerisation of *N*-(2-pyridyl) indole may be likely)⁵⁸⁻⁶¹ occurring during the catalytic cycle resulting in the formation of undesirable side products and hindering formation of the desired C-2 product (**263**).

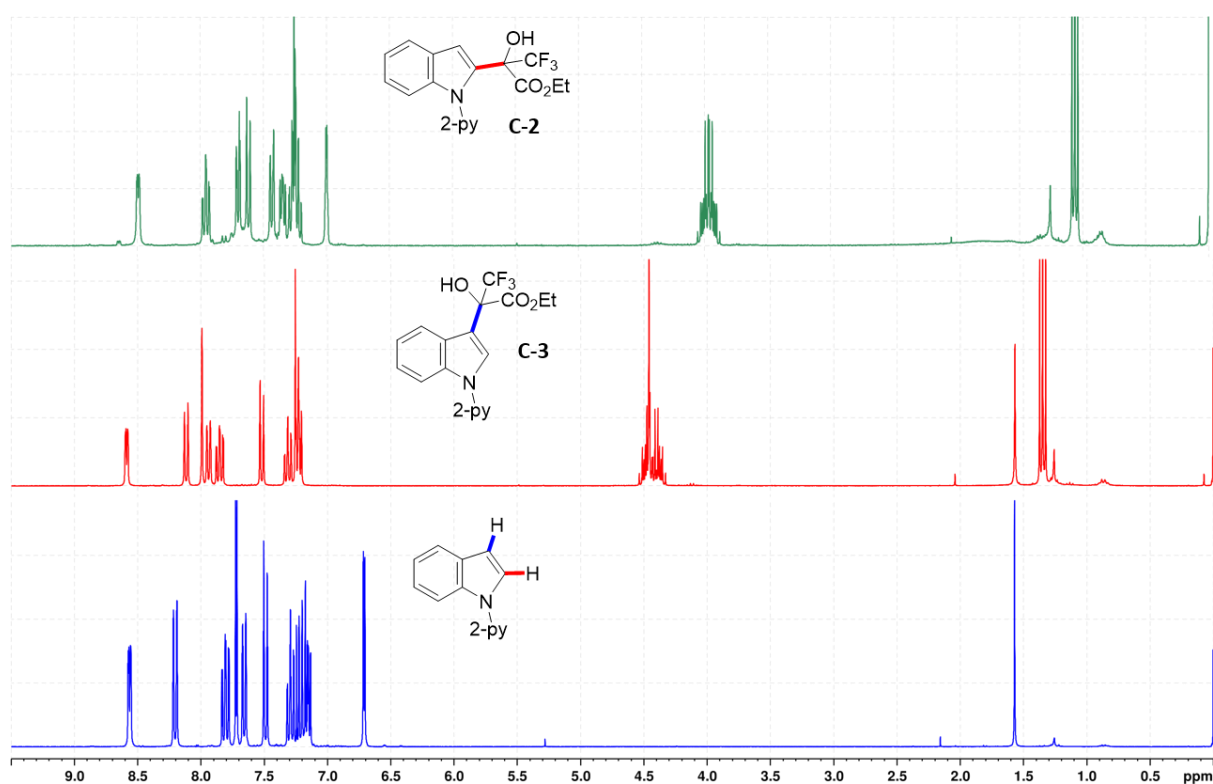


Figure 44. Stacked ^1H NMR spectra comparing *N*-(2-pyridyl) indole (**247**), C-3 product (**264**) and C-2 product (**263**).

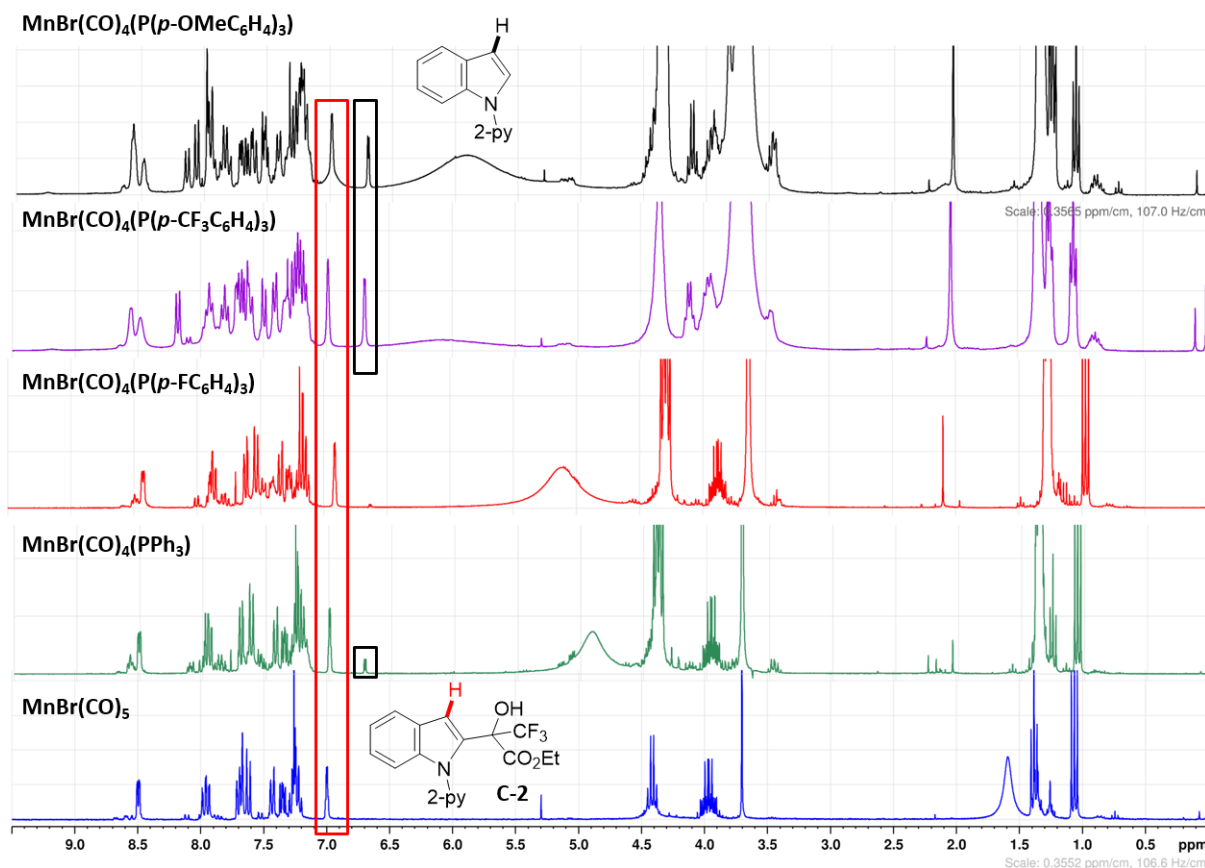


Figure 45. ^1H NMR spectra of the crude reaction mixtures corresponding to the tetracarbonyl Mn phosphine complexes **223-225**, **DJ1** versus ^1H NMR spectrum of the crude reaction mixture employing $\text{MnBr}(\text{CO})_5$ as the pre-catalyst.

Similar observations were made for the tricarbonyl Mn phosphine complexes (**226-229**) following analysis of the respective ^1H NMR spectra of the crude reaction mixtures. After 26 hours, it was observed that no di-phosphine complex (**226-229**) allowed for full consumption of indole starting material **247** (Figure 45). Interestingly, pre-catalyst complex **227** containing a *para*-fluoro group on the phosphine ligand, appeared to be the slowest pre-catalyst with regard to consumption of indole starting material **247**. After 26 hours, the ratio of starting material:C-2 product (**263:264**) was 60:40 (Table 30, entry 2). In comparison, when complexes **226-228** were used, greater consumption of starting material **247** was observed after 26 hours (Table 30, entries 1 and 3). However, greater consumption of indole starting material **247** for pre-catalyst **226** (with a triphenylphosphine group) and pre-catalyst **227** (with a *para*-methoxy group on the phosphine ligand), may be compensated for by more favourable formation of undesired side-products over clean conversion of **247** to the C-2 product **263**. This was evident from the ^1H NMR spectra of the crude reaction mixtures as it was clear that

there were extra signals present in the ^1H NMR spectra for the pre-catalyst **226** and **228** (as well as pre-catalyst **227**) which did not correspond to either starting material **247**, C-2 product **263** or the C-3 product **264**. Interestingly, when pre-catalyst **228** was used, it was evident that a doublet of doublets at 6.92 ppm was clearly visible in the ^1H NMR spectrum of the crude reaction mixture. Following column chromatography of the crude reaction mixture, a product was isolated whose respective ^1H NMR spectrum consisted of a 3H singlet at 3.82 ppm, a 6H doublet of doublets at 6.92 ppm and 6H doublet of doublets at 7.54 ppm. The ^{31}P NMR spectrum showed a single resonance at 29.3 ppm. The isolated product was identified as tris-(4-methoxyphenyl)phosphine oxide⁶² and was of particular interest, as the doublet of doublets at 6.92 ppm was observed when the reaction mixture was sampled after 4 hours and a ^1H NMR spectrum was obtained. This observation may provide important information concerning the lifetime or deactivation of the Mn carbonyl phosphine pre-catalysts (**223-229**, **DJ1**). Decomposition of the Mn carbonyl phosphine pre-catalysts (**223-229**, **DJ1**) after a small number of turnovers, could lead to loss of a phosphine ligand which could be oxidised to the corresponding phosphine oxide. Moreover, the observation of the oxide after 4 hours would suggest that the oxide is formed during the course of the reaction rather than being due to degradation of the pre-catalyst (**228**) on silica gel. In addition, the corresponding oxide derivatives (i.e. triphenyl phosphine oxide, tris-(4-fluorophenyl) phosphine oxide and tris-(trifluoromethyl phenyl) phosphine oxide) were isolated following column chromatography of the crude reaction mixtures for each pre-catalyst investigated (**223-228**, **DJ1**).

This was in stark contrast to the crude reaction mixture obtained for the commercial pre-catalyst, $\text{MnBr}(\text{CO})_5$. Examination of the ^1H NMR spectrum clearly shows only C-2 product **263**, as well as a minor amount of C-3 product **264**, in addition to mostly excess ketone starting material **262**.

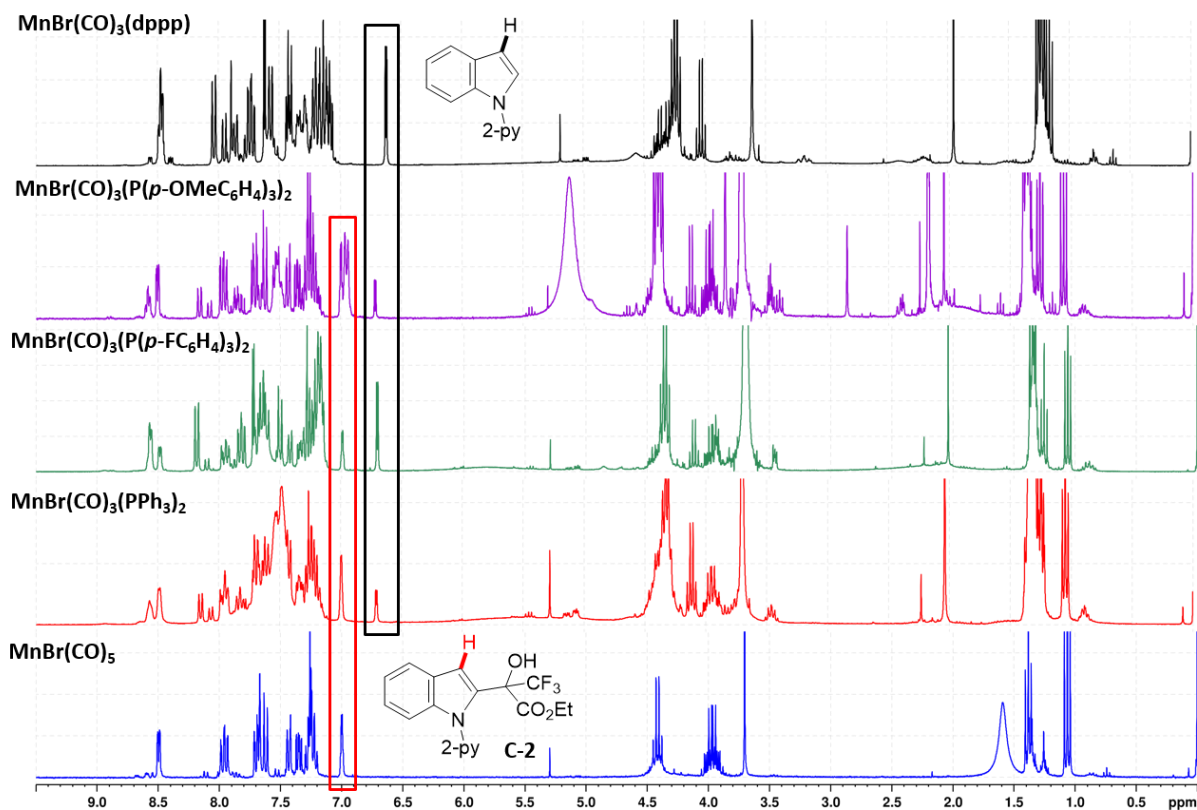


Figure 46. ^1H NMR spectra of the crude reaction mixtures corresponding to the tricarbonyl Mn phosphine complexes **226-229** versus ^1H NMR spectrum of the crude reaction mixture employing $\text{MnBr}(\text{CO})_5$ as the pre-catalyst.

Table 30. ^1H NMR ratio of C-2:C-3:SM for complexes **226-228**.

Entry	Mn Complex	C-2:C-3:SM (Ratio) ^a
1	$\text{MnBr}(\text{CO})_3(\text{PPh}_3)_2$ (226)	52:25:23
2	$\text{MnBr}(\text{CO})_3(\text{P}(p\text{-FC}_6\text{H}_4)_3)_2$ (227)	23:39:38
3	$\text{MnBr}(\text{CO})_3(\text{P}(p\text{-OMeC}_6\text{H}_4)_3)_2$ (228)	56:23:21

^aRatio of C-2:C-3:SM determined from the ^1H NMR spectrum of the crude reaction mixture.

5.5.6 Catalyst Deactivation

Overall, lower yields and an increased number of side products were obtained for the tetracarbonyl- and tricarbonyl Mn phosphine complexes relative to the commercial pre-catalyst, $\text{MnBr}(\text{CO})_5$. In their recent publications, Fairlamb and Lynam have extensively detailed how catalyst deactivation can impact greatly on product conversion.⁶³⁻⁶⁵ They suggested that “product conversion appears to tally with the TON of the Mn catalyst, with limited catalyst turnover indicating an issue in either the protonation or recycling steps

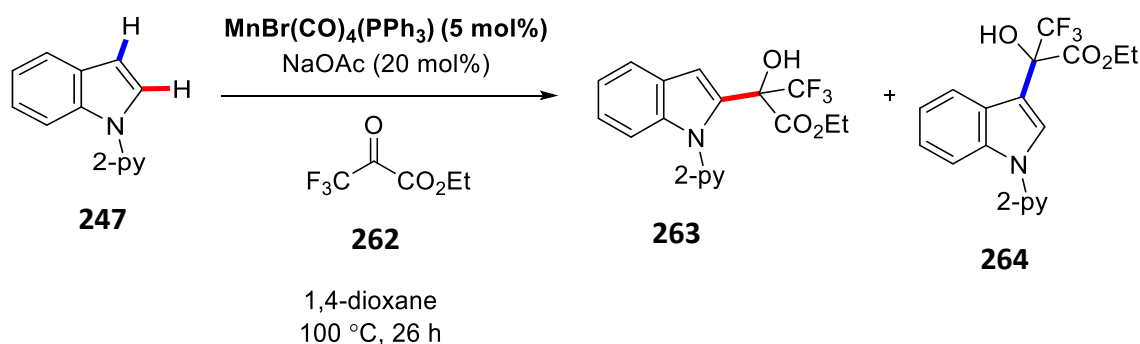
required for catalysis leading to low product conversion and rapid catalyst degradation." The lower yields obtained for the tetracarbonyl- and tricarbonyl Mn phosphine complexes maybe suggestive of lower catalyst TONs due to greater catalyst deactivation for these complexes relative to $\text{MnBr}(\text{CO})_5$.

Catalyst loadings are generally high for most reported Mn catalysed C-H transformations in the literature (usually 10 mol%), with catalyst TON numbers ranging from 5 to 9.⁶³ During the course of their work, Fairlamb and Lynam and co-workers observed the formation of catalytically inactive Mn carbonyl clusters within a few minutes of substrate turnover.⁶³ These Mn carbonyl clusters effectively provide a dead-end for catalysis. During the course of our work, a dark brown solid was observed in the reaction vessel after 24-26 hours when the reaction was stopped. Additionally, the bright yellow colour observed in the reaction vessel at the beginning of the reaction turned to a brown cloudy solution fairly rapidly. This observation was made for all the pre-catalysts investigated. The brown solid observed may be attributed to Mn carbonyl clusters, but the exact nature and composition of the Mn clusters is unknown. Of course, there may be multiple pathways for catalyst deactivation and moreover, decomposition pathways may differ among our pre-catalyst complexes (**223-229**, **DJ1**) and $\text{MnBr}(\text{CO})_5$. Decomposition be more favourable for our pre-catalysts, especially the tricarbonyl Mn phosphine complexes (**226-229**) since the poorest yields were obtained for the tricarbonyl Mn phosphine pre-catalysts. There are a number of factors that control catalyst lifetime in C-H activation reactions and as noted in a recent publication by the Glorius group, these are not clearly understood.⁶⁶ High catalyst activity, stability and the absence of catalyst poisons are all desirable in order to achieve high catalytic TONs.

Further work is required in order to gain further understanding into the relative activity and stability of the tetracarbonyl- and tricarbonyl Mn phosphine pre-catalysts (**223-229**, **DJ1**) and also how they are likely to deactivate under the reaction conditions. This will be crucial in order to develop more efficient Mn phosphine catalytic systems for future use in C-H activation reactions.

5.5.7 Reduction of catalyst loading

Mn catalysed C-H activation reactions mostly require 10 mol% of the Mn pre-catalyst.⁶³ Moreover, we were interested in determining if a reduction in catalyst loading could be possible with the carbonyl Mn phosphine pre-catalysts (**223-229**, **DJ1**). Thus, the reaction of *N*-(2-pyridyl) indole **247** with ketone **262** was investigated using 5 mol% Mn pre-catalyst **223** (**Scheme 110**). Stirring at 100 °C for 26 hours, a reduction in C-2 yield and selectivity was observed relative to when the reaction was carried out with 10 mol% Mn pre-catalyst. With 10 mol% Mn pre-catalyst, a 51% isolated yield of C-2 substituted product **263** was obtained. Additionally, the ratio of C-2:C-3 was determined to be 82:18 (**Table 29**, **entry 3**). In comparison, employing 5 mol% Mn pre-catalyst **223**, a reduced yield of 32% was observed. The ratio of C-2:C-3 product (**263:264**) was determined to be 62:38.



Scheme 110. Hydroarylation reaction investigated with 5 mol% Mn pre-catalyst **223**.

5.5.8 Mechanistic discussion

It is crucial to gain insights into the mechanisms of C-H activation reactions to allow for future development of new catalytic systems, to allow optimisation of reaction conditions and also to allow extension to new methodologies. The catalytic system employed by Ackermann and co-workers for the hydroarylation of ketones, aldehydes and imines with *N*-(2-pyridyl) indole utilised the commercial Mn(I) pre-catalysts, $\text{Mn}_2\text{CO}_{10}$ or MnBr(CO)_5 .¹⁷ Mechanistic studies carried out within the Ackermann group suggested that the catalytic cycle is initiated by facile C-H metalation to form the cyclometalated complex **I**. Coordination of the ketone generates intermediate **II**. This is followed by insertion of the ketone to form a seven membered

manganacycle **III**. Finally, proto demetalation furnishes the desired alcohol product **263** and regenerates the catalytically active Mn species **I** (Figure 47).

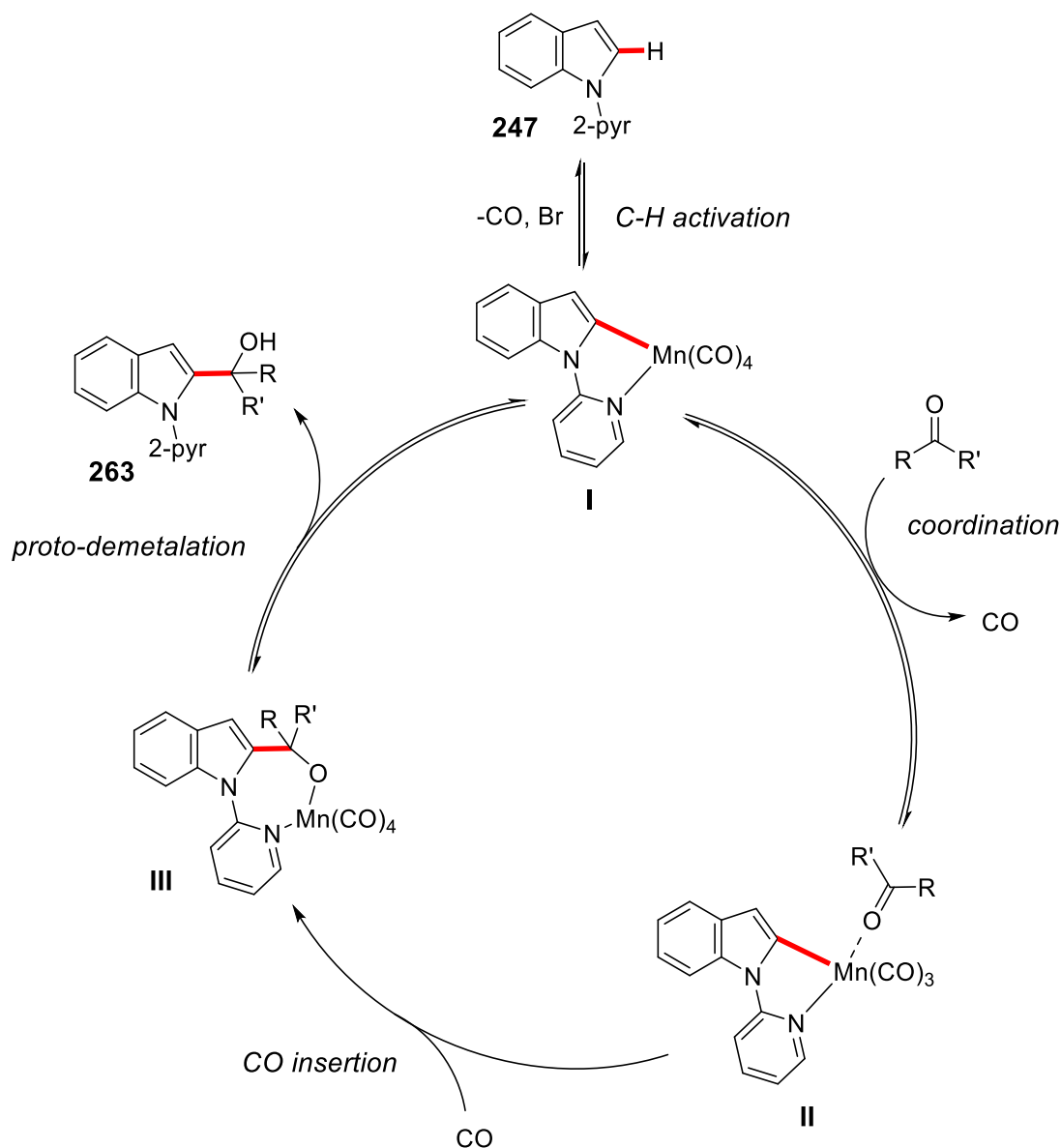
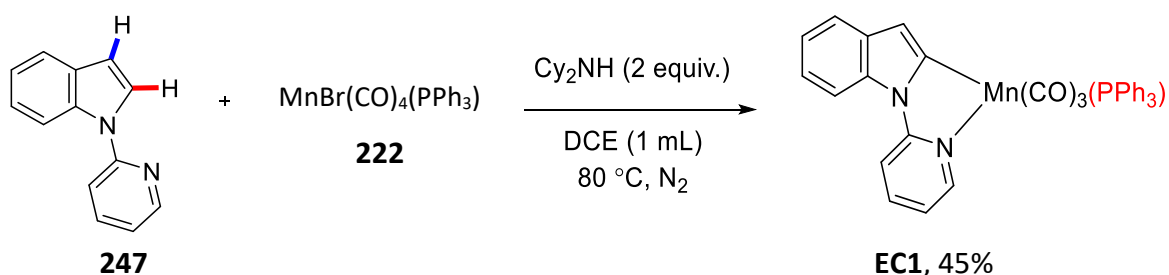
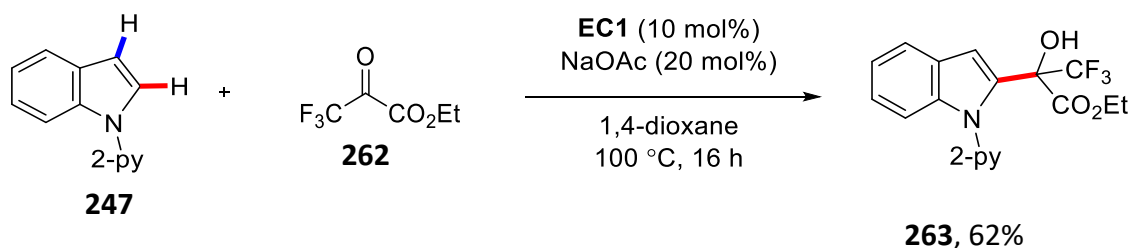


Figure 47. Catalytic cycle proposed by Ackermann and co-workers.

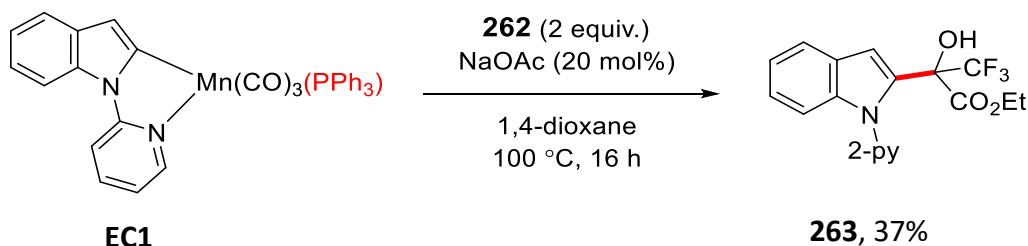
Key to further development and understanding of the hydroarylation reaction employing manganese carbonyl phosphine complexes is gaining mechanistic information on the catalytic processes, and elucidation of the role of the phosphine ligands in the reaction. Therefore, attention within the McGlacken group was turned to unravelling the nature of the catalytically active Mn species in our system. This would involve determining and understanding how the pre-catalyst complexes are activated under the reaction conditions and what are the key

catalytic species involved in the catalytic cycle. A critical question to be answered was whether or not the phosphine ligand remains coordinated to the Mn during the catalytic cycle, at what step does dissociation of the phosphine ligands occur, and how this would affect the overall rate of reaction.

To determine the nature of the catalytically active Mn species, C-H activation reactions were carried out with the cyclometalated complex **EC1**, using both catalytic and stoichiometric amounts of **EC1** (**Figure 48, b**) and **c**). (Note: this work was carried out by another member of the McGlacken group). The cyclometalated complex **EC1** was prepared in 45% yield by reaction of *N*-(2-pyridyl) indole **247** with complex **222** in DCE at 80 °C in the presence of two equivalents of Cy₂NH (**Figure 48, a**). Complex **EC1** was identified by means of ESI-MS, ³¹P NMR spectroscopy and single crystal structure X-ray analysis. Observation of a single broad resonance in the ³¹P NMR spectrum at 52 ppm clearly indicated that the phosphine ligand is still coordinated to the manganese. Hence, this indicates that the phosphine ligand remains coordinated to the Mn during the key C-H activation step, thus, resulting in the formation of the cyclometalated complex **EC1**. C-H activation reactions were also performed with cyclometalated complex **EC1**. Pleasingly, complex **EC1** proved to be competent in the catalytic as well as the stoichiometric hydroarylation reaction (**Figure 48, a**) and **b**). These findings provide strong support for the cyclometalated complex **EC1** being a catalytically competent intermediate within the catalytic cycle.

a) Synthesis of **EC1**b) Complex **EC1** as catalyst

c) Stoichiometric hydroarylation

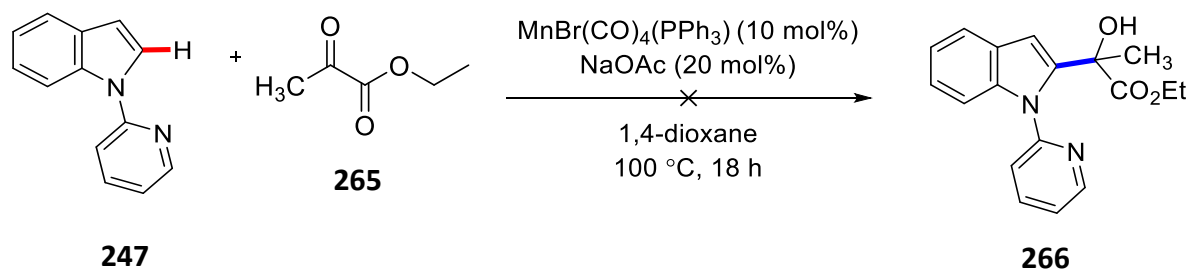
**Figure 48.** Catalytic and stoichiometric hydroarylation with cyclometalated complex **EC1**.

Preliminary work carried out within the McGlacken group has suggested that the phosphine ligands are playing an important role in the hydroarylation reaction. However, to gain further insight into the mechanistic processes occurring at the Mn centre and also to provide more information on the role of the phosphine ligands in the reaction, the McGlacken group is currently involved with an ongoing collaboration with Prof. Ian Fairlamb and Dr. Jason Lynam in York. A number of recent publications by Fairlamb and Lynam and co-workers involved using real time infrared spectroscopic analysis for studying transient manganese carbonyl species formed during C-H bond activation reactions.⁶³⁻⁶⁵ This method enabled changes in metal carbonyl absorbances to be monitored (both qualitatively and quantitatively), and thus observation of the dynamic processes occurring at the manganese centre. Moreover, it is envisaged that a similar analysis in collaboration with Fairlamb and Lynam will enable us to

determine what role the phosphine ligands are playing in the hydroarylation reaction. It is hoped that Information gathered from this work would enable further development and optimisation of Mn carbonyl phosphine pre-catalysts for application in C-H activation reactions, as well as possible applications in various other synthetic transformations.

5.5.9 Hydroarylation reaction investigated with ethyl pyruvate

In Ackermann's original publication on the hydroarylation of ketones with *N*-(2-pyridyl) indoles, the substrate scope with respect to the ketone was limited to the highly electrophilic, ethyl trifluoro pyruvate **262**.¹⁷ Thus, this represents a limitation or drawback to the work. We were therefore interested in examining whether or not the carbonyl Mn phosphine complexes synthesised in-house would facilitate reaction with a more diverse range of ketones. The reaction of *N*-(2-pyridyl) indole (**247**) with ethyl pyruvate (**265**) in the presence of 10 mol% of **223** as pre-catalyst and NaOAc as the base was examined (**Scheme 111**). Disappointingly, no conversion to the desired C-2 alcohol product **266** was observed in the ¹H NMR spectrum of the crude reaction mixture. This would indicate that the highly activated trifluoromethylated ketone **262** appears to be a key requirement for the success of this reaction.



Scheme 111. Attempted hydroarylation of ethyl pyruvate (**265**) with *N*-(2-pyridyl) indole (**247**).

5.5.10 Concluding remarks

In conclusion, although the tetracarbonyl Mn phosphine complexes (**223-225**, **DJ1**) proved to be competent catalysts in terms of selectivity for the C-2 hydroarylated product **263**, the yields were significantly lower with respect to the commercial catalyst, $\text{MnBr}(\text{CO})_5$. This may be due to side-reactions occurring, catalyst deactivation or a number of other possibilities. In terms of electronics, the pre-catalysts with electron withdrawing groups on the phosphine ligand backbone (**224**, **DJ1**) gave slightly higher yields in comparison to the pre-catalyst with

an electron donating group on the phosphine ligand (**224**). Overall, the pre-catalyst (**223**) with a 'neutral' triphenylphosphine group allowed for the highest yield (51%). Finally, the steric bulk of the tricarbonyl Mn phosphine complexes (**226-229**) had an effect on catalyst selectivity and also resulted in lower yields of **263**. Finally, complex **229** possessing the sterically bulky bidentate phosphine ligand, dppp failed to give any conversion to C-2 product. The results are summarised in **Figure 49**.

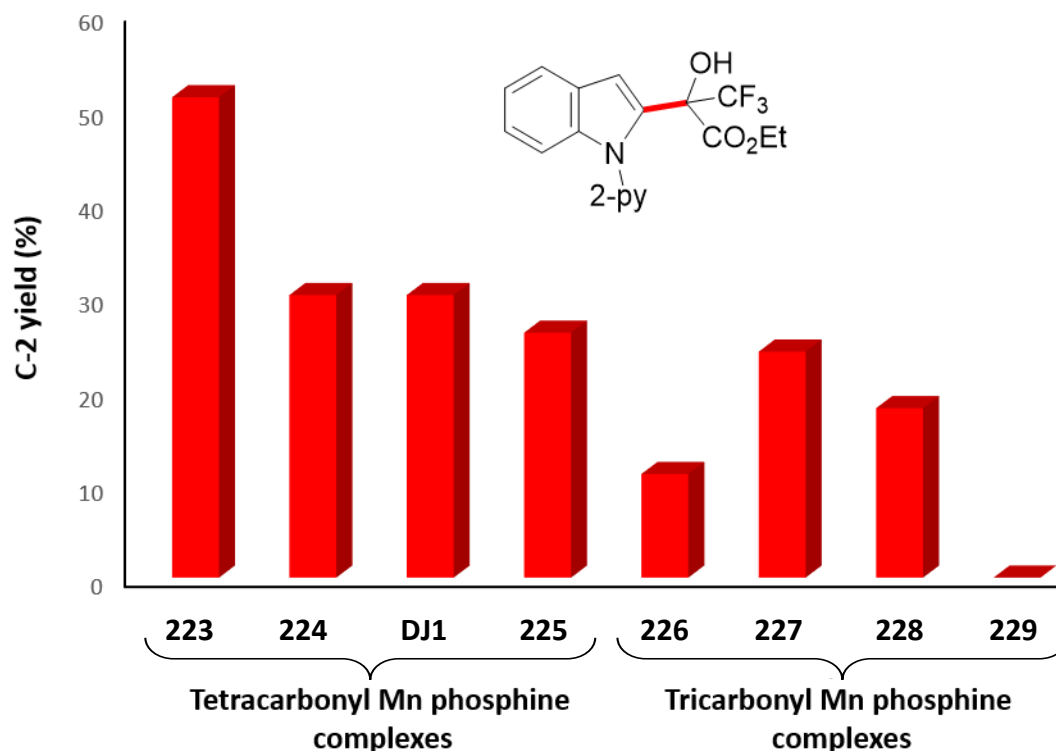
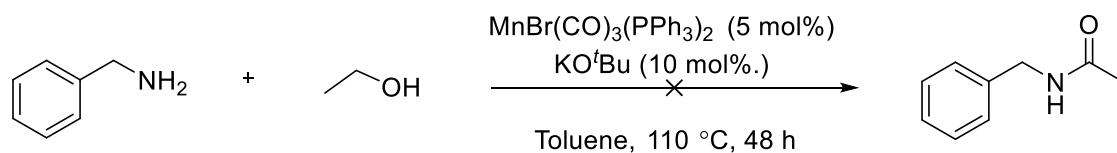


Figure 49. Comparison of tetracarbonyl Mn phosphine complexes **223-225**, **DJ1** and tricarbonyl Mn phosphine complexes **226-229** in terms of the yield of the C-2 substituted product **263**.

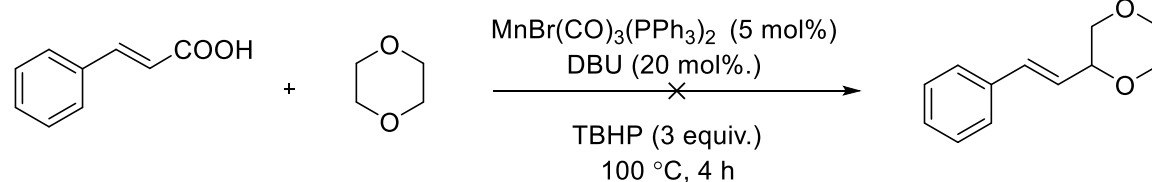
5.6 Additional reactions investigated

Numerous other transformations^{35, 67-73} were investigated with either commercially available Mn catalysts, or Mn carbonyl phosphine complexes synthesised in-house. However, no encouraging results were obtained. A summary of the reactions investigated is given in **Figure 50**.

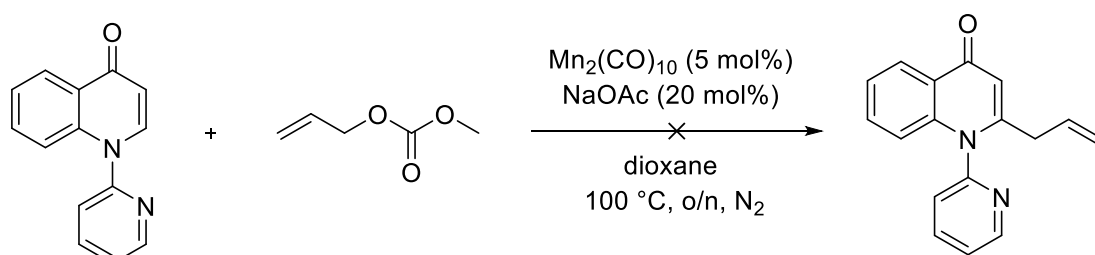
a)



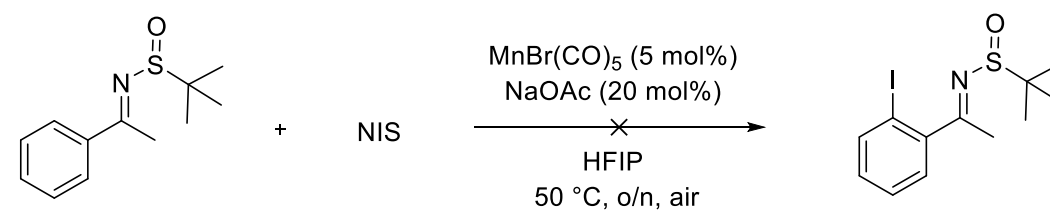
b)



c)



d)



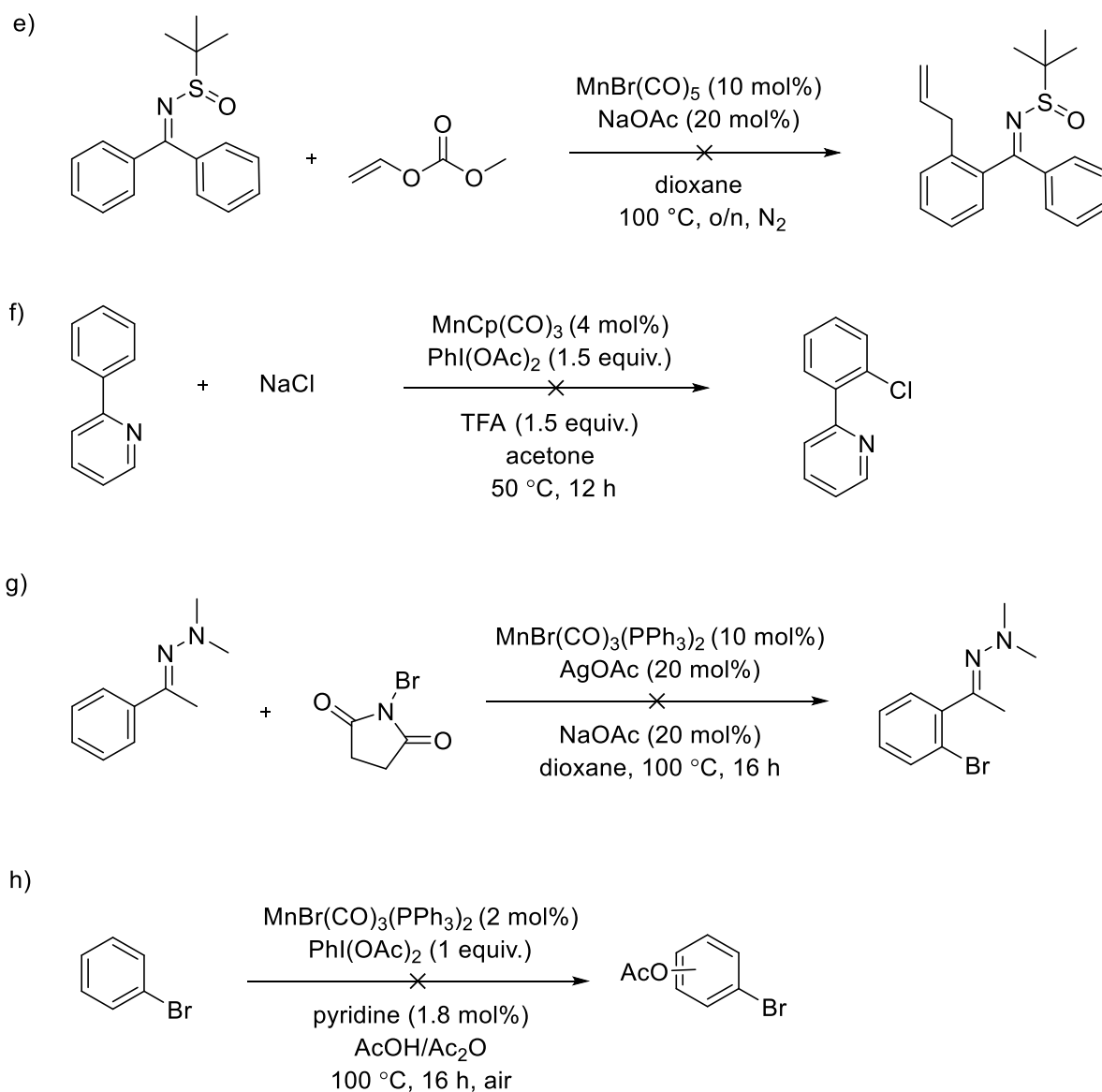


Figure 50. Various Mn catalysed transformations tested which did not yield the expected products.

5.7 Conclusion and future work

In conclusion, a number of tetracarbonyl- and tricarbonyl Mn phosphine complexes were successfully synthesised in good to excellent yields. The complexes were fully characterised by ¹H/³¹P/¹³C NMR spectroscopy, infrared spectroscopy (IR), single crystal X-ray structure analysis and elemental analysis. The pre-catalyst complexes were applied in a number of C-H activation reactions. Overall, the Mn phosphine complexes exhibited poor catalytic activity in the majority of C-H activation reactions investigated. However, application of the Mn pre-catalysts in the hydroarylation reaction of ethyl trifluoro pyruvate with *N*-(2-pyridyl) indole yielded more positive and insightful results. No discernible trend could be established with

regards to the electronic properties of the phosphine ligand ligated to the Mn centre. Steric factors appeared to play a more prominent role in achieving higher selectivity and conversion to the desired C-2 product, as the tetracarbonyl Mn phosphine complexes (**223-225**, **DJ1**) provided higher yields relative to the tricarbonyl Mn phosphine complexes (**226-229**). However, it must be noted that no Mn pre-catalyst allowed for a yield comparable to the commercial pre-catalyst $\text{MnBr}(\text{CO})_5$.

Further insight into the mechanism of action of the Mn carbonyl phosphine complexes is required to allow future applications of the complexes in C-H activation reactions. The examination of different additives may also prove fruitful in improving the efficiency of the Mn carbonyl phosphine complexes as pre-catalysts, as was recently demonstrated by Fairlamb and co-workers.⁶⁴

Future work in this area will likely be focused on carrying out an asymmetric variant of the hydroarylation reaction, which would involve using a chiral phosphine ligand (**Figure 51**). As of now, there has been no examples of an asymmetric Mn catalysed C-H activation reaction in the literature. Thus, this would represent an important advancement in the field.

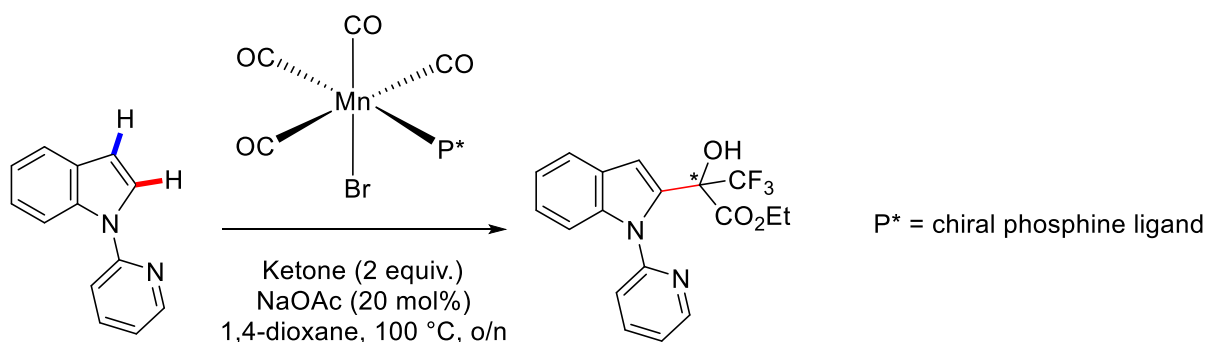


Figure 51. Asymmetric Mn catalysed hydroarylation reaction.

The exploration of ligands beyond phosphine ligands may also open up new avenues for reactivity. Mn catalysis for C-H activation is in its infancy, thus, it is hoped that new ligands for Mn will allow for the development of new and improved catalytic reactions. One such example would be phosphite ligands which are particularly interesting. The ‘carbonyl like’ π -acceptor properties of phosphites could be used to enhance the electrophilicity of the Mn centre which may allow for new reactivity to be exploited.⁷⁴ Additionally, phosphite ligands can be easily tuned for electronic and steric variations. The space that a ligand occupies

around a metal centre is an extremely important parameter for modulating and fine tuning both the stability and reactivity of metal complexes. For example, the low steric requirement of alkyl phosphites would allow for up to three (or even four) phosphite ligands to fit around the metal centre (e.g. $\text{P}(\text{OMe})_3$ has a Tolman cone angle (parameter for determining the space a ligand occupies around a metal centre) of 107° whereas PPh_3 has a cone angle of 145°).⁷⁵ Phosphite ligands are also more electron withdrawing than phosphines which makes them less sensitive to air and other oxidizing agents than phosphines.²⁹ A scattered number of Mn carbonyl phosphite complexes have previously been characterised and published in the literature,^{18, 26-29} However, their application in C-H activation reactions is unexplored. The structural diversity of phosphites (mono- and di-phosphites and heterodonor phosphite containing ligands) offer a wide variety of opportunities for derivatization. Thus, their use as ancillary ligands may have interesting effects in terms of activity and selectivity of the Mn centre in C-H activation reactions.

The investigation of various other ligand types such as multidentate pincer ligands, *N*-heterocyclic carbenes (NHCs), *N*-donor ligands such as *B*-diketiminates as well as mixed ligand systems, may also prove fruitful in allowing previously unseen reactivity for Mn to be explored and exploited, not only for C-H activation but also other areas of organic synthesis.

5.8 References

1. Engle, K. M., Yu, J.-Q. *J. Org. Chem.* **2013**, *78*, 8927-8955.
2. Pignolet, L. H. *Homogeneous Catalysis with Metal Phosphine Complexes* Springer, Boston, MA, USA, **1983**, pp. 111-135.
3. Billingsley, K., Buchwald, S. L. *J. Am. Chem. Soc.* **2007**, *129*, 3358-3366.
4. Martin, R., Buchwald, S. L. *Acc. Chem. Res.* **2008**, *41*, 1461-1473.
5. Barder, T. E., Walker, S. D., Martinelli, J. R., Buchwald, S. L. *J. Am. Chem. Soc.* **2005**, *127*, 4685-4696.
6. Yin, J., Rainka, M. P., Zhang, X.-X., Buchwald, S. L. *J. Am. Chem. Soc.* **2002**, *124*, 1162-1163.
7. Wolfe, J. P., Singer, R. A., Yang, B. H., Buchwald, S. L. *J. Am. Chem. Soc.* **1999**, *121*, 9550-9561.
8. Gelman, D., Buchwald, S. L. *Angew. Chem. Int. Ed.* **2003**, *42*, 5993-5996.
9. Okano, K., Tokuyama, H., Fukuyama, T. *J. Am. Chem. Soc.* **2006**, *128*, 7136-7137.
10. Ebran, J.-P., Hansen, A. L., Gøgsig, T. M., Skrydstrup, T. *J. Am. Chem. Soc.* **2007**, *129*, 6931-6942.
11. Cameron, M., Foster, B. S., Lynch, J. E., Shi, Y.-J., Dolling, U.-H. *Org. Process Res. Dev.* **2006**, *10*, 398-402.
12. Martin, R., Buchwald, S. L. *J. Am. Chem. Soc.* **2007**, *129*, 3844-3845.
13. Milne, J. E., Buchwald, S. L. *J. Am. Chem. Soc.* **2004**, *126*, 13028-13032.
14. Surry, D. S., Buchwald, S. L. *Angew. Chem. Int. Ed.* **2008**, *47*, 6338-6361.
15. Christmann, U., Vilar, R. *Angew. Chem. Int. Ed.* **2005**, *44*, 366-374.
16. Lafrance, M., Fagnou, K. *J. Am. Chem. Soc.* **2006**, *128*, 16496-16497.
17. Liang, Y.-F., Massignan, L., Liu, W., Ackermann, L. *Chem. Eur. J.* **2016**, *22*, 14856-14859.
18. Bond, A. M., Colton, R., McDonald, M. E. *Inorg. Chem.* **1978**, *17*, 2842-2847.
19. J. A. Pope, S., Reid, G. *J. Am. Chem. Soc., Dalton Trans.* **1999**, 1615-1622.
20. Toupadakis, A., Kubas, G. J., King, W. A., Scott, B. L., Huhmann-Vincent, J. *Organometallics* **1998**, *17*, 5315-5323.
21. Spessard, G. L., Miessler, G. L., *Organometallic Chemistry*, Oxford University Press, New York, **2010**, pp. 69-125.

22. Braga, M. *Inorg. Chem.* **1985**, *24*, 2702-2706.
23. Orpen, A. G., Connolly, N. G. *Chem. Commun.* **1985**, 1310-1311.
24. Köhl, O., *Phosphorus-31 NMR Spectroscopy*, Springer, Berlin, Germany, **2008**, pp. 83-127.
25. Grim, S. O., Yankowsky, A. W. *J. Org. Chem.* **1977**, *42*, 1236-1239.
26. Angelici, R. J., Basolo, F., Poe, A. J. *J. Am. Chem. Soc.* **1963**, *85*, 2215-2219.
27. Angelici, R. J. *J. Am. Chem. Soc.* **1962**, *84*, 2495-2499.
28. Micoli, F., Salvi, L., Salini, A., Frediani, P., Giannelli, C. *J. Organomet. Chem.* **2005**, *690*, 4867-4877.
29. Bravo, J., Castro, J., García-Fontán, S., M. Lamas, E., Seoane, P. Z. *Anorg. Allg. Chem.* **2003**, *629*, 297-302.
30. Özer, Z., Özkar, S. *Turk. J. Chem.* **1999**, *23*, 9-14.
31. Cano, R., Mackey, K., McGlacken, G. P. *Catal. Sci. Tech.* **2018**, *8*, 1251-1266.
32. Hu, Y., Zhou, B., Wang, C. *Acc. Chem. Res.* **2018**, *51*, 816-827.
33. Liu, W., Ackermann, L. *ACS Catal.* **2016**, *6*, 3743-3752.
34. Cano, R., Ramón, D. J., Yus, M. *J. Org. Chem.* **2011**, *76*, 654-660.
35. Liu, W., Richter, S. C., Zhang, Y., Ackermann, L. *Angew. Chem. Int. Ed.* **2016**, *55*, 7747-7750.
36. He, R., Huang, Z. T., Zheng, Q. Y., Wang, C. *Angew. Chem. Int. Ed.* **2014**, *53*, 4950-4953.
37. Wang, H.-W., Lu, Y., Zhang, B., He, J., Xu, H.-J., Kang, Y.-S., Sun, W.-Y., Yu, J.-Q. *Angew. Chem. Int. Ed.* **2017**, *56*, 7449-7453.
38. Zhou, B., Chen, H., Wang, C. *J. Am. Chem. Soc.* **2013**, *135*, 1264-1267.
39. Zhou, B., Ma, P., Chen, H., Wang, C. *Chem. Commun.* **2014**, *50*, 14558-14561.
40. Liu, W., Bang, J., Zhang, Y., Ackermann, L. *Angew. Chem. Int. Ed.* **2015**, *54*, 14137-14140.
41. Hummel, J. R., Ellman, J. A. *Org. Lett.* **2015**, *17*, 2400-2403.
42. Reddy, V. P., Qiu, R., Iwasaki, T., Kambe, N. *Org. Lett.* **2013**, *15*, 1290-1293.
43. Chen, S.-Y., Li, Q., Wang, H. *J. Org. Chem.* **2017**, *82*, 11173-11181.
44. Ruan, Z., Sauermann, N., Manoni, E., Ackermann, L. *Angew. Chem. Int. Ed.* **2017**, *56*, 3172-3176.

45. Zhang, S.-S., Jiang, C.-Y., Wu, J.-Q., Liu, X.-G., Li, Q., Huang, Z.-S., Li, D., Wang, H. *Chem. Commun.* **2015**, 51, 10240-10243.
46. Clarke, S. L., McGlacken, G. P. *Tetrahedron* **2015**, 71, 2906-2913.
47. Magedov, I. V., Manpadi, M., Ogasawara, M. A., Dhawan, A. S., Rogelj, S., Van slambrouck, S., Steelant, W. F. A., Evdokimov, N. M., Uglinskii, P. Y., Elias, E. M., Knee, E. J., Tongwa, P., Antipin, M. Y., Kornienko, A. *J. Med. Chem.* **2008**, 51, 2561-2570.
48. Nolan, M.-T., Bray, J. T. W., Eccles, K., Cheung, M. S., Lin, Z., Lawrence, S. E., Whitwood, A. C., Fairlamb, I. J. S., McGlacken, G. P. *Tetrahedron* **2014**, 70, 7120-7127.
49. Pardo, L. M., Prendergast, A. M., Nolan, M.-T., Ó Muimhneacháin, E., McGlacken, G. P. *Eur. J. Org. Chem.* **2015**, 2015, 3540-3550.
50. Mackey, K., Pardo, L. M., Prendergast, A. M., Nolan, M.-T., Bateman, L. M., McGlacken, G. P. *Org. Lett.* **2016**, 18, 2540-2543.
51. Das, D., Poddar, P., Maity, S., Samanta, R. *J. Org. Chem.* **2017**, 82, 3612-3621.
52. Biswas, A., Giri, D., Das, D., De, A., Patra, S. K., Samanta, R. *J. Org. Chem.* **2017**, 82, 10989-10996.
53. Wang, C., Maity, B., Cavallo, L., Rueping, M. *Org. Lett.* **2018**, 20, 3105-3108.
54. Das, D., Biswas, A., Karmakar, U., Chand, S., Samanta, R. *J. Org. Chem.* **2016**, 81, 842-848.
55. Deadman, B. J., O'Mahony, R. M., Lynch, D., Crowley, D. C., Collins, S. G., Maguire, A. R. *Org. Biomol. Chem.* **2016**, 14, 3423-3431.
56. Gandeepan, P., Müller, T., Zell, D., Cera, G., Warratz, S., Ackermann, L. *Chem. Rev.* **2019**, 119, 2192-2452.
57. Rach, S. F., Kühn, F. E. *Chem. Rev.* **2009**, 109, 2061-2080.
58. Bouldin, R. M., Singh, A., Magaletta, M., Connor, S., Kumar, J., Nagarajan, R. *Bioengineering*, **2014**, 1, 246-259.
59. Keller, P. A., Yepuri, N. R., Kelso, M. J., Mariani, M., Skelton, B. W., White, A. H. *Tetrahedron* **2008**, 64, 7787-7795.
60. Houlihan, W. J. *The Chemistry Of Heterocyclic Compounds, Indoles*, John Wiley & Sons, Canada, **2009**, pp. 586.

61. Ishii, H., Murakami, K., Sakurada, E., Hosoya, K., Murakami, Y. *J. Am. Chem. Soc., Perkin Trans. 1* **1988**, 2377-2385.
62. Denton, R. M., An, J., Adeniran, B., Blake, A. J., Lewis, W., Poulton, A. M. *J. Org. Chem.* **2011**, 76, 6749-6767.
63. Hammarback, L. A., Robinson, A., Lynam, J. M., Fairlamb, I. J. S. *J. Am. Chem. Soc.* **2019**, 141, 2316-2328.
64. Hammarback, L. A., Robinson, A., Lynam, J. M., Fairlamb, I. J. S. *Chem. Commun.* **2019**, 55, 3211-3214.
65. Hammarback, L. A., Clark, I. P., Sazanovich, I. V., Towrie, M., Robinson, A., Clarke, F., Meyer, S., Fairlamb, I. J. S., Lynam, J. M. *Nat. Catal.* **2018**, 1, 830-840.
66. Gensch, T., James, M. J., Dalton, T., Glorius, F. *Angew. Chem. Int. Ed.* **2018**, 57, 2296-2306.
67. Emmert, M. H., Cook, A. K., Xie, Y. J., Sanford, M. S. *Angew. Chem. Int. Ed.* **2011**, 50, 9409-9412.
68. Schröder, N., Wencel-Delord, J., Glorius, F. *J. Am. Chem. Soc.* **2012**, 134, 8298-8301.
69. Zhang, P., Hong, L., Li, G., Wang, R. *Adv. Syn. Catal.* **2015**, 357, 345-349.
70. Hazra, C. K., Dherbassy, Q., Wencel-Delord, J., Colobert, F. *Angew. Chem. Int. Ed.* **2014**, 53, 13871-13875.
71. Kumar, A., Espinosa-Jalapa, N. A., Leitus, G., Diskin-Posner, Y., Avram, L., Milstein, D. *Angew. Chem. Int. Ed.* **2017**, 56, 14992-14996.
72. Zhang, J.-X., Wang, Y.-J., Zhang, W., Wang, N.-X., Bai, C.-B., Xing, Y.-L., Li, Y.-H., Wen, J.-L. *Sci. Rep.* **2014**, 4, 7446.
73. Pulis, A. P., Procter, D. J. *Angew. Chem. Int. Ed.* **2016**, 55, 9842-9860.
74. Aitor, G., Goddard, C., Fuente, V. de la, Castillón *Phosphorus(III) Ligands in Homogeneous Catalysis: Design and Synthesis*, John Wiley & Sons, **2012**. pp. 81-123.
75. Tolman, C. A. *Chem. Rev.* **1977**, 77, 313-348.

Concluding remarks

In **Chapter 2** of this thesis, two sets of reaction conditions were developed, which allowed for the efficient assembly of 6*H*-benzofuro[3,2-*c*]chromen-6-one and 1*H*-pyrano[4,3-*c*]benzofuran-1-one analogues in an atom economical manner. Gratifyingly, a wide variety of 6*H*-benzofuro[3,2-*c*]chromen-6-one analogues were accessed, featuring diverse substituents, including for example halides (-F, -Cl) and a nitro group, which could undergo further derivatisation. Pleasingly, good to excellent yields were obtained for the 6*H*-benzofuro[3,2-*c*]chromen-6-one analogues with both sets of conditions. For *meta*-substituted derivatives, when **Conditions A** were employed, which utilised PivOH as reaction solvent, C-H activation occurred preferentially at the less sterically hindered position, with a single regioisomer isolated for the *meta*-methyl substrate. Overall, the regioselectivity of the double C-H activation reaction was largely dictated by steric effects, with the exception of substrates which exerted a secondary directing effect (-F, -OMe). A decrease in regioselectivity was observed when **Conditions B**, with TFA as solvent, were employed. Interestingly, a switch in regioselectivity was noted for the *meta*-methoxy substrate. For this substrate, reaction preferentially occurred the more sterically congested site. These results may be indicative of two different mechanisms operating depending on the reaction conditions employed.

A decrease in yield was observed for the 1*H*-pyrano[4,3-*c*]benzofuran-1-one products employing **Conditions A**. Furthermore, the methodology also allowed for the construction of a synthetically useful 2-quinolone analogue, albeit the yield was reduced. To our delight, the double C-H activation strategy was also exploited for the short three-step synthesis of a natural product, flemichapparin C. This is one of the most delicate molecular frameworks to have been reported for a double C-H activation protocol, which demonstrates the robustness of this transformation. Satisfyingly, this work was published in *Organic Letters* in 2016.

Encouraged by the excellent yields obtained for the coumarin and pyrone analogues, as well as some good regioselectivity observed for *meta*-substituted compounds, we then pursued the synthesis of dibenzofuran derivatives. Application of **Conditions A** efficiently delivered a number of *meta*-substituted dibenzofurans. Notably, yields of up to 99% were achieved for a range of mono- and di-substituted dibenzofurans. Overall, excellent regioselectivity was achieved for substrates with sterically bulky electron donating groups. Again, the selectivity of the double C-H activation reaction was largely governed by steric interactions. A slight

decrease in regioselectivity was observed for the *meta*-fluoro and *meta*-methoxy analogues. Additionally, the naphthyl derivative produced a mixture of regioisomers. On the contrary, application of **Conditions B** resulted in a decrease in regioselectivity and yields.

Dibenzofurans are important motifs in natural products and compounds with wide biological activity. Targeting this structural moiety using aryl–aryl bond formation, and diaryl ether precursors, is an obvious strategy. The limited current synthetic methods involving Pd catalysed C–H activation are hampered by a number of problems. Thus, **Chapter 3** of this thesis described the efficient synthesis of dibenzofurans *via* a Pd catalysed single C–H activation of *ortho*-bromo diarylethers. A catalytic amount of cheap and bench stable 6-methoxy quinoline was found to enhance the reaction. Overall, the work undertaken in this chapter addressed a number of limitations existing with current or previous protocols for the classic intramolecular C–H activation of diarylethers. This simple and efficient method allowed the synthesis of a wide range of synthetically valuable and novel dibenzofurans in good to excellent yields. Importantly, the reactions took place in air, without added phosphine or *tert*-alkyl ammonium salt. In addition, the reaction conditions allowed for the use of a pyridyl moiety and an N–H linker. Disappointingly, the reaction conditions did not facilitate full conversion to product for electron rich substrates and this led to problems during the purification step. Further optimisation of the reaction conditions did allow for an 85% conversion to product for a *para*-methoxy substrate. This was achieved using DBU as an additive. It is envisaged that a review of ligands and additives will identify a set of reaction conditions suitable for electron rich substrates. A manuscript is in preparation for this work.

A detailed review into Mn catalysed C–H activation protocols reported over the last few years, with a particular emphasis on the mechanistic aspects of the reactions, was published in *Catalysis Science and Technology* in 2018. In **Chapter 5** of this thesis, the synthesis of a number of Mn carbonyl phosphine complexes and their reactivity in C–H activation reactions was discussed. In this Chapter, a range of tetracarbonyl- and tricarbonyl Mn phosphine complexes were successfully synthesised in good to excellent yields. This work entailed the characterisation of the complexes by spectroscopic means and also by single crystal x-ray structure analysis and elemental analysis. There have been previous reports on the synthesis of Mn carbonyl phosphine complexes in the inorganic literature dating back to the 1960s. However, it is important to note that their utility in C–H activation reactions up to recently,

has been completely unexplored. Relatively little success was achieved upon the application of the pre-catalyst complexes in most of the C-H activation reactions examined. Pleasingly, success was achieved with the Mn catalysed hydroarylation reaction of ketones with indoles. This reaction was reported by Ackermann and co-workers in 2017 using the commercially available $\text{MnBr}(\text{CO})_5$ pre-catalyst. Overall, the steric properties of the complexes played an important role with regards to selectivity and conversion, with the mono-phosphine complexes displaying greater reactivity relative to the di-phosphine complexes. Relative to the commercially available pre-catalyst, $\text{MnBr}(\text{CO})_5$, which gave an 88% yield of the desired C-2 alcohol product, $\text{MnBr}(\text{CO})_4(\text{PPh}_3)$ allowed for a 51% yield of the C-2 hydroarylated product. On the contrary, the Mn carbonyl complex containing the bidentate dppp ligand exhibited very poor catalytic activity. On-going work within the McGlacken laboratory is also focused on carrying out this reaction in an asymmetric fashion using a chiral phosphine ligand, as well as examining the reactivity of the pre-catalyst complexes in other C-H activation reactions. Key to further development of this reaction involves gaining mechanistic information on the catalytic processes involving Mn and also elucidating the role of the phosphine ligands in the reaction. Furthermore, a current collaboration with Dr. Jason Lynam and Prof. Ian Fairlamb, which involves using real time infrared spectroscopic analysis for studying transient manganese carbonyl species formed during C-H bond activation reactions, is on-going. The results garnered from this collaboration will be published in due course.

Chapter 6: Experimental

6.1 General information

Solvents and reagents were used as obtained from commercial sources and without purification, with the exception of 1,4-dioxane, chloroform and dichloromethane, which were flame dried over 4Å molecular sieves (10-15% w/v) and stored in a Young's flask. Toluene was distilled from sodium/benzophenone dianion under nitrogen.

Wet flash column chromatography was carried out using Kieselgel silica gel 60, 0.040-0.063 µm (Merck). TLC was carried out on pre-coated silica gel plates (Merck 60 PF254). Visualisation was achieved by UV light. Microwave reactions were performed in a CEM Discover S-Class Synthesiser with the temperature monitored by infrared temperature control. Melting points were obtained on a uni-melt Thomas Hoover Capillary melting point apparatus.

IR spectra were recorded on Perkin-Elmer FT-IR Paragon 1000 spectrophotometer or Perkin-Elmer AT-IR spectrophotometer. Liquid samples were examined as thin films interspersed on NaCl plates. Solid samples were either recorded on Perkin-Elmer AT-IR spectrophotometer or dissolved in dichloromethane, dispersed as thin films on NaCl plates and the dichloromethane allowed to evaporate before measurement of sample on Perkin-Elmer FT-IR Paragon 1000 spectrophotometer.

NMR spectra were run in CDCl₃ using TMS as the internal standard at 25 °C unless otherwise specified. ¹H NMR (600 MHz) spectra, ¹H NMR (500 MHz) spectra and ¹H NMR (300 MHz) spectra were recorded on Bruker Avance 600, Bruker Avance 500, 0 and Bruker Avance 300 NMR spectrometers respectively. ¹³C (150 MHz) spectra, ¹³C (125 MHz) spectra, and ¹³C (75.5 MHz) spectra were recorded on Bruker Avance 600, Bruker Avance 500, and Bruker Avance 300 NMR spectrometers respectively in proton decoupled mode. ¹⁹F NMR (282 MHz) spectra were recorded on a Bruker Avance 300 NMR spectrometer in proton decoupled mode. ³¹P NMR (282 MHz) spectra were recorded on a Bruker Avance 600 NMR spectrometer in proton decoupled mode. Chemical shifts δ_H and δ_C are expressed as parts per million (ppm), positive shift being downfield from TMS; coupling constants (*J*) are expressed in hertz (Hz). Splitting patterns in ¹H NMR spectra are designated as s (singlet), *br s* (broad singlet), d (doublet), dd (doublet of doublets), dt (doublet of triplets), t (triplet), q (quartet), quin (quintet), sext

(sextet), sept (septet), and m (multiplet). For ^{13}C NMR spectra, the number of attached protons for each signal was determined using the DEPT pulse sequence run in the DEPT-90 and DEPT-135 modes.

Nominal mass spectra were recorded on a Waters Quattro Micro triple quadrupole spectrometer (QAA1202) in ESI mode using 50% acetonitrile–water containing 0.1% formic acid as eluent. High resolution mass spectra (HRMS) were recorded on a Waters LCT Premier Time of Flight spectrometer (KD160) or a Waters Vion IMS mass spectrometer (SAA055 K) in ESI mode using 50% acetonitrile–water containing 0.1% formic acid as eluent. Samples (max. 1 mg) were dissolved in acetonitrile, acetonitrile/methanol, water or 10% DMSO/acetonitrile.

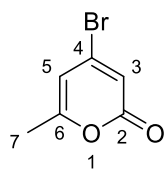
The Microanalysis Laboratory, National University of Ireland, Cork, performed elemental analysis using a Perkin-Elmer 240 and Exeter Analytical CE440 elemental analysers.

6.1.1 Analysis of known and novel compounds

^1H NMR spectra, ^{13}C NMR spectra, ^{31}P NMR spectra (where applicable) LRMS, melting point (if solid) or IR analyses were recorded for all previously prepared compounds. For novel compounds, in addition to previously mentioned analysis, ^{19}F NMR SPECTRA (where applicable), HRMS or Elemental Analysis (if possible) was also obtained. An arbitrary numbering system was employed to aid in assignment of ^1H NMR and ^{13}C NMR spectra. COSY, HSQC and HMBC experiments were used to aid in assignment.

Note: Compounds **102**, **203**, **204**, **215** and novel compounds **110**, **183**, **184**, **185** and **187** were not detected by ESI mass spectrometry under standard conditions and hence do not have a HRMS. Due to the current circumstances regarding COVID-19, I was not able to pursue this. This work however, will not be published in a journal until full characterisation is complete.

6.2 Synthesis of Starting Materials

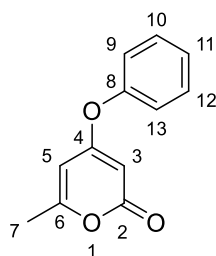
6.2.1 Preparation of 4-bromo-6-methyl-2H-pyran-2-one (**23**)¹

To a 2-necked round bottomed flask was added 4-hydroxy-6-methyl-2H-pyran-2-one (**22**) (5.0 g, 39.7 mmol, 1.0 equiv.), TBAB (14.8 g, 46.0 mmol, 1.16 equiv.), phosphorus pentoxide (13.5 g, 95.2 mmol, 2.4 equiv.) and toluene (4.0 mL/mmol). The resulting mixture was stirred in an oil bath at 94 °C for 1.5 hours. Upon cooling, the clean upper layer was separated from the lower solid layer. The lower layer was washed with toluene (2 x 30 mL). The combined organic extracts were then washed with saturated aqueous NaHCO₃ (60 mL) and brine (80 mL). The organic layer was then dried over MgSO₄, filtered and concentrated under reduced pressure. The product 4-bromo-6-methyl-2H-pyran-2-one (**23**) was isolated as an orange solid (6.4 g, 85%), m.p. 72-74 °C (lit. 73-74 °C)¹; δ_{H} (CDCl₃, 300 MHz) 2.25 (3H, d, *J* 0.5, C(7)H₃), 6.19 (1H, *t*_{app}, *J* 0.8, C(5)H), 6.46 (1H, d, *J* 0.7, C(3)H); δ_{C} (CDCl₃, 75.5 MHz) 19.7 (C(7)H₃), 108.4 (C(5)H), 114.8 (C(3)H), 141.1 (qC-4), 160.6 (qC-6), 162.1 (qC-2); *m/z* (ES⁺): Br⁷⁹ 181 [(M+H)⁺, 25%], Br⁸¹ 191 [(M+H)⁺, 98%].

Spectral characteristics were consistent with previously reported data.¹

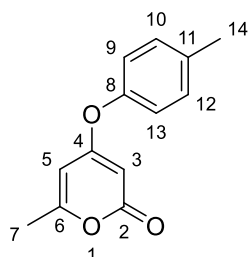
6.2.2 General procedure for preparation of 4-phenoxy-6-methyl-2H-pyran-2-ones (**24**, **30-40**)²

To a 3-necked round bottomed flask was added 4-bromo-6-methyl-2H-pyran-2-one (**23**) (1.0 equiv.), phenol (1.5 equiv.), and K₂CO₃ (1.8 equiv.) in acetone (4.0 mL/mmol). The resulting mixture was stirred in an oil bath at 65 °C for 16 hours. Upon cooling to ambient temperature, the reaction mixture was diluted with water (10 mL) and EtOAc (20 mL). The layers were separated and the aqueous layer washed with EtOAc (2 x 20 mL) and the combined organic layers were washed with aqueous NaOH (10% w/v, 2 x 20 mL). The organic layer was then dried over MgSO₄, filtered and concentrated under reduced pressure. The residues were purified by recrystallisation from EtOH.

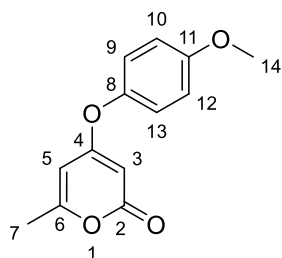
4-Phenoxy-6-methyl-2H-pyran-2-one (24)²

Synthesised according to the general procedure **6.2.2** using 4-bromo-6-methyl-2H-pyran-2-one (**23**) (2.0 g, 10.6 mmol, 1.0 equiv.) and phenol (1.5 equiv.). Yellow solid (1.69 g, 71%), m.p. 86-88 °C (lit. 86 °C); δ_{H} (CDCl₃, 300 MHz) 2.26 (3H, s, C(7)H₃), 5.21 (1H, d, *J* 2.1, C(3)H), 5.96-5.97 (1H, m, C(5)H), 7.07 (2H, d, *J* 8.0, C(9)H & C(13)H), 7.29 (1H, t, *J* 7.3, C(11)H), 7.43 (2H, t, *J* 7.8, C(10)H & C(12)H); δ_{C} (CDCl₃, 75.5 MHz) 20.0 (C(7)H₃), 91.0 (C(3)H), 99.9 (C(5)H), 121.1 (C(9)H & C(13)H), 126.5 (C(11)H), 130.2 (C(10)H & C(12)H), 152.4 (qC-8), 163.3 (qC-6), 164.6 (qC-2), 170.8 (qC-4); *m/z* (ES⁺): 203, [(M+H)⁺, 100%].

Spectral characteristics were consistent with previously reported data.²

4-(4-Methylphenoxy)-6-methyl-2H-pyran-2-one (30)²

Synthesised according to the general procedure **6.2.2** using 4-bromo-6-methyl-2H-pyran-2-one (**23**) (200 mg, 1.06 mmol, 1.0 equiv.) and 4-methyl phenol (1.5 equiv.). Cream solid (450 mg, 44%), m.p. 107-109 °C (lit. 53 °C); δ_{H} (CDCl₃, 300 MHz) 2.25 (3H, s, C(7)H₃), 2.37 (3H, s, C(14)H₃), 5.20 (1H, d, *J* 2.1, C(3)H), 5.95 (1H, *t*_{app}, *J* 1.0, C(5)H), 6.94 (2H, d, *J* 8.5, C(9)H & C(13)H), 7.21 (2H, d, *J* 8.2, C(10)H & C(12)H); δ_{C} (CDCl₃, 75.5 MHz) 20.0 (C(7)H₃), 20.9 (C(14)H₃), 90.8 (C(3)H), 99.9 (C(5)H), 120.8 (C(9)H & C(13)H), 130.7 (C(10)H & C(12)H), 136.3 (qC-11), 150.1 (qC-8), 163.2 (qC-6), 164.7 (qC-2), 171.0 (qC-4); *m/z* (ES⁻): 215, [(M-H)⁻, 16%]; HRMS (ESI-TOF): Exact mass calculated for C₁₃H₁₃O₃ [M+H⁺], 217.0865. Found 217.0869. Spectral characteristics were consistent with previously reported data.²

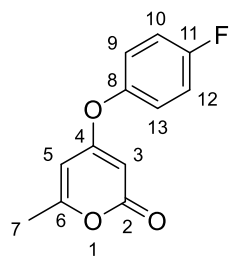
4-(4-Methoxyphenoxy)-6-methyl-2H-pyran-2-one (31)²

Synthesised according to the general procedure **6.2.2** using 4-bromo-6-methyl-2H-pyran-2-one (**23**) (200 mg, 1.06 mmol, 1.0 equiv.) and 4-methoxy phenol (1.5 equiv.). White solid (380 mg, 55%), m.p.: 106-108 °C (lit. 105-106 °C); δ_{H} (CDCl₃, 300 MHz) 2.25 (3H, t, *J* 0.7, C(7)H₃), 3.82 (3H, s, C(14)H₃), 5.19 (1H, d, *J* 2.1, C(3)H), 5.95 (1H, dd, *J* 2.2, 1.0, C(5)H), 6.89-6.94 (2H, m, C(9)H & C(13)H), 6.96-7.03 (2H, m, C(10)H & C(12)H); δ_{C} (CDCl₃, 75.5

MHz) 20.0 (C(7)H₃), 55.7 (C(14)H₃), 90.7 (C(3)H), 99.9 (C(5)H), 115.2 (C(9)H & C(13)H), 122.0 (C(10)H & C(12)H), 145.8 (qC-8), 157.8 (qC-11), 163.2 (qC-6), 164.1 (qC-2), 171.3 (qC-4); HRMS (ESI-TOF): Exact mass calculated for C₁₃H₁₃O₄ [M+H⁺], 233.0814. Found 233.0810.

Spectral characteristics were consistent with previously reported data.²

4-(4-Fluorophenoxy)-6-methyl-2H-pyran-2-one (32)²

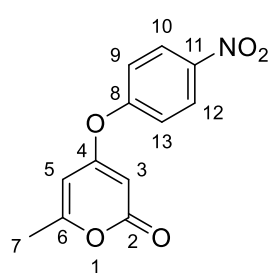


Synthesised according to the general procedure 6.2.2 using 4-bromo-6-methyl-2H-pyran-2-one (**23**) (200 mg, 1.06 mmol, 1.0 equiv.) and 4-fluorophenol (1.5 equiv.). Yellow solid (390 mg, 64%), m.p. 79-81 °C (lit. 75-76 °C); δ_H (CDCl₃, 300 MHz) 2.26 (3H, s, C(7)H₃), 5.17 (1H, d, *J* 2.4, C(3)H), 5.96 (1H, d, *J* 2.1, C(5)H), 7.01-7.16 (4H, m, C(9)H, C(10)H, C(12)H & C(13)H); δ_C

(CDCl₃, 75.5 MHz) 20.0 (C(7)H₃), 91.0 (C(3)H), 100.0 (C(5)H), 117.0 (C(10)H & C(12)H, d, *J*_{C-F} 24), 122.7 (C(9)H & C(13)H, d, *J*_{C-F} 9), 148.2 (qC-8, d, *J*_{C-F} 3), 160.5 (qC-11, d, *J*_{C-F} 247), 163.5 (qC-6), 164.4 (qC-2), 170.8 (qC-4); *m/z* (ES⁺): 221, [(M+H)⁺, 15%]; HRMS (ESI-TOF): Exact mass calculated for C₁₂H₁₀O₃F [M+H⁺], 221.0614. Found 221.0618.

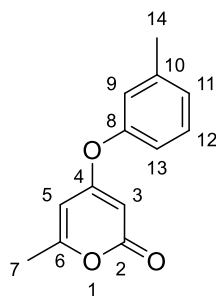
Spectral characteristics were consistent with previously reported data.²

4-(4-Nitrophenoxy)-6-methyl-2H-pyran-2-one (33)



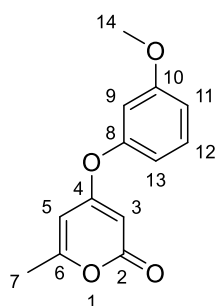
Synthesised according to the general procedure 6.2.2 using 4-bromo-6-methyl-2H-pyran-2-one (**23**) (200 mg, 1.06 mmol, 1.0 equiv.) and 4-nitrophenol (1.5 equiv.). Brown solid (130 mg, 50%), m.p. 142-144 °C; δ_H (CDCl₃, 300 MHz) 2.29 (3H, s, C(7)H₃), 5.31 (1H, d, *J* 2.1, C(3)H), 5.98 (1H, d, *J* 2.1, C(5)H), 7.24-7.28 (2H, m, C(9)H & C(13)H), 8.31-8.36 (2H, m, C(10)H & C(12)H); δ_C (CDCl₃, 75.5 MHz) 20.1 (C(7)H₃), 92.5 (C(3)H), 99.5 (C(5)H), 121.7 (C(9)H & C(13)H), 126.1 (C(10)H & C(12)H), 142.1 (qC-11), 157.2 (qC-8), 163.8 (qC-6), 164.3 (qC-2), 169.1 (qC-4); *m/z* (ES⁺): 248, [(M+H)⁺, 90%]. Anal. Calculated for C₁₂H₉NO₅: C, 58.30;

H, 3.67. Found: C, 58.60; H, 3.72.

4-(3-Methylphenoxy)-6-methyl-2H-pyran-2-one (34)

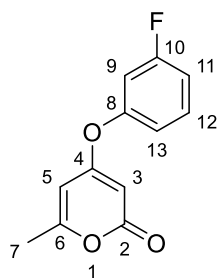
Synthesised according to the general procedure **6.2.2** using 4-bromo-6-methyl-2H-pyran-2-one (**23**) (200 mg, 1.06 mmol, 1.0 equiv.) and 3-methyl phenol (1.5 equiv.). Pale brown crystals (460 mg, 73%), m.p. 66-68 °C (lit. 59-60 °C); δ_{H} (CDCl₃, 300 MHz) 2.26 (3H, m, C(7)H₃), 2.37 (3H, s, C(14)H₃), 5.21 (1H, dd, *J* 2.2, 0.4, C(3)H), 5.96 (1H, dd, *J* 2.2, 0.9, C(5)H), 6.84-6.89 (2H, m, C(9)H & C(13)H), 7.08-7.11 (1H, m, C(11)H), 7.29 (1H, td, *J* 7.6, 1.0, C(12)H); δ_{C} (CDCl₃, 75.5 MHz) 20.0 (C(7)H₃), 21.3 (C(14)H₃), 91.0 (C(3)H), 100.0 (C(5)H), 118.0 (C(9)H), 121.6 (C(13)H), 127.3 (C(11)H), 129.9 (C(12)H), 140.6 (qC-10), 152.3 (qC-8), 163.2 (qC-6), 164.7 (qC-2), 170.8 (qC-4); *m/z* (ES⁺): 217, [(M+H)⁺, 14%]; HRMS (ESI-TOF): Exact mass calculated for C₁₃H₁₃O₃ [M+H⁺], 217.0865. Found 217.0868.

Spectral characteristics were consistent with previously reported data.²

4-(3-Methoxyphenoxy)-6-methyl-2H-pyran-2-one (35)

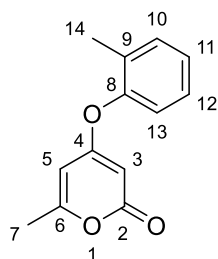
Synthesised according to the general procedure **6.2.2** using 4-bromo-6-methyl-2H-pyran-2-one (**23**) (200 mg, 1.06 mmol, 1.0 equiv.) and 3-methoxy phenol (1.5 equiv.). Yellow solid (530 mg, 58%), m.p. 99-100 °C (lit. 100 °C); δ_{H} (CDCl₃, 300 MHz) 2.26 (3H, s, C(7)H₃), 3.81 (3H, s, C(14)H₃), 5.26 (1H, d, *J* 2.1, C(3)H), 5.96 (1H, dd, *J* 2.1, 0.9, C(5)H), 6.61 (1H, t, *J* 2.3, C(9)H), 6.66 (1H, dd, *J* 8.0, 2.2, C(13)H), 6.83 (1H, dt, *J* 8.4, 2.0, C(11)H), 7.32 (1H, t, *J* 8.2, C(12)H); δ_{C} (CDCl₃, 75.5 MHz) 20.0 (C(7)H₃), 55.7 (C(14)H₃), 90.7 (C(3)H), 99.9 (C(5)H), 115.2 (C(9)H & C(13)H), 122.0 (C(11)H & C(12)H), 145.8 (qC-10), 157.8 (qC-8), 163.2 (qC-6), 164.1 (qC-2), 171.3 (qC-4); *m/z* (ES⁺): 233, [(M+H)⁺, 100%]; HRMS (ESI-TOF): Exact mass calculated for C₁₃H₁₃O₄ [M+H⁺], 233.0814. Found 233.0813.

Spectral characteristics were consistent with previously reported data.²

4-(3-Fluorophenoxy)-6-methyl-2H-pyran-2-one (36)

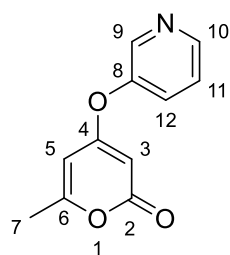
Synthesised according to the general procedure **6.2.2** using 4-bromo-6-methyl-2H-pyran-2-one (**23**) (200 mg, 1.06 mmol, 1.0 equiv.) and 3-fluorophenol (1.5 equiv.). White solid (390 mg, 21%), m.p.: 82-84 °C (lit. 77-80 °C); δ_{H} (CDCl₃, 300 MHz) 2.27 (3H, s, C(7)H₃), 5.25 (1H, d, J 2.3, C(3)H), 5.96-5.97 (1H, m, C(5)H), 6.83 (1H, dt, J 9.1, 2.3, C(13)H), 6.89 (1H, dd, J 8.2, 2.1, C(9)H), 6.99-7.02 (1H, m, C(12)H), 7.36-7.44 (1H, m, C(11)H); δ_{C} (CDCl₃, 75.5 MHz) 20.1 (C(7)H₃), 91.4 (C(3)H), 99.7 (C(5)H), 109.3 (C(9)H, d, $J_{\text{C-F}}$ 24), 113.7 (C(11)H, d, $J_{\text{C-F}}$ 21), 116.9 (C(13)H, d, $J_{\text{C-F}}$ 4), 131.2 (C(12)H, d, $J_{\text{C-F}}$ 9), 153.2 (qC-8, d, $J_{\text{C-F}}$ 11), 163.2 (qC-10, d, $J_{\text{C-F}}$ 2), 163.6 (qC-6), 164.3 (qC-2), 170.2 (qC-4); m/z (ES⁺): 221, [(M+H)⁺, 100%]; HRMS (ESI-TOF): Exact mass calculated for C₁₂H₁₀O₃F [M+H⁺], 221.0614. Found 221.0614.

Spectral characteristics were consistent with previously reported data.²

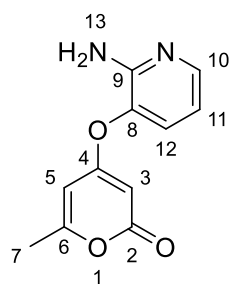
4-(2-Methylphenoxy)-6-methyl-2H-pyran-2-one (37)²

Synthesised according to the general procedure **6.2.2** using 4-bromo-6-methyl-2H-pyran-2-one (**23**) (200 mg, 1.06 mmol, 1.0 equiv.) and 2-methylphenol (1.5 equiv.). Cream solid (380 mg, 87%), m.p. 59-60 °C (lit. 59-60 °C); δ_{H} (CDCl₃, 300 MHz) 2.15 (3H, s, C(14)H₃), 2.24 (3H, s, C(7)H₃), 5.06 (1H, d, J 2.2, C(3)H), 6.00 (1H, dd, J 2.2, 0.9, C(5)H), 6.97 (1H, dd, J 7.5, 1.7, C(13)H), 7.14-7.21 (2H, m, C(10)H & C(12)H), 7.22-7.28 (1H, m, C(11)H); δ_{C} (CDCl₃, 75.5 MHz) 20.0 (C(14)H₃), 21.3 (C(7)H₃), 91.0 (C(3)H), 100.0 (C(5)H), 118.0 (C(13)H), 121.6 (C(10)H), 127.3 (C(11)H), 129.9 (C(12)H), 140.6 (qC-9), 152.3 (qC-8), 163.2 (qC-6), 164.7 (qC-2), 170.8 (qC-4); m/z (ES⁺): 217, [(M+H)⁺, 100%]; HRMS (ESI-TOF): Exact mass calculated for C₁₃H₁₃O₃ [M+H⁺], 217.0865. Found 217.0863.

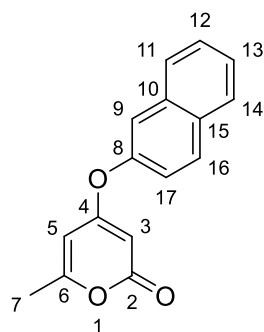
Spectral characteristics were consistent with previously reported data.²

6-Methyl-4-(pyridin-3-yloxy)-2H-pyran-2-one (38)

Synthesised according to the general procedure **6.2.2** using 4-bromo-6-methyl-2H-pyran-2-one (**23**) (200 mg, 1.06 mmol, 1.0 equiv.) and 3-pyridyl phenol (1.5 equiv.). Brown oil (140 mg, 67%); δ_{H} (CDCl_3 , 300 MHz) 2.20 (3H, s, C(7) H_3), 5.10 (1H, d, J 2.3, C(3) H), 5.93 (1H, dd, J 2.3, 0.96, C(5) H), 7.31-7.41 (2H, m, C(11) H & C(12) H), 8.37 (1H, d, J 2.7, C(9) H), 8.49 (1H, dd, J 4.5, 1.4, C(10) H); δ_{C} (CDCl_3 , 75.5 MHz) 20.0 (C(7) H_3), 91.3 (C(3) H), 99.5 (C(5) H), 124.5 (C(12) H), 128.7 (C(11) H), 143.3 (C(9) H), 147.8 (C(10) H), 149.0 (qC-8), 163.85 (qC-6), 163.9 (qC-2), 170.1 (qC-4); m/z (ES $^+$): 204, [(M+H) $^+$, 100%]; HRMS (ESI-TOF): Exact mass calculated for $\text{C}_{11}\text{H}_{10}\text{O}_3\text{N}$ [M+H $^+$], 204.1869. Found 204.1874.

4-((2-Aminopyridin-3-yl) oxy)-6-methyl-2H-pyran-2-one (39)

Synthesised according to the general procedure **6.2.2** using 4-bromo-6-methyl-2H-pyran-2-one (**23**) (200 mg, 1.06 mmol, 1.0 equiv.) and 2-amino-3-pyridyl phenol (1.5 equiv.). Yellow solid (100 mg, 43%), m.p. 145-146 °C; δ_{H} (CDCl_3 , 300 MHz) 2.27 (3H, s, C(7) H_3), 4.61 (2H, br s, N(13) H_2), 5.31 (1H, d, J 2.3, C(3) H), 5.97 (1H, dd, J 2.3, 1.3, C(5) H), 6.72 (1H, dd, J 7.9, 5.0, C(11) H), 7.22 (1H, dd, J 7.9, 1.5, C(12) H), 8.02 (1H, dd, J 4.9, 1.5, C(10) H); δ_{C} (CDCl_3 , 75.5 MHz) 20.1 (C(7) H_3), 91.1 (C(3) H), 99.2 (C(5) H), 114.4 (C(12) H), 129.1 (C(11) H), 134.2 (C(10) H), 146.2 (qC-9), 151.4 (qC-8), 163.9 (qC-6), 164.1 (qC-2), 169.2 (qC-4); m/z (ES $^+$): 219, [(M+H) $^+$, 100%]; HRMS (ESI-TOF): Exact mass calculated for $\text{C}_{11}\text{H}_{11}\text{O}_3\text{N}_2$ [M+H $^+$], 219.0770. Found 219.0766.

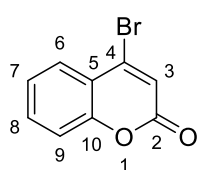
6-Methyl-4-(naphthalene-2-yloxy)-2H-pyran-2-one (40)³

Synthesised according to the general procedure **6.2.2** using 4-bromo-6-methyl-2H-pyran-2-one (**23**) (200 mg, 1.06 mmol, 1.0 equiv.) and 2-naphthol (1.5 equiv.). Brown solid (210 mg, 79%), m.p. 126-127 °C (lit. 126-127 °C); δ_{H} (CDCl_3 , 300 MHz) 2.22 (3H, s, C(7) H_3), 5.27 (1H, d, J 2.0, C(3) H), 6.01 (1H, d, J 1.1 C(5) H), 7.15-7.20 (1H, dd, J 8.9, 2.3, C(17) H), 7.45-7.59 (3H, m, C(9) H , C(13) H & C(16) H), 7.73-7.96 (3H, m, C(11) H ,

C(12)H & C(14)H); δ_c (CDCl₃, 75.5 MHz) 20.1 (C(7)H₃), 91.3 (C(3)H), 99.9 (C(5)H), 118.2 (C(9)H), 120.2 (C(17)H), 126.3 (C(16)H), 127.1 (C(13)H), 127.6 (C(12)H), 127.9 (C(14)H), 130.6 (C(11)H), 131.6 (qC-10), 133.9 (qC-15), 149.9 (qC-8), 163.4 (qC-6), 164.5 (qC-2), 170.7 (qC-4); m/z (ES+): 253, [(M+H)⁺, 100%]; HRMS (ESI-TOF): Exact mass calculated for C₁₆H₁₃O₃ [M+H⁺], 253.0865. Found 253.0865.

Spectral characteristics were consistent with previously reported data.³

6.2.3 Preparation of 4-bromo-2-coumarin (54)¹



To a 2-necked round bottomed flask was added 4-hydroxy-2-coumarin (**53**) (5.0 g, 30.83 mmol, 1.0 equiv.), TBAB (11.53 g, 35.76 mmol, 1.16 equiv.) and P₂O₅ (10.50 g, 73.99 mmol, 2.4 equiv.) in toluene (4.0 mL/mmol). The resulting mixture was stirred in an oil bath at 94 °C for 1.5 hours. Upon cooling, the clean upper layer was separated from the lower solid layer. The lower layer was washed with toluene (2 x 30 mL). The combined organic extracts were then washed with saturated aqueous NaHCO₃ (60 mL) and brine (80 mL). The organic layer was then dried over MgSO₄, filtered and concentrated under reduced pressure. The product 4-bromo-2-coumarin (**54**) was isolated as a brown solid (3.0 g, 72%), m.p. 88-89 °C (lit. 92-93°C)¹; δ_H (CDCl₃, 300 MHz) 6.87 (1H, s, C(3)H), 7.23-7.39 (2H, m, C(7)H & C(9)H), 7.57-7.63 (1H, m, C(8)H), 7.85 (1H, dd, *J* 7.9, 1.5, C(6)H); δ_c (CDCl₃, 75.5 MHz) 117.0 (C(3)H), 119.0 (qC-5), 119.6 (C(9)H), 125.0 (C(6)H), 128.1 (C(7)H), 133.2 (C(8)H), 141.5 (qC-4), 152.5 (qC-10), 158.7 (qC-2); m/z (ES+): 225, Br⁷⁹ [(M+H)⁺, 76%], 227, Br⁸¹ [(M+H)⁺, 58%].

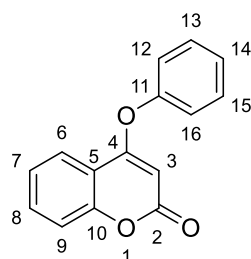
Spectral characteristics were consistent with previously reported data.¹

6.2.4 General procedure for preparation of 4-phenoxy-2-coumarins (55-68)

To a 3-necked round bottomed flask was added 4-bromo-2-coumarin (**54**) (1.0 equiv.), phenol (1.5 equiv.), and K₂CO₃ (1.8 equiv.) in acetone (4.0 mL/mmol). The resulting mixture was stirred in an oil bath at 65 °C and stirred for 16 hours. Upon cooling, the reaction mixture was diluted with water (10 mL) and EtOAc (20 mL). The mixture was extracted with EtOAc (2 x 20 mL) and the combined organic layers were washed with aqueous NaOH (10% w/v, 2 x 20 mL).

The organic layer was then dried over MgSO_4 , filtered and concentrated under reduced pressure. The residues were purified by recrystallisation from EtOH.

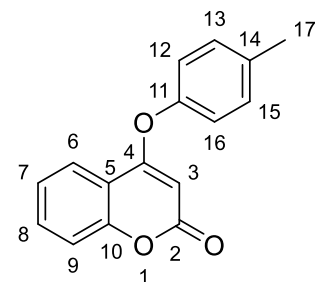
4-Phenoxy-2-coumarin (55)^{2, 4}



Synthesised according to the general procedure **6.2.4** using 4-bromo-2-coumarin (**54**) (750 mg, 3.33 mmol, 1.0 equiv.) and phenol (1.5 equiv.). Yellow solid (602 mg, 76%), m.p. 131-132 °C (lit. 131-132 °C); δ_{H} (CDCl_3 , 300 MHz) 5.42 (1H, s, C(3)H), 7.16-7.20 (2H, m, C(12)H & C(16)H), 7.32-7.38 (3H, m, C(7)H, C(9)H & C(14)H), 7.46-7.52 (2H, m, C(13)H & C(15)H), 7.59-7.65 (1H, ddd, J 8.7, 7.4, 1.6, C(8)H), 8.03 (1H, dd, J 8.0, 1.5, C(6)H); δ_{C} (CDCl_3 , 75.5 MHz) 93.5 (C(3)H), 115.4 (qC-5), 116.9 (C(9)H), 121.3 (C(12)H & C(16)H), 123.0 (C(6)H), 124.1 (C(7)H), 126.8 (C(14)H), 130.4 (C(13)H & C(15)H), 132.8 (C(8)H), 152.4 (qC-11), 153.7 (qC-10), 162.6 (qC-2), 166.4 (qC-4); m/z (ES⁺): 239, [(M+H)⁺, 100%].

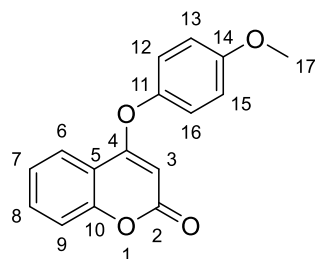
Spectral characteristics were consistent with previously reported data.^{2, 4}

4-(4-Methylphenoxy)-2H-chromene-2-one (56)³



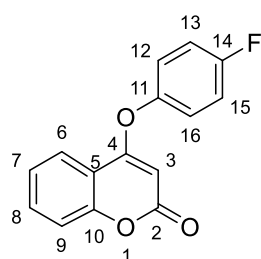
Synthesised according to the general procedure **6.2.4** using 4-bromo-2-coumarin (**54**) (4.0 g, 17.77 mmol, 1.0 equiv.) and 4-methyl phenol (1.5 equiv.). Yellow crystals (2.1 g, 48%), m.p. 132-133 °C; $\nu_{\text{max}}/\text{cm}^{-1}$ (NaCl): 1723 (ester C=O stretch), 1625 (alkene C=C stretch), 1489 (aromatic C=C stretch), 1385 (ester C-O stretch), 1227 (ether C-O stretch), 1179 (ether C-O stretch); δ_{H} (CDCl_3 , 300 MHz) 2.40 (3H, s, C(17)H₃), 5.42 (1H, s, C(3)H), 7.03-7.11 (2H, m, C(12)H & C(16)H), 7.24-7.39 (4H, m, C(7)H, C(9)H, C(13)H & C(15)H), 7.61 (1H, ddd, J 8.6, 7.2, 1.6, C(8)H), 8.03 (1H, dd, J 7.77, 1.43, C(6)H); δ_{C} (CDCl_3 , 75.5 MHz) 20.9 (C(17)H₃), 93.4 (C(3)H), 115.5 (qC-5), 116.8 (C(9)H), 120.9 (C(12)H & C(16)H), 123.1 (C(6)H), 124.0 (C(7)H), 131.0 (C(13)H & C(15)H), 132.7 (C(8)H), 136.6 (qC-14), 150.2 (qC-11), 153.7 (qC-10), 162.7 (qC-2), 166.6 (qC-4); m/z (ES⁺): 253, [(M+H)⁺, 100%]; HRMS (ESI-TOF): Exact mass calculated for $\text{C}_{16}\text{H}_{13}\text{O}_3$ [M+H⁺], 253.0861. Found 253.0865. Anal. Calculated for $\text{C}_{16}\text{H}_{12}\text{O}_3$: C, 76.18; H, 4.79. Found: C, 76.29; H, 4.81.

Spectral characteristics were consistent with previously reported data.³

4-(4-Methoxyphenoxy)-2H-chromene-2-one (57)³⁻⁴

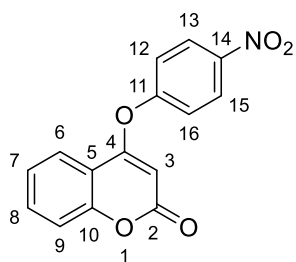
Synthesised according to the general procedure **6.2.4** using 4-bromo-2-coumarin (**54**) (4.0 g, 17.77 mmol, 1.0 equiv.) and 4-methoxy phenol (1.5 equiv.). Orange solid (3.99 g, 84%), m.p. 127-129 °C (lit. 99-101 °C); δ_{H} (CDCl₃, 300 MHz) 3.85 (3H, s, C(17)H₃), 5.42 (1H, s, C(3)H), 6.95-7.01 (2H, m, C(13)H & C(15)H), 7.06-7.12 (2H, m, C(12)H & C(16)H), 7.31-7.39 (2H, m, C(7)H & C(9)H), 7.61 (1H, ddd, *J* 8.6, 7.2, 1.6, C(8)H), 8.02 (1H, dd, *J* 7.9, 1.4, C(6)H); δ_{C} (CDCl₃, 75.5 MHz) 55.7 (C(17)H₃), 93.3 (C(3)H), 115.4 (2 x C(13)H & C(15)H), 115.4 (qC-5), 116.8 (C(9)H), 122.1 (C(12)H & C(16)H), 123.0 (C(6)H), 124.1 (C(7)H), 132.7 (C(8)H), 145.8 (qC-14), 153.7 (qC-11), 157.9 (qC-10), 162.7 (qC-2), 166.8 (qC-4); *m/z* (ES⁺): 269 [(M+H)⁺, 100%]; Anal. Calculated for C₁₆H₁₂O₄: C, 71.64; H, 4.51. Found: C, 71.69; H, 4.56.

Spectral characteristics were consistent with previously reported data³⁻⁴

4-(4-Fluorophenoxy)-2H-chromene-2-one (58)³⁻⁴

Synthesised according to the general procedure **6.2.4** using 4-bromo-2-coumarin (**54**) (4.0 g, 17.77 mmol, 1.0 equiv.) and 4-fluoro phenol (1.5 equiv.). Yellow crystals (2.2 g, 49%), m.p. 134-136 °C (lit. 118-121 °C); δ_{H} (CDCl₃, 300 MHz) 5.40 (1H, s, C(3)H), 7.13-7.23 (4H, m, C(12)H, C(13)H, C(15)H & C(16)H), 7.37 (2H, ddd, *J* 8.8, 4.2, 0.9, C(7)H & C(9)H), 7.63 (1H, ddd, *J* 8.6, 7.2, 1.6, C(8)H), 7.97-8.05 (1H, m, C(6)H); δ_{C} (CDCl₃, 75.5 MHz) 93.5 (C(3)H), 115.2 (qC-5), 117.0 (C(13)H & C(15)H, d, *J*_{C-F} 11), 117.4 (C(9)H), 122.8 (C(12)H & C(16)H, d, *J*_{C-F} 8), 123.0 (C(6)H), 124.2 (C(7)H), 132.9 (C(8)H), 148.2 (qC-11, d, *J*_{C-F} 3), 153.7 (qC-10), 160.7 (qC-14, d, *J*_{C-F} 248), 162.4 (qC-2), 166.4 (qC-4); *m/z* (ES⁺): 257, [(M+H)⁺, 40%]. Anal. Calculated for C₁₅H₉O₃F: C, 70.31; H, 3.54. Found: C, 70.15; H, 3.62.

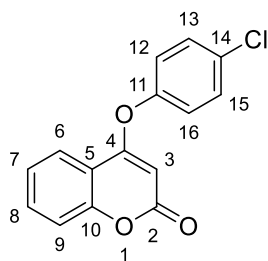
Spectral characteristics were consistent with previously reported data.³⁻⁴

4-(4-Nitrophenoxy)-2H-chromene-2-one (59)³

Synthesised according to the general procedure **6.2.4** using 4-bromo-2-coumarin (**54**) (4.0 g, 17.77 mmol, 1.0 equiv.) and 4-nitrophenol (1.5 equiv.). Yellow solid (2.9 g, 58%), m.p. 157-160 °C; $\nu_{\max}/\text{cm}^{-1}$ (NaCl): 1723 (ester C-O stretch), 1626 (alkene C=C stretch), 1522 (aromatic C=C stretch), 1485 (aromatic C=C stretch),

1346 (N=O stretch), 1230 (ester C-O stretch), 1180 (ether C-O stretch); δ_{H} (CDCl_3 , 300 MHz) 5.48 (1H, s, C(3)H), 7.34-7.46 (4H, m, C(7)H, C(9)H, C(12)H & C(16)H), 7.66 (1H, ddd, J 8.6, 7.3, 1.6, C(8)H), 7.99 (1H, dd, J 7.9, 1.4, C(6)H), 8.37-8.43 (2H, m, C(13)H & C(15)H); δ_{C} (CDCl_3 , 75.5 MHz) 94.9 (C(3)H), 114.8 (qC-5), 117.1 (C(9)H), 122.1 (C(6)H), 123.0 (C(12)H & C(16)H), 124.4 (C(7)H), 126.3 (C(13)H & C(15)H), 133.4 (C(8)H), 146.0 (qC-11), 153.7 (qC-14), 157.3 (qC-10), 161.7 (qC-2), 165.1 (qC-4); m/z (ES⁺): 284 [(M+H)⁺, 100%]; Anal. Calculated for $\text{C}_{15}\text{H}_9\text{O}_5\text{N}$: C, 63.61; H, 3.20. Found: C, 63.65; H, 3.21.

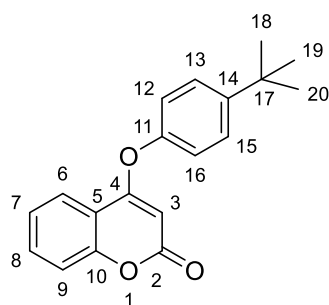
Spectral characteristics were consistent with previously reported data.³

4-(4-Chlorophenoxy)-2H-chromene-2-one (60)³

Synthesised according to the general procedure **6.2.4** using 4-bromo-2-coumarin (**54**) (2.0 g, 8.88 mmol, 1.0 equiv.) and 4-chlorophenol (1.5 equiv.). Yellow crystals (1.9 g, 79%), m.p. 124-125 °C; $\nu_{\max}/\text{cm}^{-1}$ (NaCl): 1725 (ester C-O stretch), 1626 (alkene C=C stretch) 1608 (aromatic C=C stretch), 1482 (aromatic C=C stretch), 1385 (ester C-O stretch), 1227

(ether C-O stretch), 1180 (ether C-O stretch); δ_{H} (CDCl_3 , 300 MHz) 5.41 (1H, s, C(3)H), 7.10-7.18 (2H, m, C(12)H & C(16)H), 7.32-7.41 (2H, m, C(7)H & C(9)H), 7.43-7.51 (2H, m, C(13)H & C(15)H), 7.58-7.68 (1H, m, C(8)H), 8.00 (1H, dd, J 7.9, 1.4, C(6)H); δ_{C} (CDCl_3 , 75.5 MHz) 93.7 (C(3)H), 115.2 (qC-5), 116.9 (C(9)H), 122.7 (C(6)H), 123.0 (C(12)H & C(16)H), 124.2 (C(7)H), 130.6 (C(13)H & C(15)H), 132.4 (C(8)H), 133.0 (qC-14), 150.9 (qC-11), 153.6 (qC-10), 162.3 (qC-2), 166.0 (qC-4); m/z (ES⁺): 273, [(M+H)⁺, 65%]; Anal. Calculated for $\text{C}_{15}\text{H}_9\text{O}_3\text{Cl}$: C, 66.07; H, 3.33. Found: C, 65.99; H, 3.47.

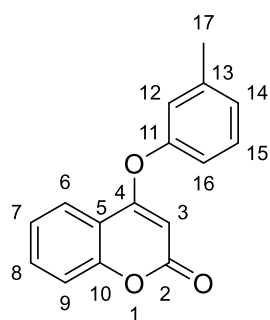
Spectral characteristics were consistent with previously reported data.³

4-(4-*Tert*-butylphenoxy)-2*H*-chromene-2-one (61)³

Synthesised according to the general procedure **6.2.4** using 4-bromo-2-coumarin (**54**) (2.0 g, 8.88 mmol, 1.0 equiv.) and 4-*tert*-butyl phenol (1.5 equiv.). Yellow solid (1.9 g, 71%), m.p. 142-144°C; $\nu_{\text{max}}/\text{cm}^{-1}$ (NaCl): 1726 (ester C=O stretch), 1625 (alkene C=C stretch), 1489 (aromatic C=C stretch), 1385 (ester C-O stretch), 1226 (ether C-O stretch), 1174 (ether C-O stretch); δ_{H}

(CDCl₃, 300 MHz) 1.36 (9H, s, C(18)H₃, C(19)H₃ & C(20)H₃), 5.44 (1H, s, C(3)H), 7.06-7.12 (2H, m, C(12)H & C(16)H), 7.31-7.39 (2H, m, C(13)H & C(15)H), 7.45-7.48 (1H, m, C(7)H), 7.49-7.51 (1H, m, C(9)H), 7.58-7.65 (1H, m, C(8)H), 8.03 (1H, dd_{app}, *J* 7.84, 1.59, C(6)H); δ_{C} (CDCl₃, 75.5 MHz) 31.4 (C(18)H₃, C(19)H₃ & C(20)H₃), 34.7 (qC-17), 93.5 (C(3)H), 115.5 (qC-5), 116.8 (C(9)H), 120.7 (C(12)H & C(16)H), 123.1 (C(6)H), 124.1 (C(7)H), 127.3 (C(13)H & C(15)H), 132.7 (C(8)H), 149.9 (qC-14), 150.0 (qC-11), 153.7 (qC-10), 162.8 (qC-2), 166.60 (qC-4); *m/z* (ES⁺): 295, [(M+H)⁺, 100%]; HRMS (ESI-TOF): Exact mass calculated for C₁₉H₁₉O₃ [M+H⁺], 295.1130. Found 295.1334. Anal. Calculated for C₁₉H₁₈O₃: C, 77.53; H, 6.16. Found: C, 77.31; H, 6.25.

Spectral characteristics were consistent with previously reported data.³

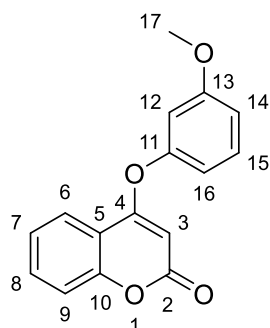
4-(3-Methylphenoxy)-2*H*-chromene-2-one (62)³⁻⁴

Synthesised according to the general procedure **6.2.4** using 4-bromo-2-coumarin (**54**) (2.0 g, 8.88 mmol, 1.0 equiv.) and 3-methyl phenol (1.5 equiv.). Pale brown solid (620 mg, 28%), m.p. 119-120 °C (lit. 118-120 °C); δ_{H} (CDCl₃, 300 MHz) 2.41 (3H, s, C(17)H₃), 5.43 (1H, s, C(3)H), 6.97 (2H, d, *J* 7.8, C(12)H & C(16)H), 7.15 (1H, d, *J* 7.5, C(14)H), 7.36 (3H, t, *J* 8.3, C(7)H, C(9)H & C(15)H), 7.62 (1H, t, *J* 7.8, C(8)H), 8.02 (1H,

d, *J* 7.6, C(6)H); δ_{C} (CDCl₃, 75.5 MHz) 21.3 (C(17)H₃), 93.5 (C(3)H), 115.6 (qC-5), 116.9 (C(9)H), 118.1 (C(16)H), 121.8 (C(12)H), 123.1 (C(6)H), 124.1 (C(7)H), 127.5 (C(14)H), 130.1 (C(15)H), 132.8 (C(8)H), 140.9 (qC-13), 152.4 (qC-11), 153.7 (qC-10), 162.7 (qC-2), 166.4 (qC-4); *m/z* (ES⁺): 253, [(M+H)⁺, 70%]; HRMS (ESI-TOF): Exact mass calculated for C₁₆H₁₃O₃ [M+H⁺], 253.0865. Found 253.0867.

Spectral characteristics were consistent with previously reported data.³⁻⁴

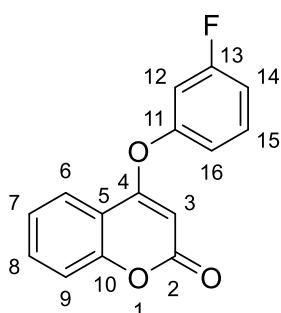
4-(3-Methoxyphenoxy)-2H-chromene-2-one (63)³



Synthesised according to the general procedure **6.2.4** using 4-bromo-2-coumarin (**54**) (2.0 g, 8.88 mmol, 1.0 equiv.) and 3-methoxy phenol (1.5 equiv.). Pale brown solid (1.8 g, 75%), m.p. 114-115 °C; $\nu_{\text{max}}/\text{cm}^{-1}$ (NaCl): 1722 (ester C=O stretch), 1625 (alkene C=C stretch), 1607 (aromatic C=C stretch), 1486 (aromatic C=C stretch), 1384 (ester C-O stretch), 1223 (ether C-O stretch), 1180 (ether C-O stretch), 1143 (ether C-O stretch); δ_{H} (CDCl_3 , 300 MHz) 3.83 (3H, s, C(17)H₃), 5.48 (1H, s, C(3)H), 6.72 (1H, t, J 2.3, C(12)H), 6.77 (1H, ddd, J 8.0, 2.2, 0.8, C(16)H), 6.88 (1H, ddd, J 8.4, 2.4, 0.8, C(14)H), 7.31-7.42 (3H, m, C(7)H, C(9)H & C(15)H), 7.62 (1H, ddd, J 8.6, 7.2, 1.6, C(8)H), 8.02 (1H, dd, J 7.9, 1.4, C(6)H); δ_{C} (CDCl_3 , 75.5 MHz) 55.6 (C(17)H₃), 93.6 (C(3)H), 107.3 (C(12)H), 112.5 (C(14)H), 113.2 (C(16)H), 115.4 (qC-5), 116.9 (C(9)H), 123.1 (C(6)H), 124.1 (C(7)H), 130.9 (C(15)H), 132.8 (C(8)H), 153.4 (qC-11), 153.7 (qC-13), 161.3 (qC-10), 162.6 (qC-2), 166.3 (qC-4); m/z (ES⁺): 269, [(M+H)⁺, 43%]; Anal. Calculated for C₁₆H₁₂O₄: C, 71.64; H, 4.51. Found: C, 71.85; H, 4.63.

Spectral characteristics were consistent with previously reported data.³

4-(3-Fluorophenoxy)-2H-chromene-2-one (64)³

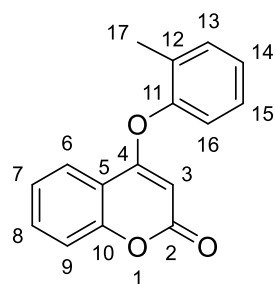


Synthesised according to the general procedure **6.2.4** using 4-bromo-2-coumarin (**54**) (600 mg, 2.67 mmol, 1.0 equiv.) and 3-fluoro phenol (1.5 equiv.). Pale brown solid (562 mg, 82%), m.p. 123-125 °C; $\nu_{\text{max}}/\text{cm}^{-1}$ (NaCl): 1719 (ester C=O stretch), 1626 (alkene C=C stretch), 1603, (aromatic C=C stretch), 1482 (aromatic C=C stretch), 1384 (ester C-O stretch), 1222 (ether C-O stretch), 1140 (ether C-O stretch), 1122 (C-F stretch); δ_{H} (CDCl_3 , 300 MHz) 5.46 (1H, s, C(3)H), 6.88-7.15 (3H, m, C(12)H, C(14)H & C(16)H), 7.32-7.53 (3H, m, C(7)H, C(9)H & C(15)H), 7.63 (1H, ddd, J 8.6, 7.3, 1.6, C(8)H), 8.00 (1H, dd, J 7.9, 1.5, C(6)H); δ_{C} (CDCl_3 , 75.5 MHz) 93.9 (C(3)H), 109.5 (C(12)H, d, $J_{\text{C-F}}$ 24), 114.0 (C(14)H, d, $J_{\text{C-F}}$ 21), 115.2 (qC-5), 116.9 (C(9)H), 117.1 (C(16)H, d, $J_{\text{C-F}}$ 4), 123.0

(C(6)H), 124.2 (C(7)H), 131.4 (C(15)H, d, J_{C-F} 10), 133.0 (C(8)H), 153.3 (qC-11, d, J_{C-F} 10), 153.7 (qC-10), 162.3 (qC-2), 163.4 (qC-13, d, J_{C-F} 250), 165.9 (qC-4); m/z (ES+): 257, [(M+H)⁺, 100%]; HRMS (ESI-TOF): Exact mass calculated for C₁₅H₁₀O₃F [M+H⁺], 257.0614. Found 257.0611.

Spectral characteristics were consistent with previously reported data.³

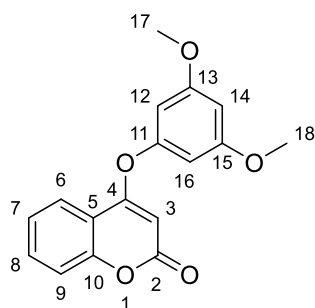
4-(2-Methylphenoxy)-2H-chromene-2-one (65)³



Synthesised according to the general procedure **6.2.4** using 4-bromo-2-coumarin (**54**) (2.0 g, 8.88 mmol, 1.0 equiv.) and 2-methyl phenol (1.5 equiv.). Off-white solid (1.2 g, 55%), m.p. 125-126 °C; $\nu_{\max}/\text{cm}^{-1}$ (NaCl): 1727 (ester C=O stretch), 1625 (alkene C=C stretch), 1608 (aromatic C=C stretch), 1487 (CH₃ bend), 1385 (ester C-O stretch), 1228 (ether C-O stretch), 1172 (ether C-O stretch); δ_{H} (CDCl₃, 300 MHz) 2.20 (3H, s, C(17)H₃), 5.31 (1H, s, C(3)H), 7.09 (1H, dd, J 7.6, 1.6, C(16)H), 7.21-7.42 (5H, m, C(7)H, C(9)H, C(13)H, C(14)H & C(15)H), 7.63 (1H, ddd, J 8.6, 7.2, 1.6, C(8)H), 8.07 (1H, dd, J 7.9, 1.4, C(6)H); δ_{C} (CDCl₃, 75.5 MHz) 15.7 (C(17)H₃), 93.0 (C(3)H), 115.3 (qC-5), 116.9 (C(9)H), 121.4 (C(16)H), 123.1 (C(6)H), 123.9 (qC-12), 124.2 (C(7)H), 127.0 (C(13)H), 127.9 (C(14)H), 132.1 (C(15)H), 132.8 (C(8)H), 150.6 (qC-11), 153.7 (qC-10), 162.7 (qC-2), 165.6 (qC-4); m/z (ES+): 253, [(M+H)⁺, 100%]; HRMS (ESI-TOF): Exact mass calculated for C₁₆H₁₃O₃ [M+H⁺], 253.0865. Found 253.0870.

Spectral characteristics were consistent with previously reported data.³

4-(3,5-Dimethoxyphenoxy)-2H-chromene-2-one (66)³⁻⁴

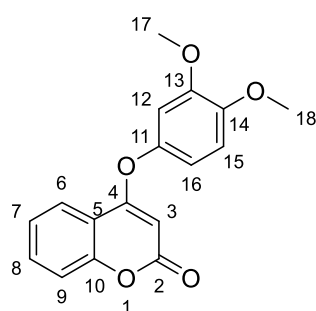


Synthesised according to the general procedure **6.2.4** using 4-bromo-2-coumarin (**54**) (2.0 g, 8.88 mmol, 1.0 equiv.) and 3,5-dimethoxy phenol (1.5 equiv.). Yellow solid (370 mg, 14%), m.p. 108-110 °C (lit. 109-113 °C); δ_{H} (CDCl₃, 300 MHz) 3.80 (6H, s, C(17)H₃ & C(18)H₃), 5.54 (1H, s, C(3)H), 6.33 (2H, d, J 2.2, C(12)H & C(16)H), 6.42 (1H, t, J 2.2, C(14)H), 7.30-7.40 (2H, m, C(7)H & C(9)H), 7.61 (1H, ddd, J 8.6, 7.3, 1.6, C(8)H), 8.00 (1H, dd, J 7.9, 1.5, C(6)H); δ_{C} (CDCl₃, 75.5 MHz) 55.6 (C(17)H₃ & C(18)H₃), 93.7 (C(3)H), 98.9 (C(14)H), 99.7 (C(12)H & C(16)H), 115.4 (qC-

5), 116.9 (C(9)H), 123.0 (C(6)H), 124.1 (C(7)H), 132.8 (C(8)H), 153.7 (qC-11), 154.0 (qC-10), 162.0 (qC-13 & qC-15), 162.6 (qC-2), 166.1 (qC-4); m/z (ES⁺): 299, [(M+H)⁺, 80%]; Anal. Calculated for C₁₇H₁₄O₅: C, 68.45; H, 4.73. Found: C, 68.14; H, 4.88.

Spectral characteristics were consistent with previously reported data.³⁻⁴

4-(3,4-Dimethoxyphenoxy)-2H-chromene-2-one (67)³



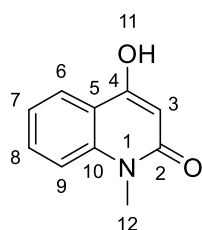
Synthesised according to the general procedure **6.2.4** using 4-bromo-2-coumarin (**54**) (2.0 g, 8.88 mmol, 1.0 equiv.) and 3,4-dimethoxy phenol (1.5 equiv.). Pale brown solid (2.4 g, 92%), m.p. 153-155 °C; $\nu_{\text{max}}/\text{cm}^{-1}$ (NaCl): 1721 (ester C=O stretch), 1625 (alkene C=C stretch), 1607 (aromatic C=C stretch), 1490 (aromatic C=C stretch), 1386 (ester C-O stretch), 1222 (ether C-O stretch),

1178 (ether C-O stretch); δ_{H} (CDCl₃, 300 MHz) 3.88 (3H, s, C(17)H₃), 3.92 (3H, s, C(18)H₃), 5.46 (1H, s, C(3)H), 6.69-6.77 (2H, m, C(12)H & C(16)H), 6.93 (1H, d, *J* 8.5, C(15)H), 7.32-7.40 (2H, m, C(7)H & C(9)H), 7.62 (1H, ddd, *J* 8.6, 7.3, 1.6, C(8)H), 8.02 (1H, dd, *J* 7.9, 1.5, C(6)H); δ_{C} (CDCl₃, 75.5 MHz) 56.1 (C(17)H₃), 56.3 (C(18)H₃), 93.3 (C(3)H), 105.1 (C(12)H), 111.7 (C(16)H), 112.6 (C(15)H), 115.4 (qC-5), 116.8 (C(9)H), 123.0 (C(6)H), 124.1 (C(7)H), 132.8 (C(8)H), 145.9 (qC-14), 147.6 (qC-13), 150.2 (qC-11), 153.6 (qC-10), 162.7 (qC-2), 166.8 (qC-4); m/z (ES⁺): 299, [(M+H)⁺, 20%]; Anal. Calculated for C₁₇H₁₄O₅: C, 68.45; H, 4.73. Found: C, 68.15; H, 4.79.

Spectral characteristics were consistent with previously reported data.³

6.2.5 Synthesis of quinolone starting materials

N-Methyl-4-hydroxy-2(1*H*)-quinolone (**93**)⁵⁻⁶



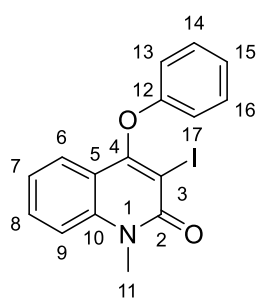
A mixture of *N*-methylantranilic acid (**92**) (5.5 g, 36.4 mmol), acetic anhydride (16.5 mL, 174.7 mmol) and acetic acid (16.3 mL) was stirred at reflux under N₂ for 4 hours. The reaction mixture was allowed to cool to room temperature and poured onto ice. A 6M aqueous sodium hydroxide solution was added until ca. pH 10 was achieved. The mixture was then

stirred at room temperature for 30 minutes after which concentrated aqueous HCl was slowly

added until *ca.* pH 5 was achieved. The mixture was allowed to cool to room temperature and the formed precipitate was isolated by suction filtration. Trituration from hot ethyl acetate afforded the product (**93**) as a tan solid (2.66 g, 42%), m.p. >230 °C (lit. 252-262 °C); δ_{H} (DMSO- d_6 , 300 MHz) 3.52 (3H, s, NC(12)H₃), 5.85 (1H, s, C(3)H), 7.21 (1H, t, *J* 7.4, C(7)H), 7.43 (1H, d *J* 8.4, C(9)H), 7.54-7.65 (1H, m, C(8)H), 7.93 (1H, dd *J* 7.9, 1.1, C(6)H); δ_{C} (DMSO- d_6 , 75.5 MHz) 29.0 (NC(12)H₃), 98.0 (C(3)H), 114.8 (C(9)H), 117.5 (qC-5), 121.4 (C(6)H), 123.8 (C(7)H), 131.5 (C(8)H), 140.5 (qC-10), 162.9 (qC-4), 163.4 (qC-2); *m/z* (ES⁻): 174, [(M-H)⁻, 100%].

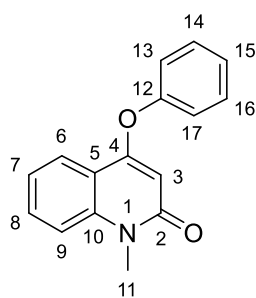
Spectral characteristics were consistent with previously reported data.⁵⁻⁶

3-Iodo-4-phenoxy-*N*-methylquinolinone (**99**)⁷



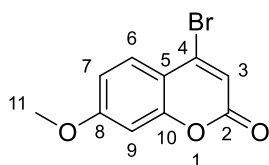
A solution of Na₂CO₃ (0.55 g, 0.9 equiv.) in EtOH (11.4 mL, 2 mL/mmol) was prepared in a 250 mL round bottomed flask. Diacetoxyiodobenzene (PIDA) (1.84 g, 5.71 mmol, 1.0 equiv.) was added and the resulting mixture was stirred at room temperature for 30 minutes. The PIDA was added to a solution containing *N*-methyl-4-hydroxy-2(1*H*)-quinolone (**93**) (1.0 g, 5.71 mmol, 1.0 equiv.), Na₂CO₃ (0.55 g, 0.9 equiv.) and EtOH (11.4 mL, 2 mL/mmol). After stirring at room temperature for 30 minutes, the precipitate was filtered off, washed with water and then triturated with MeOH. The solid was then suspended in anhydrous DMF (11 mL) in a 100 mL three-necked flask. A condenser was fitted to the flask and the flask was placed in a sand bath heated to 165 °C. After stirring at this temperature for 2 hours, the reaction mixture was quenched with water (20 mL) and the solid precipitate was filtered by suction filtration and recrystallised from MeOH to give the product **99** as an off-white solid (1.8 g, 84%), m.p. 198-201 °C (lit. 198-199 °C); δ_{H} (DMSO- d_6 , 300 MHz) 3.77 (3H, s, NC(11)H₃), 6.96 (2H, d, *J* 8.0, C(13)H & C(17)H), 7.09 (1H, t, *J* 7.0, C(15)H), 7.22 (1H, t, *J* 7.0, C(7)H), 7.35 (2H, t, *J* 8.0, C(14)H & C(16)H), 7.56 (1H, d, *J* 7.4, C(9)H), 7.64-7.76 (2H, m, C(6)H & C(8)H); δ_{C} (DMSO- d_6 , 75.5 MHz) 31.7 (NC(12)H₃), 91.7 (qC-3), 115.7 (C(13)H & C(17)H), 116.0 (C(9)H), 116.6 (qC-5), 122.9 (C(6)H), 123.3 (C(7)H), 123.8 (C(15)H), 130.6 (C(14)H & C(16)H), 132.5 (C(8)H), 140.3 (qC-10), 156.4 (qC-12), 160.4 (qC-4), 162.7 (qC-2); *m/z* (ES⁺): 377, [(M+H)⁺, 100%].

Spectral characteristics were consistent with previously reported data.⁷

1-Methyl-4-phenoxy-2(1H)-quinolinone (100)⁷

To a heated solution of 3-iodo-4-phenoxy-*N*-methylquinolinone (**99**) (200 mg, 0.53 mmol, 1.0 equiv.) in EtOH (4.44 mL) and acetic acid (4.40 mL) in a 50 mL two-necked flask was added zinc dust (1.046 g, 30 equiv.) portion wise over 1 hour until the solution turned a clear colour. A condenser was then fitted to the flask. After boiling the solution for 1 hour, the solution was filtered by gravity filtration to remove the zinc metal and the product was precipitated with water (10 mL). The solid precipitate was filtered by suction filtration and recrystallised from MeOH to afford **100** as white crystals (103 mg, 78%), m.p. 110-113 °C (lit. 113-115 °C); δ_{H} (DMSO- d_6 , 300 MHz) 3.58 (3H, s, NC(11)H₃), 5.46 (1H, s, C(3)H), 7.26-7.41 (4H, m, C(7)H, C(13)H, C(15)H, C(17)H), 7.51-7.62 (3H, m, C(9)H, C(14)H & C(16)H), 7.75 (1H, ddd, J 8.6, 7.9, 1.6, C(8)H), 8.09 (1H, dd J 8.1, 1.6, C(6)H); δ_{C} (DMSO- d_6 , 75.5 MHz) 29.3 (NC(12)H₃), 100.4 (C(3)H), 115.4 (C(9)H), 115.6 (qC-5), 121.7 (C(13)H & C(17)H), 122.4 (C(6)H), 123.2 (C(7)H), 126.6 (C(15)H), 130.9 (C(14)H & C(16)H), 132.5 (C(8)H), 140.3 (qC-10), 153.5 (qC-12), 162.3 (qC-4), 162.4 (qC-2); m/z (ES⁺): 252, [(M+H)⁺, 100%].

Spectral characteristics were consistent with previously reported data.⁷

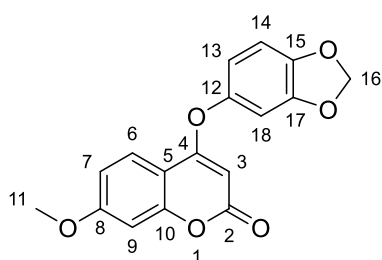
6.2.6 Preparation of 4-bromo-7-methoxy-2-coumarin (88)²⁻³

To a 2-necked round bottomed flask was added 4-hydroxy-7-methoxy-2-coumarin (**87**) (3.0 g, 15.6 mmol, 1.0 equiv.), TBAB (7.5 g, 23.4 mmol, 1.16 equiv.) and P₂O₅ (5.32 g, 37.5 mmol, 2.4 equiv.) in toluene (4.0 mL/mmol). The resulting mixture was stirred in an oil bath at 94 °C for 1.5 hours. Upon cooling, the reaction mixture was washed with toluene (2 x 30 mL). The combined organic extracts were then washed with saturated aqueous NaHCO₃ (2 x 20 mL) and H₂O (2 x 20 mL). The organic layer was then dried over MgSO₄, filtered and concentrated under reduced pressure. The product 4-bromo-7-methoxy-2-coumarin was isolated as a brown solid (703 mg, 54%), m.p. 114-117 °C; δ_{H} (CDCl₃, 300 MHz) 3.90 (3H, s, C(11)H), 6.67 (1H, s, C(3)H), 6.79 (1H, d, J 2.5, C(9)H), 6.90 (1H, dd, J 8.9, 2.5, C(7)H), 7.71 (1H, d, J 8.9, C(6)H); δ_{C} (CDCl₃, 75.5 MHz) 56.0 (C(11)H₃), 100.6 (C(9)H), 112.6 (qC-5), 113.1 (C(7)H), 116.0 (C(3)H), 129.1 (C(6)H), 141.5

(qC-4), 154.3 (qC-10), 159.2 (qC-8), 163.8 (qC-2); m/z (ES+): 255, Br⁷⁹ [(M+H)⁺, 20%], 257, Br⁸¹ [(M+H)⁺, 38%].

Spectral characteristics were consistent with previously reported data.²⁻³

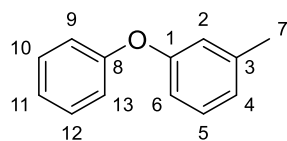
6.2.7 Preparation of 4-(benzo[d][1,3]dioxol-5-yloxy)-7-methoxy-2H-chromen-2-one (89)²⁻³



To a 3-necked round bottomed flask was added 4-bromo-7-methoxy-2-coumarin (**88**) (3.0 g, 11.76 mmol, 1.0 equiv.), sesamol (1.5 equiv.) and K₂CO₃ (1.8 equiv.) in acetone (4.0 mL/mmol). A condenser was fitted to the flask and the mixture was stirred in an oil bath at 65 °C for 16 hours. Upon

cooling, the reaction was diluted with water (10 mL) and EtOAc (20 mL). The mixture was extracted with EtOAc (2 x 20 mL) and the combined organic layers were washed with aqueous NaOH (10% w/v, 2 x 20 mL). The organic layer was then dried over MgSO₄, filtered and concentrated under reduced pressure. The residues were purified by recrystallisation from EtOH. The product was isolated as a pale yellow solid (528 mg, 84%), m.p. 174-177 °C; δ_{H} (CDCl₃, 300 MHz) 3.90 (3H, s, C(11)H₃), 5.33 (1H, s, C(3)H), 6.02 (2H, s, C(16)H₂), 6.64 (2H, dd, *J* 9.0, 5.2, C(13)H & C(18)H), 6.74-7.06 (3H, m, C(7)H, C(9)H & C(14)H), 7.87 (1H, d, *J* 9.0, C(6)H); δ_{C} (CDCl₃, 75.5 MHz) 55.8 (C(11)H₃), 90.9 (C(3)H), 100.6 (C(9)H), 102.1 (C(16)H₂), 103.3 (C(18)H), 108.6 (C(13)H), qC_{overlapping} qC-5), 112.4 (C(7)H), 113.8 (C(14)H), 124.1 (C(6)H), 146.0 (qC-15), 146.7 (qC-17), 148.7 (qC-12), 155.5 (qC-10), 163.1 (qC-8), 163.6 (qC-2), 167.0 (qC-4); m/z (ES+): 312, [(M+H)⁺, 79%].

Spectral characteristics were consistent with previously reported data.²⁻³

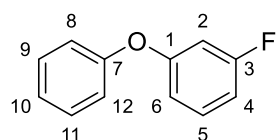
6.2.8 Preparation of mono-substituted diarylethers (**102-113**)⁸1-Methyl-3-(phenoxy) benzene (**102**)⁸

To a sealable tube equipped with a stir bar was charged phenol (150 mg, 1.594 mmol, 1 equiv.), Cs₂CO₃ (1.038 g, 3.188 mmol, 2 equiv.) and anhydrous FeCl₃ (26 mg, 0.159 mmol, 10 mol%). The aperture of the tube was then replaced with a rubber septum and a nitrogen atmosphere was then established. 3-iodo toluene (**118**) (0.30 mL, 2.391 mmol, 1.5 equiv.), 2,2,6,6-tetramethyl-3,5-heptadione (TMHD, 59 mg, 0.3188 mmol, 0.2 equiv.) and DMF (1 mL/mmol) were added by syringe. The reagents were added to three separate reaction vials. The rubber septum was replaced by a screw cap and the reaction vessel was placed in a multi reaction mantle at 135 °C. The reaction mixture was stirred at this temperature for 20 hours, after which the heterogeneous mixture was cooled to room temperature. The crude material from each vial was combined and filtered through a pad of Celite with DCM (80 mL). The filtrate was then washed with HCl (1 M, 1 x 20 mL), water (3 x 20 mL) and brine (1 x 20 mL). The organic layer was dried over MgSO₄, filtered and concentrated under reduced pressure. The crude product was purified by column chromatography (hexanes, 100%) to yield 1-methyl-3-(phenoxy) benzene (**102**). Yellow oil (457 mg, 52%); $\nu_{\text{max}}/\text{cm}^{-1}$ (NaCl): 2921 (aromatic C-H stretch), 1584 (aromatic C=C stretch), 1486 (aromatic C=C stretch), 1459 (-CH₃ bend), 1256 (ether C-O stretch), 1215 (ether C-O stretch), 936 (aromatic C-H bend), 690 (aromatic C-H bend); δ_{H} (CDCl₃, 300 MHz) 2.36 (3H, s, C(7)H₃), 6.79-6.88 (2H, m, C(2)H & C(6)H), 6.93 (1H, d, *J* 7.6, C(4)H), 6.99-7.06 (2H, m, C(9)H & C(13)H), 7.06-7.15 (1H, m, C(5)H), 7.22 (1H, t, *J* 7.7, C(11)H), 7.29-7.39 (2H, m, C(10)H & C(12)H); δ_{C} (CDCl₃, 75.5 MHz) 21.4 (C(7)H₃), 115.9 (C(6)H), 118.9 (C(9)H & C(13)H), 119.6 (C(2)H), 123.1 (C(11)H), 124.0 (C(4)H), 129.4 (C(5)H), 129.7 (C(10)H & C(12)H), 139.9 (qC-3), 157.2 (qC-1), 157.4 (qC-8). Did not ionise in HRMS (ESI-TOF).

Spectral characteristics were consistent with previously reported data.⁸

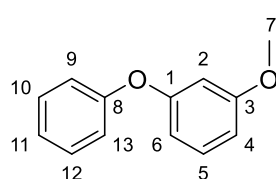
1-Fluoro-3-(phenoxy) benzene (**103**)

Compound **103** was prepared *via* the procedure described for **102** using 3-fluoro phenol (0.12 mL, 1.34 mmol, 1 equiv.) and iodobenzene (**127**) (0.22 mL, 2.01 mmol, 1.5 equiv.). The reagents were added to three separate reaction vials. After 20 hours, the crude material from



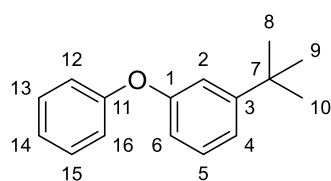
each vial was combined. The crude product was purified by column chromatography (hexanes, 100%; hexanes:Et₂O, 90:10) to yield **103** as a colourless oil (615 mg, 57%); $\nu_{\text{max}}/\text{cm}^{-1}$ (NaCl): 3073 (aromatic C-H stretch), 1594 (aromatic C=C stretch), 1483 (aromatic C=C stretch), 1271 (ether C-O stretch), 1212 (ether C-O stretch), 1071 (C-F stretch), 855 (aromatic C-H bend), 691 (aromatic C-H bend); δ_{H} (CDCl₃, 300 MHz) 6.69 (1H, dt, J 2.3, 10.4, C(4)H), 6.74-6.83 (2H, m, C(2)H & C(6)H), 6.99-7.07 (2H, m, C(8)H & C(12)H), 7.07-7.18 (1H, m, C(10)H), 7.19-7.30 (1H, m, C(5)H), 7.30-7.41 (2H, m, C(9)H & C(11)H); δ_{C} (CDCl₃, 75.5 MHz) 106.0 (C(2)H, d, $J_{\text{C-F}}$ 25), 110 (C(4)H, d, $J_{\text{C-F}}$ 22), 114.0 (C(6)H, d, $J_{\text{C-F}}$ 7), 119.0 (C(8)H or C(12)H), 120.0 (C(8)H or C(12)H), 123.2 (C(9)H or C(11)H), 124.0 (C(9)H or C(11)H), 130.0 (C(10)H), 131.0 (C(5)H, d, $J_{\text{C-F}}$ 10), 156.3 (qC-7), 159.0 (qC-1, d, $J_{\text{C-F}}$ 11), 164.0 (qC-3, d, $J_{\text{C-F}}$ 247); δ_{F} (282 MHz, CDCl₃) -111.2. HRMS (ESI-TOF): Exact mass calculated for C₁₂H₈OF [M-H], 187.0559. Found 187.0556.

1-Methoxy-3-(phenoxy) benzene (**104**)⁸



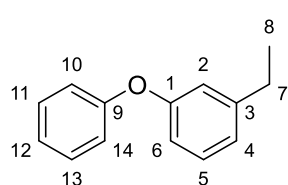
Compound **104** was prepared *via* the procedure described for **102** using 3-methoxy phenol (0.09 mL, 0.81 mmol, 1 equiv.) and iodobenzene (**127**) (0.135 mL, 1.21 mmol, 1.5 equiv.). The reagents were added to three separate reaction vials. After 20 hours, the crude material from each vial was combined. The crude product was purified by column chromatography (hexanes) to yield **104** as a colourless oil (379 mg, 78%); $\nu_{\text{max}}/\text{cm}^{-1}$ (NaCl): 1585 (aromatic C=C stretch), 1486 (aromatic C=C stretch), 1450 (-CH₃ bend), 1281 (ether C-O stretch), 1217 (ether C-O stretch), 1042 (ether C-O stretch), 951 (aromatic C-H bend), 849 (aromatic C-H bend), 688 (aromatic C-H bend); δ_{H} (CDCl₃, 300 MHz) 3.81 (3H, s, C(7)H), 6.55-6.61 (2H, m, C(2)H & C(6)H), 6.65 (1H, ddd, J 8.4, 2.3, 0.8, C(4)H), 6.98-7.06 (2H, m, C(9)H & C(13)H), 7.06-7.14 (1H, m, C(11)H), 7.17-7.26 (1H, m, C(5)H), 7.28-7.38 (2H, m, C(10)H & C(12)H); δ_{C} (CDCl₃, 75.5 MHz) 55.4 (C(7)H₃), 104.9 (C(2)H), 108.9 (C(4)H), 110.9 (C(6)H), 119.1 (C(9)H & C(13)H), 123.4 (C(11)H), 129.7 (C(10)H & C(12)H), 130.1 (C(5)H), 157.0 (qC-3), 158.5 (qC-1), 161.0 (qC-8); m/z (ES⁺): 201, [(M+H)⁺, 70%].

Spectral characteristics were consistent with previously reported data.⁸

1-*Tert*-butyl-3-(phenoxy) benzene (105)

Compound **105** was prepared *via* the procedure described for **102** using 3-*tert*-butyl phenol (150 mg, 0.999 mmol, 1 equiv.) and iodobenzene (0.17 mL, 1.499 mmol, 1.5 equiv.). The reagents were added to three separate reaction vials. After 20 hours, the

crude material from each vial was combined. The crude product was purified by column chromatography (hexanes, 100%). Colourless oil (297 mg, 44%); $\nu_{\max}/\text{cm}^{-1}$ (NaCl): 3067 (aromatic C-H stretch), 2964 (alkane C-H stretch), 1580 (aromatic C=C stretch), 1489 (aromatic C=C stretch), 1428 (-CH₃ bend), 1364 (-CH₃ bend), 1270 (ether C-O stretch), 1166 (ether C-O stretch), 928 (aromatic C-H bend), 698 (aromatic C-H bend); δ_{H} (CDCl₃, 300 MHz) 1.30 (9H, s, C(8)H, C(9)H & C(10)H), 6.78 (1H, ddd, *J* 7.9, 2.4, 1.0, C(6)H), 6.96-7.03 (2H, m, C(12)H & C(16)H), 7.03-7.16 (3H, m, C(2)H, C(4)H & C(14)H), 7.20-7.28 (1H, m, C(5)H), 7.28-7.37 (2H, m, C(13)H & C(15)H); δ_{C} (CDCl₃, 75.5 MHz) 31.9 (C(8)H₃, C(9)H₃ & C(10)H₃), 34.8 (qC-7), 115.8 (C(2)H), 116.6 (C(6)H), 118.6 (C(12)H & C(16)H), 120.4 (C(4)H), 122.9 (C(14)H), 129.2 (C(5)H), 129.5 (C(13)H & C(15)H), 153.5 (qC-3), 156.9 (qC-1), 157.6 (qC-11); *m/z* (ES⁺): 201, [(M+H)⁺, 70%].

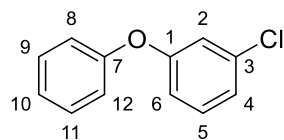
1-Ethyl-3-(phenoxy) benzene (106)

Compound **106** was prepared *via* the procedure described for **102** using 3-ethyl phenol (0.15 mL, 1.23 mmol, 1 equiv.) and iodobenzene (**127**) (0.21 mL, 1.845 mmol, 1.5 equiv.). The reagents were added to three separate reaction vials. After 20 hours, the crude material from

each vial was combined. The crude product was purified by column chromatography (hexanes, 100%) to yield **106** as a colourless oil (571 mg, 78%); $\nu_{\max}/\text{cm}^{-1}$ (NaCl): 2966 (aromatic C-H stretch), 2932 (alkane C-H stretch), 1582 (aromatic C=C stretch), 1487 (-CH₂ bend), 1445 (-CH₃ bend), 1252 (ether C-O stretch), 1214 (ether C-O stretch), 919 (aromatic C-H bend), 691 (aromatic C-H bend); δ_{H} (CDCl₃, 300 MHz) 1.26 (3H, t, *J* 7.6, C(8)H₃), 2.67 (2H, q, *J* 7.8, C(7)H₂), 6.81-6.89 (1H, m, C(6)H), 6.89-6.94 (1H, m, C(2)H), 6.98 (1H, d, *J* 7.8, C(4)H), 7.01-7.08 (2H, m, C(10)H & C(14)H), 7.08-7.17 (1H, m, C(12)H), 7.27 (1H, t, *J* 7.2, C(5)H), 7.31-7.40 (2H, m, C(11)H & C(13)H); δ_{C} (CDCl₃, 75.5 MHz) 15.4 (C(8)H₃), 28.8 (C(7)H₂), 116.1 (C(2)H), 118.5 (C(6)H), 118.8 (C(10)H & C(14)H), 122.9 (C(4)H), 123.1 (C(12)H), 129.5 (C(5)H), 129.7

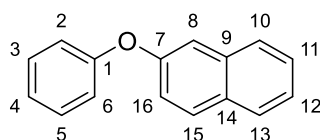
(C(11)H & C(13)H), 146.4 (qC-3), 157.3 (qC-9), 157.5 (qC-1); HRMS (ESI-TOF): Exact mass calculated for C₁₄H₁₅O [M+H⁺], 199.1123. Found 199.1123.

1-Chloro-3-(phenoxy) benzene (**107**)



Compound **107** was prepared *via* the procedure described for **102** using phenol (150 mg, 1.594 mmol, 1 equiv.) and 3-chloroiodobenzene (**127**) (0.3 mL, 2.391 mmol, 1.5 equiv.). The crude product was purified by column chromatography (hexanes, 100%; hexanes:Et₂O, 94:6) to yield **107** as a colourless oil (165 mg, 51%); $\nu_{\max}/\text{cm}^{-1}$ (NaCl): 1583 (aromatic C=C stretch), 1489 (aromatic C=C stretch), 1470 (aromatic C=C stretch), 1231 (ether C-O stretch), 1159 (ether C-O stretch), 756 (C-Cl stretch), 695 (C-Cl stretch); δ_{H} (CDCl₃, 300 MHz) 6.90 (1H, ddd, *J* 8.2, 2.3, 0.9, C(6)H), 6.97-7.12 (4H, m, C(2)H, C(4)H, C(8)H & C(12)H), 7.12-7.21 (1H, m, C(10)H), 7.22-7.30 (1H, m, C(5)H), 7.33-7.43 (2H, m, C(9)H & C(11)H); δ_{C} (CDCl₃, 75.5 MHz) 116.7 (C(6)H), 118.8 (C(2)H), 119.4 (C(8)H & C(12)H), 123.2 (C(4)H), 124.0 (C(10)H), 130.0 (C(9)H & C(11)H), 130.5 (C(5)H), 135.0 (qC-3), 156.3 (qC-7), 158.3 (qC-1); HRMS (ESI-TOF): Exact mass calculated for C₁₂H₁₀OCl [M+H⁺], 204.0264. Found 204.0257.

2-Phenoxy naphthalene (**108**)⁸

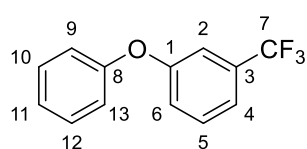


Compound **108** was prepared *via* the procedure described for **102** using 2-naphthol (150 mg, 1.040 mmol, 1 equiv.) and iodobenzene (**127**) (0.17 mL, 1.56 mmol, 1.5 equiv.). The reagents were added to four separate reaction vials. After 20 hours, the crude material from each vial was combined. The crude product was purified by column chromatography (hexanes, 100%) to yield **108** as a colourless solid (653 mg, 71%); m.p. 47-49 °C; $\nu_{\max}/\text{cm}^{-1}$ (NaCl): 3056 (aromatic C-H stretch), 1588 (aromatic C=C stretch), 1509 (aromatic C=C stretch), 1488 (aromatic C=C stretch), 1463 (aromatic C=C stretch), 1249 (ether C-O stretch), 1165 (ether C-O stretch), (aromatic C-H bend), 690 (aromatic C-H bend); δ_{H} (CDCl₃, 300 MHz) 7.00-7.18 (3H, m, C(2)H, C(6)H & C(4)H), 7.21-7.48 (6H, m, C(3)H, C(5)H, C(8)H, C(11)H, C(12)H & C(16)H), 7.68 (1H, d, *J* 8.2, C(10)H), 7.76-7.86 (2H, m, C(13)H & C(15)H); δ_{C} (CDCl₃, 75.5 MHz) 114.4 (C(8)H), 119.2 (C(2)H & C(6)H), 120.0 (C(16)H), 123.5 (C(4)H), 124.8 (C(12)H), 126.6 (C(11)H), 127.2 (C(10)H)

& **C(13)H**), 127.8 (**C(15)H**), 129.9 (**C(3)H** & **C(5)H**), 129.9 (q**C-14**), 134.4 (q**C-9**), 155.1 (q**C-7**), 157.2 (q**C-1**); Anal. Calculated for $C_{16}H_{12}O$: C, 87.31; H, 5.49. Found: C, 87.52; H, 5.62.

Spectral characteristics were consistent with previously reported data.⁸

1-Trifluoromethyl-3-(phenoxy) benzene (**109**)⁹

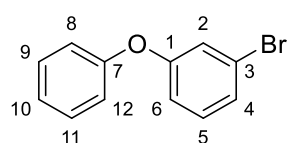


Compound **109** was prepared *via* the procedure described for **102** using 3-trifluoromethyl phenol (0.11 mL, 0.925 mmol, 1 equiv.) and iodobenzene (**127**) (0.16 mL, 1.388 mmol, 1.5 equiv.). The crude

product was purified by column chromatography (hexanes, 100%) to yield **109** as colourless oil (140 mg, 64%); $\nu_{\max}/\text{cm}^{-1}$ (NaCl): 3072 (aromatic C-H stretch), 1587 (aromatic C=C stretch), 1490 (aromatic C=C stretch), 1329 (C-F stretch), 1171 (ether C-O stretch), 1127 (ether C-O stretch), 791 (aromatic C-H bend), 693 (aromatic C-H bend); δ_{H} (CDCl_3 , 300 MHz) 6.99-7.07 (2H, m, **C(9)H** & **C(13)H**), 7.12-7.22 (2H, m, **C(11)H**), 7.22-7.27 (1H, m, **C(5)H** & **C(6)H**), 7.29-7.48 (4H, m, **C(2)H**, **C(4)H**, **C(10)H** & **C(12)H**); δ_{C} (CDCl_3 , 75.5 MHz) 115.3 (**C(2)H**, q, $J_{\text{C-F}}$ 4), 119.4 (**C(9)H** & **C(13)H**), 119.6 (**C(4)H**, q, $J_{\text{C-F}}$ 4), 121.6 (**C(11)H**), 123.7 (q**C-7**, q, $J_{\text{C-F}}$ 272), 124.2 (**C(6)H**), 130.1 (**C(10)H** & **C(12)H**), 130.3 (**C(5)H**), 132.2 (q**C-3**, q, $J_{\text{C-F}}$ 32), 156.1 (q**C-8**), 157.9 (q**C-1**); m/z (ES^+): 238, $[(\text{M}+\text{H})^+]$, 70%].

Spectral characteristics were consistent with previously reported data.⁹

1-Bromo-3-(phenoxy) benzene (**110**)

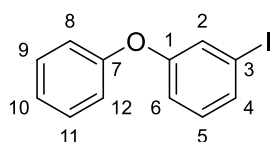


Compound **110** was prepared *via* the procedure described for **102** using 3-bromo phenol (0.092 mL, 0.867 mmol, 1 equiv.) and iodobenzene (**127**) (0.145 mL, 1.3005 mmol, 1.5 equiv.). The reagents

were added to four separate reaction vials. After 20 hours, the crude material from each vial was combined. The crude product was purified by column chromatography (hexanes, 100%) to yield **110** as a colourless oil (437 mg, 51%); $\nu_{\max}/\text{cm}^{-1}$ (NaCl): 3063 (aromatic C-H stretch), 1579 (aromatic C=C stretch), 1488 (aromatic C=C stretch), 1227 (ether C-O stretch), 1159 (ether C-O stretch), 665 (C-Br stretch); δ_{H} (CDCl_3 , 300 MHz) 6.90-6.97 (1H, m, **C(6)H**), 6.99-7.07 (2H, m, **C(2)H** & **C(4)H**), 7.11-7.25 (4H, m, **C(5)H**, **C(8)H**, **C(10)H** & **C(12)H**), 7.32-7.42 (2H, m, **C(9)H** & **C(11)H**); δ_{C} (CDCl_3 , 75.5 MHz) 117.2 (**C(6)H**), 119.3 (**C(8)H** & **C(12)H**), 121.7 (**C(2)H**),

122.9 (qC-3), 124.0 (C(4)H), 126.1 (C(10)H), 129.3 (C(9)H & C(11)H), 130.8 (C(5)H), 156.4 (qC-7), 158.4 (qC-1). Did not ionise in HRMS (ESI-TOF).

1-Iodo-3-(phenoxy) benzene (**111**)¹⁰

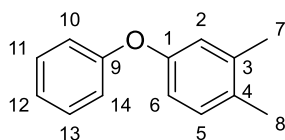


Compound **111** was prepared *via* the procedure described for **102** using 3-iodo phenol (150 mg, 0.6817 mmol, 1 equiv.) and iodobenzene (**127**). (0.11 mL, 1.023 mmol, 1.5 equiv.) The reagents were added to

three separate reaction vials. After 20 hours, the crude material from each vial was combined. The crude product was purified by column chromatography (hexanes) to yield **111** as a light pink oil (140 mg, 23%); $\nu_{\max}/\text{cm}^{-1}$ (NaCl): 3030 (aromatic C-H stretch), 1575 (aromatic C=C stretch), 1464 (aromatic C=C stretch), 1232 (ether C-O stretch), 1160 (ether C-O stretch), 692 (C-I stretch); δ_{H} (CDCl₃, 300 MHz) 6.92-7.07 (4H, m, C(2)H, C(6)H, C(8)H & C(12)H), 7.09-7.17 (1H, m, C(4)H), 7.35-7.45 (4H, m, C(5)H, C(9)H, C(10)H & C(11)H); δ_{C} (CDCl₃, 75.5 MHz) 94.2 (qC-3), 118.2 (C(6)H), 119.3 (C(8)H & C(12)H), 124.0 (C(2)H), 127.6 (C(10)H), 130.0 (C(9)H & C(11)H), 131.0 (C(4)H), 132.2 (C(5)H), 156.4 (qC-7), 158.1 (qC-1); HRMS (ESI-TOF): Exact mass calculated for C₁₂H₉IO [M+H⁺], 296.9776. Found 296.9789.

Spectral characteristics were consistent with previously reported data.¹⁰

1,6-Dimethyl-3-(phenoxy) benzene (**112**)

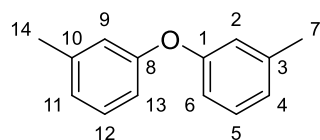


Compound **112** was prepared *via* the procedure described for **102** using 3,4-dimethyl phenol (180 mg, 1.47 mmol, 1 equiv.) and iodobenzene (**127**) (0.25 mL, 2.21 mmol, 1.5 equiv.). The crude

product was purified by column chromatography (hexanes, 100%) to yield **112** as a pale yellow oil (245 mg, 84%); $\nu_{\max}/\text{cm}^{-1}$ (NaCl): 2969 (aromatic C-H stretch), 2860 (alkane C-H stretch), 1590 (aromatic C=C stretch), 1488 (aromatic C=C stretch), 1454 (-CH₃ bend), (ether C-O stretch), 1150 (ether C-O stretch), 949 (aromatic C-H bend), 691 (aromatic C-H bend); δ_{H} (CDCl₃, 300 MHz) 2.24 (6H, s, C(7)H₃ & C(8)H₃), 6.77 (1H, dd, *J* 8.2, 2.6, C(6)H), 6.84 (1H, d, *J* 2.5, C(2)H), 6.95-7.02 (2H, m, C(10)H & C(14)H), 7.02-7.14 (2H, m, C(5)H & C(12)H), 7.27-7.37 (2H, m, C(11)H & C(13)H); δ_{C} (CDCl₃, 75.5 MHz) 19.1 (C(8)H₃), 20.0 (C(7)H₃), 116.5 (C(6)H), 118.4 (C(10)H & C(14)H), 119.5 (C(2)H), 122.7 (C(12)H), 129.7 (C(11)H & C(13)), 130.3 (C(5)H),

131.6 (qC-4), 138.2 (qC-3), 154.9 (qC-1), 157.9 (qC-9); HRMS (ESI-TOF): Exact mass calculated for $C_{14}H_{15}O$ $[M+H]^+$, 199.1123. Found 199.1131.

1-Methyl-3-(3-methylphenoxy) benzene (**113**)¹¹



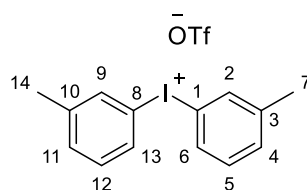
Compound **113** was prepared *via* the procedure described for **102** using 3-methyl phenol (0.15 m, 1.387 mmol, 1 equiv.) and 3-iodo toluene (**118**) (0.27 mL, 2.08 mmol, 1.5 equiv.). The reagents were

added to three separate reaction vials. After 20 hours, the crude material from each vial was combined. The crude product was purified by column chromatography (hexanes, 100%) to yield **113** as a colourless oil (423 mg, 51%); $\nu_{\max}/\text{cm}^{-1}$ (NaCl): 2919 (alkane C-H stretch), 1605 (aromatic C=C stretch), 1577 (aromatic C=C stretch), 1485 ($-\text{CH}_3$ bend), 1157 (ether C-O stretch), 1085 (ether C-O stretch), 688 (aromatic C-H bend); δ_{H} (CDCl_3 , 300 MHz) 2.32 (6H, s, C(7) H_3 & C(14) H_3), 6.79-6.87 (4H, m, C(2) H , C(6) H , C(9) H & C(13) H), 6.90-6.96 (2H, m, C(4) H & C(11) H), 7.18-7.25 (2H, m, C(5) H & C(12) H); δ_{C} (CDCl_3 , 75.5 MHz) 21.4 (C(7) H_3 & C(14) H_3), 115.9 (2C(6) H & C(13) H), 119.6 (C(2) H & C(9) H), 123.9 (C(4) H & C(11) H), 129.4 (C(5) H & C(12) H), 139.9 (qC-3 & qC-10), 157.3 (qC-1 & qC-8); m/z (ES $^+$): 199, $[(M+H)^+]$, 60%].

Spectral characteristics were consistent with previously reported data.¹¹

6.2.9 Procedure for preparation of bis(3-methylphenyl)iodonium triflate (**121**)¹²

Bis(3-methylphenyl)iodonium triflate (**121**)



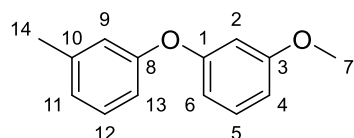
To a 250 mL equipped with a stir bar was added *m*CPBA (81% active oxidant, 958 mg, 5.55 mmol, 1.1 equiv.) and DCM (20 mL). To the solution was added 3-iodo toluene (**118**) (0.65 mL, 5.045 mmol, 1 equiv.) followed by slow addition of $\text{BF}_3 \cdot \text{OEt}_2$ (1.56 mL, 12.61

mmol, 2.5 equiv.) at room temperature. The resulting yellow solution was stirred at room temperature for 30 minutes and then cooled to 0 °C. 3-Methyl phenylboronic acid (**119**) (754 mg, 5.55 mmol, 1.1 equiv.) was added portion wise over 15 minutes. After 1 hour of stirring at room temperature, triflic acid (0.49 mL, 5.55 mmol, 1.1 equiv.) was added at 0 °C and the mixture was stirred at room temperature for an additional 15 minutes. The crude reaction mixture was then applied on a silica plug (12 g) and eluted with DCM (120 mL) to remove

unreacted 3-iodo toluene and *m*CPBA, followed by DCM:MeOH (240 mL, 20:1), to elute the product, leaving any boric acid derivatives on the column. The latter solution was concentrated and diethyl ether was added to the residue to induce a precipitation of the salt, with any iodine(III) intermediates and BF₃ derivatives remaining in solution. The solution was allowed to stir for 15 minutes and then the ether phase was decanted. The solid was washed twice more with diethyl ether and then dried *in vacuo* to give the pure bis(3-methylphenyl)iodonium triflate salt (**121**). White solid (1.20 g, 52%); m.p. 157-160 °C; δ_{H} (DMSO-*d*₆, 300 MHz) 2.35 (6H, s, C(7)H₃ & C(14)H₃), 7.42 (2H, t, *J* 7.7, C(4)H & C(11)H), 7.49 (2H, d, *J* 7.7, C(5)H & C(12)H), 8.04 (2H, d, *J* 8.0, C(6)H & C(13)H), 8.10 (2H, bs, C(2)H & C(9)H); δ_{C} (DMSO-*d*₆, 75.5 MHz) 21.2 (C(7)H₃ & C(14)H₃), 116.6 (qC-1 & qC-8), 131.9 (C(4)H & C(11)H), 132.7 (C(5)H & C(12)H), 133.2 (C(2)H & C(9)H), 135.7 (C(6)H & C(13)H), 142.3 (qC-3 & qC-10); δ_{F} (DMSO-*d*₆, 282 MHz) -77.7; *m/z* (ES⁺): 309 [(M-OTf)⁺, 100%]. HRMS (ESI-TOF): Exact mass calculated for C₁₄H₁₄I [M-OTf]⁺, 309.0135. Found 309.0136.

6.2.10 Preparation of di-substituted diarylethers (122-126) *via* bis(3-methylphenyl)iodonium triflate salt (**121**)⁹

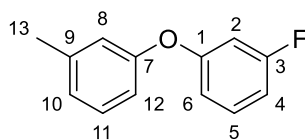
1-Methoxy-3-(3-methylphenoxy) benzene (**122**)



To a suspension of potassium *tert*-butoxide (199 mg, 1.77 mmol, 1.1 equiv.) in THF (20 mL) was added the 3-methoxy phenol (0.177 mL, 1.611 mmol, 1.0 equiv.) at 0 °C. After stirring for 1 h, the iodonium triflate salt (**121**) (884 mg, 1.93 mmol, 1.2 equiv.) was added and the resulting mixture was stirred at 40 °C overnight. The reaction mixture was quenched with water (15 mL) and the organic layer was extracted with ethyl acetate (3 × 10 mL). The organic layer was then dried over MgSO₄, filtered and concentrated under reduced pressure. The crude residue was purified by silica gel chromatography (hexanes, 100%) to yield the product **122** as a colourless oil (174 mg, 50%); ν_{max} /cm⁻¹ (NaCl): 1584 (aromatic C=C stretch), 1486 (-CH₃ bend), 1252 (ether C-O stretch), 1193 (ether C-O stretch), 1132 (ether C-O stretch), 959 (aromatic C-H stretch); δ_{H} (CDCl₃, 300 MHz) 2.34 (3H, s, C(14)H₃), 3.78 (3H, s, C(7)H₃), 6.55-6.62 (2H, m, C(2)H & C(6)H), 6.65 (1H, ddd *J* 8.3, 2.3, 0.9, C(4)H), 6.79-6.88 (2H, m, C(9)H & C(13)H), 6.89-6.96 (1H, m, C(11)H), 7.17-7.28 (2H, m, C(5)H & C(12)H); δ_{C} (CDCl₃, 75.5 MHz) 21.4 (C(14)H₃), 55.4 (C(7)H₃), 104.9 (C(2)H), 108.7 (C(4)H), 110.0 (C(6)H), 116.1 (C(13)H), 119.8 (C(9)H), 124.2

(C(11)H), 129.4 (C(12)H), 130.1 (C(5)H), 139.9 (qC-10), 156.9 (qC-8), 158.6 (qC-1), 161.0 (qC-3); HRMS (ESI-TOF) m/z : $[M+H]^+$ calcd. for $C_{14}H_{15}O_2$: 215.1067. Found 215.1065.

1-Fluoro-3-(3-methylphenoxy) benzene (**123**)¹³

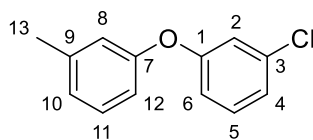


Compound **123** was prepared *via* the procedure described for **122** using 3-fluoro phenol (0.162 mL, 1.789 mmol, 1 equiv.) and **121**.

The crude product was purified by column chromatography (hexanes, 100%) followed by Kugelrohr distillation (160-180 °C) to yield **123** as a colourless liquid (207 mg, 57%); $\nu_{\max}/\text{cm}^{-1}$ (NaCl): 1596 (aromatic C=C stretch), 1586 (aromatic C=C stretch), 1448 (-CH₃ bend), 1270 (ether C-O stretch), 1162 (ether C-O stretch), 1118 (C-F stretch), 964 (aromatic C-H bend); δ_{H} (CDCl₃, 300 MHz) 2.34 (3H, s, C(13)H₃), 6.68 (1H, td, J 10.3, 2.4, C(4)H), 6.73-6.80 (2H, m, C(2)H & C(6)H), 6.80-6.88 (2H, m, C(8)H & C(12)H), 6.92-6.99 (1H, m, C(10)H), 7.19-7.30 (2H, m, C(5)H & C(11)H); δ_{C} (CDCl₃, 75.5 MHz) 21.4 (C(13)H₃), 106.0 (C(2)H, d, $J_{\text{C-F}}$ 24), 109.7 (C(4)H, d, $J_{\text{C-F}}$ 21), 113.9 (C(6)H, d, $J_{\text{C-F}}$ 3), 116.5 (C(12)H), 120.2 (C(8)H), 124.8 (C(10)H), 129.6 (C(11)H), 130.4 (C(5)H, d, $J_{\text{C-F}}$ 10), 140.2 (qC-9), 156.2 (qC-7), 159.1 (qC-1, d, $J_{\text{C-F}}$ 11), 161.5 (qC-3, d, $J_{\text{C-F}}$ 247); δ_{F} (282 MHz, CDCl₃) -111.0; HRMS (ESI-TOF) m/z : $[M]^+$ calcd. for $C_{13}H_{11}FO$: 202.0788, found 202.0783.

Spectral characteristics were consistent with previously reported data.¹³

1-Chloro-3-(3-methylphenoxy) benzene (**124**)

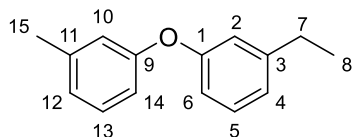


Compound **124** was prepared *via* the procedure described for **122** using 3-chloro phenol (0.16 mL, 1.56 mmol, 1 equiv.) and **121**. The

crude product was purified by column chromatography (cyclohexane, 100%; cyclohexane:EtOAc, 90:10) to yield **124** as a colourless oil (275 mg, 81%); $\nu_{\max}/\text{cm}^{-1}$ (NaCl): 1605 (aromatic C=C stretch), 1485 (aromatic C=C stretch), 1446 (-CH₃ bend), 1258 (ether C-O stretch), 1157 (ether C-O stretch); δ_{H} (CDCl₃, 300 MHz) 2.34 (3H, s, C(13)H₃), 6.78-6.85 (2H, m, C(2)H & C(8)H), 6.87 (1H, ddd, J 8.4, 2.3, 0.9, C(12)H), 6.93-6.99 (2H, m, C(4)H & C(10)H), 7.05 (1H, ddd, J 8.0, 2.0, 1.0, C(6)H), 7.18-7.27 (2H, m, C(5)H & C(11)H); δ_{C} (CDCl₃, 75.5 MHz) 21.4 (C(13)H₃), 116.4 (C(12)H), 116.7 (C(6)H), 118.7 (C(2)H), 120.1 (C(8)H), 123.0 (C(4)H), 124.8 (C(10)H), 129.6 (C(11)H), 130.4 (C(5)H), 135.0 (qC-9), 140.2 (qC-3), 156.3

(qC-7), 158.5 (qC-1); HRMS (ESI-TOF) m/z : $[M+H]^+$ calcd. for $C_{13}H_{11}ClO$: 219.0571, found 219.0572.

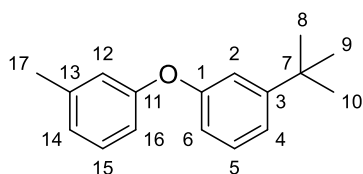
1-Ethyl-3-(3-methylphenoxy) benzene (125)



Compound **125** was prepared *via* the procedure described for **122** using 3-ethyl phenol (0.079 mL, 0.647 mmol, 1 equiv.) and **121**. The crude product was purified by column chromatography

(hexanes, 100%) followed by Kugelrohr distillation (160-180 °C) to yield **125** as a pale yellow oil (71 mg, 51%); $\nu_{\max}/\text{cm}^{-1}$ (NaCl): 3072 (aromatic C-H stretch), 2922 (alkane C-H stretch), 1606 (aromatic C=C stretch), 1596 (aromatic C=C stretch), 1586 (aromatic C=C stretch), 1483 (aromatic C=C stretch), 1448 (-CH₃ bend), 1270 (ether C-O stretch), 1147 (ether C-O stretch), 964 (aromatic C-H bend), 771 (C-Cl stretch); δ_{H} (CDCl₃, 300 MHz) 1.22 (3H, t, J 8.3, C(8)H₃), 2.33 (3H, s, C(15)H₃), 2.63 (2H, q, J 7.5, C(7)H₂), 6.76-6.88 (4H, m, C(2)H, C(6)H, C(10)H & C(14)H), 6.88-6.96 (2H, m, C(4)H & C(12)H), 7.21 (2H, q_{app}, J 7.8, C(5)H & C(13)H); δ_{C} (CDCl₃, 75.5 MHz) 15.4 (C(8)H₃), 21.4 (C(15)H₃), 28.8 (C(7)H₂), 115.8 (C(6)H), 116.1 (C(14)H), 118.5 (C(2)H), 119.5 (C(10)H), 122.7 (C(4)H), 123.9 (C(12)H), 129.4 (C(5)H), 129.5 (C(13)H), 139.9 (qC-11), 146.3 (qC-3), 157.3 (qC-1), 157.4 (qC-9); HRMS (ESI-TOF) m/z : $[M+H]^+$ calcd. for $C_{15}H_{17}O$: 212.2920, found, 212.2917.

1-*Tert*-butyl-3-(3-methylphenoxy) benzene (126)



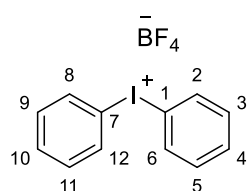
Compound **126** was prepared *via* the procedure described for **122** using 3-*tert*-butyl phenol (200 mg, 1.331 mmol, 1 equiv.) and **121**. The crude product was purified by column

chromatography (hexanes) to yield **126** as a yellow oil (201 mg, 63%); $\nu_{\max}/\text{cm}^{-1}$ (NaCl): 2963 (alkane C-H stretch), 1604 (aromatic C=C stretch), 1576 (aromatic C=C stretch), 1364 (-CH₃ bend), 1254 (ether C-O stretch), 1201 (ether C-O stretch), 779 (aromatic C-H stretch); δ_{H} (CDCl₃, 300 MHz) 1.31 (9H, s, C(8)H₃, C(9)H₃ & C(10)H₃), 2.32 (3H, s, C(17)H₃), 6.73-6.85 (3H, m, C(12)H, C(16)H & C(4)H), 6.85-6.93 (1H, m, C(14)H), 7.06-7.15 (2H, m, C(2)H & C(6)H), 7.20 (1H, t, J 7.8, C(15)H), 7.25 (1H, t, J 7.9, C(5)H); δ_{C} (CDCl₃, 75.5 MHz) 21.4 (C(17)H₃), 31.3 (C(8)H₃, C(9)H₃ & C(10)H₃), 34.8 (qC-7), 115.7 (C(12)H & C(16)H), 116.6 (C(2)H or C(6)H), 119.3 (C(4)H), 120.2 (C(2)H or C(6)H), 123.8 (C(14)H), 129.1 (C(5)H), 129.4 (C(15)H), 139.9 (qC-13), 153.5 (qC-

3), 157.0 (qC-11), 157.5 (qC-1); HRMS (ESI-TOF) m/z : $[M]^+$ calcd. for $C_{17}H_{20}O$: 240.1509, found; 240.1497.

6.2.11 Procedure for preparation of diphenyliodonium tetrafluoroborate salt (**129**)¹²

Diphenyliodonium tetrafluoroborate (**129**)¹²

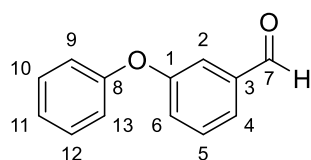


*m*CPBA (81% active oxidant, 3.3 g, 19.12 mmol, 1.1 equiv.) was dissolved in DCM (50 mL) in a 250 mL round bottomed flask equipped with a stir bar. To the solution was added iodobenzene (**127**) (1.55 mL, 13.92 mmol, 1 equiv.) followed by slow addition of $BF_3 \cdot OEt_2$ (4.25 mL, 34.45 mmol, 2.5 equiv.) at room temperature. The resulting yellow solution was stirred at room temperature for 30 minutes and then cooled to 0 °C. Phenylboronic acid (**128**) (1.85 g, 15.17 mmol, 1.1 equiv.) was subsequently added portion wise over 15 minutes. After 30 minutes of stirring at 0 °C, the crude reaction mixture was applied on a silica plug (30 g) and eluted with DCM (200 mL) to remove unreacted iodobenzene (**127**) and *m*CPBA, followed by DCM:MeOH (300 mL DCM, 15 mL MeOH), to elute the product, leaving any boric acid derivatives on the column. The latter solution was concentrated and diethyl ether was added to the residue to induce a precipitation of the salt, with any iodine(III) intermediates and BF_3 derivatives remaining in solution. The solution was allowed to stir for 15 minutes and then the ether phase was decanted. The solid was washed twice more with diethyl ether and then dried *in vacuo* to give the pure diaryliodonium tetrafluoroborate salt (**129**). White solid (3.52 g, 69%); m.p. 133-135 °C; δ_H (DMSO- d_6 , 300 MHz) 7.54 (4H, dt, J 7.5, 4.0, C(3)H, C(5)H, C(9)H & C(11)H), 7.73-7.61 (2H, m, C(4)H & C(10)H), 8.26 (4H, dt, J 3.1, 1.8, C(2)H, C(6)H, C(8)H & C(12)H); δ_C (DMSO- d_6 , 75.5 MHz) 116.9 (qC-1 & qC-7), 132.2 (C(3)H, C(5)H, C(9)H & C(11)H), 132.5 (C(4)H & C(10)H), 135.6 (C(2)H, C(6)H, C(8)H & C(12)H); δ_F (DMSO- d_6 , 282 MHz) -148.2, -148.3; m/z (ES+): 281, $[(M-BF_4)^+]$, 100%].

Spectral characteristics were consistent with previously reported data.¹²

6.2.12 Procedure for preparation of 3-Phenoxy benzaldehyde (**116**) *via* diphenyliodonium tetrafluoroborate salt (**129**)⁹

3-Phenoxy benzaldehyde (**116**)⁹



To a suspension of potassium *tert*-butoxide (101 mg, 0.90 mmol, 1.1 equiv.) in THF (4 mL) was added 3-hydroxy benzaldehyde (**130**) (100 mg, 0.8188 mmol, 1 equiv.) at 0 °C. After stirring for 1 h, the tetrafluoroborate iodonium salt (**129**) (362 mg, 0.983 mmol, 1.2 equiv.) was added and the resulting mixture was stirred at room temperature overnight. The

reagents were added to two separate 50 mL round bottomed flask. The crude material from each flask was combined after completion of the reaction. The reaction mixture was quenched with water (15 mL) and the organic layer was extracted with ethyl acetate (3 × 10 mL). The organic layer was then dried over MgSO₄, filtered and concentrated under reduced pressure. The crude product was purified by column chromatography (DCM:EtOAc, 95:5) to yield **116** as a yellow oil (153 mg, 47%); $\nu_{\text{max}}/\text{cm}^{-1}$ (NaCl): 1688 (C=O stretch aldehyde), 1585 (aromatic C=C stretch), 1488 (aromatic C=C stretch), 1308 (ether C-O stretch), 1240 (ether C-O stretch), 935 (aromatic C-H bend), 693 (aromatic C-H bend); δ_{H} (CDCl₃, 300 MHz) 7.01-7.07 (2H, m, C(9)H & C(13)H), 7.12-7.21 (1H, m, C(11)H), 7.29 (1H, ddd, *J* 8.3, 2.6, 1.2, C(6)H), 7.33-7.42 (2H, m, C(10)H & C(12)H), 7.44-7.54 (2H, m, C(2)H & C(5)H), 7.60 (1H, dt, *J* 7.5, 1.3, C(4)H), 9.96 (1H, s, C(7)H); δ_{C} (CDCl₃, 75.5 MHz) 118.2 (C(2)H), 119.5 (C(9)H & C(13)H), 124.2 (C(11)H), 124.6 (C(4)H), 124.7 (C(6)H), 130.0 (C(10)H & C(12)H), 130.4 (C(5)H), 138.1 (qC-3), 156.2 (qC-8), 158.4 (qC-1), 191.6 (qC-7); *m/z* (ES⁺): 198, [(M+2H)⁺, 60%].

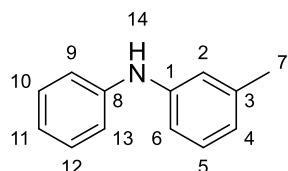
Spectral characteristics were consistent with previously reported data.⁹

6.2.13 General procedure for preparation of diphenylamines (**144-146**)¹⁴

Pd₂(dba)₃ (2.5 mol%), dppf (10 mol%) and NaO^{*t*}Bu (1.4 equiv.) were all weighed out in air and transferred to a flame dried resealable Schlenk tube. The Schlenk tube was then evacuated and back filled with N₂ three times. The stopper was then replaced with a rubber septum under a nitrogen purge and the liquid reagents were added: aniline (1 equiv.) and aryl iodide (1.2 equiv.) *via* syringe. The sides of the flask were rinsed with anhydrous toluene (2 mL/mmol) and the septum replaced by a stopper. The reaction mixture was then stirred in an oil bath at 100 °C for 48 hours. The reaction mixture was cooled to room temperature after

48 hours, diluted with ether (30 mL/mmol) and filtered through a plug of Celite. The crude product was concentrated and purified by silica gel chromatography (hexanes, 100%; hexanes:EtOAc) to yield diphenylamines **144-146**.

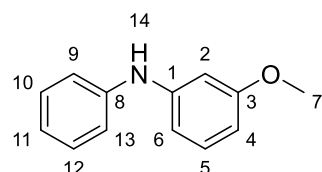
3-Methyl diphenylamine (**144**)¹⁵



Synthesised according to the general procedure **6.2.13** using aniline (0.39 mL, 4.295 mmol, 1 equiv.) and 3-iodo toluene (**118**) (0.67 mL, 5.16 mmol, 1.2 equiv.). The crude product was purified by column chromatography (hexanes, 100%) to yield **144** as a brown oil (540 mg, 69%); $\nu_{\max}/\text{cm}^{-1}$ (NaCl): 3393 (N-H stretch), 1590 (aromatic C=C stretch), 1494 (aromatic C=C stretch), 1315 (C-N stretch), 1166 (C-N stretch), 690 (aromatic C-H bend); δ_{H} (CDCl₃, 300 MHz) 2.30 (3H, s, C(7)H₃), 5.63 (1H, bs, N(14)H), 6.74 (1H, d, *J* 7.6, C(6)H), 6.83-6.96 (3H, m, C(2)H, C(4)H & C(11)H), 7.02-7.09 (2H, m, C(9)H & C(13)H), 7.10-7.19 (1H, m, C(5)H), 7.21-7.30 (2H, m, C(10)H & C(12)H); δ_{C} (CDCl₃, 75.5 MHz) 21.5 (C(7)H₃), 115.0 (C(6)H), 117.9 (C(9)H & C(13)H), 118.6 (C(2)H), 120.9 (C(4)H), 121.9 (C(11)H), 129.2 (C(5)H), 129.3 (C(10)H & C(12)H), 139.2 (qC-3), 143.1 (qC-1), 143.3 (qC-8); *m/z* (ES⁺): 184, [(M+H)⁺, 100%].

Spectral characteristics were consistent with previously reported data.¹⁵

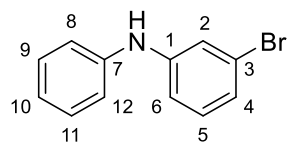
3-Methoxy diphenylamine (**145**)¹⁶



Synthesised according to the general procedure **6.2.13** using 3-methoxy aniline (0.36 mL, 3.25 mmol, 1 equiv.) and iodobenzene (**127**) (0.44 mL, 3.896 mmol, 1.2 equiv.). The crude product was purified by column chromatography (hexanes:EtOAc, 93:7) to yield **145** as a white solid (648 mg, 68%); m.p. 67-69 °C; $\nu_{\max}/\text{cm}^{-1}$ (NaCl): 3391 (N-H stretch), 1592 (aromatic C=C stretch), 1494 (aromatic C=C stretch), 1314 (C-N stretch), 1157 (C-O stretch), 1047 (C-N stretch), 756 (aromatic C-H bend); δ_{H} (CDCl₃, 300 MHz) 3.78 (3H, s, C(7)H₃), 5.69 (1H, bs, N(14)H), 6.44-6.52 (1H, m C(2)H), 6.60-6.69 (2H, m, C(4)H & C(6)H), 6.90-6.98 (1H, m, C(11)H), 7.05-7.12 (2H, m, C(9)H & C(13)H), 7.13-7.20 (1H, m, C(5)H), 7.22-7.31 (2H, m, C(10)H & C(12)H); δ_{C} (CDCl₃, 75.5 MHz) 55.2 (C(7)H₃), 103.4 (C(6)H), 106.2 (C(2)H), 110.2 (C(4)H), 118.4 (C(9)H & C(13)H), 122.3 (C(11)H), 129.3 (C(10)H & C(12)H), 130.1 (C(5)H), 142.8 (qC-1), 144.6 (qC-8), 160.7 (qC-3); *m/z* (ES⁺): 200, [(M+H)⁺, 100%].

Spectral characteristics were consistent with previously reported data.¹⁶

3-Bromo diphenylamine (**146**)¹⁶

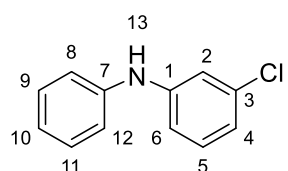


Synthesised according to the general procedure **6.2.13** using 3-bromo aniline (0.25 mL, 2.33 mmol, 1 equiv.) and iodobenzene (**127**) (0.31 mL, 2.796 mmol, 1.2 equiv.). The crude product was purified by

column chromatography (hexanes:EtOAc, 94:6) to yield **146** as a brown oil (329 mg, 57%); $\nu_{\max}/\text{cm}^{-1}$ (NaCl): 3399 (N-H stretch), 1587 (aromatic C=C stretch), 1477 (aromatic C=C stretch), 1313 (C-N stretch), 1067 (C-N stretch), 750 (aromatic C-H bend); δ_{H} (CDCl₃, 300 MHz) 5.69 (1H, bs, N(13)H), 6.93 (1H, ddd, *J* 8.0, 2.2, 1.1, C(6)H), 6.99-7.04 (2H, m, C(4)H & C(10)H), 7.04-7.13 (3H, m, C(5)H, C(8)H & C(12)H), 7.19 (1H, t, *J* 2.0, C(2)H), 7.23-7.35 (2H, m, C(9)H & C(11)H); δ_{C} (CDCl₃, 75.5 MHz) 115.6 (C(6)H), 119.0 (C(8)H & C(12)H), 119.6 (C(2)H), 122.2 (C(10)H), 123.2 (qC-3), 123.4 (C(4)H), 129.5 (C(9)H & C(11)H), 130.6 (C(5)H), 141.9 (qC-7), 145.0 (qC-1); HRMS (ESI-TOF): Exact mass calculated for C₁₂H₁₁NBr [M+H⁺], 248.0075. Found 248.0067.

Spectral characteristics were consistent with previously reported data.¹⁶

6.2.14 Procedure for preparation of 3-Chloro diphenylamine (**148**)¹⁷⁻¹⁸



To a premixed solution of ethyl acetate (0.1 M), Cu(OAc)₂ (0.2 equiv.), benzoic acid (1 equiv.) and K₂CO₃ (1 equiv.) in a 250 mL round bottomed flask was added 3-chloro aniline (**147**) (0.249 mL, 2.352 mmol, 1 equiv.) and phenyl boronic acid (**128**) (860 mg, 7.056 mmol,

3 equiv.) at room temperature. The resulting mixture was stirred at 80 °C in an oil bath until TLC analysis (3:1 hexanes:EtOAc) indicated complete consumption of the starting material. The solvent was then evaporated *in vacuo*. The residue was purified by column chromatography (hexanes: EtOAc, 90:10) to yield the final product **148** as an orange oil (293 mg, 61%); $\nu_{\max}/\text{cm}^{-1}$ (NaCl): 3402 (N-H stretch), 1590 (aromatic C=C stretch), 1480 (aromatic C=C stretch), 1314 (C-N stretch), 751 (C-Cl stretch), 681 (aromatic C-H bend); δ_{H} (CDCl₃, 300 MHz) 5.70 (1H, bs, N(13)H), 6.87 (2H, ddd, *J* 7.9, 2.1, 0.9, C(2)H & C(6)H), 6.94-7.05 (2H, m, C(8)H & C(12)H), 7.05-7.11 (2H, m, C(4)H & C(10)H), 7.14 (1H, t, *J* 8.0, C(5)H), 7.23-7.35 (2H, m, C(9)H & C(11)H); δ_{C} (CDCl₃, 75.5 MHz) 115.1 (C(6)H), 116.7 (C(2)H), 119.0 (C(8)H & C(12)H),

120.5 (C(4)H), 122.1 (C(10)H), 129.5 (C(9)H & C(11)H), 130.3 (C(5)H), 135.0 (qC-3), 142.0 (qC-7), 144.9 (qC-1); m/z (ES⁺): 204, [(M+H)⁺, 100%].

Spectral characteristics were consistent with previously reported data.¹⁷

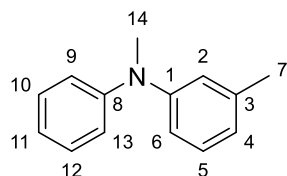
6.2.15 General procedure for preparation of *N*-methyl diphenylamines (149-151)¹⁹

A mixture of diphenylamine (1 equiv.), potassium hydroxide (6.25 equiv.) and anhydrous DMF (0.25 M) was stirred at room temperature for 1 hour. Iodomethane (2 equiv.) was added dropwise at room temperature and the resulting reaction mixture was stirred for an additional 47 hours.

Work-up conditions as per 1.35 mmol diphenylamine

The reaction mixture was then diluted with water (15 mL) and ethyl acetate (15 mL). The aqueous and organic phases were separated and the aqueous phase was washed with ethyl acetate (3 × 15 mL). The combined organic extracts were washed with brine, dried over MgSO₄, filtered and concentrated under reduced pressure. The crude mixture was purified by silica gel column chromatography (hexanes, 100%) to yield the title products.

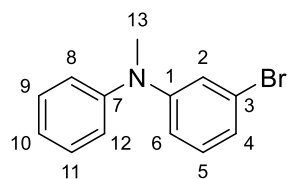
N,3-Dimethyl-*N*-phenyl benzamine (149)²⁰



Synthesised according to the general procedure **6.2.15** using 3-methyl diphenylamine (**144**) (248 mg, 1.353 mmol, 1 equiv.). The crude product was purified by column chromatography (hexanes, 100%) to yield **149** as a yellow oil (157 mg, 59%); $\nu_{\max}/\text{cm}^{-1}$ (NaCl):

2919 (N-CH₃ stretch), 1594 aromatic C=C stretch), 1494 (aromatic C=C stretch), 1343 (C-N stretch), 1126 (C-N stretch), 692 (aromatic C-H stretch); δ_{H} (CDCl₃, 300 MHz) 2.30 (3H, s, C(7)H₃), 3.30 (3H, s, C(14)H₃), 6.75-6.78 (3H, m, C(2)H, C(6)H & C(11)H), 6.92 (1H, ddd, J 8.4, 2.2, 1.1, C(4)H), 6.97-7.03 (2H, m, C(9)H & C(13)H), 7.17 (1H, t, J 8.1, C(5)H), 7.21-7.31 (2H, m, C(10)H & C(12)H); δ_{C} (CDCl₃, 75.5 MHz) 21.6 (C(7)H₃), 40.3 (C(14)H₃), 117.9 (C(6)H), 120.1 (C(9)H & C(13)H), 120.9 (C(2)H), 121.5 (C(4)H), 122.4 (C(11)H), 129.0 (C(5)H), 129.1 (C(10)H & C(12)H), 139.0 (qC-3), 149.1 (qC-1), 149.2 (qC-8); m/z (ES⁺): 198, [(M+H)⁺, 100%].

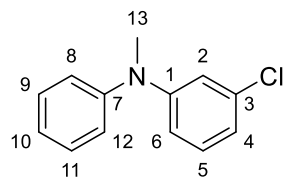
Spectral characteristics were consistent with previously reported data.²⁰

3-Bromo *N*-methyl-*N*-phenyl benzamine (150)²⁰

Synthesised according to the general procedure **6.2.15** using 3-bromo diphenylamine (**146**) (130 mg, 0.526 mmol, 1 equiv.). The crude product was purified by column chromatography (hexanes, 100%) to yield **150** as a brown oil (80 mg, 58%); $\nu_{\max}/\text{cm}^{-1}$ (NaCl):

3036 (N-CH₃ stretch), 2925 (alkane C-H stretch), 1585 (aromatic C=C stretch), 1481 (aromatic C-H stretch), 1343 (C-N stretch), 1133 (C-N stretch); δ_{H} (CDCl₃, 300 MHz) 3.29 (3H, s, C(13)H₃), 6.82 (1H, ddd, *J* 8.2 2,2, 1.0, C(6)H), 6.95-7.02 (1H, m, C(2)H), 7.03-7.08 (2H, m, C(4)H & C(10)H), 7.08-7.15 (3H, m, C(5)H, C(8)H, & C(12)H), 7.29-7.39 (2H, m, C(9)H & C(11)H); δ_{C} (CDCl₃, 75.5 MHz) 40.3 (C(13)H₃), 116.3 (C(6)H), 120.4 (C(2)H), 122.5 (C(4)H), 123.0 (qC-3), 123.3 (C(8)H & C(12)H), 123.5 (C(10)H), 129.6 (C(9)H & C(11)H), 130.2 (C(5)H), 148.2 (qC-7), 150.4 (qC-1); *m/z* (ES⁺): 262, [(M+H)⁺, 100%].

Spectral characteristics were consistent with previously reported data.²⁰

3-Chloro *N*-methyl-*N*-phenyl benzamine (151)²¹

Synthesised according to the general procedure **6.2.15** using 3-chloro diphenylamine (**148**) (60 mg, 0.29 mmol, 1 equiv.). The crude product was purified by column chromatography (hexanes, 100%) to yield **151** as a colourless oil (62 mg, 99%); $\nu_{\max}/\text{cm}^{-1}$ (NaCl):

2925 (N-CH₃ stretch), 1586 (aromatic C=C stretch), 1484 (aromatic C=C stretch), 1343 (C-N stretch), 1133 (C-N stretch), 900 (aromatic C-H stretch), 699 (C-Cl stretch); δ_{H} (CDCl₃, 300 MHz) 3.29 (3H, s, C(13)H₃), 6.79 (1H, ddd, *J* 8.3, 2.3, 0.7, C(6)H), 6.83 (1H, ddd, *J* 7.8, 1.8, 0.9, C(4)H), 6.90 (1H, t, *J* 2.1, C(2)H), 7.03-7.20 (4H, m, C(5)H, C(8)H, C(10)H & C(12)H), 7.28-7.41 (2H, m, C(9)H & C(11)H); δ_{C} (CDCl₃, 75.5 MHz) 40.3 (CH₃, C(13)H₃), 115.8 (C(6)H), 117.5 (C(2)H), 119.5 (C(4)H), 123.4 (C(8)H & C(12)H), 123.5 (C(10)H), 129.6 (C(9)H & C(11)H), 129.3 (C(5)H), 134.8 (qC-3), 148.3 (qC-7), 150.3 (qC-1); *m/z* (ES⁺): 218, [(M+H)⁺, 100%].

Spectral characteristics were consistent with previously reported data.²¹

6.3 Synthesis of starting materials for direct arylation of *ortho*-bromo diarylethers

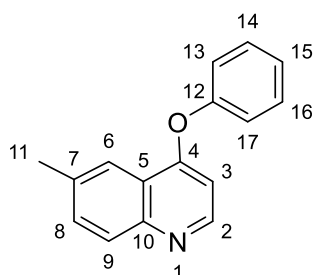
6.3.1 Procedure for Synthesis of 6-Substituted-4-Phenoxy quinoline ligands (159-161)²²

A mixture of 4-chloroquinoline (1 equiv.), phenol (5 equiv.) and NaOH (crushed pellets) (1.5 equiv.) was stirred in an oil bath at 130 °C until TLC analysis indicated complete consumption of starting material (hexanes:EtOAc, 8:2).

Work-up as per 1.6 mmol 4-chloro quinoline

The cooled reaction mixture was then diluted with 10% aq. NaOH (10 mL) and stirred at room temperature for 1 h. The aqueous phase was extracted with DCM (3 × 10 mL). The combined organics were washed with 6M NaOH (3 × 10 mL), water (10 mL) and brine (10 mL) and then dried with MgSO₄, filtered and concentrated *in vacuo*. The crude product was passed through a short pad of silica using hexanes:EtOAc (8:2) to yield the title products.

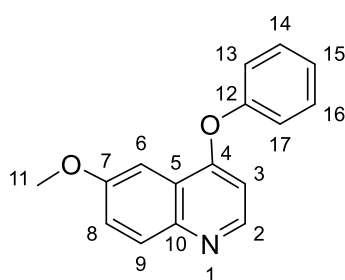
4-Phenoxy-6-methyl-quinoline (159)



Synthesised according to the general procedure **6.3.1** using 4-chloro-6-methyl quinoline (300 mg, 1.69 mmol, 1 equiv.) and phenol (**158**) (795 mg, 8.45 mmol, 5 equiv.) to yield **159** as a yellow solid (269 mg, 68%); m.p. 85-88 °C; $\nu_{\text{max}}/\text{cm}^{-1}$ (NaCl): 1596 (aromatic C=C stretch), 1490 (aromatic C=C stretch), 1466 (-CH₃

bend), 1362 (C-N stretch), 1255 (C-O stretch), 877 (aromatic C=C bend); δ_{H} (CDCl₃, 300 MHz) 2.57 (3H, s, C(11)H₃), 6.53 (1H, d, *J* 5.2, C(3)H), 7.14-7.23 (2H, m, C(13)H & C(17)H), 7.24-7.34 (1H, m, C(15)H), 7.41-7.53 (2H, m, C(14)H & C(16)H), 7.59 (1H, dd, *J* 8.5, 2.2, C(8)H), 7.99 (1H, d, *J* 8.6, C(9)H), 8.14 (1H, bs, C(6)H), 8.61 (1H, d, *J* 5.3, C(2)H); δ_{C} (CDCl₃, 75.5 MHz) 21.8 (C(11)H₃), 104.5 (C(3)H), 120.6 (C(6)H), 121.0 (C(13)H & C(17)H), 121.4 (qC-5), 125.5 (C(15)H), 128.9 (C(9)H), 130.2 (C(14)H & C(16)H), 132.3 (C(8)H), 136.1 (qC-7), 148.4 (qC-10), 150.2 (C(2)H), 154.6 (qC-12), 161.3 (qC-4); m/z (ES⁺): 236, [(M+H)⁺, 100%]. HRMS (ESI-TOF) m/z: [M+H]⁺ calcd. for C₁₆H₁₄NO: 236.1069, found 236.1071.

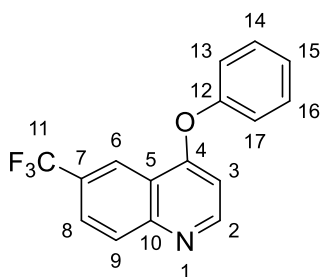
4-Phenoxy-6-methoxy-quinoline (160)



Synthesised according to the general procedure **6.3.1** using 6-methoxy-4-chloro quinoline (300 mg, 1.549 mmol, 1 equiv.) and phenol (**158**) (730 mg, 7.745 mmol, 5 equiv.) to yield **160** as a yellow solid (178 mg, 46%); m.p. 95-97 °C; $\nu_{\max}/\text{cm}^{-1}$ (NaCl): 1625 (aromatic C=C stretch), 1572 (aromatic C=C stretch), 1365

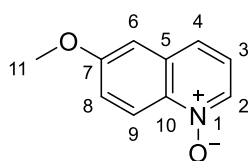
(C-N stretch), 1234 (C-O stretch), 838 (aromatic C=C bend); δ_{H} (CDCl_3 , 300 MHz) 3.96 (3H, s, C(11)H₃), 6.54 (1H, d, J 5.2, C(3)H), 7.14-7.24 (2H, m, C(13)H & C(17)H), 7.29 (1H, t, J 7.3, C(15)H), 7.40 (1H, dd, J 9.2, 2.8, C(8)H), 7.43-7.52 (2H, m, C(14)H & C(16)H), 7.59 (1H, d, J 2.8, C(6)H), 7.99 (1H, d, J 9.2, C(9)H), 8.54 (1H, d, J 5.1, C(2)H); δ_{C} (CDCl_3 , 75.5 MHz) 55.6 (C(11)H₃), 99.3 (C(6)H), 104.8 (C(3)H), 121.1 (C(13)H & C(17)H), 122.3 (qC-5), 122.8 (C(8)H), 125.5 (C(15)H), 130.3 (C(14)H & C(16)H), 130.6 (C(9)H), 145.9 (qC-10), 148.5 (C(2)H), 154.6 (qC-12), 157.7 (qC-7), 160.8 (qC-4); m/z (ES⁺): 252, [(M+H)⁺, 100%]. HRMS (ESI-TOF) m/z: [M+H]⁺ calcd. for C₁₆H₁₄NO₂: 252.1019, found 252.1019.

4-Phenoxy-6-trifluoromethyl-quinoline (161)

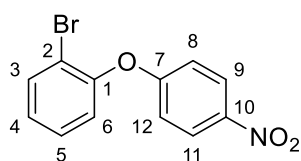


Synthesised according to the general procedure **6.3.1** using 6-trifluoromethyl-4-chloro quinoline (300 mg, 1.295 mmol, 1 equiv.) and phenol (**158**) (609 mg, 6.475 mmol, 5 equiv.) to yield **161** as an amber oil (375 mg, 66%); $\nu_{\max}/\text{cm}^{-1}$ (NaCl): 1634 (aromatic C=C stretch), 1470 (aromatic C=C stretch), 1367 (C-N stretch), 1251 (C-

O stretch), 1060 (C-F stretch), 844 (aromatic C=C bend); δ_{H} (CDCl_3 , 300 MHz) 6.62 (1H, d, J 5.3, C(3)H), 7.17-7.25 (2H, m, C(13)H & C(17)H), 7.29-7.39 (1H, m, C(15)H), 7.44-7.58 (2H, m, C(14)H & C(16)H), 7.93 (1H, dd, J 8.9, 2.1, C(8)H), 8.20 (1H, d, J 8.8, C(9)H), 8.73 (1H, bs, C(6)H), 8.76 (1H, d, J 5.3, C(2)H); δ_{C} (CDCl_3 , 75.5 MHz) 104.8 (C(3)H), 120.3 (C(6)H, q, $J_{\text{C-F}}$ 5), 120.6 (qC-5), 124.1 (qC-11, q, $J_{\text{C-F}}$ 272), 125.8 (C(8)H, q, $J_{\text{C-F}}$ 3), 126.2 (C(13)H & C(17)H), 126.2 (C(15)H), 128.0 (qC-7, q, $J_{\text{C-F}}$ 33), 130.3 (C(9)H), 130.5 (C(14)H & C(16)H), 150.7 (qC-12), 153.3 (C(2)H), 153.8 (qC-10), 162.5 (qC-4); δ_{F} (CDCl_3 , 282 MHz) -62.2; HRMS (ESI-TOF) m/z: [M+H]⁺ calcd. for C₁₆H₁₁BrF₃O: 290.0787, found 290.0788.

6.3.2 Procedure for synthesis of 6-methoxy-quinoline-*N*-oxide (**162**)

6-Methoxyquinoline (100 mg, 0.63 mmol, 1 equiv.), *m*CPBA (273 mg, 1.58 mmol, 2.5 equiv.) were weighed out in air and transferred to a reaction vial. DCM (4 mL/mmol) was added to the reaction vial which was sealed. The reaction mixture was stirred at room temperature for 24 hours. The reaction mixture was then diluted with 10% aq. NaOH (2 mL) and stirred at room temperature for 30 minutes. The aqueous phase was extracted with DCM (3 × 5 mL). The combined organics were washed with 10% aq. NaOH (2 × 5 mL), water (5 mL) and brine (5 mL) and then dried with MgSO₄, filtered and concentrated *in vacuo*. The crude product was passed through a short pad of silica using DCM:MeOH (98:2-80:20) to yield the final product **162** as a pale yellow solid. (70 mg, 64%); m.p. 75-79 °C; $\nu_{\text{max}}/\text{cm}^{-1}$ (NaCl): 1621 (aromatic C=C stretch), 1473 (aromatic C=C stretch), 1383 (C-N stretch), 1253 (C-O stretch); δ_{H} (CDCl₃, 300 MHz) 3.89 (3H, s, C(11)H₃), 7.05 (1H, d, *J* 2.7, C(6)H), 7.19 (1H, dd, *J* 8.5, 5.9, C(3)H), 7.32 (1H, dd, *J* 9.5, 2.6, C(8)H), 7.57 (1H, d, *J* 8.4, C(4)H), 8.33 (1H, d, *J* 6.0, C(2)H), 8.60 (1H, d, *J* 9.5, C(9)H); δ_{C} (CDCl₃, 75.5 MHz) 55.8 (C(11)H₃), 105.8 (C(6)H), 121.4 (C(3)H), 121.5 (C(8)H), 122.8 (C(4)H), 124.9 (C(2)H), 132.0 (qC-5), 133.8 (C(9)H), 137.3 (qC-10), 159.5 (qC-7); *m/z* (ES⁺): 176, [(M+H)⁺, 100%]; HRMS (ESI-TOF) *m/z*: [M+H]⁺ calcd. for C₁₀H₁₀NO₂: 176.0706, found 176.0705.

6.3.3 Procedure for preparation of 1-bromo-2-(4-nitrophenoxy) benzene (**163**)²³

Sodium hydride (2.4 equiv., 60%) was suspended in DMSO (1 mL/mmol) at 0 °C, 2-bromo phenol (**158**) (865 mg, 5 mmol, 2 equiv.) was added dropwise to the reaction mixture. The reaction mixture was then heated at 80 °C in a DrySyn[®] heating block for 1 h. 4-Nitro-fluoro benzene (353 mg, 2.5 mmol, 1 equiv.) was then added slowly *via* syringe. The resulting reaction mixture was stirred at R.T. for 24 h. Water was then added and the precipitated solid was collected, dried and recrystallised from ethanol to give 1-bromo-2-(4-nitrophenoxy) benzene (**163**) as a yellow solid (378 mg, 51%); m.p. 80-82 °C; δ_{H} (CDCl₃, 300 MHz) 6.95 (2H, ddd_{overlapping}, *J* 9.3, 3.2, 2.2, C(8)H & C(12)H), 7.15 (1H, dd, *J* 7.9, 1.6, C(6)H), 7.18 (1H, td, *J*, 7.8, 1.6, C(4)H), 7.39 (1H, td, *J* 7.8, 1.6, C(5)H), 7.90 (1H, dd, *J* 7.9, 1.4, C(3)H), 8.21 (2H, ddd_{overlapping}, *J* 9.3, 3.3, 2.2, C(9)H & C(11)H); δ_{C} (CDCl₃, 75.5 MHz) 116.2 (qC-2), 116.4 (C(8)H & C(12)H), 122.8 (C(6)H), 126.0 (C(9)H

& C(11)H), 127.2 (C(4)H), 129.3 (C(5)H), 134.4 (C(3)H), 142.9 (qC-10), 151.4 (qC-1), 162.5 (qC-7); HRMS (ESI-TOF) m/z: [M+H]⁺ calcd. for C₁₂H₉BrNO₃: 293.9760, found 293.9761.

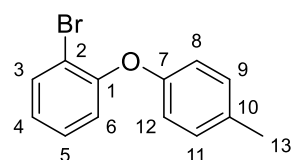
6.3.4 General procedure for preparation of 1-bromo-2-(4-methylphenoxy) benzene (166)²³ and 1-bromo-2-(4-methoxyphenoxy) benzene (167)²³

To a flame dried three-neck round bottomed flask which was evacuated and refilled with nitrogen three times was added sodium hydride (1.2 equiv) (95% dispersion in mineral oil). DMF (2 mL/mmol) was added *via* syringe at 0 °C. Phenol (1 equiv.) was then added dropwise to the reaction mixture. The reaction mixture was then stirred at 0 °C for 1 h. 2-bromo-fluoro benzene (1 equiv.) was then added slowly *via* syringe. The resulting reaction mixture was stirred under N₂ atmosphere at 120 °C in a DrySyn[®] heating block for 24 h.

Work-up as per 3.66 mmol phenol

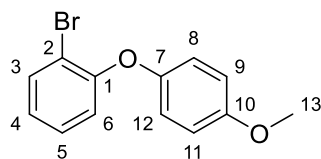
The reaction mixture was cooled to room temperature after 24 h and quenched with water (10 mL). The organic layer was extracted with ether (3 × 10 mL), washed with 2M NaOH (3 × 10 mL) and the combined organics were washed with brine (1 × 10 mL). The organic layer was then dried over MgSO₄, filtered and concentrated under reduced pressure. The residues were purified by silica gel chromatography (hexanes) to yield the title products.

1-Bromo-2-(4-methylphenoxy) benzene (166)



Synthesised according to the general procedure 6.3.4 using 2-bromo-fluorobenzene (165) (1.01 mL, 9.24 mmol, 1 equiv.) and 4-methyl phenol (1 g, 9.24 mmol, 1 equiv.). Hexanes, hexanes:EtOAc (90:10).

Colourless oil (232 mg, 10%); $\nu_{\text{max}}/\text{cm}^{-1}$ (NaCl): 1582 (aromatic C=C stretch), 1470 (aromatic C=C stretch), 1235 (ether C-O stretch), 1165 (ether C-O stretch), 872 (aromatic C-H bend), 658 (C-Br stretch); δ_{H} (CDCl₃, 300 MHz) 2.33 (3H, s, C(13)H₃), 6.83-6.93 (3H, m, C(6)H, C(8)H & C(12)H), 6.97 (1H, ddd, *J* 7.7, 7.5, 1.5, C(4)H), 7.10-7.16 (2H, m, C(9)H & C(11)H), 7.22 (1H, ddd, *J* 7.8, 6.6, 1.7, C(5)H), 7.61 (1H, dd, *J* 7.9, 1.5, C(3)H); δ_{C} (CDCl₃, 75.5 MHz) 20.7 (C(13)H₃), 114.5 (qC-2), 118.4 (C(8)H & C(12)H), 120.0 (C(6)H), 124.6 (C(4)H), 128.6 (C(5)H), 130.3 (C(9)H & C(11)H), 133.1 (qC-10), 133.8 (C(3)H), 154.2 (qC-7), 154.5 (qC-1); HRMS (ESI-TOF) m/z: [M]⁺ calcd. for C₁₃H₁₁BrO: 261.9988, found 261.9989.

1-Bromo-2-(4-methoxyphenoxy) benzene

Synthesised according to the general procedure **6.3.4** using 2-bromo fluorobenzene (**165**) (0.25 mL, 2.29 mmol, 1 equiv.) and 4-methoxy phenol (0.29 mL, 3.664 mmol, 1.6 equiv.). Colourless oil

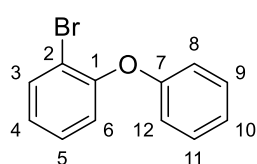
(143 mg, 22%); $\nu_{\max}/\text{cm}^{-1}$ (NaCl): 1592 (aromatic C=C stretch), 1471 (aromatic C=C stretch), 1233 (ether C-O stretch), 1030 (ether C-O stretch), 839 (aromatic C-H bend), 656 (C-Br stretch); δ_{H} (CDCl_3 , 300 MHz) 3.80 (3H, s, C(13)H₃), 6.83 (1H, dd, J 8.1, 1.5, C(6)H), 6.85-6.99 (5H, m, C(4)H, C(8)H, C(9)H, C(11)H & C(12)H), 7.20 (1H, ddd, J 8.4, 7.8, 1.6, C(5)H), 7.60 (1H, dd, J 7.9, 1.6, C(3)H); δ_{C} (CDCl_3 , 75.5 MHz) 55.7 (C(13)H₃), 113.8 (qC-2), 115.0 (C(9)H & C(11)H), 118.8 (C(6)H), 120.2 (C(8)H & C(12)H), 124.1 (C(4)H), 128.5 (C(5)H), 133.7 (C(3)H), 150.0 (qC-7), 154.9 (qC-10), 156.0 (qC-1); Anal. Calculated for $\text{C}_{13}\text{H}_{11}\text{BrO}_2$: C, 55.94 H, 3.97. Found: C, 56.18; H, 4.05.

6.3.5 General procedure for preparation of 2-bromo diarylethers via Chan-Lam-Evans coupling²⁴⁻²⁶

Phenyl boronic acid (2 equiv.), phenol (1 equiv.), $\text{Cu}(\text{OAc})_2$ (1 equiv.) and triethylamine (5 equiv.) were added to a 250 mL round bottom flask containing DCM (25 mL) and 3 Å molecular sieves. The resulting mixture was stirred at room temperature until TLC analysis indicated complete consumption of the starting material (hexanes:EtOAc, 2:1).

Work-up as per 2 mmol phenol

The reaction mixture was filtered through a pad of Celite® using DCM (60 mL). The filtrate was then washed with 3M NaOH (3 × 10 ml). The combined organics were then washed with brine (15 mL), dried with MgSO_4 and the solvent was then evaporated *in vacuo*. The residue was purified by silica gel chromatography (hexanes) to yield the title products.

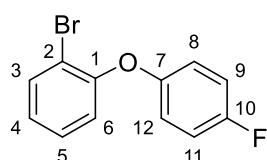
1-Bromo-2-phenoxy benzene (157**)²⁷**

Synthesised according to the general procedure **6.3.5** using 2-bromo phenol (**158**) (0.211 mL, 2 mmol, 1 equiv.) and phenyl boronic acid (490 mg, 4 mmol, 2 equiv.). Colourless solid (498 mg, 55%); m.p. 37-40 °C; $\nu_{\max}/\text{cm}^{-1}$ (NaCl): 3063 (aromatic C-H stretch), 1578 (aromatic C=C

stretch), 1470 (aromatic C=C stretch), 1261 (ether C-O stretch), 1029 (ether C-O stretch), 869 (aromatic C-H bend), 689 (C-Br stretch); δ_{H} (CDCl_3 , 300 MHz) 6.91-7.05 (4H, m, C(6)H, C(8)H, C(10)H & C(12)H), 7.06-7.15 (1H, m, C(4)H), 7.21-7.29 (1H, m, C(5)H), 7.29-7.38 (2H, m, C(9)H & C(11)H), 7.63 (1H, d, J 7.9, 1.6, C(3)H); δ_{C} (CDCl_3 , 75.5 MHz) 115.0 (qC-2), 118.1 (C(8)H & C(12)H), 120.7 (C(6)H), 123.4 (C(10)H), 125.0 (C(4)H), 128.7 (C(5)H), 129.8 (C(9)H & C(11)H), 133.9 (C(3)H), 153.7 (qC-7), 156.9 (qC-1); HRMS (ESI-TOF) m/z : $[M]^+$ calcd. for $\text{C}_{12}\text{H}_9\text{BrO}$: 247.9831, found 247.9827.

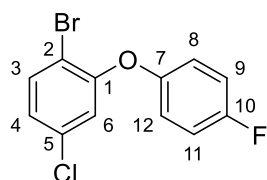
Spectral characteristics are consistent with previously reported data.²⁷

1-Bromo-2-(4-fluorophenoxy) benzene (168)



Synthesised according to the general procedure 6.3.5 using 2-bromo phenol (**158**) (0.1 mL, 0.9005 mmol, 1 equiv.) and 4-fluoro phenyl boronic acid (252 mg, 1.801 mmol, 2 equiv.). Colourless oil (173 mg, 72%); $\nu_{\text{max}}/\text{cm}^{-1}$ (NaCl): 1500 (aromatic C=C stretch), 1471 (aromatic C=C stretch), 1261 (ether C-O stretch), 1191 (ether C-O stretch), 1029 (C-F stretch), 817 (aromatic C-H bend), 658 (C-Br stretch); δ_{H} (CDCl_3 , 300 MHz) 6.85-7.09 (6H, m, C(4)H, C(6)H, C(8)H, C(9)H, C(11)H & C(12)H), 7.19-7.30 (1H, m, C(5)H), 7.63 (1H, dd, J 7.9, 1.5, C(3)H); δ_{C} (CDCl_3 , 75.5 MHz) 114.5 (qC-2), 116.3 (C(9)H & C(11)H, d, $J_{\text{C-F}}$ 24), 119.7 (C(6)H), 119.9 (C(8)H & C(12)H, d, $J_{\text{C-F}}$ 12), 124.9 (C(4)H), 128.7 (C(5)H), 133.9 (C(3)H), 152.7 (qC-7, d, $J_{\text{C-F}}$ 3), 154.1 (qC-1), 158.8 (qC-10, d, $J_{\text{C-F}}$ 243); δ_{F} (CDCl_3 , 282 MHz) -120.0; Anal. Calculated for $\text{C}_{12}\text{H}_8\text{BrFO}$: C, 53.96; H, 3.02. Found: C, 54.26; H, 3.15.

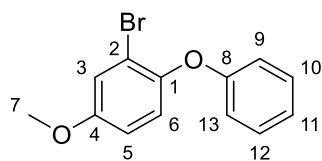
1-Bromo-4-chloro-2-(4-fluorophenoxy) benzene (169)



Synthesised according to the general procedure 6.3.5 using 2-bromo-5-chloro phenol (330 mg, 1.6 mmol, 1 equiv.) and 4-fluoro phenyl boronic acid (448 mg, 3.2 mmol, 2 equiv.). Colourless oil (150 mg, 31%); $\nu_{\text{max}}/\text{cm}^{-1}$ (NaCl): 1576 (aromatic C=C stretch), 1467 (aromatic C=C stretch), 1254 (ether C-O stretch), 1219 (ether C-O stretch), 1087 (C-F stretch), 830 (aromatic C-H bend), 682 (C-Br stretch); δ_{H} (CDCl_3 , 300 MHz) 6.82 (1H, d, J 2.4, C(6)H), 6.93-7.02 (3H, m, C(4)H, C(8)H & C(12)H), 7.02-7.12 (2H, m, C(9)H & C(11)H), 7.53 (1H, d, J 8.6, C(3)H); δ_{C} (CDCl_3 ,

75.5 MHz) 112.0 (qC-2), 116.3 (C(9)H & C(11)H, d, J_{C-F} 24), 119.9 (C(6)H), 120.2 (C(8)H & C(12)H, d, J_{C-F} 9), 125.0 (C(4)H), 134.0 (qC-5), 134.4 (C(3)H), 151.7 (qC-7, d, J_{C-F} 3), 155.0 (qC-1), 159.4 (qC-10, d, J_{C-F} 243); δ_F (CDCl₃, 282 MHz) -118.5; Anal. Calculated for C₁₂H₇BrClFO: C, 47.80; H, 2.34. Found: C, 47.83; H, 2.47. HRMS (ESI-TOF) m/z: [M]⁺ calcd. for C₁₂H₇BrClFO: 299.9347, found 299.9359.

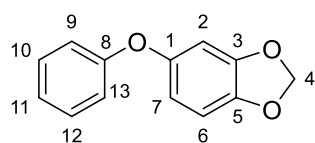
1-bromo-4-methoxy-2-(phenoxy) benzene (171)



Synthesised according to the general procedure **6.3.5** using 2-bromo-4-methoxy phenol (1 g, 4.93 mmol, 1 equiv.) and phenyl boronic acid (**128**) (1.2 g mg, 9.85 mmol, 2 equiv.). Colourless oil

(450 mg, 33%); ν_{max}/cm^{-1} (NaCl): 1605 (aromatic C=C stretch), 1484 (aromatic C=C stretch), 1216 (ether C-O stretch), 1163 (ether C-O stretch), 1038 (ether C-O stretch), 836 (aromatic C-H bend), 689 (C-Br stretch); δ_H (CDCl₃, 300 MHz) 3.81 (3H, s, C(7)H₃), 6.84 (1H, dd, J 8.9, 2.9, C(5)H), 6.86-6.92 (2H, m, C(9)H & C(13)H), 6.98 (1H, d, J 8.9, C(6)H), 7.00-7.08 (1H, m, C(11)H), 7.17 (1H, d, J 2.6, C(3)H), 7.24-7.34 (2H, m, C(10)H & C(12)H); δ_C (CDCl₃, 75.5 MHz) 55.9 (C(7)H₃), 114.6 (C(5)H), 116.1 (qC-2), 116.8 (C(6)H), 118.6 (C(9)H & C(13)H), 122.6 (C(3)H & C(11)H), 129.7 (C(10)H & C(12)H), 146.7 (qC-4), 156.7 (qC-1), 158.0 (qC-8); HRMS (ESI-TOF) m/z: [M]⁺ calcd. for C₁₃H₁₁BrO₂: 277.9937, found 277.9937.

5-phenoxy-1,3-benzodioxole (174)²⁸

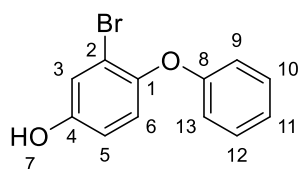


Synthesised according to the general procedure **6.3.5** using sesamol (**173**) (1 g, 7.24 mmol, 1 equiv.) and phenyl boronic acid (**128**) (1.72 g, 14.48 mmol, 2 equiv.). Colourless oil (120 mg, 29%);

ν_{max}/cm^{-1} (NaCl): 1594 (aromatic C=C stretch), 1479 (aromatic C=C stretch), 1214 (C-O stretch), 1174 (C-O stretch), 1038 (C-O stretch), 748 (aromatic C-H bend), 692 (C-Br stretch); δ_H (CDCl₃, 300 MHz) 5.96 (2H, s, C(4)H₂), 6.49 (1H, dd, J 8.3, 2.4, C(7)H), 6.58 (1H, d, J 2.4, C(2)H), 6.75 (1H, d, J 8.4, C(6)H), 6.92-6.99 (2H, m, C(9)H & C(13)H), 7.01-7.08 (1H, m, C(11)H), 7.26-7.34 (2H, m, C(10)H & C(12)H); δ_C (CDCl₃, 75.5 MHz) 101.5 (C(4)H₂), 102.2 (C(7)H), 108.3 (C(2)H), 112.0 (C(6)H), 117.9 (C(9)H & C(13)H), 122.7 (C(11)H), 129.6 (C(10)H & C(12)H), 143.8 (qC-5), 148.4 (qC-3), 151.5 (qC-1), 158.2 (qC-8); Anal. Calculated for C₁₃H₁₀O₃: C, 72.89; H, 4.71. Found: C, 72.81; H, 4.45.

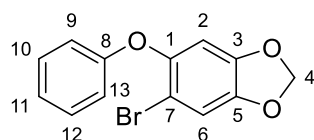
Spectral characteristics are consistent with previously reported data.²⁸

1-Bromo-3-hydroxy-2-(phenoxy) benzene (**172**)



Compound **172** was prepared *via* a procedure described by Wiegrebé *et al.*²⁹ A 250 mL 3-neck round bottomed flask was heated under vacuum and then refilled with N₂. 2-Bromo-4-methoxy diphenylether (**171**) (420 mg, 1.50 mmol, 1 equiv.) and DCM (40 mL) were added. BBr₃ (1.4 mL, 7.5 mmol, 7 equiv.) was added dropwise at 0 °C. The reaction mixture was then stirred at room temperature under N₂ atmosphere until TLC analysis indicated full consumption of starting material. The reaction mixture was quenched with water (10 mL) and the organic layer separated from the aqueous layer. The organic layer was washed with water (3 × 10 mL). The combined organics were washed with brine (10 mL), dried with MgSO₄, filtered and concentrated under reduced pressure. The residue was purified by column chromatography (hexanes:EtOAc 3:1) to yield **172** as a colourless oil (371 mg, 93%); $\nu_{\text{max}}/\text{cm}^{-1}$ (NaCl); 3378 (O-H stretch), 1589 (aromatic C=C stretch), 1490 (aromatic C=C stretch), 1211 (ether C-O stretch), 1036 (ether C-O stretch), 847 (aromatic C=C bend), 689 (C-Br stretch); δ_{H} (CDCl₃, 300 MHz) 4.97 (1H, bs, O(7)H), 6.78 (1H, dd, *J* 8.7, 2.9, C(5)H), 6.85-6.97 (3H, m, C(9)H, C(11)H & C(13)H), 7.00-7.10 (1H, m, C(6)H), 7.13 (1H, d, *J* 2.9, C(3)H), 7.24-7.34 (2H, m, C(10)H & C(12)H); δ_{C} (CDCl₃, 75.5 MHz) 115.7 (C(5)H), 116.1 (qC-2), 116.8 (C(9)H & C(13)H), 120.4 (C(3)H), 122.6 (C(6)H), 122.7 (C(11)H), 129.7 (C(10)H & C(12)H), 146.9 (qC-1), 153.0 (qC-4), 157.9 (qC-8); HRMS (ESI-TOF) *m/z*: [M-H]⁻ calcd. for C₁₂H₈BrO₂: 262.9713, found 262.9707.

5-Bromo-6-phenoxy-1,3-benzodioxole (**175**)



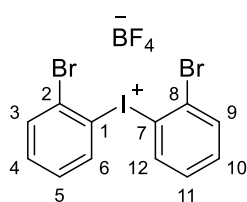
Compound **175** was prepared *via* a procedure described by Siegel *et al.*³⁰ A solution of NBS (208 mg, 1.17 mmol, 1 equiv.) in acetonitrile (2 mL) was added to a 100 mL round bottomed flask containing a stirred solution of **174** (250 mg, 1.17 mmol, 1 equiv.) in acetonitrile (2 mL) at 0 °C. After 10 minutes of stirring at this temperature, the reaction mixture was warmed to room temperature overnight. After 16 hours, the reaction was quenched with water (10 mL) and the organic layer extracted with DCM (10 mL). The organic layer was then washed with water

(3 × 10 mL), dried with MgSO₄ and concentrated under reduced pressure. The residue was flushed through a pad of silica using DCM to yield **175** as a pale pink solid (281 mg, 94%); $\nu_{\text{max}}/\text{cm}^{-1}$ (NaCl): 1590 (aromatic C=C stretch), 1471 (aromatic C=C stretch), 1208 (C-O stretch), 1116 (C-O stretch), 1036 (C-O stretch), 844 (aromatic C-H bend), 690 (C-Br stretch); δ_{H} (CDCl₃, 300 MHz) 5.99 (2H, s, C(4)H₂), 6.58 (1H, s, C(2)H), 6.85-7.11 (2H, m, C(9)H & C(13)H), 7.01-7.12 (2H, m, C(6)H & C(11)H), 7.26-7.35 (2H, m, C(10)H & C(12)H); δ_{C} (CDCl₃, 75.5 MHz) 102.2 (C(4)H₂), 103.5 (C(2)H), 106.0 (qC-7), 112.4 (C(6)H), 116.9 (C(9)H & C(13)H), 122.8 (C(11)H), 129.7 (C(10)H & C(12)H), 145.0 (qC-5), 147.5 (qC-3), 147.9 (qC-1), 157.8 (qC-8); Anal. Calculated for C₁₃H₉BrO₃: C, 53.27; H, 3.10. Found: C, 53.18; H, 3.15.

6.3.6 General procedure for preparation of diphenyliodonium tetrafluoroborate salts (**177-179**)¹²

*m*CPBA (81% active oxidant, 1.1 equiv.) was dissolved in DCM (0.25 M). To the solution was added aryl iodide (1 equiv.), followed by slow addition of BF₃ · OEt₂ (2.5 equiv.) at room temperature. The resulting yellow solution was stirred at room temperature for 45 minutes and then cooled to 0 °C. The phenylboronic acid (1.1 equiv.) was added portion wise over 15 minutes. After 30 minutes of stirring at room temperature, the crude reaction mixture was applied on a silica plug (12 g/1g aryl iodide) and eluted with DCM (120 mL/1g aryl iodide) to remove unreacted aryl iodide and *m*CPBA, followed by DCM:MeOH (20:1, 240 mL/1 g aryl iodide), to elute the product, leaving any boric acid derivatives on the column. The latter solution was concentrated and diethyl ether was added to the residue to induce a precipitation of the salt, with any iodine(III) intermediates and BF₃ derivatives remaining in solution. The solution was allowed to stir for 15 minutes and then the ether phase was decanted. The solid was washed twice more with diethyl ether and then dried *in vacuo* to give the pure diaryliodonium tetrafluoroborate salt.

Bis(2-bromophenyl)iodonium tetrafluoroborate (**177**)³¹

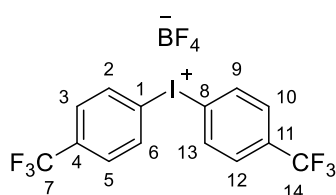


Synthesised according to the general **6.3.6** using 2-bromo iodobenzene (0.32 mL, 2.5 mmol, 1 equiv.) and 2-bromophenyl-boronic acid (**156**) (552 mg, 2.75 mmol, 1.1 equiv.). Light brown solid (799 mg, 61%); m.p. 197-200 °C; δ_{H} (DMSO-d₆, 300 MHz) 7.54 (2H, td, *J* 8.3, 1.3, C(4)H &

C(10)H), 7.63 (2H, td, J 8.3, 1.3, C(5)H & C(11)H), 7.99 (2H, dd, J 8.0, 1.1, C(3)H & C(9)H), 8.50 (2H, dd, J 8.1, 1.4, C(6)H & C(12)H); δ_c (DMSO- d_6 , 75.5 MHz) 123.2 (qC-2 & qC-8), 127.4 (qC-1 & qC-7), 131.0 (C(4)H & C(10)H), 134.5 (C(5)H & C(11)H), 135.2 (C(3)H & C(9)H), 139.7 (C(6)H & C(12)H); δ_f (DMSO- d_6 , 282 MHz) -148.3, -148.2; HRMS (ESI-TOF) m/z : $[M-BF_4]^+$ calcd. for $C_{12}H_7Br_2I$: 436.8031, found 436.8036.

Spectral characteristics are consistent with previously reported data.¹⁸³¹

Bis(4-trifluoromethylphenyl)iodonium tetrafluoroborate (178)³²

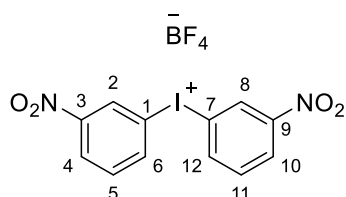


Synthesised according to the general procedure **6.3.6** using 4-iodobenzotrifluoride (0.27 mL, 1.84 mmol, 1 equiv.) and 4-trifluoromethylphenyl boronic acid (384 mg, 2.024 mmol, 1.1 equiv.). White solid (286 mg, 31%); m.p. 198-200 °C; δ_H (DMSO-

d_6 , 300 MHz) 7.95 (4H, d_{app} , J 8.3, C(3)H, C(5)H, C(10)H & C(12)H), 8.53 (4H, d_{app} , J 8.4, C(2)H, C(6)H, C(9)H & C(13)H); δ_c (DMSO- d_6 , 75.5 MHz) 121.4 (qC-1 & qC-8), 129.0 (C(3)H, C(5)H, C(10)H & C(12)H, q, J_{C-F} 4), 123.7 (qC-7 & qC-14, q, J_{C-F} 272), 132.5 (qC-4 & qC-11, q, J_{C-F} 33), 136.7 (C(2)H, C(6)H, C(9)H & C(13)H); δ_f (DMSO- d_6 , 282 MHz) -148.3, -148.2 -61.7; m/z (ES+): 417 $[(M-BF_4)^+, 100\%]$.

Spectral characteristics are consistent with previously reported data.³²

Bis(3-nitrophenyl)iodonium tetrafluoroborate (179)³¹



Synthesised according to the general procedure **6.3.6** using 3-nitroiodobenzene (600 mg, 2.41 mmol, 1 equiv.) and 3-nitrophenyl boronic acid (443 mg, 2.651 mmol, 1.1 equiv.). Light brown solid (260 mg, 24%); m.p. 188-190 °C; δ_H (DMSO- d_6 , 300

MHz) 7.85 (2H, t, J 8.1, C(5)H & C(11)H), 8.48 (2H, dd_{app} , J 8.3, 1.5, C(3)H & C(9)H), 8.74-8.78 (2H, m, C(4)H & C(10)H), 9.25-9.33 (2H, m, C(6)H & C(12)H); δ_c (DMSO- d_6 , 75.5 MHz) 117.3 (qC-1 & qC-7), 127.5 (C(5)H & C(11)H), 130.6 (C(4)H & C(10)H), 133.4 (C(2)H & C(8)H), 141.8 (C(6)H & C(12)H), 148.9 (qC-3 & qC-9); δ_f (DMSO- d_6 , 282 MHz) -148.3, -148.2; m/z (ES+): 371 $[(M-BF_4)^+, 100\%]$.

Spectral characteristics are consistent with previously reported data.³¹

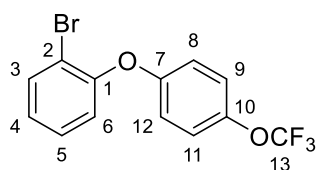
6.3.7 General procedure for preparation of 2-bromo diarylethers *via* diphenyliodonium tetrafluoroborate salts (177-182)⁹

To a suspension of potassium *tert*-butoxide (1.1 equiv.) in THF (10 mL) was added 2-bromo-phenol (substituted) at 0 °C. After stirring for 1 hour, the iodonium salt (1.2 equiv.) was added and the resulting mixture was stirred at room temperature overnight.

Work-up as per 1 mmol phenol

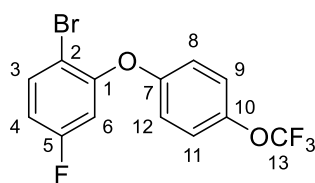
The reaction mixture was quenched with water (15 mL) and the organic layer was extracted with ethyl acetate (3 × 10 mL). The organic layer was then dried over MgSO₄, filtered and concentrated under reduced pressure. The crude residue was purified by silica gel chromatography (hexanes:EtOAc, 3:1) to yield the title products.

1-Bromo-2-(4-(trifluoromethoxy)phenoxy) benzene (183)



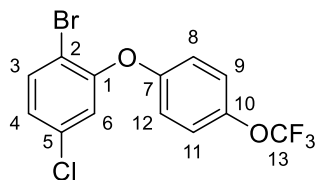
Synthesised according to the general procedure **6.3.7** using bis-(4-trifluoromethoxyphenyl)iodonium tetrafluoroborate (**180**) (500 mg, 0.933 mmol, 1.2 equiv.) and 2-bromo-phenol (0.09 mL, 0.777 mmol, 1 equiv.). Colourless oil (157 mg, 61%); $\nu_{\text{max}}/\text{cm}^{-1}$ (NaCl):

1578 (aromatic C=C stretch), 1472 (aromatic C=C stretch), 1242 (ether C-O stretch), 1102 (ether C-O stretch), 1047 (C-F stretch), 844 (aromatic C-H bend), 750 (C-Br stretch); δ_{H} (CDCl₃, 300 MHz) 6.95 (2H, ddd_{overlapping}, J 9.1, 3.6, 2.4, C(9)H & C(11)H), 6.99 (1H, dd, J 8.1, 1.6, C(6)H), 7.06 (1H, ddd, J 8.3, 7.7, 1.5, C(4)H), 7.13-7.23 (2H, m, C(8)H & C(12)H), 7.29 (1H ddd, J 8.3, 7.7, 1.5, C(5)H), 7.64 (1H dd, J 8.0, 1.6, C(3)H); δ_{C} (CDCl₃, 75.5 MHz) 115.2 (qC-2), 118.7 (C(9)H & C(11)H), 120.6 (qC-13, q, $J_{\text{C-F}}$ 261), 121.1 (C(6)H), 122.6 (C(8)H & C(12)H), 125.6 (C(4)H), 128.8 (C(5)H), 134.0 (C(3)H), 144.6 (qC-10), 153.2 (qC-7), 155.5 (qC-1); δ_{F} (CDCl₃, 282 MHz) -58.3; HRMS (ESI-TOF) m/z : [M]⁺ calcd. for C₁₃H₈BrF₃O₂: 354.9552, found 354.9562.

1-Bromo-4-fluoro-2-(4-(trifluoromethoxy)phenoxy) benzene (184)

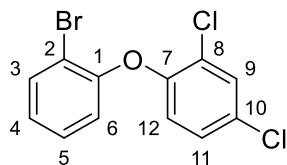
Synthesised according to the general procedure **6.3.7** using bis(4-trifluoromethoxyphenyl)iodonium tetrafluoroborate (**180**) (800 mg, 1.5 mmol, 1.2 equiv.) and 2-bromo-5-fluoro phenol (0.13 mL, 1.2 mmol, 1 equiv.). Colourless oil (98 mg, 23%); $\nu_{\max}/\text{cm}^{-1}$ (NaCl);

1596 (aromatic C=C stretch), 1502 (aromatic C=C stretch), 1478 (aromatic C=C stretch), 1262 (ether C-O stretch), 1189 (ether C-O stretch), 1042 (C-F stretch), 845 (aromatic C-H bend), 599 (C-Br stretch); δ_{H} (CDCl_3 , 300 MHz) 6.67 (1H, dd, J 9.4, 2.9, C(6)H), 6.79 (1H, ddd, J 8.9, 7.8, 3.0, C(4)H), 6.96-7.05 (2H, m, C(8)H & C(12)H), 7.17-7.25 (2H, m, C(9)H & C(11)H), 7.59 (1H, dd, J 9.0, 6.0, C(3)H); δ_{C} (CDCl_3 , 75.5 MHz) 107.9 (C(6)H, d, $J_{\text{C-F}}$ 26), 109.0 (qC-2, d, $J_{\text{C-F}}$ 4), 112.4 (C(4)H, d, $J_{\text{C-F}}$ 22), 118.8 (C(8)H & C(12)H), 120.9 (qC-13, q, $J_{\text{C-F}}$ 257), 122.8 (C(9)H & C(11)H), 134.4 (C(3)H, d, $J_{\text{C-F}}$ 9), 145.2 (qC-10, q, $J_{\text{C-F}}$ 2), 154.4 (qC-7), 154.5 (qC-1), 162.4 (qC-5, d, $J_{\text{C-F}}$ 247); δ_{F} (CDCl_3 , 282 MHz) -111.1, -58.3; HRMS (ESI-TOF) m/z : $[\text{M}]^+$ calcd. for $\text{C}_{13}\text{H}_7\text{BrF}_4\text{O}_2$: 350.1383, found 350.1384.

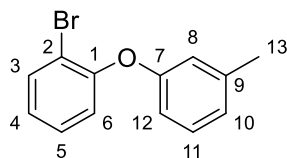
1-Bromo-4-chloro-2-(4-(trifluoromethoxy)phenoxy) benzene (185)

Synthesised according to the general procedure **6.3.7** using bis(4-trifluoromethoxyphenyl)iodonium tetrafluoroborate (**180**) (382 mg, 0.71 mmol, 1.2 equiv.) and 2-bromo-5-chloro phenol (118 mg, 0.568 mmol, 1 equiv.). Colourless oil (62 mg, 30%); $\nu_{\max}/\text{cm}^{-1}$

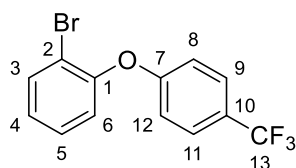
(NaCl); 1580 (aromatic C=C stretch), 1477 (aromatic C=C stretch), 1260 (ether C-O stretch), 1188 (ether C-O stretch), 1040 (C-F stretch), 840 (aromatic C-H bend), 780 (C-Cl stretch), 590 (C-Br stretch); δ_{H} (CDCl_3 , 300 MHz) 6.93 (1H, d, J 2.4, C(6)H), 6.96-7.02 (2H, m, C(9)H & C(11)H), 7.03 (1H, dd, J 8.5, 2.4, C(4)H), 7.18-7.25 (2H, m, C(8)H & C(12)H), 7.56 (1H, d, J 8.5, C(3)H); δ_{C} (CDCl_3 , 75.5 MHz) 112.9 (qC-2), 119.4 (C(9)H & C(11)H), 120.5 (qC-13, d, $J_{\text{C-F}}$ 257), 120.5 (C(6)H), 122.8 (C(4)H), 125.5 (C(3)H), 134.2 (qC-5), 134.5 (C(8)H & C(12)H), 145.2 (qC-10), 154.1 (qC-7), 154.6 (qC-1); δ_{F} (CDCl_3 , 282 MHz) -58.2. HRMS (ESI-TOF) m/z : $[\text{M}]^+$ calcd. for $\text{C}_{13}\text{H}_7\text{BrF}_3\text{O}_2$: 365.9265, found 365.9280.

1-Bromo-2-(2,4-dichlorophenoxy) benzene (187)

Synthesised according to the general procedure **6.3.7** using bis(2-bromophenyl)iodonium tetrafluoroborate (**177**) (550 mg, 1.046 mmol, 1.2 equiv.) and 2,4-dichloro phenol (**186**) (136 mg, 0.8368 mmol, 1 equiv.). Colourless oil (163 mg, 61%); $\nu_{\max}/\text{cm}^{-1}$ (NaCl): 1574 (aromatic C=C stretch), 1469 (aromatic C=C stretch), 1258 (ether C-O stretch), 1100, (ether C-O stretch), 806 (aromatic C-H bend), 773 (C-Cl stretch), 553 (C-Br stretch); δ_{H} (CDCl_3 , 300 MHz) 6.77 (1H, d, J 8.8, C(12)H), 6.86 (1H, dd, J 8.4, 1.2, C(6)H), 7.04 (1H, ddd, J 8.0, 7.7, 1.6, C(4)H), 7.16 (1H, dd, J 8.8, 2.5, C(11)H), 7.27 (1H, ddd, J 8.2, 7.8, 1.6, C(5)H), 7.47 (1H, d, J 2.5, C(9)H), 7.64 (1H, dd, J 7.9, 1.6, C(3)H); δ_{C} (CDCl_3 , 75.5 MHz) 114.3 (qC-2), 119.7 (C(6)H), 120.1 (C(12)H), 125.5 (C(4)H), 126.0 (qC-8), 128.0 (C(11)H), 128.8 (C(5)H), 129.2 (qC-10), 130.6 (C(9)H), 134.1 (C(3)H), 151.1 (qC-7), 153.0 (qC-1). Anal. Calculated for $\text{C}_{12}\text{H}_7\text{BrCl}_2\text{O}$: C, 45.33; H, 2.22. Found: C, 45.10; H, 2.50.

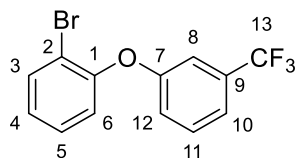
1-Bromo-2-(3-methylphenoxy) benzene (189)

Synthesised according to the general procedure **6.3.7** using bis(2-bromophenyl)iodonium tetrafluoroborate (**177**) (537 mg, 1.021 mmol, 1.2 equiv.) and *m*-cresol (**188**) (0.089 mL, 0.851 mmol, 1 equiv.). Colourless oil (113 mg, 51%); $\nu_{\max}/\text{cm}^{-1}$ (NaCl): 1607 (aromatic C=C stretch), 1485 (aromatic C=C stretch), 1441 ($-\text{CH}_3$ bend), 1252 (ether C-O stretch), 1144 (ether C-O stretch), 658 (C-Br stretch); δ_{H} (CDCl_3 , 300 MHz) 2.33 (3H, s, C(13)H₃), 6.72-6.82 (2H, m, C(8)H & C(12)H), 6.88-6.97 (2H, m, C(6)H & C(10)H), 7.00 (1H, td, J 7.6, 1.5, C(11)H), 7.21 (1H, t, J 7.2, C(4)H), 7.24 (1H, ddd, J 8.7, 7.7, 1.6, C(5)H), 7.62 (1H, dd, J 7.9, 1.6, C(3)H); δ_{C} (CDCl_3 , 75.5 MHz) 21.4 (C(13)H₃), 114.9 (qC-2), 115.1 (C(12)H), 118.9 (C(8)H), 120.6 (C(6)H), 124.2 (C(10)H), 124.8 (C(4)H), 128.6 (C(11)H), 129.5 (C(5)H), 133.8 (C(3)H), 140.0 (qC-9), 153.8 (qC-1), 156.9 (qC-7); Anal. Calculated for $\text{C}_{13}\text{H}_{11}\text{BrO}$: C, 59.34; H, 4.21. Found: C, 59.32; H, 4.35.

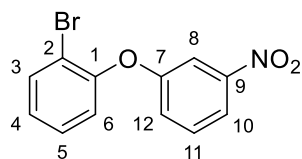
1-Bromo-2-(4-(trifluoromethyl)phenoxy) benzene (190)³³

Synthesised according to the general procedure **6.3.7** using bis(4-trifluoromethylphenyl)iodonium tetrafluoroborate (**178**) (300 mg, 0.595 mmol, 1.2 equiv.) and 2-bromo phenol (**156**) (0.058 mL, 0.497 mmol, 1 equiv.). Colourless oil (102 mg, 65%); $\nu_{\max}/\text{cm}^{-1}$ (NaCl): 1616 (aromatic C=C stretch), 1579 (aromatic C=C stretch), 1471 (aromatic C=C stretch), 1262 (ether C-O stretch), 1168 (ether C-O stretch), 1066 (C-F stretch), 874 (aromatic C-H bend), 660 (C-Br stretch); δ_{H} (CDCl_3 , 300 MHz) 6.93-7.02 (2H, m, C(8)H & C(12)H), 7.07 (1H, dd, J 7.9, 1.6, C(6)H), 7.11 (1H, td, J 7.8, 1.6, C(4)H), 7.34 (1H, td, J_{app} 7.8, 1.6, C(5)H), 7.53-7.62 (2H, m, C(9)H & C(11)H), 7.67 (1H, dd, J 8.0, 1.6, C(3)H); δ_{C} (CDCl_3 , 75.5 MHz) 115.9 (qC-2), 117.0 (C(8)H & C(12)H), 122.2 (C(6)H), 124.2 (qC-13, q, $J_{\text{C-F}}$ 272), 125.0 (qC-10, q, $J_{\text{C-F}}$ 32), 126.0 (C(4)H), 127.2 (C(9)H & C(11)H, q, $J_{\text{C-F}}$ 4), 129.0 (C(5)H), 134.2 (C(3)H), 152.2 (qC-1), 159.9 (qC-7); δ_{F} (CDCl_3 , 282 MHz) -61.8; HRMS (ESI-TOF) m/z : $[\text{M}]^+$ calcd. for $\text{C}_{13}\text{H}_8\text{BrF}_3\text{O}$: 315.9705, found 315.9705.

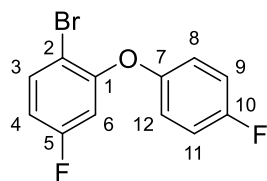
Spectral characteristics are consistent with previously reported data.³³

1-Bromo-2-(3-(trifluoromethyl)phenoxy) benzene (191)

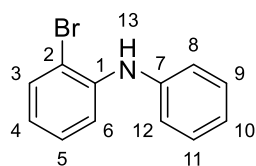
Synthesised according to the general procedure **6.3.7** using bis(3-trifluoromethyl)iodonium tetrafluoroborate (**182**) (140 mg, 0.28 mmol, 1.2 equiv.) and 2-bromo phenol (**156**) (0.03 mL, 0.23 mmol, 1 equiv.). Colourless oil (58 mg, 80%); $\nu_{\max}/\text{cm}^{-1}$ (NaCl): 1578 (aromatic C=C stretch), 1471 (aromatic C=C stretch), 1262 (ether C-O stretch), 1128 (ether C-O stretch), 1064 (C-F stretch), 696 (C-Br stretch); δ_{H} (CDCl_3 , 300 MHz): 7.03 (1H, dd, J 8.1, 1.6, C(6)H), 7.03-7.13 (2H, m, C(4)H & C(12)H), 7.17-7.23 (1H, m, C(8)H), 7.28-7.39 (2H, m, C(5)H & C(10)H), 7.43 (1H, t, J 7.9, C(11)H), 7.67 (1H, dd, J 8.0, 1.6, C(3)H); δ_{C} (CDCl_3 , 75.5 MHz) 114.5 (C(8)H, q, $J_{\text{C-F}}$ 4), 115.5 (qC-2), 119.8 (C(10)H, q, $J_{\text{C-F}}$ 4), 120.6 (C(12)H), 121.5 (C(6)H), 123.7 (qC-13, q, $J_{\text{C-F}}$ 272), 126.0 (C(4)H), 129.0 (C(5)H), 130.3 (C(3)H), 132.3 (qC-9, q, $J_{\text{C-F}}$ 32), 134.2 (C(11)H), 152.6 (qC-1), 157.4 (qC-7); δ_{F} (CDCl_3 , 282 MHz) -61.7; Anal. Calculated for $\text{C}_{13}\text{H}_8\text{BrF}_3\text{O}$: C, 49.24; H, 2.54. Found: C, 49.47; H, 2.74.

1-Bromo-2-(3-nitrophenoxy) benzene (164)²³

Synthesised according to the general procedure **6.3.7** using bis(3-nitrophenyl)iodonium tetrafluoroborate (**179**) (200 mg, 0.437 mmol, 1.2 equiv.) and 2-bromo phenol (**156**) (0.042 mL, 0.364 mmol, 1 equiv.). Pale yellow oil (72 mg, 67%); $\nu_{\max}/\text{cm}^{-1}$ (NaCl): 1578 (aromatic C=C stretch), 1469 (aromatic C=C stretch), 1352 (N=O stretch), 1261 (ether C-O stretch), 1238 (C-N stretch), 1046 (ether C-O stretch), 840 (aromatic C=C bend), 736 (C-Br stretch); δ_{H} (CDCl₃, 300 MHz) 7.09 (1H, dd, J 8.0, 1.5, C(6)H), 7.15 (1H, ddd, J 8.7, 7.5, 1.5, C(4)H), 7.27 (1H, ddd, J 8.5, 2.3, 0.9, C(12)H), 7.37 (1H, ddd, J 8.5, 7.5, 1.5, C(5)H), 7.49 (1H, t, J 8.2, C(11)H), 7.65-7.75 (2H, m, C(3)H & C(8)H), 7.95 (1H, ddd, J 8.2, 2.2, 0.9, C(10)H); δ_{C} (CDCl₃, 75.5 MHz) 112.0 (C(8)H), 115.8 (qC-2), 117.8 (C(10)H), 122.2 (C(6)H), 123.2 (C(12)H), 126.8 (C(4)H), 129.2 (C(5)H), 130.4 (C(11)H), 134.4 (C(3)H), 149.3 (qC-9), 151.9 (qC-1), 158.0 (qC-7); m/z (ES⁻): 294 [(M)⁻, 60%].

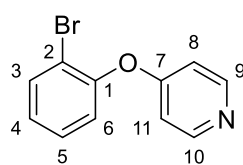
1-Bromo-4-fluoro-2-(4-fluorophenoxy) benzene (192)

Synthesised according to the general procedure **6.3.7** using bis(4-fluorophenyl)iodonium tetrafluoroborate (**181**) (500 mg, 1.24 mmol, 1.2 equiv.) and 2-bromo-5-fluoro phenol (0.11 mL, 1.03 mmol, 1 equiv.). Colourless oil (191 mg, 65%); $\nu_{\max}/\text{cm}^{-1}$ (NaCl); 1584 (aromatic C=C stretch), 1500 (aromatic C=C stretch), 1477 (aromatic C=C stretch), 1279 (ether C-O stretch), 1193 (ether C-O stretch), 1144 (ether C-O stretch), 1040 (C-F stretch), 840 (aromatic C-H bend), 599 (C-Br stretch); δ_{H} (CDCl₃, 300 MHz) 6.56 (1H, dd, J 9.6, 2.9, C(6)H), 6.73 (1H, ddd, J 9.6, 7.3, 3.0, C(4)H), 6.93-7.13 (4H, m, C(8)H, C(9)H, C(11)H & C(12)H), 7.56 (1H, dd, J 8.9, 6.1, C(3)H); δ_{C} (CDCl₃, 75.5 MHz) 106.7 (C(6)H, d, $J_{\text{C-F}}$ 26), 108.1 (qC-2, d, $J_{\text{C-F}}$ 4), 111.5 (C(4)H, d, $J_{\text{C-F}}$ 23), 116.6 (C(9)H & C(11)H, d, $J_{\text{C-F}}$ 24), 120.7 (C(8)H & C(12)H, d, $J_{\text{C-F}}$ 8), 134.2 (C(3)H, d, $J_{\text{C-F}}$ 9), 151.6 (qC-7, d, $J_{\text{C-F}}$ 2), 155.3 (qC-1, d, $J_{\text{C-F}}$ 10), 159. (qC-10, d, $J_{\text{C-F}}$ 223), 162.0 (qC-5, d, $J_{\text{C-F}}$ 227); δ_{F} (CDCl₃, 282 MHz) -118.4, -111.3; HRMS (ESI-TOF) m/z : [M]⁺ calcd. for C₁₂H₇BrF₂O: 283.9643, found 283.9645.

6.3.8 General procedure for preparation of 2-bromo diphenylamine (**195**)^{14, 34}

$\text{Pd}_2(\text{dba})_3$ (2.5 mol%), dppf (10 mol%) and NaO^tBu (1.4 equiv.) were all weighed out in air and transferred to a flame dried resealable Schlenk tube that was evacuated and refilled with N_2 three times. The stopper was then replaced with a rubber septum under a nitrogen purge and the liquid reagents were added (aniline (**193**) (800 mg, 8.59 mmol, 1 equiv.) and 2-bromoiodobenzene (**194**) (2.92 g, 10.31 mmol, 1.2 equiv.) *via* syringe. The sides of the flask were rinsed with solvent (1 mL/mmol) and the septum replaced by a stopper. The Schlenk tube was then stirred in an oil bath at 100 °C for 48 h. When TLC analysis indicated disappearance of the aniline, the reaction mixture was cooled to room temperature, diluted with DCM and filtered through a plug of Celite®. The crude residue was concentrated and purified by silica gel chromatography (hexanes, 100%) to yield 2-bromo diphenylamine (**195**). Yellow liquid (457 mg, 96%); $\nu_{\text{max}}/\text{cm}^{-1}$ (NaCl); 3396 (N-H stretch), 1583 (aromatic C=C stretch), 1464 (aromatic C=C stretch), 1311 (C-N stretch), 1020 (C-N stretch), 692 (C-Br stretch) δ_{H} (CDCl_3 , 300 MHz) 6.07 (1H, s, N(13)H), 6.72 (1H, ddd J 8.4, 7.6, 1.6, C(4)H), 6.97-7.07 (1H, m, C(10)H), 7.09-7.19 (3H, m, C(5)H, C(8)H & C(12)H), 7.23 (1H, dd, J 8.1, 1.9, C(6)H), 7.26-7.37 (2H, m, C(9)H & C(11)H), 7.51 (1H, dd, J 8.0, 1.5, C(3)H); δ_{C} (CDCl_3 , 75 .5 MHz) 112.2 (qC-2), 115.9 (C(6)H), 120.3 (C(8)H & C(12)H), 120.9 (C(4)H), 122.7 (C(10)H), 128.1 (C(5)H), 129.5 (C(9)H & C(11)H), 133.0 (C(3)H), 141.5 (qC-7), 141.6 (qC-1); HRMS (ESI-TOF) m/z : $[\text{M}+\text{H}]^+$ calcd. for $\text{C}_{12}\text{H}_{11}\text{BrN}$: 248.0069, found 248.0071.

Spectral characteristics are consistent with previously reported data.³⁴

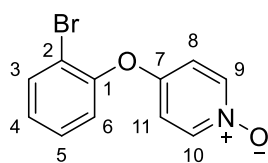
6.3.9 Procedure for synthesis of 4-(2-bromophenoxy)pyridine (**197**)²²

A mixture of 4-chloro pyridine hydrochloride (**196**) (500 mg, 3.33 mmol, 1 equiv.), 2-bromo phenol (**156**) (2.88 g, 16.65 mmol, 5 equiv.) and NaOH (200 mg, 4.99 mmol, 1.5 equiv.) was added to a 250 mL round bottomed flask and stirred at 130 °C in an oil bath until TLC analysis indicated complete consumption of starting material. The cooled reaction mixture was then diluted with 10% aq. NaOH (5 mL) and stirred at room temperature for 1 h. The aqueous phase was extracted with DCM (3 × 10 mL). The combined organics were washed with 6M NaOH (3 × 10

mL), water (10 mL) and brine (10 mL) and then dried with MgSO₄, filtered and concentrated *in vacuo*. The crude product was passed through a short pad of silica using hexanes:EtOAc (3:1) to yield the final product **197** as a yellow solid (502 mg, 60%); m.p. 63-66 °C (lit. 64-66 °C); δ_{H} (DMSO-*d*₆, 300 MHz) 6.78 (2H, d, *J* 6.0, C(8)H & C(11)H), 7.10-7.22 (2H, m, C(4)H & C(6)H), 7.37 (1H, td, *J* 7.8, 1.6, C(5)H), 7.68 (1H, dd, *J* 7.8, 1.2, C(3)H), 8.48 (2H, bs, C(9)H & C(10)H); δ_{C} (DMSO-*d*₆, 75.5 MHz) 111.6 (C(8)H & C(11)H), 116.3 (qC-2), 123.0 (C(6)H), 127.2 (C(4)H), 129.1 (C(5)H), 134.3 (C(3)H), 150.8 (qC-1), 151.5 (C(9)H & C(10)H), 164.0 (qC-7); HRMS (ESI-TOF) *m/z*: [M+H]⁺ calcd. for C₁₁H₉BrNO: 249.9862, found 249.9856.

Spectral characteristics are consistent with previously reported data.²²

6.3.10 Procedure for synthesis of 4-(2-bromophenoxy)pyridine *N*-oxide (**198**)



Synthesised according to the general procedure using 4-(2-bromophenoxy)pyridine (**197**) (150 mg, 0.599 mmol, 1 equiv.). The crude product was purified by column chromatography (DCM (100%), DCM:MeOH, 94:6). Yellow oil (149 mg, 94%); $\nu_{\text{max}}/\text{cm}^{-1}$ (NaCl): 1624 (aromatic C=C stretch), 1467 (aromatic C=C stretch), 1272 (C-O stretch), 1207 (C-N stretch), 1045 (C-O stretch), 839 (aromatic C=C bend), 715 (C-Br stretch); δ_{H} (DMSO-*d*₆, 300 MHz) 6.92-7.00 (2H, m, C(8)H & C(11)H), 7.28 (1H, ddd, *J* 8.2, 7.4, 1.6, C(4)H), 7.34 (1H, dd, *J* 8.2, 1.6, C(6)H), 7.51 (1H, ddd, *J* 8.2, 7.4, 1.6 C(5)H), 7.80 (1H, dd, *J* 8.1, 1.5, C(3)H), 8.11-8.22 (2H, m, C(9)H & C(10)H); δ_{C} (DMSO-*d*₆, 75.5 MHz) 115.1 (C(8)H & C(11)H), 115.3 (qC-2), 123.1 (C(6)H), 128.1 (C(4)H), 130.4 (C(5)H), 134.6 (C(3)H), 140.6 (C(9)H & C(10)H), 151.1 (qC-1), 154.2 (qC-7); Anal. Calculated for C₁₁H₈BrNO₂: C, 49.65; H, 3.03. Found: C, 49.47; H, 3.07.

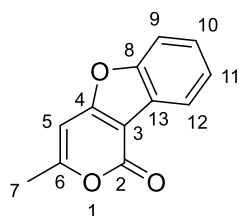
6.4 Palladium catalysed intramolecular double C-H activation

6.4.1 General procedures for intramolecular double C-H activation of 2-coumarins, 2-pyrones and related heterocycles. Synthesis of compounds 25, 41-51, 73-85.

Conditions A: Pyrone, coumarin (50 mg, 1.0 equiv.) or quinolone (50 mg, 1.0 equiv.), Pd(OAc)₂ (10 mol%), Ag₂O (1.5 equiv.), NaO^tBu (0.2 equiv.) and pivalic acid (PivOH) (0.5M) were added to a sealed reaction vial equipped with a magnetic stir bar. The resulting mixture was stirred at 140 °C under air atmosphere in a multi reaction heating mantle for 3 hours (pyrones) or 16 hours (coumarins and quinolone). Upon cooling, the mixture was diluted with DCM and filtered through a plug of Celite[®]. The reaction mixture was then diluted with DCM (15 mL) and washed with aqueous NaOH (10% w/v, 3 x 15 mL). The organic layer was then dried over MgSO₄, filtered and concentrated under reduced pressure. The residues were then flushed through silica gel using DCM as eluent to afford the title products, which were purified by recrystallisation from DCM:hexanes.

Conditions B: Pyrone, coumarin (50 mg, 1.0 equiv.) or quinolone (50 mg, 1.0 equiv.), Pd(OAc)₂ (5 mol%), Ag₂O (1.5 equiv.), K₂CO₃ (2.5 equiv.) and TFA (0.4M) were added to a sealed reaction vial equipped with a stir bar. The resulting mixture was stirred at 140 °C under air atmosphere in a multi reaction heating mantle for 16 hours (pyrones and coumarins) or 21 hours (quinolone). Upon cooling, the reaction mixture was concentrated under reduced pressure. The residue was flushed through silica gel using DCM as eluent to afford the title products, which were purified by recrystallisation from DCM:hexanes.

3-Methyl-1*H*-pyrano[4,3-*b*]benzofuran-1-one (25)²⁻³



Conditions A. White solid (74 mg, 52%)

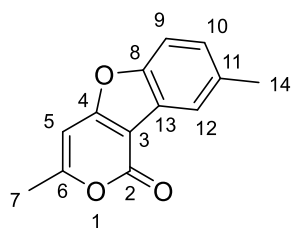
Conditions B. White solid (77 mg, 56%)

Compound **24** (141 mg, 0.70 mmol, 1.0 equiv.) was used as the substrate in the general procedure **6.4.1**. m.p. 190-191 °C (lit. 187-188 °C); δ_{H} (CDCl₃, 300 MHz) 2.43 (3H, s, C(7)H₃), 6.54 (1H, s, C(5)H), 7.36-7.47 (2H, m, C(9)H & C(11)H), 7.50-7.58 (1H, m, C(10)H), 7.97-8.10 (1H, m, C(12)H); δ_{C} (CDCl₃, 75.5 MHz) 20.6 (C(7)H₃), 95.9 (C(5)H), 103.7 (qC-

3), 111.5 (C(9)H), 121.4 (C(12)H), 122.9 (qC-13), 125.0 (C(11)H), 126.1 (C(10)H), 154.9 (qC-8), 159.5 (qC-6), 162.9 (qC-2), 164.5 (qC-4); m/z (ES⁺): 201, [(M+H)⁺, 80%].

Spectral characteristics were consistent with previously reported data.²⁻³

3,8-Dimethyl-1H-pyrano[4,3-b]benzofuran-1-one (41)²⁻³

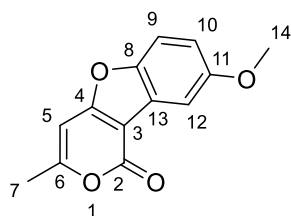


Conditions A. White solid (25 mg, 56%)

Compound **30** (45 mg, 0.21 mmol, 1.0 equiv.) was used as the substrate in the general procedure **6.4.1**. m.p. 159-160 °C (lit. 159-160 °C); δ_{H} (CDCl₃, 300 MHz) 2.41 (3H, d, *J* 0.9, C(7)H₃), 2.48 (3H, s, C(14)H₃), 6.50 (1H, d, *J* 0.9, C(5)H), 7.17-7.23 (1H, m, C(9)H), 7.40 (1H, d, *J* 8.5, C(10)H), 7.80-7.85 (1H, m, C(12)H); δ_{C} (CDCl₃, 75.5 MHz) 20.6 (C(7)H₃), 21.3 (C(14)H₃), 96.0 (C(5)H), 103.5 (qC-3), 110.9 (C(9)H), 121.2 (C(12)H), 122.9 (qC-13), 127.2 (C(10)H), 134.8 (qC-11), 153.4 (qC-8), 159.6 (qC-6), 162.6 (qC-2), 164.6 (qC-4); m/z (ES⁺): 215, [(M+H)⁺, 100%].

Spectral characteristics were consistent with previously reported data.²⁻³

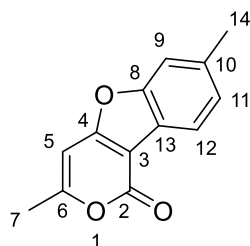
8-Methoxy-3-methyl-1H-pyrano[4,3-b]benzofuran-1-one (42)²⁻³



Conditions A. White solid (22 mg, 42%)

Compound **31** (53 mg, 0.23 mmol, 1.0 equiv.) was used as the substrate in the general procedure **6.4.1**. m.p. 152-154 °C (lit. 152-154 °C); δ_{H} (CDCl₃, 300 MHz) 2.42 (3H, s, C(7)H₃), 3.89 (3H, s, C(14)H₃), 6.50 (1H, s, C(5)H), 6.97 (1H, dd, *J* 9.0, 2.7, C(9)H), 7.45 (2H, dd, *J* 7.4, 5.8, C(10)H & C(12)H); δ_{C} (CDCl₃, 75.5 MHz) 20.6 (C(7)H₃), 56.0 (C(14)H₃), 96.0 (C(5)H), 103.3 (C(9)H), 103.9 (qC-3), 112.0 (C(12)H), 115.1 (C(10)H), 123.7 (qC-13), 149.6 (qC-11), 157.5 (qC-8), 159.6 (qC-6), 162.6 (qC-2), 165.0 (qC-4); m/z (ES⁺): 231, [(M+H)⁺, 100%].

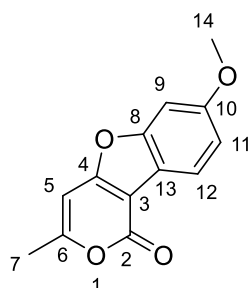
Spectral characteristics were consistent with previously reported data.²⁻³

7-Methyl-3-methyl-1*H*-pyrano[4,3-*b*]benzofuran-1-one 48a²⁻³

Conditions A. Yellow solid (65 mg, 44%)

Compound **34** (150 mg, 0.69 mmol, 1.0 equiv.) was used as the substrate in the general procedure **6.4.1**. m.p. 138-139 °C (lit. 139-141 °C); δ_{H} (CDCl₃, 300 MHz) 2.41 (3H, d, *J* 0.8, C(7)H₃), 2.50 (3H, s, C(14)H₃), 6.51 (1H, s, C(5)H), 7.23 (1H, d, *J* 7.3, C(11)H), 7.34 (1H, s, C(9)H), 7.89 (1H, d, *J* 7.9, C(12)H); δ_{C} (CDCl₃, 75.5 MHz) 20.5 (C(7)H₃), 21.8 (C(14)H₃), 96.0 (C(5)H), 103.7 (qC-3), 111.7 (C(9)H), 120.2 (qC-13), 120.8 (C(12)H), 126.2 (C(11)H), 136.7 (qC-10), 155.4 (qC-8), 159.6 (qC-6), 162.4 (qC-2), 164.2 (qC-4); *m/z* (ES⁺): 215, [(M+H)⁺, 100%].

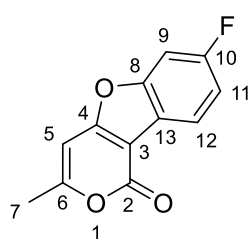
Spectral characteristics were consistent with previously reported data.²⁻³

7-Methoxy-3-methyl-1*H*-pyrano[4,3-*b*]benzofuran-1-one (49a)²⁻³

Conditions A. White solid (12 mg, 20%)

Compound **35** (60 mg, 0.26 mmol, 1.0 equiv.) was used as the substrate in the general procedure **6.4.1**. m.p. 164-166 °C (lit. 158-159 °C); δ_{H} (CDCl₃, 300 MHz) 2.41 (3H, s, C(7)H₃), 3.88 (3H, s, OC(14)H₃), 6.50 (1H, s, C(5)H), 7.01 (1H, dd, *J* 8.6, 2.2, C(11)H), 7.07 (1H, d, *J* 2.1, C(9)H), 7.88 (1H, d, *J* 8.5, C(12)H); δ_{C} (CDCl₃, 75.5 MHz) 20.5 (C(7)H₃), 55.8 (OC(14)H₃), 95.9 (C(5)H), 96.8 (C(9)H), 103.8 (qC-3), 113.0 (C(11)H), 115.9 (qC-13), 121.5 (C(12)H), 156.1 (qC-8), 159.2 (qC-10), 159.6 (qC-6), 161.7 (qC-2), 164.0 (qC-4); *m/z* (ES⁺): 231, [(M+H)⁺, 100%].

Spectral characteristics were consistent with previously reported data.²⁻³

7-Fluoro-3-methyl-1*H*-pyrano[4,3-*b*]benzofuran-1-one (50a)²⁻³

Conditions A. White solid (64 mg, 65%)

Compound **36** (100 mg, 0.45 mmol, 1.0 equiv.) was used as the substrate in the general procedure **6.4.1**. m.p. 207-209 °C (lit. 201-202 °C); δ_{H} (CDCl₃, 300 MHz) 2.43 (3H, d, *J* 0.8, C(7)H₃), 6.53 (1H, d, *J* 0.9, C(5)H),

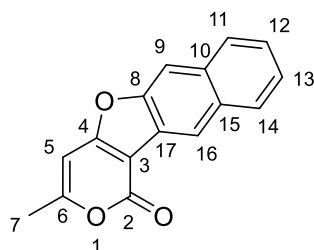
7.17 (1H, ddd, J 9.4, 8.6, 2.3, C(11)H), 7.25-7.30 (1H, m, C(9)H), 7.96 (1H, dd, J 8.6, 5.4, C(12)H); δ_{C} (CDCl₃, 75.5 MHz) 20.6 (C(7)H₃), 95.8 (C(5)H), 99.8 (C(9)H, d, $J_{\text{C-F}}$ 27), 103.5 (qC-3), 113.0 (C(11)H, d, $J_{\text{C-F}}$ 24), 119.2 (qC-13, d, $J_{\text{C-F}}$ 2), 121.8 (C(12)H, d, $J_{\text{C-F}}$ 10), 154.9 (qC-8, d, $J_{\text{C-F}}$ 20), 159.3 (qC-6), 161.5 (qC-10, d, $J_{\text{C-F}}$ 246), 162.8 (qC-2), 165.0 (qC-4); m/z (ES⁺): 219, [(M+H)⁺, 100%].

Spectral characteristics were consistent with previously reported data.²⁻³

3-Methyl-1*H*-naphtho[2',3':4,5]furo[3,2-*c*]pyran-1-one (51a)³ and 9-Methyl-7*H*-naphtho[2',1':4,5]furo[3,2-*c*]pyran-7-one (51b)³

Compound **40** (100 mg, 0.396 mmol, 1.0 equiv.) was used as the substrate in the general procedure **6.4.1**. Compounds **51a** and **51b** were obtained as a mixture with a ratio of 80:20 (**Conditions A** and **Conditions B**) determined from the ¹H NMR spectrum of the crude reaction mixture.

3-Methyl-1*H*-naphtho[2',3':4,5]furo[3,2-*c*]pyran-1-one (51a)³

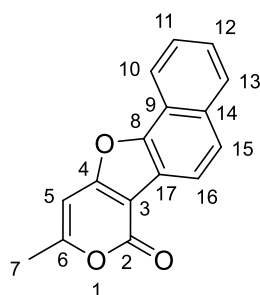


Conditions A. White solid (13 mg, 13%)

Conditions B. White solid (11 mg, 11%)

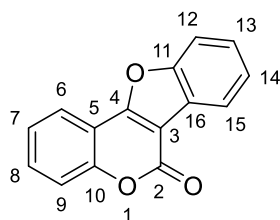
m.p. 157-159 °C; $\nu_{\text{max}}/\text{cm}^{-1}$ (NaCl): 1727 (ester C=O stretch), 1572 (alkene C=C stretch), 1261 (ester C-O stretch), 1096 (ether C-O stretch); δ_{H} (CDCl₃, 300 MHz) 2.47 (3H, d, J 0.7, C(7)H₃), 6.58 (1H, d, J 0.8, C(5)H), 7.49-7.56 (2H, m, C(12)H & C(13)H), 7.91-7.98 (2H, m, C(9)H & C(11)H), 8.00-8.06 (1H, m, C(14)H), 8.49 (1H, s, C(16)H); δ_{C} (CDCl₃, 75.5 MHz) 20.9 (C(7)H₃), 96.1 (C(5)H), 103.0 (qC-3), 107.5 (C(9)H), 119.8 (C(16)H), 122.9 (qC-17), 125.3 (C(13)H), 126.0 (C(12)H), 128.0 (C(11)H), 128.4 (C(14)H), 131.4 (qC-15), 131.9 (qC-10), 153.6 (qC-8), 159.4 (qC-6), 164.5 (qC-2), 166.9 (qC-4); m/z (ES⁺): 251, [(M+H)⁺, 10%]; HRMS (ESI-TOF) Exact mass calculated for C₁₆H₁₁O₃ [M+H⁺], 251.0708. Found 251.0713.

Spectral characteristics were consistent with previously reported data.³

9-Methyl-7H-naphtho[2',1':4,5]furo[3,2-c]pyran-7-one (51b)³**Conditions A.** White solid (25 mg, 25%)**Conditions B.** White solid (36 mg, 37%)

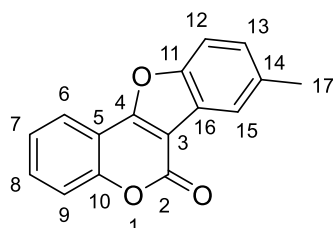
m.p. 164-167 °C; $\nu_{\text{max}}/\text{cm}^{-1}$ (NaCl): 1735 (ester C=O stretch), 1652 (alkene C=C stretch), 1566 (aromatic C=C stretch); δ_{H} (CDCl_3 , 300 MHz) 2.46 (3H, d, J 0.9, C(7) H_3), 6.60 (1H, d, J 0.9, C(5) H), 7.57 (1H, ddd, J 8.2, 6.9, 1.3, C(11) H), 7.65-7.74 (2H, m, C(12) H & C(15) H), 7.86 (1H, d, J 8.9, C(16) H), 7.95 (1H, d, J 8.2, C(13) H), 9.59-9.66 (1H, m, C(10) H); δ_{C} (CDCl_3 , 75.5 MHz) 20.4 (C(7) H_3), 96.0 (C(5) H), 105.7 (qC-3), 111.5 (C(16) H), 118.6 (qC-17), 125.7 (C(15) H), 127.1 (C(10) H), 127.3 (C(12) H), 127.8 (C(11) H), 128.0 (qC-9), 128.4 (C(13) H), 131.3 (qC-14), 152.6 (qC-8), 160.0 (qC-2), 162.0 (qC-6), 163.8 (qC-4); m/z (ES⁺): 251, [(M+H)⁺, 10%]; HRMS (ESI-TOF) Exact mass calculated for $\text{C}_{16}\text{H}_{11}\text{O}_3$ [M+H⁺], 251.0708. Found 250.0705.

Spectral characteristics were consistent with previously reported data.³

6H-Benzofuro[3,2-c]chromen-6-one (73)²⁻³**Conditions A.** White solid, (46 mg, 92%)**Conditions B.** White solid, (38 mg, 75%)

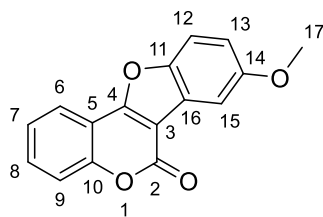
4-Phenoxy-2-coumarin (**55**) was used as the substrate in the general Procedure **6.4.1**. m.p. 177-180 °C (lit. 177-180 °C); δ_{H} (CDCl_3 , 300 MHz) 7.38-7.55 (4H, m, C(7) H , C(9) H , C(13) H & C(14) H), 7.59-7.72 (2H, m, C(8) H & C(12) H), 8.05 (1H, dd, J 7.8, 1.3, C(6) H), 8.12-8.19 (1H, m, C(15) H); δ_{C} (CDCl_3 , 75.5 MHz) 105.9 (qC-3), 111.8 (C(12) H), 112.6 (qC-5), 117.5 (C(9) H), 121.9 (C(6) H & C(15) H), 123.4 (qC-16), 124.7 (C(7) H), 125.2 (C(14) H), 126.8 (C(13) H), 132.0 (C(8) H), 153.7 (qC-10), 155.5 (qC-11), 158.1 (qC-2), 160.0 (qC-4); m/z (ES⁺): 237, [(M+H)⁺, 20%]; HRMS (ESI-TOF): Exact mass calculated for $\text{C}_{15}\text{H}_9\text{O}_3$ [M+H⁺], 237.0552. Found 237.0547.

Spectral characteristics were consistent with previously reported data.²⁻³

8-Methyl-6H-benzofuro[3,2-c]chromen-6-one (74)^{3, 35}**Conditions A.** Light brown solid, (36 mg, 72%)**Conditions B.** Light brown solid, (32 mg, 65%)

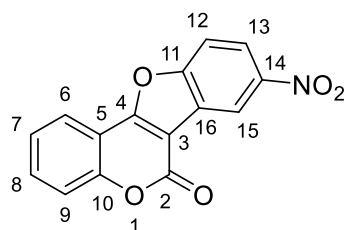
4-(4-Methylphenoxy)-2*H*-chromene-2-one (**56**) was used as the substrate in the general procedure **6.4.1**. m.p. 189-190 °C (lit. 201-202 °C); δ_{H} (CDCl₃, 300 MHz) 2.52 (3H, s, C(17)H₃), 7.27-7.31 (1H, m, C(13)H), 7.38-7.46 (1H, m, C(7)H), 7.48-7.67 (3H, m, C(7)H, C(9)H & C(15)H), 7.93-7.97 (1H, m, C(8)H), 8.03 (1H, dd, *J* 7.8, 1.5, C(6)H); δ_{C} (CDCl₃, 75.5 MHz) 21.4 (C(17)H₃), 105.7 (qC-3), 111.2 (C(12)H), 112.8 (qC-5), 117.5 (C(9)H), 121.7 (C(15)H), 121.8 (C(13)H), 123.5 (qC-16), 124.6 (C(6)H), 128.0 (C(7)H), 131.8 (C(8)H), 135.2 (qC-14), 153.6 (qC-10), 154.0 (qC-11), 158.3 (qC-2), 160.1 (qC-4); m/z (ES⁺): 251, [(M+H)⁺, 100%].

Spectral characteristics were consistent with previously reported data.^{3, 35}

8-Methoxy-6H-benzofuro[3,2-c]chromen-6-one (75)^{3, 36}**Conditions A.** Yellow solid, (38 mg, 77%)**Conditions B.** Yellow solid, (21 mg, 42%)

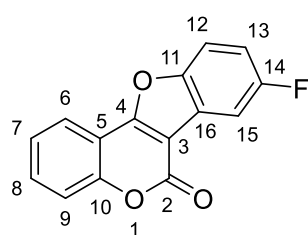
4-(4-Methoxyphenoxy)-2*H*-chromene-2-one (**57**) was used as the substrate in the general procedure **6.4.1**. m.p. 224-227 °C (lit. 229-230 °C); δ_{H} (CDCl₃, 300 MHz) 3.92 (3H, s, C(17)H₃), 7.05 (1H, dd, *J* 9.0, 2.7, C(13)H), 7.41 (1H, ddd, *J* 7.8, 7.3, 1.2, C(7)H), 7.47-7.65 (4H, m, C(6)H, C(8)H, C(9)H & C(12)H), 8.00 (1H, dd, *J* 7.8, 1.6, C(15)H); δ_{C} (CDCl₃, 75.5 MHz) 56.0 (C(17)H₃), 103.4 (C(16)H), 106.0 (qC-3), 112.4 (C(13)H), 112.8 (qC-5), 116.1 (C(12)H), 117.5 (C(9)H), 121.8 (C(6)H), 124.2 (qC-16), 124.7 (C(7)H), 131.8 (C(8)H), 150.3 (qC-14), 153.5 (qC-11), 157.6 (qC-10), 158.3 (qC-2), 160.4 (qC-4); m/z (ES⁺): 267, [(M+H)⁺, 100%].

Spectral characteristics were consistent with previously reported data.^{3, 36}

8-Nitro-6*H*-benzofuro[3,2-*c*]chromen-6-one (76)³**Conditions A.** Orange solid, (47 mg, 95%)**Conditions B.** Orange solid, (35 mg, 70%)

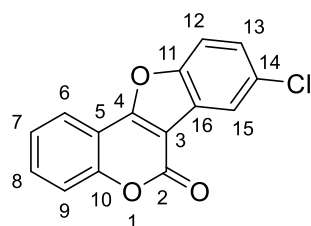
4-(4-Nitrophenoxy)-2*H*-chromene-2-one (**59**) was used as the substrate in the general procedure **6.4.1**. m.p. >230 °C; $\nu_{\text{max}}/\text{cm}^{-1}$ (NaCl): 1746 (ester C=O stretch), 1531 (aromatic C=C stretch), 1350 (N=O stretch), 1085 (ester C-O stretch), 1057 (ether C-O stretch); δ_{H} (CDCl₃, 300 MHz) 7.44-7.52 (1H, m, C(7)H), 7.56 (1H, d, *J* 7.9, C(9)H), 7.71 (1H, ddd, *J* 8.8, 7.3, 1.6, C(8)H), 7.81 (1H, d, *J* 9.1, C(12)H), 8.07 (1H, dd, *J* 7.9, 1.4, C(6)H), 8.43 (1H, dd, *J* 9.1, 2.4, C(13)H), 9.05 (1H, d, *J* 2.2, C(15)H); δ_{C} (CDCl₃, 75.5 MHz) 105.9 (qC-3), 111.9 (qC-5), 112.4 (C(12)H), 117.8 (C(9)H), 118.1 (C(15)H), 122.1 (C(6)H), 122.5 (C(13)H), 124.4 (qC-16), 125.2 (C(7)H), 133.3 (C(8)H), 145.8 (qC-14), 154.1 (qC-10), 157.0 (qC-11), 157.9 (qC-2), 162.5 (qC-4); HRMS (ESI-TOF): Exact mass calculated for C₁₅H₈NO₅ [M+H⁺], 282.0402. Found 282.0396.

Spectral characteristics were consistent with previously reported data.³

8-Fluoro-6*H*-benzofuro[3,2-*c*]chromen-6-one (77)^{3, 35}**Conditions A.** Yellow solid, (40 mg, 80%)**Conditions B.** Yellow solid, (48 mg, 85%)

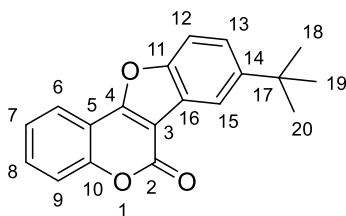
4-(4-Fluorophenoxy)-2*H*-chromene-2-one (**58**) was used as the substrate in the general procedure **6.4.1**. m.p. 224-225 °C (lit. 223-224 °C); δ_{H} (CDCl₃, 300 MHz) 7.15-7.24 (1H, td, *J* 18.0, 9.0, 2.7, C(13)H), 7.38-7.47 (1H, m, C(15)H), 7.48-7.55 (1H, dd, *J* 8.4, 0.7, C(9)H), 7.58-7.68 (2H, m, C(7)H & C(12)H), 7.77 (1H, dd_{app}, *J* 7.9, 2.7, C(8)H), 7.99-8.05 (1H, dd, *J* 7.9, 1.5, C(6)H); δ_{C} (CDCl₃, 75.5 MHz) 106.0 (qC-3, d, *J*_{C-F} 4), 107.8 (C(15)H, d, *J*_{C-F} 21), 112.7 (C(12)H, d, *J*_{C-F} 10), 112.5 (qC-5), 114.5 (C(13)H, d, *J*_{C-F} 21), 117.6 (C(9)H), 118.3 (C(6)H), 121.9 (C(7)H), 124.6 (qC-16, d, *J*_{C-F} 12), 132.4 (C(8)H), 151.6 (qC-11), 153.8 (qC-10), 157.7 (qC-2), 160.4 (qC-14, d, *J*_{C-F} 237), 161.6 (qC-4); *m/z* (ES⁺): 255, [(M+H)⁺, 20%].

Spectral characteristics were consistent with previously reported data.^{3, 35}

8-Chloro-6H-benzofuro[3,2-c]chromen-6-one (78)^{3, 35}**Conditions A.** Light brown solid, (49 mg, 99%)**Conditions B.** Light brown solid, (49 mg, 99%)

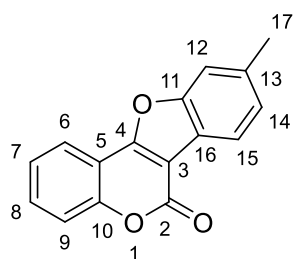
4-(4-Chlorophenoxy)-2H-chromene-2-one (**60**) was used as the substrate in the general procedure **6.4.1**. m.p. 220-222 °C (lit. 227-228 °C); δ_{H} (CDCl₃, 300 MHz) 7.39-7.46 (2H, m, C(7)H & C(13)H), 7.48-7.53 (1H, dd, *J* 8.4, 0.7, C(12)H), 7.56-7.68 (2H, m, C(8)H & C(9)H), 8.00 (1H, dd, *J* 7.8, 1.5, C(6)H), 8.09-8.12 (1H, dd_{app}, *J* 2.2, 0.4, C(15)H); δ_{C} (CDCl₃, 75.5 MHz) 105.3 (qC-3), 112.3 (qC-5), 112.8 (C(12)H), 117.6 (C(9)H), 121.6 (C(15)H), 122.0 (C(6)H), 124.9 (C(7)H), Coverlapping qC-16), 127.0 (C(13)H), 131.1 (qC-14), 132.5 (C(8)H), 153.8 (qC-10), 153.8 (qC-11), 157.6 (qC-2), 161.0 (qC-4); m/z (ES⁺): 271, [(M+H)⁺, 100%].

Spectral characteristics were consistent with previously reported data.^{3, 35}

9-Tert-butyl-6H-benzofuro[3,2-c]chromen-6-one (79)³**Conditions A.** Yellow solid (27 mg, 56%)**Conditions B.** Yellow solid, (44mg, 89%)

4-(4-Tert-butylphenoxy)-2H-chromene-2-one (**61**) was used as the substrate in the general procedure **6.4.1**. m.p. 167-171°C; ν_{max} /cm⁻¹ (NaCl): 1743 (ester C=O stretch), 1630 (alkene C=C stretch), 1451 (aromatic C=C stretch), 1080 (ether C-O stretch), 754 (alkene C-H bend); δ_{H} (CDCl₃, 300 MHz) 1.43 (9H, s, C(18)H₃, C(19)H₃ & C(20)H₃), 7.38-7.46 (1H, m, C(13)H), 7.49-7.65 (4H, m, C(7)H, C(8)H, C(9)H & C(12)H), 8.00-8.06 (1H, dd, *J* 7.88, 1.54, C(6)H), 8.13-8.16 (1H, dd_{app}, *J* 1.93, 0.66, C(15)H); δ_{C} (CDCl₃, 75.5 MHz) 31.8 (C(18)H₃, C(19)H₃ & C(20)H₃), 35.1 (qC-17), 106.0 (qC-3), 111.0 (C(12)H), 112.8 (qC-5), 117.5 (C(9)H), 118.3 (C(15)H), 121.8 (C(6)H), 123.2 (qC-16), 124.6 (C(7)H), 124.7 (C(13)H), 131.8 (C(8)H), 148.8 (qC-14), 153.6 (qC-10), 153.8 (qC-11), 158.3 (qC-2), 160.2 (qC-4); m/z (ES⁺): 293, [(M+H)⁺, 97%]; HRMS (ESI-TOF): Exact mass calculated for C₁₉H₁₇O₃ [M+H⁺], 293.1162. Found 295.1488.

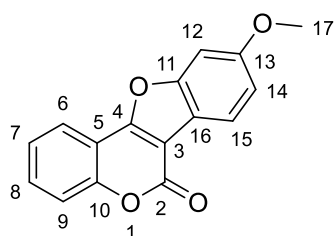
Spectral characteristics were consistent with previously reported data.³

9-Methyl-6H-benzofuro[3,2-c]chromen-6-one (80)^{3, 37}**Conditions A.** Light brown solid, (27 mg, 55%)**Conditions B.** Light brown solid, (28 mg, 57%)

4-(3-Methylphenoxy)-2*H*-chromene-2-one (**62**) was used as the substrate in the general procedure **6.4.1**. m.p. 182-185 °C (lit. 198-

200 °C); δ_{H} (CDCl₃, 300 MHz) 2.53 (3H, s, C(17)H₃), 7.22-7.29 (1H, m, C(12)H), 7.35-7.42 (1H, m, C(14)H), 7.42-7.51 (2H, m, C(7)H & C(9)H), 7.53-7.62 (1H, m, C(8)H), 7.93-8.03 (2H, m, C(6)H & C(15)H); δ_{C} (CDCl₃, 75.5 MHz) 22.0 (C(17)H₃), 106.0 (qC-3), 112.0 (C(12)H), 112.8 (qC-5), 117.3 (C(9)H), 120.8 (qC-16), 121.3 (C(14)H), 121.8 (C(6)H), 124.6 (C(7)H), 126.6 (C(15)H), 131.6 (C(8)H), 137.5 (qC-13), 153.5 (qC-10), 156.0 (qC-11), 158.2 (qC-2), 159.6 (qC-4); m/z (ES⁺): 251 [(M+H)⁺, 10%]; HRMS (ESI-TOF): Exact mass calculated for C₁₆H₁₁O₃ [M+H⁺], 251.0702. Found 251.0702.

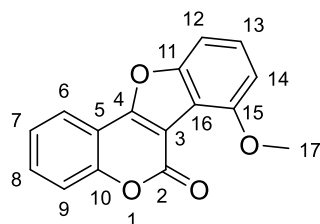
Spectral characteristics were consistent with previously reported data.^{3, 37}

9-Methoxy-6H-benzofuro[3,2-c]chromen-6-one (81a)^{3, 37}**Conditions A.** White solid, (16.4 mg, 33%)**Conditions B.** White solid, (19.2 mg, 38%)

4-(3-Methoxyphenoxy)-2*H*-chromene-2-one (**63**) was used as the substrate in the general procedure **6.4.1**. m.p. 210-211 °C (lit. 216

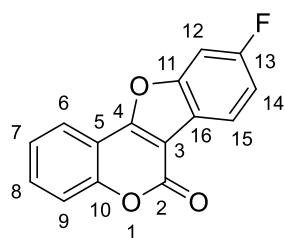
°C); δ_{H} (CDCl₃, 300 MHz) 3.92 (3H, s, C(17)H₃), 7.07 (1H, dd, *J* 8.6, 2.2, C(14)H), 7.20 (1H, d, *J* 2.2, C(12)H), 7.41 (1H, ddd, *J* 7.9, 7.2, 1.2, C(7)H), 7.50 (1H, dd, *J* 8.4, 0.8, C(9)H), 7.54-7.63 (1H, m, C(8)H), 7.96-8.03 (2H, m, C(6)H & C(15)H); δ_{C} (CDCl₃, 75.5 MHz) 56.9 (C(17)H₃), 96.8 (C(12)H), 106.1 (qC-3), 112.9 (qC-5), 113.6 (C(14)H), 116.5 (qC-16), 117.4 (C(9)H), 121.5 (C(15)H), 122.0 (C(6)H), 124.6 (C(7)H), 131.3 (C(8)H), 153.2 (qC-10), 156.8 (qC-11), 158.2 (qC-13), 159.3 (qC-2), 159.7 (qC-4); m/z (ES⁺): 267, [(M+H)⁺, 100%]; HRMS (ESI-TOF): Exact mass calculated for C₁₆H₁₁O₄ [M+H⁺], 267.0657. Found 267.0656.

Spectral characteristics were consistent with previously reported data.^{3, 37}

7-Methoxy-6H-benzofuro[3,2-c]chromen-6-one (81b)³**Conditions A.** (not isolated)**Conditions B.** White solid, (24 mg, 47%)

4-(3-Methoxyphenoxy)-2*H*-chromene-2-one (**63**) was used as the substrate in the general procedure **6.4.1**. m.p. 200-201 °C; $\nu_{\text{max}}/\text{cm}^{-1}$ (NaCl): 1746 (ester C=O stretch), 1627 (alkene C=C stretch), 1502 (aromatic C=C stretch), 1364 (ester C-O stretch), 1271 (ether C-O stretch); δ_{H} (CDCl₃, 300 MHz) 4.07 (3H, s, C(17)H₃), 6.90 (1H, d, *J* 8.1, C(14)H), 7.28 (1H, dd, *J* 8.1, 0.8, C(12)H), 7.35-7.52 (3H, m, C(7)H, C(9)H & C(13)H), 7.58 (1H, ddd, *J* 8.7, 7.2, 1.6, C(8)H), 8.01 (1H, dd, *J* 7.8, 1.2, C(6)H); δ_{C} (CDCl₃, 75.5 MHz) 55.9 (C(17)H₃), 96.7 (C(12)H), 106.0 (qC-3), 112.8 (qC-5), 113.6 (C(14)H), 116.4 (qC-16), 117.4 (C(9)H), 121.5 (C(13)H), 122.0 (C(6)H), 124.6 (C(7)H), 131.3 (C(8)H), 153.2 (qC-10), 156.8 (qC-11), 158.2 (qC-15), 159.3 (qC-2), 159.7 (qC-4); *m/z* (ES⁺): 267, [(M+H)⁺, 20%]; HRMS (ESI-TOF): Exact mass calculated for C₁₆H₁₁O₄ [M+H⁺], 267.0657. Found 267.0657.

Spectral characteristics were consistent with previously reported data.³

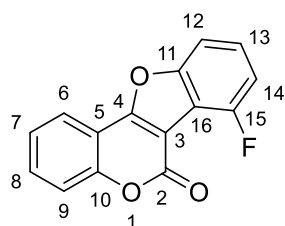
9-Fluoro-6H-benzofuro[3,2-c]chromen-6-one (82a)³**Conditions A.** White solid, (55.3 mg, 56%)**Conditions B.** White solid, (16.5 mg, 17%)

4-(3-Fluorophenoxy)-2*H*-chromene-2-one (**64**) (100 mg, 0.39 mmol, 1 equiv.) was used as the substrate in the general procedure **6.4.1**. m.p. >230 °C; $\nu_{\text{max}}/\text{cm}^{-1}$ (NaCl): 1754 (ester C=O stretch), 1632 (alkene C=C stretch), 1413 (C-F stretch), 1080 (ether C-O stretch), 750 (alkene C-H bend); δ_{H} (CDCl₃, 300 MHz) 7.22 (1H, dd, *J* 8.7, 2.2, C(14)H), 7.37-7.47 (2H, m, C(7)H & C(12)H), 7.52 (1H, d, *J* 7.7, C(9)H), 7.63 (1H, ddd, *J* 8.7, 7.3, 1.6, C(8)H), 8.02 (1H, dd, *J* 7.8, 1.5, C(6)H), 8.09 (1H, dd, *J* 8.6, 5.4, C(15)H); δ_{C} (CDCl₃, 75.5 MHz) 100.0 (C(12)H, d, *J*_{C-F} 26), 105.7 (qC-3), 112.5 (qC-5), 113.5 (C(14)H, d, *J*_{C-F} 25), 117.5 (C(9)H), 119.7 (qC-16, d, *J*_{C-F} 2), 121.7 (C(6)H), 122.4 (C(15)H, d, *J*_{C-F} 10), 124.8 (C(7)H), 132.0 (C(8)H), 153.5 (qC-10), 155.6 (qC-11, d, *J*_{C-F} 14), 157.8 (qC-2), 160.4 (qC-4, d, *J*_{C-F} 2), 163.6 (qC-

13, d, J_{C-F} 249); δ_F (CDCl₃, 282 MHz) -112.5; m/z (ES⁺): 255 [(M+H)⁺, 10%]; HRMS (ESI-TOF): Exact mass calculated for C₁₅H₈O₃F [M+H⁺], 255.0457. Found 255.0452.

Spectral characteristics were consistent with previously reported data.³

7-Fluoro-6*H*-benzofuro[3,2-*c*]chromen-6-one (82b)³



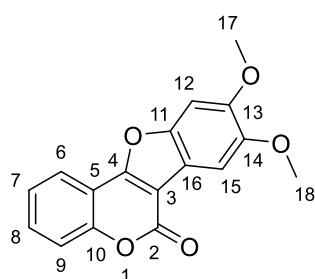
Conditions A. (12 mg, 12%)

Conditions B. White solid, (7 mg, 7%)

4-(3-Fluorophenoxy)-2*H*-chromene-2-one (**64**) was used as the substrate in the general procedure **6.4.1**. m.p. >230 °C ν_{max}/cm^{-1} (NaCl): 1748 (ester C=O stretch), 1634 (alkene C=C stretch), 1089 (ether C-O stretch), 741 (C-F stretch); δ_H (CDCl₃, 300 MHz) 7.18 (1H, ddd, J 9.0, 7.6, 1.3, C(14)H), 7.38-7.56 (4H, m, C(7)H, C(9)H, C(12)H & C(13)H), 7.64 (1H, ddd, J 8.7, 7.3, 1.6, C(8)H), 8.04 (1H, dd, J 7.8, 1.4, C(6)H); δ_C (CDCl₃, 75.5 MHz) 104.7 (qC-3, d, J_{C-F} 4), 108.0 (C(12)H, d, J_{C-F} 5), 111.9 (C(14)H, d, J_{C-F} 20), 112.1 (qC-5), 117.5 (C(9)H), 122.0 (C(6)H), 112.6 (qC-16, d, J_{C-F} 22), 124.7 (C(7)H), 127.8 (C(13)H, d, J_{C-F} 8), 132.4 (C(8)H), 154.0 (qC-10), 156.3 (qC-15, d, J_{C-F} 257), 156.6 (qC-2), 157.0 (qC-11, d, J_{C-F} 9), 160.2 (qC-4, d, J_{C-F} 1); δ_F (CDCl₃, 282 MHz) -111.0; m/z (ES⁺): 255 [(M+H)⁺, 10%]; HRMS (ESI-TOF): Exact mass calculated for C₁₅H₈O₃F [M+H⁺], 255.0457. Found 255.0455.

Spectral characteristics were consistent with previously reported data.³

8, 9-Dimethoxy-6*H*-benzofuro[3,2-*c*]chromen-6-one (83)^{3, 37}



Conditions A. Yellow solid, (38 mg, 76%)

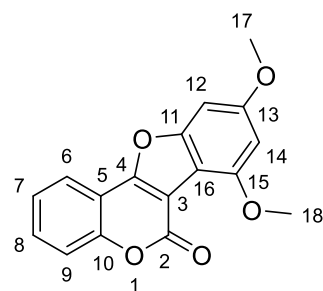
Conditions B. Yellow solid, (22 mg, 43%)

4-(3,4-Dimethoxyphenoxy)-2*H*-chromene-2-one (**67**) was used as the substrate in the general procedure **6.4.1**. m.p. 214-215 °C (lit. 219-220 °C); δ_H (CDCl₃, 300 MHz) 3.99 (3H, s, C(18)H₃), 4.01 (3H, s, C(17)H₃), 7.19 (1H, s, C(12)H), 7.35-7.43 (1H, m, C(7)H), 7.48 (1H, dd, J 8.4, 0.8, C(9)H), 7.51 (1H, s, C(15)H), 7.53-7.60 (1H, m, C(8)H) 7.95 (1H, dd, J 7.8, 1.3, C(6)H); δ_C (CDCl₃, 75.5 MHz) 56.5 (C(17)H₃ &

C(18)H₃), 95.5 (C(12)H), 102.2 (C(15)H), 106.3 (qC-3), 113.0 (qC-5), 115.4 (qC-16), 117.4 (C(9)H), 121.3 (C(6)H), 124.6 (C(7)H), 131.1 (C(8)H), 148.1 (qC-13), 149.6 (qC-14), 150.4 (qC-11), 153.0 (qC-10), 158.5 (qC-2), 158.9 (qC-4); m/z (ES⁺): 297, [(M+H)⁺, 20%].

Spectral characteristics were consistent with previously reported data.^{3, 37}

7,9-Dimethoxy-6*H*-benzofuro [3,2-*c*]chromen-6-one (84)³



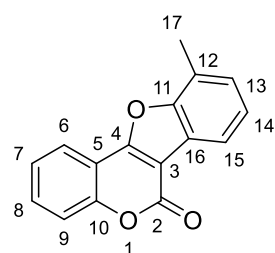
Conditions A. Orange solid, (48 mg, 98%)

Conditions B. Orange solid, (24 mg, 48%)

4-(3,5-Dimethoxyphenoxy)-2*H*-chromene-2-one (**66**) was used as the substrate in the general procedure **6.4.1**. m.p. 218-220 °C; $\nu_{\max}/\text{cm}^{-1}$ (NaCl): 1742 (ester C=O stretch), 1628 (alkene C=C stretch), 1508 (aromatic C=C stretch), 1304 (ester C-O stretch), 1149 (ether C-O stretch), 1088 (ether C-O stretch); δ_{H} (CDCl₃, 300 MHz) 3.90 (3H, s, C(17)H₃), 4.02 (3H, s, C(18)H₃), 6.48 (1H, d, *J* 2.0, C(12)H), 6.78 (1H, d, *J* 2.0, C(14)H), 7.36 (1H, ddd, *J* 8.3, 7.2, 1.3, C(7)H), 7.43-7.59 (2H, m, C(8)H & C(9)H), 7.94 (1H, dd, *J* 7.8, 1.2, C(6)H); δ_{C} (CDCl₃, 75.5 MHz) 55.9 (C(17)H₃), 56.3 (C(18)H₃), 88.6 (C(12)H), 96.5 (C(14)H), 106.1 (qC-16), 106.8 (qC-3), 112.5 (qC-5), 117.1 (C(9)H), 121.3 (C(6)H), 124.4 (C(7)H), 131.1 (C(8)H), 153.1 (qC-10), 155.0 (qC-11), 157.1 (qC-13), 157.7 (qC-15), 158.4 (qC-2), 161.0 (qC-4); m/z (ES⁺): 297, [(M+H)⁺, 100%]; HRMS (ESI-TOF): Exact mass calculated for C₁₇H₁₃O₅ [M+H⁺], 297.0763. Found 297.0758.

Spectral characteristics were consistent with previously reported data.³

10-Methyl-6*H*-benzofuro [3,2-*c*]chromen-6-one (85)³



Conditions A. Orange solid, (36 mg, 72%)

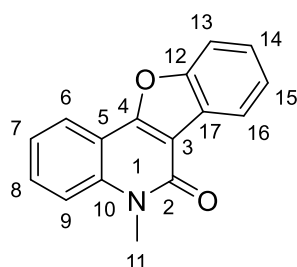
Conditions B. Orange solid, (21 mg, 41%)

4-(2-Methylphenoxy)-2*H*-chromene-2-one (**65**) was used as the substrate in the general procedure **6.4.1**. m.p. 123-125 °C $\nu_{\max}/\text{cm}^{-1}$ (NaCl): 1735 (ester C=O stretch), 1627 (alkene C=C stretch), 1597 (aromatic C=C stretch), 1371

(ester C-O stretch), 1082 (ether C-O stretch); δ_{H} (CDCl_3 , 300 MHz) 2.63 (3H, s, C(17) H_3), 7.20-7.44 (3H, m, C(7) H , C(13) H & C(14) H), 7.48 (1H, d, J 7.7, C(9) H), 7.59 (1H, ddd, J 8.7, 7.3, 1.6, C(8) H), 7.94 (1H, d, J 7.6, C(6) H), 8.04 (1H, dd, J 7.8, 1.4, C(15) H); δ_{C} (CDCl_3 , 75.5 MHz) 15.0 (C(17) H_3), 106.2 (qC-3), 112.8 (qC-5), 117.5 (C(9) H), 119.3 (C(13) H), 121.9 (C(6) H), 122.1 (qC-12), 123.0 (qC-16), 124.6 (C(7) H), 125.3 (C(15) H), 127.9 (C(14) H), 131.8 (C(8) H), 153.6 (qC-10), 154.6 (qC-11), 158.3 (qC-2), 159.7 (qC-4); m/z (ES $^+$): 251, [(M+H) $^+$, 10%]. HRMS (ESI-TOF): Exact mass calculated for $\text{C}_{16}\text{H}_{11}\text{O}_3$ [M+H $^+$], 251.0702. Found 251.0704.

Spectral characteristics were consistent with previously reported data.³

5-Methylbenzofuro[3,2-*c*]quinolin-6(5*H*)-one (**101**)^{3, 38}



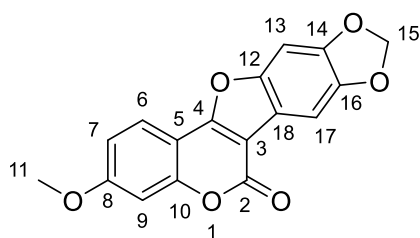
Conditions A. White solid, (26.2 mg, 30%)

Modified Conditions B. Compound **100** (50 mg, 0.20 mmol, 1.0 equiv.), Pd(OAc)₂ (5 mol%), Ag₂O (1.5 equiv.), K₂CO₃ (2.5 equiv.) and TFA (0.4 M) were added to a reaction vial. The resulting mixture was stirred at 120 °C under air atmosphere in a multi reaction

heating mantle for 21 hours. Upon cooling, the reaction mixture was concentrated under reduced pressure. The crude product was purified by column chromatography using hexanes/EtOAc, 90/10 as eluent to afford title product **101**. White solid, (26 mg, 33%), m.p.: 195-197 °C (lit. 202-204 °C); δ_{H} (CDCl_3 , 300 MHz) 3.75 (3H, s, NC(11) H_3), 7.27 (1H, t, J 7.5, C(7) H), 7.31-7.43 (3H, m, C(9) H , C(14) H & C(15) H), 7.47-7.60 (2H, m, C(13) H & C(8) H), 8.14 (2H, ddd, J 8.9, 6.4, 1.4, C(6) H & C(16) H); δ_{C} (CDCl_3 , 75.5 MHz) 29.2 (NC(11) H_3), 110.3 (qC-3), 111.3 (C(13) H), 112.8 (qC-5), 115.1 (C(9) H), 122.2 (C(6) H), 122.3 (C(15) H & C(16) H), 124.4 (C(7) H), 124.5 (qC-17), 126.1 (C(14) H), 130.7 (C(8) H), 139.4 (qC-10), 155.4 (qC-12), 157.3 (qC-2), 159.6 (qC-4); m/z (ES $^+$): 250, [(M+H) $^+$, 100%]. HRMS (ESI-TOF): Exact mass calculated for $\text{C}_{16}\text{H}_{12}\text{O}_2\text{N}$ [M+H $^+$], 250.0868. Found 250.0868.

Spectral characteristics were consistent with previously reported data.^{3, 38}

3-Methoxy-6*H*-[1,3]dioxolo[4',5':5,6]benzofuro[3,2-*c*]chromen-6-one, flemichapparin C (90a)^{2-3, 39-40}



Conditions A. Compound **89** (100 mg, 0.32 mmol, 1.0 equiv.) was used as the substrate in the general procedure **6.4.1** (stirred at 140 °C for 16 hours). Compounds **90a** and **90b** were obtained as a mixture with a ratio of 84:16 determined from the ¹H NMR spectrum of the crude

reaction mixture. After column chromatography (hexanes:EtOAc, 80:20), the major regioisomer **90a** (flemichapparin C) was isolated as a white solid (18 mg, 23%) with the remainder as an inseparable mixture (combined yield: 81 mg, 82%). m.p. >230 °C (lit. >230 °C); δ_{H} (CDCl₃, 300 MHz) 3.91 (3H, s, C(11)H₃), 6.07 (2H, s, C(15)H₂), 6.97 (2H, dd, *J* 7.9, 2.0, C(7)H & C(9)H), 7.12 (1H, s, C(13)H), 7.47 (1H, s, C(17)H), 7.85 (1H, dd, *J* 7.5, 1.6, C(6)H); δ_{C} (CDCl₃, 75.5 MHz) 56.0 (C(11)H₃), 94.0 (C(13)H), 100.2 (C(15)H₂), 101.5 (C(17)H), 102.0 (C(9)H), 104.0 (qC-3), 106.3 (qC-5), 113.0 (C(7)H), 117.1 (qC-18), 122.3 (C(6)H), 146.1 (qC-16), 147.5 (qC-14), 150.6 (qC-12), 155.0 (qC-10), 158.5 (qC-8), 160.0 (qC-2), 162.5 (qC-4); *m/z* (ES⁺): 311, [(M+H)⁺, 80%]; HRMS (ESI-TOF): Exact mass calculated for C₁₇H₁₁O₆ [M+H⁺], 311.0556. Found 311.0551.

Spectral characteristics were consistent with previously reported data.^{2-3, 39-40}

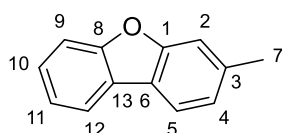
6.4.2 General procedures for intramolecular double C-H activation of diarylethers. Synthesis of compounds 131-137.

Conditions A: Diarylether (1 equiv.), Pd(OAc)₂ (10 mol%), Ag₂O (1.5 equiv.), NaO^tBu (0.2 equiv.) and pivalic acid (PivOH) (0.5M) were added to a sealed reaction vial equipped with a magnetic stir bar. The resulting reaction mixture was stirred at 140 °C under air atmosphere in a multi reaction heating mantle for 18 hours. Work-up as per 0.3 mmol diarylether: Upon cooling, the reaction was diluted with DCM (15 mL), filtered through a pipette of Celite[®] and then washed with aqueous NaOH (10% w/v, 3 x 15 mL). The organic layer was then dried over MgSO₄, filtered and concentrated under reduced pressure. The residues were then flushed through silica gel using hexanes or DCM as eluent to afford the title products.

Conditions B: Diarylether (1 equiv.), Pd(OAc)₂ (5 mol%), Ag₂O (1.5 equiv.), K₂CO₃ (2.5 equiv.) and TFA (0.4M) were added to a sealed reaction vial equipped with a magnetic stir bar. The resulting reaction mixture was stirred at 140 °C under air atmosphere in a multi reaction heating mantle for 18-24 hours. Work-up as per 0.3 mmol diarylether: Upon cooling, the reaction was diluted with DCM (15 mL), filtered through a pipette of Celite[®] and then washed with aqueous NaOH (10% w/v, 3 x 15 mL). The organic layer was then dried over MgSO₄, filtered and concentrated under reduced pressure. The residues were then flushed through silica gel using hexanes or DCM as eluent to afford the title products.

In cases where a mixture of regioisomers was obtained, the yield reflects the mixture of regioisomers. The regioisomeric ratio was determined by analysis of the ¹H NMR spectrum of the crude reaction mixture.

3-Methyl-dibenzofuran (131)⁴¹⁻⁴²



Conditions A: White solid (48 mg, 49%)

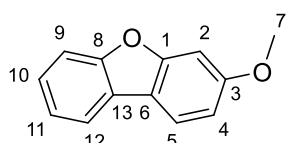
Conditions B: White solid (38 mg, 39%)

3-Methyl diphenyl ether (**102**) (100 mg, 0.543 mmol, 1 equiv.) was used as the substrate in the general procedure **6.4.2**. The residue was purified by column chromatography (DCM). m.p. 52-53 °C; $\nu_{\text{max}}/\text{cm}^{-1}$ (NaCl): 1455 (aromatic C=C stretch), 1421 (aromatic C=C stretch), 1345 (-CH₃ bend), 1261 (ether C-O stretch), 1210 (ether C-O stretch), (aromatic C-H bend); δ_{H} (CDCl₃, 300 MHz) 2.54 (3H, s, C(7)**H**₃), 7.18 (1H, d, *J* 8.0, C(4)**H**), 7.33 (1H, td, *J* 7.5, 1.0, C(11)**H**),

7.37-7.40 (1H, m, C(2)H), 7.43 (1H, td, *J* 8.2, 1.4, C(10)H), 7.56 (1H, d, *J* 8.2, C(9)H), 7.83 (1H, d, *J* 7.9, C(5)H), 7.92 (1H, dd, *J* 7.6, 0.7, C(12)H); δ_c (CDCl₃, 75.5 MHz) 22.0 (C(7)H₃), 111.6 (C(9)H), 112.0 (C(2)H), 120.2 (C(5)H), 120.3 (C(12)H), 121.7 (qC-6), 122.6 (C(11)H), 124.0 (C(4)H), 124.4 (qC-13), 126.6 (C(10)H), 137.7 (qC-3), 156.2 (qC-1), 156.7 (qC-8); Anal. Calculated for C₁₃H₁₀O: C, 85.69; H, 5.53. Found: C, 85.69; H, 5.79.

Spectral characteristics were consistent with previously reported data.⁴¹⁻⁴²

3-Methoxy-dibenzofuran (132)⁴¹



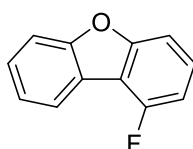
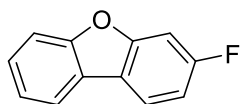
Conditions A: White solid (68 mg, 92%)

Conditions B: White solid (46 mg, 62%)

3-Methoxy diphenyl ether (**104**) (75 mg, 0.374 mmol, 1 equiv.) was used as the substrate in the general procedure **6.4.2**. The residue was purified by column chromatography (DCM). m.p. 85-87 °C; $\nu_{\max}/\text{cm}^{-1}$ (NaCl): 2948 (alkane C-H stretch), 1636 (aromatic C=C stretch), 1605 (aromatic C=C stretch), 1457 (-CH₃ bend), 1279 (ether C-O stretch), 1150 (ether C-O stretch), 1033 (ether C-O stretch), 749 (aromatic C-H bend); δ_H (CDCl₃, 300 MHz) 3.88 (3H, s, C(7)H₃), 6.92 (1H, dd, *J* 8.6, 2.3, C(4)H), 7.09 (1H, d, *J* 2.4, C(2)H), 7.30 (1H, td, *J* 7.5, 1.2, C(11)H), 7.37 (1H, td, *J* 7.4, 1.5, C(10)H), 7.49-7.54 (1H, m, C(9)H), 7.78 (1H, d, *J* 8.6, C(5)H), 7.85 (1H, ddd, *J* 7.4, 1.7, 0.5, C(12)H); δ_c (CDCl₃, 75.5 MHz) 55.7 (C(7)H₃), 96.5 (C(2)H), 111.0 (C(4)H), 111.4 (C(9)H), 117.4 (qC-6), 119.8 (C(12)H), 120.9 (C(5)H), 122.7 (C(11)H), 124.4 (qC-13), 125.7 (C(10)H), 156.4 (qC-8), 157.6 (qC-1), 160.0 (qC-3); Anal. Calculated for C₁₃H₁₀O: C, 78.77; H, 5.09. Found: C, 78.73; H, 5.24.

Spectral characteristics were consistent with previously reported data.⁴¹

3-Fluoro-dibenzofuran (133a)⁴² and 1-fluoro-dibenzofuran (133b)

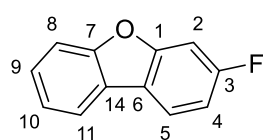


Conditions A: Yellow solid (Combined yield: 64 mg, 84%) (NMR ratio: 88:12)

Conditions B: Yellow solid (Combined yield: 36 mg, 46%) (NMR ratio: 65:35)

3-Fluoro diphenyl ether (**103**) (77 mg, 0.409 mmol, 1 equiv.) was used as the substrate in the general procedure **6.4.2 (Conditions A)** and 3-fluoro diphenyl ether (**103**) (80 mg, 0.425 mmol, 1 equiv.) was used as the substrate in the general procedure **6.4.2 (Conditions B)**. The residue was purified by column chromatography (hexanes, 100%) to afford a mixture of products **133a** and **133b**. Assignment based on ^1H NMR and ^{13}C NMR spectrum of the mixture of both regioisomers and spectral data from the literature.

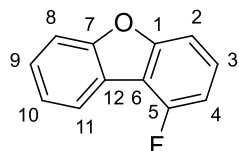
3-Fluoro-dibenzofuran (**133a**)⁴²



Major; δ_{H} (CDCl_3 , 300 MHz) 7.09 (1H, ddd, J 9.2, 8.7, 2.3, C(4)H), 7.28 (1H, dd, J 9.3, 2.3, C(2)H), 7.36 (1H, dd, J 7.7, 1.2, C(10)H), 7.44 (1H, td, J 7.3, 1.4, C(9)H), 7.53-7.58 (1H, m, C(8)H), 7.85 (1H, dd, J 5.6, 2.9, C(5)H), 7.90 (1H, dd, J 7.6, 0.7, C(11)H); δ_{C} (CDCl_3 , 75.5 MHz) 99.7 (C(2)H, d, $J_{\text{C-F}}$ 27), 110.7 (C(4)H, d, $J_{\text{C-F}}$ 22), 111.7 (C(8)H), 120.3 (C(11)H), 120.6 (qC-6, d, $J_{\text{C-F}}$ 2), 121.1 (C(5)H, d, $J_{\text{C-F}}$ 10), 123.0 (C(10)H), 123.7 (qC-14), 126.7 (C(9)H), 156.5 (qC-1, d, $J_{\text{C-F}}$ 13), 156.8 (qC-7, d, $J_{\text{C-F}}$ 2), 162.4 (qC-3, d, $J_{\text{C-F}}$ 245); δ_{F} (CDCl_3 , 282 MHz) -113.1.

Spectral characteristics were consistent with previously reported data.⁴²

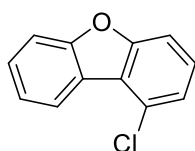
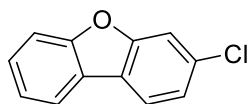
1-Fluoro-dibenzofuran (**133b**)



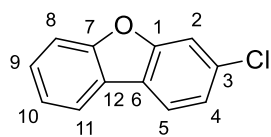
Minor; δ_{C} (CDCl_3 , 75.5 MHz) 107.6 (C(2)H, d, $J_{\text{C-F}}$ 4), 108.9 (C(4)H, d, $J_{\text{C-F}}$ 19), 111.5 (C(8)H), 113.2 (qC-6, d, $J_{\text{C-F}}$ 21), 120.6 (qC-12, d, $J_{\text{C-F}}$ 2), 122.8 (C(11)H, d, $J_{\text{C-F}}$ 3), 123.3 (C(10)H), 127.4 (C(9)H), 127.6 (C(3)H, d, $J_{\text{C-F}}$ 8), 156.1 (qC-7), 157.6 (qC-5, d, $J_{\text{C-F}}$ 276), 157.7 (qC-1, d, $J_{\text{C-F}}$ 9); δ_{F} (CDCl_3 , 282 MHz) -113.2.

3-Chloro-dibenzofuran (**134a**) and 1-Chloro-dibenzofuran (**134b**)⁴¹

Conditions A: Yellow solid (Combined yield: 71 mg, 90%) (NMR ratio: 99:1)

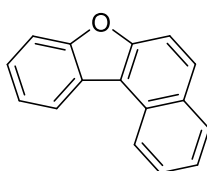
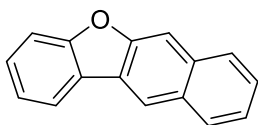


Conditions B: White solid (Combined yield: 10 mg, 31%) (NMR ratio: 87:13)

3-Chloro-dibenzofuran (134a)⁴¹

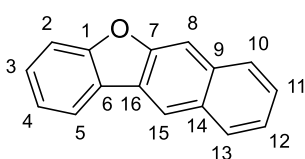
3-Chloro diphenyl ether (**107**) (80 mg, 0.392 mmol, 1 equiv.) was used as the substrate in the general procedure **6.4.2 (Conditions A)** and 3-Chloro diphenyl ether (**107**) (35 mg, 0.17 mmol, 1 equiv.) was used as the substrate in the general procedure **6.4.2 (Conditions B)**. The residue was purified by column chromatography (hexanes, 100%). m.p. 80-82 °C; $\nu_{\max}/\text{cm}^{-1}$ (NaCl): 1590 (aromatic C=C stretch), 1457 (aromatic C=C stretch), 1230 (ether C-O stretch), 1190 (ether C-O stretch), 897 (aromatic C-H bend), 599 (C-Cl stretch); δ_{H} (CDCl_3 , 300 MHz) 7.33 (1H, dd, J 8.2, 1.8, C(4)H), 7.36 (1H, td, J 7.5, 1.0, C(10)H), 7.47 (1H, td, J 7.2, 1.4, C(9)H), 7.53-7.60 (2H, m, C(2)H & C(8)H), 7.85 (1H, d, J 8.3, C(5)H), 7.91 (1H, ddd, J 7.7, 1.3, 0.6, C(11)H); δ_{C} (CDCl_3 , 75.5 MHz) 111.8 (C(8)H), 112.3 (C(2)H), 120.6 (C(11)H), 121.2 (C(5)H), 123.0 (qC-6), 123.1 (C(10)H), 123.4 (C(4)H), 123.5 (qC-12), 127.5 (C(9)H), 132.6 (qC-3), 156.3 (qC-1), 156.5 (qC-7); Anal. Calculated for $\text{C}_{12}\text{H}_7\text{OCl}$: C, 71.13; H, 3.48. Found: C, 71.30; H, 3.76.

Spectral characteristics were consistent with previously reported data.⁴¹

Benzo[*b*]naphtho[2,3-*d*]furan (135a)⁴²⁻⁴³ and Benzo[*b*]naphtha[1,2-*d*]furan (135b)

Conditions A: Yellow solid (Combined yield: 29 mg, 58%) (NMR ratio: 63:37)

2-Phenoxy naphthalene (**108**) (50 mg, 0.23 mmol, 1 equiv.) was used as the substrate in the general procedure **6.4.2**. The residue was purified by column chromatography (hexanes, 100%) to afford a mixture of products **135a** and **135b**. 8 mg of **135b** was isolated. Assignment of major and minor regioisomers based on ^1H NMR and ^{13}C NMR spectrum of the mixture of both regioisomers and deduction of signals corresponding to the minor regioisomer, in addition to spectral data available in the literature.

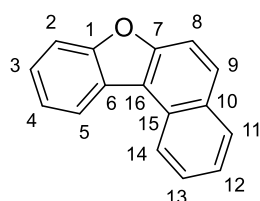
Benzo[*b*]naphtho[2,3-*d*]furan (135a)⁴²⁻⁴³

Major; δ_{H} (CDCl_3 , 600 MHz) 7.36 (1H, td, J 8.0, 1.3, C(4)H), 7.41-7.60 (4H, m, C(2)H, C(3)H, C(11)H & C(12)H), 7.91 (1H, s, C(8)H), 7.96-8.07 (3H, m, C(5)H, C(10)H & C(13)H), 8.42 (1H, s, C(15)H); δ_{C}

(CDCl₃, 150 MHz) 106.9 (C(8)H), 111.6 (C(2)H), 119.2 (C(15)H), 121.3 (C(5)H), 122.8 (C(4)H), 123.9 (qC-6), 124.4 (C(12)H), 125.4 (qC-16), 125.8 (C(11)H), 127.8 (C(3)H), 128.4 (2 × CH, C(10)H & C(13)H), 130.3 (qC-14), 133.1 (qC-9), 154.8 (qC-7), 157.6 (qC-1).

Spectral characteristics were consistent with previously reported data.⁴²⁻⁴³

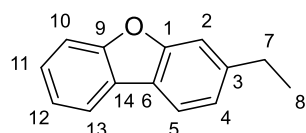
Benzo[*b*]naphtha[1,2-*d*]furan (135b)^{24, 42}



Minor; Colourless oil (8 mg isolated); $\nu_{\text{max}}/\text{cm}^{-1}$ (NaCl): 1626 (aromatic C=C stretch), 1584 (aromatic C=C stretch), 1460 (aromatic C=C stretch), 1251 (ether C-O stretch), 1214 (ether C-O stretch), 803 (aromatic C-H bend), 740 (aromatic C-H bend); δ_{H} (CDCl₃, 600 MHz) 7.44-7.51 (2H, m, C(3)H & C(4)H), 7.55 (1H, ddd, *J* 7.8, 6.7, 1.2, C(12)H), 7.68-7.75 (2H, m, C(8)H & C(13)H), 7.77 (1H, d, *J* 9.0, C(2)H), 7.93 (1H, d, *J* 9.0, C(11)H), 8.03 (1H, d, *J* 8.2, C(9)H), 8.36-8.43 (1H, m, C(5)H), 8.63 (1H, d, *J* 8.3, C(14)H); δ_{C} (CDCl₃, 150 MHz) 111.9 (C(8)H), 112.8 (C(2)H), 117.3 (qC-16), 122.0 (C(5)H), 123.2 (C(4)H), 123.5 (C(14)H), 124.4 (C(12)H), 124.9 (qC-6), 125.9 (C(3)H), 127.2 (C(13)H), 128.6 (C(11)H), 129.1 (qC-15), 129.2 (C(9)H), 130.5 (qC-10), 154.3 (qC-7), 155.9 (qC-1); *m/z* (ES⁺): 218 [(M+H)⁺, 100%].

Spectral characteristics were consistent with previously reported data.^{24, 42}

3-Ethyl-dibenzofuran (136)



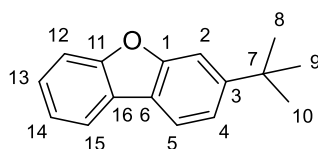
Conditions A: White solid (49 mg, 99%)

Conditions B: White solid (35 mg, 71%)

3-Ethyl diphenyl ether (**106**) (50 mg, 0.252 mmol, 1 equiv.) was used as the substrate in the general procedure **6.4.2**. The residue was purified by column chromatography (hexanes, hexanes:Et₂O, 92:8). m.p. 74-76 °C; $\nu_{\text{max}}/\text{cm}^{-1}$ (NaCl): 1457 (aromatic C=C stretch), 1420 (-CH₂ bend), 1343 (-CH₃ bend), 1230 (ether C-O stretch), 1198 (ether C-O stretch), 931 (aromatic C-H bend), 840 (aromatic C-H bend); δ_{H} (CDCl₃, 300 MHz) 1.32 (3H, t, *J* 7.6, C(8)H₃), 2.82 (2H, q, *J* 7.6, C(7)H₂), 7.15-7.22 (1H, m, C(4)H), 7.31 (1H, td, *J* 7.5, 1.2, C(12)H), 7.40 (1H, d, *J* 0.8, C(2)H), 7.41 (1H, td, *J* 7.3, 1.4, C(11)H), 7.50-7.58 (1H, m, C(10)H), 7.84 (1H, d, *J* 7.8, C(5)H), 7.90 (1H, ddd, *J* 7.6, 1.4, 0.6, C(13)H); δ_{C} (CDCl₃, 75.5 MHz) 15.1 (C(8)H₃), 29.3 (C(7)H₂), 110.7 (C(2)H), 111.5 (C(10)H), 120.29 (C(5)H), 120.3 (C(13)H), 121.9 (qC-6), 122.6 (C(12)H), 122.9

(C(4)H), 124.4 (qC-14), 126.5 (C(11)H), 144.3 (qC-3), 156.3 (qC-1), 156.7 (qC-9); Anal. Calculated for C₁₄H₁₂O: C, 85.68; H, 6.16. Found: C, 85.42; H, 6.05.

3-*Tert*-butyl-dibenzofuran (137)⁴²



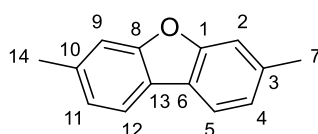
Conditions A: White solid (74 mg, 94%)

Conditions B: White solid (42 mg, 53%)

3-*Tert*-butyl diphenyl ether (**105**) (80 mg, 0.353 mmol, 1 equiv.) was used as the substrate in the general procedure **6.4.2**. The residue was purified by column chromatography (DCM). m.p. 57-60 °C; $\nu_{\max}/\text{cm}^{-1}$ (NaCl): 2964 (alkane C-H stretch), 1634 (aromatic C=C stretch), 1457 (aromatic C=C stretch), 1421 (-CH₃ bend), 1365 (-CH₃ bend), 1230 (ether C-O stretch), 1187 (ether C-O stretch), 726 (aromatic C-H bend); δ_{H} (CDCl₃, 300 MHz) 1.44 (9H, s, C(8)H₃, C(9)H₃ & C(10)H₃), 7.34 (1H, td, *J* 7.7, 0.9, C(4)H), 7.39-7.48 (2H, m, C(2)H & C(14)H), 7.54-7.61 (1H, m, C(12)H), 7.54-7.60 (1H, m, C(13)H), 7.88 (1H, d, *J* 8.2, C(5)H), 7.91-7.96 (1H, m, C(15)H); δ_{C} (CDCl₃, 75.5 MHz) 31.7 (C(8)H₃, C(9)H₃ & C(10)H₃), 35.3 (qC-7), 108.5 (C(2)H), 111.6 (C(12)H), 120.0 (C(4)H), 120.4 (C(5)H), 120.5 (C(15)H), 121.5 (qC-6), 122.6 (C(14)H), 124.3 (qC-16), 126.6 (C(13)H), 151.4 (qC-3), 156.4 (qC-1), 156.6 (qC-11); Anal. Calculated for C₁₆H₁₆O: C, 85.68; H, 7.19. Found: C, 85.36; H, 7.37.

Spectral characteristics were consistent with previously reported data.^{24, 42}

3,7-Dimethyl-dibenzofuran (138)⁴⁴



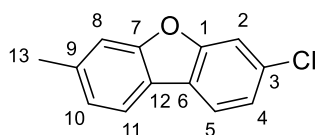
Conditions A: White solid (41 mg, 85%)

1-Methyl-3-(3-methylphenoxy) benzene (**113**) (50 mg, 0.252 mmol, 1 equiv.) was used as the substrate in the general procedure **6.4.2**. The residue was purified by column chromatography (hexanes, 100%). m.p. 76-78 °C; $\nu_{\max}/\text{cm}^{-1}$ (NaCl): 2927 (alkane C-H stretch), 1421 (aromatic C=C stretch), 1272 (ether C-O stretch), 1115 (ether C-O stretch), 800 (aromatic C-H bend); δ_{H} (CDCl₃, 300 MHz) 2.51 (6H, s, C(7)H₃ & C(14)H₃), 7.14 (2H, dd, *J* 7.8, C(4)H & C(11)H), 7.32-7.37 (1H, m, C(2)H & C(9)H), 7.76 (2H, d, *J* 7.8, C(5)H & C(12)H); δ_{C} (CDCl₃, 75.5 MHz) 21.9 (C(7)H₃ & C(14)H₃), 111.9 (C(2)H & C(9)H), 119.8 (C(5)H & C(12)H), 121.8 (qC-13 & qC-6), 123.8 (C(4)H & C(11)H), 137.0

(qC-3 & qC-10), 156.6 (qC-1 & qC-8); Anal. Calculated for C₁₄H₁₂O: C, 85.68; H, 6.16. Found: C, 85.48; H, 6.27.

Spectral characteristics were consistent with previously reported data.⁴⁴

3-Methyl-7-chloro-dibenzofuran (139)

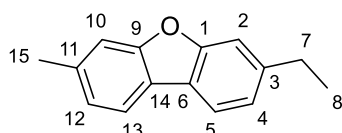


Conditions A: Light yellow solid (25 mg, 50%)

1-Chloro-3-(3-methylphenoxy) benzene (**124**) (50 mg, 0.229 mmol, 1 equiv.) was used as the substrate in the general procedure **6.4.2**.

The residue was purified by column chromatography (hexanes, 100%). m.p. 113-116 °C; $\nu_{\text{max}}/\text{cm}^{-1}$ (NaCl): 3050 (aromatic C-H stretch), 2921 (alkane C-H stretch), 1415 (aromatic C=C stretch), 1268 (ether C-O stretch), 1115 (C-O stretch), 802 (aromatic C-H bend), 600 (C-Cl stretch); δ_{H} (CDCl₃, 300 MHz) 7.15 (1H, d, *J* 7.8, C(10)H), 7.28 (1H, dd, *J* 8.4, 1.8, C(4)H), 7.34 (1H, bs, C(8)H), 7.52 (1H, d, *J* 1.6, C(2)H), 7.74 (1H, d, *J* 7.8, C(11)H), 7.77 (1H, d, *J* 8.3, C(5)H); δ_{C} (CDCl₃, 75.5 MHz) 22.0 (C(13)H₃), 112.0 (C(8)H), 112.2 (C(2)H), 120.1 (C(11)H), 120.8 (C(5)H), 120.9 (qC-12), 123.1 (qC-6), 123.2 (C(4)H), 124.4 (C(10)H), 132.0 (qC-3), 138.1 (qC-9), 156.3 (qC-1), 157.0 (qC-7); Anal. Calculated for C₁₃H₉ClO: C, 72.07; H, 4.19. Found: C, 72.21; H, 4.58.

3-Methyl-7-ethyl-dibenzofuran (140)



Conditions A: Sticky orange oil (31 mg, 77%)

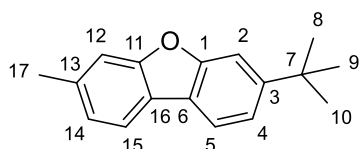
1-Ethyl-3-(3-methylphenoxy) benzene (**125**) (39.8 mg, 0.187 mmol, 1 equiv.) was used as the substrate in the general

procedure **6.4.2**. The residue was purified by column chromatography (hexanes, 100%). $\nu_{\text{max}}/\text{cm}^{-1}$ (NaCl): 2964 (aromatic C-H stretch), 2927 (alkane C-H stretch), 1609 (aromatic C=C stretch), 1473 (aromatic C=C stretch), 1432 (-CH₃ bend), 1221 (ether C-O stretch), 1130 (ether C-O stretch), 804 (aromatic C-H bend); δ_{H} (CDCl₃, 300 MHz) 1.31 (3H, t, *J* 7.7, C(8)H₃), 2.51 (3H, s, C(15)H₃), 2.80 (2H, q, *J* 7.8, C(7)H₂), 7.08-7.19 (2H, m, C(4)H & C(12)H), 7.31-7.38 (2H, m, C(2)H & C(10)H), 7.76 (1H, d, *J* 7.6, C(5)H), 7.78 (1H, d, *J* 7.7, C(13)H); δ_{C} (CDCl₃, 75.5 MHz) 15.9 (C(8)H₃), 21.9 (C(7)H₂), 29.3 (C(15)H), 110.6 (C(2)H), 111.9 (C(10)H), 119.8 (C(13)H), 119.9 (C(5)H), 121.8 (qC-14), 122.0 (qC-6), 122.7 (C(4)H), 123.8 (C(12)H), 137.0 (qC-11), 143.6 (qC-

3), 156.6 (qC-1), 156.7 (qC-9); Anal. Calculated for C₁₅H₁₄O: C, 85.68; H, 6.71. Found: C, 85.77; H, 6.89.

3-Methyl-7-*tert* butyl-dibenzofuran (**141**)

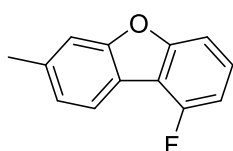
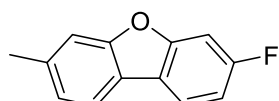
Conditions A: Sticky orange solid (38 mg, 76%)



1-*Tert*-butyl-3-(3-methylphenoxy) benzene (**126**) (50 mg, 0.021 mmol, 1 equiv.) was used as the substrate in the general procedure **6.4.2**. The residue was purified by column

chromatography (DCM). $\nu_{\max}/\text{cm}^{-1}$ (NaCl): 2964 (alkane C-H stretch), 1422 (aromatic C=C stretch), 1210 (ether C-O stretch), 806 (aromatic C-H bend); δ_{H} (CDCl₃, 300 MHz) 1.33 (9H, s, C(8)H₃, C(9)H₃ & C(10)H₃), 2.44 (3H, s, C(17)H₃), 7.08-7.15 (1H, m, C(14)H), 7.34 (1H, bs, C(12)H), 7.36 (1H, dd, J 8.2, 1.8, C(4)H), 7.55 (1H, d, J 1.5, C(2)H), 7.76 (1H, d, J 8.0, C(15)H), 7.80 (1H, d, J 8.3, C(5)H); δ_{C} (CDCl₃, 75.5 MHz) 21.9 (C(17)H₃), 31.7 (C(8)H₃, C(9)H₃ & C(10)H₃), 35.2 (qC-7), 108.4 (C(2)H), 111.8 (C(12)H), 119.6 (C(5)H), 119.9 (C(15)H), 120.2 (C(4)H), 121.7 (qC-6), 121.8 (qC-16), 123.8 (C(14)H), 137.0 (qC-13), 150.7 (qC-3), 156.7 (qC-1), 156.9 (qC-11); Anal. Calculated for C₁₇H₁₈O: C, 85.67; H, 7.61. Found: C, 84.75; H, 7.85.

3-Methyl-7-fluoro-dibenzofuran (**142a**) and 1-fluoro-7-methyl-dibenzofuran (**142b**)

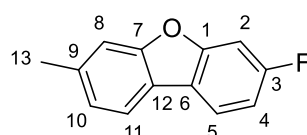


Conditions A: White solid (Combined yield: 35 mg, 70%) (NMR ratio: 84:16)

1-Fluoro-3-(3-methylphenoxy) benzene (**123**)

(70 mg, 0.346 mmol, 1 equiv.) was used as the substrate in the general procedure **6.4.2**. The residue was purified by column chromatography (hexanes, 100%) to afford a mixture of products **142a** and **142b**. Assignment of major and minor regioisomers based on ¹H NMR and ¹³C NMR spectrum of the mixture of both regioisomers.

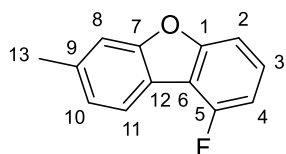
3-Methyl-7-fluoro-dibenzofuran (**142a**)



Major; δ_{H} (CDCl₃, 300 MHz) 2.52 (3H, s, C(13)H₃), 7.07 (1H, ddd, J 9.0, 2.3, 0.8, C(4)H), 7.16 (1H, ddd, J 7.9, 1.3, 0.7, C(10)H), 7.23 (1H, dd, J 9.1, 2.3, C(2)H), 7.35-7.38 (1H, m, C(8)H), 7.76 (1H, d, J 7.79, C(11)H), 7.81 (1H, dd, J 8.5, 5.5, C(5)H); δ_{C} (CDCl₃, 75.5 MHz) 21.9 (C(13)H₃), 99.6 (C(2)H, d, $J_{\text{C-F}}$ 27), 110.5 (C(4)H, d, $J_{\text{C-F}}$ 24), 112.0 (C(8)H), 119.8 (C(11)H), 120.7 (C(5)H, d, $J_{\text{C-F}}$ 10), 120.7 (qC-

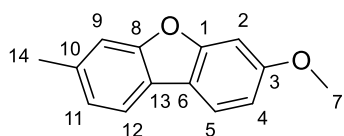
6, d, J_{C-F} 2), 124.3 (C(10)H), 124.8 (qC-12), 137.3 (qC-9), 156.5 (qC-1, d, J_{C-F} 13), 157.3 (qC-7), 162.0 (qC-3, d, J_{C-F} 244); δ_F (CDCl₃, 282 MHz) -113.9.

1-Fluoro-7-methyl-dibenzofuran (142b)



Minor; δ_C (CDCl₃, 75.5 MHz) 22.0 (C(13)H₃), 107.5 (C(2)H, d, J_{C-F} 4), 108.9 (C(4)H, d, J_{C-F} 19), 111.7 (C(8)H), 110.0 (qC-6, d, J_{C-F} 21), 121.1 (qC-12, d, J_{C-F} 1), 122.3 (C(11)H, d, J_{C-F} 3), 124.5 (C(10)H), 127.0 (C(3)H, d, J_{C-F} 8), 138.1 (qC-9), 156.2 (qC-7), 157.7 (qC-1, d, J_{C-F} 9), 157.4 (qC-5, d, J_{C-F} 250); δ_F (CDCl₃, 282 MHz) -114.0.

3-Methyl-7-methoxy-dibenzofuran (143a)



Conditions A: Orange solid (35 mg, 70%)

1-Methoxy-3-(3-methylphenoxy) benzene (**122**) (50 mg, 0.233 mmol, 1 equiv.) was used as the substrate in the general procedure **6.4.2**. The residue was purified by column chromatography (hexanes, 100%). m.p. 85-88 °C; ν_{max}/cm^{-1} (NaCl): 2948 (alkane C-H stretch), 1600 (aromatic C=C stretch), 1430 (-CH₃ bend), 1294 (ether C-O stretch), 1149 (ether C-O stretch), 1035 (ether C-O stretch), 806 (aromatic C-H bend); δ_H (CDCl₃, 300 MHz) 2.52 (3H, s, C(14)H₃), 3.91 (3H, s, C(7)H₃), 6.90 (1H, dd, J 8.6, 2.3, C(4)H), 7.06 (1H, d, J 2.2, C(2)H), 7.10-7.17 (1H, m, C(11)H), 7.30-7.33 (1H, m, C(9)H), 7.69 (1H, d, J 7.8, C(12)H), 7.73 (1H, d, J 8.6, C(5)H); δ_C (CDCl₃, 75.5 MHz) 21.9 (C(14)H₃), 55.7 (C(7)H₃), 96.6 (C(2)H), 110.7 (C(4)H), 111.7 (C(9)H), 117.5 (qC-6), 119.3 (C(12)H), 120.6 (C(5)H), 121.8 (qC-13), 123.9 (C(11)H), 136.1 (qC-10), 156.8 (qC-8), 157.5 (qC-1), 159.6 (qC-3); Anal. Calculated for C₁₄H₁₂O: C, 79.23; H, 5.70. Found: C, 78.95; H, 5.88.

6.5 Palladium catalysed intramolecular direct arylation of *ortho*-bromo diarylethers.

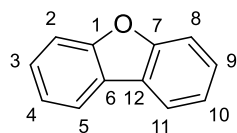
6.5.1 General procedures for intramolecular direct arylation of *ortho*-bromo diarylethers.

Synthesis of compounds **16**, **199-211**, **215**.

Diarylether (1 equiv.), Pd(OAc)₂ (5 mol%), K₂CO₃ (2.0 equiv.), 6-methoxy quinoline (10 mol%) and NMP (2.0 mL/mmol) were added to a sealed reaction vial equipped with a magnetic stir bar. The resulting mixture was stirred at 135 °C under air atmosphere in a multi reaction heating mantle for 22 hours. Work-up as per 0.1 mmol diarylether: Upon cooling, the reaction was diluted with DCM (15 mL), filtered through a plug of Celite® and the solvent was

concentrated under reduced pressure. The residues were then flushed through silica gel using hexanes as eluent to afford the title products.

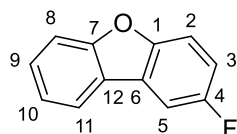
Dibenzofuran (**16**)⁴²



1-Bromo-2-phenoxybenzene (**157**) (30 mg, 0.120 mmol, 1 equiv.) was used as the substrate in the general procedure **6.5.1**. White solid (27 mg, 99%), m.p. 77-79 °C; δ_{H} (CDCl_3 , 300 MHz) 7.34 (2H, td, J 7.5, 1.1, C(4)H & C(10)H), 7.45 (2H, dd_{app}, J 7.5, 1.1, C(3)H & C(9)H), 7.54-7.60 (2H, m, C(2)H & C(8)H), 7.96 (2H, ddd, J 7.6, 1.3, 0.6, C(5)H & C(11)H); δ_{C} (CDCl_3 , 75.5 MHz) 111.7 (C(2)H & C(8)H), 120.6 (C(5)H & C(11)H), 122.7 (C(4)H & C(10)H), 124.2 (qC-6 & qC-12), 127.1 (C(3)H & C(9)H), 156.2 (qC-1 & qC-7); Anal. Calculated for $\text{C}_{12}\text{H}_8\text{O}$: C, 85.69; H, 4.79. Found: C, 85.60; H, 4.58.

Spectral characteristics are consistent with previously reported data.⁴²

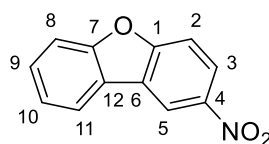
2-Fluoro-dibenzofuran (**199**)^{27, 42}



1-Bromo-2-(4-fluorophenoxy) benzene (**168**) (30 mg, 0.11 mmol, 1 equiv.) was used as the substrate in the general procedure **6.5.1**. White solid (27 mg, 99%), m.p. 83-86 °C; $\nu_{\text{max}}/\text{cm}^{-1}$ (NaCl): 1476 (aromatic C=C stretch), 1209 (ether C-O stretch), 1159 (C-F stretch), 864 (aromatic C-H bend); δ_{H} (CDCl_3 , 300 MHz) 7.15 (1H, td, J 9.0, 2.7, C(3)H), 7.34 (1H, ddd, J 7.5, 1.2, C(5)H), 7.43-7.52 (2H, m, C(9)H & C(10)H), 7.53-7.58 (1H, m, C(2)H), 7.60 (1H, dd, J 8.2, 2.5, C(8)H), 7.90 (1H, ddd, J 7.8, 1.3, 0.5, C(11)H); δ_{C} (CDCl_3 , 75.5 MHz) 107.0 (C(5)H, d, $J_{\text{C-F}}$ 25), 111.9 (C(8)H), 112.3 (C(2)H, d, $J_{\text{C-F}}$ 9), 114.4 (C(3)H, d, $J_{\text{C-F}}$ 26), 120.9 (C(11)H), 122.7 (C(10)H), 124.0 (qC-12, d, $J_{\text{C-F}}$ 4), 125.1 (qC-6, d, $J_{\text{C-F}}$ 10), 122.8 (C(9)H), 152.2 (qC-1), 157.2 (qC-7), 159.0 (qC-4, d, $J_{\text{C-F}}$ 239); m/z (ES⁺): 187 [(M+H)⁺, 50%].

Spectral characteristics are consistent with previously reported data.^{27, 43}

2-Nitro-dibenzofuran (**200**)⁴⁵

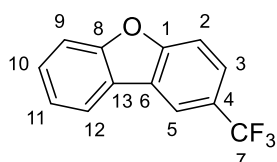


1-Bromo-2-(4-nitrophenoxy) benzene (**163**) (40 mg, 0.136 mmol, 1 equiv.) was used as the substrate in the general procedure **6.5.1**. White solid (28 mg, 97%), m.p. 150-152 °C; $\nu_{\text{max}}/\text{cm}^{-1}$ (NaCl): 1525

(aromatic C=C stretch), 1466 (aromatic C=C stretch), 1343 (N=O stretch), 1183 (ether C-O stretch), 891 (aromatic C-H bend); δ_{H} (CDCl₃, 300 MHz) 7.40-7.49 (1H, td, *J* 7.7, 1.2, C(10)H), 7.58 (1H, td, *J* 7.7, 1.3, C(9)H), 7.61-7.69 (2H, m, C(2)H & C(8)H), 8.04 (1H, ddd, *J* 7.8, 1.1, 0.6, C(11)H), 8.40 (1H, dd, *J* 9.0, 2.4, C(3)H), 8.87 (1H, d, *J* 2.3, C(5)H); δ_{C} (CDCl₃, 75.5 MHz) 112.0 (C(8)H), 112.3 (C(2)H), 117.3 (C(5)H), 121.3 (C(11)H), 123.0 (C(3)H), 123.1 (qC-12), 123.9 (C(10)H), 125.0 (qC-6), 129.0 (C(9)H), 144.0 (qC-4), 157.5 (qC-7), 159.2 (qC-1); Anal. Calculated for C₁₂H₇NO₃: C, 67.61; H, 3.31. Found: C, 67.70; H, 3.47.

Spectral characteristics are consistent with previously reported data.⁴⁵

2-Trifluoromethyl-dibenzofuran (201)²⁷



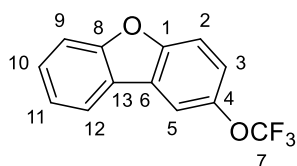
1-Bromo-2-(4-(trifluoromethoxy) benzene (190) (49.8 mg, 0.15 mmol, 1 equiv.) used as the substrate in the general procedure 6.5.1.

White solid (25 mg, 86%), m.p. 91-93 °C; $\nu_{\text{max}}/\text{cm}^{-1}$ (NaCl): 1452

(aromatic C=C stretch), 1353 (C-F stretch), 1165 (ether C-O stretch), 1099 (ether C-O stretch), 828 (aromatic C-H stretch); δ_{H} (CDCl₃, 300 MHz) 7.40 (1H, ddd, *J* 8.2, 7.4, 1.1, C(11)H), 7.53 (1H, ddd, *J* 8.4, 7.1, 1.3, C(10)H), 7.58-7.68 (2H, m, C(2)H & C(9)H), 7.73 (1H, d, *J* 8.8, 1.5, C(3)H), 7.99 (1H, ddd, *J* 7.7, 1.2, 0.6, C(12)H), 8.23 (1H, s, C(5)H); δ_{C} (CDCl₃, 125 MHz) 112.0 (C(2)H & C(9)H), 118.3 (qC-6, q, *J*_{C-F} 4), 121.0 (C(5)H), 123.3 (C(12)H), 123.4 (C(11)H), 124.2 (C(3)H, q, *J*_{C-F} 4), 124.6 (qC-13), 124.6 (qC-7, q, *J*_{C-F} 270), 125.4 (qC-4, q, *J*_{C-F} 32), 128.2 (C(10)H), 156.9 (qC-1), 157.6 (qC-6); δ_{F} (CDCl₃, 282 MHz) -60.9; Anal. Calculated for C₁₃H₇F₃O: C, 66.11; H, 2.99. Found: C, 66.40; H, 2.66.

Spectral characteristics are consistent with previously reported data.²⁷

2-Trifluoromethoxy-dibenzofuran (202)

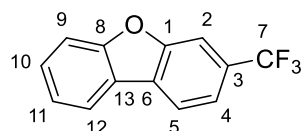


1-Bromo-2-(4-(trifluoromethoxy)phenoxy) benzene (183) (49.8 mg, 0.15 mmol, 1 equiv.) was used as the substrate in the general procedure 6.5.1. White solid (25 mg, 66%), m.p. 50-51 °C; $\nu_{\text{max}}/\text{cm}^{-1}$

(NaCl): 1445 (aromatic C=C stretch), 1307 (C-O stretch), 1211 (ether C-O stretch), 1163 (ether C-O stretch), 1147 (C-F stretch), 827 (aromatic C-H bend); δ_{H} (CDCl₃, 500 MHz) 7.28-7.42 (2H, m, C(3)H & C(11)H), 7.51 (1H, ddd, *J* 8.3, 7.2, 1.3, C(10)H), 7.54-7.62 (2H, m, C(2)H & C(9)H),

7.80 (1H, s, C(5)H), 7.91-7.96 (1H, m, C(12)H); δ_{C} (CDCl₃, 125 MHz) 112.0 (C(5)H), 112.4 (C(9)H), 113.6 (C(2)H), 120.5 (C(3)H), 120.7 (qC-7, q, $J_{\text{C-F}}$ 257), 120.9 (C(12)H), 123.1 (C(11)H), 123.6 (qC-6), 125.2 (qC-13), 128.1 (C(10)H), 144.7 (qC-4), 154.2 (qC-1), 157.1 (qC-8); δ_{F} (CDCl₃, 282 MHz) -58.2; Anal. Calculated for C₁₃H₇F₃O₂: C, 61.91; H, 2.80. Found: C, 62.15; H, 2.66.

3-Trifluoromethyl-dibenzofuran (203)⁴⁵

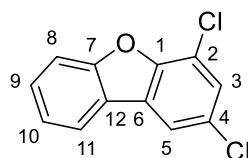


1-Bromo-2-(3-(trifluoromethyl)phenoxy) benzene (**191**) (40 mg, 0.126 mmol, 1 equiv.) was used as the substrate in the general procedure **6.5.1**. White solid (28 mg, 96%), m.p. 108-110 °C;

$\nu_{\text{max}}/\text{cm}^{-1}$ (NaCl): 1428 (aromatic C=C stretch), 1339 (C-F stretch), 1166 (ether C-O stretch), 1103 (ether C-O stretch), 831 (aromatic C-H stretch); δ_{H} (CDCl₃, 300 MHz) 7.36-7.45 (1H, m, C(4)H), 7.54 (1H, ddd, J 8.7, 7.2, 1.4, C(11)H), 7.59-7.67 (2H, m, C(9)H & C(10)H), 7.84 (1H, s, C(2)H), 7.98-8.03 (1H, m, C(5)H), 8.05 (1H, dt, J 8.1, 1.7, C(12)H); δ_{C} (CDCl₃, 75.5 MHz) 109.2 (C(2)H, q, $J_{\text{C-F}}$ 4), 112.0 (C(9)H), 119.7 (C(4)H, q, $J_{\text{C-F}}$ 4), 121.0 (C(12)H), 121.3 (C(5)H), 123.1 (qC-6), 123.3 (C(11)H), 124.3 (qC-7, q, $J_{\text{C-F}}$ 272), 128.5 (C(10)H), 127.4 (qC-13), 129.1 (qC-3, q, $J_{\text{C-F}}$ 32), 155.4 (qC-1), 157.2 (qC-8); δ_{F} (CDCl₃, 282 MHz) -61.4. HRMS (ESI-TOF) m/z : [M]⁺ calcd. for C₁₃H₇F₃O: 236.0444, found 236.0456.

Spectral characteristics are consistent with previously reported data.⁴⁵

2,4-Dichloro-dibenzofuran (204)⁴⁶

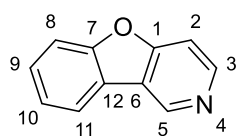


1-bromo-2-(2,4-dichlorophenoxy) benzene (**187**) (50 mg, 0.157 mmol, 1 equiv.) was used as the substrate in the general procedure **6.5.1**. White solid (26 mg, 70%), m.p. 129-132 °C; $\nu_{\text{max}}/\text{cm}^{-1}$ (NaCl): 1577 (aromatic C=C stretch), 1467 (aromatic C=C stretch), 1223 (ether C-O stretch), 1182 (ether C-O stretch), 845 (aromatic C-H bend), 745 (C-Cl stretch); δ_{H} (CDCl₃, 300 MHz) 7.37 (1H, td, J 7.6, 1.0, C(10)H), 7.44 (1H, d, J 2.0, C(3)H), 7.52 (1H, td, J 7.9, 1.3, C(9)H), 7.60-7.66 (1H, m, C(8)H), 7.79 (1H, d, J 2.0, C(5)H), 7.88 (1H, ddd, J 7.7, 1.3, 0.6, C(11)H); δ_{C} (CDCl₃, 75.5 MHz) 112.3 (C(8)H), 111.7 (qC-6), 119.0 (C(5)H), 120.8 (C(11)H), 123.2 (qC-12), 123.6 (C(10)H), 126.8 (qC-2), 127.0 (C(3)H), 128.5 (qC-4), 128.6 (C(9)H), 150.6 (qC-1), 156.7 (qC-7). Anal. Calculated for C₁₂H₆Cl₂O:

C, 60.79; H, 2.55. Found: C, 60.95; H, 2.65. HRMS (ESI-TOF) m/z : $[M]^+$ calcd. for $C_{12}H_6Cl_2O$: 235.9790, found 235.9790.

Spectral characteristics are consistent with previously reported data.⁴⁶

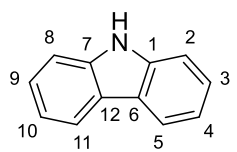
Benzofuro[3,2-*c*]pyridine (205)²²



4-(2-Bromophenoxy)pyridine (**197**) (40 mg, 0.16 mmol, 1 equiv.) was used as the substrate in the general procedure **6.5.1**. White solid (19 mg, 70%), m.p. 73-74°C (lit. 73-74 °C); δ_H (DMSO- d_6 , 300 MHz) 7.50 (1H, td, J 7.6, 1.0, C(10)H), 7.62 (1H, ddd, J 8.6, 7.7, 1.4, C(9)H), 7.76-7.83 (2H, m, C(2)H & C(8)H), 8.27 (1H, ddd, J 7.7, 1.4, 0.6, C(11)H), 8.55-8.77 (1H, m, C(3)H), 9.44 (1H, bs, C(5)H); δ_C (DMSO- d_6 , 75.5 MHz) 108.1 (C(2)H), 112.5 (C(8)H), 121.5 (qC-6 & qC-12), 122.3 (C(11)H), 124.6 (C(10)H), 129.1 (C(9)H), 144.5 (C(5)H), 148.2 (C(3)H), 155.6 (qC-7), 160.7 (qC-1); m/z (ES⁺): 170, [(M+H)⁺, 100%].

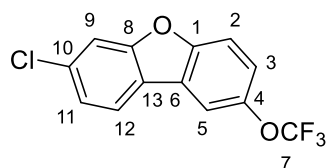
Spectral characteristics are consistent with previously reported data.²²

9H-carbazole (206)⁴⁷



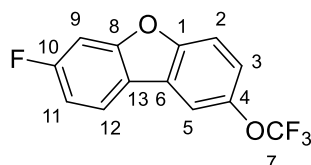
2-Bromo diphenylamine (**195**) (40 mg, 0.16 mmol, 1 equiv.) was used as the substrate in the general procedure **6.5.1**. Yellow solid (13 mg, 50%), m.p. >230 °C; ν_{max}/cm^{-1} (NaCl): 3419 (N-H stretch), 2921 (aromatic C-H stretch), 1450 (aromatic C=C stretch), 1334 (C-N stretch); δ_H (CDCl₃, 300 MHz) 7.03 (2H, ddd, J 8.5, 7.5, 1.1, C(4)H & C(10)H), 7.26 (2H, ddd, J 8.3, 7.1, 1.3, C(3)H & C(9)H), 7.33-7.41 (2H, m, C(2)H & C(9)H), 7.99 (2H, d, J 7.8, C(5)H & C(11)H); δ_C (CDCl₃, 75.5 MHz) 111.4 (C(2)H & C(8)H), 118.9 (C(4)H & C(10)H), 120.6 (C(5)H & C(11)H), 122.8 (qC-12 & qC-6), 125.9 (C(3)H & C(9)H), 140.2 (qC-1 & qC-7); m/z (ES⁺): 168, [(M+H)⁺, 30%]. HRMS (ESI-TOF) m/z : $[M+H]^+$ calcd. for $C_{12}H_9N$: 168.0808, found 168.0802.

Spectral characteristics are consistent with previously reported data.⁴⁷

2-Trifluoromethoxy-7-chloro-dibenzofuran (207)

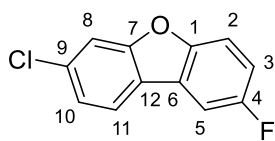
1-Bromo-4-chloro-2-(4-(trifluoromethoxy)phenoxy) benzene (**185**) (46 mg, 0.125 mmol, 1 equiv.) was used as the substrate in the general procedure **6.5.1**. White solid (32 mg, 90%), m.p. 64-65

°C; $\nu_{\max}/\text{cm}^{-1}$ (NaCl): 1596 (aromatic C=C stretch), 1483 (aromatic C=C stretch), 1277 (ether C-O stretch), 1212 (ether C-O stretch), 1185 (C-F stretch), 1163 (C-F stretch), 819 (aromatic C-H bend), 809 (C-Cl stretch); δ_{H} (CDCl_3 , 500 MHz) 7.28-7.40 (2H, m, C(3)H & C(11)H), 7.55 (1H, d, J 9.0, C(2)H), 7.58 (1H, d, J 1.8, C(9)H), 7.75 (1H, bd, J 1.1, C(5)H), 7.83 (1H, d, J 8.4, C(12)H); δ_{C} (CDCl_3 , 125 MHz) 112.6 (C(5)H & C(9)H), 113.5 (C(2)H), 120.6 (qC-7, q, $J_{\text{C-F}}$ 255), 120.8 (C(3)H), 121.5 (C(12)H), 122.3 (qC-6), 123.8 (C(11)H), 124.5 (qC-13), 133.7 (qC-10) 145.0 (qC-4, q, $J_{\text{C-F}}$ 2), 154.4 (qC-1), 157.2 (qC-8); δ_{F} (CDCl_3 , 282 MHz) -58.2; Anal. Calculated for $\text{C}_{13}\text{H}_6\text{ClF}_3\text{O}_2$: C, 54.47; H, 2.11. Found: C, 54.16; H, 2.09. HRMS (ESI-TOF) m/z : $[\text{M}]^+$ calcd. for $\text{C}_{13}\text{H}_6\text{ClF}_3\text{O}_2$: 286.0003, found 285.9993.

2-Trifluoromethoxy-7-fluoro-dibenzofuran (208)

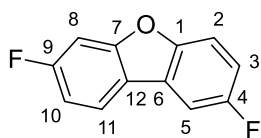
1-Bromo-4-fluoro-2-(4-(trifluoromethoxy)phenoxy) benzene (**184**) (40 mg, 0.11 mmol, 1 equiv.) was used as the substrate in the general procedure **6.5.1**. White solid (23 mg, 80%), m.p. 42-43 °C;

$\nu_{\max}/\text{cm}^{-1}$ (NaCl): 1640, 1606 (aromatic C=C stretch), 1263 (ether C-O stretch), 1162 (C-F stretch), 1130 (C-F stretch), 1098 (ether C-O stretch), 843 (aromatic C-H bend); δ_{H} (CDCl_3 , 500 MHz) 7.11 (1H, dd, J 9.4, 9.0, 2.3, C(11)H), 7.23-7.34 (2H, m, C(3)H & C(9)H), 7.53 (1H, d, J 8.9, C(2)H), 7.74 (1H, d, J 1.4, C(5)H), 7.85 (1H, dd, J 8.8, 5.4, C(12)H); δ_{C} (CDCl_3 , 125 MHz); 99.9 (C(9)H, d, $J_{\text{C-F}}$ 27), 111.3 (C(11)H, d, $J_{\text{C-F}}$ 23), 112.4 (C(5)H), 113.3 (C(2)H), 120.0 (qC-13, d, $J_{\text{C-F}}$ 3), 120.1 (C(3)H), 120.6 (qC-7, q, $J_{\text{C-F}}$ 257), 121.6 (C(12)H, d, $J_{\text{C-F}}$ 11), 124.7 (qC-6), 145.1 (qC-4, q, $J_{\text{C-F}}$ 2), 154.8 (qC-1), 157.5 (qC-8, d, $J_{\text{C-F}}$ 14), 162.8 (qC-10, d, $J_{\text{C-F}}$ 248); δ_{F} (CDCl_3 , 282 MHz) -58.2, -111.3; Anal. Calculated for $\text{C}_{13}\text{H}_6\text{F}_4\text{O}_2$: C, 57.79; H, 2.24. Found: C, 57.90; H, 2.26.

2-Fluoro-7-chloro-dibenzofuran (209)

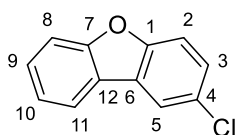
1-Bromo-4-chloro-2-(4-fluorophenoxy) benzene (**169**) (40 mg, 0.133 mmol, 1 equiv.) was used as the substrate in the general procedure

6.5.1. White solid (24 mg, 83%), m.p. 86-88 °C; $\nu_{\text{max}}/\text{cm}^{-1}$ (NaCl): 1603 (aromatic C=C stretch), 1468 (aromatic C=C stretch), 1417 (C-F stretch), 1216 (ether C-O stretch), 1164 (ether C-O stretch), 807 (aromatic C-H bend); δ_{H} (CDCl₃, 300 MHz) 7.17 (1H, td, J 9.7, 2.6, C(3)H), 7.33 (1H, dd, J 8.4, 1.6, C(10)H), 7.49 (1H, dd, J 9.1, 4.1, C(5)H), 7.52-7.61 (2H, m, C(2)H & C(8)H), 7.80 (1H, d, J 8.3, C(11)H); δ_{C} (CDCl₃, 75.5 MHz) 106.7 (C(5)H, d, $J_{\text{C-F}}$ 25), 112.5 (C(2)H, d, $J_{\text{C-F}}$ 9), 112.5 (C(8)H), 114.8 (C(3)H, d, $J_{\text{C-F}}$ 26), 121.4 (C(11)H), 122.7 (qC-6, d, $J_{\text{C-F}}$ 4), 123.5 (C(10)H), 124.5 (qC-9), 133.4 (qC-12), 152.5 (qC-1), 157.3 (qC-7), 159.2 (qC-4, d, $J_{\text{C-F}}$ 241); δ_{F} (CDCl₃, 282 MHz) -119.8; HRMS (ESI-TOF) m/z : [M]⁺ calcd. for C₁₂H₆ClFO: 220.0085, found 220.0080.

2,7-Difluoro-dibenzofuran (210)

1-Bromo-4-fluoro-2-(4-fluorophenoxy) benzene (**192**) (50 mg, 0.175 mmol, 1 equiv.) was used as the substrate in the general procedure

6.5.1. Pale yellow solid (22 mg, 63%), m.p. 89-90 °C; $\nu_{\text{max}}/\text{cm}^{-1}$ (NaCl): 1638 (aromatic C=C stretch), 1471 (aromatic C=C stretch), 1425 (C-F stretch), 1262 (ether C-O stretch), 1158 (ether C-O stretch), 845 (aromatic C-H stretch); δ_{H} (CDCl₃, 500 MHz) 7.04-7.10 (1H, m, C(10)H), 7.13 (1H, td, J 9.1, 2.7, C(3)H), 7.26 (1H, dd, J 8.9, 2.2, C(8)H), 7.47 (1H, dd, J 8.9, 3.2, C(5)H), 7.53 (1H, dd, J 8.0, 2.7, C(2)H), 7.81 (1H, dd, J 8.9, 5.3, C(11)H); δ_{C} (CDCl₃, 125 MHz) 99.8 (C(8)H, d, $J_{\text{C-F}}$ 27), 106.5 (C(5)H, d, $J_{\text{C-F}}$ 25), 111.0 (C(10)H, d, $J_{\text{C-F}}$ 24), 112.3 (C(2)H, d, $J_{\text{C-F}}$ 9), 114.0 (C(3)H, d, $J_{\text{C-F}}$ 26), 120.3 (qC-12, d, $J_{\text{C-F}}$ 1), 121.4 (C(11)H, d, $J_{\text{C-F}}$ 10), 124.6 (qC-6, d, $J_{\text{C-F}}$ 10), 152.8 (qC-7, d, $J_{\text{C-F}}$ 3), 157.5 (qC-1), 159.2 (qC-4, d, $J_{\text{C-F}}$ 240), 162.7 (qC-9, d, $J_{\text{C-F}}$ 247); δ_{F} (CDCl₃, 282 MHz) -111.8, -119.9; Anal. Calculated for C₁₂H₆F₂O: C, 70.59; H, 2.96. Found: C, 70.90; H, 3.10.

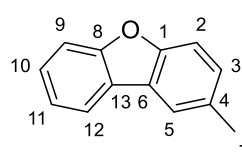
2-Chloro-dibenzofuran (211)⁴¹

1-Bromo-2-(4-chlorophenoxy) benzene (**LMP1**) (40 mg, 0.141 mmol, 1 equiv.) was used as the substrate in the general procedure **6.5.1**. White

solid (27 mg, 95%), m.p. 89-92 °C; $\nu_{\max}/\text{cm}^{-1}$ (NaCl): 1428 (aromatic C=C stretch), 1166 (ether C-O stretch), 1127 (ether C-O stretch), 831 (aromatic C-H bend), 751 (C-Cl stretch); δ_{H} (CDCl_3 , 300 MHz) 7.35 (1H, ddd, J 8.0, 7.4, 1.1, C(10)H), 7.40 (1H, dd, J 8.7, 2.1, C(3)H), 7.43-7.52 (2H, m, C(2)H & C(9)H), 7.56 (1H, dt, J 8.2, 0.9, C(8)H), 7.86-7.95 (2H, m, C(5)H & C(11)H); δ_{C} (CDCl_3 , 75.5 MHz) 111.9 (C(8)H), 112.7 (C(2)H), 120.5 (C(11)H), 120.8 (C(5)H), 123.0 (C(10)H), 123.4 (qC-6), 125.7 (qC-12), 127.2 (C(9)H), 127.9 (C(3)H), 128.2 (qC-4), 155.0 (qC-1), 156.8 (qC-7); Anal. Calcd. for $[\text{C}_{12}\text{H}_7\text{ClO}]$: C, 71.13; H, 3.48. Found: C, 70.98; H, 3.88.

Spectral characteristics are consistent with previously reported data.⁴¹

2-Methyl-dibenzofuran (215)⁴¹



1-Bromo-2-(4-methylphenoxy) benzene (**166**) (30 mg, 0.11 mmol, 1 equiv.) was used as the substrate in the general procedure **6.5.1**. White solid (8.4 mg, 42%), m.p. 35-37 °C; $\nu_{\max}/\text{cm}^{-1}$ (NaCl): 1482 (aromatic C=C stretch), 1447 (CH_3 bend), 1121 (ether C-O stretch), 1029 (ether C-O stretch), 840 (aromatic C=C bend); δ_{H} (CDCl_3 , 500 MHz) 2.52 (3H, s, C(7)H₃), 7.26 (1H, ddd, J 8.3, 1.8, 0.4, C(3)H), 7.32 (1H, td, J 8.0, 1.1, C(11)H), 7.39-7.48 (2H, m, C(2)H & C(10)H), 7.54 (1H, dt, J 8.1, 0.8, C(9)H), 7.75 (1H, t, J 0.8, C(5)H), 7.92 (1H, ddd, J 7.7, 1.3, 0.6, C(12)H); δ_{C} (CDCl_3 , 125 MHz) 21.3 (C(7)H₃), 111.1 (C(2)H), 111.6 (C(9)H), 120.5 (C(5)H), 120.6 (C(12)H), 122.5 (C(11)H), 124.2 (qC-6), 124.3 (qC-13), 126.9 (C(3)H), 128.2 (C(10)H), 132.2 (qC-4), 154.4 (qC-1), 156.5 (qC-8). HRMS (ESI-TOF) m/z : $[\text{M}]^+$ calcd. for $\text{C}_{13}\text{H}_{10}\text{O}$: 182.0726, found 182.0725.

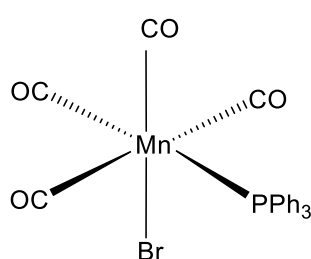
Spectral characteristics are consistent with previously reported data.⁴¹

6.6 Synthesis of manganese carbonyl phosphine complexes and their application in C-H activation reactions

6.6.1 General procedure for preparation of tetracarbonyl manganese phosphine complexes (223-225)⁴⁸

MnBr(CO)₅ (1 equiv.) and the appropriate phosphine ligand (1 equiv.) were added to a reaction vial. The reaction vial was then wrapped in tinfoil. The resulting reaction mixture was stirred in refluxing anhydrous chloroform or dichloromethane (1 mL/0.364 mmol MnBr(CO)₅) for 8 hours in a multi reaction heating mantle. After 8 hours, the reaction mixture was allowed to cool to room temperature. The compounds were isolated by evaporation of the solvent and recrystallisation from a dichloromethane/hexane mixture. (Dichloroethane could also be used as the reaction solvent and the time could be reduced to 4 hours).

cis-[MnBr(CO)₄(PPh₃)] (223)⁴⁹

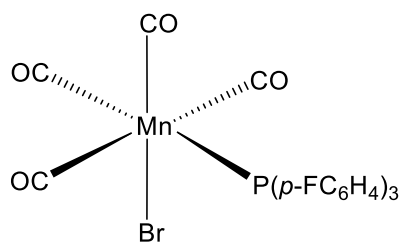


Synthesised according to the general procedure 6.6.1 using MnBr(CO)₅ (200 mg, 0.728 mmol, 1 equiv.) and triphenylphosphine (191 mg, 0.728 mmol, 1 equiv.). The solids were added to four separate reaction vials and the crude material from each vial was combined after 8 hours. Orange crystalline solid (1.41 g, 95%);

$\nu_{\max}/\text{cm}^{-1}$ IR-ATR (solid) 2086 (s, $\bar{\nu}$ CO), 2002 (s, $\bar{\nu}$ CO), 1956 (s, $\bar{\nu}$ CO); δ_{H} (CDCl₃, 600 MHz) 7.34-7.55 (9H, br m), 7.58-7.78 (6H, br m); δ_{C} (CDCl₃, 150 MHz) 128.7 (d, $J_{\text{C-P}}$ 10, *meta*-CH of Ph), 130.9 (d, $J_{\text{C-P}}$ 2, *para*-CH of Ph), 132.5 (d, $J_{\text{C-P}}$ 42, *ipso*-C of Ph), 133.6 (d, $J_{\text{C-P}}$ 10, *ortho*-CH of Ph), 210.6 (br m, CO), 211.6 (br m, CO), 216.4 (br m, CO); δ_{p} (CDCl₃, 243 MHz) 40.4; Anal. Calcd. for [C₂₂H₁₅BrMnO₄P]: C, 51.90; H, 2.97. Found: C, 51.88; H, 2.96.

Spectral characteristics are consistent with previously reported data.⁴⁹

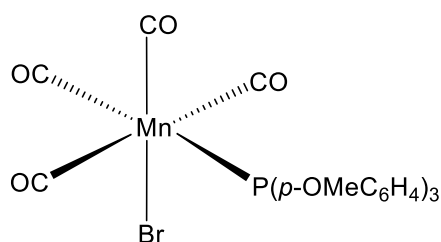
cis-[MnBr(CO)₄(P(*p*-FC₆H₄)₃)] (224)



Synthesised according to the general procedure 6.6.1 using MnBr(CO)₅ (200 mg, 0.728 mmol, 1 equiv.) and tris-(4-fluorophenyl) phosphine (230 mg, 0.728 mmol, 1 equiv.). The solids were added to four separate reaction vials and the crude material from each vial was combined after 8 hours.

Orange solid (1.40 g, 86%); $\nu_{\max}/\text{cm}^{-1}$ IR-ATR (solid) 2091 (s, $\bar{\nu}$ CO), 1998 (s, $\bar{\nu}$ CO), 1946 (s, $\bar{\nu}$ CO); δ_{H} (CDCl_3 , 600 MHz) 6.94-7.30 (6H, br m), 7.45-7.90 (6H, br m); δ_{C} (CDCl_3 , 150 MHz) 116.3 (dd, $J_{\text{C-F}}$ 21, $J_{\text{C-P}}$ 11, *meta*-CH of Ph), 128.0 (d, $J_{\text{C-P}}$ 44, *ipso*-CH of Ph), 135.6 (t_{app}, $J_{\text{C-P}}$ 10, $J_{\text{C-F}}$ 10, *ortho*-CH of Ph), 164.8 (d, $J_{\text{C-F}}$ 255, *para*-C of Ph), 210.3 (br m, CO), 211.1 (br m, CO), 216.2 (br m, CO); δ_{P} (CDCl_3 , 243 MHz) 39.43; Anal. Calcd. for $[\text{C}_{22}\text{H}_{12}\text{BrF}_3\text{MnO}_4\text{P}]$: C, 46.92; H, 2.15. Found: C, 46.54; H, 1.93.

***cis*-[MnBr(CO)₄(P(*p*-OMeC₆H₄)₃)] (225)**

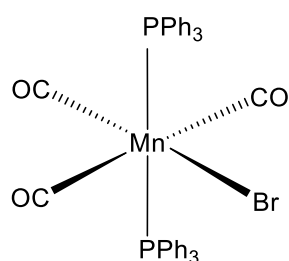


Synthesised according to the general procedure 6.6.1 using $\text{MnBr}(\text{CO})_5$ (200 mg, 0.728 mmol, 1 equiv.) and tris-(4-methoxyphenyl) phosphine (257 mg, 0.728 mmol, 1 equiv.). The solids were added to four separate reaction vials and the crude material from each vial was combined

after 8 hours. Orange solid (1.58 g, 91%); $\nu_{\max}/\text{cm}^{-1}$ IR-ATR (solid) 2083 (s, $\bar{\nu}$ CO), 1989 (s, $\bar{\nu}$ CO), 1943 (s, $\bar{\nu}$ CO); δ_{H} (CDCl_3 , 600 MHz) 3.83 (9H, s), 6.94 (6H, d J 8.5), 7.56 (6H, t J 9.2) δ_{C} (CDCl_3 , 150 MHz) 55.3 (OCH_3), 114.1 (d, $J_{\text{C-P}}$ 11, *meta*-CH of Ph), 124.0 (d, $J_{\text{C-P}}$ 47, *ipso*-CH of Ph), 135.0 (d, $J_{\text{C-P}}$ 11, *ortho*-CH of Ph), 161.3 (s, *para*-C of Ph), 210.9 (br m, CO), 211.7 (br m, CO), 216.7 (br m, CO); δ_{P} (CDCl_3 , 243 MHz) 36.09; Anal. Calcd. for $[\text{C}_{25}\text{H}_{21}\text{BrMnO}_7\text{P}]$: C, 50.11; H, 3.53. Found: C, 50.32; H, 3.51.

6.6.2 General procedure for preparation of tricarbonyl manganese phosphine complexes (226-229)⁴⁸

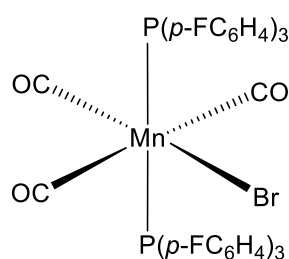
$\text{MnBr}(\text{CO})_5$ (1 equiv.) and the appropriate phosphine ligand (2 equiv.) were added to a reaction vial. The reaction vial was then wrapped in tin foil. The resulting reaction mixture was stirred in refluxing anhydrous chloroform or dichloromethane (1 mL/0.364 mmol $\text{MnBr}(\text{CO})_5$) for 16 hours in a multi reaction heating mantle. After 16 hours, the reaction mixture was allowed to cool to room temperature. The compounds were isolated by evaporation of the solvent and recrystallisation from a dichloromethane/hexane mixture.

***mer-trans*-[MnBr(CO)₃(PPh₃)₂] (**226**)⁴⁸**

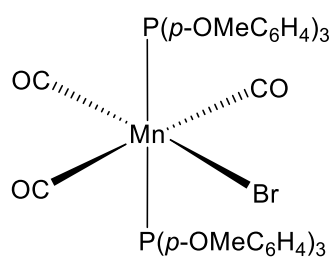
Synthesised according to the general procedure **6.6.2** using MnBr(CO)₅ (150 mg, 0.546 mmol, 1 equiv.) and triphenylphosphine (286 mg, 1.092 mmol, 2 equiv.). Yellow solid (296 mg, 73%); $\nu_{\text{max}}/\text{cm}^{-1}$ IR-ATR (solid) 2087 (s, $\bar{\nu}$ CO), 2003 (s, $\bar{\nu}$ CO), 1943 (s, $\bar{\nu}$ CO); δ_{H} (CD₂Cl₂, 600 MHz) 6.90-7.58 (18H, br m), 7.58-8.10 (12H, br m); δ_{C} (CD₂Cl₂, 150 MHz) (coupling to ³¹P not resolved) 129.4 (br m, *meta*-CH of Ph), 131.3 (br m, *para*-CH of Ph), 135.2 (br m, *ortho*-CH of Ph), 136.0 (t, $J_{\text{C-P}}$ 20, *ipso*-C of Ph), 218.1 (br m, CO), 223.5 (br m, CO); δ_{P} (CD₂Cl₂, 243 MHz) 54.3; Anal. Calcd. for [C₃₉H₃₀BrMnO₃P₂]: C, 63.01; H, 4.07. Found: C, 62.75; H, 4.07.

Spectral characteristics are consistent with previously reported data.⁴⁸

Note: ¹H NMR spectra, ¹³C NMR spectra and ³¹P NMR spectra of MnBr(CO)₃(PPh₃)₂ (**226**) were ran in CD₂Cl₂ due to observed decomposition of **266** in CDCl₃ after a short period of time.

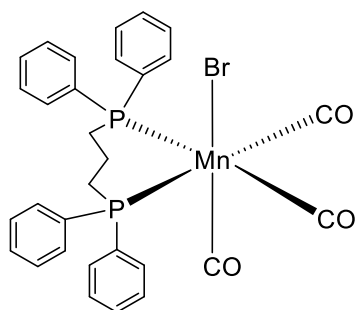
***mer-trans*-[MnBr(CO)₃(P(*p*-FC₆H₄)₂)] (**227**)**

Synthesised according to the general procedure **6.6.2** using MnBr(CO)₅ (100 mg, 0.364 mmol, 1 equiv.) and tris-(4-fluorophenyl) phosphine (241 mg, 0.762 mmol, 2 equiv.). Yellow solid (254 mg, 82%); $\nu_{\text{max}}/\text{cm}^{-1}$ IR-ATR (solid) 2036 (s, $\bar{\nu}$ CO), 1931 (s, $\bar{\nu}$ CO), 1902 (s, $\bar{\nu}$ CO); δ_{H} (CDCl₃, 600 MHz) 6.75-7.40 (12H, br m), 7.45-8.10 (12H, br m); δ_{C} (CDCl₃, 151 MHz) 115.8 (dt, $J_{\text{C-P}}$ 5, $J_{\text{C-F}}$ 21, *meta*-CH of Ph), 129.9 (t, $J_{\text{C-P}}$ 21, *ipso*-CH of Ph), 135.8 (dd_{app}, $J_{\text{C-P}}$ 12, $J_{\text{C-F}}$ 5, *ortho*-CH of Ph), 163.8 (d, $J_{\text{C-F}}$ 253, *para*-C of Ph), 216.1 (br m, CO), 221.5 (br m, CO); δ_{P} (CDCl₃, 243 MHz) 52.2; Anal. Calcd. for [C₄₀H₂₇BrF₆MnO₃P₂]: C, 55.45; H, 3.14. Found: C, 54.84; H, 2.76.

***mer-trans*-[MnBr(CO)₃(P(*p*-OMeC₆H₄)₂)] (228)**

Synthesised according to the general procedure 6.6.2 using MnBr(CO)₅ (100 mg, 0.364 mmol, 1 equiv.) and tris-(4-methoxyphenyl) phosphine (268 mg, 0.726 mmol, 2 equiv.). Yellow solid (315 mg, 94%); $\nu_{\max}/\text{cm}^{-1}$ IR-ATR (solid) 2008 (s, $\bar{\nu}$ CO), 1939 (s, $\bar{\nu}$ CO), 1908 (s, $\bar{\nu}$ CO); δ_{H} (CDCl₃, 600 MHz) 3.80 (18H, br s), 6.72-7.03 (12H, br m), 7.50-7.76 (12H, br m); δ_{C} (CDCl₃, 151 MHz) 55.3 (OCH₃), 113.6 (t, $J_{\text{C-P}}$ 5, *meta*-CH of Ph), 126.6 (t, $J_{\text{C-P}}$ 22, *ipso*-CH of Ph), 135.4 (t, $J_{\text{C-P}}$ 5, *ortho*-CH of Ph), 160.6 (br s, *para*-C of Ph), 217.0 (br m, CO), 224.6 (br m, CO); δ_{P} (CDCl₃, 243 MHz) 49.5; Anal. Calcd. for [C₄₅H₄₂BrMnO₉P₂]: C, 58.52; H, 4.58. Found: C, 58.17; H, 4.59.

Note: A few extra signals of low intensity were observed in the ¹³C NMR and ³¹P NMR spectra for **228**, which did not correspond to the free phosphine ligand nor the oxide. The signals may be due to the fluxionality of the complex in solution.

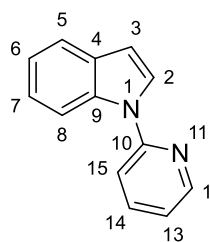
***fac-cis*-[MnBr(CO)₃(dppp)] (229)⁵⁰**

Synthesised according to the general procedure 6.6.2 using MnBr(CO)₅ (80 mg, 0.30 mmol, 1 equiv.) and dppp (256 mg, 0.62 mmol, 2 equiv.). Yellow solid (158 mg, 81%); $\nu_{\max}/\text{cm}^{-1}$ IR-ATR (solid) 2019 (s, $\bar{\nu}$ CO), 1953 (s, $\bar{\nu}$ CO), 1905 (s, $\bar{\nu}$ CO); δ_{H} (CDCl₃, 600 MHz) 1.50-1.71 (2H, m), 2.17-2.43 (2H, m), 3.29 (2H, t, J 13) [-Ph₂PCH₂CH₂CH₂PPh₂-], 7.26-7.52 (16H, m), 7.62-7.76 (4H, m)

δ_{C} (CDCl₃, 150 MHz) 19.0 (CH₂CH₂CH₂), 24.5 (t, $J_{\text{C-P}}$ 12, PCH₂CH₂CH₂P), 128.2 (t, $J_{\text{C-P}}$ 4, *meta*-CH of Ph), 128.5 (t, $J_{\text{C-P}}$ 4, *meta*-CH of Ph), 130.0 (s, *para*-CH of Ph), 130.4 (s, *para*-CH of Ph), 132.13 (t, $J_{\text{C-P}}$ 5, *ortho*-CH of Ph), 133.6 (t, $J_{\text{C-P}}$ 5, *ortho*-CH of Ph), 133.7 (t, $J_{\text{C-P}}$ 22, *ipso*-CH of Ph), 136.7 (t, $J_{\text{C-P}}$ 22.3, *ipso*-CH of Ph), 216.4 (br m, CO), 223.0 (br m, CO); δ_{P} (CDCl₃, 243 MHz) 28.3; Anal. Calcd. for [C₃₀H₂₆BrMnO₃P₂]: C, 57.08; H, 4.15. Found: C, 57.00; H, 3.74.

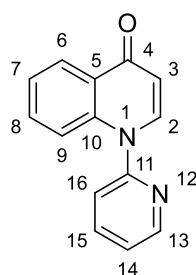
Spectral characteristics are consistent with previously reported data.⁵⁰

6.6.3 Synthesis of starting materials

***N*-(2-pyridyl)-indole (247)⁵¹**

To a 2-necked round bottomed flask was added indole (**245**) (7.03 g, 60 mmol, 1.2 equiv.), KOH (7.01 g, 125 mmol, 2.08 equiv.) and anhydrous DMSO (50 mL). The resulting mixture was stirred in a sand bath at 94 °C for 1 hour under a blanket of nitrogen. During the time, the reaction mixture turned a dark red colour indicating deprotonation of indole had occurred. 2-Bromopyridine (**246**) (7.9 g, 4.77 mL, 50 mmol, 1 equiv.) was then added *via* syringe. The reaction mixture was stirred at 135 °C in a sand bath for 48 hours. Upon cooling, the reaction mixture was diluted with ethyl acetate (200 mL) and washed with water (100 mL). The combined organic extracts were then washed with saturated aqueous NaHCO₃ (60 mL) and brine (80 mL). The organic layer was then dried over MgSO₄, filtered and concentrated under reduced pressure. The crude material was purified by column chromatography using hexanes:Et₂O (90:10) to give the product **247** as a light yellow oil (3.97 g, 41%); $\nu_{\text{max}}/\text{cm}^{-1}$ (NaCl) 1589 (aromatic C=C stretch), 1472 (aromatic C=C stretch), 1346 (C-N stretch), 1240 (C-N stretch), 761 (aromatic C-H bend); δ_{H} (CDCl₃, 300 MHz) 6.71 (1H, dd J 3.5, 0.8, C(3)H), 7.12-7.23 (2H, m, C(6)H & C(13)H), 7.31 (1H, td, J 7.8, 1.4, C(7)H), 7.49 (1H, dt J 8.4, 0.9, C(5)H), 7.66 (1H, ddd, J 7.8, 1.3, 0.6, C(8)H), 7.72 (1H, d, J 3.5, C(2)H), 7.82 (1H, ddd, J 8.3, 6.9, 2.0, C(15)H), 8.19-8.25 (1H, m, C(14)H), 8.56 (1H, ddd, J 4.8, 1.9, 0.7, C(12)H); δ_{C} (CDCl₃, 75.5 MHz) 105.5 (C(3)H), 113.0 (C(8)H), 114.6 (C(15)H), 120.0 (C(13)H), 121.1 (C(5)H), 121.3 (C(6)H), 123.1 (C(7)H), 126.0 (C(2)H), 130.5 (qC-4), 135.1 (qC-9), 138.4 (C(14)H), 149.0 (C(12)H), 152.6 (qC-10); m/z (ES⁺): 195, [(M+H)⁺, 30%].

Spectral characteristics are consistent with previously reported data.⁵¹

1-(2-pyridyl)-4-(1H)-quinolone (256)⁵²⁻⁵³

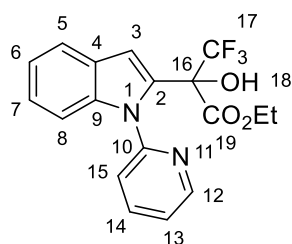
To A Schlenk tube evacuated and refilled with nitrogen three times was added 4-quinolinol (**255**) (500 mg, 3.44 mmol, 1 equiv.), CuI (65.5 mg, 0.344 mmol, 10 mol%) and K₂CO₃ (475 mg, 3.44 mmol, 1 equiv.). 2-Bromo pyridine (**246**) (0.66 mL, 6.88 mmol, 2 equiv.) was added *via* syringe followed by anhydrous DMSO (2 mL/mmol). The reaction mixture was stirred at 150 °C in a sand bath for 24 hours. Upon cooling to room temperature, the reaction

mixture was quenched with NH_4OH (20 mL) and then diluted with EtOAc (20 mL). The organic layer was separated from the aqueous layer and then washed with water (3×10 mL) and brine (20 mL). The organic layer was then dried over MgSO_4 , filtered and concentrated under reduced pressure. The crude material was purified by column chromatography using DCM: MeOH (98:2) to give the product **256** as a white solid (112 mg, 15%); m.p. 104-106 °C; $\nu_{\text{max}}/\text{cm}^{-1}$ (NaCl) 1624 (C=O stretch), 1609 (aromatic C=C stretch), 1582 (alkene C=C stretch), 1482 (aromatic C=C stretch), 1466 (C-N stretch), 1290 (C-N stretch), 757 (aromatic C-H bend); δ_{H} (CDCl_3 , 300 MHz) 6.37 (1H, d, J 7.9, C(2)H), 7.21 (1H, d, J 8.7, C(16)H), 7.31-7.40 (1H, m, C(3)H), 7.43-7.56 (3H, m, C(7)H, C(8)H & C(14)H), 7.79 (1H, d, J 8.1, C(9)H), 7.97 (1H, td, J 8.3, 2.0, C(15)H), 8.44 (1H, dd, J 8.1, 1.5, C(6)H), 8.68 (1H, dd, J 5.6, 1.9, C(13)H); δ_{C} (CDCl_3 , 75.5 MHz) 110.8 (C(3)H), 116.6 (C(14)H), 121.5 (C(16)H), 123.1 (C(9)H), 124.1 (C(6)H), 124.2 (C(7)H), 126.5 (qC-5), 126.7 (C(8)H), 139.3 (C(15)H), 140.1 (qC-10), 141.6 (C(2)H), 150.4 (C(13)H), 153.4 (qC-11), 178.4 (qC-4); m/z (ES+): 223, [(M+H)⁺, 100%].

Spectral characteristics are consistent with previously reported data.⁵²⁻⁵³

6.6.4 General procedure for preparation of compounds **263** and **264**⁵⁴

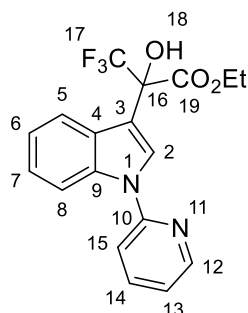
A Schlenk tube was heated under vacuum and refilled with N_2 three times. NaOAc (4.22 mg, 0.051 mmol, 20 mol%) and Mn catalyst (10 mol%) were added. The stopper was then replaced with a rubber septum. Ethyl trifluoropyruvate (**262**) (0.068 mL, 0.514 mmol, 2 equiv.) was added through a syringe. *N*-(2-pyridyl)indole (**247**) (50 mg, 0.267 mmol, 1 equiv.) was dissolved in anhydrous 1,4-dioxane (0.5 mL) in a separate 50 mL round bottomed flask under a N_2 atmosphere. This solution was then added *via* syringe to the Schlenk tube containing the solids and ketone. The rubber septum was replaced with a stopper. The resulting reaction mixture was stirred in an oil bath heated to 100 °C for 16-26 hours. After cooling to room temperature, the reaction mixture was quenched with H_2O (10 mL) and EtOAc (10 mL). The organic layer was separated from the aqueous layer and washed with H_2O (2×10 mL) and brine (10 mL). The combined organic layers were dried over MgSO_4 and filtered through a plug of Celite[®] into a 50 mL round bottomed flask. The solvent was evaporated *in vacuo*. The crude product was purified by column chromatography (hexanes:EtOAc, 70:30).

Ethyl 3,3,3-trifluoro-2-hydroxy-2-[1-(pyridin-2-yl)-1H-indol-2-yl]propanoate (263)⁵⁴

Synthesised according to the general procedure **6.6.4** using *N*-(2-pyridyl)indole (**247**) (50 mg, 0.257 mmol, 1 equiv.), ethyl trifluoropyruvate (**262**) (0.068 mL, 0.514 mmol, 2 equiv.) and $\text{MnBr}(\text{CO})_4(\text{PPh}_3)$ (**223**) (13.1 mg, 0.0357 mmol, 10 mol%). The reaction mixture was stirred at 100 °C for 26 hours. The crude

product was purified by preparative TLC (DCM:hexanes, 9:1). Colourless solid (48 mg, 51%). $\nu_{\text{max}}/\text{cm}^{-1}$ (NaCl) 1758 (ester C=O stretch), 1592 (aromatic C=C stretch), 1474 (aromatic C=C stretch), 1247 (ester C-O stretch), 1214 (C-F stretch), 1160 (ether C-O stretch), 740 (aromatic C-H bend); δ_{H} (CDCl_3 , 600 MHz) 0.98 (3H, t, J 7.6, C(21) H_3 ester), 3.77-3.99 (3H, m, O(18) H & C(20) H_2 ester), 6.89-6.95 (1H, m, C(3) H), 7.10-7.23 (2H, m, C(6) H & C(13) H), 7.26 (1H, ddd, J 7.5, 5.0, 1.1, C(7) H), 7.32-7.38 (1H, m, C(5) H), 7.53 (1H, dt, J 8.2, 0.8, C(8) H), 7.58-7.66 (1H, m, C(15) H), 7.87 (1H, ddd, J 8.2, 7.7, 1.9, C(14) H), 8.41 (1H, ddd, J 5.0, 1.9, 0.8, C(12) H); δ_{C} (CDCl_3 , 150 MHz) 13.7 (C(21) H_3 ester), 63.1 (C(20) H_2 ester), 77.0 (qC-19, q, $J_{\text{C-F}}$ 30), 107.4 (C(3) H), 110.3 (C(8) H), 120.4 (C(15) H), 121.9 (C(13) H), 122.0 (C(5) H), 122.4 (C(6) H), 123.3 (qC-17, q, $J_{\text{C-F}}$ 286), 124.2 (C(7) H), 127.8 (qC-4), 133.6 (qC-2), 136.7 (qC-9), 138.4 (C(14) H), 148.3 (C(12) H), 150.9 (qC-10), 168.1 (qC-19); δ_{F} (CDCl_3 , 600 MHz) -73.9; m/z (ES⁺): 297, [(M+H)⁺, 60%].

Spectral characteristics were consistent with previously reported data.⁵⁴

Ethyl 3,3,3-trifluoro-2-hydroxy-2-[1-(pyridin-2-yl)-1H-indol-3-yl]propanoate (264)⁵⁴

Synthesised according to the general procedure **6.6.4** using *N*-(2-pyridyl)indole (**247**) (50 mg, 0.257 mmol, 1 equiv.), ethyl trifluoropyruvate (**262**) (0.068 mL, 0.514 mmol, 2 equiv.) and $\text{MnBr}(\text{CO})_5$ (7.06 mg, 0.0257 mmol, 10 mol%). The reaction mixture was stirred at 100 °C for 16 hours. Colourless solid (82 mg, 88%). $\nu_{\text{max}}/\text{cm}^{-1}$ (NaCl) 1741 (ester C=O stretch), 1593 (aromatic C=C stretch), 1472 (aromatic C=C stretch), 1229 (C-F stretch), 1184 (ester C-O stretch), 1136 (ether C-O stretch), 745 (aromatic C-H bend); δ_{H} (CDCl_3 , 300 MHz) 1.35 (3H, t, J 7.2, C(21) H_3 ester), 4.32-4.54 (3H, m, O(18) H & C(20) H_2 ester), 7.19-7.27 (2H, m, C(6) H & C(13) H), 7.31 (1H, td, J 7.8, 1.2, C(7) H), 7.51 (1H, dt, J 8.2, 0.7, C(5) H), 7.85 (1H, ddd, J 8.2, 7.4, 1.9, C(8) H), 7.90-7.97 (1H, m, C(15) H), 7.99 (1H, s, C(2) H), 8.07-8.15 (1H, m, C(14) H), 8.59 (1H, ddd, J 4.9, 2.0, 0.8, C(12) H); δ_{C} (CDCl_3 , 75.5 MHz)

13.9 (C(21)H₃ ester), 64.4 (C(20)H₂ ester), 76.6 (qC-16, q, J_{C-F} 32), 111.0 (qC-3), 112.7 (C(8)H), 115.3 (C(15)H), 120.9 (C(13)H), 121.5 (C(5)H), 121.8 (C(6)H), 123.4 (qC-17, q, J_{C-F} 284), 123.7 (C(7)H), 126.4 (C(2)H), 127.4 (qC-4), 135.6 (qC-9), 138.5 (C(14)H), 149.2 (C(12)H), 151.8 (qC-10), 169.1 (qC-19); δ_F (CDCl₃, 300 MHz) -76.4; m/z (ES⁺): 297, [(M+H)⁺, 60%].

Spectral characteristics were consistent with previously reported data.⁵⁴

6.5 References

1. Kato, Y., Okada, S., Tomimoto, K., Mase, T. *Tetrahedron Lett.* **2001**, 42, 4849-4851.
2. Nolan, M.-T., Pardo, L. M., Prendergast, A. M., McGlacken, G. P. *J. Org. Chem.* **2015**, 80, 10904-10913.
3. Mackey, K., Pardo, L. M., Prendergast, A. M., Nolan, M.-T., Bateman, L. M., McGlacken, G. P. *Org. Lett.* **2016**, 18, 2540-2543.
4. Alizadeh, A., Ghanbaripour, R. *Synlett* **2014**, 25, 2777-2780.
5. Lutz, R. E., Codington, J. F., Rowlett, R. J., Deinet, A. J., Bailey, P. S. *J. Am. Chem. Soc.* **1946**, 68, 1810-1812.
6. Abe, I., Abe, T., Wanibuchi, K., Noguchi, H. *Org. Lett.* **2006**, 8, 6063-6065.
7. Kappe, T., Korbuly, G., Stadlbauer, W. *Chem. Ber.* **1978**, 111, 3857-3866.
8. Bistri, O., Correa, A., Bolm, C. *Angew. Chem. Int. Ed.* **2008**, 47, 586-588.
9. Jalalian, N., Ishikawa, E. E., Silva, L. F., Olofsson, B. *Org. Lett.* **2011**, 13, 1552-1555.
10. Zhao, J., Larock, R. C. *J. Org. Chem.* **2006**, 71, 5340-5348.
11. Tlili, A., Monnier, F., Taillefer, M. *Chem. Eur. J.* **2010**, 16, 12299-12302.
12. Bielawski, M., Aili, D., Olofsson, B. *J. Org. Chem.* **2008**, 73, 4602-4607.
13. Hampton, A. S., Mikulski, L., Palmer-Brown, W., Murphy, C. D., Sandford, G. *Bioorg. Med. Chem. Lett.* **2016**, 26, 2255-2258.
14. Ali, M. H., Buchwald, S. L. *J. Org. Chem.* **2001**, 66, 2560-2565.
15. Roy, S., Sarma, M. J., Kashyap, B., Phukan, P. *Chem. Commun.* **2016**, 52, 1170-1173.
16. Yu, J., Wang, Y., Zhang, P., Wu, J. *Synlett* **2013**, 24, 1448-1454.
17. Fors, B. P., Davis, N. R., Buchwald, S. L. *J. Am. Chem. Soc.* **2009**, 131, 5766-5768.
18. Wang, X., Jang, H.-Y. *Bull Korean Chem Soc.* **2012**, 33, 1785-1787.
19. Hernandez-Perez, A. C., Collins, S. K. *Angew. Chem. Int. Ed.* **2013**, 52, 12696-12700.
20. Bhojgude, S. S., Kaicharla, T., Biju, A. T. *Org. Lett.* **2013**, 15, 5452-5455.
21. Medina, J. M., Mackey, J. L., Garg, N. K., Houk, K. N. *J. Am. Chem. Soc.* **2014**, 136, 15798-15805.
22. Shanahan, R. M., Hickey, A., Reen, F. J., O'Gara, F., McGlacken, G. P. *Eur. J. Org. Chem.* **2018**, 2018, 6140-6149.
23. Ames, D. E., Opalko, A. *Synthesis* **1983**, 1983, 234-235.

24. Lam, P. Y., Clark, C. G., Saubern, S., Adams, J., Winters, M. P., Chan, D. M., Combs, A. *Tetrahedron Lett.* **1998**, 39, 2941-2944.
25. Evans, D. A., Katz, J. L., West, T. R. *Tetrahedron Lett.* **1998**, 39, 2937-2940.
26. Chan, D. M., Monaco, K. L., Wang, R.-P., Winters, M. P. *Tetrahedron Lett.* **1998**, 39, 2933-2936.
27. Lockner, J. W., Dixon, D. D., Risgaard, R., Baran, P. S. *Org. Lett.* **2011**, 13, 5628-5631.
28. Liu, X., Zhang, S. *Synlett* **2011**, 2011, 268-272.
29. Kammermeier, T., Kaiser, A., Lee, G. S., Burgemeister, T., Wiegrebe, W. *Arch. Pharm.* **1994**, 327, 207-210.
30. Colman, E. Z., Arias, K., Siegel, J. S., *Can. J. Chem.* **2009**, 87, 440-447.
31. Storr, T. E., Greaney, M. F. *Org. Lett.* **2013**, 15, 1410-1413.
32. Beaud, R., Phipps, R. J., Gaunt, M. J. *J. Am. Chem. Soc.* **2016**, 138, 13183-13186.
33. Tobisu, M., Hasegawa, J., Kita, Y., Kinuta, H., Chatani, N. *Chem. Commun.* **2012**, 48, 11437-11439.
34. Lindner, R., van den Bosch, B., Lutz, M., Reek, J. N. H., van der Vlugt, J. I. *Organometallics* **2011**, 30, 499-510.
35. Kapdi, A. R., Karbelkar, A., Naik, M., Pednekar, S., Fischer, C., Schulzke, C., Tromp, M. *RSC Adv.* **2013**, 3, 20905-20912.
36. Guo, D.-D., Li, B., Wang, D.-Y., Gao, Y.-R., Guo, S.-H., Pan, G.-F., Wang, Y.-Q. *Org. Lett.* **2017**, 19, 798-801.
37. Tang, L., Pang, Y., Yan, Q., Shi, L., Huang, J., Du, Y., Zhao, K. *J. Org. Chem.* **2011**, 76, 2744-2752.
38. Lee, Y. R., Kim, B. S., Kweon, H. I. *Tetrahedron* **2000**, 56, 3867-3874.
39. Adityachaudhury, N., Gupta, P. K. *Phytochemistry* **1973**, 12, 425-428.
40. Kamara, B. I., Brandt, E. V., Ferreira, D. *Tetrahedron* **1999**, 55, 861-868.
41. Wei, Y., Yoshikai, N. *Org. Lett.* **2011**, 13, 5504-5507.
42. Wang, C., Piel, I., Glorius, F. *J. Am. Chem. Soc.* **2009**, 131, 4194-4195.
43. Martínez, A., Fernández, M., Estévez, J. C., Estévez, R. J., Castedo, L. *Tetrahedron* **2005**, 61, 1353-1362.
44. Zhao, H., Yang, K., Zheng, H., Ding, R., Yin, F., Wang, N., Li, Y., Cheng, B., Wang, H., Zhai, H. *Org. Lett.* **2015**, 17, 5744-5747.

45. Xiao, B., Gong, T.-J., Liu, Z.-J., Liu, J.-H., Luo, D.-F., Xu, J., Liu, L. *J. Am. Chem. Soc.* **2011**, *133*, 9250-9253.
46. Chang, Y.-S., Deinzer, M. L. *Synth. Commun.* **1990**, *20*, 2501-2506.
47. Bonesi, S. M., Ponce, M. A., Erra-Balsells, R. *J. Heterocycl. Chem.* **2004**, *41*, 161-171.
48. Bond, A. M., Colton, R., McDonald, M. E. *Inorg. Chem.* **1978**, *17*, 2842-2847.
49. Angelici, R. J., Basolo, F. *J. Am. Chem. Soc.* **1962**, *84*, 2495-2499.
50. J. A. Pope, S., Reid, G. *J. Am. Chem. Soc., Dalton Trans.* **1999**, 1615-1622.
51. Cano, R., Ramón, D. J., Yus, M. *J. Org. Chem.* **2011**, *76*, 654-660.
52. Biswas, A., Giri, D., Das, D., De, A., Patra, S. K., Samanta, R. *J. Org. Chem.* **2017**, *82*, 10989-10996.
53. Das, D., Poddar, P., Maity, S., Samanta, R. *J. Org. Chem.* **2017**, *82*, 3612-3621.
54. Liang, Y.-F., Massignan, L., Liu, W., Ackermann, L. *Chem. Eur. J.* **2016**, *22*, 14856-14859.

“Nothing in the world can take the place of persistence, talent will not. Persistence and determination alone are omnipotent.”

Appendix I

Publications

"Cyclisation of 4-phenoxy-2-coumarins and 2-pyrones *via* a double C-H activation" Mackey, K., Pardo, L.M., Prendergast, A.M., Nolan, M.T., Bateman, L.M., McGlacken, G.P., *Org. Lett.*, 2016, 18, 11, 2540-2543.

"Recent advances in manganese catalysed C-H activation: scope and mechanism" Mackey, K., Cano, R., L.M., McGlacken, G.P., *Catal. Sci. Technol.*, 2018, 8, 1251-1266.

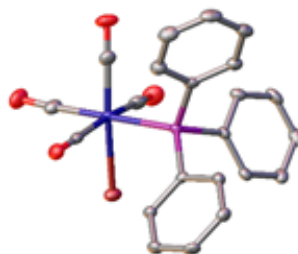
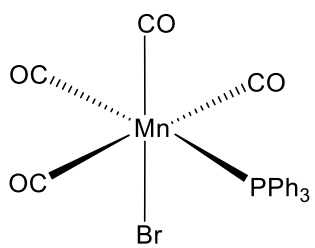
'Quinolines enhance reactivity in classic intramolecular C-H activations'. Mackey, K., Jones, D.J., Pardo, L.M., McGlacken, G.P. *manuscript in preparation*.

'Manganese carbonyl phosphine complexes in C-H activation reactions: first pre-catalyst modifications'. Mackey, K., McGlacken, G.P. *et al. manuscript in preparation*.

Appendix II

I

X-ray crystallographic data for *cis*-MnBr(CO)₄(PPh₃)

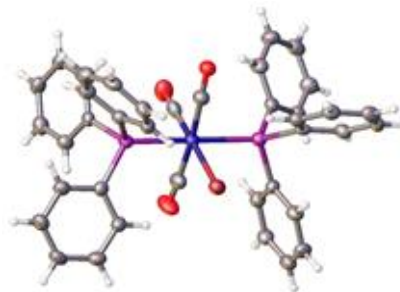
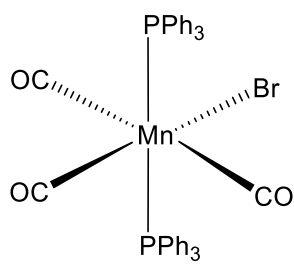


Empirical Formula	C ₂₂ H ₁₅ BrMnO ₄ P
<i>D</i>_{calc.}/ g cm⁻³	1.607
<i>μ</i>/mm⁻¹	2.627
Formula Weight	509.16
Colour	clear light yellow
Shape	block
Size/mm³	0.34×0.20×0.07
<i>T</i>/K	100(2)
Crystal System	triclinic
Space Group	<i>P</i> -1
<i>a</i>/Å	10.4449(3)
<i>b</i>/Å	14.0413(4)
<i>c</i>/Å	14.8389(5)
<i>α</i>/°	92.569(2)
<i>β</i>/°	100.099(3)
<i>γ</i>/°	99.819(3)
<i>V</i>/Å³	2104.90(11)
<i>Z</i>	4
<i>Z</i>'	2
Wavelength/Å	0.71073
Radiation type	MoK _α
<i>θ</i>_{min}/°	2.953
<i>θ</i>_{max}/°	28.499
Measured Refl.	33913
Independent Refl.	10637
Reflections with <i>I</i> > 2(<i>I</i>)	9086
<i>R</i>_{int}	0.0404
Parameters	523
Restraints	0
Largest Peak	0.789
Deepest Hole	-0.496

GooF	1.059
wR_2 (all data)	0.0805
wR_2	0.0765
R_1 (all data)	0.0493
R_1	0.0385

II

X-ray crystallographic data for *mer, trans*-MnBr(CO)₃(PPh₃)₂



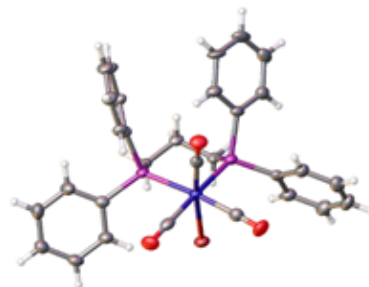
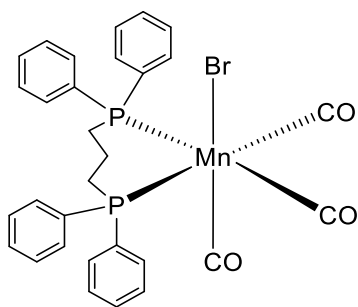
Empirical Formula	C ₃₉ H ₃₀ BrMnO ₃ P ₂
<i>D</i>_{calc.}/ g cm⁻³	1.499
<i>μ</i>/mm⁻¹	5.900
Formula Weight	743.42
Colour	clear orange
Shape	block
Size/mm³	0.22×0.12×0.09
<i>T</i>/K	120(2)
Crystal System	triclinic
Space Group	<i>P</i> -1
<i>a</i>/Å	10.2337(2)
<i>b</i>/Å	12.2596(3)
<i>c</i>/Å	14.4575(3)
<i>α</i>/°	97.164(7)
<i>β</i>/°	104.352(7)
<i>γ</i>/°	106.483(7)
<i>V</i>/Å³	1647.47(10)
<i>Z</i>	2
<i>Z</i>'	1
Wavelength/Å	1.54187
Radiation type	CuK _α
<i>θ</i>_{min}/°	3.227
<i>θ</i>_{max}/°	68.490
Measured Refl.	18722
Independent Refl.	5927
Reflections with <i>I</i> > 2(<i>I</i>)	4416
<i>R</i>_{int}	0.0594
Parameters	413
Restraints	6
Largest Peak	0.700
Deepest Hole	-0.575
Goof	1.054
<i>wR</i>₂ (all data)	0.1195
<i>wR</i>₂	0.1101
<i>R</i>₁ (all data)	0.0820

R_1

0.0579

III

X-ray crystallographic data for *fac, cis*-MnBr(CO)₃(dppp)



Empirical Formula	C ₃₀ H ₂₆ BrMnO ₃ P ₂
<i>D</i>_{calc.}/ g cm⁻³	1.521
<i>μ</i>/mm⁻¹	6.932
Formula Weight	631.30
Colour	clear light yellow
Shape	block
Size/mm³	0.25×0.11×0.06
<i>T</i>/K	120(2)
Crystal System	monoclinic
Space Group	<i>P</i> 2 ₁ / <i>n</i>
<i>a</i>/Å	10.0980(3)
<i>b</i>/Å	20.6590(6)
<i>c</i>/Å	13.7894(4)
<i>μ</i>/°	90
<i>β</i>/°	106.548(7)
<i>γ</i>/°	90
<i>V</i>/Å³	2757.52(17)
<i>Z</i>	4
<i>Z</i>'	1
Wavelength/Å	1.54187
Radiation type	CuK _α
<i>θ</i>_{min}/°	3.970
<i>θ</i>_{max}/°	68.489
Measured Refl.	30333
Independent Refl.	5010
Reflections with <i>I</i> > 2(<i>I</i>)	3816
<i>R</i>_{int}	0.1246
Parameters	334
Restraints	0
Largest Peak	0.812
Deepest Hole	-0.489
Goof	1.037
<i>wR</i>₂ (all data)	0.1496
<i>wR</i>₂	0.1372
<i>R</i>₁ (all data)	0.0830

R_1

0.0590

